DISSERTATION

ON THE NATURE AND MECHANICS OF FLOODPLAIN RESPONSE AND STABILITY IN THE SEMI-ARID ENVIRONMENT OF SOUTHERN CALIFORNIA

Submitted by

David Walter Dust

Department of Civil and Environmental Engineering

In partial fulfillment of the requirements

For the Degree of Doctor of Philosophy

Colorado State University

Fort Collins, Colorado

Fall 2009

COLORADO STATE UNIVERSITY

September 8, 2009

WE HEREBY RECOMMEND THAT THE DISSERTATION PREPARED UNDER OUR SUPERVISION BY DAVID WALTER DUST ENTITLED “ON THE NATURE AND MECHANICS OF FLOODPLAIN RESPONSE AND STABILITY IN THE SEMI-ARID ENVIRONMENT OF SOUTHERN CALIFORNIA” BE ACCEPTED AS FULFILLING IN PART REQUIREMENTS FOR THE DEGREE OF DOCTOR OF PHILOSOPHY.

Committee of Graduate Work

Neil S. Grigg

Chester C. Watson

Ellen E. Wohl

Adviser – Brian P. Bledsoe

Department Head – Luis A. Garcia

ABSTRACT OF DISSERTATION

ON THE NATURE AND MECHANICS OF FLOODPLAIN RESPONSE AND STABILITY IN THE SEMI-ARID ENVIRONMENT OF SOUTHERN CALIFORNIA

The core research questions motivating this dissertation are: (1) *How can we assess the existing stability state of a floodplain?* ; and (2) *How can we estimate the trend and magnitude of the change in floodplain geometry due to urbanization?* Field investigations conducted early in this research indicated that it was essential to build a basic framework of understanding for the fluvial systems in the semi-arid environment of southern California, prior to addressing the core research questions. To build this framework, various classification systems and conceptual models have been developed to characterize the nature and form of floodplains at multiple spatial scales.

A reach-scale classification system and conceptual model were created to synthesize the observed floodplain forms into three basic floodplain continuums (armored, non-armored, and active-regional alluvial fan), where each of these continuums are comprised of three to five alluvial floodplain forms (cascade, step-pool, plane-coarse-bed, plane-mixed-bed, plane-fine-bed, pool-riffle, braided, and dune-ripple). A catchment-scale conceptual model was created to describe the interrelationship between the three basic floodplain continuums in terms of climatic and geologic metrics. This conceptual model provided the basis to develop a practical GIS-based technique for predicting the floodplain continuum type within a catchment.

For the non-armored and armored floodplain continuums, floodplain state plots have been generated to quantitatively describe the natural downstream progression of

floodplain forms, using specific stream power and the width-to-depth ratio as the state and shape metrics. These floodplain state plots provided the bases to create *conceptual models for intra-catchment processes* and to develop techniques for assessing the stability state of a floodplain.

Using the series of conceptual models as a framework, regime-type modeling tools have been developed for estimating the trend and magnitude of the change in floodplain geometry due to changes in water and sediment supply. At the core of these tools are the basic flow relationships of continuity, flow resistance, and sediment transport for floodplains with trapezoidal geometry. To factor in bank erosional resistance and stability characteristics, the basic flow relationships are coupled with floodplain response and stability constraints developed from the *conceptual models for intra-catchment processes*.

David Walter Dust
Department of Civil and Environmental Engineering
Colorado State University
Fort Collins, CO 80523
Fall 2009

Acknowledgements

Though the work documented in this dissertation represents my contribution to the SCCWRP Hydromodification Project, the opportunity and the resources that have made completion of this dissertation possible are due to the efforts of many. First, I would like to thank the sponsors for the Southern California Coastal Water Research Project (SCCWRP) Hydromodification Project: California State Water Resources Control Board (via Proposition 50 funding)and the Counties of Los Angeles, Orange, Riverside, San Bernardino, San Diego, and Ventura. In addition, I want to thank the principle investigators for the project, Eric Stein (SCCWRP) and Brian Bledsoe (Colorado State University), for providing me the opportunity to participate in the project.

An extensive set of field data was the basis for this dissertation and collecting this field data involved months of rather arduous effort by myself and many others. First, I want to thank the following SCCWRP personnel for making the field data collection efforts both exceptionally productive and "good fun": Liesl Tiefenthaler, Greg Lyon, Jeff Brown, and Becky Schaefer. These individuals also provided an invaluable sense of camaraderie to the data collection efforts for which I am sincerely appreciative and forever in their debt. Second, I want to thank fellow student, Bob Hawley, and the personnel from Stillwater Sciences and the Riverside County Flood Control and Water Conservation District for their key roles in the data collection efforts.

I believe that key elements of this dissertation are the conceptual models describing the form and nature of the floodplains observed in the semi-arid environment of southern California. For providing both the encouragement and technical support to pursue development of these conceptual models, I want to sincerely thank my committee members:

Ellen Wohl, Chester Watson, and Neil Grigg. For without your encouragement and support, development of the conceptual models may never have been part of this dissertation.

For helping me formulate and bounce around ideas, I want to thank my friends and colleagues Kristin Bunte, Seema-Shah Fairbank, Lina Polvi, Tew-Fik Mahdi, and Jack Moody. Our hours of discussions were influential to my investigations and greatly appreciated.

Last but not least, I want to give special thanks to my wife, Diane, and my mother-in-law, Marjorie Franklin, for providing both moral support and encouragement throughout my studies at Colorado State University.

Table of Contents

List of Appendices

List of Figures

List of Tables

List of Symbols

Greek Symbols	
α	kinetic energy coefficient ≈ 1.15
β_0	intercept
β_1 & β_2	partial slope coefficients
γ	specific weight of water = 9810 (kg/m^{2}s^2)
γ_s	specific weight of sediment = 25,967 (kg/m^{2}s^2)
υ	kinematic viscosity = 1.0x10^{-6} (m^2/s) at 20^o C.
ϕ_i	Shear stress to reference shear stress ratio
ρ_s	density of sediment =2647(kg/m^3)
τ	total boundary shear stress (Pa = kg/ms^2)
τ^*	Shields parameter
τ^*_{ri}	dimensionless reference shear stress
$\left(\tau^*_{ri}\right)_j$	dimensionless incipient motion criteria for *i* = s or g and *j* = 0 or 1
ω	specific stream power (W/m^2)
ω_f	fall velocity (m/s)
Ω	total stream power (W/m)
Symbols	
A	flow area (m^2)
A_c	catchment area (km^2 or mi^2)
A_{pi}	area for precipitation polygon "*i*" (km^{2}or mi^2)
A_{Gi}	area for *Geo-Soil* polygon "*i*" (km^{2}or mi^2)
b	bottom width of a trapezoidal or rectangular channel (m)
C_{ts}	total sand concentration (ppm by weight)
C_{tg}	total gravel concentration (ppm by weight)
$D=A/W$	hydraulic depth (m)
d	maximum flow depth (m)
d_{gs}	grain size (m)
d_{50}	particle size for which 50% of the particles in the sample are smaller(mm or m)
d_{84}	particle size for which 84% of the particles in the sample are smaller(mm or m)
d_m	median grain size or particle diameter (m)
d_i	characteristic grain size for size fraction "*i*" (m)
d_s	characteristic grain size for sand fraction (m)
d_g	characteristic grain size for gravel fraction (m)
D_e	embedded depth of largest or dominant grain size in surface layer

ff	friction factor
F_r	Froude Number
F_s	sand fraction of surface bed material (range 0 to 1)
F_g	gravel fraction of surface bed material (0 to 1)
g	acceleration of gravity = 9.81 (m/s^2)
$G = \gamma_s / \gamma$	specific gravity of sediment = 2.65
G_{aw}	Area-Weighted *Geo-Soil* Score (range 1 to 3)
G_i	*Geo-Soil Value* for *Geo-Soil* polygon "*i*" (range 1 to 3)
h	bank height
h_c	critical bank height
L	reach length
M	percentage of silt and clay in the perimeter of the channel
n	Manning's roughness coefficient
$P(Y= S_A)$	probability that dependent variable *Y* is in *State A*
$P(Y= S_B)$	probability that dependent variable *Y* is in *State B*
P_{AW}	area-weighted average annual precipitation (m or in)
P_i	average annual precipitation for polygon "*i*" (m or in)
P_w	wetted perimeter (m)
q_{bi}	volumetric transport rate per unit width for $i = s$ or g (m^2/s)
q_{bt}	total unit transport rate (m^2/s)
Q_{bt}	Total volumetric transport rate (m^3/s)
Q_T	peak flow rate with return period T years (m^3/s or ft^3/s)
Q	flow rate (m^3/s)
Q_s	sediment transport rate (units vary) or inflowing sediment supply
$R = A / P_w$	hydraulic radius (m)
S_A & S_B	*State A* and *State B* are the dichotomous states of dependent variable *Y*
S_b	bed or bottom slope (m/m)
S_f	energy line or friction slope (m/m)
S_w	water surface slope (m/m)
S_v	valley slope
SE_i	standard error of coefficient "*i*" in logistic regression analyses
$\mathrm{T} = W / d$	width-to-depth ratio or dimensionless shape factor
U_*	shear velocity (m/s)
V	flow velocity (m/s)
V_{S1} & V_{S2}	volume of sediment represented by hydrograph
V_{W1} & V_{W2}	volume of water represented by hydrograph
V_{cr} / ω_f	critical dimensionless unit stream power

W	topwidth of flow area (m)
W_c	topwidth of channel (m)
X_1 & X_2	independent variable
Y	dependent variable
z	dimensionless side slope in term of z horizontal : 1 vertical units
Z_i	"Z" statistic for coefficient "i" in logistic regression analyses

Chapter 1: Introduction

1.1 Overview

This dissertation was prepared in partial fulfillment of the requirements for the degree of Doctor of Philosophy. The objectives of this introductory chapter are to:

- describe the practical and applied research questions at the core of this research study;
- provide descriptions of key terms and concepts that are at the base of this research;
- provide a brief description of the geopolitical boundaries for the study area;
- describe the overall methodology and approach for the investigations described in this dissertation; and
- provide an overview of the structure of this dissertation.

1.1.1 The Hydromodification Project and the Practical Research Questions Motivating This Research

This dissertation represents my principal contributions to the Southern California Coastal Water Research Project (SCCWRP) "Hydromodification Project", lead by Dr. Eric Stein (SCCWRP) and Dr. Brian Bledsoe (Colorado State University). In the context of this study, "hydromodification" is used to refer to the changes in sediment yield and runoff characteristics for a catchment associated with urbanization.

For this dissertation it is useful to recognize that there are the three basic types of questions that researchers can ask (Turabian, 2007):

- Practical Questions: *What should we do?*
- Applied Questions: *What must we understand before we know what we should do?*

- Conceptual Questions: *What should we think?*

When put in the form of a *practical* research question, the primary objective of the SCCWRP Hydromodification Project is to address: ***How should we evaluate and then mitigate the potential risk for severe floodplain instability, due to urbanization/hydromodification?***

For the SCCWRP Hydromodification Project, the principle investigators proposed the approach of developing a series of "tools" to address the aforementioned practical research question. More specifically, the following series of tools were proposed for evaluating and mitigating the potential risk for severe floodplain instability in response to hydromodification:

- "Screening Tools" for identifying the risk for and the potential trend of severe floodplain instability.
- "Modeling Tools" for evaluating the trend and magnitude of the change in floodplain geometry due to urbanization/hydromodification.
- "Mitigation Tools" for guiding recommended mitigation and management measures, including "Monitoring Protocol" for future data collection efforts.

In general terms, the geometry of a floodplain may change in terms of width, depth, and/or bed slope. Hence, the "trend" of the geomorphic response of a floodplain would be described in terms of the changes in the width, depth, and/or bed slope of the floodplain.

Like most dissertations prepared by engineering students, this dissertation has at its core the goal of addressing a *practical* research question. I was asked to make the task of developing the "Modeling Tools" the primary focus of my research; hence, the practical research question motivating my research is: ***How can we estimate the trend and magnitude of the change in floodplain geometry due to urbanization or***

hydromodification? However, I found over the course of my research that it was essential to have a basic understanding of the existing stability state of a floodplain prior to assessing the potential response of a floodplain. Therefore, addressing the following practical research question became inherently and inextricably tied to the overall motivation for my research: ***How can we assess the existing stability state of a floodplain?***

In order to discuss these two practical research questions effectively, it is imperative to have clear definitions for the terms "floodplain" and "severe instability"; hence, the following two sections discuss the meanings of these terms in the context of this dissertation.

1.1.2 Floodplains From an Engineering Perspective

In dictionaries and the literature, the term "floodplain" can have a wide range of typically overlapping definitions and can be spelled as one word, two words, or hyphenated (Graf 1988). Graf (1988) has identified a total of six different perspectives from which to view "floodplains", with the following being brief descriptions of the perspectives being most pertinent to this study:

- From a geomorphic perspective, the noun "flood plain" is used to describe "that portion of a river, adjacent to the channel, which is built of sediment deposited during the present regime of the river and is covered with water when the river overflows its banks at flood stages" (Bates and Jackson, 1984).
- From a hydrologic perspective, a cross section of a river has a channel flanked by "flood plains" that are inundated by water with a given return period (Graf, 1988; Ward, 1978).
- From an engineering perspective, the term "floodplain" is used to describe the land surface inundated by a flow event with a specific return period (e.g. 100 years) and a specific water surface profile. The water surface profile corresponding to the

floodplain is typically assessed with computer programs HEC-2 or HEC-RAS. Within these programs, a river cross section is typically divided into the *main channel* and the *right and left overbanks* (from the perspective of looking downstream) for computational purposes (Brunner, 2008).

Since this dissertation is concerned with floodplains from primarily an engineering perspective, the single word spelling of "floodplain" is used and the engineering perspective is intended, which is consistent with the Federal Emergency Management Agency's (FEMA) national flood insurance program (FEMA, 1986). When the term "floodplain" is intended to have a perspective different from the engineering perspective, the perspective will be specifically noted.

The engineering perspective of floodplains is illustrated in Figure 1.1 for a general downstream progression of floodplain forms observed in southern California. As illustrated in Figure 1.1, floodplains in southern California may be comprised of just a single-thread channel or floodplain, a compound floodplain comprised of a main channel and overbanks, and a braided floodplain with multiple channels and migrating bars.

1.1.3 The Applicability of Equilibrium Concepts and Defining States of Stability in the Semi-Arid Environment

In the context of this dissertation, it is important to ask: *Does the concept of* ***equilibrium*** *even apply to the perennial, ephemeral, or intermittent watercourses in the semi-arid environment, such as that in southern California?* I have debated the answer to this question with both fellow engineering students and professional colleagues on numerous occasions over the years, because it is generally well recognized that floodplains in the semi-arid environment can be rather dynamic in nature. During these debates, it was generally agreed that the concept of equilibrium can be useful from both an engineering and geomorphic perspective, when attempting to evaluate flooding and erosion hazards in the semi-arid environment. However, it was also agreed that it was absolutely essential when invoking equilibrium concepts to both: (a) clearly define *equilibrium* and the associated stability states specifically in terms of the semi-arid environment; and (b) acknowledge the limitations of doing such.

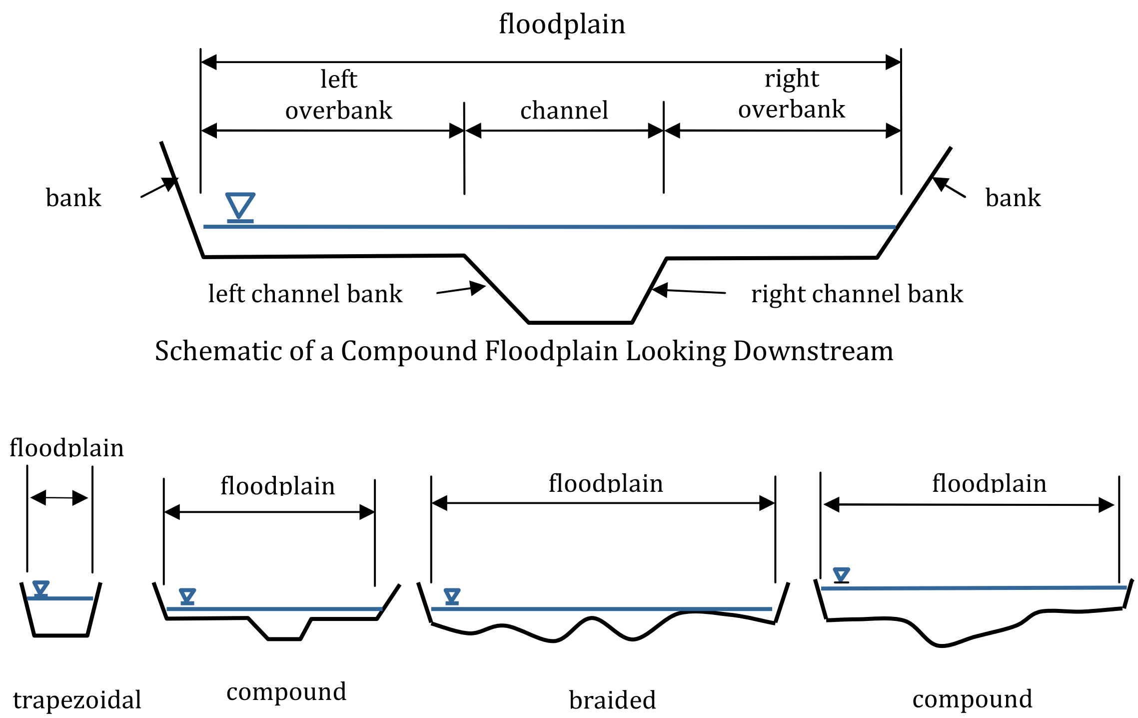

Figure 1.1 – Schematic illustrating the engineering perspective of a floodplain for a range of floodplain geometries

These investigations have found that equilibrium concepts can be useful for evaluating both the probability for floodplain instability and estimating the response of floodplains to changes in intra-catchment processes. Therefore, the objective of this section is to define how this author is invoking equilibrium concepts in the context of the semi-arid environment.

The fundamental fluvial geomorphic concept underlying the evaluation of watercourse stability is that an alluvial system can over time establish and maintain an equilibrium condition, where the geomorphic characteristics of a floodplain remain relatively stable over time (Tanner, 1968; Shen, 1979; Dingman, 1984). However, the geometry of a stable watercourse does not have to be static over time and may temporarily change in response to low flow events and/or natural variations in water and sediment supply. Therefore, the key characteristic of a stable watercourse is that fluvial processes, during floodplain formative flows, restore the geomorphic characteristics of a floodplain rather than perpetuating and amplifying changes in geomorphic characteristics (Watson, Biedenharn, and Thorne, 2005).

This type of stability is often referred to as ***dynamic equilibrium***. The basic assumption underlying the concept of dynamic equilibrium is that the geometry of a floodplain will adjust to convey both the water and sediment supplied from the upstream catchment, while maintaining a balance with the erosional resistance and stability characteristics of the banks within and/or along the periphery of the floodplain (Schumm, 1977).

Herein, the term ***severe instability*** is used to describe the state of a watercourse that is ***unstable*** and is **not** in a state of dynamic equilibrium. Hence, the key characteristic of a watercourse that is in the state of *severe instability* is that fluvial processes do not restore the geomorphic characteristics of the floodplain, but instead perpetuate and/or amplify changes in the geomorphic characteristics of the floodplain and permanently (in an engineering timescale) alter the water and/or sediment supply to the fluvial system. I contend that when the intra-catchment processes that govern the geomorphic characteristics of a floodplain are sufficiently perturbed and a state of severe instability is induced, the intra-catchment processes will undergo a long-term and complex transition. During this long-term transition period of potentially several decades to even centuries, the watercourse may undergo a complex series of significant, if not dramatic, changes in geomorphic characteristics. I believe that this definition for the state of *severe instability* is consistent, if not overlapping, with concepts described by Graf (1988) and other authors regarding temporal and spatial characteristics of flood plains (from a geomorphic perspective) along arid-region rivers, where a key concept is that "arid-region rivers … may not exhibit long-term (several decades) tendencies toward some equilibrium condition (Stevens, Simons, and Richardson, 1975; Graf, 1981)."

In a semi-arid environment where most watercourses are ephemeral in nature, the concept of *dynamic equilibrium* is further complicated by potentially long response times, because flow events are typically sporadic and characterized as having relatively short durations and high peaks. Hence, it is important to recognize that it may take years or maybe even decades for a floodplain to even begin to respond to significant changes in the catchment (such as urbanization), depending upon the number and magnitude of floodplain-forming flow events that have occurred since the changes in the catchment. During the period when a watercourse is responding to some perturbation in the catchment, the watercourse will be referred to as ***responding*** and in a state of ***dynamic response***. If the perturbation to the intra-catchment processes results in the watercourse passing some stability threshold, the watercourse will then become unstable and shift into the state of *severe instability*, for decades if not centuries, until the watercourse re-attains a new state of *dynamic equilibrium*. If the perturbation does not result in the watercourse passing some stability threshold, the geometry of the watercourse will adjust and attain a new state of *dynamic equilibrium* relatively quickly.

To summarize, I contend that within an engineering timescale a watercourse is in one of the following three stability states, as illustrated in Figure 1.2:

- ***Stable*** and in a state of ***dynamic equilibrium***: In this state, fluvial processes restore the geomorphic characteristics of the floodplain rather than perpetuating and amplifying changes in geomorphic characteristics, during floodplain formative flows (Watson, et al., 2005).

- ***Responding*** and in a state of ***dynamic response***: In this state, a watercourse is responding to a perturbation in the catchment, which may not be immediately or fully reflected in its geomorphic characteristics due to relatively long response times. If the cumulative influence of the perturbations are relatively minor, the watercourse will adjust in a relatively short period of time (i.e., years or decades) and obtain a new state of dynamic equilibrium. However, in cases where the cumulative influence of the perturbations cause the watercourse to exceed a threshold, the watercourse may become *unstable* and shift into a state of *severe instability.*
- ***Unstable*** and in a state of ***severe instability***: In this state, fluvial processes do not restore the geomorphic characteristics of the floodplain, but instead perpetuate and/or amplify changes in the geomorphic characteristics of the floodplain and permanently (in an engineering timescale) alter the water and/or sediment supply to the fluvial system. A watercourse may be in a state of *severe instability* for a long period of time (i.e., decades or centuries) before eventually attaining a new state of dynamic equilibrium, during which time the watercourse may undergo a complex series of dramatic changes in geomorphic characteristics.

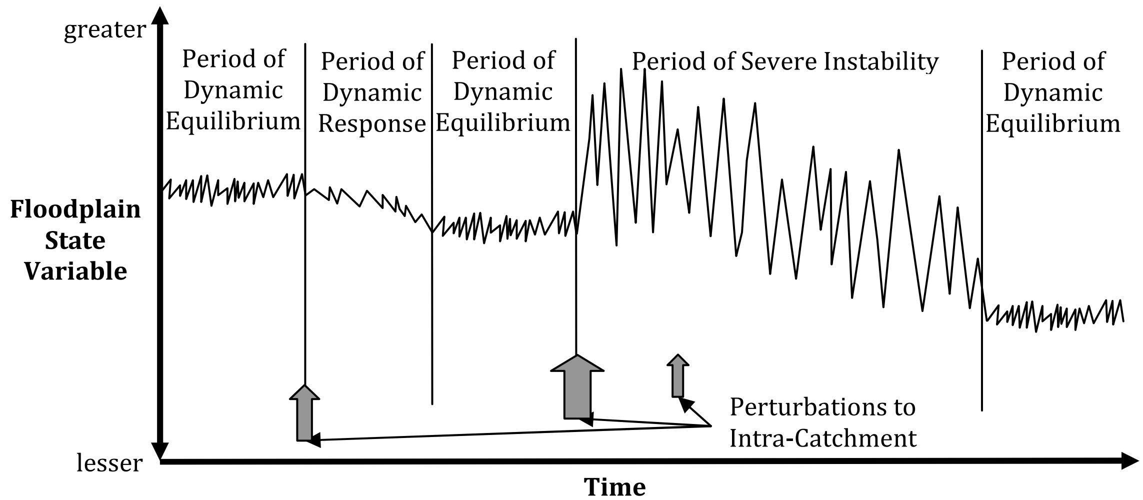

Figure 1.2 – Schematic illustrating the three stability states of dynamic equilibrium, dynamic response, and severe instability

Bull (1979) described the philosophical differences between the threshold and graded stream conceptual framework as follows:

"*Both approaches consider the interaction between process and form, but the threshold concept emphasizes the possibility of change in a fluvial system. Those using the threshold approach are more likely to be interested in when and where change occurs in fluvial systems and the reasons for change, rather than searching for approximations of equilibrium. The graded stream approach generally encourages study of self-regulating feedback mechanisms, but the threshold approach generally encourages study of self enhancing feedback mechanisms.*"

Given this description of the threshold conceptual framework, it is clear that the definitions of the three stability states, described herein, have been tailored to fit within the threshold conceptual framework.

Within the literature, there is a wide range of frameworks set forth for describing the stability states for watercourses. The stability state framework used in this research contains elements that are based on, consistent with, and/or similar to previous stability state frameworks, in addition to those already mentioned. Though posed in a slightly different context, it is believed that the stability state framework used in this research is consistent with the framework that "*within any landscape there are eroding, stable, healing, and potentially unstable landforms…*" as described by Schumm, Harvey, and Watson (1984). In addition, the stability states used in this research are also similar in some respects to the "*equilibrium, disequilibrium, and non-equilibrium*" landforms defined by Renwick (1992); however, there are also distinct differences.

This discussion of stability states leads to a very important point regarding the practical research questions motivating this research. To assess the trend and magnitude of the change in the geometry of a floodplain due to some perturbation in water and/or sediment supply, it is essential to be able to assess the current or existing stability state of the floodplain. This is why the following two practical research questions motivating this research are inherently and inextricably linked:

- How can we assess the existing stability state of a floodplain?
- How can we estimate the trend and magnitude of the change in floodplain geometry due to perturbations in intra-catchment processes associated with urbanization/hydromodification?

These practical research questions are addressed in Chapters 3 and 4, respectively.

1.1.4 Geopolitical Boundaries for This Study

As defined in the Hydromodification Project's scope of work, the study area was limited to the six southern-most counties in southern California with watersheds that drain to the Pacific Ocean. Hence, the study area includes portions of Ventura, Los Angeles, San Bernardino, Riverside, Orange, and San Diego Counties (as shown in Figure 1.3).

Figure 1.3 – Map showing geopolitical boundaries for this study within the State of California

1.2 Overall Approach and Methodology

1.2.1 Initial Site Investigations and Formulation of Applied Research Questions

As a member of the SCCWRP Hydromodification Project team, I was asked to make the task of developing "Modeling Tools" the primary focus of my research. As described earlier in this Chapter, I reformulated this task into the following interrelated *practical* research questions that are, therefore, at the core of my research and investigations:

- How can we assess the existing stability state of a floodplain?
- How can we estimate the trend and magnitude of the change in floodplain geometry due to perturbations in intra-catchment processes associated with urbanization/hydromodification?

Given these *practical* research questions, I then found it necessary to identify the underlying *applied* research question. That is, ***What must we understand before we know what to do?*** I found it necessary to at least attempt to "***understand the key processes and***

mechanisms that govern floodplain formation, response, and stability in southern California" before I could really begin to address the *practical* research questions at the core of this research.

The task of trying to identify and understand the key processes and mechanisms that govern floodplain formation, response, and stability in southern California is both daunting and complex. In the course of my career, I have found it is best to approach complex tasks by breaking them up into first logical and then manageable pieces. To do this effectively, it is imperative to have a basic understanding of the scope and bounds of the task. To gain this basic understanding for the project team, I (and Mr. Robert Hawley) conducted initial site investigations at fifty two (52) individual sites within the study area. These initial site investigations were primarily conducted at locations recommended by Dr. Eric Stein (a principle investigator) and the county floodplain administrators involved with the project. However, additional initial site investigations were conducted along reaches of watercourses identified either while in transit between the recommended sites or in aerial photographs while I was preparing to visit the recommended sites, when time and site access permitted. Hence, the initial site investigations were conducted at a combination of sites that were either pre-selected by others (and thereby, typically associated with instability issues) or essentially randomly identified.

During the initial site investigations, I made several key observations regarding the floodplain-reach morphologies for watercourses in the semi-arid environment of southern California, as listed in Table 1.1. However, the observation regarding the three basic floodplain continuums has been by far the most influential in terms of the approach and methodology adopted for this research.

Table 1.1 – Summary of key observations from initial site investigations

ID	Key Observations Regarding Floodplain Morphologies in the Semi-Arid Environment of Southern California
a	Though potentially more complex and/or significantly different than other regions of the United States, southern California catchments appear to have at least three basic floodplain continuums that are comprised of multiple floodplain forms which have a typical sequence along the length of the watercourse.
b	Catchments within the study area varied greatly in terms of both relief and the predominant sedimentation processes, which appear to be the direct result of the complex geologic history for the region.
c	The observed floodplain continuums and forms appear indicative of intra-catchment sedimentation processes, which can be impacted by hydromodification, floodplain encroachment, and/or base level changes.
d	Each of the various floodplain continuums and forms appear to have different response thresholds and mechanisms when impacted by hydromodification, floodplain encroachment, and/or base level changes.
f	The potential for and the magnitude of the change in the geometry of a floodplain in response to perturbations in water and/or sediment supply appear to be influenced by the catchment characteristics and the corresponding floodplain continuums.
e	Most, if not essentially all, watercourses naturally pass through a floodplain braiding threshold, where: • the threshold typically corresponds to a significant transition in both floodplain geometry and associated hydraulic characteristics; and • the spatial location of the corresponding floodplain transition can move upstream or downstream in response to both natural and/or induced perturbations to intra-catchment processes.

Armed with these observations and the knowledge gained from the initial site investigations, I then broke up the original task of *identifying the key processes and mechanisms associated with floodplain formation, response, and stability* into logical pieces by formulating the following series of *applied* research questions (i.e., what must we understand before we know what to do?):

- What are the forms and nature (i.e., geomorphic properties) of floodplains in southern California?
- What are the primary "process drivers" that govern the type of floodplain continuum within a catchment?
- What are the intra-catchment processes that govern the natural downstream floodplain form progression, including specifically the transition from single-thread to braided floodplains?

- What is the impact of urbanization on the primary intra-catchment processes that govern the natural downstream floodplain form progression?

The overall objective of formulating and addressing the aforementioned *applied* research questions is to obtain the insights and understanding needed to attempt to break up the task of addressing the *practical* research questions at the core of this into manageable pieces. To address the four applied research questions listed above, it was necessary to develop and execute an effective field data collection and analyses program.

1.2.2 Field Data Collection and Analyses Program

Following the initial site investigations and formulation of the applied research questions, the next key step was to develop the field data collection program. The primary elements of the field data collection program are as follows:

- Selection of the number and location of study sites.
- Identification of the level, extent, and format of the qualitative data collected at each study site.
- Identification of the level and extent of quantitative data collected at each study site.

As with essentially all projects, there was a limit to the time and effort that could be allocated to data collection. To get the most comprehensive data set for the given budget, significant effort and thought was given to the site selection process. During the initial site investigations, basic information was collected for each of the initial fifty two (52) sites, allowing them to be categorized and ranked. The Hydromodification Project Team determined that the budget allowed for data collection at approximately thirty (30) sites, if two (i.e., *screening* and *modeling*) levels of data collection were used. Thirty (30) data collection sites were selected by the project team, based on the criteria listed in Table 1.2.

Table 1.2 – Study site selection criteria

ID	Study Site Selection Criteria
1	Approximately 50% of sites should exhibit signs of instability, with the cause(s) or history of the instability being relatively identifiable or definable. That is, sites with long and/or complex histories of instability should not be considered.
2	Data sites should provide a representative range of: • Catchment urbanization levels. • Floodplain or channel forms. • Bed material composition. • Channel vegetation densities.
3	Sites should be representative of geo-political boundaries.
4	Most of the sites should have catchments less than 20 km^2 and all catchments should be less than 70 km^2.
5	Sites with floodplain form transitions and/or confluences are given priority.
6	Approximately 50% of the sites should be suitable for post flow event and/or long-term monitoring.
7	Sites where legal permission to access the site was either confirmed or obtained prior to the selection process are given priority.

As indicated in the previous paragraph, the Hydromodification Project Team determined that more sites could be included in the study, if two levels of data collection were employed. These two levels of field data collection are referred to as *screening* and *modeling* levels. As implied by the name, the *modeling* level of field data collection is intended to provide sufficient data to permit hydraulic modeling with rigid bed, movable bed, and/or movable boundary models. However, the primary difference between the two levels of data collection is that only one to three cross sections were surveyed at *screening* level sites; whereas, five to eighteen cross sections were surveyed at *modeling* level sites. The field data collection protocol for *screening* and *modeling* level sites are summarized in Table 1.3.

Table 1.3 – Summary of field data collection protocol

Field Data Collection Protocol
Qualitative data collected at each cross section within sites via a multiple-choice formatted data collection form: • Observed floodplain forms and sequences. • Estimation of Manning's roughness coefficient (*n*) for floodplain. • Bank characteristics, including a visual assessment of stability and/or modes of failure. • Basic bed material characteristics, including basic rock types, size ranges, and the level/extent of bed armoring. • Preliminary assessment of current stability state in terms of the Channel Evolution Model (CEM) Phases (Schumm, 1981; Schumm et al., 1984). • The level, extent, and characteristics of the vegetation within the floodplain. • Digital photographs of study reach documenting bed material, bed forms, bank conditions, and vegetation characteristics

Quantitative Data Collected at *Screening* Level Sites:
• 1 to 3 bed material gradations, based on pebble count and/or dry sieve analyses of bed material samples.
• Survey/geometry data collected using a pole mounted hand-level and Pocket Rod.
  o 1 to 3 floodplain cross sections.
  o bed profile extending approximately 50 meters upstream and downstream of cross section(s).

Quantitative Data Collected at *Modeling* Level Sites:
• 2 to 3 bed material gradations, based on pebble count and/or dry sieve analyses of bed samples.
• Survey/geometry data collected using either a total station or a survey level global positioning system by either Stillwater Consultants or Riverside County Public Works Department.
  o 5 to 18 floodplain cross sections
  o bed profile extending approximately 50 meters upstream and downstream of cross sections.

To provide the basis for developing and evaluating both conceptual models and computational procedures for estimating floodplain responses, the field data were used to compile a *hydraulic analysis* database. This hydraulic analysis database contains records for six flow conditions for each of the 124 surveyed cross sections, thereby creating a database with 744 records. Each record in this database has the following information or fields:

- Basic site data, including: floodplain form, bed slope, valley slope, valley width, existing stability state in terms of CEM stage, d_{50}, and a visually estimated value for Manning's roughness coefficient (n).

- Computed hydraulic parameters, including stage or maximum flow depth, wetted perimeter, hydraulic radius, hydraulic depth, topwidth, width-to-depth ratio, total boundary shear stress, Shields parameter, Froude Number, specific stream power, and total stream power.

1.2.3 Classification Systems and Conceptual Models

Key elements of this dissertation are the classification systems and conceptual models. A useful classification system provides a framework for identifying, describing, and organizing observed parameters and/or patterns. Whereas, "conceptual models" are a simplified representation of some aspect of the "real world". In the context of this dissertation, conceptual models can take the form of graphs, charts, tables, diagrams, proportionalities, and/or flow charts.

In this dissertation, conceptual models are used to address many of the "applied" research questions posed earlier in this chapter. In general terms, the objectives of the conceptual model are to:

- provide a useful visualization of a complex concept or system;
- describe the interactions or interrelationships between the observed floodplain forms and continuums;
- describe the interrelationships between the observed floodplain forms and continuums with intra-catchment process and/or process drivers;
- provide an effective method to identify and describe geomorphic thresholds and the associated physical processes or mechanisms;
- provide a framework for identifying and describing the observed downstream progression of floodplain forms, both qualitatively and quantitatively; and
- provide a framework for identifying and describing both the magnitude and trend of the change in floodplain geometry in response to urbanization or hydromodification.

1.2.4 Probabilistic Approach to Geomorphic Thresholds and a Regime-Type Approach for the Modeling Tools

Probabilistic Approach to Geomorphic Thresholds

Though it is more common for logistic regression analyses to be applied in the behavioral and health sciences, Tung (1985) and Bledsoe and Watson (2001) have applied logistic regression techniques in the evaluation and definition of geomorphic thresholds. In context of this research, a *binary linear logistic regression analysis* is a statistical technique that can be used to define geomorphic thresholds in terms of probability; hence, using this technique at least acknowledges that there maybe transition zones or natural variability associated with geomorphic thresholds.

When sufficient data existed, binary linear logistic regression analysis techniques have been applied to define stability and braiding thresholds. As described in Chapter 3, the approach adopted in these investigation was to attempt to define stability and braiding thresholds in terms of a *state* and a *shape* metric for floodplains. Like Nanson and Croke (1992), the primary state metrics considered in these investigations were specific stream power and total boundary shear stress, while the width-to-depth ratio was the primary shape metric considered.

Regime-Type Approach for the Modeling Tools

The basic assumption underlying the concept of dynamic equilibrium is that the geometry of a floodplain will adjust to convey both the water and sediment supplied from the upstream catchment, while maintaining a balance with the erosional resistance and stability characteristics of the banks (Schumm, 1977). Hence, it is generally argued that the basic flow relationships of continuity, resistance, and sediment transport are not sufficient to describe the processes by which the hydraulic geometry (including bed slope) of a watercourse adjusts to maintain dynamic equilibrium, because the basic flow relationships do not reflect the influence of the erosional resistance and stability characteristics of the banks (as argued and described by Laursen (1958) and Henderson (1966)). Therefore, the challenge in applying a regime-type modeling approach is to identify a relationship or constraint that defines how the width, depth, and slope of a floodplain adjust simultaneously to take into account the influence of the erosional resistance and stability characteristics of the banks.

A regime-type modeling approach has been adopted in this research to develop *modeling tools* for estimating the trend and magnitude of the change in floodplain geometry, where the solution of the basic flow relationships is facilitated by incorporating into the solution procedure what are referred to herein as *floodplain response constraints*. These *floodplain response constraints* are intended to take into account bank characteristics and have been derived from analysis of field data for a wide range of floodplain geometries, within the semi-arid environment of southern California. Similar to the geomorphic thresholds, the *floodplain response constraints* have also been defined in terms of state and shape metrics (e.g., specific stream power and width-to-depth ratio).

The solution procedures for the modeling tools include steps where what are referred to as ***floodplain stability constraints*** are used to assess the stability state of the floodplain and, thereby, evaluate the basic applicability of the regime-type modeling approach under specific conditions. Where possible, the *floodplain stability constraints* are quantitative in nature and are based on stability threshold defined by logistic regression analyses; otherwise, the *floodplain stability constraints* are qualitative in nature and are based on the comparison with field data.

1.3 Structure of This Dissertation

With the exception of this “Introduction” and the “Conclusions” chapter, each chapter describes classification systems, conceptual models, and/or modeling tools. The chapters have been organized in a progression such that each chapter builds on the concepts developed in the previous chapters.

To aid the reader in applying the equations and techniques provided in the text, definitions for variables or symbols are provided in the "list of symbols" near the front of this document and with each reference by an equation. In addition, equations that are referenced in multiple chapters are provided in each chapter with a new equation number; for example, the Manning equation is provided as both Equations 3.12 and 4.3. Furthermore, equations are often grouped into tables for ease of reference and application.

Within this document, Chapters 2, 3, and 4 are comprised of the following sections:

- An ***Overview*** section, which includes both an abstract and introduction for the chapter.
- A ***Previous Studies*** or literature review section.
- A ***Study Area*** section that describes key aspects of the study area pertinent to the specific chapter
- A ***Methods*** section that describes the field, computational, and/or statistical techniques pertinent to the chapter.
- A ***Results and Discussion*** section that presents the key findings and addresses the limitations and potential applications of the key findings.
- A ***Conclusions*** section that summarizes and relates the key findings back to both the practical and applied research questions at the core of this study, plus describes potential avenues for further investigations.

Chapter 2: Reach and Catchment Scale Conceptual Models Describing the Form and Nature of Floodplains in Southern California

2.1 Chapter Overview

2.1.1 Abstract

With the overall goal of building a framework for developing modeling tools for estimating the trend and magnitude of the change in floodplain geometry due to hydromodification, classification systems and conceptual models have been developed to characterize the nature and form of floodplains (i.e., channel plus overbank areas) at various scales in the semi-arid environment of southern California. To provide a basic spatial scale for comparing floodplain properties, a hierarchy of spatial scales was developed specifically for southern California. From the largest to the smallest scale, this hierarchy is comprised of the watershed, geomorphic province, catchment or valley segment, floodplain reach, and floodplain unit scales. A reach-scale classification system and conceptual model were created to synthesize the observed floodplain forms into three basic floodplain continuums (armored, non-armored, and active-regional alluvial fan), where each of these continuums are comprised of three to five alluvial floodplain forms (cascade, step-pool, plane-coarse-bed, plane-mixed-bed, plane-fine-bed, pool-riffle, braided, and dune-ripple). A catchment-scale conceptual model was developed to describe the interrelationship between the three basic floodplain continuums in terms of climatic and geologic metrics for a catchment. This conceptual model provided the basis to develop a practical GIS-based technique for predicting the floodplain continuum type within a catchment, utilizing GIS data available for the region.

2.1.2 Introduction/Research Questions

The fundamental fluvial geomorphic concept underlying the evaluation of watercourse stability is that an alluvial system can over time establish and maintain an equilibrium condition, where the geomorphic characteristics of the floodplain remain relatively stable over time (Tanner, 1968; Shen, 1979; Dingman, 1984). Another fundamental fluvial geomorphic concept pertinent to the evaluation of watercourse stability is that the natural downstream progression of alluvial floodplain forms represents a continuum rather than just discrete floodplain forms (Ferguson, 1987; Nanson and Croke, 1992; Montgomery and Buffington, 1997). Initial field investigations indicated that:

- Though potentially more complex and/or significantly different than other regions of the United States, southern California catchments do appear to have typical floodplain forms that are comprised of multiple continuums of floodplain forms. In this context, continuum is used to describe a coherent whole that is characterized by a sequence or progression of elements.
- Each of the various floodplain forms and continuums appear to have different response thresholds and mechanisms when impacted by hydromodification, floodplain encroachment, and/or base level changes.

Hence, these observations indicate that it is essential to have a basic understanding of the geomorphic characteristics of the floodplains to provide a framework for further investigating methods for estimating the changes in floodplain geometry due to urbanization or hydromodification. Therefore, the objectives of the investigations described in this chapter are to address the following applied research questions:

- What are the forms and nature of floodplains in southern California on both a catchment and a reach scale?

- What are the primary geomorphic province-scale parameters or ”process drivers” that govern floodplain forms and continuums on a valley segment or catchment-scale?

To address these questions, the objectives of the investigations described in this chapter were to develop classification systems and conceptual models to characterize the form and nature of floodplains at various spatial scales for the semi-arid environment of southern California. More specifically, the objectives were to:

- Establish a hierarchical classification system, specific for southern California, to provide a basic framework for comparing floodplain properties at varying spatial scales, including catchment and reach scales.
- Develop a reach-scale classification system and a conceptual model that synthesizes the observed floodplain forms into basic floodplain sequences or continuums.
- Develop a catchment-scale conceptual model that describes the interrelationship between the basic floodplain sequences or continuums in terms of the dominant process drivers.
- Quantify the catchment-scale conceptual model to develop a GIS-based technique or planning-level tool for predicting the floodplain continuum within a catchment using available GIS layers.

2.2 Previous Classification Systems and Conceptual Models for Channel and Floodplain Morphologies

There are a number of classification systems and conceptual models, documented in the literature, for floodplain (geomorphic perspective) and channel morphologies. Generally, the classification systems are used to identify and organize the key elements of the fluvial systems; whereas, conceptual models are typically used to describe interrelationships between key elements of the fluvial system and/or the relationship between key elements with dominant processes. The variety and complexity of the classification systems and conceptual models attests to both the variety and complexity exhibited by alluvial floodplain systems and the variety of purposes for which they may be useful. Since this study is primarily concerned with stream stability and geomorphic response to urbanization in high gradient systems (> 0.5 % slopes), classification systems that are fluvial process based and segregate floodplain forms in a manner consistent with response mechanisms are the most pertinent to this study. The following classification systems and/or conceptual models provided a starting point and a basis for developing the conceptual models for the floodplain morphologies observed in southern California:

- The "hierarchical channel classification" described by Montgomery and Buffington (1998).
- "Channel-reach morphology in mountain drainage basins" by Montgomery and Buffington (1997)
- "A genetic classification of floodplains" by Nanson and Croke (1992).

The following sections provide brief descriptions of these classification systems and conceptual models and how they pertain to the conceptual models developed for alluvial floodplains in southern California.

2.2.1 Spatial Scales of Hierarchical Levels of Floodplain Classification

The basic objective of a hierarchical approach to floodplain classification is to relate the various factors influencing floodplain properties to a range of spatial scales. For an area in the Pacific Northwest (Olympic Peninsula, Washington), Montgomery and Buffington (1998) developed a hierarchy of spatial scales that reflects differences in processes and controls on channel morphology using the following six scales: Geomorphic Provinces (> 1000 km^2), Watersheds (50 to 500 km^2), Valley Segments (10^2 to 10^4 m), Channel Reaches (10^1 to 10^3 m), and Channel Units (10^0 to 10^1 m).

This type of hierarchy provides a framework for comparing channel (and floodplain) properties at various spatial scales. However, Montgomery and Buffington (1998) recognized and explicitly indicated that aspects of this hierarchical approach to channel classification are site dependent. Hence, an important step for investigating the properties of floodplains in southern California was to define a hierarchy of spatial scales appropriate for the study area. As documented in the "Results" section, the hierarchy of spatial scale defined for this study is comprised of the same basic elements defined by Montgomery and Buffington (1998); however, the order and spatial scales of the elements have been adjusted to meet the site-specific conditions in southern California.

2.2.2 Previous Classification System and Conceptual Model for Channel-Reach Morphology in Mountain Streams

Montgomery and Buffington (1997) developed a classification system for reach-scale channel morphologies in mountain streams. This classification system identifies three basic valley segment types: colluvial, bedrock, and alluvial. The alluvial valley segment type is further divided into five reach-scale channel types: cascade, step-pool, plane-bed, pool-riffle, and dune-ripple. As illustrated in Figure 2.1, Montgomery and Buffington (1997) developed a watershed-scale conceptual model of reach morphology by linking the spatial distribution of reach-scale morphologies to key intrabasin processes.

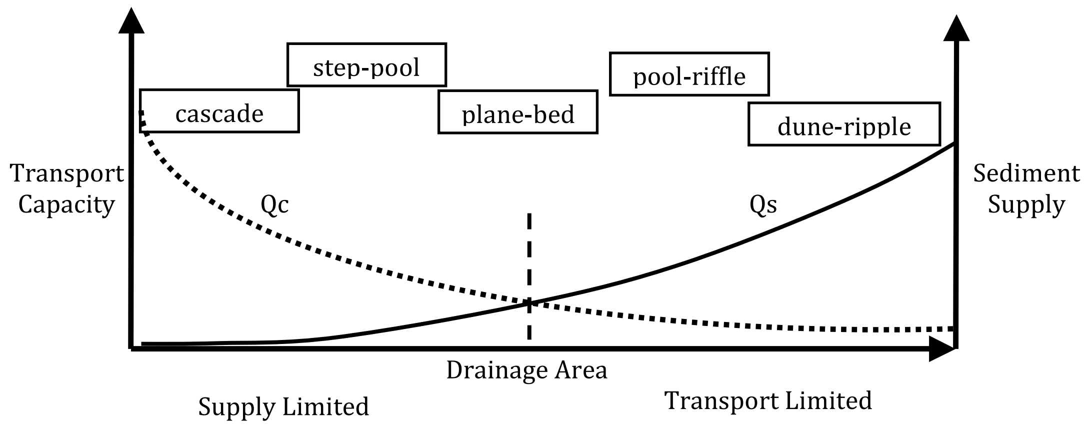

Figure 2.1 – Schematic of watershed-scale conceptual model relating reach types and generalized trends in sediment supply and transport capacity in mountain drainage basins (after Montgomery and Buffington (1997))

Even though the climatic and geologic conditions for the Pacific Southwest are significantly different than those for the Pacific Northwest, there is one type of alluvial floodplain continuum observed in southern California that exhibits a very similar catchment and reach-scale morphology to that described by Montgomery and Buffington (1997). In addition, the bedform-based nomenclature used in their reach-scale classification system was found to be very appropriate for this study since it is: (a) descriptive, (b) intuitive with respect to field identification, and (c) easily adaptable to the wider range of bedforms observed in the semi-arid environment. Therefore, the classification system and corresponding conceptual models documented herein are considered by this author to be an extension of the Montgomery and Buffington (1997) concepts to the semi-arid environment of southern California.

2.2.3 Previous Classification of Floodplains From a Geomorphic Perspective

Nanson and Croke (1992) developed a "genetic classification of floodplains" based on the concept that floodplains (geomorphic perspective) are formed by a complex interaction of fluvial processes; however, floodplain properties are primarily a function of specific stream power and sediment character. This genetic classification system is comprised of three valley segment scale classes: Class A – high-energy non-cohesive; Class B – medium-energy non-cohesive; and Class C – low energy cohesive floodplains. These classes are further divided into thirteen (13) reach-scale "orders and sub-orders" that range from confined, coarse grained, and non-cohesive floodplains in high specific stream power environments to unconfined, fine grained cohesive floodplains in low specific energy environments.

The genetic classification system defined by Nanson and Croke (1992) is unique in that it identifies braided floodplains as "Class B – medium energy", with non-braided floodplains being in both higher and lower energy classes. This is an important distinction that is directly pertinent to these investigations and the downstream progression of floodplain forms observed in the semi-arid environment of southern California.

2.3 Study Area

2.3.1 Geographical Boundary for This Study

The geographical boundary for this study was defined by two constraints. First, the study area was limited to the six southern-most counties in southern California with watersheds that drain to the Pacific Ocean. Hence, the study area includes portions of Ventura, Los Angeles, San Bernardino, Riverside, Orange and San Diego Counties. Second, the study area was further limited to those watersheds that drain to the ocean. The geographical boundary for the study area, based on these two constraints, is shown in Figure 2.2. As indicated in Figure 2.2, the study area includes essentially all of the large metropolitan areas south of the City of Santa Barbara.

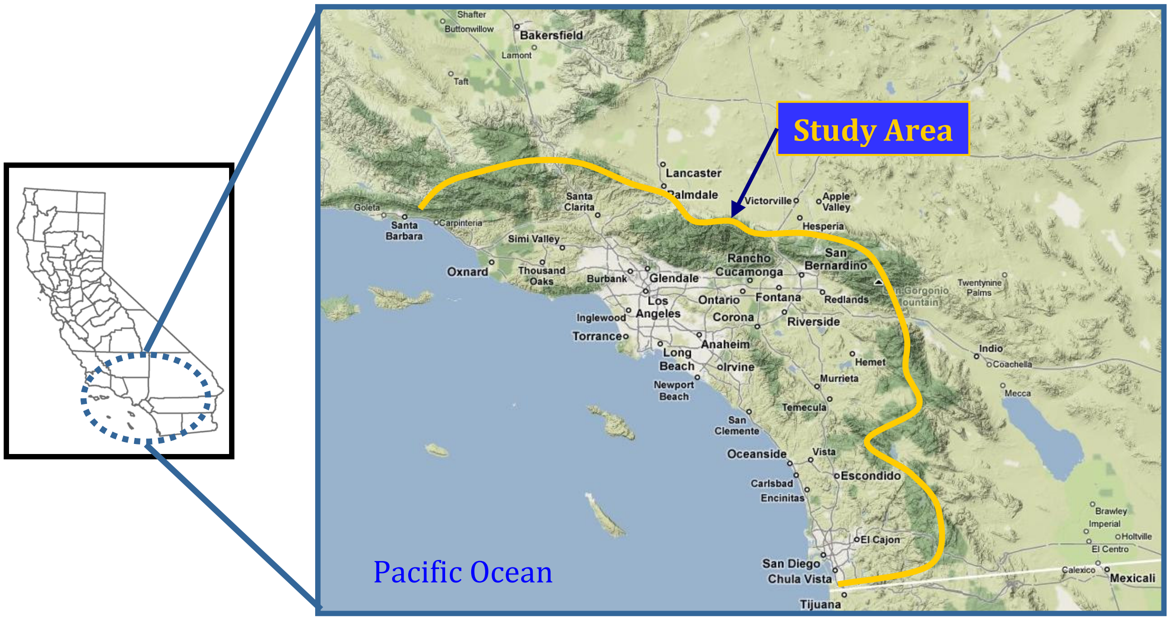

Figure 2.2 – Map showing geographical boundaries for this study within the State of California (relief map via Google Maps)

2.3.2 Geologic Setting – Geologic Province and Watershed Scale

In terms of the geologic provinces defined by the U. S. Geological Survey (USGS), the study area is located within the Pacific Province and includes the Transverse and Peninsular Ranges, as shown in Figure 2.3. The Transverse and Peninsular Ranges are the result of the complex interaction of the North American Plate and the Pacific Plate along the San Andreas Fault system over approximately the past 20 to 30 million years (Mount, 1995).

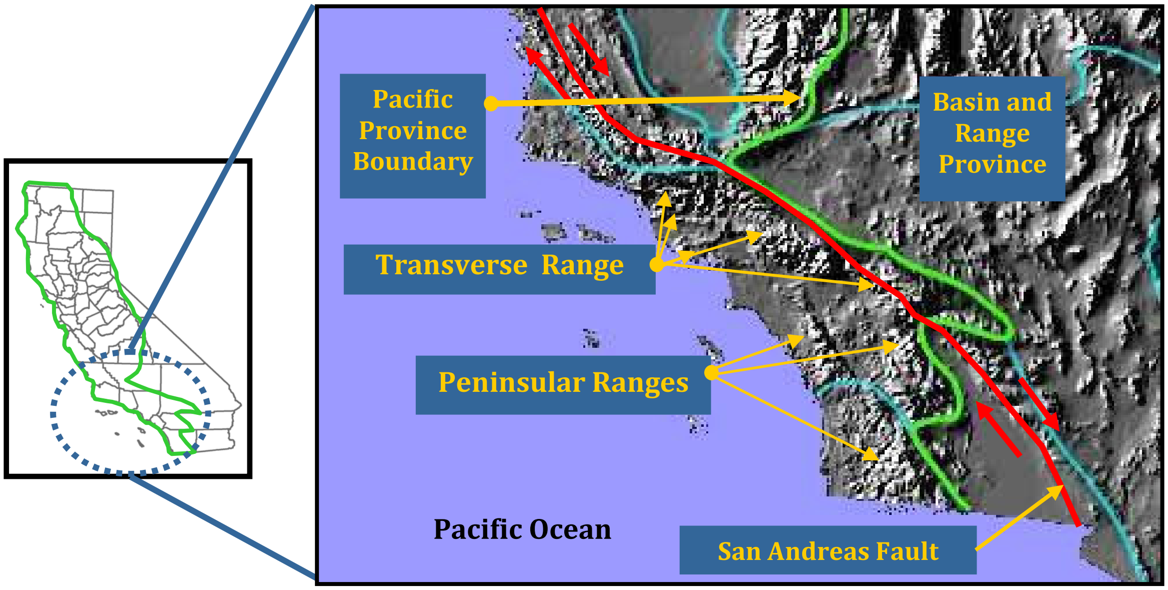

Figure 2.3 – Map showing geologic provinces and primary mountain ranges in the vicinity of the study area (San Andreas fault alignment and province boundaries after USGS (2009))

The Transverse Ranges are oriented along an east-west axis, as opposed to the southeast to northwest orientation typical of most California Ranges. Within the study area, the Los Angeles or Transverse Ranges include the Topatopa Mountains, the Santa Susana Mountains, Simi Hills, and the Santa Monica Mountains. The Topatopa Mountains (Ventura County), the Santa Susana Mountains (Ventura and Los Angeles Counties), Simi Hills (Ventura County), and the Santa Monica Mountains (Ventura and Los Angeles Counties) are composed primarily of sedimentary rock and have peaks as high as 2,047 meters (6,716 feet). The San Gabriel Mountains (Los Angeles and San Bernardino Counties) and the San Bernardino Mountains (San Bernardino and Riverside Counties) are composed of primarily igneous and metamorphic rock and have peaks as high as 3,505 meters (11,499 feet).

The Peninsular Ranges include the Santa Ana , the San Jacinto and the Laguna Mountain ranges. The Santa Ana Mountains (Orange, Riverside, and San Diego Counties) have a predominantly southeast to northwest orientation, are composed primarily of igneous and metamorphic rock, and have peaks as high as 1,733 meters (5,687 feet). The

San Jacinto Mountains (Riverside and San Diego Counties) and Laguna Mountains (San Diego County) have a predominantly a north-south orientation, are composed primarily of metamorphic and igneous rock, and have peaks as high as 3,302 meters (10,833 feet).

2.4 Methods

2.4.1 Study Catchment Selection

An objective of this study was to identify and describe the stable floodplain forms and continuums for the study area. Hence, it was imperative to investigate and evaluate a representative sample of watercourses at both a reach and catchment-scale. As with any study, there is a limit to the amount of resources that can be allocated to the site selection and data collection process. Therefore, a systematic and multi-step process (Table 2.1) was employed to select both the most representative study catchments and the most advantageous level of data collection at each study site.

In all, the site selection process yielded a total of fifty one (51) study catchments corresponding to thirty seven (37) individual watercourses. Of these, eight watercourses have multiple (i.e., 2 to 5) sub-catchments. As indicated in Figure 2.4, the fifty one (51) study catchments are relatively evenly distributed within the study area and at least one of the study catchments is located in each of the major mountain ranges within the Transverse and Peninsular Ranges.

Table 2.1 – Summary of study catchment selection process

Steps in Study Catchment Selection Process
Initial Site Investigations: Conduct *initial site investigations* at as many locations as possible (within an allotted time period), with the objective of collecting sufficient information to evaluate the potential study sites in terms of the follow key characteristics or considerations: • floodplain form, including floodplain form transitions; • bedform, including extent and degree of bed armoring; • degree of upstream urbanization; • current stability state (i.e., CEM stage or phase); and • site accessibility constraints and geo-political location.
Site Evaluation and Selection: Based on the data collected at fifty two (52) locations during the initial site investigation, key aspects of the potential study sites were tabulated and 30 study sites or reaches were selected to provide as representative a range of the key characteristics as possible, while taking into consideration site accessibility constraints.
Level of Data Collection: The level of data collection, at a reach scale, for each site was then selected to include as many floodplain form transitions as possible. Study catchments corresponding to both the upstream and downstream limits were delineated for the study sites with relatively long study reaches.
Additional Catchments: Two additional study catchments were included based on a study of step-pool floodplains in the Santa Monica Mountains by Chin (2002).
Alluvial Fan Continuum: The alluvial fan floodplain continuum was intentionally excluded from the reach-scale site selection process; however, it was important to include the alluvial fan continuum in this study on at least a catchment-scale. Therefore, aerial photographs and Google Earth were used to identify six active-regional alluvial fans within the study area.

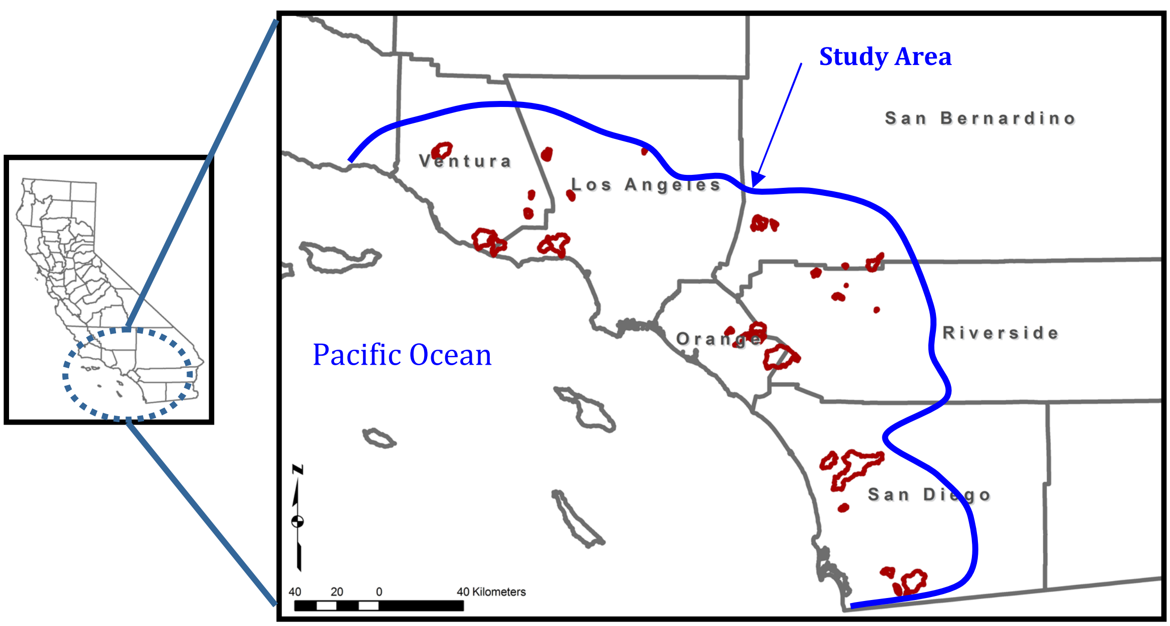

Figure 2.4 – Study area map showing the county boundaries and the locations of the 51 study catchments in southern California

2.4.2 GIS Methods and Techniques for Quantifying Process Drivers

For the Pacific Northwest, Buffington, Woodsmith, Booth, and Montgomery (2003) identified geology, climate, fire, and land-use as the "process drivers" essentially responsible for channel characteristics and types within the one channel continuum defined for the Pacific Northwest. It is believed that the same process drivers govern floodplain forms, at a reach-scale level, in the Pacific Southwest; however, climatic and geologic characteristics appear to be the primary process drivers governing which of the three floodplain continuums exists on a catchment-scale, in relatively undeveloped catchments. To provide a basis for developing a Geographical Information System (GIS) based technique for predicting the floodplain continuum within a catchment, indices appropriate for quantifying the climatic and geologic process drivers were investigated.

To quantify the process drivers, the first step requires defining both the most pertinent characteristic of the process driver to be quantified and a quantitative metric for that particular characteristic. In the case of the climate, the pertinent characteristic was selected to be a measure of "how conducive the climate is to the weathering of bedrock and the generation of a flow regime capable of transporting larger diameter bed material (e.g., coarse gravels and cobbles)", with *average annual precipitation* being a quantitative metric. In the case of the geologic process driver, the pertinent characteristic was selected to be a measure of "how conducive the bedrock is to the generation of larger diameter bed material capable of armoring channel beds", with a quantitative metric being based on either a measure of the cementation-level of the rock or rock type. The reasoning behind selecting these characteristics and corresponding metrics to represent the dominant process drivers is further described in Section 2.5.3.

The following government-sponsored data gateways were explored to find GIS layers corresponding to each of the potential metrics for the process drivers:

- The United States Department of Agriculture (USDA) - National Resource Conservation Service (NRCS) "Geospatial Data Gateway" (http://datagateway.nrcs.usda.gov/GatewayHome.html).
- The United States Geological Survey (USGS) "Preliminary integrated geologic map databases for the United States" (http://pubs.usgs.gov/of/2005/1305/#CA).

Area-Weighted Average Annual Precipitation

Average annual precipitation data compiled by the USDA/NRCS - National Cartography and Geospatial Center is available via the USDA Geospatial Data Gateway. The GIS data set is based on precipitation records for 1961 through 1990 (USDA/NRCS, 1998) and provides a complete layer for the study area. Meta data provided with the data set indicate that the data set was generated as part of the "NRCS PRISM Climate Mapping Project". The Parameter-elevation Regressions on Independent Slopes Model (PRISM) "uses point measurements of climate data and a digital elevation model (DEM) to generate estimates of annual, monthly and event-based climatic elements" USDA/NRCS (1998). Hence, an important characteristic of this precipitation data is that they reflect, to some degree, both regional and orographic variations in precipitation.

The ESRI ArcGIS ® software package was used to estimate the area-weighted mean annual precipitation by using "overlay/intersect" functionality to first compute the area associated with each "precipitation" polygon within the catchment polygon. Then the area-weighted *average annual precipitation* was computed using Equation 2.1.

$$P_{aw} = \frac{\sum_i P_i \cdot A_{pi}}{\sum_i A_{pi}}$$ Equation 2.1

where: P_{aw} = area-weighted *average annual precipitation*

A_{pi} = area for precipitation polygon "*i*"

P_i = *average annual precipitation* for precipitation polygon "*i*"

Area-Weighted Geo-Soil Score

To quantify the geologic process driver, two parameters were used: (a) the cementation-level of the underlying strata provided in the "SSURGO" soil data (USDA/NRCS, 2007) and (b) "rock types 1 and 2" provided in the "Preliminary integrated geologic map databases" (USGS, 2005). The cementation-level data have been used as the primary parameter to quantify the geologic process driver, because the cementation-level data are the most detailed information. The *rock type* data have only been used as supplemental data source, when a cementation-level is not specified for a soil unit.

The *rock type* data are a direct attribute in the USGS's geology layer. However, the cementation-level data are provided in the stand-alone SSURGO database and are not an attribute directly in the soil data GIS layer. Furthermore, the soil data GIS layer does not have a "1 to 1" relationship with the cementation-level data, because each soil unit polygon is defined by a composition of specific soil types (which each have a cementation-level). Therefore, a 1 to 1 (as opposed to a 1 to many) relationship between the individual soil units and the cementation-level data had to be defined to use the cementation-level data directly in a GIS application.

The cementation-level data were extracted from the SSURGO database for each soil type composition in each soil unit. Based on the composition percentages for each of the soil types within each of the soil units, a 1 to 1 relationship table was developed relating the

1632 individual soil units, within the study area, with a representative cementation level. The cementation-level data are provided in the SSURGO database as seven levels of descriptive values ranging from “extremely weakly cemented” to “indurated”.

A scoring system had to be devised to quantify the cementation-level and rock type data, because the cementation-level and rock-type data associated with the GIS layers are descriptive in nature. The quantitative metric created to reflect the geologic process driver for a catchment is referred to as the *Geo-Soil Score*. The scoring system developed to quantify the cementation-level and rock type data is provided in Table 2.2. As indicated in Table 2.2, the *Geo-Soil Value* ranges from 1 to 3, with a value of “1” being assigned to “extremely weakly cemented” and a value of “3” being assigned to “indurated”. When a soil unit was not assigned a cementation-level in the SSURGO database (i.e., the field was blank), rock type attributes were used to assign a *Geo-Soil Value* as specified in Table 2.2.

The following procedure was used to compute an area-weighted *Geo-Soil Score* for each of the study catchments:

- Using the “overlay/intersect” functionality within ESRI ArcGIS ®, the catchment polygon was intersected with both the geology and soil data layers, thereby dividing the catchment into a group of *geo-soil* polygons that have a unique soil unit and rock type attributes. The area for each of these *geo-soil* polygons was computed using ArcGIS ® functionality.
- Using the 1 to 1 relationship table relating soil units to cementation levels, a cementation level was assigned to each of the *geo-soil* polygons comprising the catchment.
- A geo-soil value was assigned to each *geo-soil* polygon using the scoring system provided in Table 2.2.

- The area-weighted *Geo-Soil Score* was then computed for the catchment using Equation 2.2.

$$G_{aw} = \frac{\sum_i G_i \cdot A_{Gi}}{\sum_i A_{Gi}} \qquad \text{Equation 2.2}$$

where: G_{aw} = area-weighted *Geo-Soil Score*

A_{Gi} = area for *Geo-Soil* polygon "*i*"

G_i = *Geo-Soil Value* for *Geo-Soil* polygon "*i*"

Table 2.2 – Geo-Soil Values assigned to soil and geologic data

"Cementation Level" Attribute From SSURGO Soil Database	"Rock Types 1 - 2" Attributes From USGS Integrated Geologic Map Database for California	Geo-Soil Value (G_i)
Extremely Weakly Cemented	"Any Rock Type"	1.00
Very Weakly Cemented	"Any Rock Type"	1.33
Weakly Cemented	"Any Rock Type"	1.66
Moderately Cemented	"Any Rock Type"	2.00
Strongly Cemented	"Any Rock Type"	2.33
Very Strongly Cemented	"Any Rock Type"	2.66
Indurated	"Any Rock Type"	3.00
"blank"	Alluvium-Terrace (Alluvium)	1.00
"blank"	Mudstone-Sandstone (Sedimentary)	1.00
"blank"	Sandstone-Mudstone (Sedimentary)	1.00
"blank"	Sandstone- Conglomerate (Sedimentary)	1.33
"blank"	Conglomerate-Sandstone (Sedimentary)	1.66
"blank"	Argillite-Greywacke (Metamorphic)	2.00
"blank"	Schist-Gneiss (Metamorphic)	2.00
"blank"	Gneiss-Granitoid (Metamorphic/Igneous)	2.00
"blank"	Rhyolite-Tuff (Igneous)	2.66
"blank"	Gabbro-Diorite (Igneous)	3.00
"blank"	Plutonic Rock (phaneritic)-Gneiss (Igneous/Metamorphic)	3.00
"blank"	Tonalite-Quartz Diorite (Igneous)	3.00
"blank"	Granodiorite-Quartz Monzonite(Igneous)	3.00
"blank"	Felsic Volcanic Rock-Intermediate Volcanic Rock (Igneous)	3.00
"blank"	Basalt-Andesite (Igneous)	3.00

2.5 Results and Discussion

2.5.1 Hierarchy of Spatial Scales for Southern California

The basic objective of a hierarchical approach to floodplain classification is to relate the various factors influencing floodplain properties to a range of spatial scales. For southern California, this type of hierarchy of spatial scales provides an important framework for classifying and comparing floodplain properties at various spatial scales. Based on the classification system developed by Montgomery and Buffington (1998) for a region in the Pacific Northwest, a hierarchy of spatial scales was developed specifically for southern California that reflects differences in processes and controls on floodplain morphology. This hierarchy of spatial scales is comprised of and defined by the five levels listed and illustrated in Table 2.3.

Due to the complex geologic history for the study area and a relatively strong orographic effect on precipitation, a significant percentage of even the moderate sized study catchments (i.e., approximately 20 to 100 km^2) are comprised of multiple geomorphic provinces. Hence, the hierarchy of spatial scales developed for southern California has geomorphic province-scale being smaller than the watershed-scale, unlike the hierarchy of spatial scales developed for the Pacific Northwest (Montgomery and Buffington, 1998).

Table 2.3 – Hierarchy of spatial scales for watercourses in southern California

Scale	Description	Schematic
Watershed (>~500 km²)	A watershed encompasses the drainage area for a major watercourse that either drains into the Pacific Ocean or drains into a land-locked lake.	Watershed 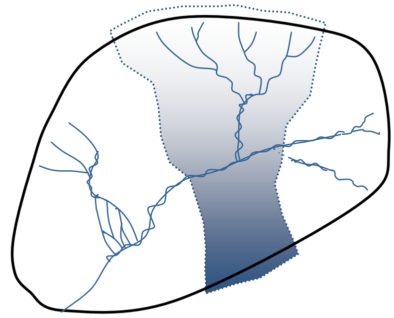
Geomorphic Province (< 500 km²)	Geomorphic Provinces, as defined by Montgomery and Buffington (1998), are “regions with similar land forms that reflect comparable hydrologic, erosional, and tectonic processes”.	Geomorphic Province 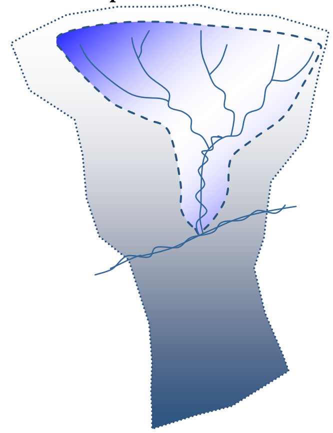
Catchment (< 500 km²) or **Valley Segment** (10^2 to 10^5 m)	This level in the hierarchy of spatial scales is unique in that it can be described as either a length of a watercourse or in terms of the corresponding drainage area. A valley segment is a portion of a drainage network that has related floodplain form and nature; whereas, a catchment is the drainage area corresponding to a point on a valley segment or floodplain reach. If the valley segment or floodplain reach is located near the terminus of the watercourse, the catchment is essentially the same as the watershed; however, a catchment is always a subset of the watershed. In the context of southern California, valley segments are comprised of three primary types: colluvial, bedrock, and alluvial. The alluvial valley segment is further divided into “non-armored” (Type 1), “armored” (Type 2), and “active-regional regional alluvial fan” (Type 3) continuums (Section 2.5.2).	Catchment 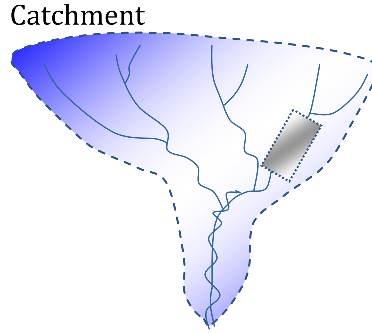
Floodplain Reach (10^1 to 10^3 m)	Floodplain reaches are defined primarily by dominant bedforms and are sub-divided into three main categories, as with the valley segments: colluvial, bedrock, and alluvial. Alluvial reaches are further divided into cascade, step-pool, plane-coarse-bed, plane-mixed-bed, plane-fine-bed, pool-riffle, braided, dune-ripple reaches, and floodout reaches (Section 2.5.2).	Floodplain Reach 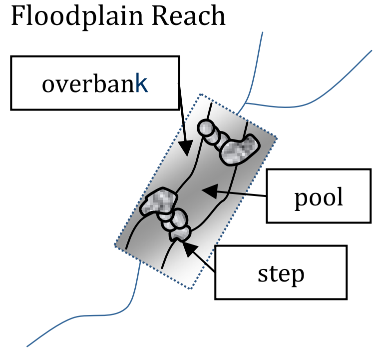
Floodplain Unit (10^0 to 10^1 m)	Floodplain units include various types of pools, bars, banks, overbanks, primary and secondary channels, riffles, and shallows.	

2.5.2 *Reach-Scale Classification System and Conceptual Model for Floodplain Forms*

The concept that there is a continuum of bedforms, channel forms, or floodplain forms along a fluvial system is not new. However, researchers have typically focused on investigating watercourse characteristics at various scales along a single continuum. For example, Naden and Brayshaw (1987), Bluck (1987), Richards and Clifford (1991), Montgomery and Buffington (1997, 1998), Chin (1998, 2002), and Thompson, Croke, Ogden, and Wallbrink (2006) have investigated the form and characteristics associated with "gravel-bed rivers" or "mountain streams". Whereas, Cooke and Reeves (1976), Schumm et al. (1984), and Graf (1988) have investigated "arroyos". Within southern California, multiple watercourse continuums occur and often occur within one watershed. , Therefore, it is important to recognize which continuums occur, basic characteristics of the floodplain forms in each continuum, and how these continuums interrelate on both a reach and catchment-scale.

Montgomery and Buffington (1997, 1998) developed a classification system for reach-scale channel morphology that uses the dominant bedform as the basic nomenclature for defining specific alluvial reach types within the "mountain stream" continuum (Figure 2.1). This approach has been both adapted and extended to apply to the floodplain morphology observed in southern California as follows:

- First, the Montgomery and Buffington (1997, 1998) classification system has been adapted to apply to "floodplains", from an engineering perspective, as opposed to just channels. I contend that it is essential to consider both the form and processes associated with the entire active portion of the fluvial system during a flood, because the stability of watercourses from an engineering perspective is at the core of this study. Hence, the nomenclature of the classification system described herein is based on bedform, but is used to refer to the entire floodplain (i.e., channel plus overbanks).

- Secondly, the Montgomery and Buffington (1997, 1998) classification system has been extended to include multiple watercourse continuums, not just one, and a wider range of floodplain forms.

More specifically, three basic floodplain continuums or typical floodplain sequences have been identified in southern California: *non-armored* (Type 1), *armored* (Type 2), and *active-regional alluvial fan* (Type 3). These three basic continuums and the typical interrelationships between these continuums are shown schematically in Figure 2.5. The remainder of this section is used to describe the three basic continuums, the floodplain forms within each continuum, and other interrelationships or characteristics that are shown schematically in Figure 2.5.

As illustrated schematically in Figure 2.5, I contend that the three continuums are comprised of three or more reach-scale floodplain forms. In this context, the term "continuum" is intended to describe a coherent whole that is characterized by a sequence or progression of elements with distinct characteristics; however, the term is **not** intended to imply that there is a smooth or gradual transition from one element (or floodplain form) to another, as implied in the typical dictionary definition of the term. Quite to the contrary, it is the pronounced and often rapid transition from one floodplain form to another (such as the transition from a single-thread to a braided floodplain form) that is of interest in these investigations.

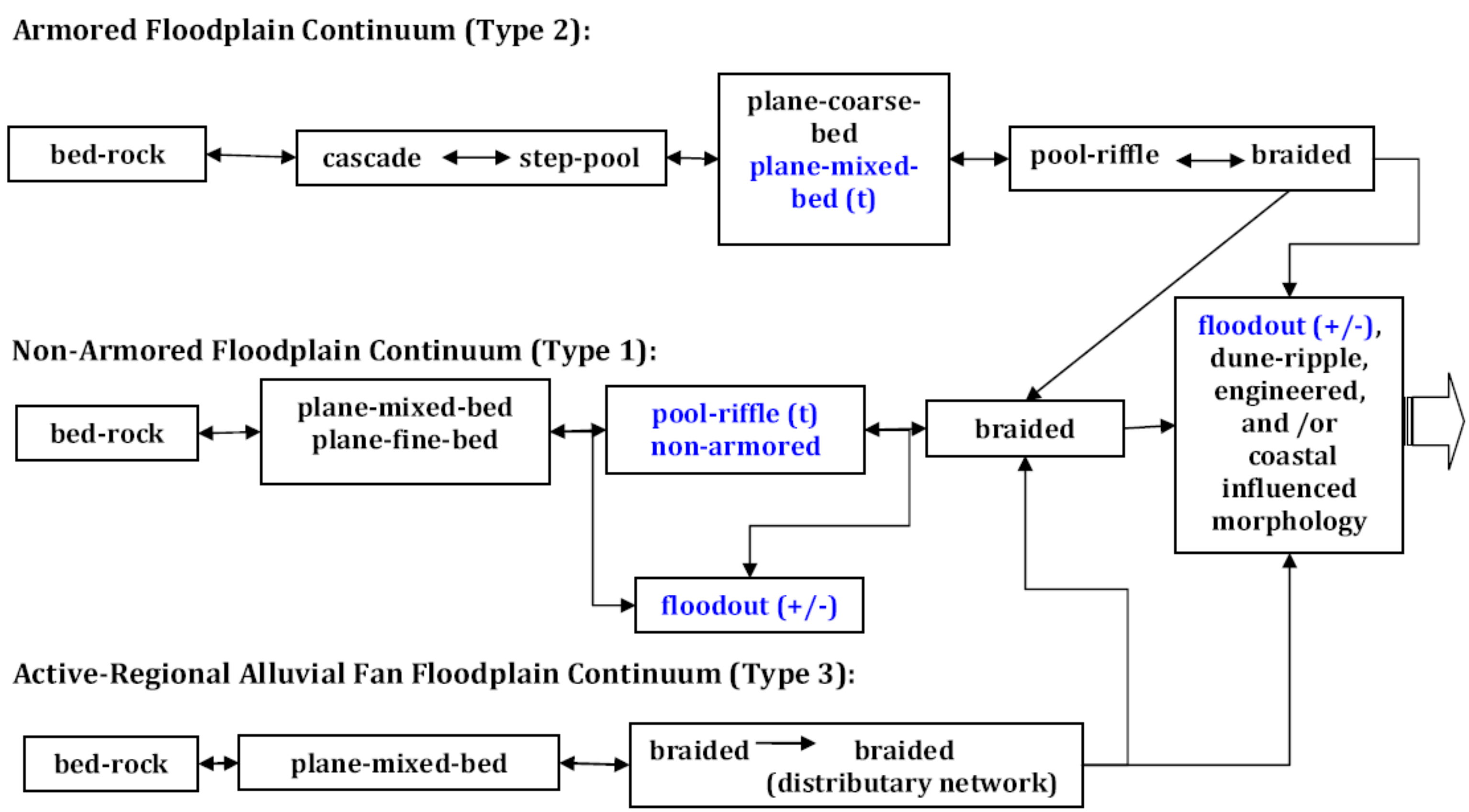

Figure 2.5 – Reach-scale conceptual model for floodplain continuums in the semi-arid environment of southern California

The terms *non-armored*, *armored*, and *active-regional alluvial fan* are intended to be form-oriented, and thereby consistent with the bedform-oriented nomenclature adapted for the floodplain forms. Furthermore, a nomenclature for the continuums oriented on bed material size, such as sand- and gravel-bed, seemed inadequate and susceptible to confusion, because coarse gravel and cobble sized particles can be quite prevalent in the bed and banks of floodplain forms in the *non-armored* continuum.

As shown schematically in Figure 2.5, the progression of floodplain forms for each of the continuums represents the typical sequence for a watercourse. Due to the complex geologic history for the study area, it is simply not practical, nor useful, to try to show schematically all of the possible permutations of floodplain transitions. Hence, it is fully recognized that the continuums shown schematically in Figure 2.5 may not specifically illustrate all of the floodplain form transitions that do or can occur along a major watercourse within the study area. Furthermore, Figure 2.5 is intended to only represent the continuums associated with relatively stable watercourses. For a watercourse in a state of severe instability, the sequence of floodplain forms may be quite complex and change significantly during individual flow events (Schumm et al., 1984); hence, in this case the floodplain forms shown for each continuum in Figure 2.5 simply represent the range of forms the floodplain may exhibit.

In addition to the three basic floodplain continuums, Figure 2.5 is also intended to illustrate schematically several important aspects of the floodplain continuums observed in southern California:

- ***Transitory Floodplain Forms***: Transitory floodplain forms typically occur on a sporadic basis in both space and time. In terms of stability, they are a "responding" floodplain form and represent a state of *dynamic response*. Transitory floodplain forms are designated by "(t)" in Figure 2.5 and include the Type 1 pool-riffle and the Type 2 plane-mixed-bed floodplain forms.

- ***Floodouts***: As defined by Pickup (1991), the term "floodout" is used to describe the circumstance when the surface relief associated with a floodplain form terminates, typically within an alluvial fill valley (Figure 3.2b). Though not a true reach type or floodplain form, the potential for "floodouts" to occur along the various continuums is also shown in Figure 2.5. Floodouts were only observed to occur in association with the non-armored (Type 1) and active-regional alluvial fan (Type 3) continuums; however, it is possible for a floodout to be associated with the armored (Type 2) continuum. Floodouts are indicated with "(+/-)" in Figure 2.5 to signify that this is not a typical floodplain form and typically does not occur along a watercourse.
- ***Reverse Transitions***: It is recognized that a wide range of external controls may alter the downstream sequence of floodplain forms from the typical sequence shown in Figure 2.5. For example, it was observed along Santiago Wash (Orange County) that when the valley walls narrowed, the braided floodplain transitioned to a pool-riffle floodplain; however, the floodplain transitioned back to a braided floodplain as the valley walls widened again. To reflect the potential for this type of reverse transition in form, double ended arrows are used in Figure 2.5 to connect the floodplain forms where this type of reverse transition can potentially occur.
- ***Type 1 and Type 2 Braided Floodplains***: In the conceptual model shown in Figure 2.5, a distinction is made between non-armored and armored braided floodplains. Bristow and Best (1993) noted that "*within the geology and geomorphology oriented literature has been a long held distinction between gravel-bed braided rivers and sand-bed braided rivers*." The distinction between *armored* and *non-armored* braided floodplains is similar to but not completely analogous to the distinction between

"gravel-bed braided rivers and sand-bed braided rivers." However, Bristow and Best (1993) also noted that the terminology of "gravel-bed braided rivers and sand-bed braided rivers" is not always that distinctive with the following statement: *"… many natural gravel bed rivers include those with bedloads of sand, granule, pebble, cobble and even boulder grade material while fine-grained sand-bed rivers braided rivers are held to contain less than 25% gravel* (Bluck, 1979)."

- ***Type 1 to Type 2 Continuum Transition***: As show schematically in Figure 2.5 with an arrow, Type 2- braided floodplains will typically transition into a Type 1- braided floodplain, as the bed gradation fines and the armor layer in the low flow channel(s) fails or disintegrates.
- ***Intermixed and Complex Morphology***: At the far right side of Figure 2.5, there is a box in the flow diagram at the terminus of all three continuums containing "floodout, dune-ripple, engineered, and/or coastal influenced morphology". This box is used to simply acknowledge the wide range of floodplain forms that occur in the metropolitan and coastal areas. The term *engineered* floodplain is used to describe the condition where all or part of the floodplain has been stabilized with concrete, dumped rip-rap, grouted rip-rap, soil cement, and/or other materials. Whereas, the term "coastal influenced morphology" is used to describe floodplains and estuaries where the morphology is significantly influenced by a combination of fluvial processes, tidal patterns, and/or near shore processes.

As indicated by the names, the *armored* and *non-armored* floodplain sequences are primarily distinguished by the presence of bed armoring within the floodplain or the lack thereof, respectively. Whereas, the *active-regional alluvial fan* continuum is distinguished strictly by its unique floodplain sequence, which is by definition and nature in a state of perpetual non-equilibrium. From a floodplain stability and management standpoint, it is very important to recognize and to differentiate between the three basic floodplain continuums, since field observations and analyses presented in later sections indicate that:

- The trend and magnitude of the change in floodplain geometry, due to urbanization, appear significantly different for each of the continuums.
- The probability for and the magnitude of floodplain instability appear significantly different for each of the continuums.
- The threshold for and the mechanisms associated with floodplain braiding appear different for each of the continuums.
- The observed floodplain forms in each of the continuums appear indicative of catchment runoff and sedimentation processes, which can be impacted by urbanization.

These are key points of these investigations and each of these points is further defined and described in later sections or chapters.

Non-Armored Floodplain Continuum (Type 1)

Based on field observations, the non-armored floodplain sequence appears to be both the most common and the most extensive continuum within southern California. The non-armored floodplain continuum is intended to include all watercourses that have insufficient coarse bed material to allow bed armoring to occur, excluding only active-regional alluvial fan systems.

Watercourses that fall within the non-armored continuum may be in a state of dynamic equilibrium; however, watercourses in this continuum are typically highly susceptible to transitioning into a state of severe instability. Watercourses within the non-armored continuum and in a state of severe instability are often referred to as "arroyos", “incised channels”, and/or “gullies” in the literature. Specific definitions for these terms are as follows:

- “Arroyos” are described by Cooke and Reeves (1976) as “valley bottom gullies characterized by steeply sloping or vertical walls in cohesive, fine sediments and by flat and generally sandy floors.”
- “Incised channels” are described by Schumm et al. (1984) as channels that “have lowered their bed by degradation, thereby setting in motion a period of considerable channel instability with the potential for serious damage …”.
- “Gullies” are described by Harvey, Watson, and Schumm (1985) as “incised channels that form where no well-defined channel previously existed.”

An example of a catchment with a non-armored floodplain continuum is shown in Figure 2.6. Figure 2.6 shows the floodplain form at two locations within the catchment, where the upstream channel is believed to be in a state of dynamic equilibrium; whereas, the downstream cross section was assessed as being in a state of severe instability. Key characteristics and geometry of the floodplain forms defining the non-armored continuum are described and illustrated in Table 2.4. Within Table 2.4 reference is made to Type 1a and 1b catchments. Definitions and descriptions for these catchment types are provided in Section 2.5.3 - “Geomorphic Province-Scale Model for Floodplain Continuums”.

Hasley Canyon – Los Angeles Co.

Photo-Relief via Google Earth

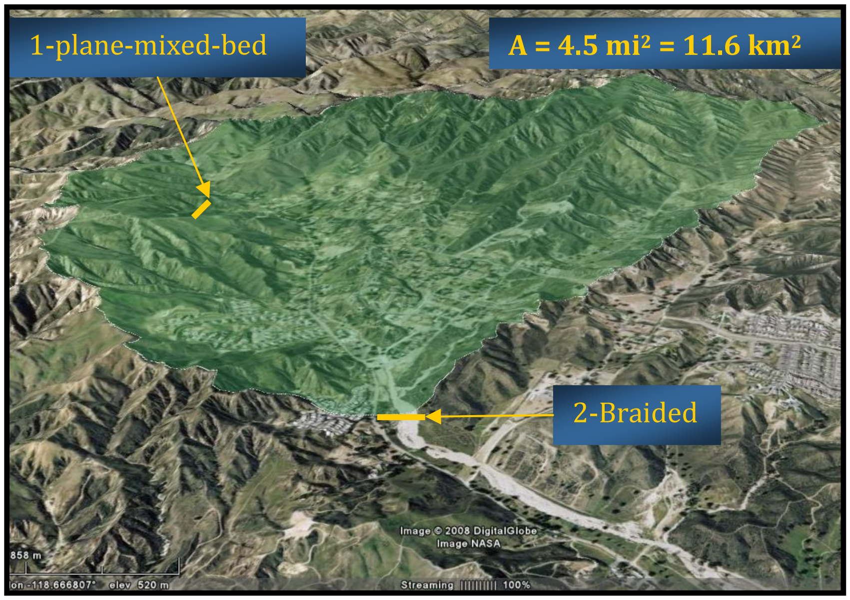

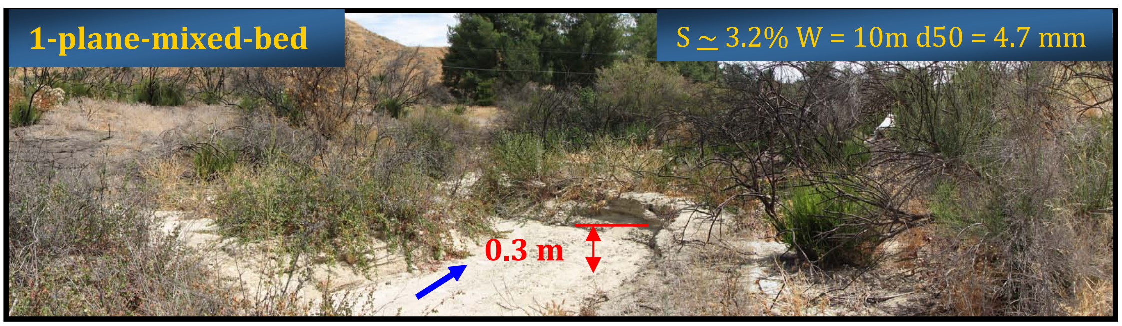

bed-rock ↔ plane-mixed-bed / plane-fine-bed ↔ pool-riffle (t) / non-armored ↔ braided ⇒

Figure 2.6 – Illustration of the *non-armored* (Type 1) floodplain continuum

Table 2.4a – Floodplain field identification table for bedrock and plane-mixed-bed floodplains in the non-armored continuum

ID	Key Characteristics	Geometry
1-BR	**Bedrock (BR) - General**: Bedrock reaches can occur intermittently along a valley segment and disrupt the general downstream transition in floodplain forms. In Type 1a catchments, the bedrock is predominantly sedimentary rock; whereas, in Type 1b catchments it is predominantly metamorphic and/or igneous rock. **Planform**: Planform is typically straight or meandering, with low to moderate sinuosity. **Cross Section**: Cross section is typically trapezoidal, but may vary. **Bedform**: The bedform can vary significantly depending upon the hardness and extent of the exposed bedrock. **Bed Material**: The bed material is predominantly exposed bedrock; however, there is typically a thin veneer of sand, gravel, and/or cobbles. **Example**: Santiago Creek, Orange County (Type 1a)	 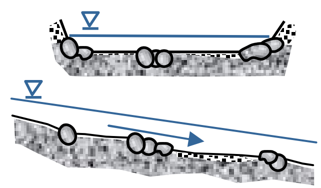
1-PMB	**Plane-Mixed-Bed(PMB) – General**: Type 1 “PMB” floodplains differ from “PFB” floodplains in that the bed material is a “mixture” of sand, gravel, cobbles, and possibly small boulders. **Planform**: Typically meandering, with varying sinuosity. **Cross Section**: Cross section is typically compound, but can be trapezoidal. **Bedform**: Bedform is non-armored plane or flat bed with only relatively minor irregularities or bars (< 10mm). However, groupings of small boulders (256-512 mm) and/or cobbles (64-256 mm) may form small steps (< ~250 mm) that are irregularly spaced. These small groupings of coarse material may have small downstream local scour holes; however, there isn't a pool located upstream of the boulder and/or cobble groupings. **Bed Material**: Channel and overbank material is a mixture of sand, gravel, cobbles, and possibly small boulders; however, there are insufficient quantities of coarse material to armor the bed. **Example**: Hicks Canyon Wash (HCMR), Orange County	 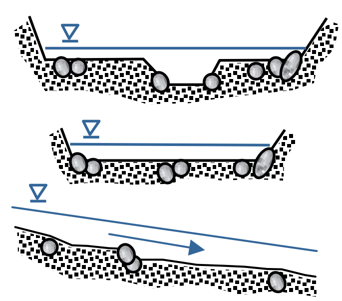

Table 2.4b – Floodplain field identification table for plane-fine-bed and pool-riffle floodplains in the non-armored continuum

ID	Key Characteristics	Geometry
1-PFB	**Plane-Fine-Bed(PFB) - General**: One unique characteristic of plane-fine-bed floodplains is that none were observed to have a compound geometry. **Planform**: Meandering, typically with varying sinuosity. **Cross Section**: Rectangular to trapezoidal cross section depending upon bank material properties and/or current stability condition. Valley section may have compound configuration; however, high magnitude flow events (including 100 year event) are confined to the rectangular or trapezoidal channel. **Bedform**: Bed form is plane or flat bed with only relatively minor irregularities or bars (< 10 mm). **Bed Material**: Bed material is primarily composed of sands (0.062-2 mm) to fine gravel (4-8 mm), with few (if any) coarser material. **Example**: Un-named wash (PLSB) in Lake Perris State Recreational Area, Riverside County	 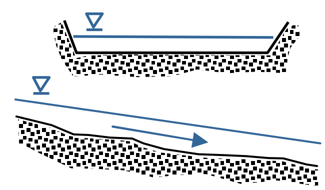
1-PR	**Pool-Riffle (PR) - General**: A Type 1 pool-riffle floodplain was only observed at one study site. This appears to be a transitory floodplain form (for the Type 1 floodplain continuum) and may only form during the falling limb of high or infrequent flow events. **Planform**: Meandering, typically with varying sinuosity. **Cross Section**: Rectangular to trapezoidal cross section depending upon bank material properties and the current stability state. **Bedform**: Subtle, but measurable, pool-riffle sequence with non-armored riffles and very shallow pools (< 10 cm). **Bed Material**: Bed material is primarily composed of sands (0.062-2 mm) to fine gravel (4-8 mm), with few (if any) coarser material. Essentially no gradation difference between pool and riffle sections. **Example**: Un-named wash (SJBL), Riverside County	 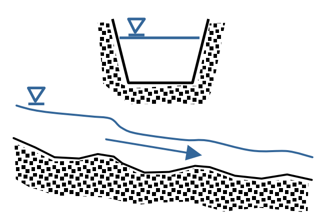

Table 2.4c – Floodplain field identification table for braided and dune-ripple floodplains in the non-armored continuum

ID	Key Characteristics	Geometry
1-BF	**Braided Floodplain(BF) – General**: This appears to be the most prevalent floodplain form within the study area. **Planform**: Straight, with undulating bank lines and meandering low-flow channels. Low flow channels are transitory and shift locations during flow events. **Cross Section**: Braided cross section with multiple low flow channels. **Bedform**: Plane-bed with varying degrees of bar development. Relatively stable braided floodplains (CEM 1,2, and 5) typically have a complex system of bars, with some of the bars being low to moderately vegetated. In unstable braided floodplains (CEM 3 and 4) the bar formation is typically associated with pulses of sediment into the channel, often due to bank failures and confluences. (See Table 3.4 regarding CEM phases.) **Bed Material**: Bed material can be a mixture of sand, gravel, cobbles, and possibly small boulders; however, the coarse gravels, cobbles, and/or small boulders are in insufficient quantities to armor the bed. **Example**: Hasley Canyon (HCSA) Los Angeles County	 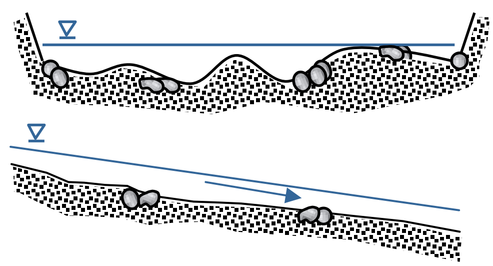
1-DR	**Dune-Ripple (DR) - General**: The dune-ripple floodplain form is common to both Type 1 and 2 floodplain continuums. This floodplain form was only observed at or near the coast. **Planform**: Meandering, typically with varying sinuosity. **Cross Section**: Typically compound. **Bedform**: Predominantly sand bed forms including dunes and ripples. **Bed Material**: Channel and overbank material is composed primarily of sands (0.062-2 mm) and fine gravel (4-8 mm). **Example**: Santa Ana River, Orange County	 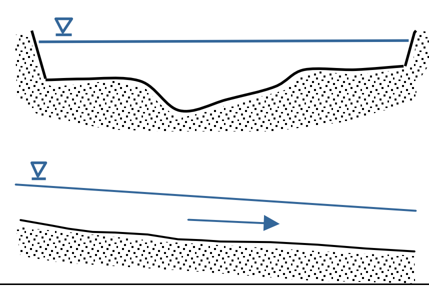

Armored Floodplain Continuum (Type 2)

Comparison of Figures 2.1 and 2.5 indicates that the reach-scale channel morphology identified by Montgomery and Buffington (1997, 1998) is most similar to the "armored" floodplain continuum shown in Figure 2.5. However, it is important to recognize that even though the floodplain forms in Figures 2.1 and 2.5 may share the same name and general bedform characteristics, many other aspects of the floodplain forms may be significantly different, due to regional differences in climatic and geologic conditions.

As would be expected, the distinguishing characteristic of floodplain forms in the armored continuum is the presence of a well developed armor layer along the thalweg of the watercourse. The term *armoring* is used describe the process associated with the surface coarsening of the bed material and the formation of an armor layer (Knighton, 1998, p. 131; Bunte and Abt, 2001, p. 188). Hence, an armored channel bed or overbank has a coarse surface layer overlaying a significantly finer substrate. The thickness of an armor layer is often defined as extending from the bed surface plane down to the embedded depth (D_e) of the largest or dominant grain size in the surface layer, as illustrated in Figure 2.7.

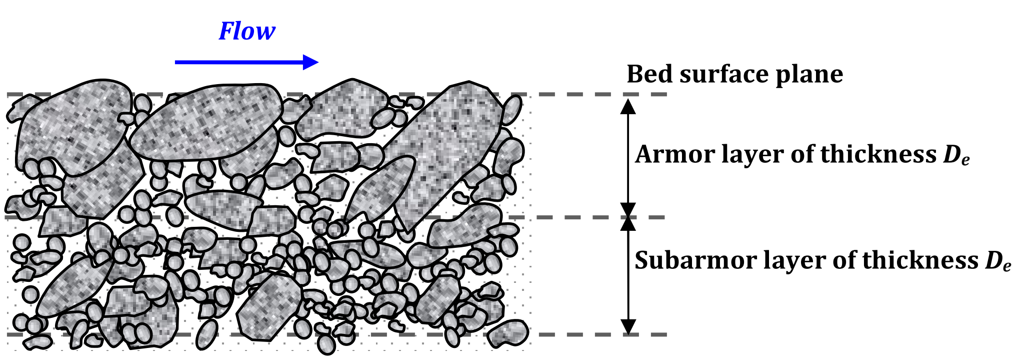

Figure 2.7 – Illustration of an armor layer (after Bunte and Abt (2001))

In a semi-arid environment with a complex geologic history, I contend that the following two conditions must occur for an armored floodplain sequence to form and persist on a catchment-scale:

- Climatic conditions are conducive to the weathering of bedrock and the generation of a flow regime capable of transporting larger diameter bed material, such as coarse gravels and cobbles.
- Geologic and lithologic conditions are conducive to the generation of larger diameter bed material capable of armoring channel beds and/or overbanks.

As discussed in Section 2.5.3, both of these conditions really represent a continuum. Hence, there are catchments where one condition is completely met, while the other condition may only be marginally met. As a result, there are many catchments within the study area that have an armored floodplain sequence; however, the floodplains with organized bedforms (i.e., step-pool and pool-riffle floodplains) may not be as persistent in time and space as their counterparts in the Pacific Northwest.

Another significant difference between the armored floodplain continuum observed in southern California and the "mountain stream" continuum (Montgomery and Buffington, 1997) is that stable or relatively stable braided floodplains occur and are prominent in southern California. Montgomery and Buffington (1998) did observe that pool-riffle channels may temporarily become braided in response to massive inputs of sediment, such as from a landslide. Buffington et al. (2003) further recognized that braided channels in the Pacific Northwest commonly occur (a) "as glacial outwash channels", (b) "in alluvial valleys where banks have been destabilized by riparian cutting and livestock trampling", and (c) "in semi-arid regions with insufficient riparian vegetation to stabilize banks composed of cohesionless sediments". Hence, braided floodplains appear to be primarily a transitory, unstable, or "special case" floodplain form in the humid regions of the Pacific Northwest. As indicated in item (c) above by Buffington et al. (2003), I also contend that the vegetation growth along the banks and in overbank areas, supported by the more humid conditions, provides an important stabilizing effect and, thereby, may prevent the braided floodplain form from being part of the typical floodplain continuum in the Pacific Northwest

An example of a catchment with the armored floodplain continuum is shown in Figure 2.8. Figure 2.8 shows the floodplain form at three locations within the catchment. Key characteristics and geometry of the floodplain forms defining the armored continuum are described and illustrated in Table 2.5.

Active-Regional Alluvial Fan Continuum (Type 3)

The active-regional alluvial fan or Type 3 continuum is unique in that it is inherently and by definition in a state of "dynamic response" and does not have a stable state in an engineering timeframe (i.e., typically 50 to 100 years). This continuum is intended to only describe those watercourses that have fan surfaces that are actively aggrading during flow events and are "regional" in the sense that the fan surfaces are larger than approximately 1 km^2 .

This continuum was not the focus of this study, since active alluvial fan floodplains have unique flood hazards and are highly regulated under the FEMA flood insurance program. However, the alluvial fan continuum was included in the conceptual model shown in Figure 2.5 in recognition that it is a prevalent continuum in the tectonically active and semi-arid environment of southern California.

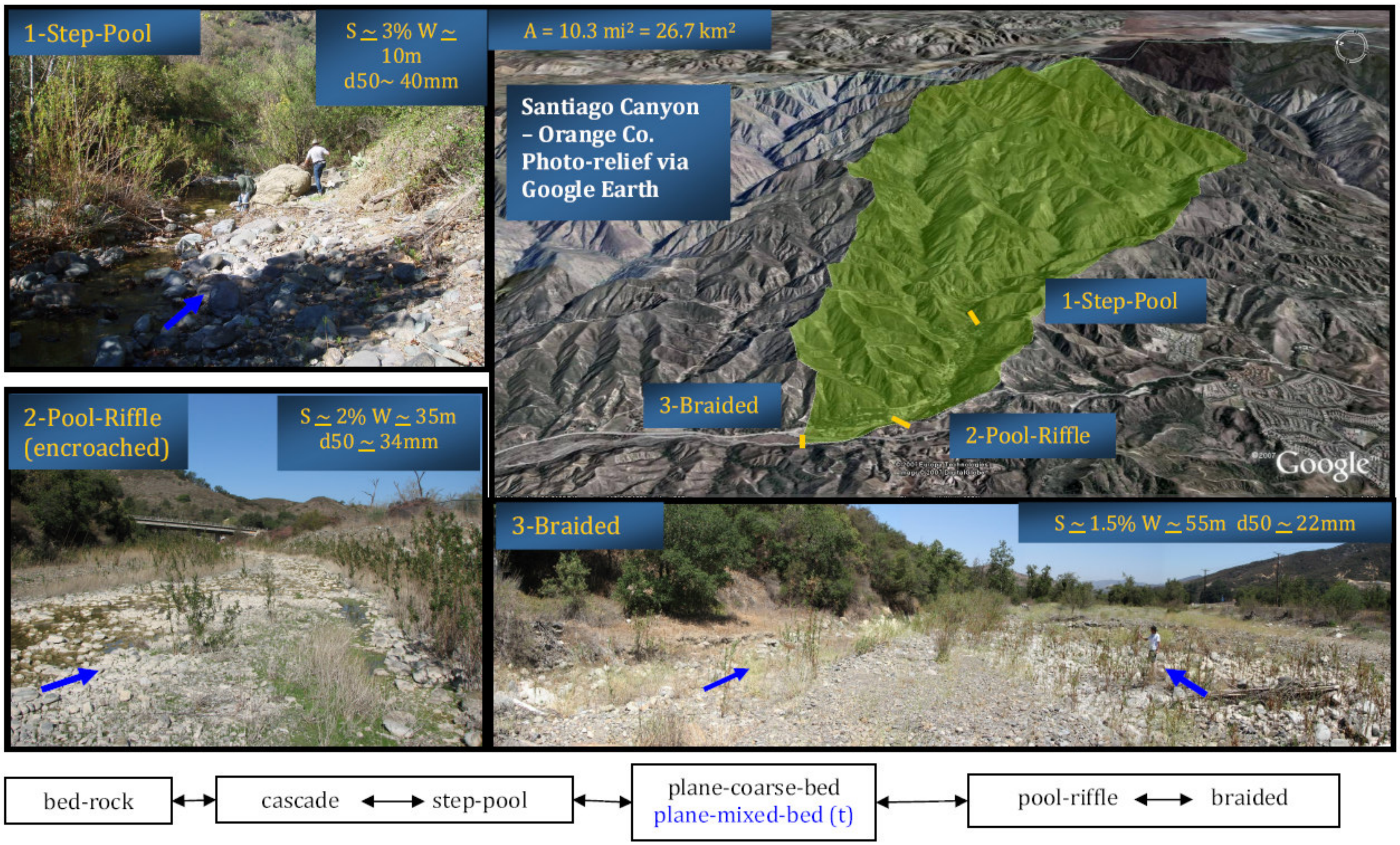

Figure 2.8 – Illustration of the *armored* (Type 2) floodplain continuum

Table 2.5a – Floodplain field identification table for bedrock and cascade floodplains in the armored continuum

ID	Key Characteristics	Geometry
2-BR	**Bedrock (BR) - General**: Bedrock reaches can occur intermittently along a valley segment and disrupt the general downstream transition in floodplain forms. In Type 2 catchments the bedrock may be sedimentary, metamorphic, and/or igneous. **Planform**: Planform is typically straight or meandering with low to moderate sinuosity. This floodplain is typically confined by valley walls or hill slopes. **Cross Section**: Cross section is typically trapezoidal, but may vary. **Bedform**: The bedform can vary significantly depending upon the hardness and extent of the exposed bedrock. **Bed Material**: The bed material is predominantly exposed bedrock; however, there may often be a relatively thin veneer of sand, gravel, cobbles, and boulders.. **Example**: Silverado Creek (SCOL), Orange County	 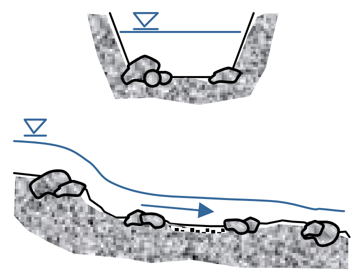
2-CA	**Cascade(CA) - General**: A key distinguishing characteristic of cascade reaches is that the flow depth is generally shallow relative to the large bed material; hence, the flow has circuitous paths over and around individual cobbles and boulders. **Planform**: Planform is typically straight or meandering, with low to moderate sinuosity. **Cross Section**: The effective cross section is primarily irregular in shape due to the irregular distribution of large diameter clasts within the cross section. **Bedform**: The bedform is characterized by large diameter bed material that is not organized either longitudinally or laterally (Montgomery and Buffington, 1997). However, cascade reaches typically have small pools, that only partially span the cross section, during low to moderate flows. **Bed Material**: Bed material is typically dominated by cobbles (64-256 mm) to very large boulders (128-4096 mm). **Example**: Stewart Canyon Wash (SCNS), Ventura County	 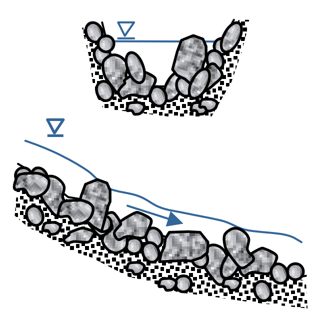

Table 2.5b – Floodplain field identification table for step-pool and plane-coarse-bed floodplains in the armored continuum

ID	Key Characteristics	Geometry
2-SP	**Step-Pool (SP) - General**: The distinguishing characteristic of step-pool floodplains is the rhythmic spacing of discrete channel spanning accumulations (i.e., steps) that separate pools composed of finer bed material (Montgomery and Buffington, 1997; Chin, 2002). **Planform**: The planform is typically straight to meandering, with low to moderate sinuosity. **Cross Section**: The cross section may be compound or trapezoidal. **Bedform**: The bedform is a rhythmic sequence of discrete channel spanning steps that separate pools comprised of finer bed material. The periodicity of step-pool sequences in the Santa Monica Mountains has been investigated by Chin (2002). **Bed Material**: The steps in a step-pool sequence are primarily composed of cobbles (64-256 mm) and boulders (256-4096 mm). The pools and overbanks are armored with coarse gravels and/or cobbles, but will often have a veneer of sand and gravel. **Example**: Silverado Creek (SCOL), Orange County	 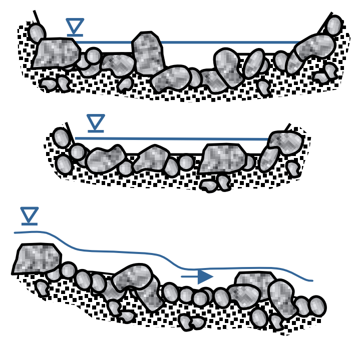
2-PCB	**Plane-Coarse-Bed(PCB) - General**: The plane-coarse-bed floodplain is comparable in nature and form to the "plane-bed channel" described by Montgomery and Buffington (1987). This does not appear to be a common floodplain form and was only observed at one study site. **Planform**: The planform is typically straight to meandering, with low to moderate sinuosity. **Cross Section**: The cross section may be compound or trapezoidal. **Bedform**: The bedform is planar and typically relatively featureless for at least several floodplain topwidths. **Bed Material**: The bed is typically armored with coarse gravel (16-64 mm), cobbles (64-256 mm), and potentially small boulders (256-512 mm). **Example:** Little Cedar Canyon (LCOL), San Diego County	 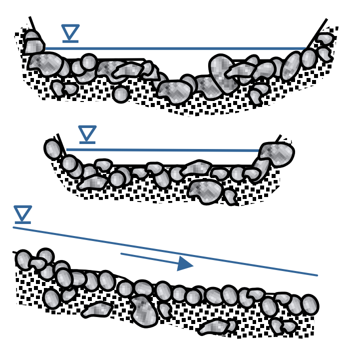

Table 2.5c – Floodplain field identification table for plane-mixed-bed and pool-riffle floodplains in the armored continuum

ID	Key Characteristics	Geometry
2-PMB	**Plane-Mixed-Bed (PMB) – General**: This is strictly a transitory floodplain form in the "armored" floodplain continuum and was observed at locations subjected to large influxes of sediment associated with rainfall events following recent fires. **Planform**: Like the underlying step-pool, plane-coarse-bed, or pool-riffle floodplain, the planform is typically meandering, with low to moderate sinuosity. **Cross Section**: May have a compound or trapezoidal cross section. **Bedform**: Non-armored plane or flat bed with only relatively minor irregularities or bars (< 10 cm); however, the bed may have multiple head-cuts that actively advance during even low and shallow flows. Base flow or low flow events actively transport the bed material, even though the flow depth may be less than 10 cm. **Bed Material**: There is a relatively thin surface layer (0.5 to 0.65 m thick observed at the site shown in the photograph), composed primarily of sand and gravels, overlaying the armored bed surface of the buried channel bed. **Example**: Santiago Creek (SCSC), Orange County	 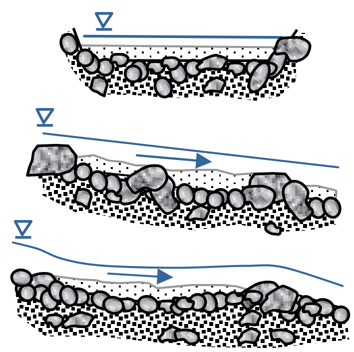
2-PR	**Pool-Riffle(PR) - General**: Though they share a general geometry, pool-riffle floodplains in southern California appear to have significantly shallower pools sections and much coarser bed material than their humid region counterpart (Montgomery and Buffington 1987). **Planform**: Planform is meandering (with low to moderate sinuosity) with distinct point bars adjacent to the pool sections. **Cross Section**: A compound cross section is typical; however, the floodplain may be more trapezoidal in cross section, when confined by valley walls or embankments.. **Bedform**: The bedform is undulating with a sequence of pools and riffles. **Bed Material**: The bed is typically armored with coarse gravel (16-64 mm), cobbles (64-256 mm), and potentially small boulders (256-512 mm). **Example:** Santiago Creek (SCSA) Orange, County	 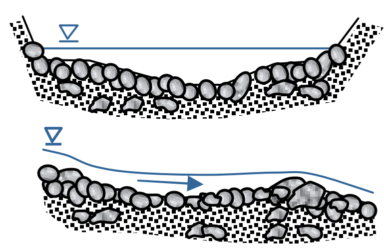

Table 2.5d – Floodplain field identification table for braided floodplains in the armored continuum

ID	Key Characteristics	Geometry
2-BF	**Braided Floodplain(BF) - General**: The Type 2 – braided floodplain is less common than Type 1 braided floodplains and differs from the Type 1- braided floodplain in that at least one of the low flow channels has bed armoring. As indicated in Figure 2.5, the Type 2- braided floodplain will typically transition into a Type 1- braided floodplain as the bed gradation fines and the armor layer in the low flow channel(s) fail or disintegrate. **Planform**: Planform is typically straight, with undulating bank lines. Low-flow channel(s) typically meander with low to moderate sinuosity. The low flow channels are relatively transitory and may shift locations during high magnitude flow events. **Cross Section**: Braided cross section with multiple low flow channels. One of the low flow channels is typically dominant in that it conveys all or most of the base and low flows. **Bedform**: The low flow channels, especially the dominant low flow channel, may have a wide range of bedforms, including step-pool, plane-coarse-bed, and/or pool-riffle. **Bed Material**: Bed material is typically a mixture of sand, gravel, cobbles, and possibly small to medium boulders. The coarse gravels, cobbles, and/or boulders are in sufficient quantities to at least armor the dominant low flow channel. **Example:** Santiago Creek (SCSA) Orange, County	 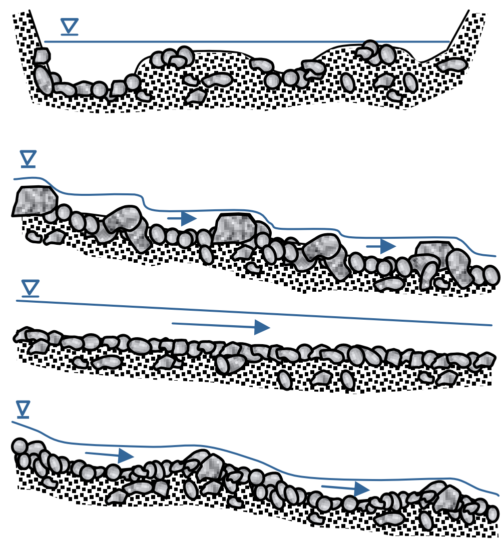
		

As is reflected in Figure 2.5, the Type 3 continuum is in many aspects a subset of the non-armored continuum, since almost all of the floodplain forms are essentially the same. However it is important to note that even though the Type 1 and Type 3 continuums share floodplain forms, Type 3 floodplains have been observed to have much higher bed slopes than their Type 1 counterparts. More specifically, braided channels in the Type 3 continuum were observed to have slopes greater than 10 percent; whereas, Type 1 braided floodplains typically have slopes between 1 and 3 percent. Another unique aspect of the Type 3 continuum is that on the fan surface it is common to have a distributary network of braided floodplains, as shown in Figure 2.9.

2.5.3 Catchment-Scale Conceptual Model for Floodplain Continuums

For the Pacific Northwest, Buffington et al. (2003) identified geology, climate, fire, and land-use as the "process drivers" essentially responsible for channel characteristics and types within their one channel continuum. It is believed that the same process drivers control floodplain forms, at a reach-scale level, in the Pacific Southwest; however, climate and geology are the primary process drivers dictating which of the three floodplain continuums exists on a catchment-scale.

Of course, the primary difference between the "non-armored" and "armored" floodplain continuum is the presence of bed armoring. In terms of the geologic and climatic process drivers, the conditions required for the formation of bed armoring can be described as follows:

- Climatic conditions are conducive to the weathering of bedrock and the generation of a flow regime capable of transporting larger diameter bed material, such as coarse gravels and cobbles.
- Geologic and lithologic conditions are conducive to the generation of larger diameter bed material capable of armoring channel beds.

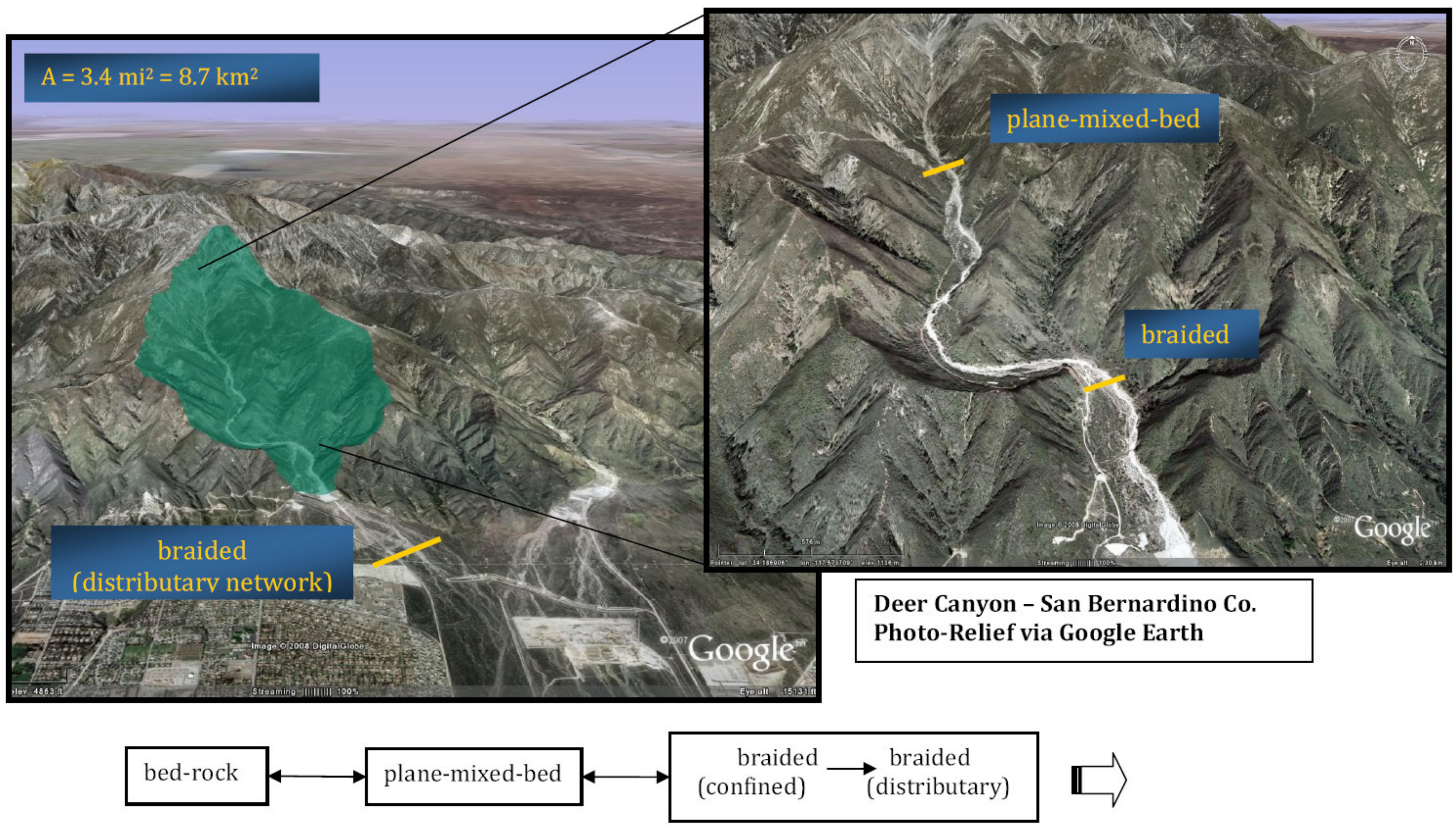

Figure 2.9 – Illustration of the *active-regional alluvial fan* (Type 3) floodplain continuum

Similarly, I contend that the conditions most conducive to the formation of large and active alluvial fans can be described in terms of the process drivers as follows:

- Geologic and lithologic conditions are conducive to the generation of the maximum sediment yield from a catchment. That is, the bedrock must be soft enough to weather and generate sediment; yet, the bedrock must be hard enough to maintain steep hill-slopes and generate the maximum runoff during a precipitation event.
- Climatic conditions are conducive to the weathering of bedrock and the generation of a flow regime with the maximum transport capacity.

Based on these assessments of conditions most conducive to the formation of each of the three basic floodplain continuums, a conceptual model showing the interrelationship of the three floodplain continuums, on a catchment-scale, can be hypothesized in terms of process drivers as shown in Figure 2.10.

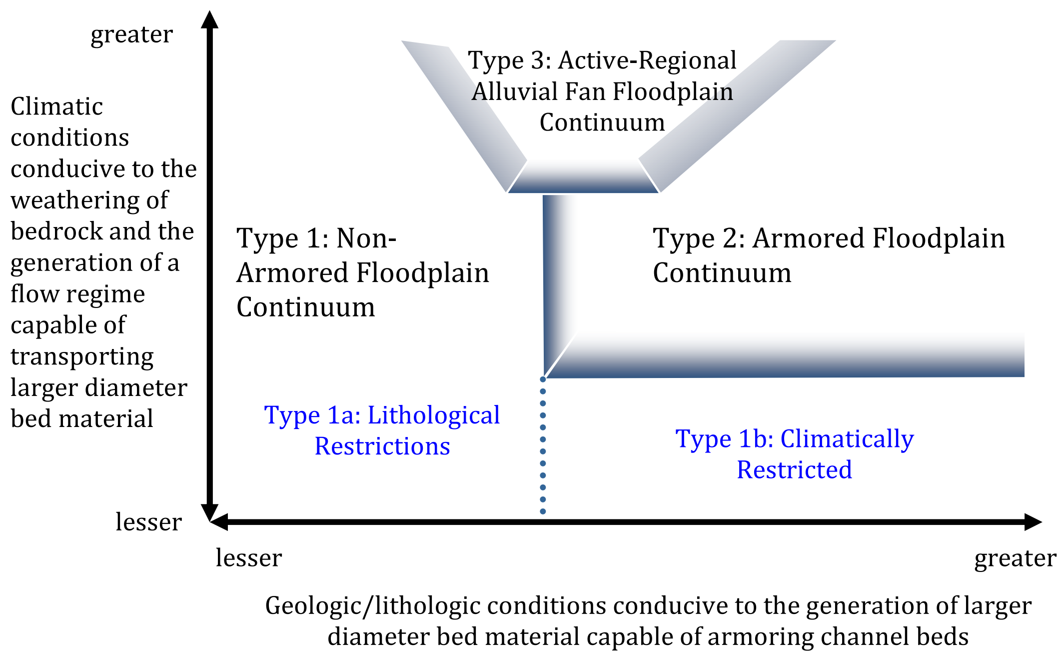

Figure 2.10 – Catchment or valley segment-scale conceptual model for floodplain continuums

In Figure 2.10, "Type 1 Catchments" are those catchments with non-armored floodplain sequences; whereas, "Type 2 Catchments" are those catchments with armored floodplain sequences. "Type 1a Catchments" are those catchments with a non-armored floodplain sequence due to the geologic and lithologic properties of the catchment being not conducive to the formation of coarser bed material required for bed armoring. "Type 1b Catchments" are those with climatic conditions not conducive (i.e., very low precipitation) to the generation of a flow regime capable of transporting larger diameter bed material and forming an armor layer.

In Figure 2.10, the boundaries between the three basic catchment types are intentionally shown with indefinite boundaries to illustrate that there are probably bands where catchment types can overlap. It is further anticipated that within the band between Type 1 and Type 2 catchments, the bed forms characteristic of the armored floodplain continuum can be less well developed, since the conditions can be less than ideal for the formation of armor layers.

2.5.4 Interrelationship of Floodplain Continuums in Terms of Quantifiable Metrics for Dominant Process Drivers

Figure 2.10 is a qualitative conceptual model relating the three basic floodplain continuums to the two dominant process drivers on a catchment or valley segment scale. However, it was recognized that the conceptual model shown in Figure 2.10 could provide a useful planning-level tool for predicting the floodplain continuum at a catchment-scale, if metrics for the two dominant process drivers could be quantified using available Geographical Information System (GIS) data.

In the case of the climatic process driver, the objective for the metric is to quantify both flow regime and weathering of bedrock characteristics. Area-weighted *average annual* *precipitation* was identified as a metric for the climatic process driver for two primary reasons:

- *Average annual precipitation* is directly related to the flow regime for a catchment.
- Due to the orographic effect captured in the precipitation data layer (USDA/NRCS, 1998), the higher annual precipitation rates almost always correspond to higher altitudes, where freeze-thaw effects can be significant with respect to the weathering of bedrock.

In the case of the geologic process driver, the objective for the metric is to quantify how conducive the underlying strata is to the generation of larger diameter bed material capable of armoring channel beds". The *Geo-Soil Score*, as defined in the "Methods" section of this chapter, is the metric developed for the geologic process driver. The effectiveness of the *Geo-Soil Score* as a metric for the geologic process driver is based on the general accuracy of the following two contentions:

- Contention #1: Underlying strata with higher levels of cementation, as defined in the soil data layer (USDA/NRCS, 1998), are more likely to weather into larger diameter clasts under conducive climatic conditions.
- Contention #2: In terms of the three basic rock types, igneous rocks generally have a higher probability of weathering into larger diameter clasts than metamorphic and sedimentary rocks; whereas, metamorphic rocks generally have a higher probability of weathering into larger diameter clasts than sedimentary rocks.

Both of these points of contention are generally consistent with field observations regarding the rock types comprising the bed armor layers at the study sites. However, Contention #1 is deemed the be less prone to error and/or less subject to exceptions; hence, the cementation-level data were used as the primary data source for computing the *Geo-Soil*

Score for a catchment, as indicated in Table 2.2. It was further recognized that there are some special cases regarding Contention #2; hence, the *Geo-Soil Value* assigned to various rock types in Table 2.2 was adjusted, within a limited degree, to reflect the potential for these special cases. For example, the *Geo-Soil Score* for "conglomerate" sedimentary rock was set at 1.66 (as opposed to 1.00 like most sedimentary rocks), because it was recognized that many of the conglomerates within in the study area are composed of and weather to granitic gravels, cobbles, and boulders.

Based on field observations and/or aerial photography, the floodplain continuum was identified for each of the study catchments. The computed catchment area, *average annual precipitation*, and Geo-Soil Score parameters for the study catchments are summarized in Table 2.6. (Table A.1 in Appendix A lists catchment area, precipitation data, and the Geo-Soil Score for each of the fifty one study catchments.) Figure 2.11 is a plot of *average annual precipitation* versus *Geo-Soil Score* for each of the fifty one (51) study catchments; hence, Figure 2.11 is a quantified version of the qualitative conceptual model provided in Figure 2.10.

Table 2.6 – Summary of study catchment parameters

Catchment Type	**Catchment Area (km^2)**			**Average Annual Precipitation (m)**			**Geo-Soil Score (Range 1 to 3)**		
	Min.	Max.	Mean	Min.	Max.	Mean	Min.	Max.	Mean
1a	0.15	16.80	5.11	0.36	0.60	0.43	1.00	1.94	1.50
1b	0.14	26.28	4.81	0.28	0.38	0.34	1.88	2.76	2.28
2	0.76	155.05	41.01	0.36	0.68	0.50	1.98	2.97	2.39
3	1.72	12.43	5.45	0.92	1.07	0.92	2.11	2.64	2.11

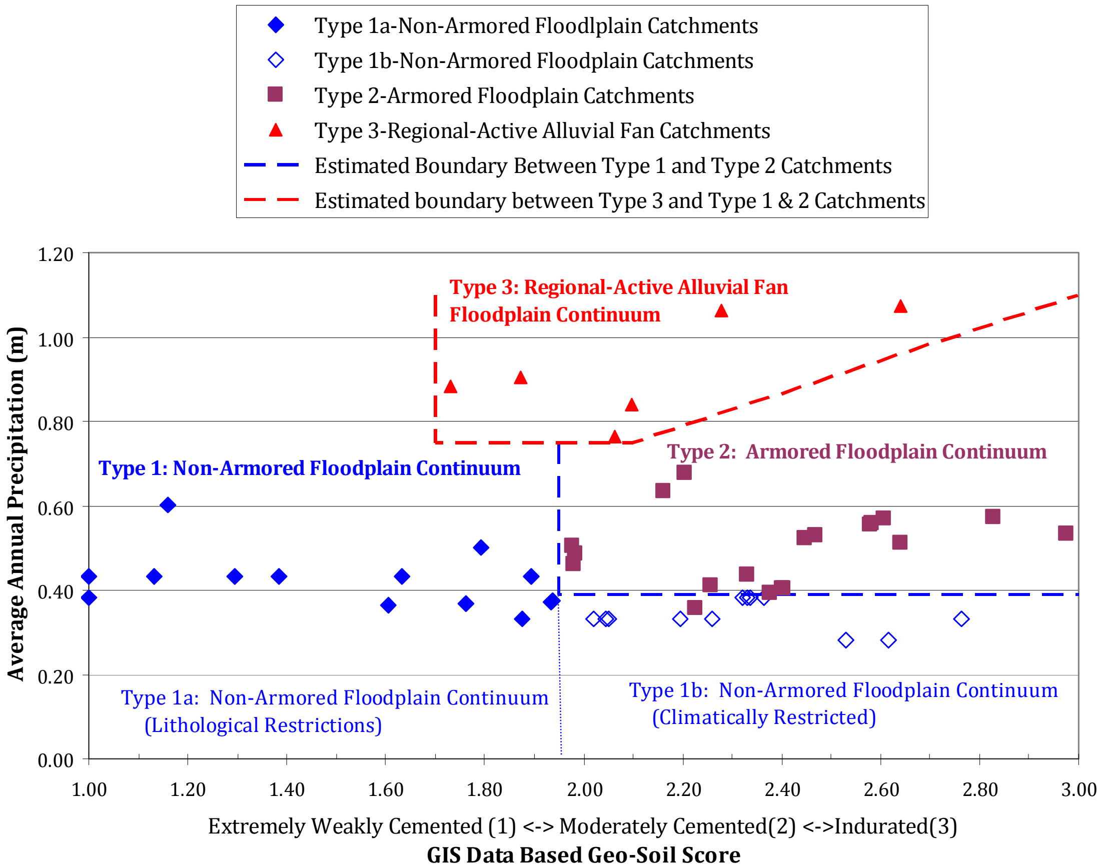

Figure 2.11 – Interrelationship of floodplain continuums in terms of average annual precipitation versus Geo-Soil Score

From a statistical standpoint, the data sets for the classes of study catchments shown in Figure 2.11 are relatively cohesive and isolated, in a statistical sense as described by Gordon (1999, p. 4). Furthermore, the pattern of the data points is rather complex and is, thereby, not conducive to the application of discriminant analysis techniques. Hence, the boundaries shown in Figure 2.11 separating the various floodplain continuums have been visually estimated based on the readily observable and clear breaks in the data points. The boundary shown between the Type 2 and Type 1b floodplain continuums corresponds to an *average annual precipitation* value of 0.39 m; whereas, the boundary shown between the Type 1a and Type 2 floodplain continuums corresponds to a *Geo-Soil Score* of 1.95.

All of the data points corresponding to the active-regional alluvial fan floodplain continuum have *average annual precipitation* values greater than 0.75 m. As can be clearly seen in Figure 2.11, this study does not include a sufficient number of study catchments to meaningfully describe the boundary between the active-regional alluvial fan continuum and the other continuums. Hence, the boundary shown in Figure 2.11 only represents a working hypothesis as to where the actual transitions may occur.

Close inspection of Figure 2.11 indicates that only one of the 51 data points (i.e., 98% accuracy) is not in the appropriate region of the graph. That is, the Type 2 data point at coordinate *Geo-Soil Score* = 2.22 and *average annual precipitation* = 0.355 meters is in the Type 1b floodplain continuum region. This data point corresponds to the Escondido Creek catchment and is unique in that this study catchment has the largest area (155 km^2) and the highest level of urbanization, with the majority of the metropolitan area of Escondido is within the catchment. I contend that the high level urbanization has altered the flow regime for Escondido Creek; hence, the area-weighted average annual rainfall for the catchment is no longer a meaningful metric for the climatic process driver. However this data point is useful for illustrating: (a) the potential impact of urbanization on even a floodplain continuum level; and (b) the limitation associated with using *average annual precipitation* as a metric for the climatic process driver in a large and highly urbanized catchment.

2.5.5 Application and Applicability of the GIS-Based Technique for Floodplain Continuum Identification

Application of the GIS-Based Technique for Predicting the Floodplain Continuums

The boundaries separating the three basic floodplain continuums shown in Figure 2.11 provide a means for predicting the floodplain continuum within a catchment in terms of *average annual precipitation* and *Geo-Soil Score*. Field observations and literature (Schumm et al., 1984; Harvey et al., 1985) suggest that the non-armored floodplain continuum has a significantly higher relative risk for transitioning to a state of severe instability in response to hydromodification than the armored floodplain continuum; hence, the GIS-based technique for predicting the floodplain continuum within a catchment may be a useful planning-level tool for assessing the relative risk for watercourse instability in response to hydromodification on a regional basis.

As with any GIS-based technique, there are limitations to its application. The following are basic guidelines for applying the GIS technique (illustrated in Figure 2.11) for predicting the floodplain continuum within a catchment:

- **Analyze Watercourses Individually**: Due primarily to the complexity of the geology within southern California, it is recommended that catchments for individual watercourses be evaluated individually; that is, do not compute the metrics for one polygon that includes catchments for multiple adjacent watercourses.
- **Maximum Catchment Size**: If the watercourse of interest has a catchment greater than 50 km^2, analyze the catchment as a series of increasing and overlapping catchments, where the upstream-most catchment is less than 25 km^2 and the incremental increase in area of the series of catchments is less than 25 km^2. For example: if the watercourse of interest has a catchment that is approximately 100 km^2, divide the catchment into 4 overlapping catchments that have areas of approximately 25 km^2, 50 km^2, 75 km^2, and 100 km^2.
- **Field Verification of Predicted Floodplain Continuums**: It is essential to develop a program for field verifying the predicted floodplain continuums. The percentage and locations of the predicted floodplain continuums to be field verified should be based on both the level of completeness of the GIS data and the range of variation in both the precipitation and *Geo-Soil Score* metrics.

- **Verification of the Level of Completeness of the Cementation-Level Attribute**: As described in the Methods section, SSURGO soil data are the primary source of data for computing the *Geo-Soil Score*. Since the cementation-level attribute within the SSURGO soil data is not fully populated and the SSURGO soil data do not provide complete coverage for southern California, it is important to assess the level of completeness of the cementation-level data when applying the GIS technique for predicting floodplain continuums. An approach for verifying the completeness of the SSURGO soil data is described in the following section.

Verification of the Level of Completeness of the SSURGO Soil Data

The applicability of any GIS-based technique can be limited by: (a) the degree of completeness of individual attributes within in the GIS data, and/or (b) the extent of the geographical coverage of the GIS layer. The floodplain continuum prediction tool illustrated in Figure 2.11, utilizes three GIS layers to compute the metrics for the process drivers as follows:

- **Climatic Process Driver**: The *average annual precipitation* data compiled by the USDA/NRCS (1998).
- **Geologic Process Driver**: The *cementation-level* attribute provided in the "SSURGO" soil data (USDA/NRCS, 2007) and the rock type attribute provided in the "Preliminary integrated geologic map databases" (USGS, 2005).

The precipitation data and the USGS geology data layers provide fully attributed and complete coverage for California. However, the SSURGO soil data are provided in separate layers corresponding to individual soil reports and do not provide complete coverage for all of southern California. Furthermore, the *cementation-level* attribute within the SSURGO soil data is not fully attributed, which is why the USGS geology data have been used to supplement the soil data when computing the *Geo-Soil Score* in this research. Hence, it is important to assess the level of completeness of the *cementation-level* attribute when applying the GIS-based technique for predicting the floodplain continuum type within a catchment.

The SSURGO soil data do provide complete coverage for the 51 study catchments and a high level of coverage for the study area shown in Figure 2.1, with only minor overlap or sliver issues. As described in Section 2.4.2, the geology layer data are used to supplement the SSURGO *cementation-level* attribute data during computation of the *Geo-Soil Score*, since the *cementation-level* attribute data are not completely populated. To assess the completeness of the SSURGO *cementation-level* data, the percentage of each study catchment that does not have a *cementation-level* attribute specified and the corresponding rock type from the USGS database were tabulated and evaluated. The results of these analyses are summarized in Table 2.7 and provided in detail in Table A.2. In general terms, the analyses summarized in Table 2.7 indicate that the *cementation-level* attribute has a relatively high level of completeness within the study catchments. More specifically, the results of the analyses summarized in Table 2.7 indicate that:

- The SSURGO *cementation-level* attribute data have a relatively high level of completeness (i.e., 85% complete), by area, within the 51 study catchments.
- On an individual study catchment basis, the percentage (by area) of a study catchment without a *cementation-level* attribute specified ranges from 0.00 to 96.7%. This indicates that the level of completeness of the *cementation-level* attribute varies widely on a geographical basis, even though the overall level of completeness for the study catchments is relatively high (i.e., 85% complete).
- Comparison of statistics 2a through 2d in Table 2.7 indicates that, within the study catchments, the *cementation-level* attribute is least complete (i.e., 9.86 % incomplete) when the geology *rock type* attribute is "igneous". This may simply indicate that

when the soil scientists were conducting the soil studies and assessing the cementation level of the underlying strata, they were unsure how to assess igneous rock. The *cementation-level* attribute data are probably most pertinent when the underlying strata are composed of sedimentary rock, since the *cementation-level* attribute can typically vary more widely for sedimentary rock than an other general rock type. In the case of sedimentary rock, the *cementation-level* attribute is only 1.54% incomplete.

Table 2.7 – Summary of statistics used to evaluate the completeness of the SSURGO *cementation-level* attribute data for the study catchments

Statistic ID	Statistic	Value
1	The percentage of the total study catchments area (933.7 km^2) **with** a cementation-level specified in the SSURGO database	85.4 %
2a	The percentage of the total study catchments area (933.7 km^2) **without** a cementation-level attribute specified in the SSURGO database and with an “Alluvium” rock type-1 attribute per the USGS database:	1.04 %
2b	The percentage of the total study catchments area (933.7 km^2) **without** a cementation-level attribute specified in the SSURGO database and with a “Sedimentary” rock type-1 attribute per the USGS database:	1.54 %
2c	The percentage of the total study catchments area (933.7 km^2) **without** a cementation-level attribute specified in the SSURGO database and with a “metamorphic” rock type-1 attribute per the USGS database:	2.17 %
2d	The percentage of the total study catchments area (933.7 km^2) **without** a cementation-level attribute specified in the SSURGO database and with an “Igneous” rock type-1 attribute per the USGS database:	9.86 %
3a	The minimum percentage of a study catchment **without** a cementation-level attribute specified in the SSURGO database:	0.00 %
3b	The maximum percentage of a study catchment **without** a cementation-level attribute specified in the SSURGO database:	96.7 %
3c	The mean percentage of a study catchment **without** a cementation-level attribute specified in the SSURGO database:	23.9 %
3d	The standard deviation of the percentage of a study catchment **without** a cementation-level attribute specified in the SSURGO database:	26.0 %

2.6 Summary and Conclusions

2.6.1 Primary Findings

The primary objectives of the investigations described in this chapter were to develop classification systems and conceptual models to characterize the nature and form of floodplains at various scales in the semi-arid environment of southern California. Due to the complex geologic history, the hierarchy of spatial scales developed for southern California emphasizes that watersheds and even catchments often encompass multiple geomorphic provinces, unlike in the Pacific Northwest.

The complex geologic history of southern California is also reflected in the reach-scale classification system and conceptual model. That is, the region's watercourses have been characterized with a complex interrelationship of three basic floodplain continuums and twelve basic alluvial floodplain forms. The classification system developed for southern California is an adaptation and extension of the classification system developed by Montgomery and Buffington (1997) to include three continuums (instead of just one), apply to floodplains (not just channels), and a wider range of floodplain forms. In addition, the reach-scale classification system, developed for southern California, incorporates a key concept regarding the braided floodplain form described by Nanson and Croke (1992); that is, braided floodplains have two thresholds: an upstream and a downstream threshold.

The complex geologic history of southern California is even further reflected in the catchment-scale conceptual model that relates the three basic continuums to the dominant process drivers of climate and geology. In southern California these two process drivers are strongly interlinked in the sense that plate tectonic activity has resulted in the formation of several high mountain ranges, which have in turn altered the climate and, more specifically, the geographic precipitation patterns. Hence, the wide range in annual precipitation, a metric for the climatic process driver, currently observed in the study area is directly linked to the geologic history for the region. Furthermore, the complex geologic history has also resulted in the mountain ranges being composed of a wide range of rock types. Therefore, the wide range in values for both of the dominant process drivers are directly linked to southern California's complex geologic history.

At the beginning of this chapter, I stated that the classification systems and conceptual models are intended to provide a framework for further investigating methods for estimating the trend and magnitude of changes in the geometry of a floodplain due to urbanization. The conceptual models and the GIS technique described in this chapter provide this essential framework by distinguishing the three basic floodplain continuums at multiple spatial scales and by providing multiple means for identifying the continuum within which a floodplain form is a member. By describing and characterizing the differences in floodplain forms in each of the floodplain continuums, the conceptual models also lead to the following series of important working hypotheses:

- The three basic floodplain continuums have different sequences of floodplain forms, due to differences in the corresponding intra-catchment runoff and sedimentation processes.
- The natural downstream floodplain geometry transitions are a direct reflection of the natural downstream changes in intra-catchment runoff and sedimentation processes, which can be significantly altered by urbanization.
- Each of the floodplain continuums can have different stability thresholds, floodplain form transition thresholds (e.g., braiding thresholds), and, most importantly, response mechanisms.

Therefore, the conceptual models described in this chapter provide an important "process oriented" framework for further investigating the mechanics and geomorphic thresholds associated with the natural downstream progression of floodplain forms.

2.6.2 Avenues for Further Investigation

GIS Tool for Relating Floodplain Continuum to Process Drivers

In Sections 2.4.2 and 2.5.4, a GIS-based technique is described for quantitatively relating the floodplain continuum to two process drivers on a catchment-scale. From a floodplain management perspective, this GIS-based technique is potentially a useful planning tool because it may provide a relatively efficient and accurate means to assess the floodplain continuum type for watercourses on a catchment to a regional scale. The potential value of this tool is demonstrated by findings in later chapters, which indicate that the potential for severe instability and the geomorphic response of a floodplain (in both trend and magnitude) to urbanization are distinctly different for the non-armored and armored floodplain continuums.

From a fluvial geomorphic standpoint, the GIS technique developed as part of this research may provide a unique tool for investigating the interrelationships between the floodplain continuums and the corresponding thresholds, in terms of process drivers on a catchment-scale. One geomorphic threshold of interest that the GIS-based technique may be useful for evaluating is the transition of a "Type 2" braided floodplain to a "Type 1" braided floodplain; however, this research did not collect any data to permit investigations into this geomorphic threshold.

Though these investigations have sufficient data to demonstrate the feasibility of the technique and define the boundaries between some of the continuums reasonably well, I fully recognize that there clearly are not sufficient data to describe all of the boundaries well. Therefore, there are several avenues for further investigations involving the GIS-based technique described in Section 2.5.5, in terms of both further refinement and potential applications.

Chapter 3: Conceptual Models for Intra-Catchment Processes that Govern the Downstream Progression of Floodplain Forms and Methods for Assessing the Current Stability State for a Floodplain

3.1 Chapter Overview

3.1.1 Abstract

For the non-armored and armored floodplain continuums, floodplain state plots have been generated to quantitatively describe the natural downstream progression of floodplain forms using specific stream power and width-to-depth ratio as the state and shape metrics, respectively. Based on the premise that the observed natural downstream progression of floodplain forms is a direct reflection of changes in intra-catchment runoff and sedimentation processes, these floodplain state plots provided the basis to: (a) develop techniques to assess the stability of a floodplain; (b) assess general floodplain response trends; (c) infer the interaction of key intra-catchment processes that govern the downstream progression of floodplain forms; and (d) develop hypotheses regarding the mechanisms governing the upstream braiding threshold for non-armored and armored floodplains. These finding were compiled diagrammatically to create *conceptual models for intra-catchment* process for the non-armored and armored floodplain continuums. In terms of the practical research questions at the core of these investigations, these conceptual models provide: (a) a means to assess the stability state of a floodplain; and (b) a framework within which to develop methods for estimating the trend and magnitude of the change in floodplain geometry due to urbanization.

3.1.2 Introduction/Research Questions

The core *practical* research questions motivating the research documented in this dissertation are:

- How can we quantitatively assess the existing stability state of a floodplain?
- How can we estimate the trend and magnitude of the change in floodplain geometry due to perturbations in intra-catchment processes associated with urbanization/hydromodification?

To address these core questions it was first important to develop a basic understanding of the form and nature of the floodplains in the semi-arid environment of southern California. As described in Chapter 2, three basic floodplain continuums have been identified for southern California: *non-armored*, *armored*, and *active-regional alluvial fan*. As shown in Figure 2.5, each of these continuums are comprised of three or more alluvial floodplain forms that have a general downstream sequence in stable systems. If it is argued or assumed that the observed natural downstream progression of floodplain forms is a direct reflection of natural changes in intra-catchment runoff and sedimentation processes, it is then logical to conclude that developing conceptual models describing key intra-catchment processes should provide a framework for addressing the *practical* research questions at the core of this research.

Therefore, the primary objective of the research documented in this chapter was to develop conceptual models describing key intra-catchment processes by addressing the following *applied* research questions:

- What are the intra-catchment processes that govern the observed downstream progression of floodplain forms in a stable system, including specifically the progression from single-thread to braided floodplains?

- How do the erosional resistance and stability characteristics of the banks influence the natural downstream progression of floodplain geometry and can this influence be quantified into general floodplain response trends and constraints?
- What is the interrelationship between the stability state with the form and geometry of a floodplain, under various hydraulic conditions?
- What is the impact of urbanization on the primary intra-catchment processes that govern the natural downstream floodplain form progression?

The research described in this chapter strictly focuses on the non-armored and armored floodplain continuums. The active-regional alluvial fan continuum has been included in this research on a qualitative and conceptual level, for the sake of completeness. However, this floodplain continuum has been excluded from quantitative reach-scale investigation in this research, since active alluvial fan floodplains are already highly regulated by FEMA and/or local agency guidelines.

3.1.3 The Threshold Approach and the Search for State and Shape Metrics That Quantitatively Describe the Natural Downstream Progression of Floodplain Forms

The approach adopted in this research was to first find a quantitative method to describe the natural downstream progression of floodplain forms, then use these findings to infer the key intra-catchment processes for the non-armored and armored floodplain continuums. This approach is based on the fundamental concept that the observed natural downstream progression of floodplain forms is a direct reflection of natural changes in intra-catchment runoff and sedimentation processes. Though posed in slightly different wording and context, this concept appears to be consistent with the threshold conceptual framework described by Bull (1979) as follows: "… the threshold concept emphasizes the possibility of change in a fluvial system. Those using the threshold approach are more likely to be interested in when and where change occurs in fluvial systems and the reasons for change, rather than searching for approximations of equilibrium. The graded stream approach generally encourages study of self-regulating feedback mechanisms, but the threshold approach generally encourages study of self enhancing feedback mechanisms."

Having adopted the threshold approach, the objective of these investigations was to quantitatively describe the natural downstream progression of floodplain forms. My approach involved searching for two quantitative metrics that described the natural progression of floodplain forms in terms of topwidth, depth, and bed slope. The objective of one metric is to quantify the *state* of a floodplain, in a manner related to both the stability state and the geometry of the floodplain; while the objective of the second metric is to quantify a key aspect of the *shape* or geometry of a floodplain form. To be of practical use, these metrics should be readily computable from field measurements of a floodplain and/or GIS-based measurements of the corresponding catchment. In addition, at least one of these metrics should be capable of reflecting the impacts of urbanization on the intra-catchment processes. Therefore, a critical objective of this research involved finding metrics that can quantify the *state* and *shape* of a floodplain.

3.2 Previous Studies: State and Shape Metrics for Floodplains

The concept of using state and/or shape metrics for describing floodplains and channels has a relatively long history and, as a result, a wide range of metrics has been evaluated in the literature. However, the work done by several researchers has strongly influenced the approach adopted in these investigations. This section briefly describes key aspects of these previous investigations into geomorphic thresholds, influential to this research, and the metrics used to describe these thresholds. The equations for each of the *state* and *shape* metrics described in this section are listed in Table 3.1.

Table 3.1 – List of *state* and *shape* metrics evaluated in the literature

Total Stream Power (Bagnold, 1973; Bagnold, 1977):

$\Omega = \gamma Q S_f$ in (W/m) Equation 3.1

Specific Stream Power (Bull, 1979):

$\omega = \gamma \frac{Q}{W} S_f$ in (W/m^2) Equation 3.2

Total Boundary Shear Stress (Chow, 1959):

$\tau = \gamma R S_f$ in (Pa = kg/ms^2) Equation 3.3

Slope/Froude Number (Parker, 1976):

$S_f / F_r = \frac{S_f (gd)^{1/2}}{V}$ Equation 3.4

Width-to-Depth Ratio for Channels (Harvey, Watson and Schumm, 1985):

$W_C / d = 255 \cdot M^{-1.08}$ Equation 3.5

where: Q = flow rate (m^3/s)

S_f = friction slope (m/m)

γ = 9810 (kg/m^{2}s^2) = specific weight of water

W = topwidth of flow area (m)

$R = A / P_w$ = hydraulic radius (m)

A = flow area (m^2)

P_w = wetted perimeter (m)

d = maximum flow depth (m)

V = flow velocity (m/s)

g = 9.81 (m/s^2) = acceleration of gravity

W_C = topwidth of channel (m)

M = percentage of silt and clay in the perimeter of the channel

The Concept of a Critical Power Threshold

Bagnold (1973, 1977) argued the concept that watercourses are primarily "sediment-transporting machines" that can be considered in terms of the availability of stream power (per Equation 3.1 in Table 3.1) to do work. Based on this concept, Bull (1979) developed the concept of a *critical-power threshold* that separates "*the modes of erosion and deposition in streams and is dependent on the relative magnitudes of power needed to transport the average sediment load and on the stream power available to transport the load*." That is, Bull (1979) used stream power as a *state* metric and considered stream power in terms of both *total stream power* (per Equation 3.1 in Table 3.1) and *total stream power per unit area of streambed* (or specific stream power per Equation 3.2 in Table 3.1).

Classification of Floodplains Based on Specific Stream Power

Nanson and Croke (1992) developed a "genetic classification of floodplains" based on the concept that floodplains (geomorphic perspective) are formed by a complex interaction of fluvial processes; however, their properties are primarily a function of specific stream power and sediment character (i.e., cohesive versus non-cohesive). That is, they used specific stream power (per Equation 3.2 in Table 3.1) as a *state* metric and identified thresholds for differentiating between the various floodplain forms.

The classification system defined by Nanson and Croke (1992) is unique in that it describes an array of floodplain forms (from a geomorphic perspective) and links them into potential continuums using identified ranges of specific stream power. Furthermore, their classification system identifies braided floodplains as "Class B – medium energy", with non-braided floodplains being in both higher and lower energy classes. Hence, a logical (if not direct) implication of their classification system is that braided floodplains have both an upstream and downstream braiding threshold, as observed in southern California. This is an important distinction to this research, because other investigations into braiding thresholds in the literature only show braided floodplains as having higher power or energy levels than non-braided (or typically meandering) floodplains (Parker, 1976; Chang, 1988, p. 278; van den Burg, 1995; Bledsoe and Watson, 2001).

It was influential to this research that Nanson and Croke (1992) indicated that they would have preferred to use specific stream power values specifically for the floodplains (geomorphic perspective) in their classification system; however, they had to use specific stream power values computed for bankfull flow conditions within the channel as a surrogate. They further indicated they also considered evaluating boundary shear stress (per Equation 3.3 in Table 3.1) as a *state* metric ; however, they also lacked sufficient hydraulic data with which to estimate boundary shear stress.

Parker (1976) State Diagram and Braiding Threshold

Parker (1976) developed a state diagram for differentiating meandering, braided, and straight channels at formative discharges. For this state diagram, the *state* metric is defined as slope divided by the Froude Number (Equation 3.4 in Table 3.1) and the *shape* metric is the inverse of the width-to-depth ratio. It is important to note that this state diagram is strictly for the downstream braiding threshold, where the braided channel has the higher *state* metric for a given value of the *shape* metric. However, this state diagram clearly demonstrates the concept of defining geomorphic thresholds in terms of a *state* and a *shape* metric, even though the author didn't specifically describe it in these terms.

Shape Metric for Describing Downstream Changes in Channel Geometry

Cooke and Reeves (1976) and Tooth (2000) used width-to-depth ratios (and cross section plots) to describe downstream changes in channel geometry for arroyos in the American Southwest and dryland river channels in the northern plains of arid central Australia, respectively. In both of these publications, the width-to-depth ratio was in reference to bankfull conditions; however, their research clearly demonstrated that the width-to-depth ratio may be a useful *shape* metric in the arid and semi-arid environment.

Width-to-depth Ratio as a Reflection of Bank Characteristics

Schumm (1977) and Harvey et al. (1985) observed and quantified a relationship between *width-to-depth* ratio and the percentage of silt and clay in the channel perimeter (Equation 3.5 in Table 3.1). In regards to Equation 3.5, the authors emphasized that the percentage of silt and clay in the perimeter of the channel represents both a metric of the type of sediment being transported within the channel and an indication of stability characteristics of the bank material. Hence, this implies that the observed width-to-depth ratio, in ***stable fluvial systems***, is also a metric of the erosional resistance and/or stability characteristics of the bank material, to some degree.

3.3 Study Area: Geomorphic Limits and Geologic Setting

3.3.1 Geomorphic Limits for This Study

The geographical boundary for this study was defined by two constraints. First, the study area was limited to the six southern-most counties in southern California with watersheds that drain to the Pacific Ocean. Second, the study area was further limited to those watersheds that drain to the ocean. The geographical boundary for the study area, based on these two constraints, is shown in Figure 2.2.

Since urbanization in southern California is now extending into the upper reaches of the watersheds, this research intentionally focused on studying the upper reaches of non-armored and armored watercourses, which have relatively small catchments. This focus resulted in essentially a geomorphic limit being imposed on the range of floodplain forms included in this study. As illustrated in Figure 3.1, this geomorphic limit encompasses the braided and upstream floodplain forms for the armored and non-armored floodplain continuums shown in Figure 2.5.

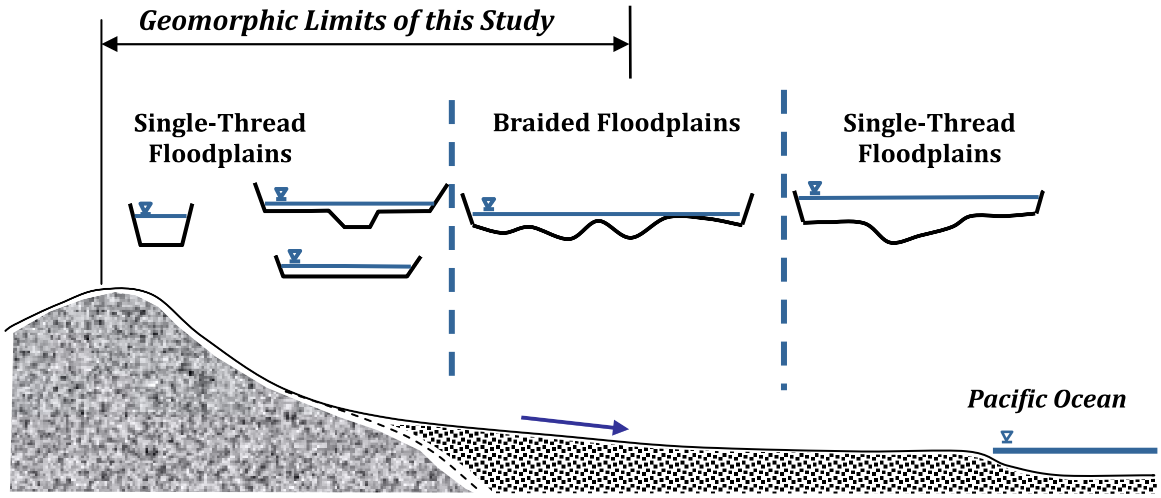

Figure 3.1 – Schematic illustrating a general floodplain continuum and the geomorphic limits for this study

3.3.2 Geologic Setting – Geomorphic Province and Catchment Scale

The study area is located within the Pacific Province and includes the Transverse and Peninsular Ranges, as shown in Figure 2.3. The Transverse and Peninsular Ranges are the result of the complex interaction of the North American Plate and the Pacific Plate along the San Andreas Fault system over approximately the past 20 to 30 million years (Mount, 1995).

This complex geologic history has resulted in the mountain ranges within the study being composed of a wide variety of sedimentary, metamorphic, and igneous rocks. In addition, the study area has an extensive network of fault lines. As a result, the geologic setting within the study area can be complex on even the catchment or valley segment scale.

On a very general level, there are two basic valley types within the study area:

- river valleys, where fluvial processes have been the dominant driver in the formation of the drainage network within the valley (Figure 3.2a); and

- alluvial fill valleys, where a combination of active faults and fluvial processes are currently and have been the dominant drivers in the formation of the valley (Figure 3.2b).

These two basic types of valleys are illustrated in Figure 3.2. It is important to recognize that these representations are highly simplified, especially in terms of the sub-surface features. That is, there may also be faulting associated with river valleys, even though this faulting is not depicted in Figure 3.2a; however, these faults may be relatively inactive and occur in areas where the geologic and climatic conditions are not exceptionally conducive to the formation of alluvial fans. Figure 3.2b depicts an alluvial fill valley with alluvial fans and reverse or thrust faulting , which is representative of the south front of the eastern San Gabriel Mountains, as also shown in Figure 2.9 (Crooks, Allen, Kamb, Payne, and Proctor, 1987; Cramer and Harrington, 1987); however, the faulting associated with the major alluvial fill valleys within the study area is actually a complex network of normal, reverse, and transform faults (USGS, 1987).

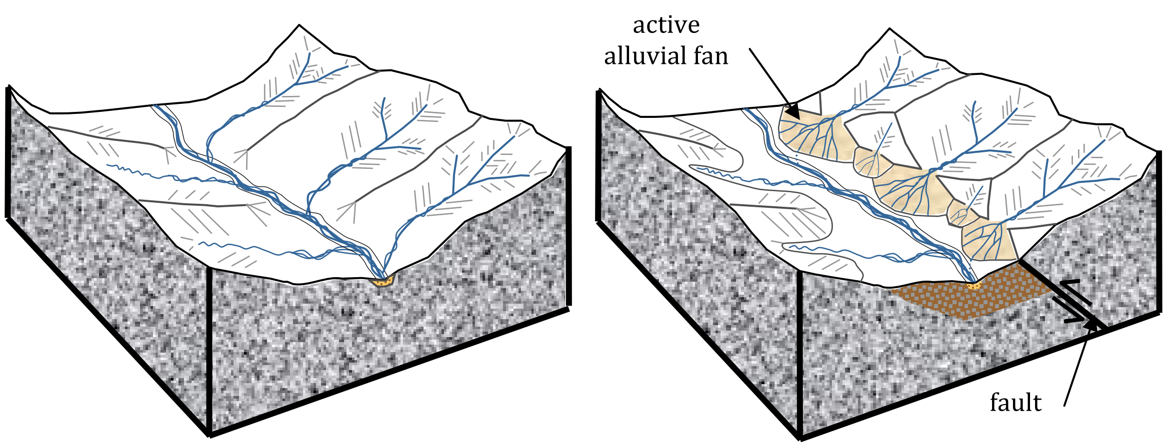

Figure 3.2 a: *River valley*

Figure 3.2 b: *Alluvial fill valley* showing reverse fault and alluvial fans

Figure 3.2 – Schematic illustrating *river* and *alluvial fill* valley types

Figure 3.2 illustrates the key characteristics of, and key differences between, the two basic valley types. As depicted in Figure 3.2a, river valleys have relatively narrow valley bottoms and typically do not have active alluvial fans, such as the valleys associated with the Santa Clara River, Escondido Creek, and Dulzura Creek. Whereas, alluvial fill valleys (as depicted in Figure 3.2b) have relatively broad valley floors with deep alluvium, such as the San Fernando, Simi, San Gabriel, Pomona, San Bernardino, Perris, and San Jacinto Valleys. In addition, alluvial fill valleys may often have alluvial fans along the mountain fronts with active faulting, as depicted in Figure 3.2b.

3.4 Methods

3.4.1 Site Selection Process

An objective of this research is to describe the geomorphic characteristics for both the stable and unstable floodplain forms within the armored and non-armored floodplain continuums. Hence, it was imperative to investigate and evaluate a representative sample of watercourses on both a reach- and catchment-scale basis. As with any study, there is a limit to the amount of resources that can be allocated to the site selection and data collection process. Therefore, a systematic and multi-step process was employed to select both the most representative study sites and the most advantageous level of data collection at each site.

Based on the data collected at fifty two (52) locations during the initial reconnaissance-level site investigations, key aspects of the potential study sites were tabulated and 30 study sites or reaches were selected to provide as representative a range of the key floodplain characteristics as possible using the criteria summarized in Table 3.2. The level of data collection, at a reach scale, for each site was then selected to include as many floodplain form transitions as possible.

Table 3.2 – Summary of study site selection criteria

Criteria	Study Site Selection Criteria
1	Approximately 50% of sites should exhibit signs of instability, with the cause(s) or history of the instability being relatively identifiable or definable. That is, sites with very complex histories of instability should not be considered
2	Sites with floodplain form transitions and/or confluences are given priority.
3	Data sites should provide a representative range of: • Catchment urbanization levels between none to moderate. • Floodplain or channel forms. • Bed material composition. • Floodplain (i.e., channel and overbank) vegetation densities.
4	Most of the sites should have catchments less than 20 km^2 and all catchments should be less than approximately 70 km^2.
5	Approximately 50% of the sites should be suitable for post flow event and/or long-term monitoring.
6	Sites where legal permission to access the site was either confirmed or obtained prior to the site selection process are given priority.
7	Sites should be representative of the geo-political boundaries within the study area.

3.4.2 Field Data Collection

Due to the wide range of geomorphic conditions at each of the thirty (30) study sites, it was determined that a wider range of field data could be collected, if two levels of data collection were employed. These two levels of field data collection are referred to as "screening" and "modeling" levels. As implied by the name, the "modeling" level of field data collection is intended to provide sufficient data to permit hydraulic modeling with both rigid bed hydraulic models and/or movable boundary models. However, the primary difference between the two levels of data collection is that only one to three cross sections were surveyed at screening-level sites; whereas, five to eighteen cross sections were surveyed at modeling-level sites. The field data collected at both the screening-level and modeling-level sites are summarized in Table 3.3.

Table 3.3 – Summary of the levels of field data collection for each type of study site

Site Type	Levels of Field Data Collection for Each Type of Study Site
All	**Qualitative data collected at each cross section within sites via a multiple-choice formatted data collection form**: • Observed floodplain forms within the reach. • Estimation of Manning-n values for channels and overbanks. • Bank characteristics, including a visual assessment of stability and/or modes of failure. • Basic bed material characteristics, including basic rock types, size ranges, and the level/extent of bed armoring. • Field assessment of the current stability state of the floodplain, per criteria in Table 3.4. • The level, extent, and characteristics of the vegetation within the floodplain. • Digital photographs of study reach documenting bed material, bed forms, bank conditions, and vegetation characteristics

Screening Level Sites	**Quantitative Data Collected at "Screening-Level" Sites:**
	• 1 to 3 bed material gradations, based on pebble count and/or dry sieve analyses bed samples.
	• Survey/geometry data collected using a pole mounted hand-level and Pocket Rod.
	    ○ 1 to 3 floodplain cross sections.
	    ○ bed profile extending a minimum of approximately 50 meters upstream and downstream of cross section(s).

Modeling Level Sites	**Quantitative Data Collected at "Modeling-Level" Sites:**
	• 2 to 3 bed material gradations, based on pebble count and/or dry sieve analyses of bed samples.
	• Survey/geometry data collected using either a total station or a survey level global positioning system by either Stillwater Consultants or Riverside County Public Works Department.
	    ○ 5 to 18 floodplain cross sections
	    ○ bed profile extending a minimum of approximately 50 meters upstream and downstream of the cross sections.

Criteria for Field Identification of Current Stability State of a Floodplains

A critical step in the field data collection involved assessing the current stability state of the floodplains at each of the study sites. Schumm, Harvey, and Watson (1981, 1984) recognized that incised floodplains have transitioned through a sequence of forms and employed the technique termed *location-for-time substitution* to develop a Channel Evolution Model (CEM) for Oaklimeter Creek in northern Mississippi. This CEM is defined in terms of five evolutionary phases typically encountered in an incised floodplain, with each CEM phase being defined in terms of the dominant fluvial processes. Using the CEM phases as a basis, the field observation criteria listed in Table 3.4 have been developed and used to assess the CEM phase and the corresponding current stability state at each of the cross sections within the study sites.

It is important to note that the CEM phases described in Table 3.4 have been modified and adapted to be applicable to the floodplain continuums observed in the semi-arid environment of southern California and compatible with the three states of stability described in Section 1.3.1. The most notable difference between the CEM phases described in Table 3.4 and the original CEM is that the *primary* head-cut or knickpoint appears in Phase III as opposed to Phase II. This modification was done in recognition that floodplains may experience relatively minor head-cut migrations that do not significantly destabilize the banks, in response to natural perturbations in the runoff and sediment supply within the catchment. As listed in Table 3.4, this modification also assisted in distributing the five CEM phases into the three states of stability as follows:

- Stable and in a state of dynamic equilibrium includes CEM Phases I, Ia, and V.
- Responding and in a state of dynamic response includes CEM Phase II.
- Unstable and in a state of severe instability includes CEM Phases III and IV.

The Classification and Stability of Braided Floodplains

It is important to recognize that during the course of the field data collection, both stable and unstable braided floodplains were observed and included in these investigations. In addition, stable and unstable braided floodplain were observed to have distinguishing characteristics. Unstable braided floodplains were distinguished by clear evidence of floodplain degradation, accompanied by severe and extensive bank failures.

Table 3.4 – Field observation criteria used to assess the current stability state of a floodplain in the semi-arid environment of southern California

CEM Stage & Stability State	Dominant Processes: Fluvial	Dominant Processes: Banks/Terraces	Indicators for Assessing CEM Stage or Phase
I Pre-Modified (***Stable*** – *State of Dynamic Equilibrium*)	Floodplain in dynamic equilibrium.	Bank alignments relatively unchanged in engineering time scale. Bank height less than or equal to critical ($h < h_c$).	No evidence of head-cut migration. Only minor bank cutting.
Ia Constructed (***Stable*** – *State of Dynamic Equilibrium*)	Floodplain in dynamic equilibrium	Floodplain/channel improvements are in good condition with no evidence of under-cutting.	Floodplain improvements functioning and in good condition, with no evidence of significant aggradation or degradation.
II Degrading (***Responding*** – *State of Dynamic Response*)	Channel degradation, in response to a small head-cut or knickpoint migration. This head-cut may or may not be a precursor for a primary head-cut.	Heightening and steepening of banks. Bank height less than critical ($h < h_c$).	Evidence of minor head-cut migration. Limited or intermittent shear erosion or under-cutting of banks. Intermittent or minor slab and/or slump bank failures.
III Threshold (***Unstable*** – *State of Severe Instability*)	Channel degradation and widening, with primary and/or secondary head-cut or knickpoint migration.	Bank retreat and scalloping occurring. Thalweg **low** relative to top of bank. Bank height greater than critical ($h > h_c$).	Evidence of substantial head-cut migration. Vertical bank surfaces. Frequent or extensive shear erosion or under-cutting of banks. Significant slab, slump and/or rotational bank failures
IV Aggrading (***Unstable*** – *State of Severe Instability*)	Channel aggradation and widening. Initial development of bars within channel. Re-working of material from bank failures.	Bank retreat and scalloping. Vertical bank surfaces, but slopes beginning to flatten in locations. Thalweg **low** relative to top of bank. Bank height greater than or equal to critical ($h \geq h_c$).	Limited or intermittent shear erosion or under-cutting of banks. Slab, slump and/or rotational bank failures; however, evidence of bank healing or re- stabilizing.
V Re-Stabilized (***Stable*** – *State of Dynamic Equilibrium*)	Minor channel aggradation. Continuing development of bars within channel. Continued re-working of material from bank failures.	Bank healing and re-vegetation occurring. Continued flattening of bank angles. Thalweg **high** relative to top of bank. Bank alignments have stabilized. Bank height less than critical ($h < h_c$).	No evidence of active head-cut migration. Banks are or are nearly healed and re-stabilized

The concept that there are stable and unstable braided floodplains is not new. In terms of the classification system developed by Lane (1957), the stable braided floodplains observed in these investigations would be an example of "Type 2" braiding, while the unstable braided floodplains would be an example of "Type 1" braiding per Table 3.5.

Table 3.5 – Classification of braided watercourses by Lane (1957).

Braided Streams	I. Braiding due to steep slopes	1. Braiding due to steep slope with degradation
		2. Braiding due to steep slope with approximate equilibrium
	II. Braiding due to aggradation	3. Braiding due to steep slope with aggradation
		4. Braiding due to moderate slope with aggradation
		5. Braiding due to low slope with aggradation

Bed Material Gradation Analyses

As reflected in the floodplain descriptions in Tables 2.4 and 2.5, the watercourses studied in these investigations have a wide range of bed material compositions. Hence an assortment of bed material sampling and analysis techniques had to employed. The conditions under which the various sampling and analyses techniques have been employed are summarized in Table 3.6.

3.4.3 Estimation of a Range of Flow Rates

As indicated in Section 3.2, essentially all of the candidates for the state and shape metrics for a floodplain are hydraulic parameters and are, therefore, associated with specific flow conditions; hence, estimation of these metrics requires hydraulic computations corresponding to a specific flow rate or a range of flow rates. In addition, field observations imply that relatively infrequent, high magnitude flow events are probably responsible for both forming and maintaining the geometry of floodplains in the semi-arid environment; hence, it was deemed important to at least initially consider and evaluate candidates for state and shape metrics over a relatively wide range of flow rates. Therefore, finding a systematic method for estimating a range of flow rates for a floodplain and corresponding catchment became a critical step in the search for finding useful state and shape metrics for a floodplain.

Table 3.6 – Bed material sampling and analysis techniques

Method	**Bed Material Composition**	**Sampling Technique**	**Analysis Technique**
1	Mixture of gravel, cobbles, and/or boulders, and bed armoring is prevalent. ***Note***: Applied this method only if the pebble count indicated that less than 10% of the bed material is less than 2 mm in diameter.	Surface sample (pebble count) per Bunte and Abt (2001).	Percent passing for a range of sizes obtained directly from pebble count.
2	Mixture of sand, gravel, and cobbles, with no evidence of bed armoring. ***Note***: Applied this method when the pebble count indicated that more than 10% of the bed material is less than 2 mm in diameter and there are coarse gravel or larger material present.	Surface sample (pebble count) and volumetric sample, per Bunte and Abt (2001).	Percent passing for a range of particle diameters obtained from pebble count and dry sieve analyses. Use *Flexible Combination* analysis procedure to combine data to obtain a single gradation, per Bunte and Abt (2001).
3	Sand and/or fine to medium gravel, with no evidence of bed armoring.	Volumetric sample, per Bunte and Abt (2001).	Dry sieve analysis to obtain the percent passing for a range of particle diameters.

Many studies have used catchment area alone, or a relationship based on catchment area, as a surrogate for flow rate when trying to identify state variables for a watercourse. As described in section 2.4.2, average annual precipitation varies widely and has strong orographic patterns; therefore, catchment area alone is not an appropriate surrogate for discharge within the study area.

Several methods for systematically identifying a reasonable range of flow rates for a given cross section of a floodplain were considered, including the "regional flood-frequency equations" developed for several regions in California by the USGS (Waananen and Crippen, 1977). As indicated in Table 3.7, the regional flood-frequency equations for the “South Coast Region” include both catchment area and average annual precipitation as input parameters; in addition, equations have been developed for a wide range of return periods, including the 2, 5, 10, 25, 50, and 100 year events. It is recognized that these equations represent a simplified approach for estimating discharges corresponding to specific return periods and may be prone to significant error. However, the objective of using the USGS regional flood-frequency equations in this study is to identify the range of flows associated with the formation and/or maintenance of the floodplain and not to identify a peak flow rate associated with a specific return period; therefore, the equations were deemed a reasonable approach for estimating a range of discharges for a given catchment and have been used in this study.

3.4.4 Hydraulic Analyses and Development of Hydraulic Database

To address both the practical research questions at the core of this research and the corresponding applied research question regarding the intra-catchment processes that cause natural floodplain transitions, one approach is to find both *state* and *shape* metrics to quantitatively describe the downstream progression of floodplain forms. As described in Section 3.2, essentially all of the candidates for the *state* and *shape* metrics for a floodplain are associated with specific flow conditions.

Table 3.7 - Regional flood-frequency equations for the California South Coast Region (Waananen and Crippen, 1977)

Regional Flood-Frequency Equations in English Units

$Q_2 = 0.41 A_C^{0.72} P_{aw}^{1.62}$ in (ft³/s) Equation 3.6a

$Q_5 = 0.40 A_C^{0.77} P_{aw}^{1.69}$ in (ft³/s) Equation 3.7a

$Q_{10} = 0.63 A_C^{0.79} P_{aw}^{1.75}$ in (ft³/s) Equation 3.8a

$Q_{25} = 1.10 A_C^{0.81} P_{aw}^{1.81}$ in (ft³/s) Equation 3.9a

$Q_{50} = 1.50 A_C^{0.82} P_{aw}^{1.85}$ in (ft³/s) Equation 3.10a

$Q_{100} = 1.95 A_C^{0.83} P_{aw}^{1.87}$ in (ft³/s) Equation 3.11a

where: Q_T = flow rate for return period T years (ft³/s)

A_C = catchment area, in square miles (mi²)

P_{aw} = area-weighted average annual precipitation per Equation 2.1 (in)

Regional Flood-Frequency Equations Converted into Metric Units

$Q_2 = 2.246 A_C^{0.72} P_{aw}^{1.62}$ in (m³/s) Equation 3.6b

$Q_5 = 2.702 A_C^{0.77} P_{aw}^{1.69}$ in (m³/s) Equation 3.7b

$Q_{10} = 5.205 A_C^{0.79} P_{aw}^{1.75}$ in (m³/s) Equation 3.8b

$Q_{25} = 11.115 A_C^{0.81} P_{aw}^{1.81}$ in (m³/s) Equation 3.9b

$Q_{50} = 17.390 A_C^{0.82} P_{aw}^{1.85}$ in (m³/s) Equation 3.10b

$Q_{100} = 24.099 A_C^{0.83} P_{aw}^{1.87}$ in (m³/s) Equation 3.11b

where: Q_T = flow rate for return period T years (m³/s)

A_C = catchment area, in square miles (km²)

P_{aw} = area-weighted average annual precipitation per Equation 2.1 (m)

Under ideal conditions, it would be best to compute state and shape metrics based on field measurements of flow rate, flow depth, topwidth, friction slope, flow velocity, and other hydraulic parameters for a wide range of flow conditions at each of the study sites. However, this simply isn't practical and/or possible in the semi-arid environment of southern California, especially at locations where the floodplain is in a state of severe instability and the geometry of the floodplain changes during each significant flow event. Hence, estimation of state and shape metrics requires hydraulic computations to estimate flow depth, topwidth, and other hydraulic parameters corresponding to a field- measured cross section and a range of flow rates.

To provide a basis for evaluating various hydraulic parameters as potential state and shape metrics for floodplains, the Manning equation (Equation 3.14 in Table 3.8) was selected to be the basis for the hydraulic analyses used to estimate hydraulic parameters for each of the study cross sections, given field-measured geometry and estimated *n* value. Technically speaking, the Manning equation is only applicable to steady uniform flow conditions; that is, the flow conditions are such that: (a) the flow depth does not change with time; (b) the flow depth, area, velocity, and rate are constant in space over a significant reach length; and (c) the energy line or friction slope (S_f), water surface slope (S_w), and bed slope (S_b) are all parallel (Chow, 1959). It is fully recognized that strict uniform flow conditions rarely occur in natural watercourses and essentially cannot strictly occur in watercourses in the armored floodplain continuum, where the floodplain has pronounced bedforms with respect to flow depths. However, the primary objective in this study for applying the Manning equation is to estimate reach-averaged state and shape metrics associated with a given floodplain geometry. Therefore, it is recognized that the results from these hydraulic analyses are approximate and general.

The results of the individual hydraulic analyses for each of the study cross sections (provided in Appendix B) have been compiled to create one *hydraulic analyses* database. This *hydraulic analyses* database contains records for six flow conditions for each of the 124 surveyed cross sections, thereby creating a database with 744 records. Each record in this database has the following information:

- Basic site data, including floodplain form, bed slope, valley slope, valley width, existing stability state in terms of CEM stage, d_{50}, and an estimated Manning-n value.

- The hydraulic parameters listed in Table 3.8, including stage or maximum flow depth (d), wetted perimeter (P_w), hydraulic radius (R), hydraulic depth (D), topwidth (W), width-to-depth ratio (W/d), total boundary shear stress (Equation 3.3), Shields parameter (Equation 3.17), and specific stream power (Equation 3.2), and Froude Number (Equation 3.18).

The *hydraulic analyses* database was compiled within a spreadsheet application. To aid in the graphic analyses of the data within the *hydraulic analyses* database, Visual Basic ® macros were coded to perform user specified-queries and to rapidly generate complex plots of the data.

3.4.5 Binary Linear Logistic Regression Analysis

Though it is more common for logistic regression analyses to be applied in the behavioral and health sciences, Tung (1985) and Bledsoe and Watson (2001) have applied logistic regression techniques in the evaluation of geomorphic thresholds. The binary linear logistic regression analysis technique is an extension of linear regression techniques and its application can be best illustrated with an example.

Basic Concept Illustrated with an Example

As illustrated in Figure 3.3, consider the case when there are two sets of two dimensional data points, where each set of data points corresponds to one of two known states for a dichotomous dependent variable Y. In this case, the two qualitative states of the dichotomous dependent variable Y are *State A* and *State B*; and, the two dimensions are defined by independent variables X_1 and X_2 .

Table 3.8 – List of the primary hydraulic parameters in the hydraulic database for each cross section and a range of flow rates

Hydraulic Depth — Equation 3.12

$$D = A / W \quad \text{in (m)}$$

Hydraulic Radius — Equation 3.13

$$R = A / P_w \quad \text{in (m)}$$

Manning Equation (Chow, 1959): — Equation 3.14

$$V = \frac{1}{n} R^{2/3} S_f^{1/2} \quad \text{in (m/s)}$$

Continuity Equation (Chow, 1959): — Equation 3.15

$$Q = V \cdot A \quad \text{in (m}^3\text{/s)}$$

Width-to-Depth Ratio (Knighton, 1998): — Equation 3.16

$$\mathrm{T} = (W / d) = \text{Width-to-Depth Ratio (m/m)}$$

Total Boundary Shear Stress (Chow, 1959): — Equation 3.3

$$\tau = \gamma R S_f \quad \text{in (Pa = kg/ms}^2\text{)}$$

Shields Parameter (Chow, 1959): — Equation 3.17

$$\tau^* = \frac{\gamma R S_f}{(\gamma_s - \gamma) d_{gs}}$$

Specific Stream Power (Bull, 1979): — Equation 3.2

$$\omega = \gamma \frac{Q}{W} S_f \quad \text{in (W/m}^2\text{)}$$

Froude Number (Chow, 1959): — Equation 3.18

$$F_r = \frac{V}{\sqrt{\frac{gD}{\alpha}}}$$

where:
- V = flow velocity (m/s)
- n = Manning's roughness coefficient
- A = flow area (m^2)
- P_w = wetted perimeter (m)
- S_f = friction slope (m/m)
- d_{gs} = grain size (m)
- Q = flow rate (m^3/s)
- W = topwidth of flow area (m)
- d = maximum flow depth (m)
- γ = 9810 (kg/m^{2}s^2) = specific weight of water
- γ_s = 25,967 (kg/m^{2}s^2) = specific weight of sediment
- g = 9.81 (m/s^2) = acceleration of gravity
- $\alpha \approx 1.15$ = kinetic energy coefficient

If the two data sets are relatively cohesive and overlap (as shown in Figure 3.3a), a binary linear logistic regression analysis can be used to identify a series of lines, where each line has an estimated probability of being in one of the two states (Menard, 1995). That is, the example logistic regression line labeled "$P(Y= S_A) = 90\%$", in Figure 3.3b, represents the values of coordinate pairs of variables X_1 and X_2 , where the probability of being in state A is 90%. Hence, this line also corresponds to a probability of being in state B of 10% (i.e., 100% - 90%), because this is a binary logistic regression model. Therefore, a *binary linear logistic regression analysis* is a statistical technique that can be used to define geomorphic thresholds in terms of probability; hence, using this technique at least acknowledges that there may be transition zones or natural variability associated with geomorphic thresholds.

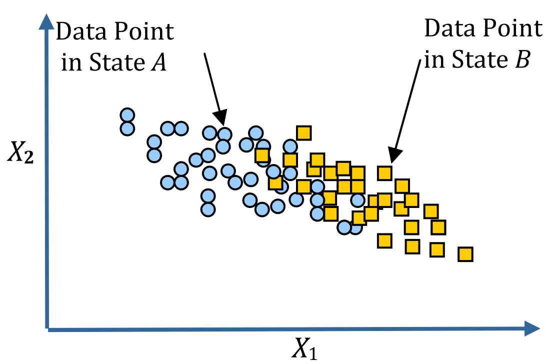

Figure 3.3a – Plot of two data sets

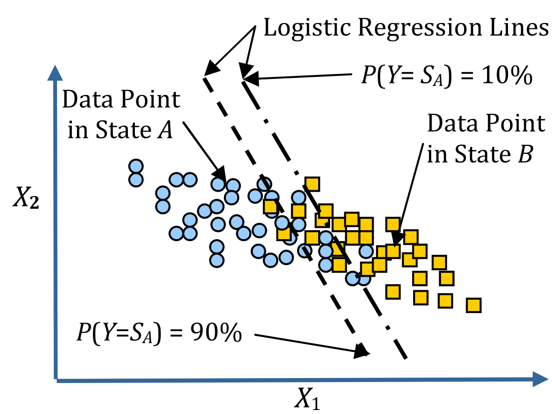

Figure 3.3b – Plot with logistic regression lines

Figure 3.3 – Illustration showing an example application of a binary linear logistic regression analysis

Transformation of the Linear Regression Equation into a Binary Logistic Regression Model

The basis for the *binary linear logistic regression model* lies in the *multiple linear regression equation* for a *continuous* dependent variable. The *multiple linear regression* equation for a *continuous* dependent variable Y in terms of independent variables X_1 and X_2 can be expressed as (Menard, 1995):

$$Y = \beta_0 + \beta_1 X_1 + \beta_2 X_2 \qquad \text{Equation 3.19}$$

where: β_0 is called the *intercept*

β_1 and β_2 are called partial slope coefficients

In the case of a *dichotomous* or *binary* dependent variable Y as depicted in Figure 3.3, the definition or actual numerical value of variable Y is arbitrary and not intrinsically meaningful. However, the probability of Y being in *State A* or *B*, in terms of the independent variables X_1 and X_2, can be intrinsically interesting and the basis for defining geomorphic thresholds in terms of probability. To transform Equation 3.19 into a logistic regression equation with which the intercept and partial slope coefficients can be solved as a function of the probability of Y being in *State A* (i.e., $P(Y = S_A)$), it is necessary to transform the dependent variable (left side of Equation 3.19) into a function of the $P(Y = S_A)$. To make the logistic regression equation useful in this context, it is also necessary that the transformed dependent variable varies from $-\infty$ to $+\infty$ as $P(Y = S_A)$ varies from 0 to 1. The *logit* function provides a transformation that meets this requirement and is expressed as (Menard, 1995):

$$logit(Y) = \ln\left[\frac{P(Y = S_A)}{1 - P(Y = S_A)}\right] \qquad \text{Equation 3.20}$$

where: $P(Y = S_A)$ is the probability of variable Y being in *State A*

Substituting the *logit* of Y (i.e., *logit*(Y) per Eq. 3.20) for the dependent variable Y in Equation 3.19 yields the following *binary linear logistic regression model* for two independent variables X_1 and X_2:

$$logit(Y) = \ln\left[\frac{P(Y = S_A)}{1 - P(Y = S_A)}\right] = \beta_0 + \beta_1 X_1 + \beta_2 X_2 \qquad \text{Equation 3.21}$$

where: S_A and S_B are the dichotomous states of variable Y

$P(Y = S_B) = 1 - P(Y = S_A)$

$P(Y = S_B)$ is the probability of variable Y being in *State B*

The objective of a *binary linear logistic regression analysis* is to find the values of the intercept and the partial slope coefficients (i.e., β_0, β_1, and β_2) that best satisfy Equation 3.21 for observed sets of independent variables X_1 and X_2. Unlike typical linear regression analyses, the intercept and the partial slope coefficients cannot be solved directly for logistic regression analyses and an iterative solution technique must be used. In this study, the Minitab-15 ® software package was used to perform the binary logistic regression analyses. The Minitab-15 ® software package uses an iterative reweighted least squares algorithm to obtain maximum likelihood estimates for the intercept and the partial slope coefficients (Minitab, 2007).

Interpretation and Application of Logistic Regression Analysis Results

The primary results of a logistic regression analysis are the intercept and the partial slope coefficients (i.e., β_0, β_1, and β_2). As shown in Equation 3.21, these coefficients define the linear relationship between the *logit* of *Y* function and the independent variables X_1 and X_2, where the *logit* of *Y* is a function of the probability of independent variable *Y* being in *State A*. Hence, Equation 3.21 can be used to generate a series of parallel lines, in terms of X_1 and X_2 coordinates, where each line corresponds to a given probability of variable *Y* being in *State A* (as shown in Figure 3.3b).

In addition, the results of the logistic regression analysis also provide the means for estimating the probability of being in *State A* (or *State B*) associated with any given coordinate pair of independent variables X_1 and X_2. That is, Equation 3.21 can be solved for the probability of variable *Y* being in *State A* (i.e., $P(Y = S_A)$) to yield Equation 3.22, and Equation 3.22 can then be used directly to estimate $P(Y = S_A)$ given the regression coefficients and values for X_1 and X_2 .

$$P(Y = S_A) = \frac{e^{\beta_0 + \beta_1 X_1 + \beta_2 X_2}}{1 + e^{\beta_0 + \beta_1 X_1 + \beta_2 X_2}}$$ Equation 3.22

where: S_A and S_B are the dichotomous states of variable Y
$P(Y = S_B) = 1 - P(Y = S_A)$
$P(Y = S_A)$ is the probability of variable Y being in *State A*
$P(Y = S_B)$ is the probability of variable Y being in *State B*

Basic Evaluation of the Statistical Significance of a Logistic Regression Analysis

As with any statistical model, it is essential to evaluate the statistical significance of the model. In the case of logistic regression analyses, the evaluation of the resulting statistical model can be complex and authors have described the process as being "more of an art than a science" (Menard, 1995; Bledsoe and Watson; 2001). As a direct reflection of this, the Minitab-15 ® software package provides no less than eight measures of the "characteristics of the estimated equation", eight "diagnostic measures", four "goodness-of-fit statistics", and four "measures of association" (Minitab, 2007). Since the objective herein is to describe how logistic regression analyses can be used to define geomorphic thresholds and ***not*** how to actually perform logistic regression analyses, this section simply includes a discussion of one basic measure for evaluating the basic *statistical significance* of a logistic model.

One basic measure for evaluating the statistical significance of a logistic regression analysis (based on a relatively large sample size) involves identifying whether or not each of the independent variables (i.e., X_1 and X_2) are ***related*** to the dependent or response variable (i.e., *logit*(Y)). Within the Minitab-15 ® software package, this measure is referred to as the "Z" statistic and is defined as follows (Minitab, 2007):

$$Z_i = \frac{\beta_i}{SE_i}$$ Equation 3.23

where: β_i are the intercept and the partial slope coefficients
SE_i is the standard error of coefficient "i"
(Agresti, 1990; Menard, 1995).

Larger absolute values of Z_i indicate that there is a significant relationship between the "i^{th}" independent variable (i.e., X_i) and the dependent variable. In this study, an absolute value of Z_i greater than two (2) was deemed to indicate that there is a significant relationship (Minitab, 2007).

Evaluation of the Physical Basis for Logistic Regression Type Thresholds

Like any statistical model, logistic regression models can be very misleading and may only be an artifact of a limited sample size, even if the model is statistically significant. Hence, it is very important to evaluate statistical models in terms of the physical processes or mechanisms governing the threshold being modeled. In the case of linear logistic regression models, it is important to evaluate both the relative position of the regressions lines, in terms of the vertical or horizontal axes, and the slope of the regression lines.

3.5 Results and Discussion

3.5.1 Floodplain State Plots for the Non-Armored and Armored Floodplain Continuums

The approach adopted in this research was to first find a quantitative means by which to describe the natural downstream progression of floodplain forms, then use these findings to infer the key intra-catchment processes for the non-armored and armored floodplain continuums. This approach is based on the fundamental concept that the observed natural downstream progression of floodplain forms is a direct reflection of natural changes in intra-catchment runoff and sedimentation processes (i.e., spatial variations in water and sediment supply).

As described in Section 3.4.4, a database was developed by performing hydraulic analyses for six flow conditions for each of the 124 surveyed cross sections, thereby creating a database with 744 records. To aid in the evaluation of the data within this *hydraulic analyses* database, Visual Basic ® macros were coded to perform user-specified queries and to rapidly generate complex plots of the data.

Initial Floodplain State Plots Utilizing All Data Points

A graphical approach was initially used to evaluate which combination of state and shape metrics may provide a quantitative means by which to describe the natural downstream progression of floodplain forms. These initial graphic analyses involved plotting all of the data points on shape versus state metric plots for various combinations of metrics, where each point was symbol/color coded by floodplain form. The results of these initial graphic analyses identified two combinations of shape and state metrics that appear to provide a basic means to quantitatively describe the downstream progression of floodplain forms. As shown in Figure 3.4, these two combinations of state and shape metrics are:

- Figure 3.4a: Width-to-Depth Ratio (Eq. 3.16) vs. Specific Stream Power (Eq. 3.2)
- Figure 3.4b: Width-to-Depth Ratio (Eq. 3.16) vs. Boundary Shear Stress (Eq. 3.3).

As can be seen in Figure 3.4, the data points corresponding to the same floodplain forms (i.e., cascade, step-pool, plane-coarse-bed, plane-mixed-bed, plane-fine-bed, pool-riffle, and braided) are relatively cohesive, but are not isolated. It also can be seen in Figure 3.4 that the distribution of the data points within the *floodplain state* plots for the two combinations of metrics are very similar.

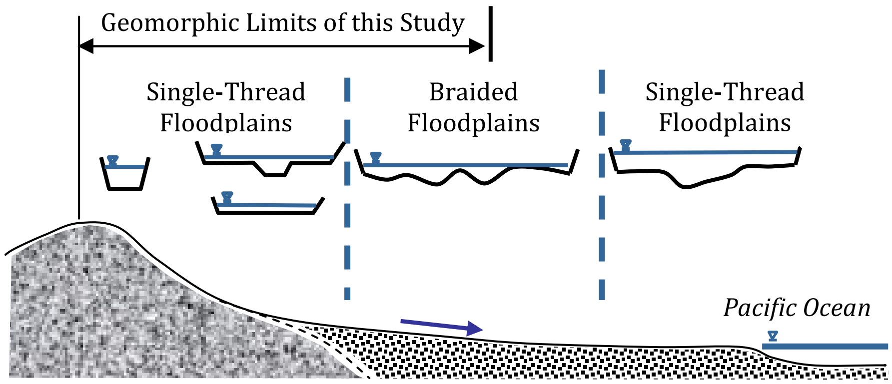

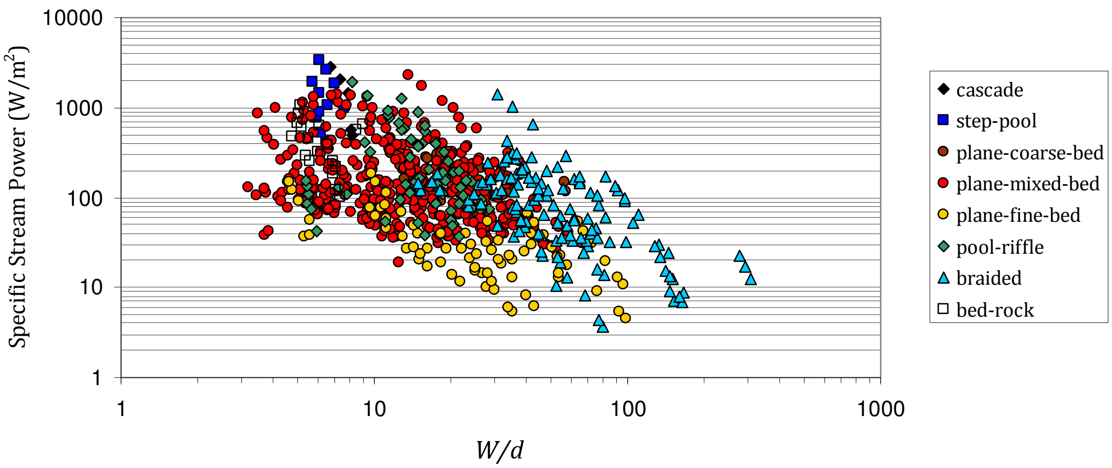

Figure 3.4a - Width-to-depth ratio vs. Specific stream power (Eq. 3.2)

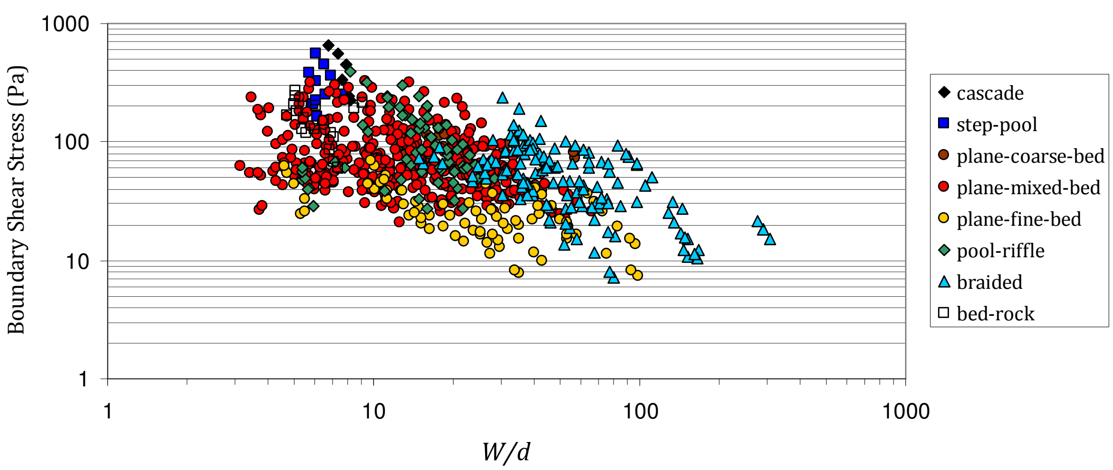

Figure 3.4b - Width-to-depth ratio vs. Boundary shear stress (Eq. 3.3)

Figure 3.4 – Initial floodplain state plots utilizing all data points for both *non-armored* and *armored* floodplain continuums

Refinement of Floodplain State Plots

The floodplain state plots shown in Figure 3.4 may provide a useful means for quantitatively describing the downstream progression of floodplains. However, the data points for each of the floodplain forms are not isolated; hence, it is difficult to interpret the results shown in Figure 3.4 in terms of observed floodplain form progressions. To aid in the interpretation and improve the usefulness of the floodplain state plot, the following approaches and criteria for either segregating or distinguishing the data points were employed:

- **Non-Armored vs. Armored Floodplain Continuum**: Based on field observations, it had been anticipated that there would be different thresholds associated with the different floodplain continuums; hence, the data points were segregated based on the floodplain continuums described in Chapter 2.
- **Stable vs. Unstable Floodplain States**: An objective at the core of this research is to develop a technique for either qualitatively or quantitatively assessing the current stability state for a floodplain; hence, the data points were distinguished in terms of their current stability state, per the criteria provided Table 3.4.
- **Flows that Form and Maintain Floodplains**: I contend that it is the higher magnitude and less frequent flow events that form and maintain the floodplain. While performing the hydraulic analyses described in Section 3.4.4, it was observed that only the estimated peak discharges, with return periods greater than or equal to approximately 25 years, fully inundated all of the various floodplain forms. Hence, it is argued that flow events with return periods of approximately 25 years and greater are the flow events primarily responsible for forming and maintaining the geometry of a floodplain in the semi-arid environment of southern California. Therefore, the

data points corresponding to peak flow rates with return periods less than 25 years were excluded from further analysis.

Segregating and distinguishing the data points per the aforementioned approaches and criteria yield the two floodplain state plots shown in Figures 3.5a and 3.5b. The floodplain state plots in Figures 3.5a and 3.5b are in terms of specific stream power (Equation 3.2) as the state metric; however, very similar plots can also be generated using total boundary shear stress (Equation 3.3) as the state metric.

As can be seen in Figure 3.5a, the data points corresponding to a) stable and unstable floodplains and b) non-braided and braided floodplains in the *non-armored* or Type 1 floodplain continuum are both relatively cohesive and relatively isolated. However in Figure 3.5b, the data points are only cohesive and relatively isolated in terms of floodplain form under stable conditions. Yet in both cases these floodplain state plots provide important insights into the intra-catchment processes and mechanisms associated with the natural downstream progression of floodplain forms. In addition, these plots also provide a basis for assessing stability and braiding thresholds.

To aid in the interpretation of the floodplain state plots shown in Figure 3.5, the natural downstream progression of floodplain geometry for stable systems is shown schematically at the top of the figure. To further illustrate that the natural downstream progression of floodplain forms is left to right in the floodplain state plots, arrows have been used to connect data points along select individual watercourses. The example watercourses shown with *solid* arrows in Figure 3.5 are for stable watercourses; whereas, the *dashed* arrows are paths associated with unstable or responding watercourses. As would be expected based on the geometry changes described in Table 3.4 for unstable watercourses (i.e., CEM Phases III and IV), the path associated with unstable watercourses

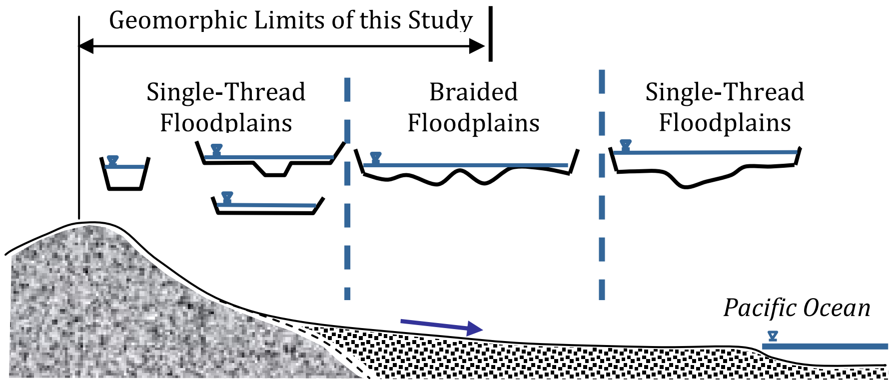

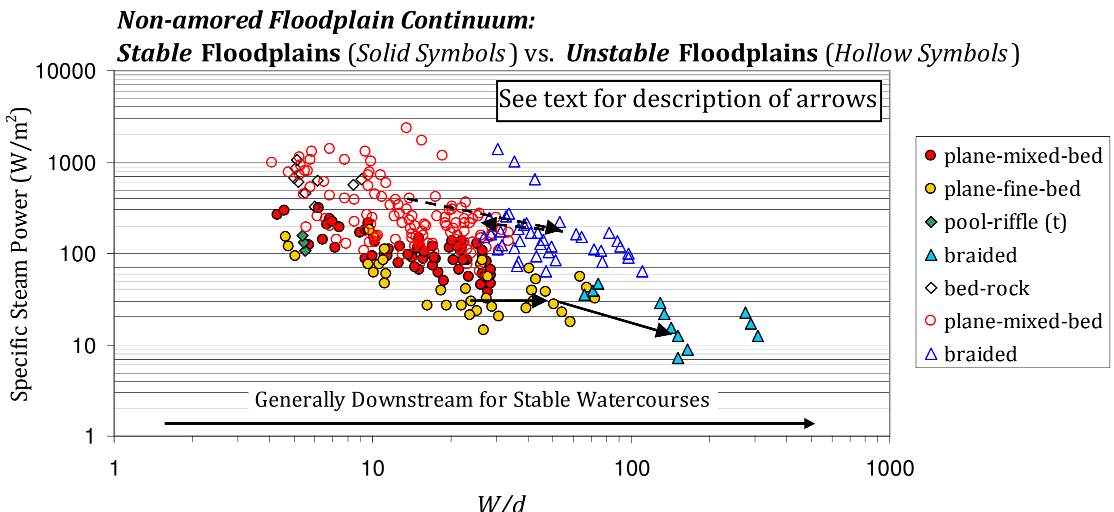

Figure 3.5a - Width-to-depth ratio vs. Specific stream power (Eq. 3.2)

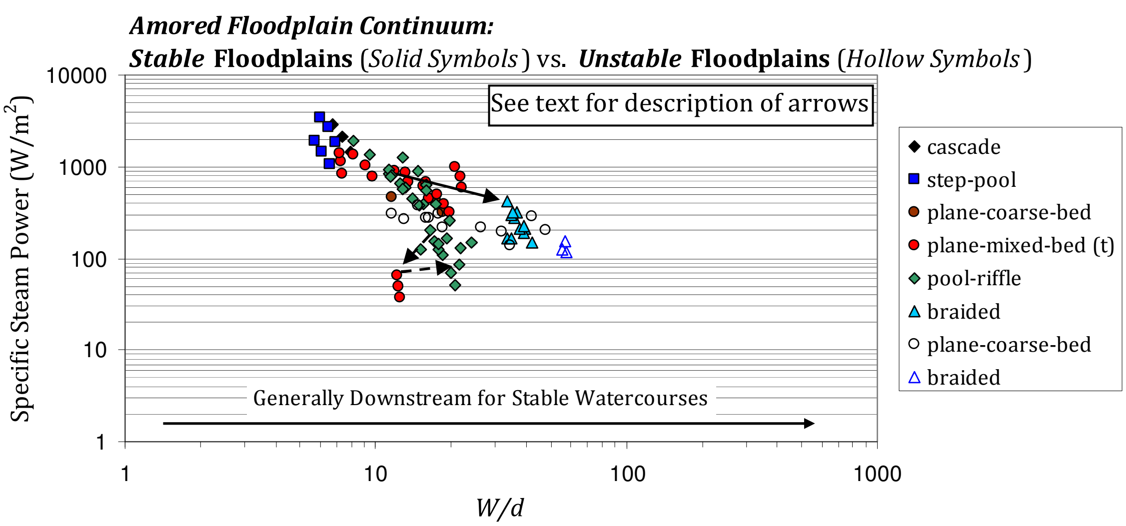

Figure 3.5b - Width-to-depth ratio vs. Specific stream power (Eq. 3.2)

Figure 3.5 – Floodplain state plots for *non-armored* and *armored* floodplain continuums that illustrate the natural downstream progression of floodplain geometry

can be quite complex when plotted on the floodplain state plots and would be expected to change significantly following a high magnitude flow event.

3.5.2 Interpretation of Floodplain State Plots In Terms of Intra-Catchment Processes and Hydraulic Controls of Floodplain Form

An important step in all research involves questioning and critically evaluating all findings and analyses. In the process of critically evaluating the floodplain state plots (Figure 3.5), implications of the data analyzed during this research led to the development of three *working hypotheses* regarding the downstream progression of floodplain geometry and forms. These working hypotheses can be summarized as follows:

- Water to sediment supply divergence process;
- *Self enhancing feedback mechanisms* to the hypothesized *water to sediment supply divergence process*; and
- Floodplain braiding mechanisms in terms of the hypothesized *water to sediment supply divergence process* and associated *self enhancing feedback mechanisms*.

As can be ascertained from the preceding list, all of these hypotheses are interrelated and build upon each other. The remainder of this section describes these hypotheses, in the order listed above, and their physical premise in terms of the observed patterns in floodplain state plots and field observations.

Hypothesis for the Water to Sediment Supply Divergence Process

Figure 3.5 provides a useful means to compare and evaluate the hydraulic controls associated with the various floodplain forms. For both the non-armored and armored continuums, the floodplain state plots (Figure 3.5) indicate that that the *width-to-depth* ratios for ***stable*** watercourses generally increase in the downstream direction, within the geomorphic limits of this study. As demonstrated in Chapter 4 - Section 4.5.3 with multiple transport functions, the transport capacity for a trapezoidal cross section ***decreases*** as the *width-to-depth* ratio ***increases***. Therefore, the floodplain state plots imply that the geometry of ***stable*** floodplains adjusts to become ***less efficient*** at transporting sediment in the downstream direction (within the geomorphic limits of this study).

The question then becomes: *What intra-catchment processes could necessitate that the geometry of a watercourse must adjust to become* ***less efficient*** *at transporting sediment in the downstream direction to maintain stability*? One possible answer involves considering the downstream trend in water and inflowing sediment supply along a watercourse, during a high magnitude flow event in a relatively small catchment. If the peak flow rate in a watercourse increases in the downstream direction during a flow event and the inflowing sediment supply initially increases and then levels off (as illustrated in Figure 3.6), the *geometry of the watercourse must adjust to become* ***less efficient*** *at transporting sediment in the downstream direction to maintain a state of dynamic equilibrium.* To facilitate further discussion, this hypothesized divergence between the flow regime and the sediment supply will be referred to herein as the *water to sediment supply divergence process*.

The next logical question then becomes: *Can natural intra-catchment runoff and soil erosion processes explain and provide a basis for the hypothesized* ***water to sediment supply divergence process*** *and, if yes, how?* I contend that the answer to this question can typically be ***yes***, due to the interrelationship between hillslope processes and floodplains in the upper reaches of a catchment.

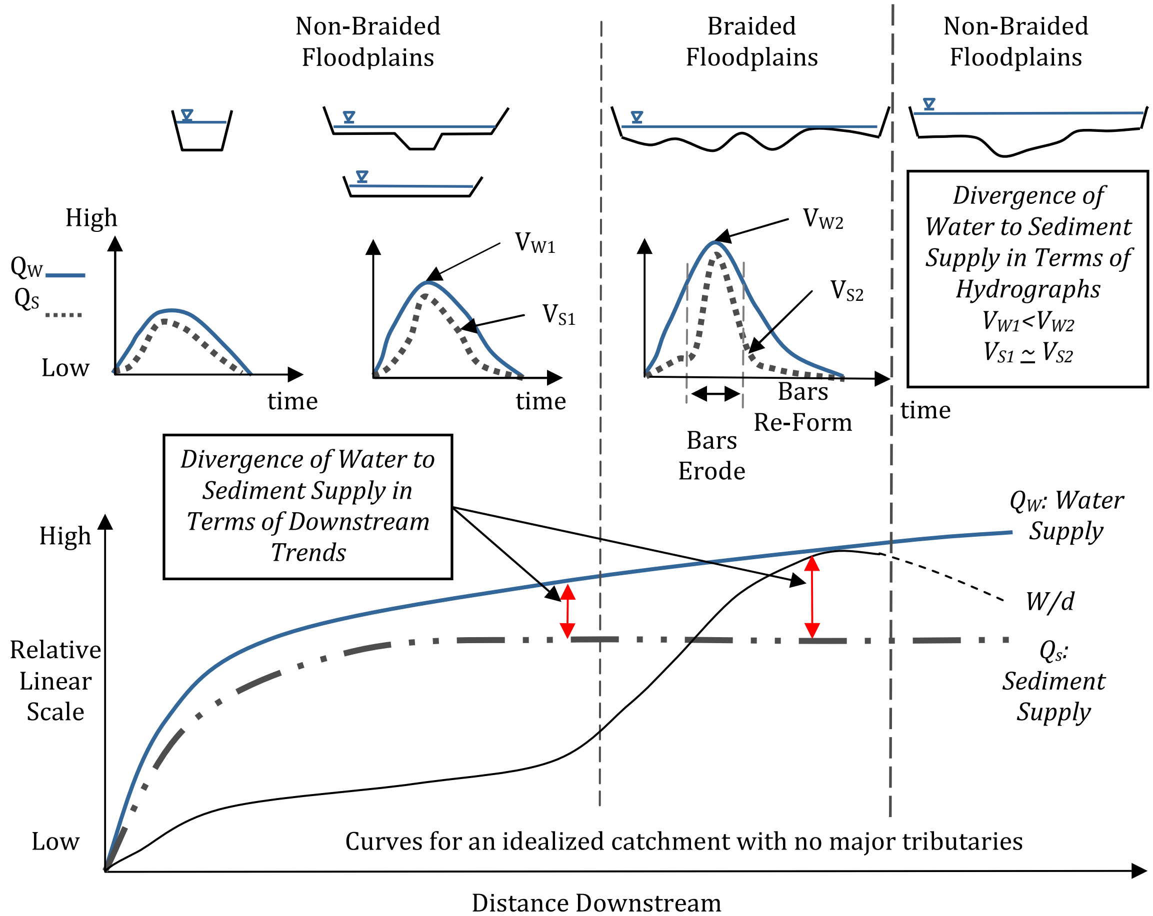

Figure 3.6 – Schematic illustrating the hypothesis for the mechanism behind the *water to sediment supply divergence process* in terms of hydrographs for a single major event and downstream trends

As illustrated in Figure 3.7, a watercourse is often in close contact with hillslope processes that deliver both water and sediment to the watercourse during rainfall events, in the upper reaches of a catchment. However, as the river valley widens, the extent of close contact between the watercourse and hillslope processes decreases, yet water is still being delivered to the watercourse as sub-surface flow and direct rainfall (Horton, 1945; Zaslavsky and Sinai, 1981; Knighton, 1998). Therefore, the net result can be the divergence between the flow rate and the sediment supply in the watercourse.

It is important to recognize that this hypothesis of the *water to sediment supply divergence process* can be viewed from and described in many timeframes; however, I contend that this divergence of flow rate to sediment supply may be most important on a timeframe as small as a single flow event of sufficient magnitude to inundate the entire active floodplain. Schematics illustrating this hypothesized *water to sediment supply divergence process* on a flow event basis are also provided in Figure 3.6.

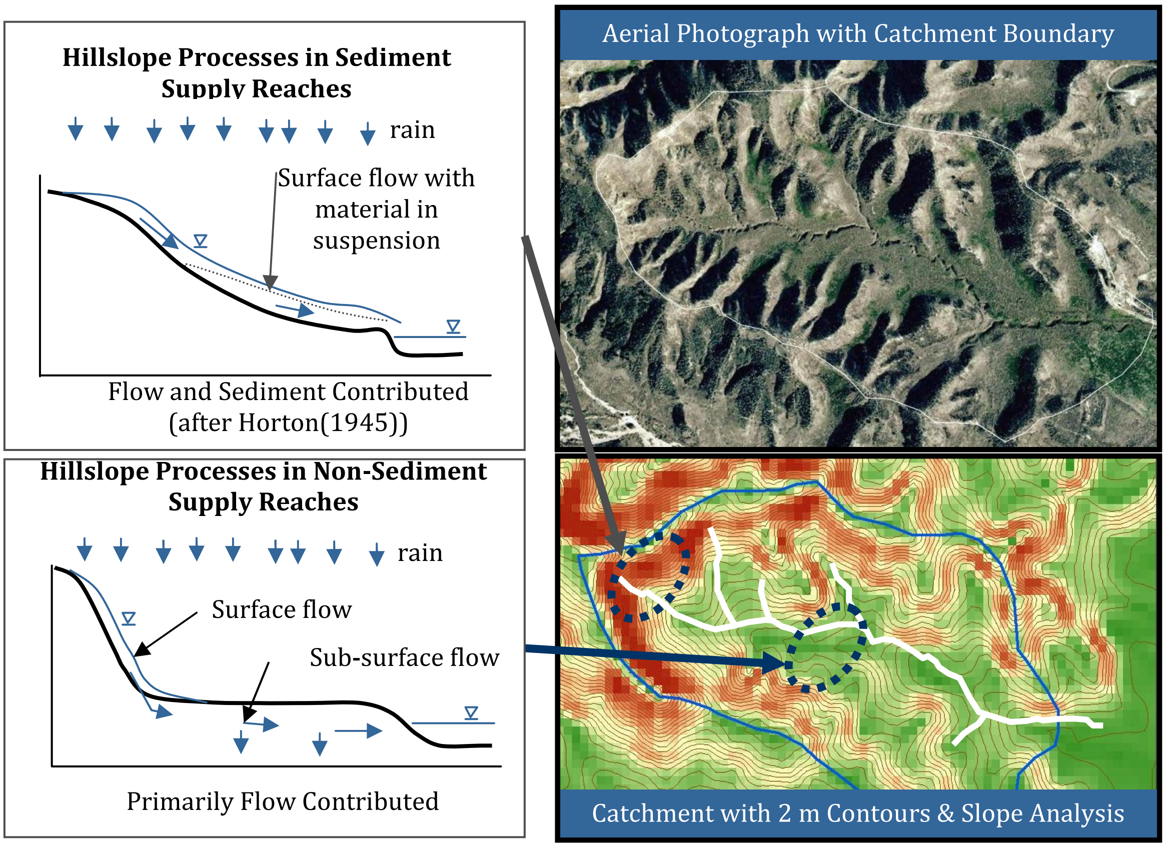

Figure 3.7 – Schematic illustrating the hypothesis for the mechanism behind the *water to sediment supply divergence process* in terms of hillslope processes

I recognize that this hypothesized *water to sediment supply divergence process* in the "real world" would have to be far more complex in both space and time than reflected in Figures 3.6 and 3.7. Moreover, field observations imply that the actual rate of *water to sediment supply divergence* would probably vary dramatically depending upon the geomorphic and geologic characteristics of the catchment. As described in Sections 2.3.2 and 3.3.2, the semi-arid environment of southern California has a complex geologic history and, as a result, the catchments within the study area have a very wide range of geomorphic and geologic characteristics, as illustrated in Figure 3.2. Therefore, it would be expected that quantitatively assessing this hypothesized *water to sediment supply divergence process* using catchment parameters would be challenging.

Quantitative investigations into the hypothesized *water to sediment supply divergence process* are beyond the scope of these investigations. Hence, the preceding discussion is only intended to represent a "working hypothesis" and, thereby, potentially provide a starting point for further research.

Furthermore, the geomorphic limits of this study are quite narrow (and possibly unique) in that almost all of the study sites are located well within the foothills region and have relatively small catchments. Hence, it is recognized that the hypothesized *water to sediment supply divergence process* may only be of significance within the geomorphic confines of this study and within the semi-arid environment.

However, the value of the preceding discussion of the hypothesized *water to sediment supply divergence process* to this research is that it may provide a framework for identifying the interrelationship between the typical impacts of urbanization with the intra-catchment processes that may govern or at least influence the downstream progression of floodplain geometry and form, as observed in the field data.

Hypotheses for Self Enhancing Feedback Mechanisms

If it is argued or assumed, for the sake of discussion, that the hypothesized *water to sediment supply divergence process* (as illustrated in Figure 3.6) is the or one of the primary intra-catchment processes that governs the downstream progression of floodplain forms, then any *self enhancing feedback mechanisms* to this process may have a significant effect on floodplain geometry and stability. A *self enhancing feedback mechanism* to the *water to sediment supply divergence process* would include any intra-catchment process that increases sediment transport capacity, while not proportionately increasing sediment supply to the watercourse. These investigations identified downstream bed material fining in armored floodplains, confluences, and the impacts of urbanization as having the potential to be *self enhancing feedback mechanisms* to the hypothesized *water to sediment supply divergence process*. The following paragraphs describe each of these "mechanisms" in terms of how and under which circumstances they may be *self enhancing feedback mechanisms* to the hypothesized *water to sediment supply divergence process.*

- **Bed Material Fining in Armored Floodplains**: In the context of braided gravel-bed rivers, Ferguson (1993, p. 83) noted that: "Sediment sorting in braided rivers does not only occur at the local scale. Downstream fining is usually apparent and can be very pronounced and rapid." In reference to investigations by Dawson (1988), Ferguson (1993), further noted that: "*Downstream fining in this and other braided rivers can be orders of magnitude more rapid than can be accounted for by abrasion … and by bedload, so is conventionally attributed to selective transport*."

  Furthermore, Wilcock and Kenworthy (2002) identified and quantified the non-linear effect of sand content on gravel transport rates for watercourses with the bed material composed of sand/gravel mixtures. That is, the investigations by Wilcock and Kenworthy (2002) predict a large increase in the sediment transport capacity of the coarser bed material, when the percent sand in the surface layer reaches approximately 6 to 26 % in a sand/gravel mixture. Hence, the introduction of fine material (i.e., sand and other particles less than approximately 2 mm in diameter) into an armored floodplain can significantly increase sediment transport capacity, when the supply of fine material reaches a threshold level.

  This implies that selective transport can be induced in an armored floodplain by the introduction of relatively fine material (via possibly a tributary) and can have the net impact of increasing the bed material transport capacity and breaking up the armor layer, while not proportionately increasing the sediment supply rate from upstream. Therefore, downstream bed material fining can be both a distinct characteristic of braided gravel bed rivers and a *self enhancing feedback mechanism* to the hypothesized *water to sediment supply divergence process*.

- **Confluences:** A confluence with a tributary can increase the difference between the water and the sediment supply in a watercourse, when the flow in the tributary has a higher water to sediment supply divergence level than the flow in the main watercourse. Therefore, confluences can, under certain circumstances, disproportionately increase the sediment transport capacity in a watercourse, while contributing relatively little to the sediment supply to the watercourse.
- **Impacts of Urbanization**: In the absence of retention or detention basins, urbanization typically results in increasing the magnitude and duration of flow events in the long-term, without proportionately contributing sediment supply. Therefore, the net impact of urbanization can be to directly increase the water to sediment supply divergence along a watercourse.

In summary, this section provides basic arguments for how and under which circumstances bed material fining, confluences, and the impacts of urbanization can be *self enhancing feedback mechanisms* to the hypothesized *water to sediment supply divergence process*. It is generally recognized and was observed as part of this research that bed material fining, confluences, and the impacts of urbanization are often associated with changes in the geometry and/or form of the downstream floodplains; hence, it is possible, if not logical, that they could be *self enhancing feedback mechanisms* to an underlying intra-catchment process responsible for the downstream progression of floodplain geometry.

Hypotheses for Floodplain Braiding Mechanisms in Terms of Intra-Catchment Processes

Figure 3.5 provides a useful means to compare and evaluate the hydraulic controls associated with the various floodplain forms within the non-armored and armored floodplain continuums. Comparison of Figures 3.5a with 3.5b clearly illustrates that the downstream progression of floodplain forms differs dramatically between the *non-armored* and *armored* floodplain continuums in terms of the state metric (i.e., specific stream power or boundary shear stress). This, in turn, implies that that the processes and mechanisms associated with the downstream progression of floodplain forms differs significantly between the *non-armored* and *armored* floodplain continuums. Using the preceding discussions for the hypothesized water to sediment supply divergence process and the associated *self enhancing feedback mechanisms* as a foundation, the following working hypotheses have been developed to describe the braiding mechanisms for stable watercourses in terms of intra-catchment processes:

- **Braiding Mechanism for Stable Non-Armored Floodplains**: I hypothesize that the water to sediment supply divergence process alone may be the intra-catchment process governing the downstream progression of floodplain forms for stable non-armored watercourses, within the geomorphic limits of this study. Hence, the braiding threshold for non-armored floodplains corresponds to the condition where the water to sediment supply divergence is of sufficient magnitude that the formation and erosion of bars are required to maintain a sediment balance within the floodplain, during the course of a flow event and/or over long periods of time. As emphasized in the above discussion, I contend that there are both stable and unstable braided floodplains, as described by Lane (1957) and in Section 3.4.2. In the case of braiding in unstable floodplains, braiding can result strictly from bank erosion and channel widening, as described and compiled by Bridge (1993, p. 16).

- **Braiding Mechanism for Stable Armored Floodplains**: Based on the distribution of the data points corresponding to pool-riffle and braided floodplains shown in Figure 3.5b, it is apparent that the hypothesized water to sediment supply divergence process cannot alone be responsible for the transition of pool-riffle to braided floodplains and the corresponding "jump" in width-to-depth ratios. That is, the data points shown in Figure 3.5b for the pool-riffle and braided floodplains are isolated and cohesive, with no overlapping in terms of width-to-depth ratio. Based on field observations and the data in Figure 3.5b, I hypothesize that the effects of bed material fining (i.e., an increase in the percent sand in the surface layer) acting in conjunction with the water to sediment supply divergence process may be the mechanisms responsible for the transition of pool-riffle to braided floodplains. As described by Ferguson (1993) and as I directly observed during these investigations, downstream bed material fining within the braided floodplain can be pronounced and rapid.

  As described in the preceding sub-section, bed material fining may also be a self enhancing feedback mechanism to the process of water to sediment supply divergence, when there is sufficient fine material in the surface layer. As shown in Figure 3.9, the braided channels in the armored floodplain continuum were estimated to have percent sand values ranging from 11% to 20 % in the surface layer. This observed range of percent sand values is within the range of percent sand (i.e., 6% to 26%) where Wilcock and Kenworthy (2002) predict a large increase in the sediment transport capacity of the coarser bed material. It is also important to note that the data in Figure 3.9 also indicate that percentage of sand alone is not a good indicator for floodplain braiding, which is why I contend that the hypothesized water to sediment supply divergence process in conjunction with bed material fining may be the two intra-catchment processes responsible for stable floodplain braiding in the armored continuum.

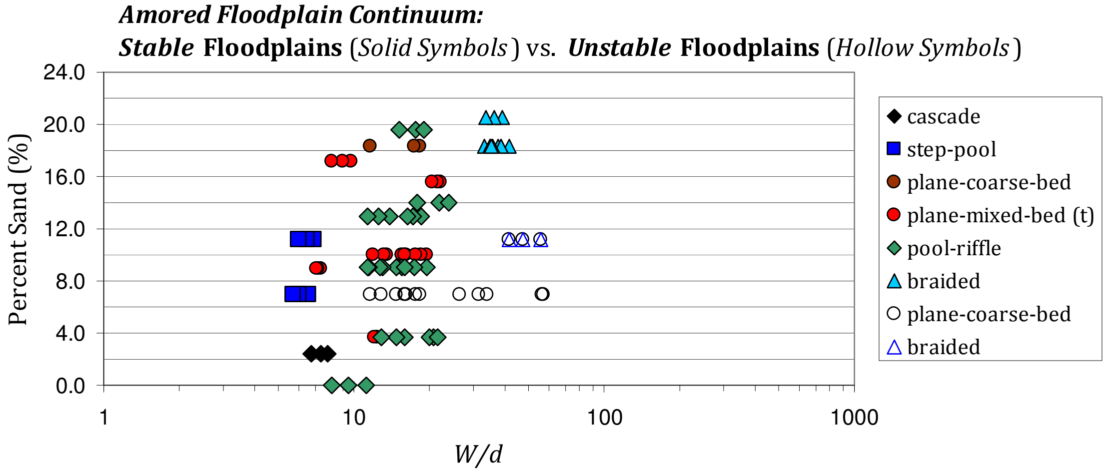

Figure 3.9 – Width-to-depth ratio versus percent sand for armored floodplains

In general, the catchment-scale processes associated with floodplain braiding, described herein, are believed to be complementary to the reach or floodplain unit-scale conceptual models for the mechanisms of braid development described by Leopold and Wolman (1957), Ashmore (1991), Bridge (1993), and Ferguson (1993). That is, these conceptual models for mechanisms of braid development focus on "***How** do rivers braid?*;" whereas, the working hypotheses developed by this author focus on "***Why** do rivers braid?*" in terms of intra-catchment processes.

3.5.3 Non-Armored Floodplain Continuum: Stability and Braiding Thresholds

The floodplain state plots shown in Figure 3.5 quantitatively describe the natural downstream progression of floodplain forms using *specific stream power* (Equation 3.2) and *width-to-depth* ratio as the *state* and *shape* metrics. In addition, Figure 3.5a also provides a means to quantitatively differentiate between stable and unstable floodplains. As a result, the floodplain state plots thereby provide a basis for defining both stability and braiding thresholds using *binary linear logistic regression analysis* techniques, as described in Section 3.4.5.

Based on the data set shown in Figure 3.5a, logistic regression analyses have been performed to quantify both stability and braiding thresholds for the non-armored floodplain continuum, as shown in Figure 3.10. The logistic regression analyses are also summarized in Table 3.9. As indicated in Table 3.9, evaluation of the regression coefficients indicates that the logistic regression models are statistically significant. As described previously, the distribution of data points within the floodplain state plots for *W/d versus **Specific Stream Power*** and *W/d versus **Boundary Shear Stress*** are very similar; hence, logistic regression analyses have also been performed with *boundary shear stress* (Equation 3.3) as the *state* metric. The results of these analyses are also provided in Figure 3.10 and Table 3.9. It is very important to recognize that the floodplain state diagrams shown in Figure 3.10 only apply to the geomorphic limits for this research, as described and shown in Section 3.3.1 and Figure 3.1.

Interpretation and Physical Basis for the Non-Armored Continuum Stability Thresholds

The floodplain state diagrams provided in Figure 3.10 can be used to address one of the two *practical* research questions at the core of these investigations: *How can we quantitatively assess the existing stability state of a floodplain?* That is, Equation 3.22, plus the intercept and partial slope coefficients (i.e., β_0, β_1, and β_2) given in Table 3.9, can be used to estimate the *probability that the floodplain is unstable and in a state of severe instability* (i.e., $P(Y = S_A)$) using values for the state and shape metrics based on cross section and flow data for a floodplain. Hence, the *probability that the floodplain is stable and*

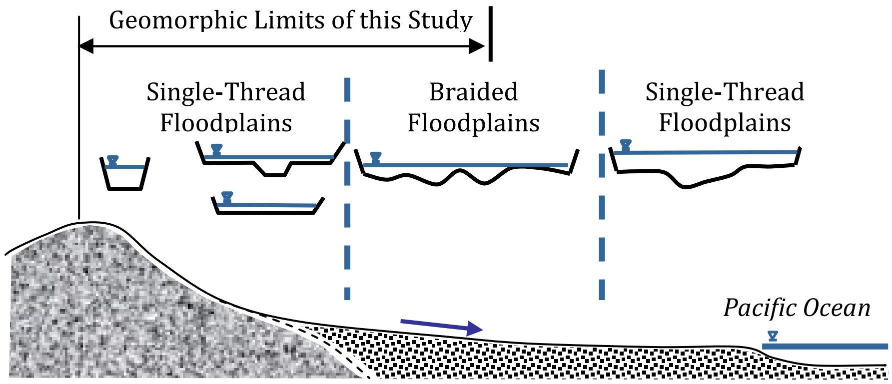

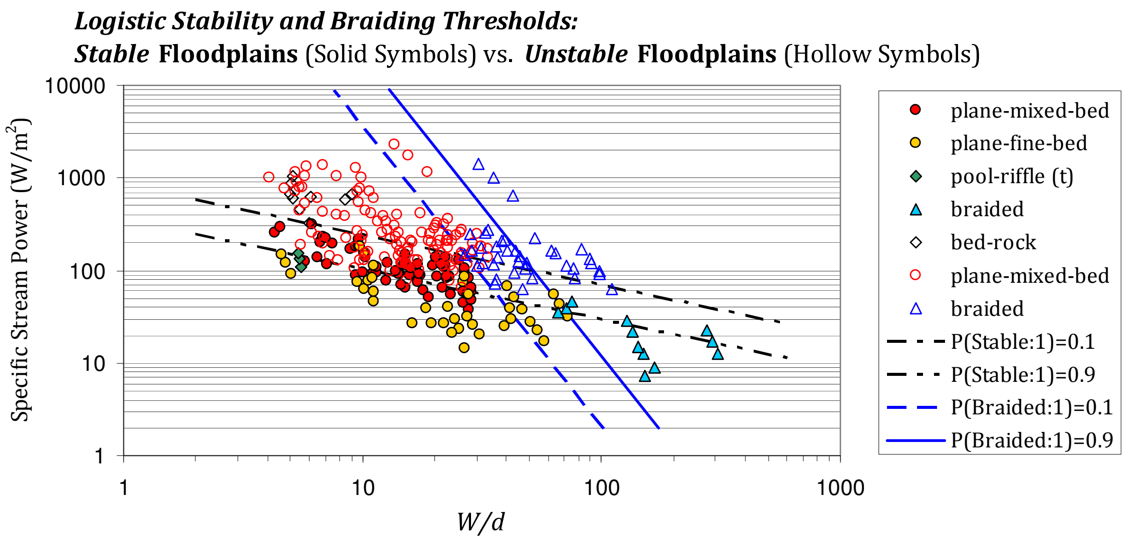

Figure 3.10a - Width-to-depth ratio vs. Specific stream power (Eq. 3.2)

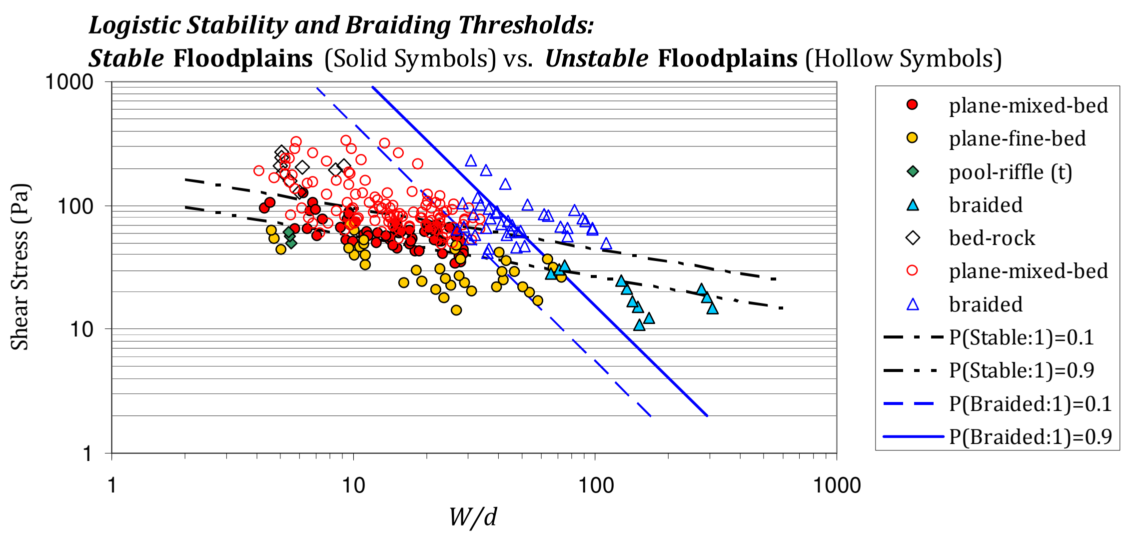

Figure 3.10b - Width-to-depth ratio vs. Boundary shear stress (Eq. 3.3)

Figure 3.10 – Floodplain stability and braiding threshold diagrams for the non-armored continuum within the geomorphic limits of this research

Table 3.9 – Results of the logistic regression analyses: Non-armored floodplain continuum stability and braiding thresholds

Logistic Regression Parameters and Results	Non-Armored or Type 1 Floodplain Continuum Stability and Braiding Thresholds			
Threshold Type & ID	**Stability-ω-1**	**Braiding- ω-1**	**Stability-τ-1**	**Braiding-τ-1**
Figure Shown	Figure 3.10a	Figure 3.10a	Figure 3.10b	Figure 3.10b
***Shape* Metric**	W/d (Eq. 3.16)	W/d (Eq. 3.16)	W/d (Eq. 3.16)	W/d (Eq. 3.16)
***State* Metric**	ω (Eq. 3.2)	ω (Eq. 3.2)	τ (Eq. 3.3)	τ (Eq. 3.3)
***State A* (S_A)**	unstable	non-braided	unstable	non-braided
***State B* (S_B)**	stable	braided	stable	braided
Total Sample Size (n)	273	273	273	273
Sample Size in *State A*	156	222	156	222
Samples Size in *State B*	117	51	117	51
X_1	$log_{10}(W/d)$	$log_{10}(W/d)$	$log_{10}(W/d)$	$log_{10}(W/d)$
X_2	$log_{10}(\omega)$	$log_{10}(\omega)$	$log_{10}(\tau)$	$log_{10}(\tau)$
β_0	-32.7596	42.1887	-43.2234	48.0928
β_1	6.4391	-19.0285	6.4544	-19.2031
β_2	11.9589	-5.8813	19.6626	-10.0109
Slope $= -\beta_1 / \beta_2$	-0.538	-3.235	-0.328	-1.918
Z_0 (Eq. 3.23)	-7.59	5.57	-7.50	5.66
Z_1 (Eq. 3.23)	6.15	-5.65	5.78	-5.87
Z_2 (Eq. 3.23)	7.75	-4.56	7.66	-4.62
Statistically Significant: $\lvert Z_i \rvert >> 2$? For i = 0 to 2	yes	yes	yes	yes

in a state of dynamic equilibrium (i.e., $P(Y = S_B)$) can then be estimated by the following equation: $P(Y = S_B) = 1 - P(Y = S_A)$.

To evaluate the physical significance of the stability thresholds, it is important to evaluate both the intercept (i.e., position of the regressions lines in relation to the vertical axis) and the slope of the regression lines in terms of physical processes. First consider the position of the stability threshold lines (shown in Figure 3.10) in terms of the *y-axis* or *state* metric. As described in Section 3.4.2, the criteria used to differentiate between stable and unstable floodplains in the field were based on the degree/extent of bank failures and head-cut migrations. Hence, the position of the stability threshold lines should be directly related to both the erosional resistance and stability characteristics of the banks, as similarly observed by Schumm (1977) and Harvey et al. (1985). Therefore, it would be anticipated that the probability for the floodplain to be unstable would increase as the specific stream power or boundary shear stress increases, as shown in Figure 3.10.

Secondly, consider the slope of the stability threshold lines, which indicates that the specific stream power (or boundary shear stress) decreases as the width-to-depth ratio increases for stable systems. This indicates that the slope of the stability threshold lines are consistent with the general downstream trends along a watercourse (within the geomorphic limits of this study), where specific stream power decreases as width-to-depth ratio increases. It is demonstrated in detail in Section 4.5.3 that the slope of the stability threshold lines appear to have a unique correlation with the basic flow relationships of continuity and flow resistance.

Interpretation and Physical Basis for the Non-Armored Continuum Braiding Thresholds

As with the stability thresholds, the results from the logistic regression analyses for the braiding thresholds can be used to estimate the *probability that the floodplain is single-thread or non-braided* (i.e., $P(Y = S_A)$), via Equation 3.22 plus the intercept and partial slope coefficients (i.e., β_0, β_1, and β_2) given in Table 3.9. Hence, the *probability that the floodplain is braided* (i.e., $P(Y = S_B)$) can then be estimated by the following equation: $P(Y = S_B) = 1 - P(Y = S_A)$.

As described in Section 3.3.1 and shown in Figure 3.1, the geomorphic limits associated with this research encompass the upstream braiding threshold. That is, a concerted effort was given to selecting study reaches where high gradient single-thread floodplains transitioned into braided floodplains, and for this reason this research may be relatively unique. The braiding thresholds shown in Figure 3.10 are also unique in that they are superimposed on the stability thresholds.

In terms of the physical significance of the braiding threshold, the positions of the braiding threshold lines in Figure 3.10 are consistent with the general downstream directionality (i.e., left to right) of Figure 3.10. As also would be expected and as correctly reflected in the slope of the logistic regression lines for the braiding thresholds (Figure 3.10), the data indicate that the progression of a single-thread (i.e., non-braided) to a braided floodplain occurs at significantly lower *width-to-depth* ratios and at higher specific stream power for *unstable* watercourses than for *stable* watercourses.

3.5.4 Armored Floodplain Continuum: Stability and Braiding Thresholds

The floodplain state plots shown in Figure 3.5 quantitatively describe the natural downstream progression of floodplain forms using *specific stream power* (Equation 3.2) as the *state* metric and the *width-to-depth* ratio as the *shape* metric. Comparison of Figures 3.5a with 3.5b clearly illustrates that the downstream progression of floodplain forms differs dramatically between the *non-armored* and *armored* floodplain continuums in terms of the state metric (i.e., specific stream power or boundary shear stress). This, in turn, implies that that the processes and mechanisms associated with the downstream progression of floodplain forms differ significantly between the *non-armored* and *armored* floodplain continuums, as would be expected.

It is important to recognize that in the armored floodplain continuum, the *plane-mixed-bed* is by definition a transitory floodplain form and describes the condition when an underlying armored floodplain form is temporarily buried by a relatively thin layer of finer, but still relatively coarse, material. During the course of this research, *plane-mixed-bed* floodplain forms developed along several watercourses as a result of a combination of recent wildfires and significant rainfall events. This floodplain form is considered "transitory" instead of "unstable", since field observations suggest that the finer fill material is transported away, during even relatively low magnitude flow events, leaving the original floodplain form essentially unaltered. As indicated in Figure 3.5b, the *plane-mixed-bed* floodplain form has shape and state metrics that overlap with cascade, step-pool, plane-coarse-bed, and pool-riffle floodplain forms.

Unlike the non-armored continuum, Figure 3.5b does **not** provide a means to quantitatively differentiate between stable and unstable floodplains in the armored continuum. That is, the data points corresponding to *unstable* floodplains are not cohesive in terms of the state and shape metrics used for Figure 3.5b. This implies that the processes and mechanisms associated with floodplain stability are more complex in the armored continuum than in the non-armored continuum, as described by Chin(1998).

However, Figures 3.5b and 3.11a provide a basis for characterizing the state/shape metrics for ***stable*** floodplain forms in the armored floodplain continuum (as summarized in Table 3.10) and, thereby, provide a qualitative means for evaluating the stability state of a floodplain.

Also unlike the non-armor continuum, Figure 3.5b does **not** provide a means to quantitatively define a braiding threshold for armored floodplains using logistic regression techniques, since there is not an overlap of data points for stable non-braided and braided floodplains. However, it can be deduced from Figure 3.4 by the general proximity of the data points for all of the braided floodplains, regardless of floodplain continuum, that there may be at least a basic correlation between the braiding thresholds for non-armored and armored floodplains.

Table 3.10 – Summary of width-to-depth ratios for floodplain forms in the armored continuum

Floodplain Form	Width-To-Depth Ratio (W/d)		Specific Stream Power (Eq. 3.2) (W/m^2)		Mean Armor Layer Diameter - d_{50} (mm)	
	Range	Mean	Range	Mean	Range	Mean
cascade and step-pool (stable only)	5.7-7.9	6.6	1051-3412	2083	124-152	139
plane-coarse-bed (stable only)	11.6-18.5	15.8	317-463	404	22-22	22
plane-coarse-bed (stable and unstable)	11.6-57.3	24.1	116-464	271	20-22	21
plane-mixed-bed (transitory)	7.1-22.1	13.9	37-1412	686	7.2-51	19.7
pool-riffle (stable only)	8.2-24	15.8	50-1915	504	34-100	55.4
braided (stable only)	33.4-41.8	36.7	149-425	244	22-34	25
braided (stable and unstable)	33.4-55.7	39.1	127-425	237	16-34	23

To test this deduction, logistic regression techniques were used to evaluate a braiding threshold using data points corresponding to both the non-armored and armored floodplain continuums. The results of this regression analysis are provided in Figure 3.11b and Table 3.11. In Figure 3.11a, two sets of the logistic regression lines for the braiding threshold are compared and superimposed with the floodplain state plot for the armored floodplain continuum. These two sets of regression lines correspond to: (a) an analysis of just the data points for the non-armored (i.e., Type 1) floodplain continuum (Figure 3.10a and Tables 3.7 and 3.9); and (b) an analysis of data points for both the non-armored and armored (i.e., Type 1 and 2) floodplain continuums. As indicated in Figure 3.11a and Table 3.11, the results of the logistic regression analyses for these two data sets are very nearly identical and may imply that the braiding thresholds for the non-armored and armored floodplain continuums are one in the same (in terms of the state and shape metrics used in this research), even though I contend that the mechanisms associated with the initiation of braiding in the two different floodplain continuums are significantly different. However,

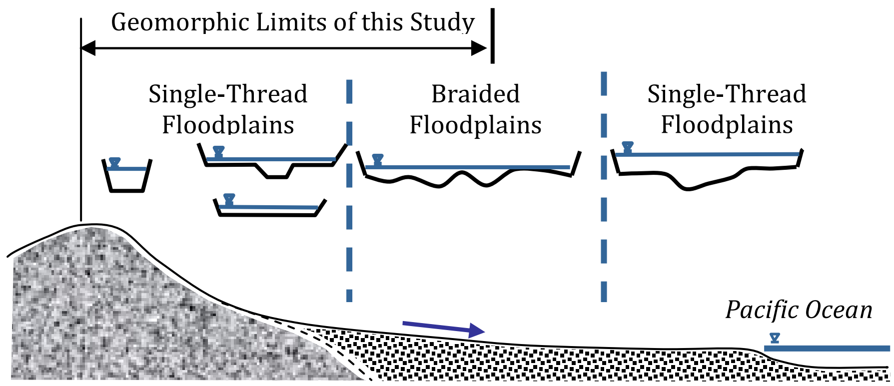

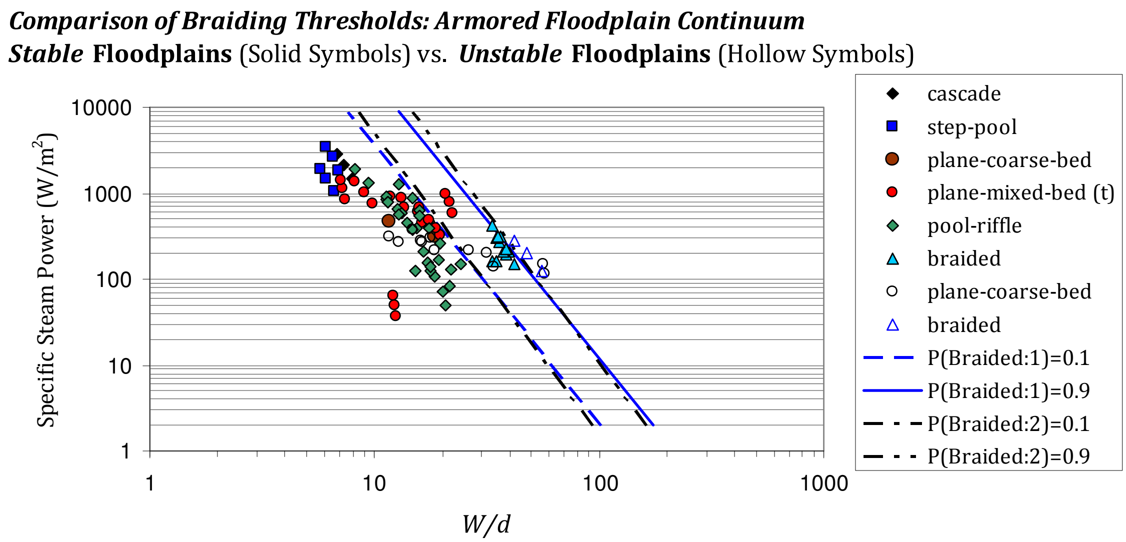

Figure 3.11a - Width-to-depth ratio vs. Specific stream power (Eq. 3.2)

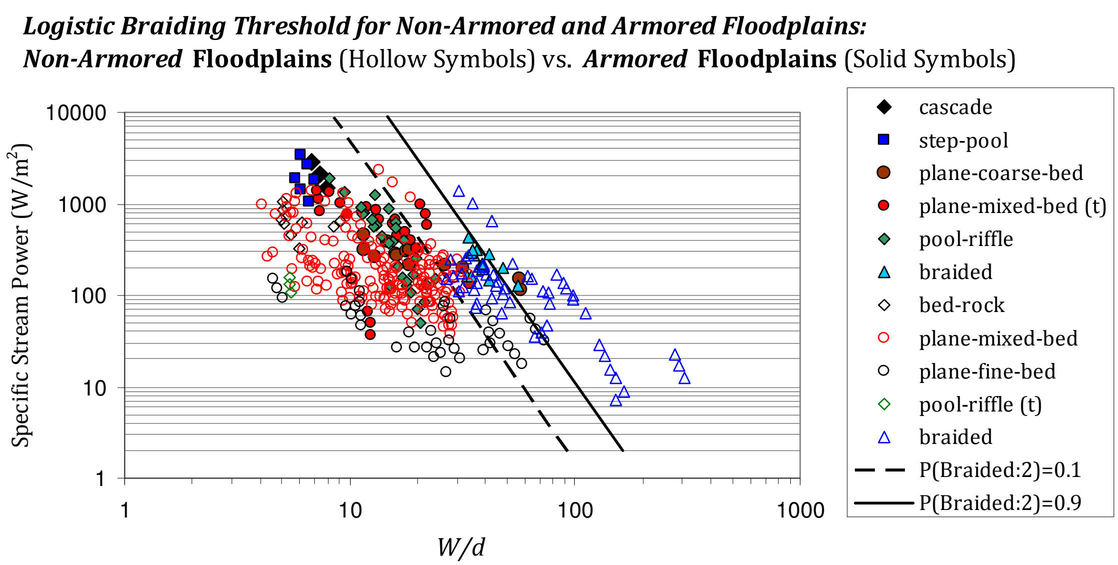

Figure 3.11b - Width-to-depth ratio vs. Specific stream power (Eq. 3.2)

Figure 3.11 – Comparison of logistic regression analyses for the non-armored floodplain continuum vs. the non-armored and armored floodplain continuums

this comparison is not entirely conclusive, since the number of data points corresponding to armored-braided floodplains represents only 4 percent of the total sample size (i.e., 15 out of 354 per Table 3.11).

Gradation data were collected at multiple locations at each of the study sites; that is, an upstream and a downstream sediment sample were typically collected at each site. However, it was time-prohibitive to collect gradation data at each cross section; hence, gradation data were assigned to groups of cross sections. Attempts were made to include the measured "percent sand" (i.e., the percentage of the particles smaller than 2 mm) as a third independent variable in the logistic regression analyses; however, these analyses did not successfully converge. I suspect that assigning gradation data to groups of cross sections prevented the logistic regression analyses from converging.

Table 3.11 – Comparison of logistic regression analyses for the non-armored floodplain continuum vs. the non-armored and armored floodplain continuums

Logistic Regression Parameters and Results	Braiding Threshold for Only the Non-Armored Floodplain Continuum	Braiding Threshold Based on Data Points for Both the Non-Armored and Armored Floodplain Continuums
Threshold Type & ID	**Braiding-ω-1**	**Braiding-ω-2**
Figure Shown	Figure 3.10a & 3.11a	Figure 3.11a & 3.11b
Line IDs in Figure 3.11	P(Braided T1)	P(Braid T1-2)
***Shape* Metric**	W/d (Eq. 3.16)	W/d (Eq. 3.16)
***State* Metric**	ω (Eq. 3.2)	ω (Eq. 3.2)
***State A* (S_A)**	non-braided	non-braided
***State B* (S_B)**	braided	braided
Total Sample Size (n)	273	354
Sample Size in *State A*	222	288
Samples Size in *State B*	51	66
X_1	$log_{10}(W/d)$	$log_{10}(W/d)$
X_2	$log_{10}(\omega)$	$log_{10}(\omega)$
β_0	42.1887	39.7135
β_1	-19.0285	-18.2570
β_2	-5.8813	-5.2022
Slope = $-\beta_1 / \beta_2$	-3.235	-3.509
Z_0 (Eq. 3.23)	5.57	6.77
Z_1 (Eq. 3.23)	-5.65	-7.02
Z_2 (Eq. 3.23)	-4.56	-5.13
Statistically Significant: $\|Z_i\| >> 2$? For i = 0 to 3	yes	yes

3.5.5 Conceptual Models for Intra-Catchment Processes

To summarize the key findings of this research in terms of intra-catchment processes, the results of these investigations have been compiled into *conceptual models for intra-catchment processes*. The *conceptual model for intra-catchment processes* for the *non-armored* and *armored* floodplain continuum are provided in Figures 3.12 and 3.13, respectively. The objectives of these conceptual models are to illustrate in one figure:

- the natural downstream progression of floodplain forms in terms of the specific stream power and width-to-depth ratio (i.e., state and shape metrics);
- the inferred downstream trends for key intra-catchment parameters (i.e., water supply or peak flow rate, width-to-depth ratio, sediment supply, specific stream power, bed slope, and percent sand) corresponding to the downstream progression of floodplain forms;
- the logistic stability and braiding thresholds, for the non-armored continuum, defined in terms of specific stream power (Equation 3.2) and the width-to-depth ratio (W/d); and
- the logistic braiding threshold for the non-armored floodplain continuum superimposed onto the data points for the armored continuum, for reference purposes only.

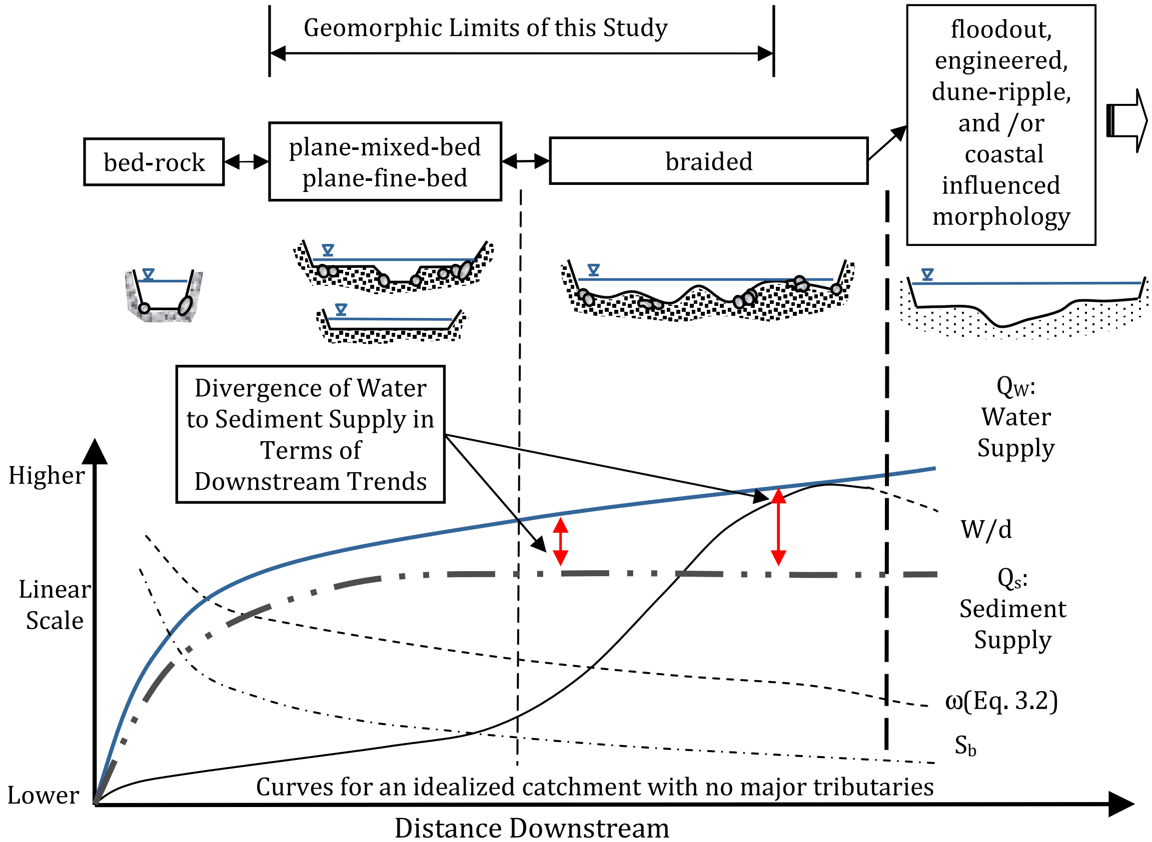

Figure 3.12a: Floodplain geometries and downstream trends

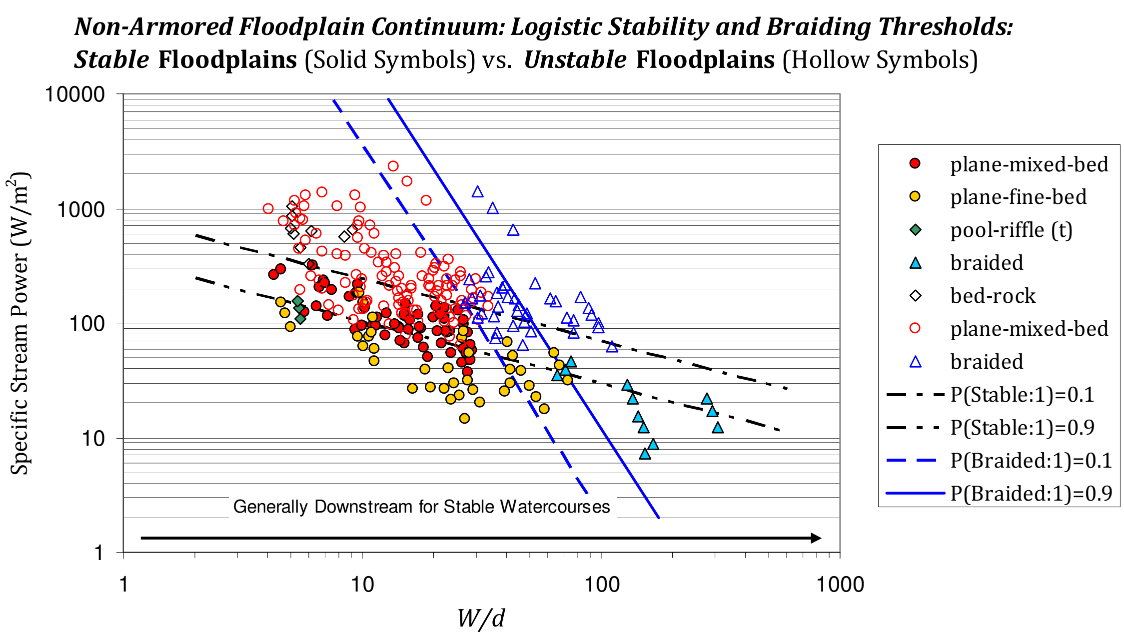

Figure 3.12b - Width-to-depth ratio vs. Specific stream power (Eq. 3.2)

Figure 3.12 – Non-armored floodplain continuum: conceptual model for intra-catchment processes: including typical floodplain geometries, downstream trends, and braiding/stability thresholds

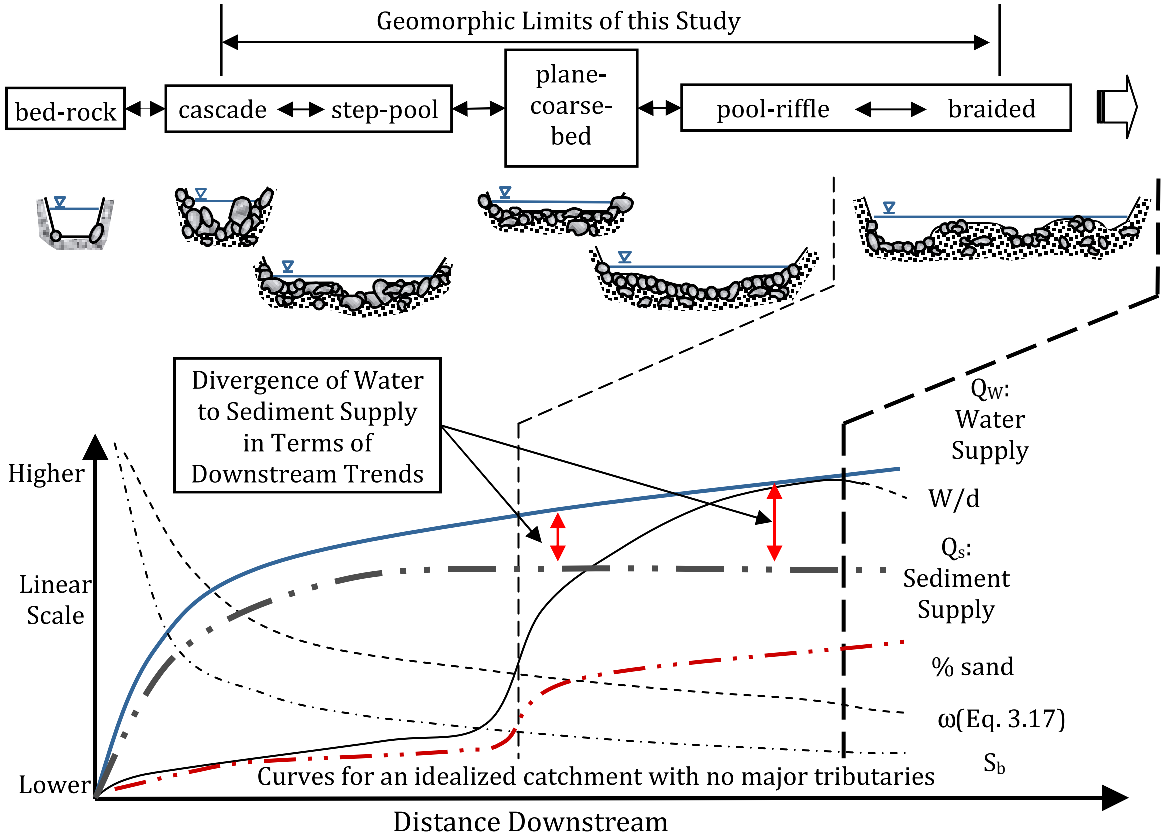

Figure 3.13a: Floodplain geometries and downstream trends

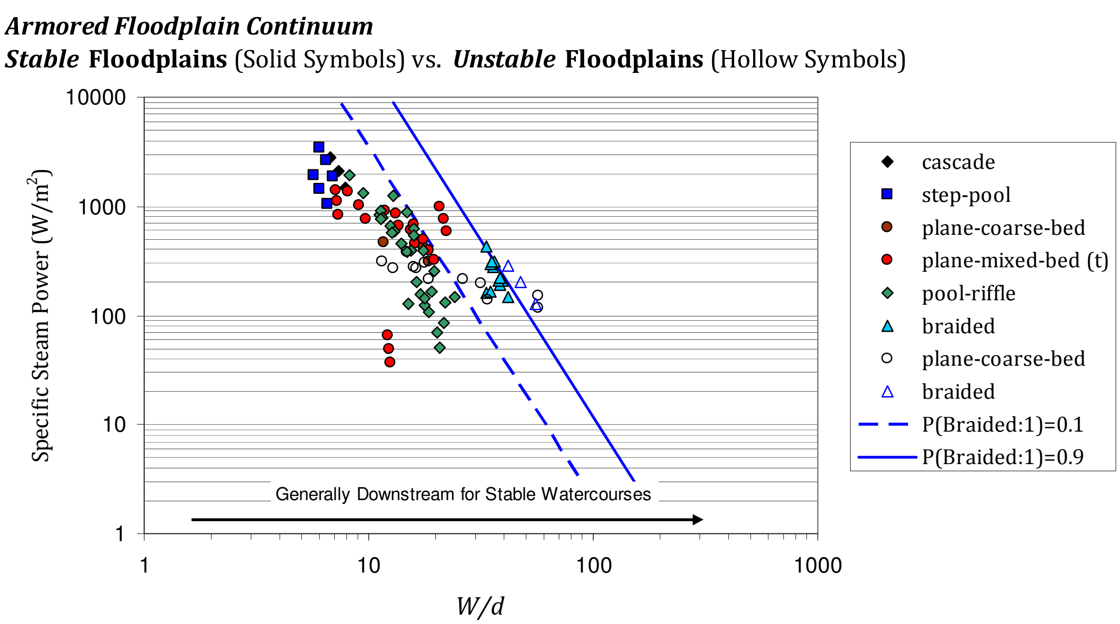

Figure 3.13b - Width-to-depth ratio vs. Specific stream power (Eq. 3.2)

Figure 3.13 – Armored floodplain continuum: conceptual model for intra-catchment processes including typical floodplain geometries, downstream trends, and braiding thresholds

3.5.6 *Floodplain Response Trends and Constraints Associated With Incremental Increases in Flow Rate*

The basic assumption underlying the concept of dynamic equilibrium is that the geometry of a floodplain will adjust to convey both the water and sediment discharges supplied from the upstream catchment, while maintaining a balance with the erosional resistance and stability characteristics of the banks (Schumm, 1977). Since the floodplain state plots shown in Figure 3.5 quantitatively describe the natural downstream progression of floodplain geometry, comparison of Figures 3.5a with 3.5b should be useful for gaining insights into the response trends and constraints associated with relatively small increases in flow rates for each of the floodplain continuums.

First consider the non-armored continuum. In Figure 3.12b, the data points for the stable non-armored floodplains have values for specific stream power ranging from approximately 300 to 10 (W/m^2), while the width-to-depth ratio varies from approximately 4 to 310. Clearly, both the slope and the width-to-depth ratio vary in the downstream direction within the geomorphic limits of this study; however, these data also illustrate that the primary response trend of non-armored floodplains to incremental increases in flow rate(i.e., < 10%) is to increase the width-to-depth ratio of the floodplain. In addition, this trend is reflected when the data points along an individual (stable) watercourse are overlaid onto the state diagram (as shown in Figure 3.5a). This floodplain response trend can be expressed as a *floodplain response constraint* as follows:

$$S_f \cong S_b \cong \textit{constant} \qquad \text{Equation 3.24}$$

where: S_f = energy or friction slope (m/m)

S_b = bed slope (m/m)

It is important to recognize that the preceding discussion and the *floodplain response constraint* for floodplains in the non-armored continuum are not intended to imply that non-armored floodplains are not susceptible to degradation or incising. To the contrary, non-armored floodplains are very susceptible to shifting into a state of severe instability (as described in Chapter 1). When unstable, non-armored floodplains may undergo severe degradation and the upstream migration of multiple head-cuts, as described in the Channel Evolution Model (CEM) developed by Schumm et al. (1981, 1984). This is why these investigations have focused on finding a means to assess the stability state of a floodplain.

However, a non-armored floodplain may undergo significant changes in geometry in response to changes in water and sediment supply without shifting into a state of severe instability, as demonstrated by the observed downstream progression of floodplain forms illustrated in Figure 3.12. It is under this scenario that the *floodplain response constraint* (Equation 3.24) is of importance and value.

The data points for pool-riffle floodplains (in Figure 3.13b) have values for specific stream power ranging from approximately 1,900 to 50 (W/m^2), while the width-to-depth ratio only varies from approximately 8 to 24. Since the range of specific stream power is so wide in comparison to the range of the width to depth ratios, the data shown in Figure 3.5b imply that the primary response of pool-riffle floodplains, to small increases flow rate, is to decrease the bed slope; however, the changes in width-to-depth ratios are also relatively significant. The slope of the pool-riffle data points shown in the floodplain state diagram parallels that of the braiding threshold shown in Figure 3.13b and can be expressed as a *floodplain response constraint* as follows:

$$\frac{\Delta \log(\omega)}{\Delta \log(W/d)} \cong -3.2 \qquad \text{Equation 3.25}$$

where: ω = specific stream power (Equation 3.2)
W/d = width-to-depth ratio

The value of "-3.2" corresponds to the slope (i.e., $-\beta_1/\beta_2$) of the "Braiding-ω-1" threshold, as shown in Figure 3.13b and Table 3.11. (Another method for setting the value for the floodplain response constraint is discussed in Section 4.5.4.) Unfortunately, there are an insufficient number of data points to identify any basic trends for cascade, step-pool, or braided floodplains in the armored floodplain continuum, as can be seen in Figure 3.13b..

The significance, application, and validity of these floodplain response constraints (i.e., Eq. 3.25) are further addressed in Chapter 4; however, it is fully recognized that the empirical *floodplain response constraints* defined by Equations 3.25 and 3.26 are simple representations of the very complex processes by which the erosion and stability characteristics of the banks influence the trend of the width, depth, and/or slope adjustments of a floodplain. It is further recognized that these floodplain response constraints are regional in nature and only reflect the characteristics of the banks within the study area.

3.5.7 Comparison of Floodplain State and Shape Metrics with Previous Studies

As reflected in Figures 3.12 and 3.13, these investigations focused on the upstream braiding threshold where high gradient single-thread floodplains transition to lower gradient braided floodplains, in the semi-arid environment of southern California. In addition, these investigations focused on "floodplains," as opposed to channels, and differentiated between:

- Stable and unstable floodplains as defined in Table 3.4; and
- Floodplains in the non-armored and armored continuums per Figure 2.5 and Tables 2.4 and 2.5, which are similar to but not completely analogous to "sand-bed" and "gravel-bed" rivers.

As a result, it is difficult to make direct comparisons to data from previous studies in terms of the state and shape metrics used in these investigations.

Within the literature, the previous study most analogous to these investigations is by Nanson and Croke (1992), within which they describe "A genetic classification of floodplains." The classification system defined by Nanson and Croke (1992) is unique in that it describes an array of floodplain forms (from a geomorphic perspective) and links them into potential continuums using identified ranges of specific stream power.

In Tables 3.12a and 3.12b, the values of specific stream power estimated for the floodplains included in this study are summarized and compared with those compiled by Nanson and Croke (1992). It is important to note that this is **not** a direct comparison. That is, the values of specific stream power (ω) computed in this study correspond to a range of reference flows that inundate the entire active floodplain (i.e., estimates for Q_{25}, Q_{50}, and Q_{100}); whereas, the values of "ω" reported by Nanson and Croke (1992) correspond to bankfull flow conditions within the channel, which were used as a surrogate for the floodplain. In addition, Nanson and Croke (1992) do not differentiate their floodplains (geomorphic perspective) in terms of their stability state or the presence of bed armoring, as was done in this study.

In spite of this differences, there is relatively close agreement between the estimated values of "ω" for both the braided and non-braided floodplain forms in many respects, as indicated in Tables 3.12a and 3.12b. That is, Nanson and Croke (1992) report a range of 50 to 300 (W/m^2) for braided floodplains, whereas the data for this study indicate a range of approximately 10 to 430 (W/m^2) for stable braided floodplains and a range of 60 to 1400 (W/m^2) for unstable braided floodplains. For the non-braided floodplains, the estimated range of values for "ω" overlap; however, the range of values estimated for this study extend an order of magnitude lower than that reported by Nanson and Croke (1992). This may at least be in part due to how the values of "ω" have been computed (i.e., floodplain vs. channel) and/or due to the influence of bed armoring.

Table 3.12a – Comparison of state and shape metrics for braided floodplains with previous studies

Description	State Metric Specific Stream Power (ω) (W/m²)		Shape Metric Width-to-Depth Ratio (W/d)	
Braided Floodplains This Study (1)	**Range**	**Mean**	**Range**	**Mean**
Non-armored	7 to 1397	165	27 to 308	78
Stable	*7 to 46*	*22*	*66 to 308*	*164*
Unstable	*63 to 1397*	*209*	*27 to 111*	*51*
Armored	127 to 425	236	33 to 56	39
Stable	*148 to 425*	*245*	*33 to 42*	*37*
Unstable	*127 to 285*	*204*	*42 to 56*	*48*
Non-Armored and Armored	7 to 1397		27 to 308	
Braided Floodplains Previous Studies	50 to 300 (2)		> ~ 50 to 60 (3)	

Notes: (1) Estimated state and shape metrics correspond to Q_{25}, Q_{50}, and Q_{100}.
(2) Nanson and Croke (1992) based on estimated bankfull conditions for Class B braided floodplains
(3) Theoretical analyses by Engelund and Skovgaard (1973), Fredsoe (1978), Fukuoka (1989)

Table 3.12b – Comparison of state and shape metrics for non-braided floodplains with previous studies

Description	State Metric Specific Stream Power (ω) (W/m²)		Shape Metric Width-to-Depth Ratio (W/d)	
Non-Braided Floodplains This Study(1)	**Range**	**Mean**	**Range**	**Mean**
Non-armored	15 to 2300	15	4 to 73	18
Stable	*15 to 318*	*94*	*4 to 73*	*21*
Unstable	*65 to 2300*	*383*	*4 to 33*	*15*
Armored	37 to 3412	698	6 to 57	16
Stable	*37 to 3412*	*785*	*6 to 24*	*14*
Unstable	*116 to 381*	*238*	*12 to 57*	*26*
Non-Armored and Armored	15 to 3412		4 to 73	
Non-Braided Floodplains Previous Studies	> ~ 300 (2)		< ~ 50 to 60 (3)	

Notes: (1) Estimated state and shape metrics correspond to Q_{25}, Q_{50}, and Q_{100}.
(2) Nanson and Croke (1992) based on estimated bankfull conditions for Class A floodplains
(3) Theoretical analyses by Engelund and Skovgaard (1973), Fredsoe (1978), Fukuoka (1989)

For the width-to-depth ratio (W/d), the findings of these investigations are compared in Tables 3.12a and 3.12b with the theoretical analyses by Engelund and Skovgaard (1973), Fredsoe (1978), and Fukuoka (1989). These theoretical analyses indicate that the major control on braiding is the width-to-depth ratio and that braiding occurs when $W/d > \sim 50$ to 60. As also noted by Bridge (1993), the theoretical threshold for braiding (i.e., $W/d > \sim 50$ to 60) can be influenced to a limited degree by bed material mobility criteria, bedform via roughness coefficient values (Fredsoe, 1978), and slope (Fukuoka, 1989).

As indicated in Tables 3.12a and 3.12b, the results of this study are for the most part consistent with the theoretical threshold of $W/d > \sim 50$ to 60. However, the results of these investigations indicate that braiding may occur at significantly lower width-to-depth ratios for unstable and/or armored braided floodplains, as listed in Table 3.12a and illustrated in Figures 3.12b and 3.13b. This point is further reflected by the "negative" slope for the logistic braiding threshold lines shown in Figure 3.12b, which indicates that braiding may occur at lower width-to-depth ratios as specific stream power increases.

3.6 Summary and Conclusions

3.6.1 Primary Findings

The primary objective of the research documented in this chapter was to develop conceptual models describing key intra-catchment processes by addressing the following *applied* research questions:

- What are the intra-catchment processes that govern the observed downstream progression of floodplain forms in a stable system, including specifically the progression from single-thread to braided floodplains?

- How do the erosional resistance and stability characteristics of the banks influence the natural downstream progression of floodplain geometry and can this influence be quantified into general floodplain response trends and constraints?
- What is the interrelationship between the stability state with the form and geometry of a floodplain, under various hydraulic conditions?
- What is the impact of urbanization on the primary intra-catchment processes that govern the natural downstream floodplain form progression?

To develop *conceptual models for intra-catchment processes*, the approach adopted in this research was to use field data to first find a quantitative means to describe the natural downstream progression of floodplain forms, then use these findings to infer the key intra-catchment processes for the non-armored and armored floodplain continuums that govern the downstream progression of floodplain forms. This approach is based on the fundamental concept that the observed natural downstream progression of floodplain forms is a direct reflection of natural changes in intra-catchment runoff and sedimentation processes in alluvial or mostly alluvial floodplains.

In Figures 3.12 and 3.13, the primary findings of the research described in this chapter have been compiled into conceptual models that illustrate the interrelationship of intra-catchment processes with the downstream progression of floodplain forms for both the non-armored and armored floodplain continuums. For the ***non-armored*** floodplain continuum, the floodplain state diagrams within the conceptual model provided the bases to:

- develop logistic stability and braiding thresholds (Figure 3.5 and Figure 3.12b) that provide a means to quantitatively assess the state of a floodplain in terms of both stability and braiding; and

- infer that the primary response of a non-armored floodplain to incremental increases in flow (while the sediment supply is relatively unchanged) is an increase in the width-to-depth ratio and, thereby, provide a means to define a floodplain response constraint (Equation 3.24).

For the ***armored*** floodplain continuum, these floodplain state diagrams provided the bases to:

- qualitatively assess the state of a floodplain in terms of both stability and braiding; and
- define a floodplain response constraint (Equation 3.25) in terms of changes in specific stream power and width-to-depth ratio, for pool-riffle floodplains.

Therefore, the *conceptual models for intra-catchment processes* directly address, to a reasonable degree, the first of the practical research questions at the core of this research: *How can we assess the existing stability state of a floodplain?* Via the floodplain response constraints, the conceptual models also provide a framework for addressing the second practical research question at the core of this research: *How can we estimate the trend and magnitude of the change in floodplain geometry?*

3.6.2 Avenues for Further Investigation

Further Investigations for Armored Floodplain Forms

I fully recognizes that the *conceptual model for intra-catchment processes* is significantly more developed for the non-armored floodplain continuum than for the armored. This is a direct result of the fact that far more data were collected for floodplains in non-armored continuum than any of the other continuums. It is believed that this primarily stems from the non-armored continuum being generally the most prevalent continuum in study area and by far the most prevalent continuum in the areas that have the higher levels of urbanization.

As part of these investigations, sufficient data have been collected to assess a *floodplain response constraint* for only the pool-riffle floodplain form, with reasonable confidence. Unfortunately, these investigation did not collect sufficient data to assess floodplain response trends and constraints for all other floodplain forms, with braided being the most important of the floodplain forms in terms of floodplain management. There are also insufficient data to quantitatively assess the braiding threshold for the armored floodplains using logistic regression techniques, with the independent variables being ω, W/d, and some metric for the bed material gradation. Therefore, there are multiple avenues for further investigations of the armored floodplain continuum.

The Hypothesized Water to Sediment Supply Divergence Process and Self Enhancing Feedback Mechanisms

The objective of the discussion in Section 3.5.2 is to simply describe a plausible, if not logical, interpretation of key aspects of the floodplain state plots (Figure 3.5), in terms of basic intra-catchment processes. Hence, the discussions of the *water to sediment supply divergence process* (Section 3.5.2) and the corresponding *self enhancing feedback mechanisms* are basically an attempt to relate the typical impacts of urbanization to the intra-catchment processes that may be responsible for the downstream progression of floodplain geometry and forms. However, I strongly believe that further investigation into and quantification of the hypothesized *water to sediment supply divergence process*, and its interrelationship with floodplain response mechanisms and braiding thresholds, could prove interesting from both a fluvial geomorphology and a floodplain management perspective.

Chapter 4: Modeling Tools for Estimating the Trend and Magnitude of the Change in Floodplain Geometry Due to Incremental Changes in Water and Sediment Supply

4.1 Chapter Overview

4.1.1 Abstract

For the non-armored and armored floodplain continuums observed in the semi-arid environment of southern California, regime-type modeling tools have been developed for estimating the trend and magnitude of the change in floodplain geometry, due to changes in water and sediment supply. At the core of these techniques are the basic flow relationships of continuity, flow resistance, and sediment transport for floodplains with trapezoidal geometry. To factor in bank erosional resistance and stability characteristics, the basic flow relationships are coupled with floodplain response constraints derived from the *conceptual models for intra-catchment processes* and the corresponding floodplain state diagrams, provided in Chapter 3. Since I contend that the response of a floodplain to changes in water and sediment supply can differ depending upon the initial stability state of the floodplain, the modeling tools also incorporate techniques for assessing both the initial and projected stability state for a floodplain.

4.1.2 Introduction/Research Questions

The core *practical* research questions motivating the investigations documented in this dissertation are:

- How can we assess the existing stability state of a floodplain?
- How can we estimate the trend and magnitude of the change in floodplain geometry due to perturbations in intra-catchment processes associated with urbanization?

To address these core questions it was first important to gain a basic understanding of the form and nature of the floodplains in the semi-arid environment of southern California. As described in Chapter 2, three basic floodplain continuums have been identified for southern California: *non-armored*, *armored*, and *active-regional alluvial fan*. As shown in Figure 2.5, each of these continuums are comprised of three or more alluvial floodplain forms that have a general downstream progression in stable systems.

Based on the argument that the observed natural downstream progression of floodplain forms is a direct reflection of natural changes in intra-catchment runoff and sedimentation processes, the next step taken to address the core practical research questions involved searching for a quantitative means to describe this observed progression of floodplain forms in terms of a state and a shape metric. This search led to the development of floodplain state diagrams, where the downstream progression of floodplain forms is described in terms of specific stream power (or boundary stress) and the width-to-depth ratio. These floodplain state diagrams provided the basis to: (a) assess the stability state of a floodplain; (b) assess general floodplain response trends; (c) describe the interaction of key intra-catchment processes that govern the downstream progression of floodplain forms; and (d) develop hypotheses regarding the mechanisms governing the upstream braiding threshold for non-armored and armored floodplains. As described in Chapter 3, these findings were compiled diagrammatically to create conceptual models for intra-catchment process for the non-armored and armored floodplain continuums. In terms of the practical research questions at the core of these investigations, these conceptual models provide: (a) a means to assess the current stability state of a floodplain; and (b) a framework within which to develop methods for estimating the trend and magnitude of the change in floodplain geometry due to perturbations in the catchment associated with urbanization.

Based on the framework described in Chapter 3, the objective of this chapter is to address the second and final practical research question at the core of these investigations: ***How can we estimate the trend and magnitude of the change in floodplain geometry due to perturbations in intra-catchment processes associated with urbanization?*** This research question is only addressed for the non-armored (or Type 1) and armored (i.e., Type 2) floodplain continuums. The active-regional alluvial fan continuum has been included in this research on a qualitative and conceptual level (in Chapter 2) for the sake of completeness. However, this floodplain continuum has been excluded from quantitative reach-scale investigation in this research, since active alluvial fan floodplains are already highly regulated by FEMA and/or local agency guidelines.

4.1.3 Modeling Tool Objectives, Approach, and Physical Basis

Modeling Tool Objectives

The fundamental fluvial geomorphic concept underlying the evaluation of watercourse stability and response is that an alluvial system can over time establish and maintain an equilibrium condition, where the geomorphic characteristics of a floodplain remain relatively stable over time (Tanner, 1968; Shen, 1979; Dingman, 1984). However, the geometry of stable watercourses do not have to be static over time and may temporarily change in response to temporal variations in water and sediment supply. Therefore, the key characteristic of a stable watercourse is that fluvial processes, during channel and/or floodplain formative flows, restore the geomorphic characteristics of a floodplain rather than perpetuating and amplifying changes in geomorphic characteristics (Watson, et al., 2005).

Inherent in this definition of stability and equilibrium is that a watercourse has a critical stability threshold, such that when exceeded the watercourse will undergo a long-term and complex series of significant (if not dramatic) changes in geomorphic characteristics. Conversely, I contend that incremental spatial variations in water and sediment supply are responsible for the natural downstream progression of floodplain forms in stable watercourses, as described in Chapters 2 and 3. When considering the response of a watercourse to changes in water and sediment supply associated with urbanization, it is, therefore, essential to be able to differentiate between a change that results in:

- severe instability and potentially a dramatic change in geomorphic characteristics once equilibrium is ultimately re-achieved; or
- a relatively minor adjustment in floodplain form, from a geomorphic perspective.

However, it is important to recognize that "a relatively minor adjustment in floodplain form, from a geomorphic perspective" may be a very significant adjustment from a floodplain management perspective.

Further inherent in the aforementioned definition of stability and dynamic equilibrium is that stable and unstable watercourses will respond differently to a new perturbation in water and/or sediment supply. Therefore, it is also essential to be able to assess the initial stability state of a watercourse, when evaluating the potential change in the geometry of a floodplain due to changes in water and sediment supply.

The objective of the research documented in this chapter was to develop a technique or *modeling tool* for estimating the trend and magnitude of the change in floodplain geometry due to changes in intra-catchment processes associated with urbanization. Inherent in this objective for the modeling tool is the constraint that the initial floodplain is stable (or relatively stable) and the corresponding floodplain geometry is known. Hence, it is essential that the modeling tool include a means to assess the stability state of both the initial and the projected floodplain geometry.

Regime-Type Approach for the Modeling Tools

The basic assumption underlying the concept of dynamic equilibrium is that the geometry of a floodplain will adjust to convey both the water and sediment discharges supplied from the upstream catchment, while maintaining a balance with the erosional resistance and stability characteristics of the banks within and/or along the periphery of the floodplain (Schumm, 1977). Hence, it is generally argued that the basic flow relationships of continuity, resistance, and sediment transport are not sufficient to describe the processes by which the hydraulic geometry (including bed slope) of a watercourse adjust to maintain dynamic equilibrium, because the basic flow relationships do not reflect the influence of the erosional resistance and stability characteristics of the banks, as argued and described by Laursen (1958) and Henderson (1966). Therefore, the challenge in applying a regime-type modeling approach is to identify a constraint that defines how the width, depth, and/or slope of a floodplain adjusts simultaneously to take into account the influence of the erosional resistance and stability characteristics of the banks.

A regime-type modeling approach has been adopted to develop *modeling tools* for estimating the trend and magnitude of the change in floodplain geometry, where the solution of the basic flow relationships is facilitated by incorporating into the solution procedure what are referred to herein as ***floodplain response constraints***. The *floodplain response constraints* are intended to account for the erosional resistance and stability characteristics of the banks. As reflected in the floodplain state diagrams for the non-armored and armored floodplain continuums (Figures 3.12b and 3.13b), the *floodplain response constraints* have been derived from analyses of field data for a wide range of floodplain geometries within the semi-arid environment of southern California, as described in Chapter 3.

Within the regime-type modeling approach for the modeling tools, what are referred to as ***floodplain stability constraints*** are used to assess the stability state of the floodplain and, thereby, evaluate the basic applicability of the regime-type modeling approach. The form of the *floodplain stability constraints* is dependent on the continuum of the floodplain being evaluated.

Physical Basis: Floodplain Response and Stability Constraints

To provide a framework for developing modeling tools, the *reach-scale conceptual model for stable floodplain continuums* and *conceptual models for intra-catchment processes* have been developed and are described in Chapters 2 and 3, respectively. The *reach-scale conceptual model for stable floodplain continuums* (as illustrated in Figure 2.5), in conjunction with Tables 2.4 and 2.5, provides the framework required to assess whether a given floodplain is within the non-armored or armored floodplain continuum.

The *conceptual models for intra-catchment processes* (as illustrated in Figures 3.12 and 3.13) provide the framework for assessing both the ***floodplain response constraints*** and ***floodplain stability constraints*** . As described in Section 3.5.6, the *floodplain response constraints* for stable non-armored and armored floodplains have been defined as follows:

- For stable floodplains in the non-armored continuum, the floodplain response constraint is such that the primary response to incremental increases in flow is to increase the width-to-depth ratio, while holding the bed slope relatively constant. This floodplain response constraint can be expressed as follows:

$$S_f \cong S_b \cong \textit{constant} \qquad \text{Equation 4.1a}$$

where: S_f = energy or friction slope (m/m)

S_b = bed slope (m/m)

- For pool-riffle floodplains in the armored floodplain continuum, the floodplain response constraint can be expressed as follows:

$$\frac{\Delta \log(\omega)}{\Delta \log(W/d)} \cong -3.2 \qquad \text{Equation 4.1b}$$

where: ω = specific stream power (Equation 3.2)
W/d = width-to-depth ratio

As described in Sections 3.5.3 and 3.5.4, the floodplain state diagrams within the conceptual models (Figure 3.12b and 3.13b) have provided a means for assessing the stability state for both initial and projected floodplain geometries, within the geomorphic limits of this study. The following paragraphs summarize the findings described in Sections 3.5.3 and 3.5.4, and the specific techniques developed for assessing the stability state of floodplains within the non-armored and armored continuums:

- For the non-armored floodplain continuum, the floodplain state plots (Figure 3.5) provided the basis to develop a probabilistic and quantitative means to assess the stability state of a floodplain using logistic regressions techniques. The results from the logistic regression analyses for the stability threshold can be used to estimate the probability that the floodplain is unstable and in state of severe instability (i.e., $P(Y = S_A)$) via Equation 3.22 and the intercept and the partial slope coefficients (i.e., β_0, β_1, and β_2) given in Table 3.9. Conversely, the probability that the floodplain is stable and in a state of dynamic equilibrium (i.e., $P(Y = S_B)$) can then be estimated with the following equation: $P(Y = S_B) = 1 - P(Y = S_A)$.
- For the armored floodplain continuum, the floodplain state diagram (Figure 3.13b) provides a qualitative means to assess stability state for both the initial and projected floodplain geometries. That is, Figure 3.13b illustrates the graphical regions associated with observed stable and unstable floodplain forms in terms of

specific stream power (as a state metric) and width-to-depth ratios (as a shape metric).

Key components of the modeling tools described in this chapter are the floodplain state diagrams that quantitatively describe the natural downstream progression of floodplain forms in terms of specific stream power and the width-to-depth ratio. Based on field observation and evaluation of the field data collected as part of these investigations, it is important to recognize that I argue that that flow events with return periods of approximately 25 years and greater are the flow events primarily responsible for forming and maintaining the geometry and form of a floodplain in the semi-arid environment of southern California. Therefore, the floodplain state diagrams in Figures 3.12 and 3.13 only include data points corresponding to estimated peak flow rates with return periods of 25, 50, and 100 years. Hence, the modeling tools described in this chapter are based on using a reference discharge that has a return period of approximately 25 years or greater.

Physical Basis: The Role of Bed Gradation in the Modeling Tools

It is generally agreed that bed material gradation has a direct effect on the geometry, form, and stability characteristics of a floodplain. However, it is also reasonable to say that the specific relationships between bed material gradation and the geometry, form, and stability characteristics of a floodplain are very complex and not necessarily well understood. Hence, some state-type diagrams for watercourses have a metric reflecting the bed material gradation, such as d_{50} (van den Burg, 1995; Bledsoe and Watson, 2001).

It is important to recognize that bed material gradation is also specifically, but more subtly, reflected in the state diagrams (Figures 3.12b and 3.13b) developed as part of these investigations and used as a framework for the *modeling tools* described in this chapter. That is, the influence of the bed material gradations for the study sites are indirectly reflected in every aspect of the state diagrams (Figures 3.12b and 3.13b) as follows:

- As described in Chapter 2, the floodplain forms are inherently related to both bedforms and the associated bed material gradation; hence, bed gradation is specifically reflected in the state diagrams (Figures 3.12b and 3.13b) via the different symbols for each of the floodplain forms.
- As described in Chapter 3, both the state and shape metrics (i.e., specific stream power and width-to-depth ratio) used to define the state diagrams are hydraulic parameters; therefore, both metrics reflect the influence of bed material gradation in terms of the Manning's roughness coefficient (n) and the surveyed cross sectional geometry used in the hydraulic computations.

In terms of the *modeling tools* described in this chapter, bed material gradation has both a direct and an indirect role. That is, metrics based on bed gradation data are directly used in sediment transport computations within the *modeling tools*; whereas, bed material gradation has an indirect role in determining the whether the modeling tools for the non-armored or armored floodplain continuum are appropriate for a specific application. Therefore, the state diagrams and the modeling tools developed as part of these investigations directly reflect the influence of bed material gradation, even though a metric specifically based on bed material gradation data is not prominent in the state diagrams (Figures 3.12b and 3.13b) which form the framework for the modeling tools described in this chapter.

4.2 Previous Studies: Empirical, Analytical, and Rational Regime Modeling Approaches

Regime models are the category of models that are predicated on the assumption that the cross sectional form of an alluvial channel or floodplain can be predicted, with some level of confidence, based on a single reference flow rate and the corresponding sediment transport rate. At the foundation of regime models are the basic flow relationships of continuity, resistance, and sediment transport; however, it is generally agreed that the basic flow relationships alone are not sufficient to describe the processes by which the hydraulic geometry of a watercourse is adjusted to maintain dynamic equilibrium and, therefore, cannot identify a unique floodplain geometry associated with a given set of hydraulic conditions.

Numerous quantitative analysis techniques have been devised to resolve this issue. However, these techniques basically fall into three basic approaches: empirical, analytical, and rational regime modeling approaches (Eaton and Millar, 2004). There are, of course, some hybrid approaches which use a combination of these approaches.

Empirical Regime Modeling Approach

In the empirical modeling or "hydraulic geometry" approach, statistical analysis techniques are used to estimate empirical relationships relating geomorphic characteristics (typically channel width, depth, and slope) to a state variable (typically bankfull or dominant discharge), as developed by Leopold and Maddock (1953), Leopold and Wolman (1957), and Hey and Thorne (1986). These empirical relationships generally fall into two sub-categories: *downstream* or *at-a-station* hydraulic geometry. The objective of a *downstream* hydraulic geometry relationship is to quantify spatial variations in channel properties along the longitudinal profile of the watercourse; whereas, the objective of *at-a-station* relationships is to quantify temporal variations in flow variables at a cross section. Even though these two sub-categories of empirical relationships have distinctly different objectives, these relationships can have basically the same power function form (Knighton, 1998).

Analytical Regime Modeling Approach

In the analytical regime modeling or stable-channel approach, the basic flow relationships are supplemented by a bank stability criterion as described by Laursen (1958) and Henderson (1966). In this approach, the bank stability criterion is defined in terms of incipient motion via critical shear stress at various bank slopes; hence, the approach does not identify a unique channel geometry, but instead identifies the channel geometry such that the bank material is at the threshold of motion (Henderson 1966).

Rational Regime Modeling Approach

In the rational regime modeling approach, the basic flow relationships are supplemented by various optimality criterion collectively referred to as "extremal hypotheses" to allow the solution of a unique floodplain geometry (Knighton, 1998). The fundamental premise of the extremal hypotheses, with a physical basis, is that there is a metric that describes a key aspect of the state of a watercourse that is either minimized or maximized in stable watercourses. Some of the predominant extremal hypotheses, with a physical basis, are based on the following premises:

- minimize unit stream power (VS_f) – by Yang (1976);
- minimize total stream power (γQS_f) – by Chang (1979);
- minimize the energy dissipation rate ($(Q\gamma+Q_s\gamma_s)LS_f$) – by Yang, Song, and Woldenberg (1981);
- maximize sediment transport efficiency ($Q_s/(\rho QS_f)$) – by Kirby (1977) and Millar (2005);
- maximize sediment transport rate or capacity (Q_s) – by White, Bettess, and Paris (1982) and Eaton and Millar (2004);
- maximize friction factor (ff) – by Davies and Sutherland (1983); and
- maximize resistance to flow in the fluvial system ($f_{sys} = f_{grain}+f_{channel}+f_{sinuosity}= (8gRS_v)/V^2$) – by Eaton, Church, and Millar (2004).

Though these principles may appear to be distinctly different, it has been shown that a couple of these principles are the same or closely related under certain conditions (Huang and Nanson, 2000; Millar, 2005).

Regime Modeling Approach Adopted for These Investigations

In the context of previous studies, I contend that the approach adopted in these investigations is basically a hybrid regime modeling approach. That is, the basis of the approach is analytical in the sense that the solution of the basic flow relationships includes relationships intended to account for observed bank erosion and stability characteristics and floodplain stability thresholds (i.e., the floodplain response and stability constraints). However, these constraints are empirical in nature and are different for the non-armored and armored continuums. In addition, the approach adopted herein is notably unique in that regime techniques are used to find the "projected" floodplain geometry given both the change in the reference discharge and the "initial" floodplain geometry. Inherent in this approach is the concept that the stable geometry at a point along a watercourse is influenced by the upstream floodplain geometry, within the geomorphic limits of this study.

It also worth noting that the findings of these investigations (as illustrated in Figures 3.12) appear to be generally consistent with some aspects of various extremal hypotheses. However, extremal hypotheses have not been invoked in the development of the modeling tools described herein.

4.3 Study Area: Geomorphic Limits and Range of Application

As described in Chapter 1, this research intentionally focused on watercourses with relatively small catchments and, as a result, the field data collection efforts only encompassed the upper reaches of non-armored and armored watercourses. This focus on relatively small catchments resulted in a geomorphic limit being imposed on the range of floodplain forms included in this study. As illustrated in Figure 4.1, this geomorphic limit encompasses the braided and upstream floodplain forms for the armored and non-armored floodplain continuums shown in Figure 2.5. Since the modeling tools described herein incorporate empirical relationships solely derived from the field data collected and analyzed as part of this research, the range of application of the modeling tools developed as part of this study are strictly limited to the geomorphic limits shown in Figure 4.1.

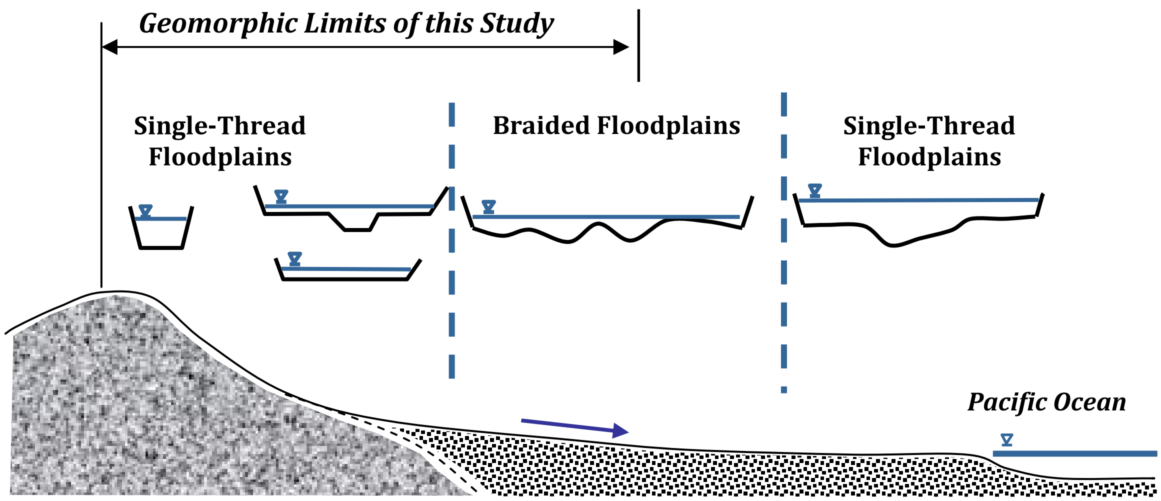

Figure 4.1 – Schematic illustrating a general floodplain continuum and the geomorphic limits for this study

4.4 Methods

4.4.1 Basic Flow Relationships of Continuity and Resistance for a Trapezoidal Floodplain

At the core of the modeling tools described in this chapter are the basic flow relationships of continuity and flow resistance for steady uniform flow, as follows:

Continuity Equation for one-dimensional steady flow

$$Q = AV \qquad \text{Equation 4.2}$$

Manning Equation (Chow, 1959):

$$V = \frac{1}{n} R^{2/3} S_f^{1/2} \quad \text{in (m/s)} \qquad \text{Equation 4.3}$$

where: V = flow velocity (m/s)
n = Manning's roughness coefficient
$R = A / P_w$ = hydraulic radius (m)
A = flow area (m²)
P_w = wetted perimeter (m)
S_f = friction slope (m/m)
Q = flow rate (m³/s)

For a floodplain with a trapezoidal cross section (as illustrated in Figure 4.2), the relationships for flow area, wetted perimeter, topwidth, and hydraulic radius can be expressed as follows:

$$A = (b + z \cdot d)d \qquad \text{Equation 4.4}$$

$$P_w = b + (2 \cdot d)\sqrt{1 + z^2} \qquad \text{Equation 4.5}$$

$$b = (W - (2 \cdot z \cdot d)) \qquad \text{Equation 4.6a}$$

$$W = (b + (2 \cdot z \cdot d)) \qquad \text{Equation 4.6b}$$

$$R = A / P_w = \frac{(b + z \cdot d)d}{b + (2 \cdot d)\sqrt{1 + z^2}} \qquad \text{Equation 4.7}$$

where: b = bottom width (m)
d = flow depth (m)
z = side slope (z horizontal : 1 vertical units)
R = hydraulic radius (m)
A = flow area (m²)
P_w = wetted perimeter (m)
W = topwidth (m)

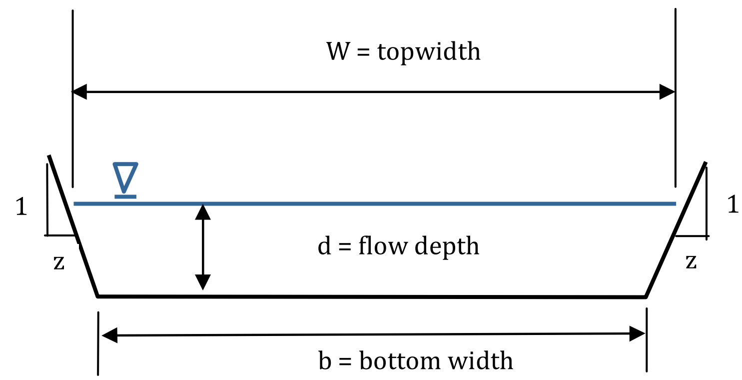

Figure 4.2 – Schematic illustrating elements of a trapezoidal cross section

4.4.2 Floodplain Response Trajectory Relationship for Non-Armored Floodplains

At this point, the width-to-depth ratio ($\mathrm{T} = (W/d)$) is introduced to facilitate the solution of the basic flow relationships and allow superimposing the hydraulic analyses onto the floodplain state diagrams (Figures 3.12b and 3.13b). Solving Equations 4.4 through 4.7 in terms of the width-to-depth ratio yields:

For $\mathrm{T} = (W/d)$: Equation 4.8

$$A = (\mathrm{T} - z)d^2 \quad \text{Equation 4.9}$$

$$P_w = d\left((\mathrm{T} - 2 \cdot z) + \left(2\sqrt{1+z^2}\right)\right) \quad \text{Equation 4.10}$$

$$b = (\mathrm{T} - (2 \cdot z))d \quad \text{Equation 4.11}$$

$$R = A/P_w = \frac{(\mathrm{T} - z)d}{(\mathrm{T} - 2 \cdot z) + \left(2\sqrt{1+z^2}\right)} \quad \text{Equation 4.12}$$

where: b = bottom width (m)
d = flow depth (m)
z = side slope (z horizontal : 1 vertical units)
R = hydraulic radius (m)
A = flow area (m^2)
P_w = wetted perimeter (m)
W = topwidth (m)

Substituting Equation 4.3 into Equation 4.2 yields Equation 4.13. Substituting Equations 4.9 and 4.12 into Equation 4.13 yields Equation 4.14 as follows:

$$Q = \frac{1}{n} A R^{2/3} S_f^{1/2} \qquad \text{Equation 4.13}$$

$$Q = \frac{(\mathrm{T}-z)d^2}{n}\left(\frac{(\mathrm{T}-z)d}{(\mathrm{T}-2\cdot z)+\left(2\sqrt{1+z^2}\right)}\right)^{(2/3)} S_f^{1/2} \qquad \text{Equation 4.14}$$

Solving Eq. 4.14 for flow depth (d) yields:

$$d = \left[\frac{Q\cdot n}{(\mathrm{T}-z)S_f^{1/2}}\left(\frac{(\mathrm{T}-z)}{(\mathrm{T}-2\cdot z)+\left(2\sqrt{1+z^2}\right)}\right)^{-2/3}\right]^{3/8} \qquad \text{Equation 4.15}$$

Substituting Equation 4.15 into Equation 4.8 and solving for topwidth yields:

$$W = \mathrm{T}\left[\frac{Q\cdot n}{(\mathrm{T}-z)S_f^{1/2}}\left(\frac{(\mathrm{T}-z)}{(\mathrm{T}-2\cdot z)+\left(2\sqrt{1+z^2}\right)}\right)^{-2/3}\right]^{3/8} \qquad \text{Equation 4.16}$$

Furthermore, substituting Equation 4.16 into the equation for specific stream power (Equation 3.2) yields:

$$\omega = \gamma\frac{Q}{W}S_f = \gamma Q S_f\left[\mathrm{T}\left[\frac{Q\cdot n}{(\mathrm{T}-z)S_f^{1/2}}\left(\frac{(\mathrm{T}-z)}{(\mathrm{T}-2\cdot z)+\left(2\sqrt{1+z^2}\right)}\right)^{-2/3}\right]^{3/8}\right]^{-1} \qquad \text{Equation 4.17}$$

where:
n = Manning's roughness coefficient
d = flow depth (m)
z = side slope (z horizontal : 1 vertical units)
S_f = friction slope (m/m)
Q = flow rate (m^3/s)
ω = specific stream power (W/m^2)
$\mathrm{T} = (W/d)$ = width-to-depth ratio

Though cumbersome to apply, Equation 4.17 does allow specific stream power to be computed directly as a function of width-to-depth ratio (W/d), discharge (Q), side slope (z), Manning's roughness coefficient (n), and friction slope (S_f). For relatively trapezoidal floodplains in the non-armored continuum, Equation 4.17 can be used to generate what are referred to herein as *floodplain response trajectories*, that can be plotted directly onto the floodplain state diagram (3.12b). Floodplain response trajectories are curves that describe the range of geomorphic characteristics (in terms of ω and W/d) that a trapezoidal floodplain may have for a constant Q, n, z, and S_f. It is important to recognize that the response trajectory for non-armored floodplains described with Equation 4.17 incorporates the constraint that the primary response to incremental increases in discharge is an increase in the width-to-depth ratio, while the bed slope remains relatively constant.

4.4.3 Sediment Transport Relationships

As described in Chapters 2 and 3, the floodplain forms observed in southern California are diverse in both form and bed material composition. Since all sediment transport relationships have inherent limitations in their range of application in terms of bed material composition, it is recognized that no one sediment transport relationship would be appropriate in all cases. It is further recognized that the ability to accurately compute the sediment transport rate for a reach is also influenced by many factors including the natural variations in floodplain geometry, bed material composition, and hydraulic conditions; therefore, the modeling techniques documented herein consider the ratio of sediment transport rates for initial and projected conditions, as opposed to an absolute transport rate.

For the non-armored floodplain continuum, two sediment transport relationships developed by Yang (2003) have been used in these investigations. As indicated in Table 4.1, Equation 4.18 is for sand bed watercourses, while Equation 4.19 is for watercourses with beds composed of medium to fine gravel. Within the proposed modeling tool approach for non-armored floodplains, the selection of either Equation 4.18 or 4.19 is based upon the d_{50} or median grain size for the bed material, as indicated in Table 4.1.

Table 4.1 – Sediment transport relationships for sand or gravel beds by Yang (2003, p. 158 & p. 167)

For sand bed floodplains (0.062 mm < d_m < 2 mm):

$$\log C_{ts} = 5.435 - 0.286\log\frac{\omega_f d_m}{\upsilon} - 0.457\log\frac{U_*}{\omega_f}:$$
$$+\left(1.799 - 0.409\log\frac{\omega_f d_m}{\upsilon} - 0.314\log\frac{U_*}{\omega_f}\right)\log\left(\frac{VS_f}{\omega_f} - \frac{V_{cr}S_f}{\omega_f}\right) \qquad \text{Equation 4.18}$$

For gravel bed floodplains (2mm < d_m < 10 mm):

$$\log C_{tg} = 6.681 - 0.633\log\frac{\omega_f d_m}{\upsilon} - 4.816\log\frac{U_*}{\omega_f}:$$
$$+\left(2.784 - 0.305\log\frac{\omega_f d_m}{\upsilon} - 0.282\log\frac{U_*}{\omega_f}\right)\log\left(\frac{VS_f}{\omega_f} - \frac{V_{cr}S_f}{\omega_f}\right) \qquad \text{Equation 4.19}$$

For shear velocity: Equation 4.20

$$U_* = \left(gRS_f\right)^{1/2}$$

For critical dimensionless unit stream power:

$$\frac{V_{cr}}{\omega_f} = \frac{2.5}{\log\left(\frac{U_* d_m}{\upsilon}\right) - 0.06} + 0.66 \quad \text{for } 1.2 < \frac{U_* d_m}{\upsilon} < 70 \qquad \text{Equation 4.21}$$

or

$$\frac{V_{cr}}{\omega_f} = 2.05 \qquad \text{for } 70 \le \frac{U_* d_m}{\upsilon} \qquad \text{Equation 4.22}$$

Conversion of C_t *in* (ppm) to Q_s in (m³/s), for ρ_s =2647(kg/m³):

$$Q_s\,(\text{m}^3/\text{s}) = Q\,(\text{m}^3/\text{s}) \cdot \frac{1}{2647}\,(\text{m}^3/\text{kg}) \cdot 10^3\,(\text{l}/\text{m}^3) \cdot \frac{1}{10^6}\,(\text{kg}/\text{mg}) \cdot Q_s\,(\text{mg}/\text{l}) \qquad \text{Equation 4.23}$$

$$Q_s\,(\text{mg}/\text{l}) = \left(\frac{G \cdot C}{G + \left((1-G)10^{-6} \cdot C\right)}\right) \qquad \text{For } G = \frac{\gamma_s}{\gamma} = 2.65$$

where:
- C_{ts} = total sand concentration (ppm by weight)
- C_{tg} = total gravel concentration (ppm by weight)
- ω_f = fall velocity (m/s)
- d_m = median particle diameter (m)
- S_f = friction or energy slope (m/m)
- R = hydraulic radius (m)
- V = flow velocity (m/s)
- υ = kinematic viscosity = 1.0x10⁻⁶ (m²/s) at 20° C.
- g = acceleration of gravity = 9.81 (m/s²)

For the armored floodplain continuum, the two-fraction sediment transport relationships developed by Wilcock and Kenworthy (2002) have been used in these investigations. The equations and the steps for applying this sediment transport relationship are provided in Table 4.2. The two-fraction approach adopted by Wilcock and Kenworthy (2002) is unique in that it is able to capture variations in sand and gravel transport rates, as well as interactions between the two size fractions in a sand/gravel mixture. As reflected in Table 4.2, the added detail associated with the two-fraction approach is gained at the expense of greater computational complexity and the requirement of a full size distribution for the bed material.

4.5 Results and Discussion

4.5.1 Modeling Tool Solution Procedures for Non-Armored and Armored Floodplains

The core objective of this research was to develop *modeling tools* for estimating the trend and magnitude of the change in floodplain geometry due to an incremental change in intra-catchment processes (i.e., water and/or sediment supply). The approach adopted in this research is considered to be a hybrid regime modeling approach. To take into account the erosional resistance and stability characteristics of the banks, empirically based *floodplain response constraints* are used to define the interrelationship between adjustments in floodplain width, depth, and bed slope. These floodplain response constraints allow the computations to converge on a unique floodplain geometry for a given set of hydraulic conditions, when used in conjunction with the basic flow relationships of continuity, flow resistance, and sediment transport. The floodplain response constraints have been defined based on the analysis of field data for a wide range of floodplain geometries, within the semi-arid environment of southern California.

Table 4.2 – Two fraction sediment transport relationship for a surface layer composed of a sand/gravel mixture by Wilcock and Kenworthy (2002)

Step 1: *Compute Dimensionless Incipient Motion Criteria* $\left(\tau_{ri}^{*}\right)$

for i = sand (s) and gravel (g), given d_g, d_s, and F_s:

$$\tau_{ri}^{*} = \left(\tau_{ri}^{*}\right)_1 + \left(\left(\tau_{ri}^{*}\right)_0 - \left(\tau_{ri}^{*}\right)_1\right)e^{-14F_s} \qquad \text{Equation 4.24}$$

where $$\left(\tau_{rs}^{*}\right)_0 = \left(\tau_{rg}^{*}\right)_0\left(\frac{d_g}{d_s}\right) \qquad \text{Equation 4.25}$$

Constants per Table 3 in Wilcock and Kenworthy(2001, p. 12-10)

$$\left(\tau_{rs}^{*}\right)_1 = 0.065 \qquad \left(\tau_{rg}^{*}\right)_0 = 0.035 \qquad \left(\tau_{rg}^{*}\right)_1 = 0.011$$

Step 2: *Compute Shear Stress-to-Reference Shear Stress Ratio* (ϕ_i)

for i = sand (s) and gravel (g), given *total shear stress* (τ):

$$\phi_i = \frac{\tau}{\tau_{ri}}: \qquad \text{Equation 4.26}$$

where $$\tau = \gamma R S_f \qquad \text{Equation 4.27}$$

$$\tau_{ri} = \tau_{ri}^{*}(G-1)\gamma d_i \qquad \text{Equation 4.28}$$

Step 3: *Compute Volumetric Transport Rate per Unit Width* (q_{bi})

for i = sand (s) and gravel (g), with constants based on field data (p. 12-6):

$$\text{For } \phi_i = \frac{\tau}{\tau_{ri}} < 1.27: \quad q_{bi} = \left(\frac{0.002 \cdot F_i}{g(G-1)}\right) \cdot \left(\frac{\tau}{\rho}\right)^{3/2} \cdot (\phi_i)^{7.5} \qquad \text{Equation 4.29}$$

$$\text{For } \phi_i = \frac{\tau}{\tau_{ri}} \geq 1.27: \quad q_{bi} = \left(\frac{115 \cdot F_i}{g(G-1)}\right) \cdot \left(\frac{\tau}{\rho}\right)^{3/2} \cdot \left(1 - \frac{0.923}{(\phi_i)^{0.25}}\right)^{4.5} \qquad \text{Equation 4.30}$$

$Q_{bi} = W \cdot q_{bi}$ = volumetric transport rate (m³/s) Equation 4.31

where: q_{bi} = volumetric transport rate per unit width for i = sand (s) or gravel (g) fraction (m²/s)

$q_{bt} = q_{bs} + q_{bg}$ = total unit transport rate (m²/s)

F_s = sand fraction of surface bed material (range 0 to 1)

$F_g = 1 - F_s$ = gravel fraction of surface bed material (0 to 1)

d_i = characteristic grain size for the surface fraction "i" (m)

S_f = friction or energy slope (m/m)

R = hydraulic radius (m)

ρ = 1000 (kg/m³) = density of water at 20° C.

g = acceleration of gravity = 9.81 (m/s²)

$G = \gamma_s / \gamma = 2.65$ = specific gravity

γ = 9810 (kg/m²s²) = specific weight of water

In summary, the solution procedures for the *modeling tools* developed for the non-armored and armored floodplain continuums are comprised of the following four basic steps:

1. hydraulic and sediment transport computations for "initial" conditions;
2. identification and evaluation of a "best fit" trapezoidal cross section;
3. identification of the "projected" floodplain geometry; and
4. computation of the floodplain response trajectory.

Due in part to the geomorphic limits of this study (Figure 4.1) and the regime-type approach adopted in these investigations, the range of applicability of the modeling tools is limited to:

- floodplains that are at least initially stable and in a state of dynamic equilibrium;
- floodplains that can be reasonably well represented with a trapezoidal cross section;
- plane-fine-bed, plane-mixed-bed, pool-riffle, or braided floodplains in the non-armored floodplain continuum; and
- pool-riffle floodplains in the armored continuum.

The detailed solution procedures for the modeling tools are provided in Tables 4.3 and 4.5 for the non-armored armored floodplain continuums, respectively. To minimize the opportunity for misapplication, the modeling tool solution procedures (in Tables 4.3 and 4.5) include procedures to assess the initial stability state of the floodplain and to verify that that the floodplain can be represented with a trapezoidal cross section.

To illustrate the application of the *modeling tools*, example sets of computations are provided for a non-armored and armored floodplain in Tables 4.4 and 4.5, respectively. Each example set of computations use the data for one of the study sites and correspond to a 10 percent increase in the reference flow rate (i.e., Q_{100} in these cases), with no change in sediment supply.

Table 4.3a – Modeling tool solution procedure for non-armored floodplains

Step	Data Requirements and Solution Procedures – Part 1 of 2
A	**Data Requirements**: Initial condition floodplain cross sectional data and bed slope, estimated Manning's roughness coefficient *(n)* for the floodplain, bed gradation (i.e., d_{50}), and a reference flow rate.
1	**Analyses for Initial Conditions**: The objectives of this step are to a. ***Hydraulic Analysis for Initial Conditions***: For the reference flow rate and given floodplain geometry, compute flow velocity (V), flow depth (d), hydraulic radius (R), topwidth (W), width-to-depth ratio (W/d), and specific stream power (ω). This can be accomplished iteratively using Manning Equation (Eq. 4.3) or with various hydraulic software packages. b. ***Compute Sediment Transport Rate/Capacity***: Compute/estimate the sediment transport rate for initial conditions $(Q_s)_{initial}$, in (m^3/s) using Equations 4.18 or 4.19 and 4.23 per steps in Table 4.1. c. ***Compute Stability State for Initial Conditions***: For $X_1 = log_{10}(W/d)$ and $X_2 = log_{10}(\omega)$, compute the *probability that the floodplain is unstable and in state of severe instability* (i.e., $P(Y=S_A)$) using Equation 3.22 plus the intercept and partial slope coefficients (β_0=-32.7596, β_1 = 6.4391, and β_2=11.9589) given in Table 3.9. If the value for P(Y=S_A=unstable) is substantial (say > 30%), the floodplain may be unstable and this regime-type approach may be inappropriate for assessing potential floodplain responses.
2	**Identification and Evaluation of "Best Fit" Trapezoidal Cross Section**: The objectives of this step are to (i) identify the "Best Fit" trapezoidal section for the natural cross section in terms of width-to-depth ratio (W/d) and side-slope (z); and (ii) assess if the trapezoidal cross section assumption is valid. a. ***Identification of "Best Fit" Trapezoidal Section***: This step requires an iterative solution for W/d and z as follows, for given values of Q, n, and S_f: • For initial values of W/d and z, compute values of d, W, R, A, V, and ω using Equations 4.15, 4.16, 4.12, 4.9, 4.3, and 4.17, respectively. Use these hydraulic parameters and d_{50} to compute Q_s in (m^3/s) using Equations 4.18 or 4.19 and 4.23 per steps in Table 4.1. • Vary values for W/d and z until the following constraints are met: $$\left(\frac{(Q_s)_{initial}}{(Q_s)_{best-fit}}\right) \cong \left(\frac{(W)_{initial}}{(W)_{best-fit}}\right) \cong \left(\frac{(d)_{initial}}{(d)_{best-fit}}\right) \cong 1$$ where "*initial*" refers to values computed in Step 1 "*best-fit*" refers to values computed in this step This step can be accomplished using Solver in Excel ® by setting the cells for W/d and z as the "changing cells", while setting the "target" cell to that with the sum of the absolute or squared value for the cumulative error associated with the ratios for Q_s, W, and d. b. ***Compute Stability State for Initial Conditions***: For $X_1 = log_{10}(W/d)$ and $X_2 = log_{10}(\omega)$, compute the *probability that the floodplain is unstable and in state of severe instability* (i.e., $P(Y=S_A)$) using Equation 3.22 plus the intercept and partial slope coefficients (β_0=-32.7596, β_1 = 6.4391, and β_2=11.9589) given in Table 3.9. c. ***Compute Probability for Floodplain Braiding***: For $X_1 = log_{10}(W/d)$ and $X_2 = log_{10}(\omega)$, compute the *probability that the floodplain is braided* (i.e., $P(Y=S_B)$) using Equation 3.22, plus the intercept and partial slope coefficients (β_0= 42.1887, β_1 = -19.0285, and β_2=-5.8813) given in Table 3.9. d. ***Assess "Best Fit" Floodplain Geometry***: The assumption of a trapezoidal cross section is valid only if: (i) the ratios for the values of Qs , W, and d computed in Step 2a are nearly 1; and (ii) the values for P(Y=S_A=unstable) computed in Steps 1c and 2b are nearly equal.

Table 4.3b – Modeling tool solution procedure for non-armored floodplains

<table>
<tr><th>Step</th><th>Data Requirements and Solution Procedure – Part 2 of 2</th></tr>
<tr><td>3</td><td>Compute and Assess Floodplain Response: The objective of this step is to identify the projected floodplain geometry (in terms of W/d) corresponding to a new flow discharge and the same sediment transport rate computed in Step 2e.
a. Identification of “Projected” Floodplain Geometry: This step requires an iterative solution for W/d as follows, for given values of $(Q)_{projected}$, z (from Step 3a), n, and S_f:
• For an initial value of W/d , compute values of d, W, R, A, V, and ω using Equations 4.15, 4.16, 4.12, 4.9, 4.3, and 4.17, respectively. Use these hydraulic parameters to compute Q_s in (m^3/s) using Equations 4.18 or 4.19 and 4.23 per steps in Table 4.1.
• Vary the values for values W d, until the following constraint is met:
$\left(\frac{(Q_s)_{initial}}{(Q_s)_{computed}}\right)=1$
where “initial” refers to values computed in Step 1
“computed” refers to values computed in this step
This step can be accomplished using Solver in Excel ® by setting the cell for W/d as the “changing cell”, while setting the “target” cell to that with the absolute or squared value for the error associated with the ratio for Q_s .
• Note: this step is simplified by the floodplain response constraint identified for the non-armored floodplain continuum that specifies: For incremental increases in flow rate, the <u>width-to-depth ratio varies </u>, while the bed slope remains relatively constant (as described in Section 3.5.6).
b. Compute Stability State for Project Floodplain Geometry: For $X_1 = log_{10}(W/d)$ and $X_2 = log_{10}(\omega)$, compute the probability that the floodplain is unstable and in state of severe instability (i.e., $P(Y{=}S_A)$) using Equation 3.22 plus the intercept and partial slope coefficients (β_0=-32.7596, β_1 = 6.4391, and β_2 =11.9589) given in Table 3.9.
c. Compute Probability for Floodplain Braiding: For $X_1 = log_{10}(W/d)$ and $X_2 = log_{10}(\omega)$, compute the probability that the floodplain is braided (i.e., $P(Y{=}S_B)$) using Equation 3.22, plus the intercept and partial slope coefficients (β_0 = 42.1887, β_1 = -19.0285, and β_2 =-5.8813) given in Table 3.9.</td></tr>
<tr><td>5</td><td>Compute and Plot Floodplain Response Trajectories (optional step): Floodplain response trajectories are a curve that describes the range of geomorphic characteristics (in terms of ω and W/d) that a trapezoidal floodplain may have for a constant Q, n, z, and S_f. Response trajectories can provide a useful visual reference for evaluating the results of this modeling tool; however, they are not required.
a. Computation of Floodplain Response Trajectory: For given values of Q, n, z, and Sf; compute ω for a range of W/d values using Equation 4.17. The range of W/d values should start at approximately the same value of W/d computed in Step 1a.
b. Plotting of Floodplain Response Trajectory: The floodplain response trajectory curve can be plotted on the floodplain state diagram (3.12b) for non-armored floodplains and should pass through the point corresponding to the projected floodplain geometry.</td></tr>
</table>

Table 4.4a – Example floodplain response analysis for a non-armored floodplain

Step 1a: Hydraulic Analysis for Initial Conditions									
Site/Prof. ID	*Q* (m^3/s)	*n*	S_f	*V* (m/s)	*d* (m)	*R* (m)	*W* (m)	*W/d*	*ω* (W/m^2)
PLSD03P06	6.18	0.030	0.0056	1.29	0.57	0.356	12.57	22.06	26.8

Step 1b: Sediment Transport Rate/Capacity for Initial Conditions						
d_m (m)	ω_f (m/s)	$(U_* d_m)/\nu$	V_{cr}/ω_f	$Log(C_{ppm})$	C_{ppm}	$(Q_s)_{initial}$ (m^3/s)
0.00076	0.0703	108.8	2.05	3.76	5792.7	0.0135

Step 1c: Stability State for Initial Conditions					
β_0	β_1	β_2	X_1=log(W/d)	X_2=log(ω)	*P(Unstable)*
-32.7596	6.4391	119589	1.344	1.427	0.088 %

Step 2a: Identification of "Best Fit" Trapezoidal Section (See cross section plot below)										
Changing Cells		*Computed Parameters*								
W/d	***z***	*d* (m)	*W* (m)	*R* (m)	*A* (m^2)	*V* (m/s)	*ω* (W/m^2)	$(U_* d_m)/\nu$	$Log(C_{ppm})$	$(Q_s)_{best\ fit}$ (m^3/s)
22.06	7.388	0.57	12.5	0.377	4.77	1.30	26.8	108.9	3.76	0.0136

Step 2a: Constraint Ratios and Error Target Cell			
Constraint Ratios			***Target Cell***
Q_s Ratio	*W* Ratio	*d* Ratio	Error (sum of the errors squared)
1.002	1.000	1.000	3.6×10^{-6}

Steps 2b & 2c: Stability State and Probability for Braiding: "Best Fit" Floodplain Geometry							
Threshold	β_0	β_1	β_2	X_1=log(W/d)	X_2=log(ω)	*P(Unstable)*	*P(Braided)*
Stability	-32.7596	6.4391	119589	1.344	1.427	0.088 %	
Braiding	42.1887	-19.0285	-5.8813	1.344	1.427		0.026 %

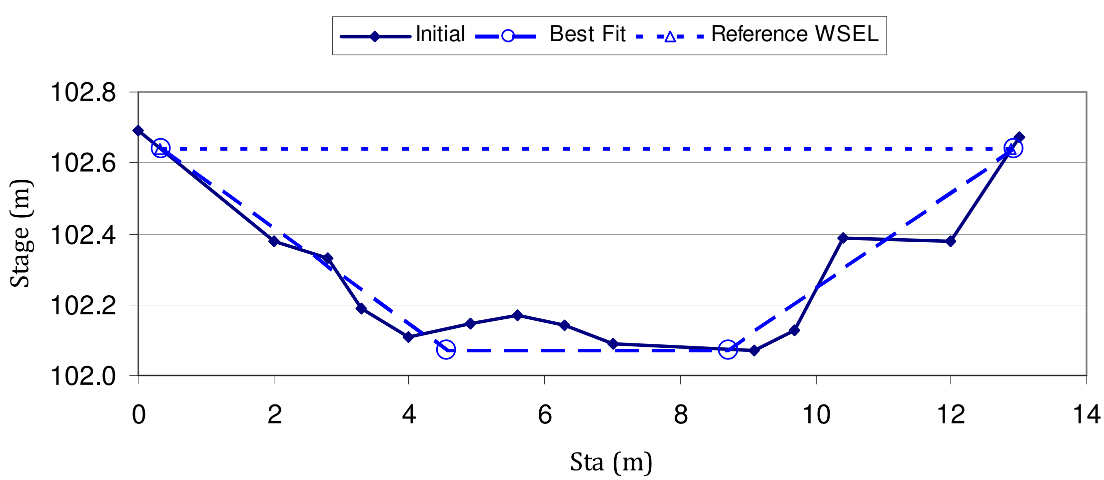

Step2a - Cross Section Plot (PLSD03): "Best Fit" vs. Existing

Table 4.4b – Example floodplain response analysis for a non-armored floodplain

Step 3a: Identification of "Projected" Floodplain Geometry (See plots below)										
$(Q)_{new}$ = 6.80 (m^3/s) : an increase of approximately 10%										
Changing Cells		*Computed Parameters*								
W/d	***z***	*d* (m)	*W* (m)	*R* (m)	*A* (m^2)	*V* (m/s)	*ω* (W/m^2)	$(U_* d_m)/\nu$	$Log(C_{ppm})$	$(Q_s)_{Projected}$ (m^3/s)
44.5	7.388	0.39	17.5	0.327	5.75	1.18	21.1	101.5	3.72	0.0135

Step 3a: Constraint Ratios and Error Target Cell	
Constraint Ratio	***Target Cell***
Q_s Ratio	Error (sum of the errors squared)
1.0000	8.9×10^{-20}

Steps 3b & 3c: Stability State and Probability for Braiding: "Projected" Floodplain Geometry							
Threshold	β_0	β_1	β_2	X_1=log(W/d)	X_2=log(ω)	*P(Unstable)*	*P(Braided)*
Stability	-32.7596	6.4391	119589	1.648	1.325	0.18 %	
Braiding	42.1887	-19.0285	-5.8813	1.648	1.325		4.60 %

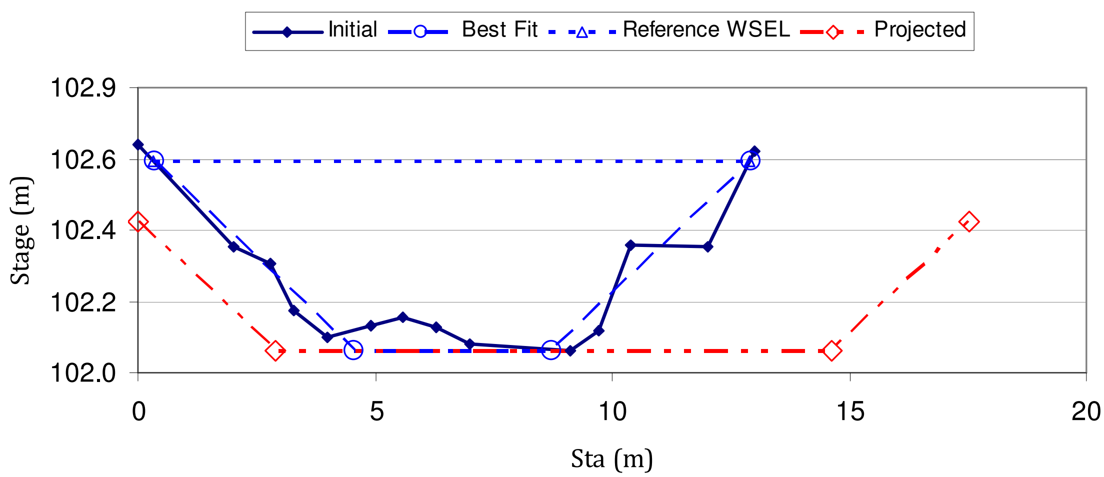

Step3a - Cross Section Plot (PLSD03): "Projected" vs. Existing

Logistic Stability and Braiding Thresholds:
***Stable* Floodplains** (Solid Symbols) vs. ***Unstable* Floodplains** (Hollow Symbols)

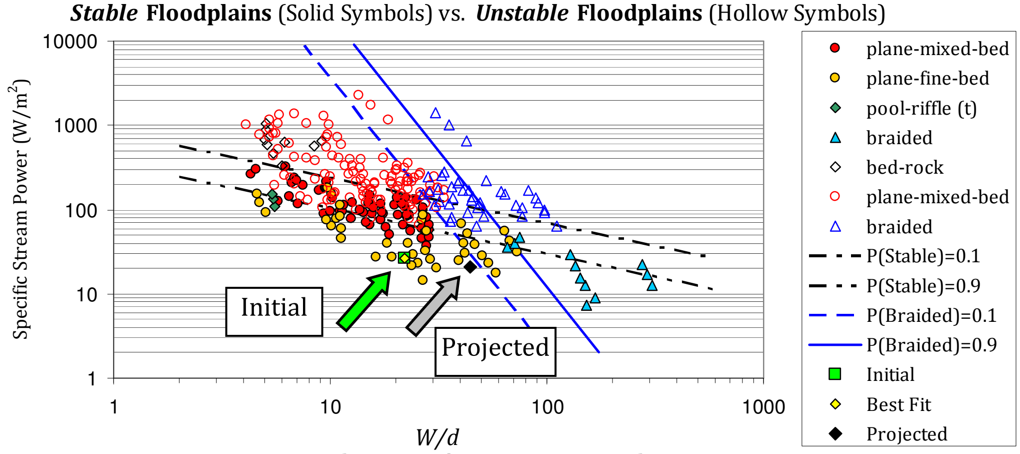

Step 3a - Regime diagram for non-armored continuum

Table 4.4c – Example floodplain response analysis for a non-armored floodplain

Step 4a: Computation of Floodplain Response Trajectory (See plot below)			
$(Q)_{new}$ (m³/s)	*n*	*z*	S_f
6.80	0.030	7.388	0.00556
W/d	*d* (m)	*W* (m)	ω (W/m²)
22	0.592	13.02	28.5
25	0.544	13.59	27.3
50	0.372	18.60	20.0
100	0.272	27.22	13.6
200	0.205	41.00	9.0
400	0.156	62.41	5.9
600	0.134	80.10	4.6

Logistic Stability and Braiding Thresholds:
***Stable* Floodplains** (Solid Symbols) vs. ***Unstable* Floodplains** (Hollow Symbols)

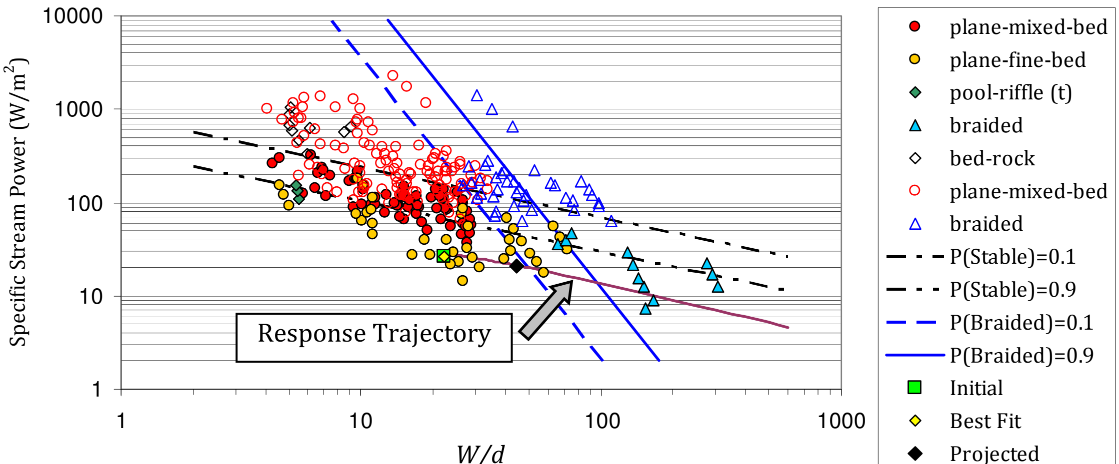

Step 4a - Regime diagram for non-armored continuum

Table 4.5a – Modeling tool solution procedure for armored floodplains

<table>
<tr><th>Step</th><th>Modeling Tool for Armored Floodplains:
Data Requirements and Solution Procedure – Part 1 of 3</th></tr>
<tr><td>A</td><td>Data Requirements: Initial condition floodplain cross sectional data and bed slope, estimated Manning n-value for floodplain, bed gradation data (i.e., F_s, F_g, d_s, and d_g), and a reference flow rate.</td></tr>
<tr><td>1</td><td>Analyses for Initial Conditions: The objectives of this step are to
a. Hydraulic Analysis for Initial Conditions: For the reference flow rate and given floodplain geometry, compute flow velocity (V), flow depth (d), hydraulic radius (R), topwidth (W), width-to-depth ratio (W/d), and specific stream power (ω). This can be accomplished iteratively using Manning Equation (Eq. 4.3) or with various hydraulic software packages.
b. Compute Sediment Transport Rate/Capacity: Compute/estimate the sediment transport rate for initial conditions (i.e., $(Q_{bs})_{initial}$ and $(Q_{bg})_{initial}$, in (m^3/s)) using Equations 4.29 or 4.30 and Equation 4.31 per procedure in Table 4.2.
c. Assess Stability State for Initial Conditions: Using the values computed for W/d and ω, plot this point on the floodplain state diagram for the armored floodplain continuum (Figure 3.13b). If this point lies outside of the general regions defined by the data points for the pool-riffle floodplain form, then the floodplain may be either unstable or not a pool-riffle floodplain. In either of these cases, this regime-type modeling approach may be inappropriate.</td></tr>
<tr><td>2</td><td>Identification and Evaluation of "Best Fit" Trapezoidal Cross Section: The objectives of this step are to (i) identify the "Best Fit" trapezoidal section for the natural cross section in terms of width-to-depth ratio (W/d) and side-slope (z); and (ii) assess if the trapezoidal cross section assumption is valid.
a. Identification of "Best Fit" Trapezoidal Section: This step requires an iterative solution for W/d and z as follows, for given values of Q, n, and S_f:
• For initial values of W/d and z , compute values of d, W, R, A, V, and ω using Equations 4.15, 4.16, 4.12, 4.9, 4.3, and 4.17, respectively. Use these hydraulic and gradation parameters to compute Q_{bs} and Q_{bg} in (m^3/s) using Equations 4.29 or 4.30 and Equation 4.31 per the procedure in Table 4.2.
• Vary values for W/d and z until the following constraints are met:
$$\left(\frac{(Q_{bs})_{initial}}{(Q_{bs})_{best-fit}}\right)=\left(\frac{(Q_{bg})_{initial}}{(Q_{bg})_{best-fit}}\right)=\left(\frac{(W)_{initial}}{(W)_{best-fit}}\right)=\left(\frac{(d)_{initial}}{(d)_{best-fit}}\right)=1$$
where "initial" refers to values computed in Step 1
"best-fit" refers to values computed in this step
This step can be accomplished using Solver in Excel ® by setting the cells for W/d and z as the "changing cells", while setting the "target" cell to that with the sum of the absolute or squared value for the cumulative error associated with the ratios for Q_{bs} , Q_{bg} , W, and d .
b. Assess "Best Fit" Floodplain Geometry: The assumption of a trapezoidal cross section is valid only if the ratios for the values of Q_s , W, and d computed in Step 3a are nearly 1.</td></tr>
</table>

Table 4.5b – Modeling tool solution procedure for armored floodplains

<table>
<tr><th>Step</th><th>Modeling Tool for Armored Floodplains:
Data Requirements and Solution Procedure – Part 2 of 3</th></tr>
<tr><td>3</td><td>Compute and Assess Floodplain Response: The objective of this step is to identify the projected floodplain geometry (in terms of W/d) corresponding to a new flow discharge and the same sediment transport rate computed in Step 2e.
a. Identification of “Projected” Floodplain Geometry: This step requires an iterative solution for W/d as follows, for given values of $(Q)_{projected}$, z (from Step 3a), and n, :
• For initial values b, d, and S_f; compute values of W, R, A, W/d, Q, and ω, using Equations 4.6, 4.7, 4.4, 4.8, 4.13, and 4.17, respectively. Use these hydraulic and gradation parameters to compute Q_{bs} and Q_{bg} in (m^3/s) using Equations 4.29 or 4.30 and Equation 4.31 per the procedure in Table 4.2.
• Vary the values for values b, d, and S_f until the following constraints are met:
$$\left(\frac{(Q_{bs})_{initial}}{(Q_{bs})_{computed}}\right)=\left(\frac{(Q_{bg})_{initial}}{(Q_{bg})_{computed}}\right)=\left(\frac{(Q)_{projected}}{(Q)_{computed}}\right)=1 \text{ and}$$
$$C_R=\frac{\left(\log(\omega)_{computed}-\log(\omega)_{initial}\right)}{\left(\log(\mathrm{T})_{computed}-\log(\mathrm{T})_{initial}\right)}\cong -3.2$$
where “initial” refers to values computed in Step 1
“computed” refers to values computed in this step
“C_R “ constraint ratio per Equation 4.1b.
This step can be accomplished using Solver in Excel ® by setting the cells for b, d, and S_f as the “changing cells”, while setting the “target” cell to that with the absolute or squared value for the cumulative error associated with the four constraints listed above.
b. Assess Stability State for Project Floodplain Geometry: Using the values computed for W/d and ω, plot this point on the floodplain state diagram for the armored floodplain continuum (Figure 3.13b). If this point lies outside of the general regions defined by the data points for the pool-riffle floodplain form, then the floodplain may be either unstable or not a pool-riffle floodplain. In either of these cases, this regime-type modeling approach may be inappropriate.
c. Visual Assessment of “Projected” Floodplain Geometry: Given W/d and ω for both the initial and projected floodplain geometries, points corresponding to both the initial and projected floodplain geometries can be plotted on Figure 3.21b to provide a visual assessment of the floodplain in terms of both the stability and braiding thresholds. Potential for Braiding: As described in Section 3.5.4, this author contends that the effects of bed material fining (i.e., an increase in the percent sand in the surface layer) acting in conjunction with the hypothesized water to sediment supply divergence process are the two mechanisms responsible for floodplain braiding in the armored floodplain continuum. Hence it is important to recognize that even though the logistic braiding thresholds shown in Figure 3.13b may provide a useful visual reference, the logistic braiding thresholds should not be used alone to assess the probability for floodplain braiding, since the logistic analysis did not consider the influence of bed material gradation. The data shown in Figure 3.9 suggests that as the percentage of sand sized particles in the surface layer increases above approximately 8 to 12 percent, the probability that a pool-riffle floodplain will transition to a braided floodplain increases significantly. Therefore, this modeling tool may be inappropriate if the percentage of sand sized particles in the bed gradation is > ~ 10% .</td></tr>
</table>

Table 4.5c – Modeling tool solution procedure for armored floodplains

Step	Modeling Tool for Armored Floodplains: Data Requirements and Solution Procedure – Part 3 of 3
4	**Compute and Plot Floodplain Response Trajectories (optional step)**: Floodplain response trajectories are a curve that describes the range of geomorphic characteristics (in terms of ω and W/d) that a trapezoidal floodplain may have for a constant Q, n, and z. Response trajectories can provide a useful visual reference for evaluating the results of this modeling tool; however, they are not required. a. ***Computation of Floodplain Response Trajectory***: This step requires an iterative solution for W/d as follows, for given values of $(Q)_{projected}$, z , and n, : • For initial values b and d, compute values of W, R, A, W/d, Q, and ω using Equations 4.6, 4.7, 4.4, 4.8, 4.13, and 4.17, for a range of bed slopes that span the initial bed slope. • Vary the values for values b, d, and S_f until the following constraints are met: $\left(\frac{(Q)_{projected}}{(Q)_{computed}}\right) = 1$ and $C_R = \frac{\left(\log(\omega)_{computed} - \log(\omega)_{initial}\right)}{\left(\log(\mathrm{T})_{computed} - \log(\mathrm{T})_{initial}\right)} \cong -3.2$ where "*initial*" refers to values computed in Step 1 "*computed*" refers to values computed in this step "C_R " = constraint ratio per Equation 4.1b This step can be accomplished using Solver in Excel ® by setting the cells for b and d as the "changing cells", while setting the "target" cell to that with the absolute or squared value for the cumulative error associated with the two constraints listed above. b. ***Plotting of Floodplain Response Trajectory***: The floodplain response trajectory curve can be plotted on the floodplain state diagram (3.13b) for armored floodplains and should pass through the point corresponding to the projected floodplain geometry.

Table 4.6a – Example floodplain response analysis for an armored floodplain

Step 1a: Hydraulic Analysis for Initial Conditions									
Site/Prof. ID	Q (m^3/s)	n	S_f	V (m/s)	d (m)	R (m)	W (m)	W/d	ω (W/m^2)
SCSA07P06	135.95	0.04	0.014	3.8	2.03	1.46	23.4	11.54	797.9

Step 1b: Sediment Transport Rate/Capacity for Initial Conditions							
F_s	d_s (m)	τ^*_{rs}	τ (Pa = kg/ms^2)	τ_{rs} (Pa = kg/ms^2)	ϕ_s	q_{bs} (m^2/s)	$(Q_{bs})_{initial}$ (m^3/s)
0.0909	0.001	0.4487	199.95	7.26	27.53	0.00567	0.1327
F_g	d_g (m)	τ^*_{rg}	τ (Pa = kg/ms^2)	τ_{rg} (Pa = kg/ms^2)	ϕ_g	q_{bg} (m^2/s)	$(Q_{bg})_{initial}$ (m^3/s)
0.9091	0.041	0.0177	199.95	11.76	17.00	0.03775	0.8834

Step 2a: Identification of "Best Fit" Trapezoidal Section										
Changing Cells		*Computed Parameters*								
W/d	***z***	d (m)	W (m)	R (m)	ω (W/m^2)	τ (Pa=kg/ms^2)	ϕ_s	$(Q_{bs})_{best\ fit}$ (m^3/s)	ϕ_g	$(Q_{bg})_{best\ fit}$ (m^3/s)
11.71	3.02	2.03	23.7	1.46	787.3	200.96	27.67	0.1360	17.08	0.9064

Step 2a: Constraint Ratios and Error Target Cell				
Constraint Ratios				***Target Cell***
Q_{bs} Ratio	Q_{bg} Ratio	W Ratio	d Ratio	Error (sum of the errors squared)
0.975	0.976	0.987	1.001	1.4×10^{-3}

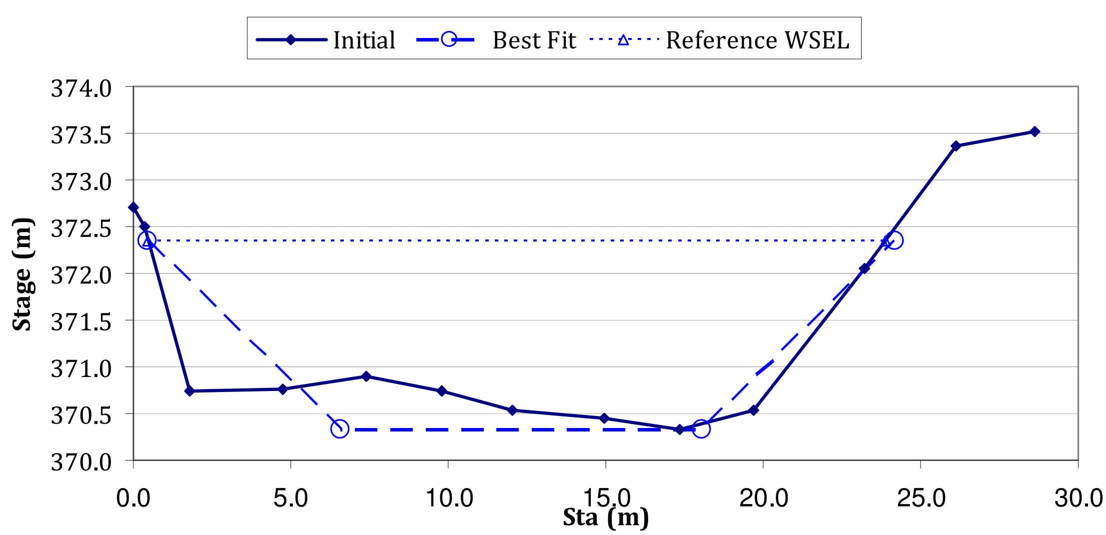

Step 2a - Cross Section Plot (SCSA07): "Best Fit" vs. Existing

Table 4.6b – Example floodplain response analysis for an armored floodplain

Step 3a: Identification of "Projected" Floodplain Geometry											
$(Q)_{new}$ = 149.55 (m^3/s) : an increase of approximately 10%											
Changing Cells			*Computed Parameters*								
S_f	b (m)	d (m)	W (m)	R (m)	W/d	A (m^2)	Q (m^3/s)	ω (W/m^2)	τ (Pa=kg/ms^2)	$(Q_{bs})_{Prj}$ (m^3/s)	$(Q_{bg})_{Prj}$ (m^3/s)
0.0131	12.20	2.12	24.98	1.53	11.8	39.3	149.5	767.6	196.6	0.1363	0.9047

Step 3a: Constraint Ratios and Error Target Cell				
Constraint Ratios				***Target Cell***
Q_{bs} Ratio	Q_{bg} Ratio	Q Ratio	C_R	Error (sum of the errors squared)
0.9979	1.0019	1.0002	-3.20	7.8x10^{-6}

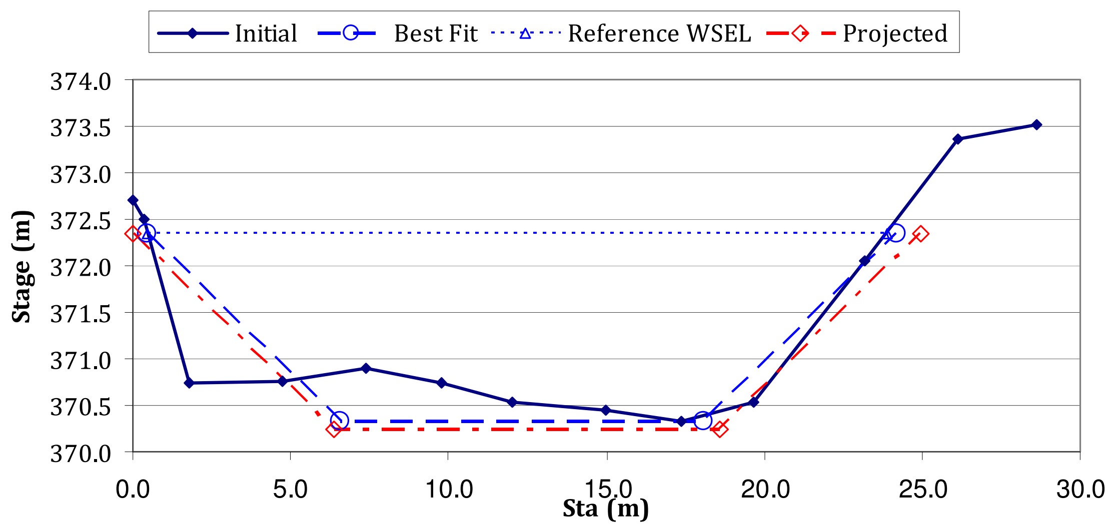

Step 3a - Cross Section Plot (SCSA07): "Projected" vs. Existing

***Stable* Floodplains** (Solid Symbols) vs. ***Unstable* Floodplains** (Hollow Symbols)

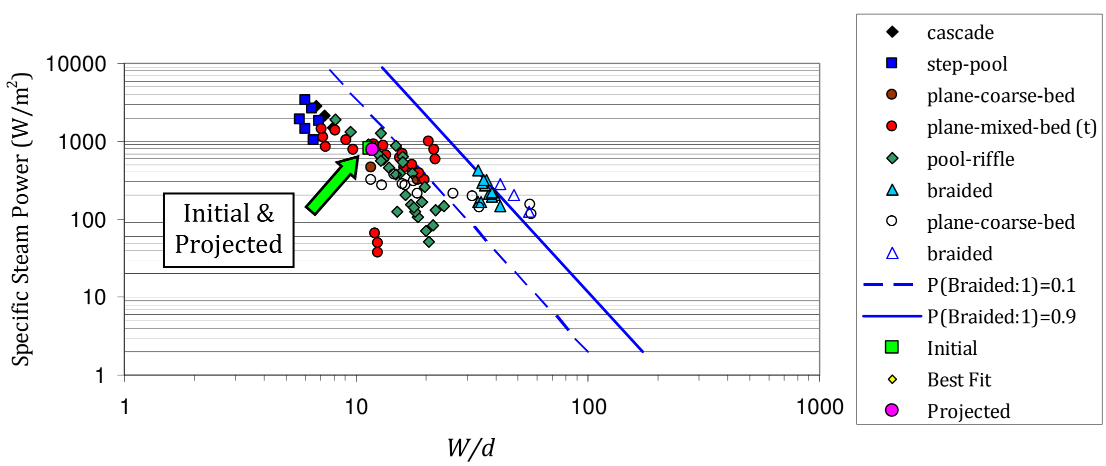

Step 3a - Regime diagram for armored floodplain continuum

Table 4.6c – Example floodplain response analysis for an armored floodplain

Step 4a: Compute Floodplain Response Trajectory (See plot below)											
(Q)$(Q)_{new}$ = 149.55 (m³/s) : an increase of approximately 10%											
Set	***Changing Cells***		*Computed Parameters*						*Constraint Ratios*		*Error*
S_f	*b* (m)	*d* (m)	*W* (m)	*R* (m)	*W/d*	A (m²)	*Q* (m³/s)	*ω* (W/m²)	*Q* Ratio	C_R	
0.01600	10.30	2.15	23.3	1.5	10.8	36.0	149.5	1009.2	1.000	-3.200	2.4E-10
0.01500	10.89	2.14	23.8	1.5	11.1	37.0	149.5	925.2	1.000	-3.200	3.1E-10
0.01400	11.54	2.13	24.4	1.5	11.5	38.2	149.5	842.7	1.000	-3.200	5.1E-11
0.01300	12.26	2.12	25.0	1.5	11.8	39.4	149.5	762.1	1.000	-3.200	1.0E-10
0.01200	13.06	2.10	25.8	1.5	12.2	40.9	149.5	683.4	1.000	-3.200	4.7E-09
0.01100	13.96	2.09	26.6	1.6	12.7	42.5	149.5	606.8	1.000	-3.200	4.6E-10
0.01000	14.99	2.08	27.6	1.6	13.2	44.3	149.5	532.4	1.000	-3.200	4.5E-10
0.00900	16.17	2.07	28.7	1.6	13.8	46.4	149.5	460.5	1.000	-3.200	1.2E-10
0.00800	17.57	2.06	30.0	1.6	14.6	49.0	149.5	391.4	1.000	-3.200	1.3E-09
0.00700	19.24	2.05	31.6	1.6	15.4	52.0	149.5	325.1	1.000	-3.200	5.9E-11
									Sum of Errors =		7.8E-09
											Target

Stable **Floodplains** (Solid Symbols) vs. ***Unstable*** **Floodplains** (Hollow Symbols)

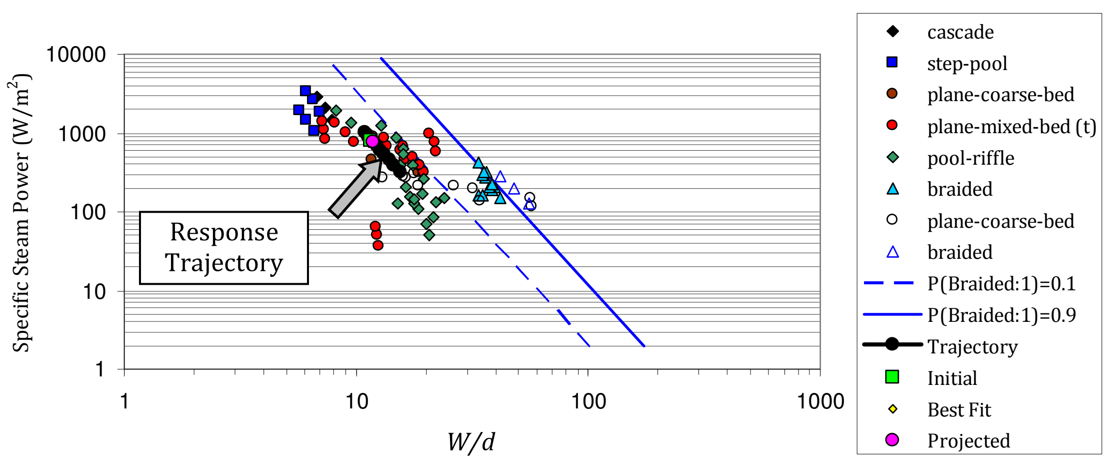

Step 4a - Regime diagram for armored floodplain continuum

Sections 4.5.2 through 4.5.5 describe investigations into both the validity and implications of the *modeling tools* and the associated *floodplain response constraints*. More specifically, Section 4.5.2 describes the comparison of the results from the modeling tools with the observed downstream progression of floodplain geometry for the non-armored floodplain featured in the example computations (Table 4.4). Sections 4.5.3 and 4.5.4 describe the significance and implications of the interrelationships between the *floodplain response trajectories* and the geomorphic thresholds for the non-armored and armored floodplain continuums. Whereas, the results from the two sets of example computations for the *non-armored* and *armored* floodplain are compared and discussed in Section 4.5.5.

4.5.2 Comparison of Projected and Natural Downstream Progression of Floodplain Geometry

The core objective of this research was to develop *modeling tools* for estimating the trend and magnitude of the change in floodplain geometry, due to an incremental change in intra-catchment processes. However, the results from applying the modeling tool can be viewed from two perspectives: *at-a-station* and *downstream*. From an *at-a-station* perspective, the results of applying the modeling tool are interpreted to reflect the changes in floodplain geometry anticipated at a specific location over time, due to the impacts of urbanization; however, the results can also be viewed to reflect the anticipated changes in floodplain geometry in a *downstream* direction along a watercourse.

As with any computational tool, it is important to test and validate the applicability of the tool. Though survey controls have been established to allow the collection of data at the *modeling level* sites over time, these investigations did not include collecting field data that could be used to assess the results of the *modeling tools* in terms of an *at-a-station* response. However, sufficient data were collected to allow at least the qualitative comparison of the results of the modeling tool with *downstream* changes in floodplain geometry.

Using observed *downstream* changes in floodplain geometry as a substitution for *at-a-station* changes in floodplain geometry is typically referred to as a "space for time" substitution and has been employed by other researchers in a similar context (Schumm et al., 1984). Furthermore, I contend that the primary impact of urbanization is a self enhancing feedback mechanism to the intra-catchment processes that may govern the downstream progression of floodplain geometry, based on the arguments provided in Section 3.5.2. If this contention is reasonably accurate, then the "space for time" substitution is also reasonable in this context. In the example case study described in the remainder of this section, the "observed" downstream progression of floodplain geometry for a watercourse is compared with "projected" geometry changes estimated with the *modeling tools* (Table 4.3) for incremental increases in the reference discharge, which in this case is the estimated 100 year event.

The example floodplain response analysis, included in Table 4.4, is for a study site located within the Lake Perris State Recreation Area (Riverside County). At this study site, data were collected for three cross sections along the un-named watercourse. More specifically, the analysis in Table 4.4 is for the upstream most cross section, at the study site, and corresponds to an increase in the reference flow rate of 10 percent. In addition, floodplain response analyses have been performed corresponding to increases in the reference flow rate of 20, 30, and 40 percent. The results for these four analyses are shown in Figure 4.3, along with the *floodplain response trajectory* corresponding to an increase in the reference flow rate of 30 percent.

To allow comparison of the "projected" and "observed" downstream progression of floodplain geometry, the observed floodplain progression for the same study site is also shown in Figure 4.3, where the two downstream floodplain geometries correspond to increases in the reference flow rate of approximately 20 and 30 percent. Since the analyses for the "projected" floodplain geometries only consider increases in water supply, it is important to recognize that this isn't entirely a direct comparison, due to the tributaries within the study reach that contribute both water and sediment supply. Yet even with this limitation in the analyses, there is still relatively close agreement between the "projected" and "observed" progression of floodplain geometry in terms of both trend and magnitude, as can be seen in Figure 4.3b.

Though the case study described in this section may provide a compelling argument, it is fully recognized that this one case study does not thoroughly validate the *modeling tools*; hence, other means of testing the validity of various aspects of the *modeling tools* have been explored. In Sections 4.5.3 and 4.5.4, the floodplain response trajectories associated with the *modeling tools* are compared in terms of the field data and the geomorphic thresholds.

4.5.3 Floodplain Response Trajectories in Terms of the Stability Thresholds and Sediment Transport Rates for Non-Armored Floodplains

For floodplains with a relatively trapezoidal cross section in the non-armored continuum, Equation 4.17 can be used to generate *floodplain response trajectories* that can be plotted directly onto the floodplain state diagram (3.12b). Equation 4.17 incorporates the *floodplain response constraint* that indicates that the primary response to incremental increases in discharge is an increase in the width-to-depth ratio, while the bed slope remains relatively constant.

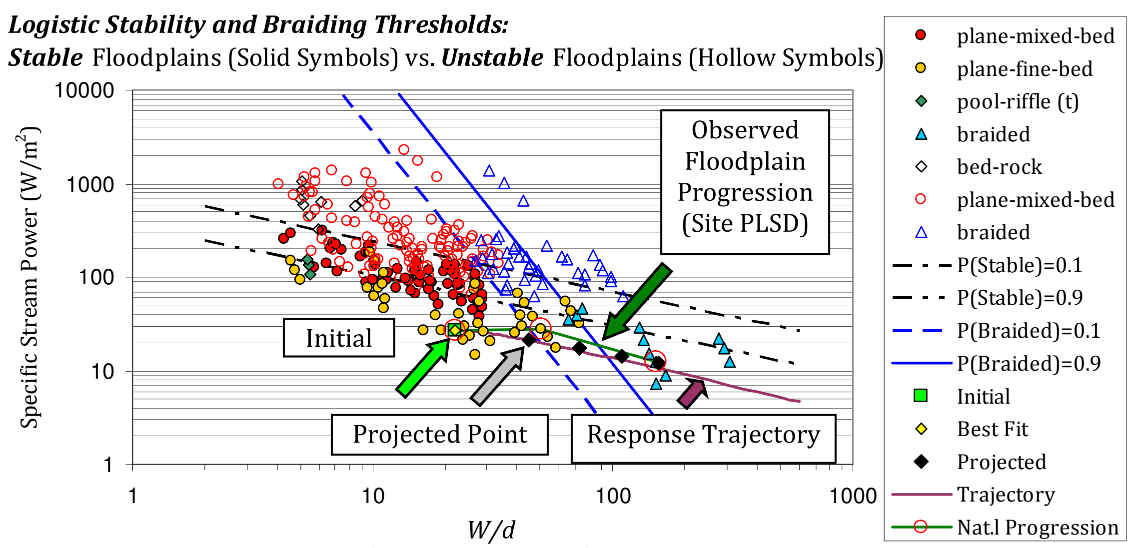

Figure 4.3a: Regime diagram for non-armored floodplain continuum

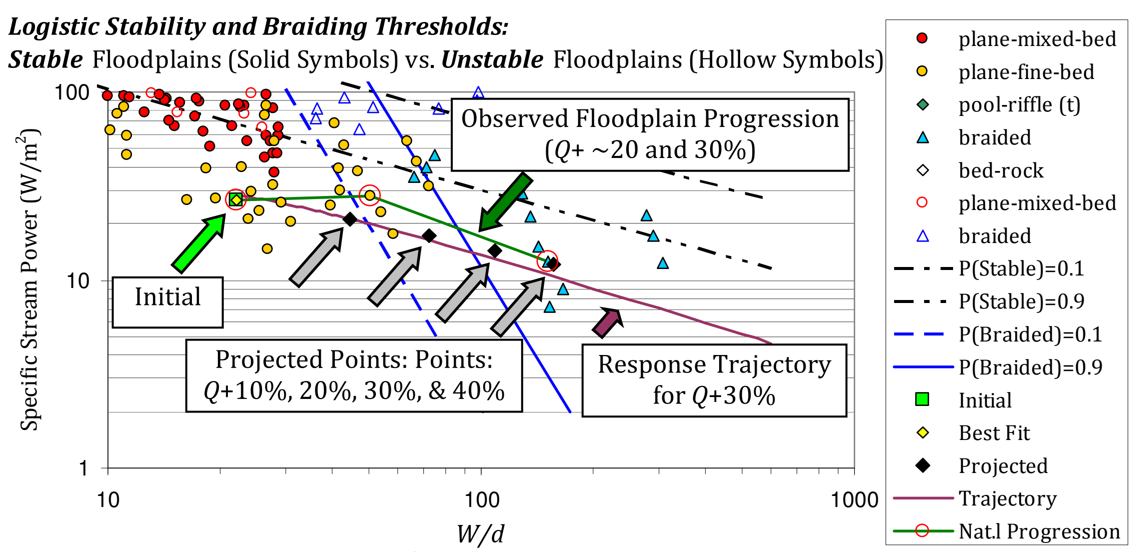

Figure 4.3b: "Zoom-in" on part of regime diagram (non-armored)

Figure 4.3 – Comparison of the results for the example floodplain response analysis with the natural floodplain progression

In Figure 4.4a, the results from the example floodplain response analyses provided in Table 4.4 are shown, including the floodplain response trajectory computed with Equation 4.17. In addition, the computed sediment transport capacity corresponding to the floodplain geometry reflected in the response trajectory is also shown in Figure 4.4a. The following two key observations can be made from Figure 4.4a:

- The floodplain response trajectory is a gentle curve that is essentially parallel to the logistic stability thresholds. If the floodplain trajectory curve (based on Equation 4.17) crossed the logistic stability threshold lines, this would be a clear indication that either the floodplain response constraint incorporated into Equation 4.17 is invalid or the slope of the logistic stability thresholds are inconsistent with the basic flow relationships of continuity and resistance. The logic behind this interpretation is that the probability that a floodplain geometry is unstable should not increase simply because the width-to-depth ratio increases, which would be the case if the floodplain trajectory crossed the stability threshold lines. Therefore, the observation that the floodplain response trajectories and the floodplain stability thresholds are nearly parallel indicates that the stability thresholds have a unique correlation with the basic flow relationships.
- The computed sediment transport capacity distinctly decreases with increasing width-to-depth (W/d) ratio; that is, a trapezoidal cross section becomes less efficient at transporting sediment as the width-to-depth ratio increases, while Q, n, and S_f are held constant. As described in Section 3.5.2, recognizing this phenomena provided the basis for identifying the potential influence of the *water to sediment supply divergence process* on floodplain geometry.

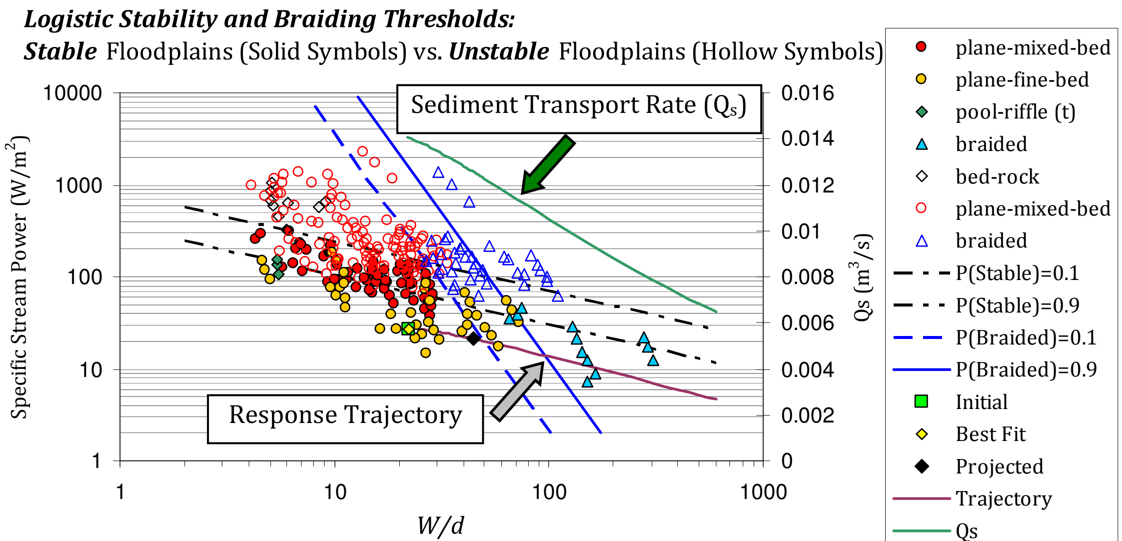

Figure 4.4a: Regime diagram for non-armored floodplain continuum

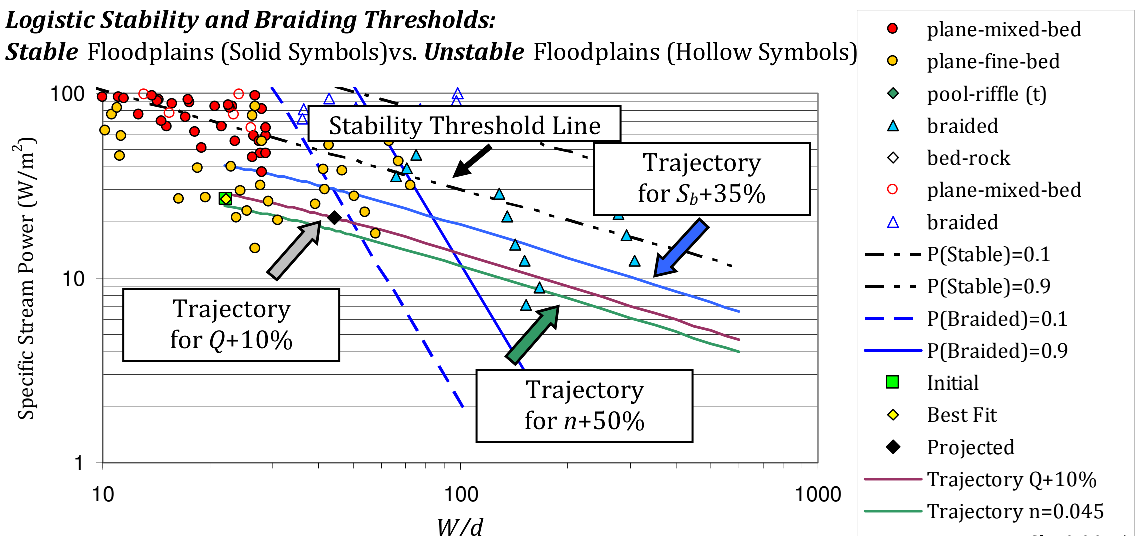

Figure 4.4b: "Zoom-in" on portion of regime diagram (non-armored)

Figure 4.4 – Comparison of floodplain response trajectories with stability thresholds and computed sediment transport rates for the non-armored floodplain continuum

In Figure 4.4b, the results from the example floodplain response analyses provided in Table 4.4 are shown; however, two additional floodplain response trajectories are also shown. These two additional trajectories correspond to the same hydraulic conditions as the first except: (a) one trajectory corresponds to an increased value for the slope (S_f), and (b)the other trajectory corresponds to an increased value for the Manning n. The two additional curves are intended to illustrate that changing the values for Q, n, or S_f results in a family of concentric response trajectories that remain nearly parallel to the logistic stability thresholds. The following two key observations can be made from Figures 4.4a and 4.4b:

- For a given floodplain geometry, increasing Q or S_f directly increases the probability for floodplain instability, as would be expected. The inverse is true for Manning n-value; that is, decreasing the floodplain roughness directly increases the probability for floodplain instability, which is also as would be expected. (In the preceding sentences, the term "directly" is used to indicate movement perpendicular to the logistic stability lines in Figure 4.4a.)
- To directly increase the probability for braiding (i.e., move perpendicularly toward the logistic braiding threshold lines in Figures 4.4a and 4.4b), a combination of things must happen: (a) Q, $(1/n)$, and/or S_f must increase; and (b) the sediment transport rate (corresponding to the new values of Q, $(1/n)$, and/or S_f) must decrease.

The first of these observations demonstrates a consistency between the modeling tools and the logistic stability thresholds that have been derived from the field data for the non-armored floodplains. The second observation listed above may not be intuitive, but it is consistent with the discussions in Section 3.5.2 and the observed downstream progression of floodplain geometry. The second observation may not be intuitive because a common conception is that floodplain braiding is only associated with excessive amounts of sediment being supplied to a watercourse, thereby resulting in the deposition of bars. As described in Section 3.5.2, I contend that this is only the case in *unstable* braided floodplains and that floodplain braiding is in essence a temporary sediment storage mechanism needed to compensate for temporal imbalances between water and sediment supply, in relatively stable systems within the geomorphic limits of this study.

In summary, the comparisons described this section demonstrate a consistency between the *floodplain response trajectories* with the field data and the corresponding geomorphic thresholds. That is, increases in Q, $(1/n)$, and/or S_f result in increasing the probability for both floodplain instability and braiding, as would be expected. The comparisons further demonstrated that the logistic braiding thresholds are related to changes in both hydraulic and sediment transport characteristics of a floodplain, whereas the stability threshold is primarily related to the hydraulic characteristics of a floodplain. Therefore, these comparisons demonstrate a consistency between the "projected" trend in floodplain geometry and form changes (as computed via the modeling tool procedures) with both the field data and the corresponding geomorphic thresholds.

4.5.4 Floodplain Response Trajectories in Terms of Braiding Thresholds and Sediment Transport Rates for Armored Floodplains

As described in Section 3.5.6, the floodplain response constraint for pool-riffle floodplains in the armored floodplain continuum was set such that the floodplain response trajectories are parallel to the braiding threshold lines. The logic behind this is that incremental increases in flow, while holding the sediment supply and gradation constant, are not sufficient alone to transition a pool-riffle floodplain into a braided floodplain; hence, the floodplain response constraint was set as the slope of the logistic braiding thresholds (per Equation 4.1b and Table 3.11), thereby resulting in response trajectories that are parallel to and will not cross the braiding thresholds.

Another approach for setting the slope for the floodplain response trajectories would be to set the floodplain response constraint based on fitting a power function to the pool-riffle floodplain data points. As illustrated in Figure 4.5a, fitting a power function to the pool-riffle data points results in a line on the log-log plot that has a slope of -3.25 and a correlation coefficient (R^2) of 0.75. As indicated in Table 3.11, the logistic braiding thresholds shown in Figure 4.5a have a slope of -3.24. Hence, the slopes corresponding to the braiding thresholds and the regression line for the pool-riffle data points are both approximately equal to -3.2, as specified in the floodplain response constraint defined by Equation 4.1b.

As described in Section 3.5.4, I hypothesize that the effects of bed material fining (i.e., an increase in the *percent sand* in the surface layer) acting in conjunction with the hypothesized *water to sediment supply divergence process* are the two mechanisms responsible for floodplain braiding in the armored floodplain continuum. It is important to recognize that even though the logistic braiding thresholds shown in Figure 4.5 may provide a useful visual reference, the logistic braiding thresholds should **not** be used alone to assess the probability for floodplain braiding, since the logistic analysis did not consider the influence of bed material fining. The field data shown in Figure 3.9 suggest that as the percentage of sand sized particles in the surface increases above approximately ten to twelve percent, the probability that a pool-riffle floodplain will transition to a braided floodplain increases significantly. Therefore, the percentage of sand sized particles in the surface layer should also be considered when assessing the potential for floodplain braiding, for floodplains in the armored continuum.

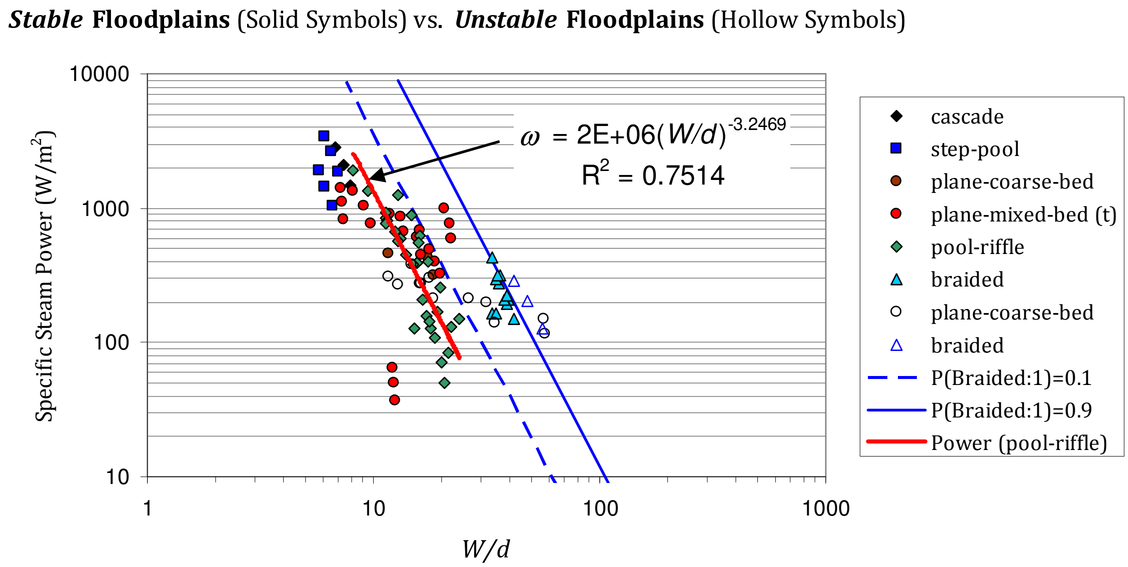

Figure 4.5a - Regime diagram for armored floodplain continuum

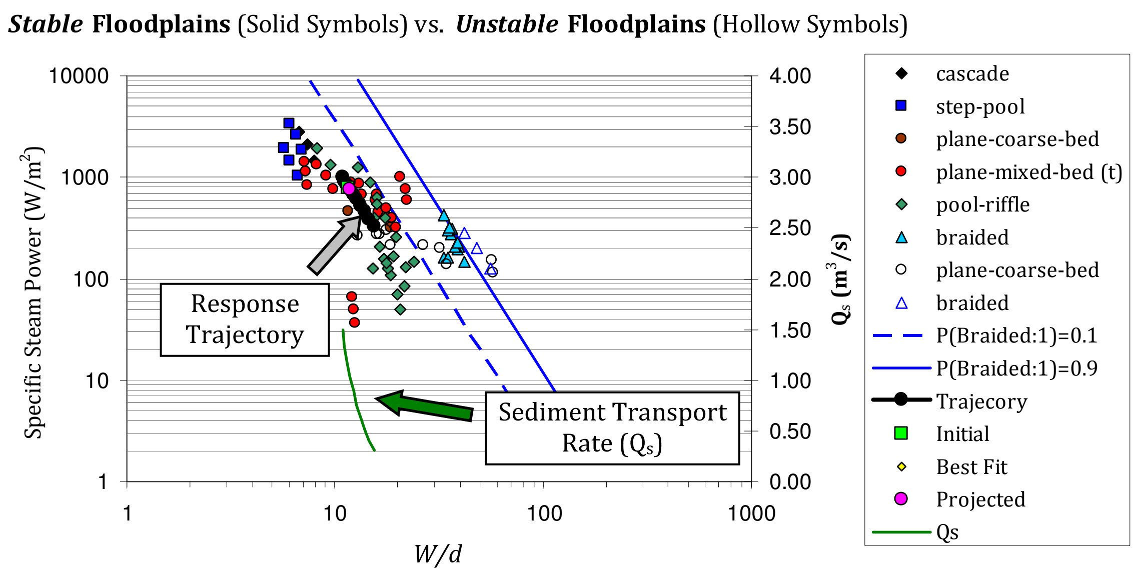

Figure 4.5b - Regime diagram for armored floodplain continuum

Figure 4.5 – Comparison of floodplain response trajectories with braiding thresholds and computed sediment transport rates for the armored floodplain continuum

In Figure 4.5b, the results from the example floodplain response analyses provided in Table 4.6 are shown, including the floodplain response trajectory. In addition, the computed sediment transport capacity corresponding to the floodplain geometry reflected in the response trajectory is shown in Figure 4.5b. As indicated in Figure 4.5, the sediment transport capacity decreases rapidly as the slope decreases and the width-to-depth ratio increases. This means that only relatively small adjustments in floodplain geometry (including bed slope) are needed to compensate for incremental increases in flow, while the inflowing sediment load is held relatively constant. Though not definitive, this is consistent with the general observations by myself and by other researchers (Simons and Simons, 1987).

4.5.5 Comparison of Example Floodplain Response Analyses for Non-Armored and Armored Floodplains

The results from the two sets of example floodplain response analyses are summarized and compared in Table 4.7. As indicated in Table 4.7, the *projected* floodplain response (in terms of the width-to-depth ratio) for the non-armored floodplain is two orders of magnitude greater than that for the armored floodplain for the same incremental increase in flow rate of 10 percent.

This differential between the magnitude of computed responses associated with the two floodplain continuums is consistent with both field observations and the visual comparison of the field data illustrated in Figures 3.5a and 3.5b. That is, the field data plotted in Figures 3.5a and 3.5b indicate that the width-to-depth ratio for stable non-armored floodplains ranges from 4 to 310, while specific stream power only ranges from 330 to 7 (W/m^2); whereas, the width-to-depth ratio for pool-riffle/armored floodplains only ranges from 8 to 24, while specific stream power ranges from 1915 to 50 (W/m^2).

Therefore, the relative *projected* changes in floodplain geometry between non-armored and armored floodplains are consistent with field observations and the field data.

Table 4.7 – Comparison of the example floodplain response analyses for a non-armored and an armored floodplain

Floodplain Continuum	**Non-Armored Floodplain**	**Armored Floodplain**
Example Computations	**Table 4.4**	**Table 4.6**
Site/Prof. ID	PLSD03P06	SCSA07P06
Initial Parameters		
$\boldsymbol{Q}$ (cms)	6.2	136.0
$\boldsymbol{\omega}$ (W/m^2)	26.8	797.9
$\boldsymbol{W/d}$	22.06	11.54
$\boldsymbol{W}$ (m)	12.57	23.40
$\boldsymbol{d}$ (m)	0.57	2.03
$\boldsymbol{S_b \approx S_f}$	0.00556	0.014
$\boldsymbol{z}$	7.39	3.02
$\boldsymbol{d_{50}}$ (m)	0.00076	0.034
Projected Parameters		
$\boldsymbol{Q}$ (cms)	6.8	149.6
$\boldsymbol{\omega}$ (W/m^2)	21.1	767.6
$\boldsymbol{W/d}$	44.49	11.54
$\boldsymbol{W}$ (m)	17.53	23.40
$\boldsymbol{d}$ (m)	0.39	2.03
$\boldsymbol{S_b \approx S_f}$	0.00556	0.0131
Projected Parameters in Terms of Change From Initial Conditions		
Increase in $\boldsymbol{Q}$ (given)	10 %	10 %
Change in $\boldsymbol{\omega}$ (W/m^2)	-5.6	-30.3
Change in ($\boldsymbol{W/d}$)	22.4	0.27
Change in $\boldsymbol{W}$ (m)	4.95	1.57
Change in $\boldsymbol{d}$ (m)	-0.18	0.09
Change in $\boldsymbol{S_f}$	0	-0.00093
Percent Change in $\boldsymbol{\omega}$	21 %	-3.8
Percent Change in ($\boldsymbol{W/d}$)	102 %	2.3 %
Percent Change in $\boldsymbol{W}$	39 %	6.7 %
Percent Change in $\boldsymbol{d}$	-30 %	4.3 %
Percent Change in $\boldsymbol{S_f}$	0 %	-6.7 %

4.5.6 Adapting the Modeling Tool for Assessing Other Potential Impacts

In a general context, the impacts of urbanization on a watercourse can be indirect and/or direct; in addition, the impacts of urbanization can also be long-term or short-term. Indirect impacts include changes to the water and sediment supply to the watercourse; whereas, direct impacts can take a wide range of forms that include floodplain encroachments, bank stabilization, channelization, bridges, culverts, and/or in-line detention basins. Short-term impacts are those associated with construction activities; whereas, long-term impacts are those associated with the end result of the construction activities.

In this context, the modeling tool solution procedures provided in Tables 4.4 and 4.6 indicate how to estimate the trend and magnitude of the change in floodplain geometry associated with the long-term and indirect impact of increasing the water supply to a reach, while the net sediment supply is relatively constant. This was chosen as the primary scenario for the modeling tool solution procedure, since it is believed that the long-term increase in water supply is the predominant indirect impact of urbanization.

However, the modeling tool solution procedures can be relatively easily adapted to also include known or estimated changes in sediment supply, if it is reasonable to assume that the bed gradation for the watercourse will not change significantly as a result. This can be accomplished by changing the "$(Q_s)_{initial}$" in Step 3a (in Tables 4.4 and 4.6) to reflect the change in inflowing sediment load associated with the reference discharge.

The modeling tools are based on using *floodplain response constraints* intended to reflect the erosional resistance and stability characteristics of the natural bank material within the region. Hence, the modeling tool solution procedures are not generally conducive to evaluating the direct impacts to watercourses typically associated with urbanization, such as bank stabilization and grade control structures.

4.5.7 Limitations to the Applicability of the Regime-Type Modeling Tools

The regime-type modeling tools described in this chapter are predicated on the assumption that the cross sectional form of a floodplain can be predicted based on a single reference flow rate and the corresponding sediment transport rate. At best, this assumption at the core of regime-type models is a dramatic simplification of the complex runoff and sediment supply processes within a catchment, especially in semi-arid environments where temporal fluctuations in discharge are typically very significant. However, the primary objective of the modeling tools is to provide a relatively non-intensive computational means to **estimate** the trend and magnitude of the change in floodplain geometry due to incremental changes in water and sediment supply. Initial evaluations of the modeling tools, with available data, indicate that this primary objective has been reasonably met.

The applicability of the modeling tools described in this chapter is limited to stable floodplains that have a relatively trapezoidal cross section. Though the active-regional alluvial fan continuum is described qualitatively in Chapter 2 and appears similar in many ways to the non-armored floodplain continuum, the applicability of the modeling tools described in this chapter is strictly limited to non-armored floodplains and pool-riffle floodplains in the armored continuum, within the geomorphic limits of this study (Figure 4.1).

In Chapter 1 of this dissertation, the question was raised regarding whether ***equilibrium*** concepts are even applicable to the perennial, ephemeral, or intermittent watercourses in the semi-arid environment of southern California. I contend that the investigations presented in this dissertation (and especially the modeling tools described and assessed in Chapter 4) demonstrate that equilibrium and the related regime concepts can be useful for evaluating floodplain response and stability hazards in the semi-arid environment. However as part of invoking equilibrium and regime concepts, I made a diligent effort to both define "equilibrium" in the context of the semi-arid environment and acknowledge the limitations in doing so. More specifically, Section 1.1.3 is dedicated to defining *equilibrium* and the associated stability states; whereas, this section and the floodplain stability assessments embedded directly into the *modeling tools* solution procedures are intended to both acknowledge and prevent violation of the equilibrium concepts invoked during development of the modeling tools.

4.6 Summary and Conclusions

4.6.1 Primary Findings

The core *practical* research question motivating the investigations documented in this chapter is: ***How can we estimate the trend and magnitude of the change in floodplain geometry, due to perturbations in intra-catchment processes associated with urbanization?*** Using the conceptual models described in Chapters 2 and 3 as a framework, regime-type modeling tools have been developed for estimating the trend and magnitude of the change in floodplain geometry associated with incremental variations in intra-catchment runoff and sedimentation processes, for the non-armored and armored floodplain continuums observed in the semi-arid environment of southern California.

At the core of the modeling tools are the basic flow relationships of continuity, flow resistance, and sediment transport for floodplains with trapezoidal geometry. To factor in bank erosional resistance and stability characteristics, the basic flow relationships are coupled with floodplain response constraints. The nature and form of the *floodplain response constraints* are dependent upon the continuum of the floodplain being evaluated and have been inferred from analysis of field data for a wide range of floodplain geometries, as reflected in the floodplain state diagrams for the non-armored and armored floodplain continuums (Figures 3.12b and 3.13b).

Since the response of a floodplain to changes in water and sediment supply can be influenced by the "initial" stability state of the floodplain, the modeling tools include a quantitative means for non-armored floodplains and a qualitative means for armored floodplains for assessing the "initial" stability state for a floodplain.

The applicability of the modeling tools is limited to initially stable floodplains, with a relatively trapezoidal cross section. Though the active-regional alluvial fan continuum appears similar in many ways to the non-armored floodplain continuum, the modeling tools described in this chapter are strictly limited to floodplain forms in the non-armored and armored continuums.

4.6.2 Avenues for Further Investigation

One of the practical research questions at the core of these investigations was to develop modeling tools for estimating the trend and magnitude of the change in floodplain geometry due to urbanization. It is believed that this objective has been reasonably well achieved; however, the modeling tools have distinct limits of applicability, as described in Section 4.5.7. Therefore, there are multiple avenues for further investigations involving the: (a) refinement of the tools to include more armored bedforms; (b) extension of the tools to include compound channel geometries; (c) automation of the tools described in this dissertation; and (d) collection of additional field data to allow further and more detailed verification of the *modeling tools*.

With respect to item "d" above, there are two basic methods to validate the modeling tools: (a) monitor the changes in floodplain geometry over time at a location and use the *modeling tools* to estimate the observed changes based on estimated changes in water and/or sediment supply overtime; and (b) measure the floodplain geometry of a relatively stable watercourse at several locations and use the modeling tools to estimate the downstream changes in floodplain geometry based on downstream changes in water and/or sediment supply, as described in Section 4.5.2. However, implementation of either of these methods poses significant challenges.

In the first method, changes in floodplain geometry are monitored over time and the primary challenge lies in estimating the long-term changes in water and/or sediment supply at a given location, due to upstream urbanization and/or land-use changes. Implementing this method will probably require performing both hydrologic and sediment yield analyses to estimate the long-term changes in water and/or sediment supply. It is important to recognize that attempting to implement this method has the following two distinct disadvantages:

- The watercourse may have to be monitored for a substantial period of time, due to the lag time required for changes in the catchment to be reflected in the geometry of the floodplain (as described in Section 1.1.3).
- If the changes in the changes in the water and/or sediment supply are too severe, the watercourse may become unstable and transition into a state of severe instability, in which case application of the *modeling tools* is no longer appropriate and the field data could not be used to verify the *modeling tools*.

In the second method, downstream changes in floodplain geometry are measured and the primary challenge lies in estimating the downstream changes in water and/or sediment supply. Implementing this method will probably involve collecting cross sectional data for major tributaries, in addition to performing hydrologic and sediment yield analyses to characterize the downstream changes in water and/or sediment supply.

As reflected in the preceding discussions, the second or “space for time” substitution method for validating the *modeling tools* is significantly more practical to implement. However, it is clear that the “space for time” substitution method is an indirect method for inferring the potential response of a floodplain to the impacts of urbanization; hence, it is reasonable to question whether the “space for time” substitution method is appropriate in this context. Based on the arguments provided in Section 3.5.2, I contend that the primary impact of urbanization is a self enhancing feedback mechanism to the intra-catchment processes that may govern the downstream progression of floodplain geometry, within the geomorphic limits of these investigations. If this contention is reasonably accurate, then the second or “space for time” substitution method for validating the *modeling tools* is also reasonable.

Chapter 5: Conclusions

5.1 Summary of Dissertation

The core ***practical*** research questions motivating the investigations documented in this dissertation are:

- How can we assess the existing stability state of a floodplain?
- How can we estimate the trend and magnitude of the change in floodplain geometry due to perturbations in intra-catchment processes associated with urbanization?

Field investigations conducted early in this research helped identify a series of ***applied*** research questions that I believe were essential to address and, thereby, provide the framework required to address the ***practical*** research questions at the core of this research. These *applied* research questions that I identified are:

- What are the forms and nature of floodplains in the semi-arid environment of southern California?
- What are the primary *process drivers* that govern the type of floodplain continuum within a catchment?
- What are the intra-catchment processes that govern the natural downstream floodplain form progression, including specifically the transition from single-thread to braided floodplains?
- What is the impact of urbanization on the primary intra-catchment processes that govern the natural downstream floodplain form progression?

The chapters in this dissertation have been organized to address both the core *practical* and the associated *applied* research questions in what I believe is a logical progression. Logical in the sense that the subject matter in each chapter builds on the previous; in addition, the analysis tools presented herein are in the most probable order in which they would be applied to assess the stability state and the geomorphic response of a floodplain to changes in water and sediment supply. The following is a brief summary of the key topics addressed in each of the chapters of this dissertation:

- **Chapter 1** introduces the research questions and defines key concepts at the core of these investigations. The two key concepts described in Chapter 1 include the concepts of :
    - The engineering perspective of a *floodplain*, which by definition encompasses both the overbank areas and the main channel.
    - *Dynamic equilibrium* in terms of the semi-arid environment and the corresponding three stability states: *stable*, *responding*, and *unstable*.
- **Chapter 2** describes the ***Reach-Scale Classification System and Conceptual Model for Floodplain Continuums in the Semi-Arid Environment*** (Figure 2.5) and the means to identify the floodplain forms and continuum within a catchment. These means to identify a floodplain form and/or continuum include:
    - ***Floodplain Field Identification Tables*** (Tables 2.4 and 2.5) that describe and illustrate key characteristics for each of the floodplain forms in both the ***non-armored*** and ***armored*** floodplain continuums.
    - ***GIS-Based Technique*** (Figure 2.11) for identifying the floodplain continuum within a catchment based on ***mean annual precipitation*** and a metric, called ***Geo-Soil Score***, that quantifies geologic characteristics of the catchment.

- **Chapter 3** describes the ***Conceptual Models for Intra-Catchment Processes*** for catchments with floodplains in either the non-armored or armored continuums. These conceptual models provide a basic framework for the modeling tools, described in Chapter 4, and are comprised of the following components:
  - State diagrams that quantitatively describe the downstream progression of floodplain forms.
  - Hypotheses for floodplain braiding mechanisms in terms of intra-catchment processes and self enhancing feedback mechanisms.
  - Either quantitative or qualitative methods for assessing the *initial* and *projected* floodplain stability state.
  - *Floodplain Response Constraints* in terms of S_b, ω and/or W/d ratio.
- **Chapter 4** describes the regime-type ***Modeling Tools*** developed for estimating the trend and magnitude of the change in floodplain geometry, due to incremental increases in water and/or sediment supply to a reach.

5.2 Applicability of Movable Bed and Boundary Models to Fluvial Systems in Southern California

In the search for a means to estimate the trend and magnitude of changes in floodplain geometry due to urbanization, several paths were initially considered. One path involved evaluating the potential applicability of various movable bed and/or boundary models, including HEC-RAS (Brunner, 2008)), Concepts (Langendoen, 2000), and Fluvial 12 (Chang, 2006). It was recognized from the onset that the hydraulic and geomorphic characteristics of the floodplains, within the geomorphic limits of this study, would be quite challenging to simulate with available models.

The tests with these models involved using test files for a prismatic floodplain that had the geometry, bed slope, and bed gradation corresponding to the downstream-most cross section for the Hasley Canyon study site (i.e., site and cross section ID HCSA01). This cross section corresponds to a non-armored braided floodplain with a bed slope of 0.0258 and a d_{50} = 1.6 mm (as provided in Appendix B, page 252). Normal depth computations (via an iterative solution of Equation 4.13) for this cross section indicate that the Froude Number (Equation 3.18) ranges from approximated 0.97 to 1.14 for estimated flows corresponding to the 2 through 100 year events.

Unfortunately, this path proved to be not very productive, since computational stability issues (i.e., oscillations) appeared to be encountered with multiple models, for conditions typical or representative of the non-armored floodplain continuum: hence, tests were discontinued. The oscillations in the computations appeared to be initiated in the hydraulic computations; however, the precise cause of the oscillations were not ascertained.

The lessons learned from these model tests and from these investigations as a whole have been incorporated into a matrix outlining what I believe are the key modeling considerations for each of the floodplain forms within the geomorphic limits of these investigations. This matrix, as provided in Tables 5.1a and 5.1b, was developed with the intent of providing information helpful to future modeling efforts. That is, the matrix provides a list of the key model functionality, in terms of physical processes, that I believe is potentially essential for adequately simulating floodplain geometry changes due to urbanization. As reflected in Tables 5.1a and 5.1b, these key modeling considerations have been divided into three categories: hydraulic, sediment transport, and movable-boundary modeling considerations. Furthermore, modeling considerations are provided for both the non-armored and armored floodplain continuums, in general, plus specific considerations for each of the floodplain forms.

Table 5.1a – Key considerations for movable boundary modeling of floodplains in the non-armored continuum

Floodplain Continuum and Form	Hydraulic Modeling Considerations	Sediment Transport Modeling Considerations	Movable Boundary Modeling Considerations
Non-Armored Continuum	These investigations indicate that near critical and supercritical flow conditions are typical within geomorphic limits of this study.	The bed material ranges from fine sands to cobbles in size, in addition mixtures of sands and gravels are a common bed material composition.	Predominant response to increases in Q is floodplain widening or increases in W/d ratio. In addition, field observations indicate that the primary modes of bank erosion include fluvial entrainment, undercutting, sloughing, and slab failure (Brierley and Fryirs, 2005, p. 98). Hence, a full mobile boundary model is appropriate.
plane-mixed-bed	One dimensional flow analyses may be insufficient due multiple critical depths associated with compound floodplain geometry at near critical or supercritical flow conditions.	Bed and overbank material is typically a mixture of sand, gravel, and/or cobbles; hence, two fraction sediment transport relationships may be appropriate.	Typical floodplain geometry is compound, thereby complicating the task of defining limits and characteristics of banks/movable boundary.
plane-fine-bed	Near critical and/or supercritical flow conditions are typical.	Bed material is typically composed of medium sands to medium gravels(0.25 to 16 mm); hence, sediment transport relationships should be appropriate for both sand and gravel.	Field observations indicate that plane-fine-bed watercourses are especially susceptible to bank erosion via fluvial entrainment, undercutting, sloughing, and slab failure (Brierley and Fryirs, 2005, p. 98).
braided	Near critical and/or supercritical flow conditions are typical.	Bed material can be a mixture of sand, gravel, and/or cobbles; hence, two fraction sediment transport relationships may be appropriate in some cases.	Field observations indicate that plane-fine-bed watercourses are highly susceptible to bank erosion via fluvial entrainment, undercutting, sloughing, and slab failure (Brierley and Fryirs, 2005, p. 98).

Table 5.1b –Key considerations for movable boundary modeling of floodplains in the armored continuum

Floodplain Continuum and Form	**Hydraulic Modeling Considerations**	**Sediment Transport Modeling Considerations**	**Movable Boundary Modeling Considerations**
Armored Continuum	These investigations indicate that near critical and supercritical flow conditions are typical within geomorphic limits of this study.	Bed and overbank material is typically a mixture of sand, gravel, cobbles, and/or boulders; hence, two or multiple fraction sediment transport relationships are appropriate.	Floodplains in the armored continuum are primarily defined by the characteristics of their bed forms, where the characteristics of these bedforms are related to both hydraulic conditions and the interaction of individual particles within a cross section.
cascade and step-pool	Combination of gradually varied and rapidly varied flow conditions prevail. In addition, the pools associated with the bed forms result in head losses that vary with discharge.	The transport and interaction of cobble and boulder sized particles are of special importance to these floodplain forms.	The results of these investigation indicate that the downstream progression of floodplain forms involves both bed slope and width-to-depth ratio adjustments.
pool-riffle	Near critical and/or supercritical flow conditions are typical.	This author contends that the effects of *bed material fining* acting in conjunction with the *water to sediment supply divergence process* are the mechanisms responsible for the transition of pool-riffle to braided floodplains.	The results of these investigation indicate that the downstream progression of floodplain forms involves both bed slope and width-to-depth ratio adjustments.
braided	It is anticipated that divided flow conditions are prevalent, during significant portions of both the rising and falling limbs of a hydrograph for a major flow event. In addition, near critical and/or supercritical flow conditions are typical.	Bed material is typically a mixture of sand, gravel, cobbles, and possibly small to medium boulders. The coarse gravels, cobbles, and/or boulders are in sufficient quantities to typically armor the dominant low flow channel. Due to the mixture of bed material two fraction sediment transport relationships are appropriate.	The low flow channels, especially the dominant low flow channel, may have a wide range of bedforms, including step-pool, plane-coarse-bed, and/or pool-riffle. That is, only portions of the bed are typically armored. Hence, models that permit spatial variations in characteristics of the armor layer within a cross section may be appropriate.

5.3 Overall Vision of Project Tools

As described in Chapter 1, the principle investigators proposed the following series of *tools* as the deliverables for the SCCWRP Hydromodification Project:

- "Screening Tools" for identifying the risk for and the potential trend of severe floodplain instability.
- "Modeling Tools" for evaluating the trend and magnitude of the change in floodplain geometry due to urbanization/hydromodification.
- "Mitigation Tools" for guiding recommended mitigation and management measures, including "Monitoring Protocol" for future data collection efforts.

This section briefly describes how I believe the techniques described in this dissertation fit into the overall framework of the various tools proposed as the deliverables for the SCCWRP Hydromodification Project.

Screening Tools

The basic objectives for *Screening Tools* are to identify the risk for instability and the potential trend of the change in floodplain geometry, due to the potential impacts of urbanization. Hence, in terms of a screening level assessment, the investigations described in this dissertation had several important findings:

- Non-armored floodplains are susceptible to transitioning into a state of severe instability at much lower levels of specific stream power than floodplains in the armored continuum, as can be determined by comparing Figures 3.12b and 3.13b.
- Non-armored floodplains have the predominant tendency to widen (i.e., increases in W/d ratio) in response to incremental increases in water supply and decreases in sediment supply, as indicated by the results for the example analysis summarized in Table 4.7.

- Pool-riffle floodplains in the armored continuum may adjust their slope and width in nearly equal proportions in response to incremental increases in water supply and decreases in sediment supply, as indicated by the results for the example analysis summarized in Table 4.7.
- The magnitude of the change in floodplain geometry (due to changes in water and/or sediment supply) associated with a non-armored floodplain is potentially orders of magnitude greater than that for a floodplain in the armored continuum (as described in Chapter 4), even if the floodplain does ***not*** become unstable and transition into the state of severe instability.

Based on these findings, I envision that identifying the floodplain continuum associated with the catchment in question would be a key step in any screening level assessment. It is important to note that I contend that the "d_{50}" value for a bed gradation is **not** necessarily a reliable indicator of whether a floodplain has an armored bed or not, in the semi-arid environment of southern California. As described in Chapter 2, these investigations found that non-armored and armored plane-mixed-bed floodplains can have very similar surface material gradations (and d_{50} values), yet have very different morphological characteristics and stability hazards. This is one of the reasons why I choose to differentiate between the "non-armored" and "armored" floodplain continuums with a term that is both form and process oriented.

In Chapter 2 both a direct and indirect method for assessing the continuum of a floodplain are described and in both cases bed gradation data are not required. The direct method involves using the ***Floodplain Field Identification Tables*** (Tables 2.4 and 2.5) in conjunction with a site visit to identify both the floodplain form and continuum representative of the reach in question. The indirect method described in Section 2.5.4 is a GIS-based technique that uses available GIS layers to predict the floodplain continuum based on catchment characteristics. Therefore, I envision that one or both of these methods would be used to assess the floodplain continuum within a catchment, as an initial step in the screening level assessment.

I would also envision that the screening level assessment would include assessing the initial stability state of the floodplain in question. An initial assessment of the stability state of the floodplain could be accomplished by identifying the CEM phase for the floodplain via field observations and the criteria listed in Table 3.4. However, I would also include assessing the stability state of the floodplain using the *floodplain state diagrams* (Figures 3.12 and 3.13) via the techniques described in Steps 1a and 1c of the *modeling tools* (Tables 4.3a and 4.5a).

To employ the *floodplain state diagrams* (Figures 3.12 and 3.13), floodplain geometry, including bed slope, and an estimated reference discharge are required. The floodplain geometry data could be obtained from either: (a) a relatively cost efficient field survey utilizing a measuring tape and a hand level; (b) detailed field survey using more sophisticated survey techniques; or (c) detailed topographic mapping, such as that used for floodplain delineation studies. The reference discharge, such as Q_{100}, can be estimated using the equations provided in Table 3.7, for catchments with little to no urbanization, or by the various hydrologic analysis techniques adopted and documented in the drainage manuals for each of the counties within the study area.

In summary, I envision that identifying the floodplain continuum associated with the catchment and assessing the initial stability state of the floodplain in question would be key initial steps in any screening level assessment. I further envision that the screening level assessment tools would also include means for assessing:

- The susceptibility of the floodplain to bank failure, by evaluating the erosional resistance and stability characteristics of the natural banks and/or bank protection improvements;
- The susceptibility of the floodplain to base level changes, by evaluating the location and condition of any natural or man-made hard points in the channel bed that may be controlling the bed profile for the watercourse; and
- The susceptibility of the floodplain to future changes in water and sediment supply due to upstream urbanization and/or flood control facilities.

Modeling Tools

The primary objective of these investigations was to develop *modeling tools* for estimating the trend and magnitude of the change in floodplain geometry, due to urbanization. I believe that this objective has been reasonably well achieved and that the *modeling tools* described in this dissertation provide a very useful means for assessing both the stability state and the potential response of a floodplain to changes in water and/or sediment supply. Therefore, I envision that the *modeling tools* described in this dissertation will form the core of the final *modeling tools* for the SCCWRP Hydromodification Project.

Mitigation Tools

Just as the conceptual models described in Chapters 2 and 3 provided the framework for developing the *modeling tools* described in Chapter 4, I envision that the conceptual models and *modeling tools* described in this dissertation will provide the framework for developing the *mitigation tools*. More specifically, I envision that there will be mitigation tools tailored to each of the floodplain forms and/or continuums. I further envision that the *modeling tools* described in this dissertation will be essential in the development of the *mitigation tools* by providing a means for assessing and testing the effectiveness of specific mitigation measures under a range of conditions.

5.4 Concluding Remarks

As described in Chapter 1, this dissertation has at its core the goal of addressing the *practical* research question: ***How can we estimate the trend and magnitude of the change in floodplain geometry due to urbanization or hydromodification?*** The approach I developed to attain this goal involved first building a framework in the form of classification systems and an array of conceptual models to describe the nature and form of floodplains in the semi-arid environment of southern California. This framework of classification systems and conceptual models has been built based on both my direct field observations and analysis of the field data collected as part of the SCCWRP Hydromodification Project.

As reflected in the *Floodplain Field Identification Tables* (Tables 2.4 and 2.5) and the *Conceptual Models for Intra-Catchment Processes* (Figures 3.12 and 3.13), an extensive set of field data has been collected as part of the SCCWRP Hydromodification Project and I consider myself fortunate to have had the opportunity to select each of the study sites and be involved with every aspect of the data collection process. Through this involvement in the data collection process, I developed a deep appreciation for both the high level of effort put forth by the entire project team to collect such a high quality set of field data and the unique opportunity that this data set provided for these investigations. Hence, the approach I developed for addressing the practical research question at the core of my research involved utilizing the field data to the fullest extent possible. Therefore, I believe that the research documented in this dissertation is securely founded in an extensive set of field data and, thereby, provides a solid framework from which to base both the three hydromodification project *tools* and future investigations.

Chapter 6: References

Agresti, A. (1990). *Categorical data analysis*, John Wiley & Sons, New York.

Ashmore, P. E. (1991). "How do gravel-bed rivers braid?" *Canadian Journal of Earth Sciences*, 28, 326-341.

Bagnold, R. A. (1973). "The nature of saltation and of bed-load transport in water." *Royal Society of London Proceedings*, ser. A, 473-504.

Bagnold, R. A. (1977). "Bed load transport by natural rivers." *Water Resources Research*, v. 13, 303-312.

Bates, R. L., and Jackson, J. A. (1984). "Dictionary of geological terms." T. A. G. Institute, ed., Anchor Books Doubleday, New York.

Bledsoe, B. P., and Watson, C. C. (2001). "Logistic analysis of channel pattern threshold: meandering, braiding, and incising." *Geomorphology*, 38, 281-300.

Bluck, B. J. (1987). "Bed forms and clast size changes in gravel-bed rivers." River channels: environment and process, K. Richards, ed., Basil Blackwell, Oxford, United Kingdom, 159-178.

Bridge, J. S. (1993). "The interaction between channel geometry, water flow, sediment transport and deposition in braided rivers." Braided Rivers, J. L. Best and C. S. Bristow, eds., The Geological Society, London.

Brierley, G. J., and Fryirs, K. A. (2005). *Geomorphology and river management: application of the river styles framework*, Blackwell Publishing, Malden, MA.

Bristow, C. S., and Best, J. L. (1993). "Braided rivers: perspectives and problems." Braided rivers, J. L. Best and C. S. Bristow, eds., The Geological Society, London.

Brunner, G. W. (2008). "HEC-RAS, River analysis system user's manual: Version 4.0." US Army Corps of Engineers, Hydrologic Engineering Center (HEC), Davis CA, 747.

Buffington, J. M., Woodsmith, R. D., Booth, D. B., and Montgomery, D. R. (2003). "Fluvial processes in Puget Sound rivers and the Pacific Northwest." Restoration of Puget Sound rivers, D. R. Montgomery, S. Bolton, D. B. Booth, and L. Wall, eds., University of Washington Press, Seattle, WA, 46-78.

Bull, W. B. (1979). "Threshold of critical power in streams." *Bulletin of the Geological Society of America*, 90, 453-464.

Bunte, K., and Abt, S. R. (2001). "Sampling surface and subsurface particle-size distributions in wadable gravel- and cobble-bed streams for analyses in sediment transport, hydraulics, and streambed monitoring." General Technical Report RMRS-GTR-74, Fort Collins, CO: U.S. Department of Agriculture, Forest Service, Rocky Mountain Research Station, 428.

Chang, H. H. (1979). "Minimum stream power and river channel patterns." *Journal of Hydrology*, 41, 303-327.

Chang, H. H. (1988). *Fluvial processes in river engineering*, John Wiley and Sons, New York.

Chang, H. H. (2006). "Fluvial-12: Mathematical model for erodible channels: users manual." Chang Consultants, Rancho Santa Fe, California.

Chin, A. (1998). "On the stability of step-pool mountain streams." The Journal of Geology, 106, 59-69.

Chin, A. (2002). "The periodic nature of step-pool mountain streams." American Journal of Science, 302, 144-167.

Chow, V. T. (1959). *Open-channel hydraulics*, McGraw-Hill Book Company, New York.

Cooke, R. U., and Reeves, R. W. (1976). *Arroyos and environmental change in the American South-West*, Oxford University Press, London.

Crooks, R., Allen, C. R., Kamb, B., Payne, C. M., and Proctor, R. J. (1987). "Quaternary geology and seismic hazard of the Sierra Madre and associated faults, Western San Gabriel Mountains." Recent reverse faulting in the Transverse Ranges, California, U.S. Geological Survey Professional Paper 1339, U.S. Government Printing Office, Washington D.C.

Cramer, C. H., and Harrington, J. M. (1987). "Seismicity and tectonics of the Cucamonga Fault and the Eastern San Gabriel Mountains, San Bernardino County." Recent reverse faulting in the Transverse Ranges, California, U.S. Geological Survey Professional Paper 1339, U.S. Government Printing Office, Washington D.C.

Davies, T. R. H., and Sutherland, A. J. (1983). "Extremal hypotheses for river behavior." *Water Resources Research*, 19(1), 141-148.

Dawson, M. D. (1988). "Sediment size variations in a braided reach of the Sunwapta River, Alberta Canada." *Earth Surface Processes and Landforms*, 13, 599-618.

Dingman, S. L. (1984). *Fluvial hydrology*, Freeman, New York.

Eaton, B. C., and Millar, R. G. (2004). "Optimal alluvial channel width under a bank stability constraint." *Geomorphology*, 62.

Eaton, B. C., Church, M., and Millar, R. G. (2004). "Rational regime model of alluvial channel morphology and response." *Earth Surface Processes and Landforms*, 29, 511-529.

Engelund, F., and Skovgaard, O. (1973). "On the origin of meandering and braiding in alluvial streams." *Journal of Fluid Mechanics*, 57, 289-302.

FEMA. (1986). "A unified national program for floodplain management." FEMA 100, Interagency Task Force on Floodplain Management, Federal Emergency Management Agency, Washington, D.C.

Ferguson, R. I. (1987). "Hydraulic and sedimentary controls on channel patterns." River channels: environment and process, K. S. Richards, ed., Blackwell, Oxford, 129-158.

Ferguson, R. I. (1993). "Understanding braiding processes in gravel-bed rivers: progress and unsolved problems." Braided rivers, J. L. Best and C. S. Bristow, eds., The Geological Society, London.

Fredsoe, J. (1978). "Meandering and braiding of rivers." *Journal of Fluid Mechanics*, 84, 609-624.

Fukuoka, S. (1989). "Finite amplitude development of alternate bars." River meandering, S. Ikeda and G. Parker, eds., American Geophysical Union, Water Resources Monographs, 237-265.

Gordon, A. D. (1999). *Classification*, Chapman & Hall/CRC, London.

Graf, W. L. (1981). "Channel instability in a sand-bed river." *Water Resources Research*, 17, 1087-1094.

Graf, W. L. (1988). "Definition of flood plains along arid-region rivers." Flood Geomorphology, V. R. Baker, R. C. Kochel, and P. C. Patton, eds., John Wiley & Sons, New York, 231-242.

Harvey, M. D., Watson, C. C., and Schumm, S. A. (1985). "Technical Note 366: Gully erosion: ." Bureau of Land Management, 181.

Henderson, F. M. (1966). *Open channel flow*, Macmillan Publishing Co. Inc., New York.

Hey, R. D., and Thorne, C. R. (1986). "Stable channels with mobile gravel beds." *Journal of Hydraulic Engineering*, 112, 671-689.

Horton, R. E. (1945). "Erosional development of streams and their drainage basins: hydrophysical approach to quantitative morphology." *Bulletin of the Geological Society of America*, 88, 1177-1182.

Huang, H. Q., and Nanson, G. C. (2000). "Hydraulic geometry and maximum flow efficiency as products of the principle of least action." *Earth Surface Processes and Landforms*, 25, 1-16.

Kirkby, M. J. (1977). "Maximum sediment efficiency as a criterion for alluvial channels." River Channel Changes, K. J. Gregory, ed., John Wiley, Chichester, 429-442.

Knighton, D. (1998). *Fluvial forms and processes: A New Perspective*, Oxford University Press, Inc., New York.

Lane, E. W. (1957). "A study of the shape of channels formed by natural streams flowing in erodible material." Missouri River Division Sediment Series No. 9. U. S. Army Engineering Division, Missouri River Corps of Engineers, Omaha, NE.

Langendoen, E. J. (2000). "CONCEPTS - conservational channel evolution and pollutant transport system: Stream Corridor Version 1.0:Research Report No.16." USDA-ARS, Oxford, Mississippi.

Laursen, E. M. (1958). "Sediment-transport mechanics in stable-channel design." *Transactions of the American Society of Civil Engineers*, vol. 123, 195.

Leopold, L. B., and Maddock Jr., T. (1953). "The hydraulic geometry of stream channels and some physiographic implications." U. S. Geological Survey Professional Paper 252, Washington D.C., 57 pp.

Leopold, L. B., and Wolman, M. G. (1957). "River channel patterns - braiding, meandering and straight." U. S. Geological Survey Professional Paper 282B, Washington D.C., 39-85.

Limerinos, J. T. (1970). "Determination of the Manning Coefficient from measured bed roughness in natural channels." USGS, Water Supply Paper 1898-B, Reston, VA, 47.

Menard, S. W. (1995). *Applied logistic regression analysis*, Sage Publications, Thousand Oaks, CA.

Millar, R. (2005). "Theoretical regime equations for mobile gravel-bed rivers with stable banks." *Geomorphology*, 64, 207-220.

Montgomery, D. R., and Buffington, J. M. (1997). "Channel –reach morphology in mountain streams." Geological Society of America Bulletin, 109(5), 16.

Montgomery, D. R., and Buffington, J. M. (1998). "Channel processes, classification, and response." River ecology and management, R. Naiman and R. Billby, eds., Springer-Verlag New York, Inc., New York, NY, 13-42.

Mount, J. F. (1995). *California rivers and streams: the conflict between fluvial process and land use*, University of California Press, Los Angeles.

Naden, P. S., and Brayshaw, A. C. (1987). "Small- and medium-scale bedforms in gravel-bed rivers." River channels: environment and process, K. Richards, ed., Basil Blackwell, Oxford, United Kingdom, 391.

Nanson, G. C., and Croke, J. C. (1992). "A genetic classification of floodplains." *Geomorphology*, 4, 459-486.

Parker, G. (1976). "On the cause and characteristic scales of meandering and braiding in rivers." Journal of Fluid Mechanics, 76(part 3), 457-480.

Pickup, G. (1991). "Event Frequency and Landscape Stability on the Floodplain Systems of Arid Central Australia." Quaternary Science Reviews, 10, 463-473.

Renwick, W. H. (1992). "Equilibrium, disequilibrium, and nonequilibrium landforms in the landscape." *Geomorphology*, 5, 265-276.

Richards, K., and Clifford, N. (1991). "Fluvial geomorphology: structured beds in gravelly rivers." *Progress in Physical Geography*, 15(4), 407-422.

Schumm, S. A. (1977). *The fluvial system*, John Wiley and Sons, New York.

Schumm, S. A. (1981). "Evolution and response of the fluvial system, sedimentologic implications." Society of Economic Paleontologists and Mineralogists, Special Publication No.1, 19-29.

Schumm, S. A., Harvey, M. D., and Watson, C. C. (1981). "Yazoo Basin geomorphology." Soil Conservation Service, Project SCS-23-MS-80, 483.

Schumm, S. A., Harvey, M. D., and Watson, C. C. (1984). *Incised channels: morphology, dynamics, and control*, Water Resources Publications, Littleton, Colorado.

Shen, H. W. (1979). *Modeling of rivers*, Wiley, New York.

Simons, D. B., and Simons, R. K. (1987). "Differences between gravel- and sand- bed rivers." Gravel bed rivers, C. R. Thorne, J. C. Bathurst, and R. D. Hey, eds., John Wiley & Sons Ltd., New York, 3-15.

Stevens, M. A., Simons, D. B., and Richardson, E. V. (1975). "Non-equilibrium river form." *Journal of the Hydraulics Division American Society of Civil Engineers*, 101, 557-566.

Tanner, W. F. (1968). "Equilibrium in geomorphology." The Encyclopedia of Geomorphology, R. W. Fairbridge, ed., Reinhold, New York, 315-316.

Thompson, C. J., Croke, L., Ogden, R., and Wallbrink, P. (2006). "A morpho-statistical classification of mountain stream reach types in southeastern Australia." *Geomorphology*, 81, 43-65.

Tooth, S. (2000). "Downstream changes in dryland river channels: the northern plains of arid central Australia." *Geomorphology*, 34, 33-54.

Tung, Y. (1985). "Channel scouring potential using logistic analysis." *Journal of Hydraulic Engineering*, 111(2), 194-205.

Turabian, K. L. (2007). "A Manual for Writers or Research Papers, Theses, and Dissertations." W. C. Booth, G. G. Colomb, and J. M. Williams, eds., The University of Chicago Press, Chicago.

USDA/NRCS. (1998). "Processed annual precipitation data: 1961-90." National Cartography & Geospatial Center: USDA Geospatial Data Gateway.

USDA/NRCS. (2007). "SSURGO - Geographic soil survey database." U.S. Department of Agriculture, Natural Resources Conservation Service: USDA Geospatial Data Gateway, Fort Worth, Texas.

USGS. (1987). "Recent reverse faulting in the Transverse Ranges, California." U.S. Geological Survey Professional Paper 1339, U.S. Government Printing Office, Washington, D.C.

USGS. (2005). "Preliminary integrated databases for the United States - western states: California, Nevada, Arizona, and Washington." S. Ludington, B. C. Moring, R. J. Miller, K. S. Flynn, P. A. Stone, and D. R. Bedford, eds., U.S. Geological Survey.

USGS. (2009). "Geologic provinces of the United States: Records of an active earth." United States Geological Survey, Retrieved August 2009, from http://geomaps.wr.usgs.gov/parks/province/index.html.

van den Berg, J. H. (1995). "Prediction of alluvial channel pattern of perennial rivers." *Geomorphology*, 12, 259-279.

Wilcock, P. R., and Kenworthy, S. T. (2002). "A two-fraction model for the transport of sand/gravel mixtures." *Water Resources Research*, 38(10), 1194.

Waananen, A. O., and Crippen, J. R. (1977). "Magnitude of frequency of floods in California." Water Resources Investigations 77-21, U.S. Geological Survey, Washington, D.C.

Ward, R. (1978). *Floods: a geographical perspective*, Wiley, New York.

Watson, C. C., Biedenharn, D. S., and Thorne, C. R. (2005). *Stream rehabilitation*, Cottonwood Research LLC, Fort Collins, Colorado.

White, W. R., Bettess, R., and Paris, E. (1982). "Analytical approach to river regime." *Journal of the hydraulics Division American Society of Civil Engineers*, 108, 1179-1193.

Yang, C. T. (1976). "Minimum unit stream power and fluvial hydraulics." *Journal of the Hydraulics Division American Society of Civil Engineers*, 102, 769-784.

Yang, C. T. (2003). *Sediment transport: theory and practice*, Krieger Publishing Company, Malabar, Florida.

Yang, C. T., Song, C. C. S., and Woldenberg, M. J. (1981). "Hydraulic geometry and minimum rate of energy Dissipation." *Water Resources Research*, 17(4), 1014-1018.

Zaslavsky, D., and Sinai, G. (1981). "Surface hydrology: I - Explanation of phenomena; II - Distribution of raindrops, III - Causes of lateral flow; IV - Flow in sloping, layered soil; V - In-surface transient flow." *Journal of the Hydraulics Division American Society of Civil Engineers*, 107(HY1), 1-93.

Appendix A– Data for Study Catchments

Table A.1a –Average annual precipitation and Geo-Soil Score data for study catchments

Site ID	Site Description	Co. (1)	Type (2)	Catchment Area (km^2)	Ave. Annual Precipitation (m)	Geo-Soil Score (1-3)
YTLC00	Yucaipa Crk Trib @ Live Oak	SB	1a	1.45	0.381	1.00
HCSC00	Hasley Canyon Site 3/C	LA	1a	0.36	0.432	1.00
HCSB00	Hasley Canyon Site 1/B	LA	1a	4.47	0.432	1.13
YCMG00	Yucaipa Crk at Mesa Grande	SB	1a	16.80	0.601	1.16
HCSA0T	Romero Cnyn @ Hasely Cnyn	LA	1a	8.07	0.432	1.30
HCSA00	Hasley Canyon Site 2/A	LA	1a	11.64	0.432	1.38
SJBL00	San Jacinto Trib - Bad Lands	R	1a	0.15	0.362	1.61
RCSA00	Romero Canyon Site A	LA	1a	0.70	0.432	1.63
BCCD00	Borrego Canyon	O	1a	7.04	0.368	1.76
ACLA00	Aliso Canyon @ Hovnanian	LA	1a	5.31	0.501	1.79
DCAD00	Dry Canyon	V	1a	3.18	0.432	1.89
HCSR00	Hicks Canyon D/S	O	1a	3.88	0.372	1.93
HCMR1T	Hicks Canyon U/S	O	1a	3.45	0.376	1.94
PLSB00	Perris Lake Site 2/B	R	1b	0.14	0.330	1.88
MCCS00	McGonigle Canyon	SD	1b	5.14	0.330	2.02
PLSD00	Perris Lake Site 4/D	R	1b	2.06	0.330	2.05
PLSA00	Perris Lake Site 1/A	R	1b	0.45	0.330	2.05
AHMD00	Agua Hedionda	SD	1b	26.28	0.330	2.20
PLSC00	Perris Lake Site 3/C	R	1b	1.46	0.330	2.26
PPSA00	Pigeon Pass Site A - D/S	R	1b	6.42	0.381	2.32
PVPV1T	Proctor Valley West Trib.	SD	1b	1.97	0.381	2.33
PVPV00	Proctor Valley	SD	1b	11.28	0.381	2.34
PPSB00	Pigeon Pass Site B - U/S	R	1b	3.50	0.381	2.36
SCAT1T	Santa Clara Trib @ Acton U/S	LA	1b	1.35	0.279	2.53
SCAT00	Santa Clara Trib @ Acton D/S	LA	1b	2.03	0.279	2.61
PLSD1T	Perris Lake Site 4/D Trib.	R	1b	0.43	0.330	2.76
LSCSMM	Little Sycamore Creek	LA	2	28.04	0.506	1.98
BSCSMM	Big Sycamore Crk-Chin(2002)	V	2	54.10	0.461	1.98
TCBD00	Topanga Canyon	LA	2	49.89	0.634	2.16
CCMCSM	Cold Creek-Chin(2002)	LA	2	21.06	0.676	2.20
SJOH00	San Juan Creek D/S	O	2	104.93	0.402	2.40
SJOH1T	San Juan Creek U/S	O	2	103.57	0.403	2.40
SCSA00DS	Santiago Canyon @ Bridge D/S	O	2	34.95	0.524	2.45
SCSA00	Santiago Canyon @ Bridge U/S	O	2	33.66	0.529	2.47
SCSB00	Santiago Canyon Tucker	O	2	17.87	0.557	2.58
SCSC00	Santiago Canyon @ Nat. Load.	O	2	17.26	0.560	2.58
SCSD00	Santiago Site D	O	2	16.22	0.569	2.61
SCOL00	Silverado Cnyn @ Nat. Loading	O	2	20.65	0.512	2.64
SAOA00	San Antonio Crk @ E Ojai Ave.	V	2	31.64	0.574	2.83
SCNS00	Stewart Canyon	V	2	4.72	0.533	2.97
BCLC00	Bus Canyon @ Challenger Park	V	2	7.29	0.487	1.98
ECLF00	Escondido Creek	SD	2	155.05	0.355	2.22
DCCR00	Dulzura Creek @ Hwy 94	SD	2	70.28	0.412	2.26
SJSR00	San Jacinto Trib @ Soboba	R	2	0.76	0.436	2.33
LCOL00	Little Cedar Canyon	SD	2	7.22	0.392	2.38

Table A.1b –Average annual precipitation and Geo-Soil Score data for study catchments

Site ID	Site Description	Co. (1)	Type (2)	Catchment Area (km^2)	Ave. Annual Precipitation (m)	Geo-Soil Score (1-3)
AF1SGM	Alluvial Fan1 SG Mnts	SB	3	1.72	0.882	1.73
AF2SGM	Alluvial Fan2 SG Mnts	SB	3	1.94	0.904	1.87
FCOG00	Un-Named Creek @ Oak Glen	SB	3	1.81	0.763	2.06
AF4SGM	Alluvial Fan4 SG Mnts	SB	3	5.18	0.839	2.10
DCHR00	Deer Canyon	SB	3	9.65	1.063	2.28
AF3SGM	Alluvial Fan3 SG Mnts	SB	3	12.43	1.074	2.64

Notes: (1) LA = Los Angeles County
O = Orange County
R = Riverside County
SD = San Diego County
SB = San Bernardino County
V = Ventura County
(2) Types 1a and 1b = Non-Armored Floodplain Continuum
Type2 = Armored Floodplain Continuum
Type 3 = Active-Regional Alluvial Fan Continuum

Table A.2a – Rock-Type and Geo-Soil Score data for study catchments

Site ID	Floodplain Continuum per Field Observation		Percent Alluvium	Percent Sedimentary	Percent Metamorphic	Percent Igneous	Geo-Soil Score (1-3)
YTLC00	1a	non-armored	100%	0%	0%	0%	1.00
HCSC00	1a	non-armored	0%	100%	0%	0%	1.00
HCSB00	1a	non-armored	0%	100%	0%	0%	1.13
YCMG00	1a	non-armored	31%	0%	69%	0%	1.16
HCSA0T	1a	non-armored	0%	100%	0%	0%	1.30
HCSA00	1a	non-armored	0%	100%	0%	0%	1.38
SJBL00	1a	non-armored	0%	100%	0%	0%	1.61
RCSA00	1a	non-armored	0%	100%	0%	0%	1.63
BCCD00	1a	non-armored	0%	100%	0%	0%	1.76
ACLA00	1a	non-armored	0%	100%	0%	0%	1.79
DCAD00	1a	non-armored	0%	100%	0%	0%	1.89
HCSR00	1a	non-armored	0%	100%	0%	0%	1.93
HCMR1T	1a	non-armored	0%	100%	0%	0%	1.94
PLSB00	1b	non-armored	100%	0%	0%	0%	1.88
MCCS00	1b	non-armored	19%	18%	0%	63%	2.02
PLSD00	1b	non-armored	57%	0%	0%	43%	2.05
PLSA00	1b	non-armored	77%	0%	0%	23%	2.05
AHMD00	1b	non-armored	0%	18%	7%	75%	2.20
PLSC00	1b	non-armored	30%	0%	0%	70%	2.26
PPSA00	1b	non-armored	31%	0%	0%	69%	2.32
PVPV1T	1b	non-armored	0%	0%	0%	100%	2.33
PVPV00	1b	non-armored	0%	0%	0%	100%	2.34
PPSB00	1b	non-armored	29%	0%	0%	71%	2.36
SCAT1T	1b	non-armored	0%	0%	0%	100%	2.53
SCAT00	1b	non-armored	0%	0%	0%	100%	2.61
PLSD1T	1b	non-armored	15%	0%	0%	85%	2.76
LSCSMM	2	armored	0%	25%	0%	75%	1.98
BSCSMM	2	armored	0%	58%	0%	42%	1.98
TCBD00	2	armored	0%	91%	0%	9%	2.16
CCMCSM	2	armored	0%	52%	0%	48%	2.20
SJOH00	2	armored	0%	1%	35%	64%	2.40
SJOH1T	2	armored	0%	1%	35%	64%	2.40
SCSA00DS	2	armored	0%	18%	51%	31%	2.45
SCSA00	2	armored	0%	15%	53%	32%	2.47
SCSB00	2	armored	0%	6%	49%	45%	2.58
SCSC00	2	armored	0%	6%	48%	46%	2.58
SCSD00	2	armored	0%	2%	49%	49%	2.61
SCOL00	2	armored	0%	0%	92%	8%	2.64
SAOA00	2	armored	8%	92%	0%	0%	2.83
SCNS00	2	armored	0%	100%	0%	0%	2.97
BCLC00	2	armored	0%	100%	0%	0%	1.98
ECLF00	2	armored	0%	0%	8%	92%	2.22
DCCR00	2	armored	0%	0%	0%	100%	2.26
SJSR00	2	armored	0%	0%	0%	100%	2.33
LCOL00	2	armored	0%	0%	0%	100%	2.38

Table A.2b – Rock-Type and Geo-Soil Score data for study catchments

Site ID	Floodplain Continuum per Field Observation		Percent Alluvium	Percent Sedimentary	Percent Metamorphic	Percent Igneous	Geo-Soil Score (1-3)
AF1SGM	3	alluvial fan	7%	0%	93%	0%	1.73
AF2SGM	3	alluvial fan	2%	0%	98%	0%	1.87
FCOG00	3	alluvial fan	12%	0%	67%	21%	2.06
AF4SGM	3	alluvial fan	2%	0%	66%	31%	2.10
DCHR00	3	alluvial fan	2%	0%	68%	31%	2.28
AF3SGM	3	alluvial fan	3%	0%	32%	65%	2.64

Appendix B– Hydraulic Analyses for Field Sites

Table B.1 – List of the primary hydraulic parameters in the hydraulic database for each cross section and a range of flow rates

Hydraulic Depth	Eq. B.1
$D = A/W$ in (m)	
Hydraulic Radius	Eq. B.2
$R = A/P_w$ in (m)	
Manning Equation (Chow, 1959):	
$V = \frac{1}{n} R^{2/3} S_f^{1/2}$ in (m/s)	Eq. B.3
Continuity Equation (Chow, 1959):	
$Q = V \cdot A$ in (m³/s)	Eq. B.4
Width-to-Depth Ratio (Knighton, 1998):	
$\mathrm{T} = (W/d) =$ Width-to-Depth Ratio (m/m)	Eq. B.5
Total Boundary Shear Stress (Chow, 1959):	
$\tau = \gamma R S_f$ in (Pa = kg/ms²)	Eq. B.6
Shields Parameter (Chow, 1959):	
$\tau^* = \frac{\gamma R S_f}{(\gamma_s - \gamma) d_{gs}}$	Eq. B.7
Specific Stream Power (Bull, 1979):	
$\omega = (\gamma Q S_f)/W$ in (W/m²)	Eq. B.8
Froude Number (Chow, 1959):	
$F_r = \frac{V}{\sqrt{(gD)/\alpha}}$	Eq. B.9
Estimation of Manning n value per Limerinos (1970)	
$n = \frac{0.113 d^{1/6}}{1.16 + 2 \cdot \log(d/d_{84})}$	Eq. B.10

where: V = flow velocity (m/s)
n = Manning's roughness coefficient
A = flow area (m²)
P_w = wetted perimeter (m)
S_f = friction slope (m/m)
d_{gs} = grain size (m)
d_{84} = particle size for which 84% of the particles are smaller
Q = flow rate (m³/s)
W = topwidth of flow area (m)
d = maximum flow depth (m)
γ = 9810 (kg/m²s²) = specific weight of water
γ_s = 25,967 (kg/m²s²) = specific weight of sediment
g = 9.81 (m/s²) = acceleration of gravity
$\alpha \approx 1.15$ = kinetic energy coefficient

Cross Section Hydraulic Analyses: Aliso Creek at Hovnanian

Floodplain/Site Description: Aliso Canyon near the Hovnanian development. Photo views looking downstream and upstream, respectively.

Location ID	ACLA01
d_{50} (mm) =	36.68
d_{84} (mm) =	157.05
So = Sf =	0.0514

Pt #	Sta (m)	Elev. (m)
1	1.69	387.05
2	2.78	386.96
3	4.28	386.65
4	5.28	386.52
5	5.57	386.27
6	6.26	385.94
7	6.83	385.63
8	7.23	385.33
9	7.68	385.17
10	8.07	385.27
11	8.46	385.52
12	9.01	385.83
13	9.30	386.22
14	10.39	386.48
15	11.47	386.43
16	12.68	386.61
17	13.72	387.28
18	14.34	387.44
19	15.00	387.45
20		
21		
22		
23		
24		
25		
26		
27		
28		
29		
30		
31		
32		
33		
34		
35		
min. Stage =	385.17	
Continuum	1	
CEM	3	

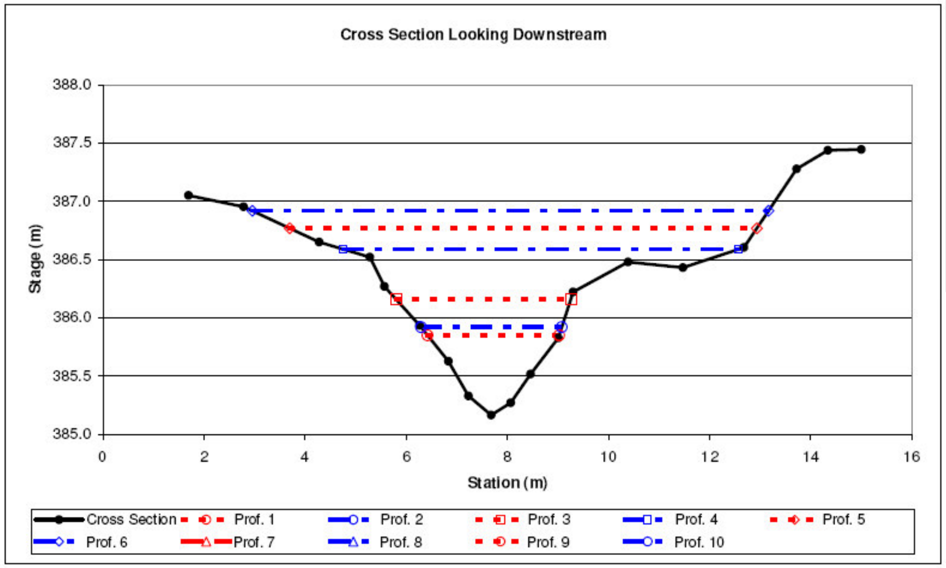

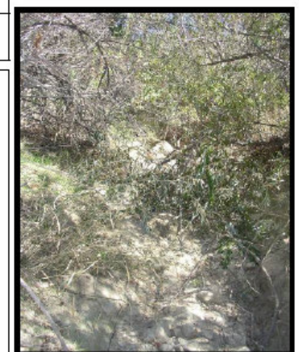

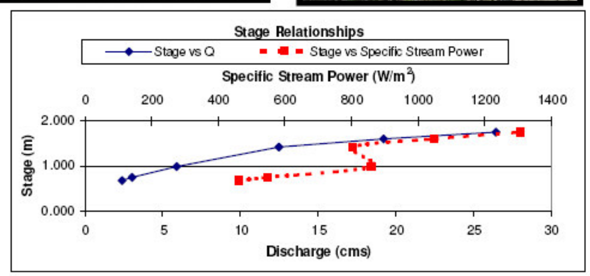

Prof. ID	Estimated n-value	L-Limit	R-Limit	WS (m)	Depth (m)	Left Sta (m)	Right Sta (m)	P_w (m)	Area (m^2)	W (m)	R (m)	D (m)	W/d	V (m/s)	Q (m^3/s)	U* (m/s)	τ (kg/ms²)	τ*	ω (W/m²)	Ω (W/m)	F_r	R/d_{84}	n-value per Limerino	Floodplain Form
ACLA01P01	0.045			385.85	0.685	6.42	9.03	2.97	0.99	2.60	0.33	0.38	3.8	2.4	2.38	0.41	167.6	0.283	462	1202	1.34	2.1	0.050	PMB
ACLA01P02	0.045			385.92	0.755	6.29	9.08	3.20	1.17	2.78	0.37	0.42	3.7	2.6	3.03	0.43	185.0	0.312	549	1529	1.36	2.3	0.048	PMB
ACLA01P03	0.045			386.16	0.995	5.80	9.26	4.05	1.92	3.46	0.47	0.56	3.5	3.1	5.90	0.49	239.4	0.404	860	2973	1.41	3.0	0.045	PMB
ACLA01P04	0.045			386.59	1.425	4.75	12.57	8.61	4.08	7.82	0.47	0.52	5.5	3.1	12.5	0.49	238.8	0.403	805	6296	1.45	3.0	0.046	PMB
ACLA01P05	0.045			386.77	1.605	3.69	12.93	10.10	5.63	9.24	0.56	0.61	5.8	3.4	19.2	0.53	281.3	0.475	1049	9693	1.50	3.6	0.044	PMB
ACLA01P06	0.045			386.92	1.755	2.96	13.17	11.12	7.09	10.21	0.64	0.69	5.8	3.7	26.5	0.57	321.3	0.542	1306	13338	1.53	4.1	0.043	PMB
ACLA01P07	0.045																							PMB
ACLA01P08	0.045																							PMB
ACLA01P09	0.045																							PMB
ACLA01P10	0.045																							PMB
	Valley Slope =	0.0417																						
	Valley Width (m) =	14.00																						

Cross Section Hydraulic Analyses: Aliso Creek at Hovnanian

Floodplain/Site Description: Aliso Canyon near the Hovnanian development. Photo view looking downstream.

Location ID	ACLA02
d_{50} (mm) =	36.68
d_{84} (mm) =	157.05
So = Sf =	0.0514

Pt #	Sta (m)	Elev. (m)
1	0.00	388.09
2	1.05	387.92
3	2.46	387.64
4	3.44	387.19
5	4.04	386.71
6	4.32	386.54
7	5.51	386.17
8	6.70	386.14
9	7.58	386.18
10	8.97	386.48
11	10.43	386.69
12	12.13	386.87
13	14.30	387.38
14	16.32	387.97
15	18.17	388.02
16	20.39	388.12
17	21.25	388.25
18	21.91	388.49
19		
20		
21		
22		
23		
24		
25		
26		
27		
28		
29		
30		
31		
32		
33		
34		
35		
min. Stage =	386.14	
Continuum	1	
CEM	3	

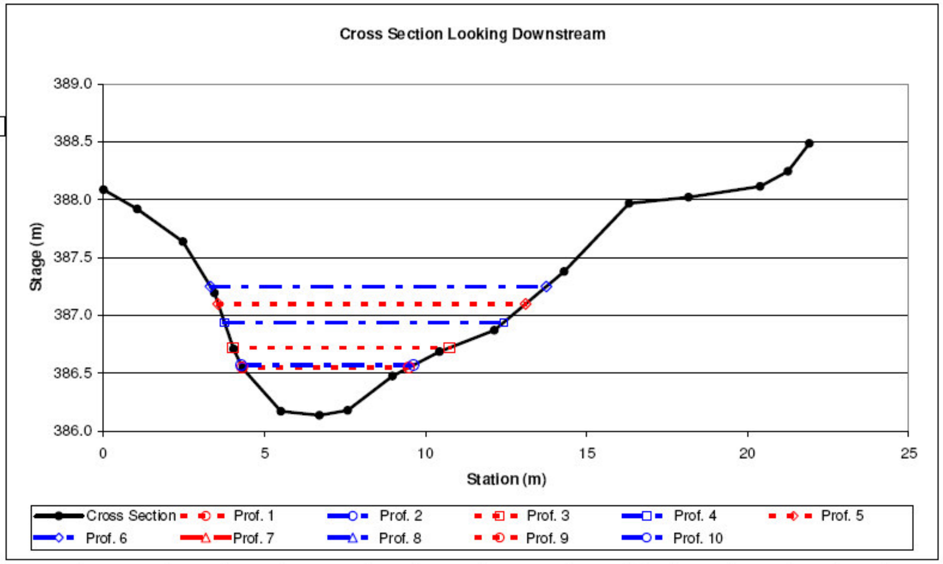

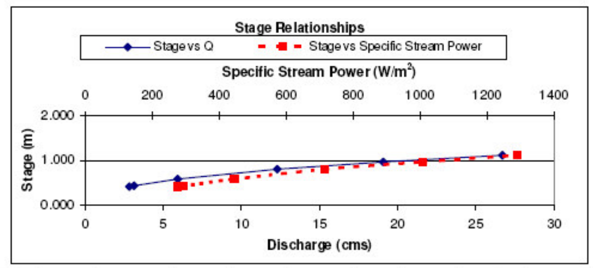

Prof. ID	Estimated n-value	L-Limit	R-Limit	WS (m)	Depth (m)	Left Sta (m)	Right Sta (m)	P_w (m)	Area (m^2)	W (m)	R (m)	D (m)	W/d	V (m/s)	Q (m^3/s)	U* (m/s)	τ (kg/ms²)	τ*	ω (W/m²)	Ω (W/m)	F_r	R/d_{84}	n-value per Limerino	Floodplain Form
ACLA02P01	0.045			386.55	0.414	4.31	9.48	5.27	1.38	5.18	0.26	0.27	12.5	2.1	2.8	0.36	131.6	0.222	276	1429	1.37	1.7	0.056	PMB
ACLA02P02	0.045			386.57	0.434	4.27	9.62	5.45	1.48	5.35	0.27	0.28	12.3	2.1	3.1	0.37	137.1	0.231	295	1580	1.38	1.7	0.055	PMB
ACLA02P03	0.045			386.72	0.584	4.03	10.74	6.87	2.38	6.71	0.35	0.36	11.5	2.5	5.9	0.42	175.0	0.295	446	2989	1.43	2.2	0.051	PMB
ACLA02P04	0.045			386.94	0.804	3.76	12.42	8.92	4.10	8.67	0.46	0.47	10.8	3.0	12.3	0.48	231.8	0.391	716	6204	1.49	2.9	0.047	PMB
ACLA02P05	0.045			387.10	0.964	3.56	13.11	9.87	5.56	9.55	0.56	0.58	9.9	3.4	19.1	0.53	283.8	0.479	1008	9623	1.54	3.6	0.045	PMB
ACLA02P06	0.045			387.25	1.114	3.32	13.75	10.81	7.05	10.43	0.65	0.68	9.4	3.8	26.7	0.57	328.8	0.555	1292	13472	1.58	4.2	0.044	PMB
ACLA02P07	0.045																							PMB
ACLA02P08	0.045																							PMB
ACLA02P09	0.045																							PMB
ACLA02P10	0.045																							PMB

Valley Slope =	0.0417
Valley Width (m) =	19.00

Cross Section Hydraulic Analyses: Aliso Creek at Hovnanian

Floodplain/Site Description: Aliso Canyon near the Hovnanian development. Photo view looking downstream.

Location ID	ACLA03
d_{50} (mm) =	16.00
d_{84} (mm) =	173.31
So = Sf =	0.0200

Pt #	Sta (m)	Elev. (m)
1	0.00	389.60
2	1.48	389.69
3	3.34	389.66
4	4.45	389.23
5	5.22	388.58
6	5.86	388.36
7	6.56	388.24
8	7.76	387.68
9	8.61	387.49
10	9.69	387.87
11	10.62	387.95
12	11.39	388.01
13	12.20	388.56
14	13.46	389.33
15	15.88	389.28
16	17.67	389.36
17	19.21	389.34
18	21.14	389.36
19		
20		
21		
22		
23		
24		
25		
26		
27		
28		
29		
30		
31		
32		
33		
34		
35		
min. Stage =		387.49
Continuum		1
CEM		3

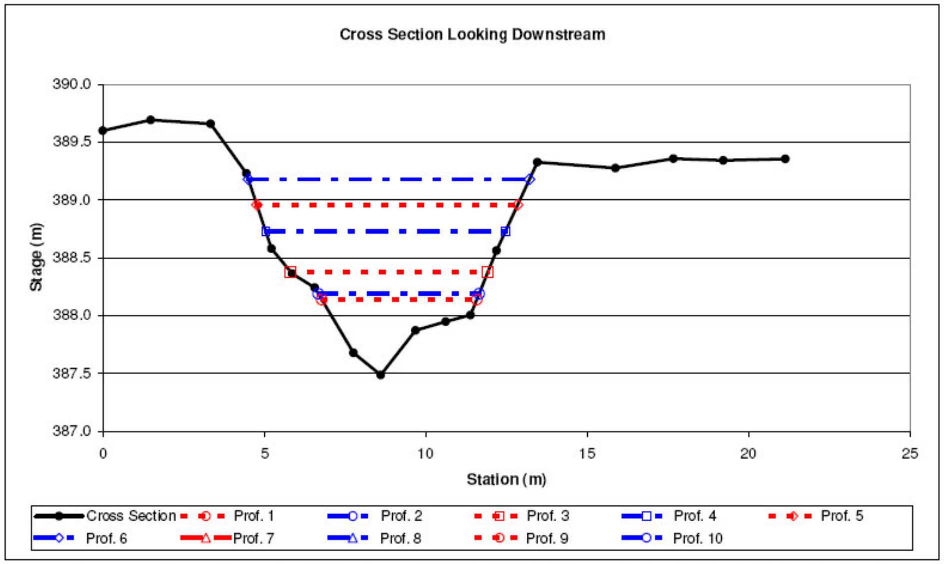

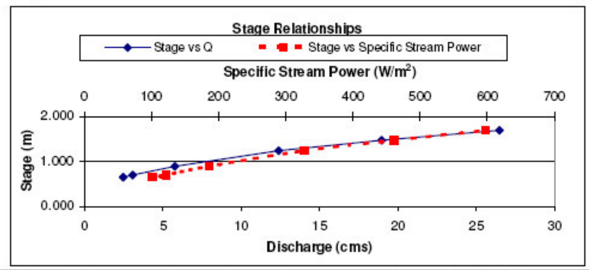

Prof. ID	Estimated n-value	L-Limit	R-Limit	WS (m)	Depth (m)	Left Sta (m)	Right Sta (m)	P_w (m)	Area (m^2)	W (m)	R (m)	D (m)	W/d	V (m/s)	Q (m^3/s)	U* (m/s)	τ (kg/ms^2)	τ*	ω (W/m^2)	Ω (W/m)	F_r	R/d_{84}	n-value per Limerino	Floodplain Form
ACLA03P01	0.040			388.14	0.652	6.78	11.58	5.04	1.54	4.80	0.31	0.32	7.4	1.6	2.48	0.25	60.1	0.233	101	487	0.97	1.8	0.055	BR
ACLA03P02	0.040			388.19	0.702	6.68	11.66	5.24	1.79	4.98	0.34	0.36	7.1	1.7	3.09	0.26	66.9	0.259	122	606	0.99	2.0	0.053	BR
ACLA03P03	0.040			388.38	0.892	5.82	11.93	6.46	2.83	6.12	0.44	0.46	6.9	2.0	5.8	0.29	86.0	0.333	185	1134	1.03	2.5	0.049	BR
ACLA03P04	0.045			388.73	1.242	5.05	12.47	7.96	5.23	7.42	0.66	0.70	6.0	2.4	12.4	0.36	128.7	0.498	328	2433	0.97	3.8	0.045	BR
ACLA03P05	0.045			388.96	1.472	4.77	12.85	8.76	7.01	8.08	0.80	0.87	5.5	2.7	19.0	0.40	156.9	0.607	461	3723	1.00	4.6	0.043	BR
ACLA03P06	0.045			389.18	1.692	4.51	13.21	9.53	8.85	8.70	0.93	1.02	5.1	3.0	26.5	0.43	182.3	0.705	597	5198	1.02	5.4	0.042	BR
ACLA03P07	0.045																							BR
ACLA03P08	0.045																							BR
ACLA03P09	0.045																							BR
ACLA03P10	0.045																							BR

Valley Slope =	0.0417
Valley Width (m) =	20.00

Cross Section Hydraulic Analyses: Aliso Creek at Hovnanian

Floodplain/Site Description: Aliso Canyon near the Hovnanian development. Photo view looking downstream.

Location ID	ACLA04
d_{50} (mm) =	16.00
d_{84} (mm) =	173.31
So = Sf =	0.0348

Pt #	Sta (m)	Elev. (m)
1	0.00	392.89
2	1.41	392.88
3	1.92	392.72
4	2.83	392.43
5	3.77	392.28
6	4.26	392.11
7	4.95	391.64
8	5.73	391.32
9	6.57	391.19
10	7.40	391.40
11	7.97	391.71
12	8.57	392.13
13	9.08	392.44
14	9.41	392.59
15	10.98	393.35
16	12.00	393.31
17		
18		
19		
20		
21		
22		
23		
24		
25		
26		
27		
28		
29		
30		
31		
32		
33		
34		
35		
min. Stage =	391.19	
Continuum	1	
CEM	3.0	

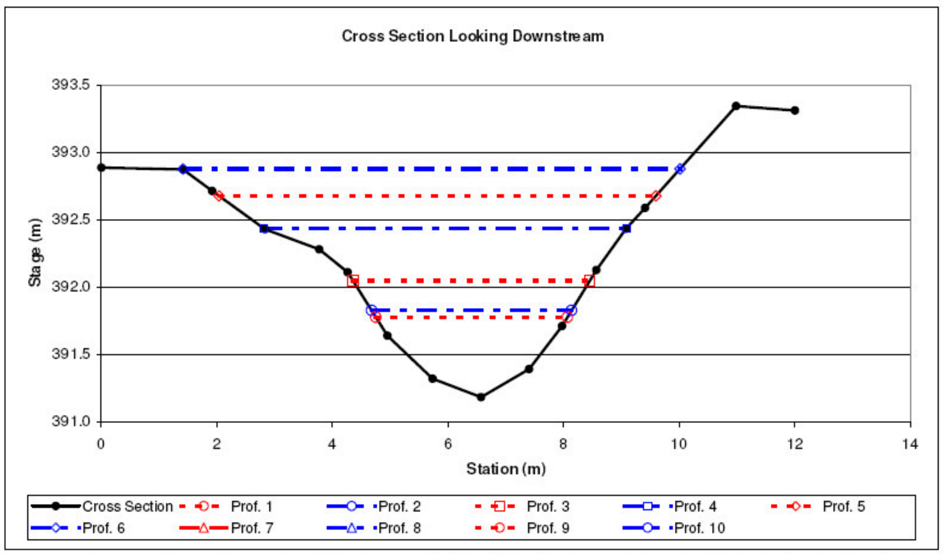

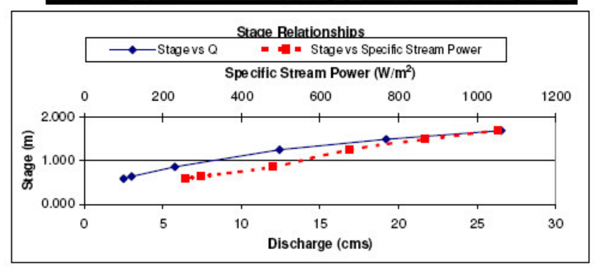

Prof. ID	Estimated n-value	L-Limit	R-Limit	WS (m)	Depth (m)	Left Sta (m)	Right Sta (m)	P_w (m)	Area (m^2)	W (m)	R (m)	D (m)	W/d	V (m/s)	Q (m^3/s)	U* (m/s)	τ (kg/ms²)	τ*	ω (W/m²)	Ω (W/m)	F_r	R/d_{84}	n-value per Limerino	Floodplain Form
ACLA04P01	0.045			391.78	0.594	4.75	8.06	3.56	1.23	3.32	0.34	0.37	5.6	2.0	2.5	0.34	117.4	0.454	257	851	1.15	2.0	0.053	BR
ACLA04P02	0.045			391.83	0.644	4.68	8.14	3.74	1.39	3.46	0.37	0.40	5.4	2.1	3.0	0.36	127.4	0.493	296	1023	1.16	2.2	0.051	BR
ACLA04P03	0.045			392.05	0.864	4.35	8.45	4.51	2.23	4.10	0.49	0.54	4.7	2.6	5.8	0.41	168.4	0.652	480	1967	1.20	2.8	0.047	BR
ACLA04P04	0.045			392.44	1.254	2.81	9.08	6.86	4.17	6.27	0.61	0.67	5.0	3.0	12.4	0.46	207.6	0.803	676	4239	1.25	3.5	0.045	BR
ACLA04P05	0.045			392.68	1.494	2.04	9.59	8.24	5.83	7.56	0.71	0.77	5.1	3.3	19.2	0.49	241.8	0.935	868	6560	1.28	4.1	0.044	BR
ACLA04P06	0.045	1.41		392.88	1.694	1.41	10.01	9.35	7.45	8.60	0.80	0.87	5.1	3.6	26.5	0.52	272.0	1.052	1054	9063	1.31	4.6	0.043	BR
ACLA04P07	0.045																							BR
ACLA04P08	0.045																							BR
ACLA04P09	0.045																							BR
ACLA04P10	0.045																							BR

Valley Slope =	0.04167
Valley Width (m) =	14.00

Cross Section Hydraulic Analyses: Aliso Creek at Hovnanian

Floodplain/Site Description: Aliso Canyon near the Hovnanian development. Photo view looking downstream.

Location ID	ACLA05
d_{50} (mm) =	16.00
d_{84} (mm) =	173.31
So = Sf =	0.0348

Pt #	Sta (m)	Elev. (m)
1	0.00	396.20
2	0.96	395.89
3	2.00	395.60
4	2.47	395.07
5	3.48	393.92
6	3.90	393.56
7	4.94	393.39
8	5.60	392.98
9	6.49	392.68
10	7.54	392.15
11	8.47	392.03
12	9.18	392.15
13	10.50	392.56
14	11.32	392.85
15	12.29	393.22
16	14.06	393.11
17	15.95	393.33
18	17.87	393.57
19		
20		
21		
22		
23		
24		
25		
26		
27		
28		
29		
30		
31		
32		
33		
34		
35		
min. Stage =	392.03	
Continuum	1	
CEM	3.0	

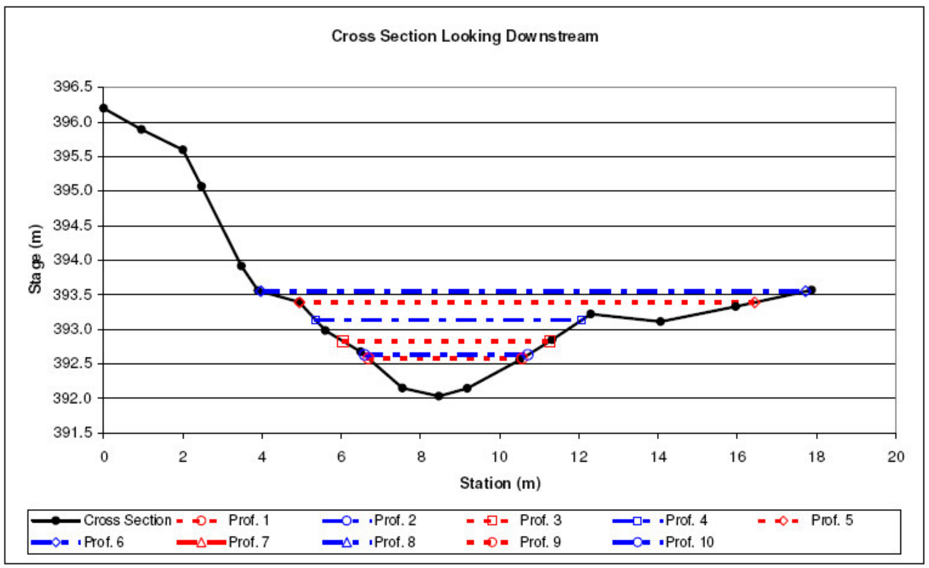

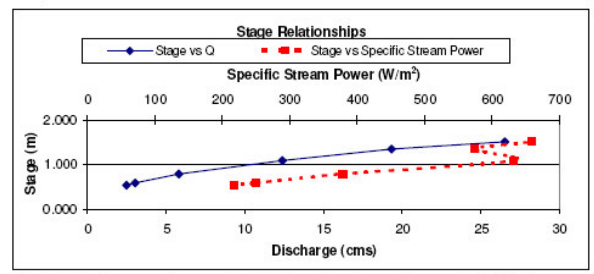

Prof. ID	Estimated n-value	L-Limit	R-Limit	WS (m)	Depth (m)	Left Sta (m)	Right Sta (m)	P_w (m)	Area (m^2)	W (m)	R (m)	D (m)	W/d	V (m/s)	Q (m^3/s)	U* (m/s)	τ (kg/ms²)	τ*	ω (W/m²)	Ω (W/m)	F_r	R/d_{84}	n-value per Limerino	Floodplain Form
ACLA05P01	0.045			392.58	0.547	6.68	10.57	4.07	1.29	3.88	0.32	0.33	7.1	1.9	2.5	0.33	108.1	0.418	218	847	1.14	1.8	0.054	BR
ACLA05P02	0.045			392.63	0.597	6.58	10.71	4.33	1.49	4.12	0.34	0.36	6.9	2.0	3.0	0.34	117.4	0.454	251	1034	1.16	2.0	0.053	BR
ACLA05P03	0.045			392.83	0.797	6.04	11.27	5.51	2.42	5.23	0.44	0.46	6.6	2.4	5.8	0.39	150.1	0.581	379	1981	1.21	2.5	0.049	BR
ACLA05P04	0.045		12.29	393.13	1.097	5.36	12.06	7.10	4.23	6.70	0.60	0.63	6.1	2.9	12.4	0.45	203.1	0.786	631	4231	1.26	3.4	0.046	BR
ACLA05P05	0.045			393.39	1.357	4.94	16.43	12.00	6.81	11.49	0.57	0.59	8.5	2.8	19.3	0.44	193.6	0.749	574	6600	1.26	3.3	0.046	BR
ACLA05P06	0.045			393.55	1.517	3.97	17.72	14.29	8.83	13.75	0.62	0.64	9.1	3.0	26.5	0.46	210.9	0.816	659	9059	1.29	3.6	0.046	BR
ACLA05P07	0.045																							BR
ACLA05P08	0.045																							BR
ACLA05P09	0.045																							BR
ACLA05P10	0.045																							BR

Valley Slope =	0.0417
Valley Width (m) =	18.00

Cross Section Hydraulic Analyses: Bus Canyon at Challenger Park

Floodplain/Site Description: Bus Canyon Creek within Challenger Park. Photo shows downstream cross section looking downstream (Jan 08). Cross section extended based on photographs to include Q100.

Location ID		BCLC01
d_{50} (mm) =		51.20
d_{84} (mm) =		112.70
So = Sf =		0.0107
Pt #	Sta (m)	Stage (m)
1	0.00	100.40
2	10.00	100.00
3	10.60	100.05
4	11.60	99.97
5	12.60	99.87
6	13.60	99.67
7	14.60	99.52
8	15.70	99.24
9	15.80	98.41
10	16.00	98.26
11	16.70	98.28
12	17.20	98.33
13	17.80	98.30
14	18.10	98.47
15	18.50	98.63
16	19.00	98.87
17	19.70	98.94
18	20.70	99.22
19	22.00	99.36
20	24.00	99.42
21	34.00	99.65
22	44.00	99.65
23	48.00	100.31
24		
25		
26		
27		
28		
29		
30		
31		
32		
33		
34		
35		
min. Stage =		98.26
Continuum		2
CEM		1

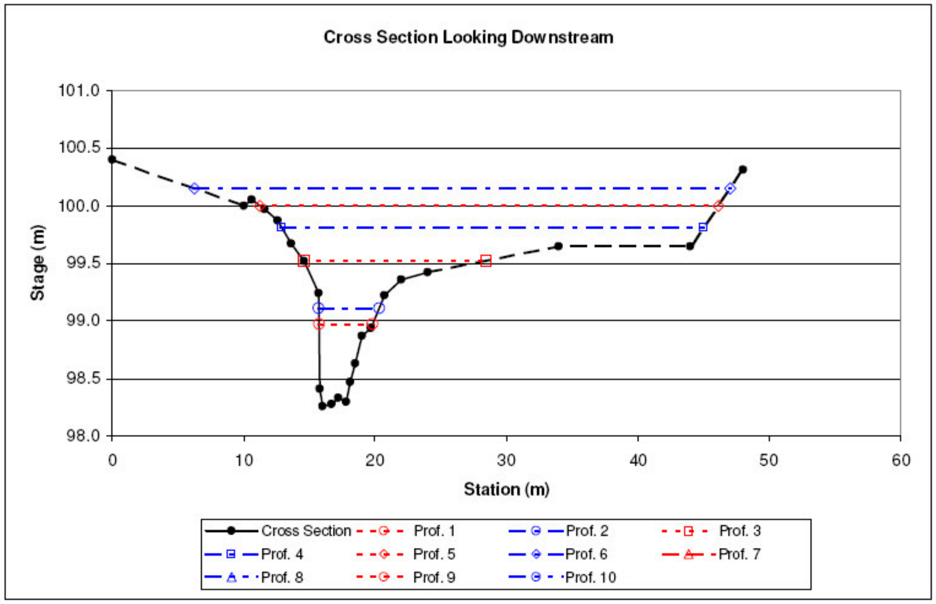

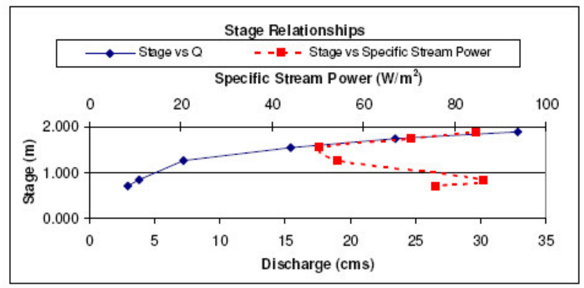

Prof. ID	Estimated n-value	L-Limit	R-Limit	WS (m)	Depth (m)	Left Sta (m)	Right Sta (m)	P_w (m)	Area (m^2)	W (m)	R (m)	D (m)	W/d	V (m/s)	Q (m^3/s)	U* (m/s)	τ (kg/ms²)	τ*	ω (W/m²)	Ω (W/m)	F_r	R/d_{84}	n-value per Limerino	Floodplain Form
BCLC01P01	0.035			98.97	0.710	15.73	19.81	4.76	1.86	4.07	0.39	0.46	5.7	1.6	2.9	0.20	41.0	0.050	76	309	0.80	3.5	0.042	PR
BCLC01P02	0.040			99.11	0.850	15.72	20.31	5.42	2.47	4.59	0.46	0.54	5.4	1.5	3.8	0.22	47.8	0.058	86	397	0.71	4.0	0.040	PR
BCLC01P03	0.040			99.52	1.260	14.60	28.44	14.85	5.43	13.84	0.37	0.39	11.0	1.3	7.2	0.20	38.4	0.046	54	754	0.72	3.2	0.043	PR
BCLC01P04	0.045			99.81	1.550	12.90	44.99	33.14	12.71	32.09	0.38	0.40	20.7	1.2	15.4	0.20	40.2	0.049	50	1618	0.66	3.4	0.043	PR
BCLC01P05	0.055			100.00	1.740	11.23	46.13	35.98	19.04	34.90	0.53	0.55	20.1	1.2	23.4	0.24	55.6	0.067	70	2460	0.57	4.7	0.040	PR
BCLC01P06	0.055			100.15	1.890	6.25	47.03	41.87	24.78	40.78	0.59	0.61	21.6	1.3	32.9	0.25	62.1	0.075	85	3449	0.58	5.3	0.040	PR
BCLC01P07	0.045																							PR
BCLC01P08	0.045																							PR
BCLC01P09	0.045																							PR
BCLC01P10	0.045																							PR

Cross Section Hydraulic Analyses: Bus Canyon at Challenger Park

Floodplain/Site Description: Photo shows middle cross section looking D/S from head-cuts (Jan 08). This reach appears to be responding to the urban outfall located ~ 50 meters upstream and the relatively flat bed slope may not be representative of the reach. Estimated gradation.

Location ID	BCLC02
d_{50} (mm) =	51.20
d_{84} (mm) =	112.70
So = Sf =	0.0061

Pt #	Sta (m)	Stage (m)
1	0.00	103.26
2	5.00	102.43
3	6.50	102.56
4	8.00	102.45
5	9.00	101.99
6	9.80	101.81
7	10.00	100.95
8	10.50	100.88
9	11.30	101.01
10	11.50	101.53
11	11.80	101.77
12	12.80	101.97
13	14.00	102.35
14	15.00	102.52
15	25.00	102.52
16	30.00	103.35
17		
18		
19		
20		
21		
22		
23		
24		
25		
26		
27		
28		
29		
30		
31		
32		
33		
34		
35		
min. Stage =	100.88	
Continuum	2	
CEM	2	

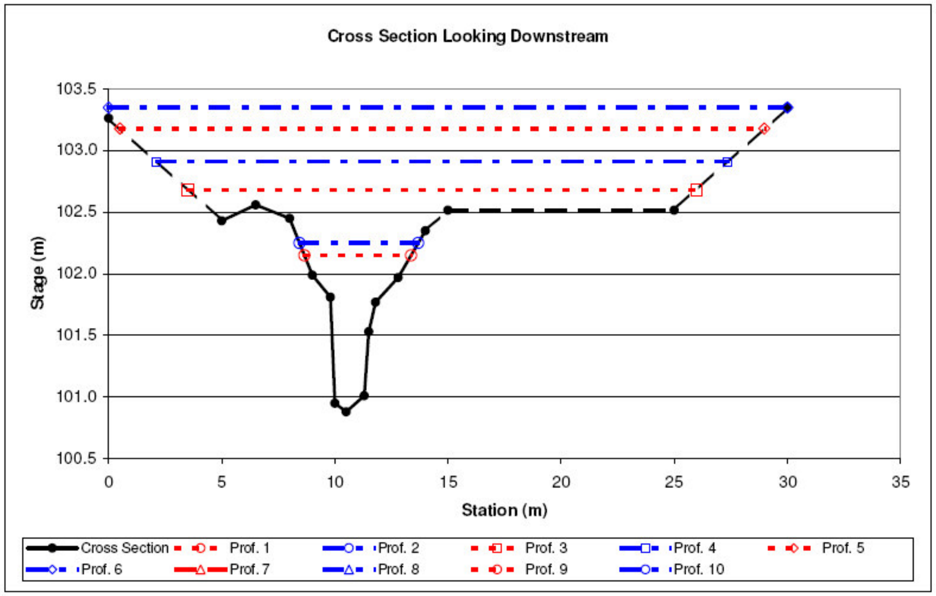

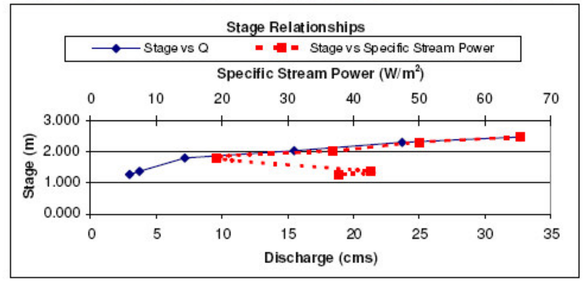

Prof. ID	Estimated n-value	L-Limit	R-Limit	WS (m)	Depth (m)	Left Sta (m)	Right Sta (m)	P_w (m)	Area (m^2)	W (m)	R (m)	D (m)	W/d	V (m/s)	Q (m^3/s)	U* (m/s)	τ (kg/ms^2)	τ*	ω (W/m^2)	Ω (W/m)	F_r	R/d_{84}	n-value per Limerino	Floodplain Form
BCLC02P01	0.040			102.15	1.270	8.65	13.37	5.96	2.62	4.72	0.44	0.56	3.7	1.1	3.0	0.16	26.4	0.032	38	178	0.52	3.9	0.040	PMB
BCLC02P02	0.040			102.25	1.370	8.43	13.68	6.53	3.12	5.25	0.48	0.59	3.8	1.2	3.7	0.17	28.7	0.035	43	224	0.53	4.2	0.040	PMB
BCLC02P03	0.045			102.68	1.800	3.50	25.98	23.88	8.33	22.48	0.35	0.37	12.5	0.9	7.2	0.14	20.9	0.025	19	431	0.48	3.1	0.044	PMB
BCLC02P04	0.045			102.91	2.030	2.12	27.36	26.67	13.81	25.24	0.52	0.55	12.4	1.1	15.5	0.18	31.1	0.038	37	930	0.52	4.6	0.040	PMB
BCLC02P05	0.055			103.18	2.300	0.50	28.98	29.96	21.07	28.48	0.70	0.74	12.4	1.1	23.7	0.21	42.2	0.051	50	1423	0.45	6.2	0.038	PMB
BCLC02P06	0.055			103.35	2.470	0.00	30.00	31.50	26.06	30.00	0.83	0.87	12.1	1.3	32.7	0.22	49.7	0.060	65	1962	0.46	7.3	0.038	PMB
BCLC02P07	0.045																							PMB
BCLC02P08	0.045																							PMB
BCLC02P09	0.045																							PMB
BCLC02P10	0.045																							PMB

Cross Section Hydraulic Analyses: Bus Canyon at Challenger Park

Floodplain/Site Description: Bus Canyon Creek within Challenger Park. Photo shows upstream cross section looking upstream (Jan 08).

Location ID	BCLC03
d_{50} (mm) =	69.70
d_{84} (mm) =	151.80
So = Sf =	0.0166

Pt #	Sta (m)	Stage (m)
1	0.00	106.26
2	3.00	105.26
3	4.90	105.25
4	6.10	105.08
5	6.40	104.80
6	7.10	104.61
7	7.50	104.37
8	8.10	104.51
9	8.50	104.49
10	8.70	104.39
11	9.15	104.38
12	9.70	104.51
13	10.10	104.55
14	10.50	104.76
15	11.30	105.35
16	13.30	105.35
17	23.30	105.35
18	28.30	106.18
19		
20		
21		
22		
23		
24		
25		
26		
27		
28		
29		
30		
31		
32		
33		
34		
35		
min. Stage =		104.37
Continuum		2
CEM		1

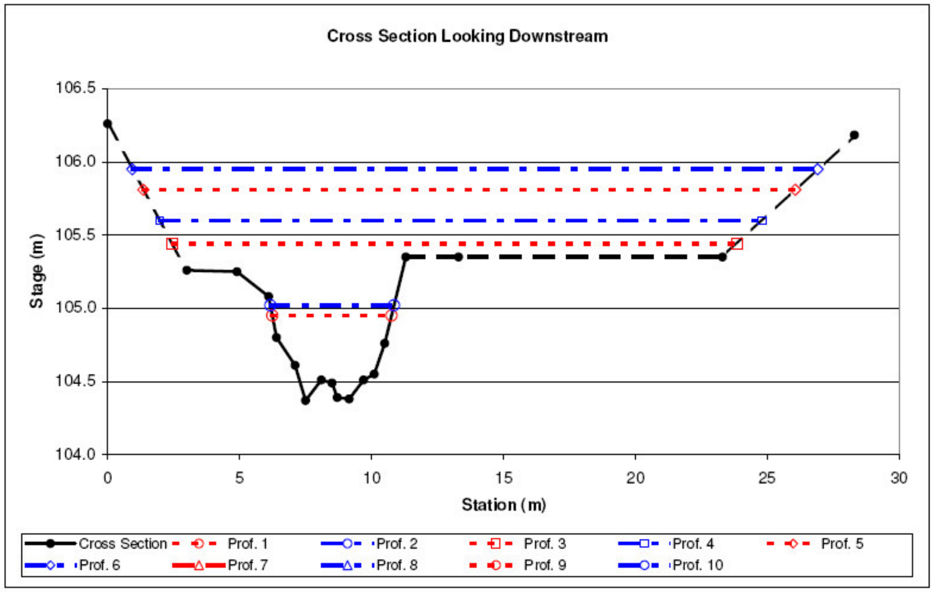

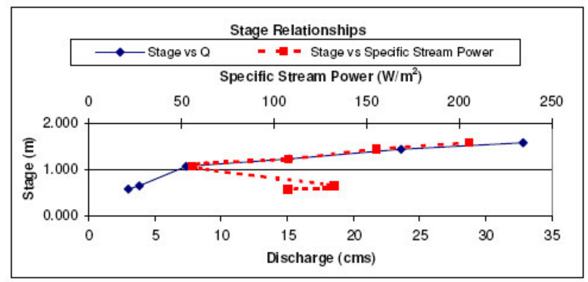

Prof. ID	Estimated n-value	L-Limit	R-Limit	WS (m)	Depth (m)	Left Sta (m)	Right Sta (m)	P_w (m)	Area (m^2)	W (m)	R (m)	D (m)	W/d	V (m/s)	Q (m^3/s)	U* (m/s)	τ (kg/ms^2)	τ^*	ω (W/m^2)	Ω (W/m)	F_r	R/d_{84}	n-value per Limerino	Floodplain Form
BCLC03P01	0.040			104.95	0.580	6.24	10.76	4.84	1.80	4.52	0.37	0.40	7.8	1.7	3.0	0.25	60.3	0.054	107	486	0.90	2.4	0.048	PR
BCLC03P02	0.040			105.02	0.650	6.16	10.85	5.06	2.12	4.69	0.42	0.45	7.2	1.8	3.8	0.26	68.1	0.060	132	620	0.92	2.8	0.047	PR
BCLC03P03	0.045			105.44	1.070	2.46	23.84	21.93	6.06	21.38	0.28	0.28	20.0	1.2	7.4	0.21	44.9	0.040	56	1195	0.78	1.8	0.054	PR
BCLC03P04	0.045			105.60	1.230	1.98	24.80	23.41	9.60	22.82	0.41	0.42	18.6	1.6	15.1	0.26	66.6	0.059	108	2461	0.83	2.7	0.048	PR
BCLC03P05	0.055			105.81	1.440	1.35	26.06	25.35	14.59	24.71	0.58	0.59	17.2	1.6	23.6	0.31	93.5	0.083	155	3837	0.72	3.8	0.044	PR
BCLC03P06	0.055			105.95	1.580	0.93	26.90	26.65	18.14	25.97	0.68	0.70	16.4	1.8	32.8	0.33	110.6	0.098	205	5334	0.74	4.5	0.043	PR
BCLC03P07	0.045																							PR
BCLC03P08	0.045																							PR
BCLC03P09	0.045																							PR
BCLC03P10	0.045																							PR

Cross Section Hydraulic Analyses: Dry Canyon

Floodplain/Site Description: Photo view looking downstream from right overbank.

Location ID		DCAD01
d_{50} (mm) =		0.73
d_{84} (mm) =		1.34
So = Sf =		0.0248
Pt #	Sta (m)	Stage (m)
1	1.14	327.25
2	2.51	327.08
3	3.67	327.06
4	5.12	327.05
5	5.97	326.96
6	6.98	326.84
7	7.22	325.94
8	7.75	325.52
9	8.22	325.27
10	9.14	325.27
11	10.25	325.33
12	11.26	325.27
13	11.79	325.12
14	12.68	325.10
15	13.59	325.06
16	14.46	325.01
17	15.35	325.02
18	16.09	325.05
19	16.93	325.04
20	17.44	325.04
21	17.98	325.08
22	18.61	325.41
23	19.39	325.73
24	19.81	326.13
25	20.26	326.15
26	20.49	326.24
27	20.85	326.53
28	21.28	326.63
29	21.80	326.72
30	22.31	326.76
31		
32		
33		
34		
35		
min. Stage =		325.01
Continuum		1
CEM		4

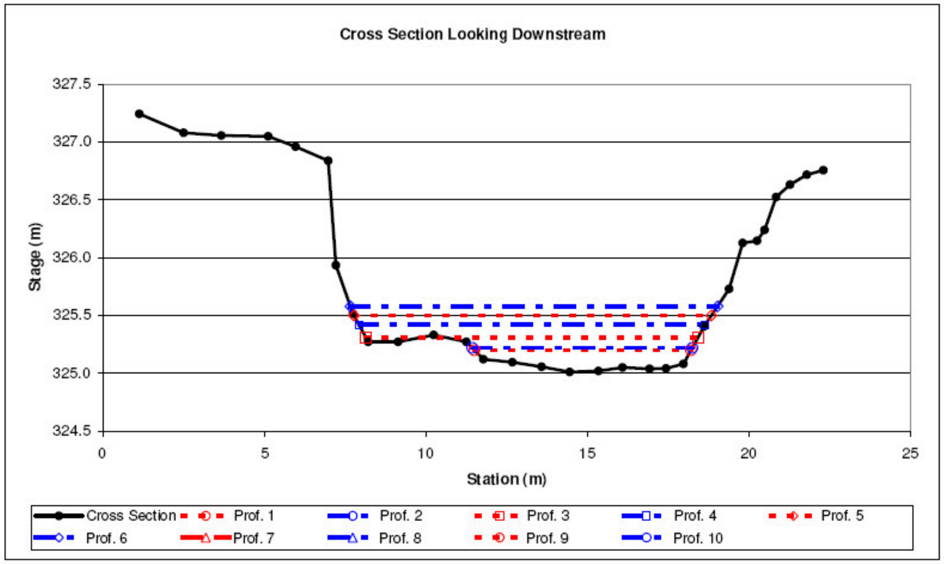

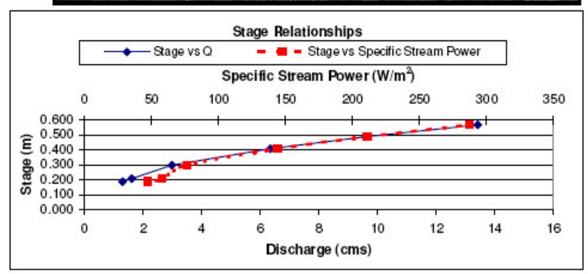

Prof. ID	Estimated n-value	L-Limit	R-Limit	WS (m)	Depth (m)	Left Sta (m)	Right Sta (m)	P_w (m)	Area (m^2)	W (m)	R (m)	D (m)	W/d	V (m/s)	Q (m^3/s)	U* (m/s)	τ (kg/ms^2)	τ*	ω (W/m^2)	Ω (W/m)	F_r	R/d_{84}	n-value per Limerino	Floodplain Form
DCAD01P01	0.030			325.20	0.189	11.51	18.21	6.75	0.94	6.70	0.14	0.14	35.5	1.4	1.32	0.18	33.8	2.879	48	322	1.29	103.5	0.016	PMB
DCAD01P02	0.030			325.22	0.209	11.44	18.25	6.86	1.07	6.81	0.16	0.16	32.6	1.5	1.64	0.20	38.0	3.237	58	398	1.31	116.4	0.016	PMB
DCAD01P03	0.030			325.31	0.299	8.15	18.43	9.60	1.77	9.51	0.18	0.19	31.8	1.7	3.00	0.21	44.8	3.813	77	731	1.35	137.0	0.016	PMB
DCAD01P04	0.030			325.42	0.409	7.93	18.65	10.86	2.91	10.72	0.27	0.27	26.2	2.2	6.4	0.26	65.3	5.554	144	1548	1.43	199.6	0.016	PMB
DCAD01P05	0.030			325.50	0.489	7.78	18.84	11.24	3.79	11.06	0.34	0.34	22.6	2.5	9.6	0.29	81.9	6.970	211	2340	1.49	250.5	0.016	PMB
DCAD01P06	0.030			325.58	0.569	7.67	19.03	11.59	4.68	11.37	0.40	0.41	20.0	2.9	13.4	0.31	98.3	8.365	288	3269	1.53	300.6	0.016	PMB
DCAD01P07	0.030																							PMB
DCAD01P08	0.030																							PMB
DCAD01P09	0.030																							PMB
DCAD01P10	0.030																							PMB

Cross Section Hydraulic Analyses: Dry Canyon

Floodplain/Site Description: Photo view looking downstream.

Location ID	DCAD02
d_{50} (mm) =	0.73
d_{84} (mm) =	1.34
So = Sf =	0.0248

Pt #	Sta (m)	Stage (m)
1	0.00	331.34
2	0.76	331.33
3	1.60	331.27
4	2.52	331.15
5	3.22	331.01
6	3.74	330.85
7	5.51	329.90
8	7.68	328.59
9	9.84	327.79
10	12.61	327.68
11	14.43	327.63
12	15.13	327.08
13	15.96	326.68
14	17.68	326.67
15	19.69	326.60
16	22.62	326.42
17	25.28	326.13
18	25.38	326.01
19	28.42	325.91
20	30.31	325.97
21	33.99	325.90
22	35.36	325.95
23	35.99	327.18
24	38.40	327.03
25	42.09	326.90
26	42.91	327.13
27	45.00	327.04
28	47.44	327.10
29	49.02	328.11
30	51.41	330.19
31	52.27	330.20
32		
33		
34		
35		
min. Stage =		325.90
Continuum		1
CEM		4

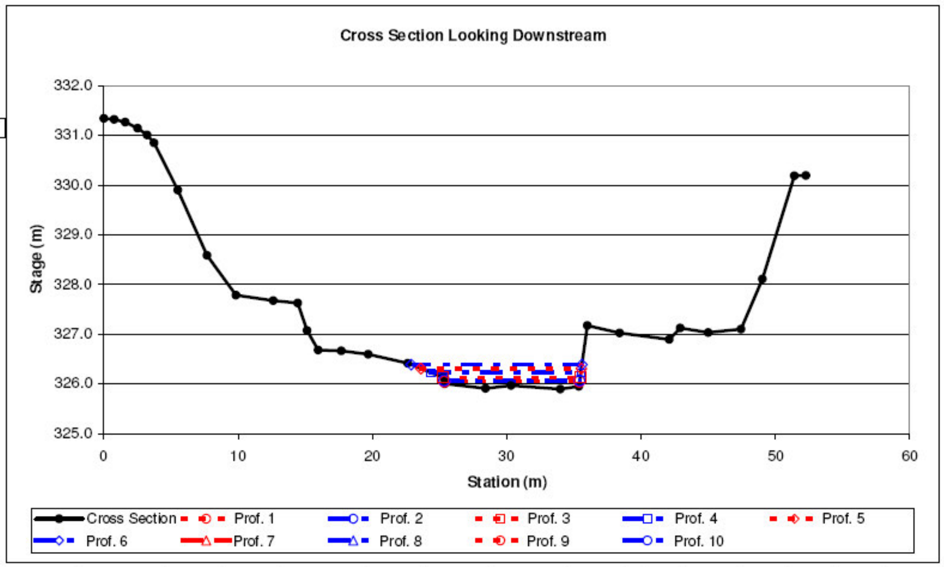

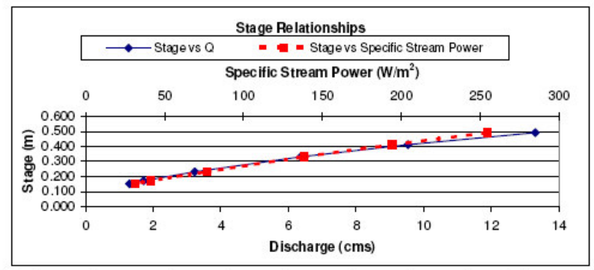

Prof. ID	Estimated n-value	L-Limit	R-Limit	WS (m)	Depth (m)	Left Sta (m)	Right Sta (m)	P_w (m)	Area (m^2)	W (m)	R (m)	D (m)	W/d	V (m/s)	Q (m^3/s)	U* (m/s)	τ (kg/ms²)	τ*	ω (W/m²)	Ω (W/m)	F_r	R/d_{84}	n-value per Limerino	Floodplain Form
DCAD02P01	0.030			326.05	0.152	25.34	35.41	10.15	1.09	10.07	0.11	0.11	66.2	1.2	1.3	0.16	26.2	2.231	31	317	1.23	80.2	0.016	PMB
DCAD02P02	0.030			326.07	0.172	25.33	35.42	10.20	1.30	10.10	0.13	0.13	58.7	1.3	1.7	0.18	30.9	2.630	41	418	1.27	94.5	0.016	PMB
DCAD02P03	0.030			326.13	0.232	25.26	35.46	10.37	1.90	10.20	0.18	0.19	44.0	1.7	3.2	0.21	44.7	3.801	77	786	1.34	136.6	0.016	PMB
DCAD02P04	0.030			326.23	0.332	24.34	35.51	11.40	2.97	11.16	0.26	0.27	33.6	2.1	6.4	0.25	63.4	5.396	139	1549	1.42	194.0	0.016	PMB
DCAD02P05	0.030			326.31	0.412	23.61	35.55	12.23	3.90	11.94	0.32	0.33	29.0	2.4	9.5	0.28	77.5	6.596	194	2321	1.47	237.1	0.016	PMB
DCAD02P06	0.030			326.39	0.492	22.88	35.59	13.05	4.88	12.71	0.37	0.38	25.8	2.7	13.3	0.30	91.0	7.742	255	3237	1.51	278.3	0.016	PMB
DCAD02P07	0.030																							PMB
DCAD02P08	0.030																							PMB
DCAD02P09	0.030																							PMB
DCAD02P10	0.030																							PMB

Cross Section Hydraulic Analyses: Dry Canyon

Floodplain/Site Description: Photo view looking upstream from right overbank.

Location ID	DCAD03	
d_{50} (mm) =	0.73	
d_{84} (mm) =	1.34	
So = Sf =	0.0168	
Pt #	Sta (m)	Stage (m)
1	0.00	327.96
2	1.10	327.95
3	2.16	327.97
4	3.47	327.98
5	4.34	327.89
6	5.34	327.90
7	6.70	327.90
8	7.88	327.97
9	9.08	327.96
10	10.27	327.99
11	11.78	327.94
12	12.76	327.96
13	13.79	327.96
14	14.62	327.86
15	15.14	327.07
16	15.70	326.66
17	16.20	326.52
18	17.08	326.30
19	18.11	326.26
20	19.13	326.25
21	20.10	326.25
22	20.83	326.22
23	21.64	326.19
24	22.46	326.15
25	23.07	326.15
26	23.61	326.25
27	25.37	328.97
28	26.09	329.39
29	26.69	329.96
30	27.53	330.36
31	27.98	330.51
32	28.42	330.66
33	28.99	330.64
34	29.63	330.89
35	30.47	330.92
min. Stage =	326.15	
Continuum	1	
CEM	4	

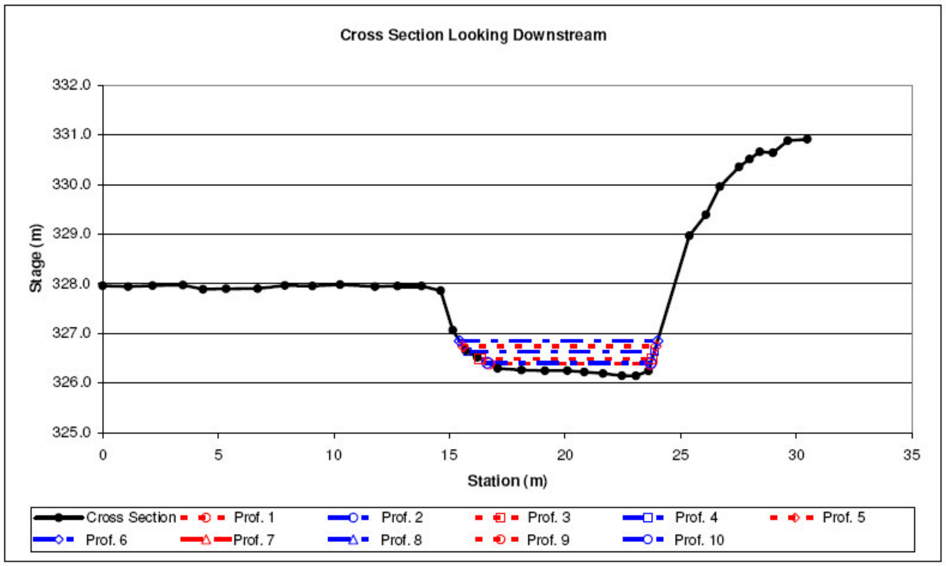

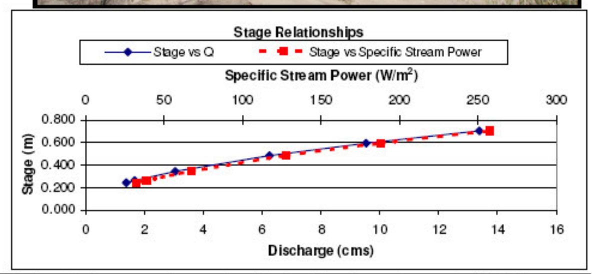

Prof. ID	Estimated n-value	L-Limit	R-Limit	WS (m)	Depth (m)	Left Sta (m)	Right Sta (m)	P_w (m)	Area (m^2)	W (m)	R (m)	D (m)	W/d	V (m/s)	Q (m^3/s)	U* (m/s)	τ (kg/ms²)	τ*	ω (W/m²)	Ω (W/m)	F_r	R/d_{84}	n-value per Limerino	Floodplain Form
DCAD03P01	0.030			326.39	0.245	16.71	23.70	7.10	1.11	6.99	0.16	0.16	28.5	1.3	1.38	0.16	25.7	2.186	33	228	1.08	115.9	0.016	PMB
DCAD03P02	0.030			326.41	0.265	16.63	23.72	7.20	1.25	7.08	0.17	0.18	26.7	1.3	1.67	0.17	28.5	2.428	39	276	1.10	128.8	0.016	PMB
DCAD03P03	0.030			326.49	0.345	16.32	23.77	7.62	1.83	7.45	0.24	0.25	21.6	1.7	3.0	0.20	39.5	3.365	67	503	1.15	178.5	0.016	PMB
DCAD03P04	0.030			326.63	0.485	15.80	23.86	8.33	2.91	8.06	0.35	0.36	16.6	2.1	6.3	0.24	57.7	4.910	128	1031	1.22	260.4	0.016	PMB
DCAD03P05	0.030			326.74	0.595	15.59	23.93	8.70	3.82	8.34	0.44	0.46	14.0	2.5	9.5	0.27	72.4	6.160	188	1572	1.26	326.7	0.016	PMB
DCAD03P06	0.030			326.85	0.705	15.44	24.00	9.01	4.75	8.56	0.53	0.55	12.1	2.8	13.4	0.29	86.8	7.390	258	2207	1.30	391.9	0.016	PMB
DCAD03P07	0.030																							PMB
DCAD03P08	0.030																							PMB
DCAD03P09	0.030																							PMB
DCAD03P10	0.030																							PMB

Cross Section Hydraulic Analyses: Dry Canyon

Floodplain/Site Description: Photo view looking downstream.

Location ID	DCAD04
d_{50} (mm) =	0.73
d_{84} (mm) =	1.34
So = Sf =	0.0168

Pt #	Sta (m)	Stage (m)
1	5.51	328.43
2	6.14	328.41
3	6.83	328.27
4	7.61	327.87
5	7.98	327.82
6	8.98	327.74
7	9.60	327.74
8	10.04	327.58
9	10.44	327.37
10	10.67	326.95
11	11.07	326.77
12	11.50	326.58
13	12.53	326.61
14	13.88	326.62
15	14.96	326.68
16	15.96	326.72
17	16.91	326.76
18	17.83	326.77
19	18.51	326.86
20	19.03	326.73
21	20.21	326.69
22	21.23	326.71
23	22.23	326.72
24	23.31	326.71
25	23.73	326.75
26	24.46	326.87
27	25.09	327.13
28	26.16	327.53
29	27.63	328.21
30	29.48	329.28
31	30.02	329.50
32	30.87	329.75
33	31.83	331.98
34	32.99	332.05
35	33.50	332.15
min. Stage =		326.58
Continuum		1
CEM		4.0

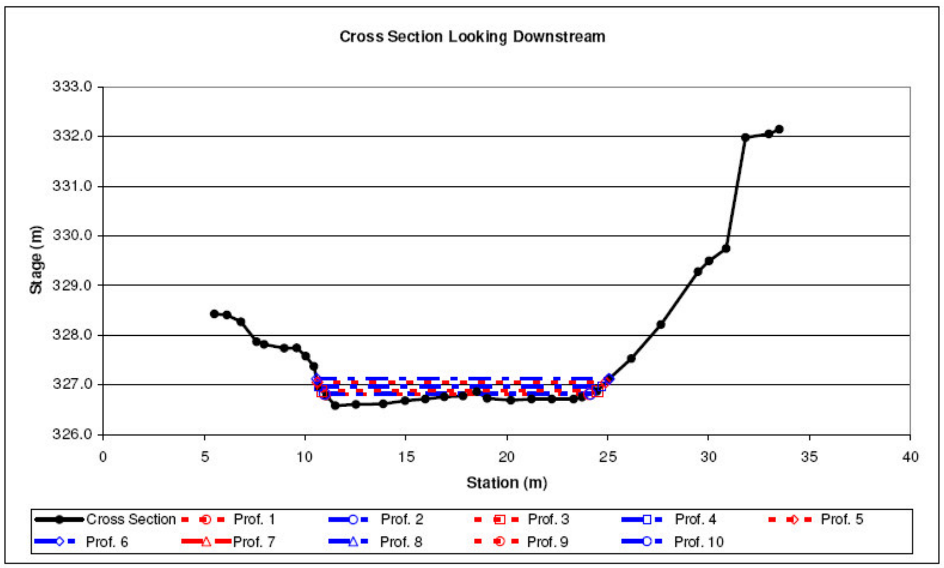

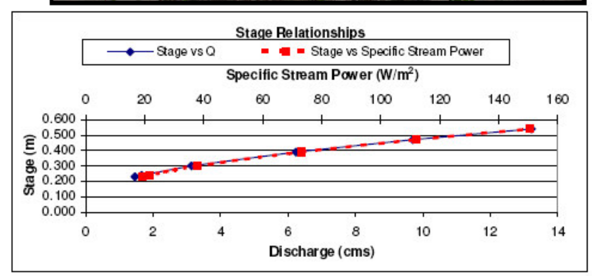

Prof. ID	Estimated n-value	L-Limit	R-Limit	WS (m)	Depth (m)	Left Sta (m)	Right Sta (m)	P_w (m)	Area (m^2)	W (m)	R (m)	D (m)	W/d	V (m/s)	Q (m^3/s)	U* (m/s)	τ (kg/ms²)	τ*	ω (W/m²)	Ω (W/m)	F_r	R/d_{84}	n-value per Limerino	Floodplain Form
DCAD04P01	0.030			326.81	0.230	10.99	24.09	12.56	1.43	12.48	0.11	0.11	54.3	1.0	1.5	0.14	18.8	1.601	19	240	1.03	84.9	0.016	BF
DCAD04P02	0.030			326.82	0.240	10.97	24.15	12.76	1.56	12.68	0.12	0.12	52.8	1.1	1.7	0.14	20.1	1.714	22	274	1.04	90.9	0.016	BF
DCAD04P03	0.030			326.88	0.300	10.83	24.49	13.76	2.35	13.65	0.17	0.17	45.5	1.3	3.1	0.17	28.2	2.400	38	517	1.10	127.3	0.016	BF
DCAD04P04	0.030			326.97	0.390	10.66	24.70	14.19	3.60	14.04	0.25	0.26	36.0	1.7	6.2	0.20	41.8	3.561	73	1029	1.17	188.9	0.016	BF
DCAD04P05	0.030			327.05	0.470	10.62	24.89	14.49	4.73	14.27	0.33	0.33	30.4	2.1	9.7	0.23	53.9	4.584	112	1600	1.22	243.1	0.016	BF
DCAD04P06	0.030			327.12	0.540	10.58	25.06	14.75	5.74	14.48	0.39	0.40	26.8	2.3	13.2	0.25	64.2	5.460	151	2180	1.25	289.6	0.016	BF
DCAD04P07	0.030																							BF
DCAD04P08	0.030																							BF
DCAD04P09	0.030																							BF
DCAD04P10	0.030																							BF

Cross Section Hydraulic Analyses: Dry Canyon

Floodplain/Site Description: Photo view looking downstream.

Pt #	Sta (m)	Stage (m)
Location ID		DCAD05
d_{50} (mm) =		0.73
d_{84} (mm) =		1.34
So = Sf =		0.0247
1	0.00	329.29
2	2.47	329.19
3	4.55	329.21
4	6.06	329.16
5	6.84	328.74
6	7.56	328.43
7	8.05	328.36
8	8.23	327.72
9	9.06	327.50
10	9.75	327.32
11	10.48	327.33
12	11.47	327.32
13	12.35	327.28
14	13.09	327.27
15	13.45	327.29
16	13.60	327.35
17	14.02	327.37
18	14.42	327.35
19	14.56	327.33
20	14.71	327.40
21	15.45	327.69
22	16.47	327.98
23	18.17	327.98
24	19.34	328.06
25	20.22	328.15
26	21.13	328.23
27	22.07	328.61
28	23.02	328.86
29	23.70	329.42
30	24.58	330.19
31	25.08	330.47
32	25.94	331.86
33	26.90	332.00
34	28.29	332.47
35	30.31	332.45
min. Stage =		327.27
Continuum		1
CEM		3.0

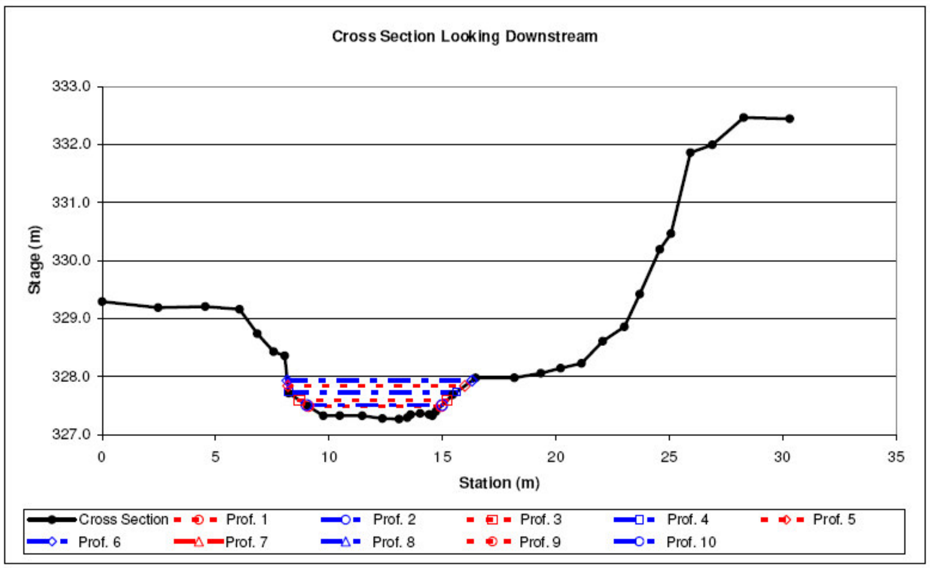

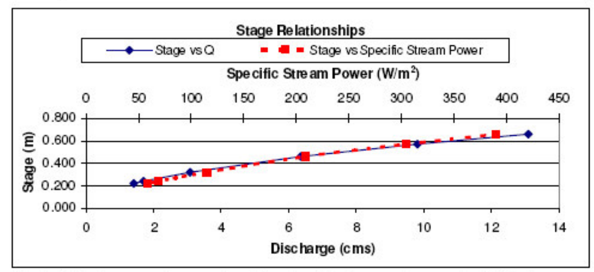

Prof. ID	Estimated n-value	L-Limit	R-Limit	WS (m)	Depth (m)	Left Sta (m)	Right Sta (m)	P_w (m)	Area (m^2)	W (m)	R (m)	D (m)	W/d	V (m/s)	Q (m^3/s)	U* (m/s)	τ (kg/ms^2)	τ*	ω (W/m^2)	Ω (W/m)	F_r	R/d_{84}	n-value per Limerino	Floodplain Form
DCAD05P01	0.030			327.49	0.221	9.09	14.95	5.93	0.93	5.86	0.16	0.16	26.5	1.5	1.4	0.19	37.9	3.227	58	342	1.31	116.5	0.016	PMB
DCAD05P02	0.030			327.51	0.241	9.01	15.00	6.07	1.05	5.99	0.17	0.17	24.9	1.6	1.7	0.20	41.8	3.558	69	412	1.33	128.4	0.016	PMB
DCAD05P03	0.030			327.59	0.321	8.71	15.21	6.60	1.55	6.50	0.23	0.24	20.3	2.0	3.1	0.24	56.8	4.831	115	746	1.40	174.4	0.016	PMB
DCAD05P04	0.030			327.73	0.461	8.22	15.61	7.54	2.52	7.39	0.33	0.34	16.0	2.5	6.4	0.28	81.0	6.894	209	1541	1.48	248.8	0.016	PMB
DCAD05P05	0.030			327.84	0.571	8.19	15.99	8.05	3.36	7.80	0.42	0.43	13.7	2.9	9.8	0.32	101.0	8.594	305	2376	1.53	310.1	0.016	PMB
DCAD05P06	0.030			327.93	0.661	8.17	16.31	8.47	4.07	8.14	0.48	0.50	12.3	3.2	13.1	0.34	116.5	9.914	390	3173	1.56	357.8	0.016	PMB
DCAD05P07	0.030																							PMB
DCAD05P08	0.030																							PMB
DCAD05P09	0.030																							PMB
DCAD05P10	0.030																							PMB

Cross Section Hydraulic Analyses: Dry Canyon

Floodplain/Site Description: Photo view looking downstream.

Location ID		DCAD06
d_{50} (mm) =		0.73
d_{84} (mm) =		1.34
So = Sf =		0.0247
Pt #	Sta (m)	Stage (m)
1	0.00	329.29
2	2.52	329.34
3	4.65	329.37
4	5.80	329.36
5	6.73	329.07
6	7.91	328.74
7	8.84	328.69
8	10.08	328.54
9	10.56	328.50
10	10.70	328.27
11	11.28	327.93
12	12.07	327.62
13	12.59	327.71
14	13.21	327.56
15	13.68	327.54
16	14.00	327.57
17	14.45	327.72
18	14.93	327.73
19	15.37	327.74
20	15.62	327.66
21	16.67	327.59
22	17.83	327.58
23	18.73	331.66
24	20.01	332.51
25	21.12	332.98
26	23.73	332.97
27		
28		
29		
30		
31		
32		
33		
34		
35		
min. Stage =		327.54
Continuum		1
CEM		3

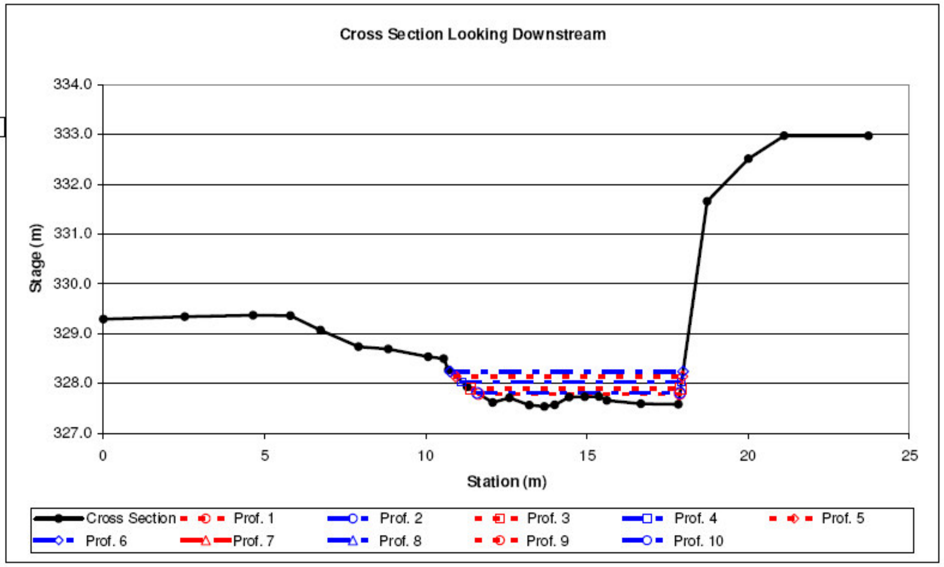

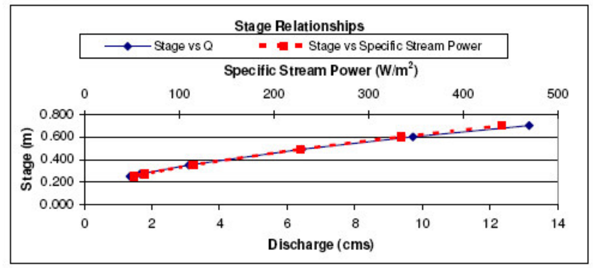

Prof. ID	Estimated n-value	L-Limit	R-Limit	WS (m)	Depth (m)	Left Sta (m)	Right Sta (m)	P_w (m)	Area (m^2)	W (m)	R (m)	D (m)	W/d	V (m/s)	Q (m^3/s)	U* (m/s)	τ (kg/ms²)	τ*	ω (W/m²)	Ω (W/m)	F_r	R/d_{84}	n-value per Limerino	Floodplain Form
DCAD06P01	0.030			327.79	0.252	11.64	17.88	6.51	0.94	6.24	0.14	0.15	24.8	1.4	1.4	0.19	35.0	2.975	53	328	1.27	107.4	0.016	PMB
DCAD06P02	0.030			327.81	0.272	11.59	17.88	6.58	1.06	6.29	0.16	0.17	23.1	1.6	1.7	0.20	39.2	3.334	64	401	1.29	120.3	0.016	PMB
DCAD06P03	0.030			327.89	0.352	11.39	17.90	6.88	1.58	6.51	0.23	0.24	18.5	2.0	3.1	0.24	55.5	4.724	115	749	1.36	170.5	0.016	PMB
DCAD06P04	0.030			328.03	0.492	11.11	17.93	7.33	2.51	6.82	0.34	0.37	13.9	2.6	6.4	0.29	83.0	7.059	229	1560	1.45	254.8	0.016	PMB
DCAD06P05	0.030			328.14	0.602	10.92	17.96	7.67	3.27	7.03	0.43	0.47	11.7	3.0	9.7	0.32	103.4	8.803	335	2356	1.49	317.7	0.016	PMB
DCAD06P06	0.030			328.24	0.702	10.75	17.98	7.97	3.99	7.23	0.50	0.55	10.3	3.3	13.2	0.35	121.2	10.314	441	3189	1.52	372.2	0.016	PMB
DCAD06P07	0.030																							PMB
DCAD06P08	0.030																							PMB
DCAD06P09	0.030																							PMB
DCAD06P10	0.030																							PMB

Cross Section Hydraulic Analyses: Dry Canyon

Floodplain/Site Description: Photo view looking downstream.

Location ID	DCAD07	
d_{50} (mm) =	0.73	
d_{84} (mm) =	1.34	
So = Sf =	0.0247	
Pt #	Sta (m)	Stage (m)
1	0.00	333.31
2	1.50	333.32
3	3.44	333.20
4	8.45	328.33
5	9.34	328.34
6	10.11	328.39
7	10.65	328.49
8	12.52	328.39
9	14.43	328.15
10	15.88	328.19
11	16.77	328.26
12	17.64	328.46
13	18.98	328.39
14	20.06	328.32
15	21.95	328.24
16	23.12	328.13
17	24.41	328.13
18	25.28	328.14
19	26.92	328.54
20	28.62	328.82
21	31.57	329.09
22	33.64	329.32
23	35.72	329.30
24	37.88	329.38
25	39.88	330.64
26	39.79	332.10
27	41.37	332.75
28	42.98	333.17
29	44.26	333.39
30		
31		
32		
33		
34		
35		
min. Stage =		328.13
Continuum		1
CEM		3

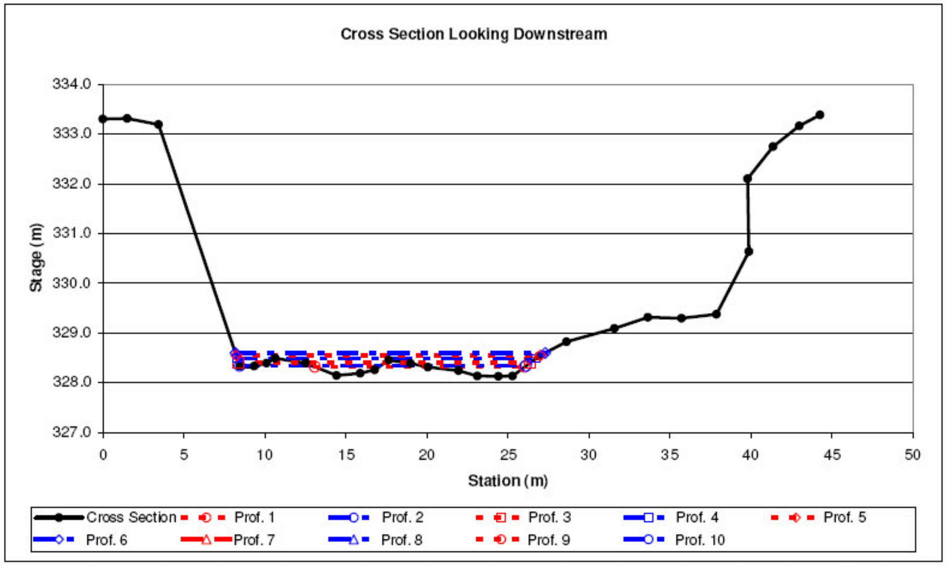

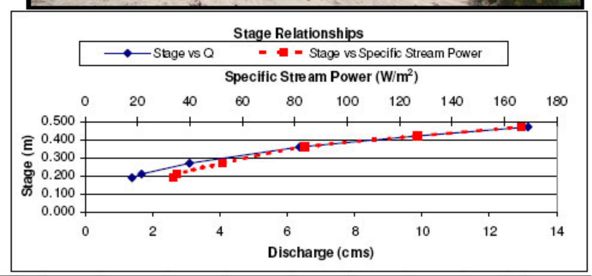

Prof. ID	Estimated n-value	L-Limit	R-Limit	WS (m)	Depth (m)	Left Sta (m)	Right Sta (m)	P_w (m)	Area (m^2)	W (m)	R (m)	D (m)	W/d	V (m/s)	Q (m^3/s)	U* (m/s)	τ (kg/ms²)	τ*	ω (W/m²)	Ω (W/m)	F_r	R/d_{84}	n-value per Limerino	Floodplain Form
DCAD07P01	0.030			328.32	0.190	13.09	26.04	10.05	1.14	10.00	0.11	0.11	52.6	1.2	1.39	0.17	27.4	2.331	34	337	1.24	84.1	0.016	BF
DCAD07P02	0.030			328.34	0.210	8.45	26.12	11.63	1.35	11.57	0.12	0.12	55.1	1.2	1.68	0.17	28.1	2.388	35	406	1.25	86.2	0.016	BF
DCAD07P03	0.030			328.40	0.270	8.38	26.36	14.43	2.12	14.32	0.15	0.15	53.1	1.5	3.1	0.19	35.6	3.032	52	750	1.30	109.4	0.016	BF
DCAD07P04	0.030			328.49	0.360	8.29	26.73	18.59	3.62	18.41	0.19	0.20	51.2	1.8	6.4	0.22	47.2	4.013	84	1543	1.36	144.8	0.016	BF
DCAD07P05	0.030			328.55	0.420	8.23	27.00	18.97	4.73	18.77	0.25	0.25	44.7	2.1	9.8	0.25	60.4	5.144	127	2381	1.42	185.6	0.016	BF
DCAD07P06	0.030			328.60	0.470	8.18	27.30	19.34	5.68	19.12	0.29	0.30	40.7	2.3	13.1	0.27	71.2	6.054	167	3186	1.45	218.5	0.016	BF
DCAD07P07	0.030																							BF
DCAD07P08	0.030																							BF
DCAD07P09	0.030																							BF
DCAD07P10	0.030																							BF

Cross Section Hydraulic Analyses: Dry Canyon

Floodplain/Site Description: Photo view looking downstream.

Location ID	DCAD08	
d_{50} (mm) =	0.73	
d_{84} (mm) =	1.34	
So = Sf =	0.0198	
Pt #	Sta (m)	Stage (m)
1	0.00	334.19
2	3.04	334.54
3	7.50	332.62
4	9.96	331.38
5	12.42	330.76
6	15.07	330.72
7	15.98	330.89
8	18.46	330.85
9	21.27	330.77
10	23.76	330.81
11	25.76	330.54
12	27.47	330.58
13	28.86	330.32
14	30.22	329.78
15	32.24	329.74
16	34.25	329.57
17	36.01	329.50
18	37.62	329.09
19	39.11	329.11
20	40.45	329.12
21	42.35	329.20
22	43.67	329.24
23	44.61	329.68
24	44.81	330.57
25	46.10	331.19
26	47.46	332.25
27	49.49	333.21
28	50.87	333.58
29		
30		
31		
32		
33		
34		
35		
min. Stage =		329.09
Continuum		1
CEM		3.0

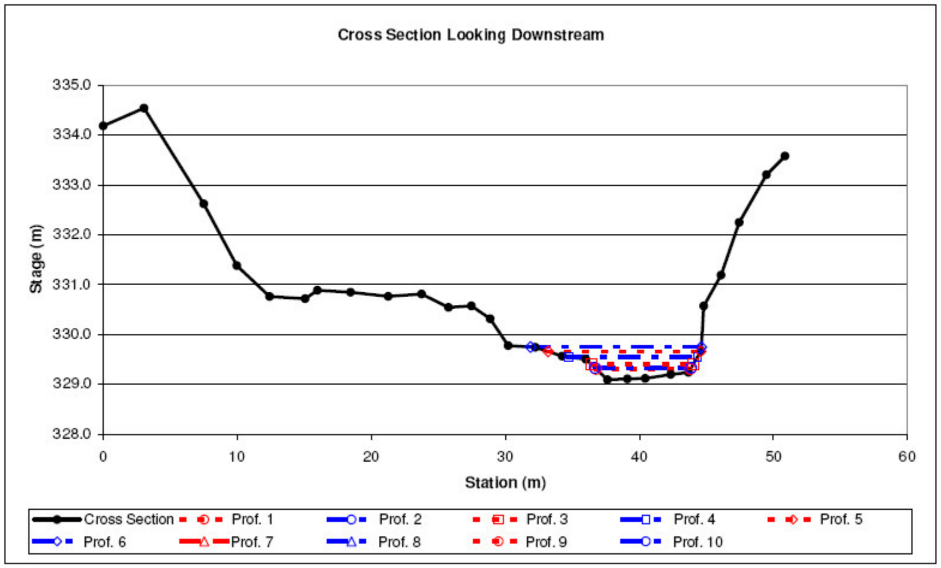

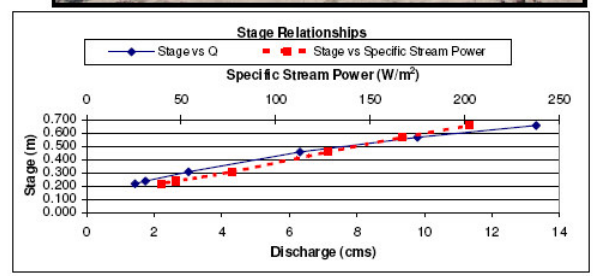

Prof. ID	Estimated n-value	L-Limit	R-Limit	WS (m)	Depth (m)	Left Sta (m)	Right Sta (m)	P_w (m)	Area (m^2)	W (m)	R (m)	D (m)	W/d	V (m/s)	Q (m^3/s)	U* (m/s)	τ (kg/ms²)	τ*	ω (W/m²)	Ω (W/m)	F_r	R/d_{84}	n-value per Limerino	Floodplain Form
DCAD08P01	0.030			329.31	0.217	36.77	43.82	7.10	1.08	7.05	0.15	0.15	32.5	1.3	1.4	0.17	29.4	2.503	39	278	1.17	112.9	0.016	PMB
DCAD08P02	0.030			329.33	0.237	36.69	43.86	7.23	1.22	7.18	0.17	0.17	30.3	1.4	1.7	0.18	32.7	2.784	47	338	1.19	125.5	0.016	PMB
DCAD08P03	0.030			329.40	0.307	36.41	44.01	7.68	1.74	7.60	0.23	0.23	24.8	1.7	3.0	0.21	43.9	3.732	77	586	1.25	168.3	0.016	PMB
DCAD08P04	0.030			329.55	0.457	34.74	44.34	9.73	2.97	9.60	0.31	0.31	21.0	2.1	6.3	0.24	59.2	5.040	128	1225	1.31	227.3	0.016	PMB
DCAD08P05	0.030			329.66	0.567	33.20	44.57	11.53	4.14	11.38	0.36	0.36	20.1	2.4	9.8	0.26	69.6	5.922	167	1899	1.34	267.0	0.016	PMB
DCAD08P06	0.030			329.75	0.657	31.88	44.63	12.96	5.21	12.75	0.40	0.41	19.4	2.6	13.3	0.28	78.0	6.634	202	2580	1.37	299.2	0.016	PMB
DCAD08P07	0.030																							PMB
DCAD08P08	0.030																							PMB
DCAD08P09	0.030																							PMB
DCAD08P10	0.030																							PMB

Cross Section Hydraulic Analyses: Dry Canyon

Floodplain/Site Description: Photo view looking downstream from DCAD10 toward DCAD09.

Location ID	DCAD09
d_{50} (mm) =	0.73
d_{84} (mm) =	1.34
So = Sf =	0.0198

Pt #	Sta (m)	Stage (m)
1	0.00	331.94
2	1.57	331.63
3	4.22	331.65
4	8.02	331.65
5	10.99	331.62
6	13.20	331.61
7	15.29	331.61
8	16.03	330.29
9	16.87	330.01
10	17.75	329.95
11	18.61	329.86
12	19.75	329.88
13	20.77	329.84
14	21.71	329.88
15	22.41	329.90
16	23.59	329.85
17	24.07	329.83
18	24.88	329.96
19	25.72	329.96
20	26.61	330.07
21	27.04	331.37
22	29.05	331.55
23	31.67	331.71
24	33.70	331.80
25	36.81	331.63
26	39.78	331.78
27	41.99	331.87
28		
29		
30		
31		
32		
33		
34		
35		
min. Stage =		329.83
Continuum		1
CEM		3.0

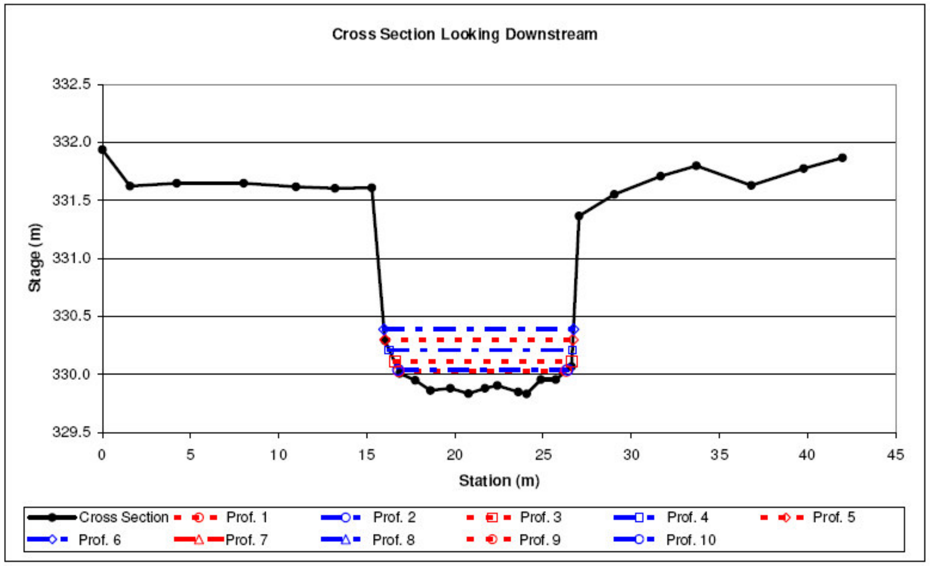

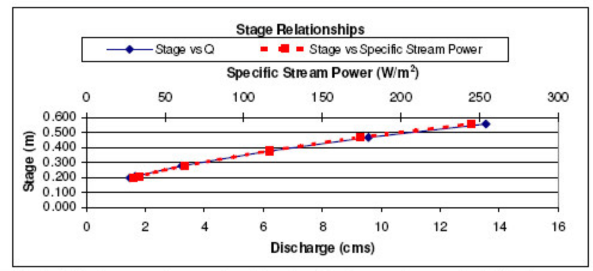

Prof. ID	Estimated n-value	L-Limit	R-Limit	WS (m)	Depth (m)	Left Sta (m)	Right Sta (m)	P_w (m)	Area (m^2)	W (m)	R (m)	D (m)	W/d	V (m/s)	Q (m^3/s)	U* (m/s)	τ (kg/ms²)	τ*	ω (W/m²)	Ω (W/m)	F_r	R/d_{84}	n-value per Limerino	Floodplain Form
DCAD09P01	0.030			330.03	0.198	16.81	26.32	9.53	1.23	9.51	0.13	0.13	48.0	1.2	1.5	0.16	25.1	2.134	30	287	1.14	96.2	0.016	PMB
DCAD09P02	0.030			330.04	0.208	16.78	26.40	9.65	1.33	9.62	0.14	0.14	46.2	1.2	1.7	0.16	26.7	2.272	33	322	1.15	102.5	0.016	PMB
DCAD09P03	0.030			330.11	0.278	16.57	26.63	10.13	2.02	10.05	0.20	0.20	36.2	1.6	3.2	0.20	38.7	3.293	62	627	1.22	148.5	0.016	PMB
DCAD09P04	0.030			330.21	0.378	16.28	26.66	10.55	3.04	10.38	0.29	0.29	27.5	2.0	6.2	0.24	56.0	4.761	116	1208	1.29	214.7	0.016	PMB
DCAD09P05	0.030			330.30	0.468	16.03	26.69	10.91	3.99	10.66	0.37	0.37	22.8	2.4	9.6	0.27	71.0	6.038	174	1856	1.34	272.3	0.016	PMB
DCAD09P06	0.030			330.39	0.558	15.98	26.72	11.11	4.95	10.74	0.45	0.46	19.2	2.7	13.6	0.29	86.5	7.361	245	2629	1.38	331.9	0.016	PMB
DCAD09P07	0.030																							PMB
DCAD09P08	0.030																							PMB
DCAD09P09	0.030																							PMB
DCAD09P10	0.030																							PMB

Cross Section Hydraulic Analyses: Dry Canyon

Floodplain/Site Description: Photo view looking downstream toward DCAD10.

Location ID	DCAD10	
d_{50} (mm) =	0.73	
d_{84} (mm) =	1.34	
So = Sf =	0.0198	
Pt #	Sta (m)	Stage (m)
1	0.00	333.61
2	2.26	333.35
3	4.38	333.02
4	6.63	332.70
5	8.49	332.49
6	10.76	332.33
7	13.70	332.20
8	14.43	330.46
9	14.93	330.32
10	16.17	330.32
11	16.87	330.42
12	17.73	330.36
13	18.55	330.36
14	19.42	330.33
15	19.72	330.35
16	21.12	330.53
17	21.48	330.47
18	22.58	330.46
19	23.50	330.46
20	24.14	330.46
21	25.07	330.49
22	25.51	330.49
23	26.54	330.81
24	27.25	331.16
25	27.55	331.76
26	28.36	332.19
27	30.94	332.30
28	33.80	332.43
29	36.61	332.60
30	38.45	332.85
31		
32		
33		
34		
35		
min. Stage =	330.32	
Continuum	1	
CEM	3	

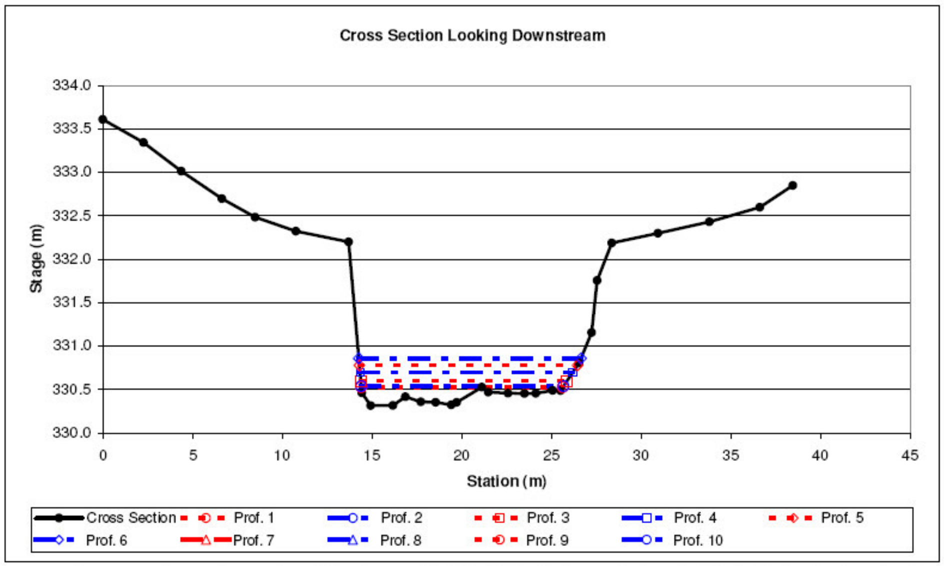

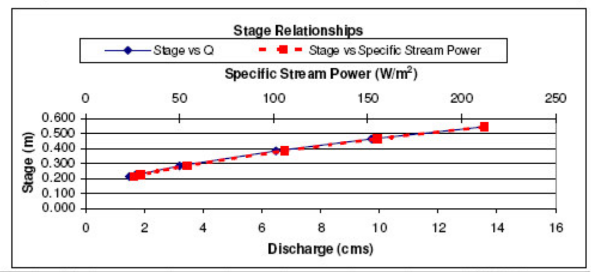

Prof. ID	Estimated n-value	L-Limit	R-Limit	WS (m)	Depth (m)	Left Sta (m)	Right Sta (m)	P_w (m)	Area (m^2)	W (m)	R (m)	D (m)	W/d	V (m/s)	Q (m^3/s)	U* (m/s)	τ (kg/ms²)	τ*	ω (W/m²)	Ω (W/m)	F_r	R/d_{84}	n-value per Limerino	Floodplain Form
DCAD10P01	0.030			330.53	0.214	14.40	25.64	11.34	1.33	11.24	0.12	0.12	52.5	1.1	1.49	0.15	22.7	1.933	26	289	1.12	87.2	0.016	PMB
DCAD10P02	0.030			330.54	0.224	14.40	25.67	11.38	1.44	11.27	0.13	0.13	50.3	1.2	1.70	0.16	24.5	2.089	29	330	1.13	94.2	0.016	PMB
DCAD10P03	0.030			330.60	0.284	14.37	25.87	11.65	2.12	11.50	0.18	0.18	40.5	1.5	3.2	0.19	35.3	3.008	54	621	1.20	135.6	0.016	PMB
DCAD10P04	0.030			330.70	0.384	14.33	26.19	12.10	3.29	11.86	0.27	0.28	30.9	2.0	6.5	0.23	52.8	4.489	106	1256	1.28	202.4	0.016	PMB
DCAD10P05	0.030			330.78	0.464	14.30	26.45	12.46	4.25	12.16	0.34	0.35	26.2	2.3	9.7	0.26	66.2	5.632	155	1887	1.32	253.9	0.016	PMB
DCAD10P06	0.030			330.86	0.544	14.27	26.65	12.76	5.24	12.38	0.41	0.42	22.8	2.6	13.5	0.28	79.6	6.772	212	2627	1.36	305.4	0.016	PMB
DCAD10P07	0.030																							PMB
DCAD10P08	0.030																							PMB
DCAD10P09	0.030																							PMB
DCAD10P10	0.030																							PMB

Cross Section Hydraulic Analyses: Dry Canyon

Floodplain/Site Description: Photo view looking from right overbank toward left overbank.

Location ID	DCAD11	
d_{50} (mm) =	0.75	
d_{84} (mm) =	7.37	
So = Sf =	0.0198	
Pt #	Sta (m)	Stage (m)
1	0.00	336.62
2	2.63	336.17
3	4.22	335.27
4	5.68	334.53
5	7.00	333.99
6	8.15	331.17
7	8.84	330.95
8	9.99	330.98
9	11.06	331.07
10	12.11	331.08
11	13.25	331.12
12	14.71	331.19
13	15.97	331.15
14	16.77	331.16
15	17.36	331.08
16	18.41	331.15
17	20.17	331.24
18	21.10	331.30
19	21.56	331.24
20	22.14	331.26
21	22.51	331.17
22	23.24	331.24
23	24.24	331.59
24	25.07	331.80
25	25.68	332.80
26	26.50	332.96
27	27.54	333.42
28	28.93	334.21
29	30.08	334.92
30	31.16	335.43
31	33.45	335.54
32	35.86	335.62
33		
34		
35		
min. Stage =		330.95
Continuum		1
CEM		3.0

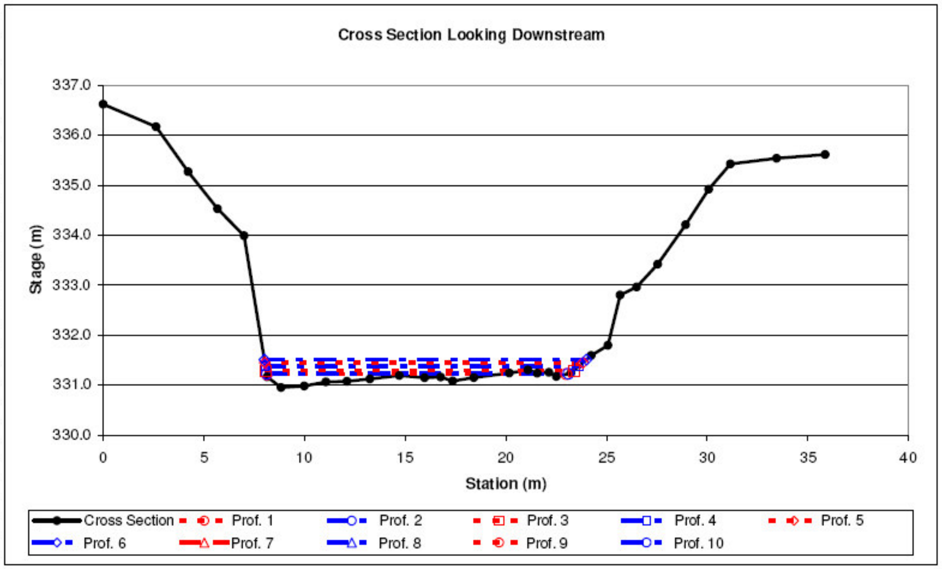

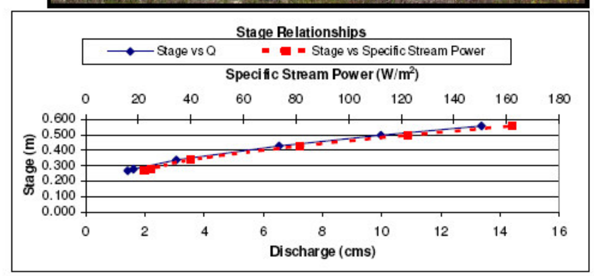

Prof. ID	Estimated n-value	L-Limit	R-Limit	WS (m)	Depth (m)	Left Sta (m)	Right Sta (m)	P_w (m)	Area (m^2)	W (m)	R (m)	D (m)	W/d	V (m/s)	Q (m^3/s)	U* (m/s)	τ (kg/ms²)	τ*	ω (W/m²)	Ω (W/m)	F_r	R/d_{84}	n-value per Limerino	Floodplain Form
DCAD11P01	0.030			331.22	0.267	8.13	23.00	12.37	1.34	12.28	0.11	0.11	46.0	1.1	1.4	0.14	20.9	1.719	22	275	1.10	14.6	0.022	BF
DCAD11P02	0.030			331.23	0.277	8.12	23.11	12.73	1.46	12.62	0.11	0.12	45.6	1.1	1.6	0.15	22.2	1.827	25	313	1.11	15.6	0.022	BF
DCAD11P03	0.030			331.29	0.337	8.10	23.37	15.12	2.30	14.96	0.15	0.15	44.4	1.3	3.1	0.17	29.5	2.420	40	595	1.17	20.6	0.022	BF
DCAD11P04	0.030			331.38	0.427	8.06	23.63	15.80	3.68	15.57	0.23	0.24	36.5	1.8	6.5	0.21	45.2	3.711	81	1268	1.25	31.6	0.021	BF
DCAD11P05	0.030			331.45	0.497	8.03	23.83	16.09	4.78	15.80	0.30	0.30	31.8	2.1	10.0	0.24	57.6	4.731	122	1934	1.30	40.3	0.021	BF
DCAD11P06	0.030			331.51	0.557	8.01	24.00	16.34	5.73	15.99	0.35	0.36	28.7	2.3	13.4	0.26	68.1	5.589	162	2593	1.33	47.6	0.021	BF
DCAD11P07	0.030																							BF
DCAD11P08	0.030																							BF
DCAD11P09	0.030																							BF
DCAD11P10	0.030																							BF

Cross Section Hydraulic Analyses: Dry Canyon

Floodplain/Site Description: Photo view looking downstream along main Floodplain.

Location ID	DCAD12
d_{50} (mm) =	0.75
d_{84} (mm) =	7.37
So = Sf =	0.0198

Pt #	Sta (m)	Stage (m)
1	0.00	333.30
2	1.72	333.30
3	3.04	333.40
4	4.17	332.66
5	5.41	332.01
6	6.47	331.63
7	7.64	331.49
8	8.27	331.58
9	9.03	331.50
10	9.71	331.47
11	10.74	331.54
12	11.77	331.56
13	12.42	331.54
14	12.52	331.56
15	13.10	331.55
16	13.20	331.49
17	14.44	331.51
18	15.32	331.53
19	17.06	336.40
20	18.15	336.40
21	19.29	336.43
22	21.13	336.36
23	22.29	336.29
24		
25		
26		
27		
28		
29		
30		
31		
32		
33		
34		
35		
min. Stage =	331.47	
Continuum	1	
CEM	3.0	

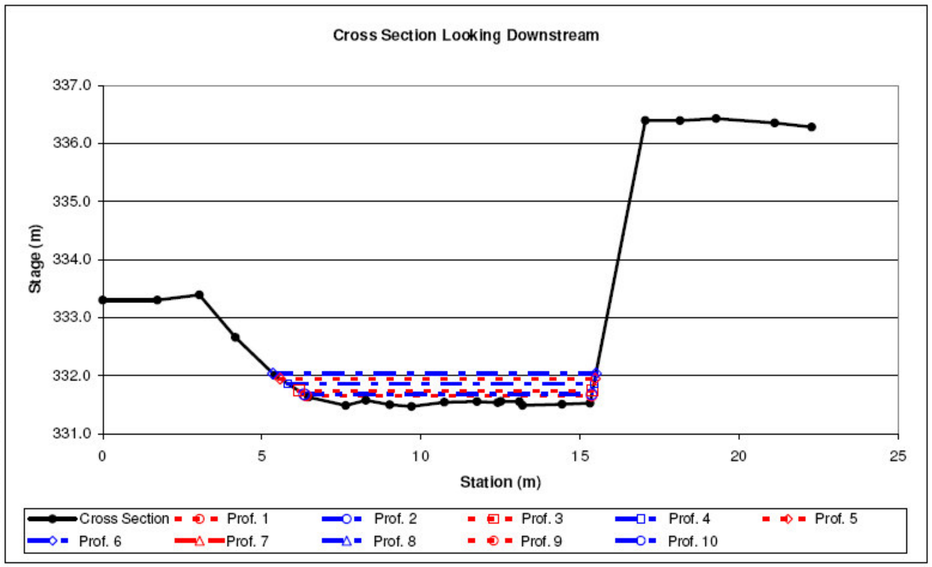

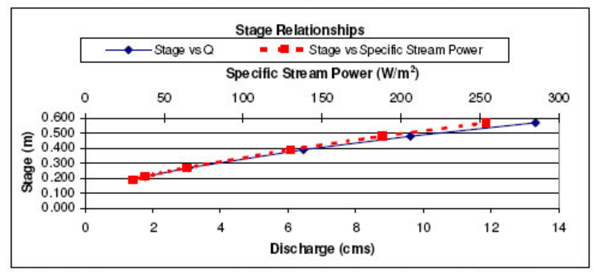

Prof. ID	Estimated n-value	L-Limit	R-Limit	WS (m)	Depth (m)	Left Sta (m)	Right Sta (m)	P_w (m)	Area (m^2)	W (m)	R (m)	D (m)	W/d	V (m/s)	Q (m^3/s)	U* (m/s)	τ (kg/ms²)	τ*	ω (W/m²)	Ω (W/m)	F_r	R/d_{84}	n-value per Limerino	Floodplain Form
DCAD12P01	0.030			331.66	0.191	6.39	15.37	9.13	1.17	8.98	0.13	0.13	47.0	1.2	1.4	0.16	25.0	2.050	30	272	1.13	17.5	0.022	PMB
DCAD12P02	0.030			331.68	0.211	6.33	15.38	9.21	1.36	9.05	0.15	0.15	42.9	1.3	1.8	0.17	28.5	2.344	38	343	1.16	20.0	0.022	PMB
DCAD12P03	0.030			331.74	0.271	6.16	15.40	9.45	1.90	9.24	0.20	0.21	34.1	1.6	3.1	0.20	39.1	3.208	64	594	1.21	27.3	0.021	PMB
DCAD12P04	0.030			331.86	0.391	5.83	15.44	9.94	3.03	9.62	0.31	0.32	24.6	2.1	6.5	0.24	59.2	4.864	130	1251	1.30	41.4	0.021	PMB
DCAD12P05	0.030			331.95	0.481	5.57	15.47	10.30	3.91	9.90	0.38	0.40	20.6	2.5	9.6	0.27	73.7	6.049	188	1865	1.34	51.5	0.021	PMB
DCAD12P06	0.030			332.04	0.571	5.35	15.51	10.64	4.82	10.16	0.45	0.47	17.8	2.8	13.3	0.30	87.8	7.211	254	2581	1.37	61.4	0.021	PMB
DCAD12P07	0.030																							PMB
DCAD12P08	0.030																							PMB
DCAD12P09	0.030																							PMB
DCAD12P10	0.030																							PMB

Cross Section Hydraulic Analyses: Dry Canyon

Floodplain/Site Description: Photo view looking downstream along main Floodplain.

Location ID	DCAD13
d_{50} (mm) =	0.75
d_{84} (mm) =	7.37
So = Sf =	0.0198

Pt #	Sta (m)	Stage (m)
1	0.00	333.63
2	1.52	333.58
3	3.01	333.68
4	4.12	333.53
5	5.71	333.49
6	7.35	333.40
7	8.43	332.76
8	9.53	332.23
9	10.81	332.13
10	12.22	332.10
11	13.61	332.11
12	14.35	331.79
13	14.81	331.74
14	15.19	331.73
15	15.57	331.69
16	16.14	331.72
17	17.20	331.71
18	18.09	331.70
19	18.89	331.69
20	19.38	331.76
21	20.18	331.81
22	20.57	331.89
23	21.47	332.01
24	22.78	336.49
25	23.84	336.55
26	24.95	336.65
27	25.73	336.64
28		
29		
30		
31		
32		
33		
34		
35		
min. Stage =		331.69
Continuum		1
CEM		3.0

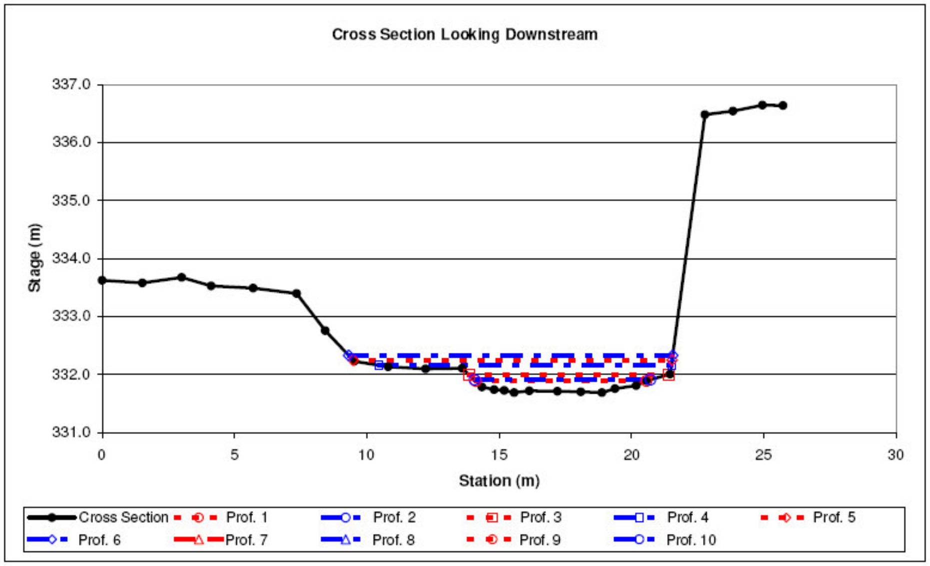

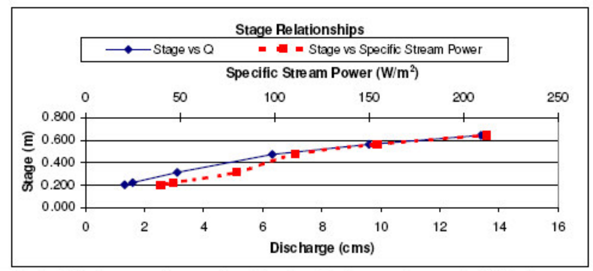

Prof. ID	Estimated n-value	L-Limit	R-Limit	WS (m)	Depth (m)	Left Sta (m)	Right Sta (m)	P_w (m)	Area (m^2)	W (m)	R (m)	D (m)	W/d	V (m/s)	Q (m^3/s)	U* (m/s)	τ (kg/ms²)	τ*	ω (W/m²)	Ω (W/m)	F_r	R/d_{84}	n-value per Limerino	Floodplain Form
DCAD13P01	0.030			331.89	0.203	14.11	20.57	6.50	0.99	6.46	0.15	0.15	42	1.3	1.3	0.17	29.6	2.430	40	257	1.09	20.7	0.022	PMB
DCAD13P02	0.030			331.91	0.223	14.07	20.72	6.70	1.12	6.65	0.17	0.17	39	1.4	1.6	0.18	32.5	2.669	47	310	1.11	22.7	0.022	PMB
DCAD13P03	0.030			332.00	0.313	13.86	21.41	7.62	1.76	7.55	0.23	0.23	32	1.8	3.1	0.21	44.8	3.682	80	603	1.17	31.4	0.021	PMB
DCAD13P04	0.030			332.16	0.473	10.46	21.51	11.27	3.15	11.06	0.28	0.29	39	2.0	6.3	0.23	54.3	4.457	111	1226	1.20	38.0	0.021	PMB
DCAD13P05	0.030			332.25	0.563	9.48	21.54	12.34	4.20	12.05	0.34	0.35	35	2.3	9.6	0.26	66.0	5.422	154	1862	1.24	46.2	0.021	PMB
DCAD13P06	0.030			332.33	0.643	9.32	21.56	12.61	5.17	12.24	0.41	0.42	29	2.6	13.4	0.28	79.6	6.535	212	2597	1.27	55.7	0.021	PMB
DCAD13P07	0.030																							PMB
DCAD13P08	0.030																							PMB
DCAD13P09	0.030																							PMB
DCAD13P10	0.030																							PMB

Cross Section Hydraulic Analyses: Dulzura Creek at Hwy 94/Campo Rd.

Floodplain/Site Description: Dulzura Creek downstream of Campo Road (Hwy 94). Downstream cross section looking along the cross section from the right overbank (note can covering rebar in foreground). Cross section extended at 20:1 to contain 50 and 100 year events.

Location ID	DCCR01
d_{50} (mm) =	34.60
d_{84} (mm) =	81.30
So = Sf =	0.0060

Pt #	Sta (m)	Stage (m)
1	0.00	101.00
2	20.00	100.00
3	22.20	99.89
4	23.30	99.65
5	25.15	98.50
6	26.25	98.50
7	27.80	98.33
8	29.55	98.37
9	30.60	98.44
10	31.30	98.65
11	32.10	98.78
12	34.00	98.89
13	37.00	98.95
14	39.00	98.98
15	42.00	99.00
16	44.00	99.28
17	47.00	99.78
18	49.00	100.18
19	69.00	101.18
20		
21		
22		
23		
24		
25		
26		
27		
28		
29		
30		
31		
32		
33		
34		
35		
min. Stage =		98.33
Continuum		2
CEM		1

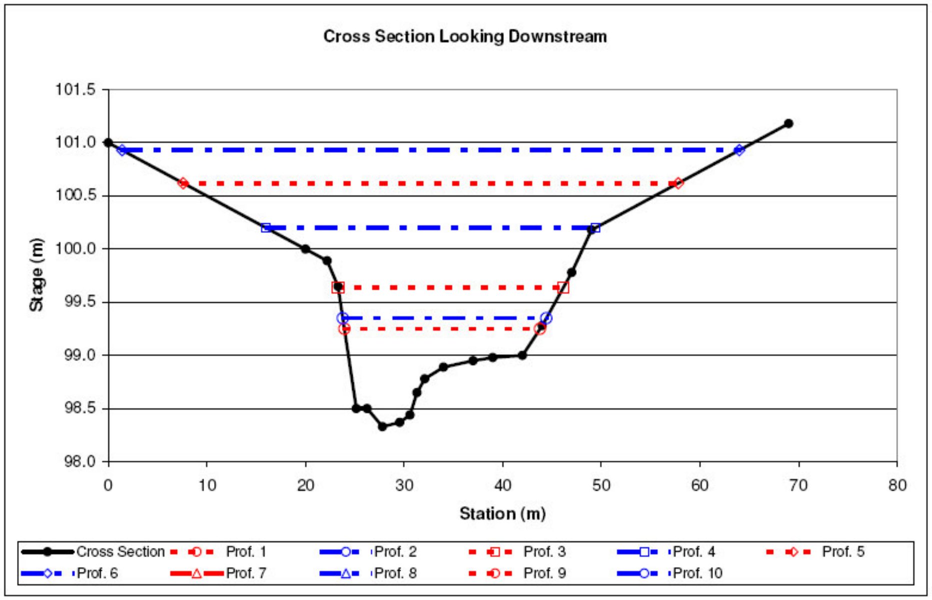

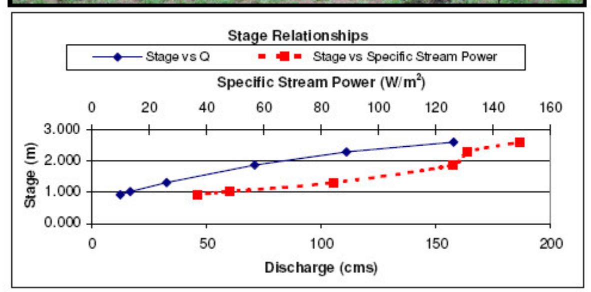

Prof. ID	Estimated n-value	L-Limit	R-Limit	WS (m)	Depth (m)	Left Sta (m)	Right Sta (m)	P_w (m)	Area (m^2)	W (m)	R (m)	D (m)	W/d	V (m/s)	Q (m^3/s)	U* (m/s)	τ (kg/ms²)	τ*	ω (W/m²)	Ω (W/m)	F_r	R/d_{84}	n-value per Limerino	Floodplain Form
DCCR01P01	0.035			99.25	0.920	23.94	43.79	20.13	9.31	19.84	0.46	0.47	21.6	1.3	12.4	0.17	27.4	0.049	37	732	0.66	5.7	0.037	PR
DCCR01P02	0.035			99.35	1.020	23.78	44.42	20.96	11.33	20.64	0.54	0.55	20.2	1.5	16.7	0.18	32.0	0.057	48	989	0.68	6.6	0.036	PR
DCCR01P03	0.035			99.64	1.310	23.32	46.16	23.28	17.64	22.84	0.76	0.77	17.4	1.8	32.5	0.21	44.9	0.080	84	1928	0.72	9.3	0.035	PR
DCCR01P04	0.035			100.20	1.870	16.00	49.40	33.92	32.73	33.40	0.96	0.98	17.9	2.2	71.0	0.24	57.2	0.102	126	4204	0.75	11.9	0.034	PR
DCCR01P05	0.035			100.62	2.290	7.60	57.80	50.74	50.28	50.20	0.99	1.00	21.9	2.2	111.0	0.24	58.7	0.105	131	6575	0.76	12.2	0.034	PR
DCCR01P06	0.035			100.93	2.600	1.40	64.00	63.16	67.77	62.60	1.07	1.08	24.1	2.3	157.7	0.25	63.6	0.114	149	9343	0.77	13.2	0.034	PR
DCCR01P07	0.035																							PR
DCCR01P08	0.035																							PR
DCCR01P09	0.035																							PR
DCCR01P10	0.035																							PR

Cross Section Hydraulic Analyses: Dulzura Creek at Hwy 94/Campo Rd.

Floodplain/Site Description: Dulzura Creek downstream of Campo Road (Hwy 94). Upstream cross section looking downstream in June of 07 before the fires in the fall.

Location ID	DCCR02
d_{50} (mm) =	47.70
d_{84} (mm) =	129.40
So = Sf =	0.0060

Pt #	Sta (m)	Stage (m)
1	0.00	101.00
2	20.00	100.00
3	20.50	100.05
4	23.20	98.62
5	24.60	99.00
6	27.00	99.13
7	31.00	99.20
8	33.20	99.05
9	33.21	99.07
10	33.60	98.88
11	34.60	98.39
12	35.85	98.23
13	37.80	98.32
14	38.60	98.58
15	39.00	98.95
16	40.50	99.75
17	43.00	100.10
18	46.00	100.65
19	66.00	101.65
20		
21		
22		
23		
24		
25		
26		
27		
28		
29		
30		
31		
32		
33		
34		
35		
min. Stage =		98.23
Continuum		2
CEM		1

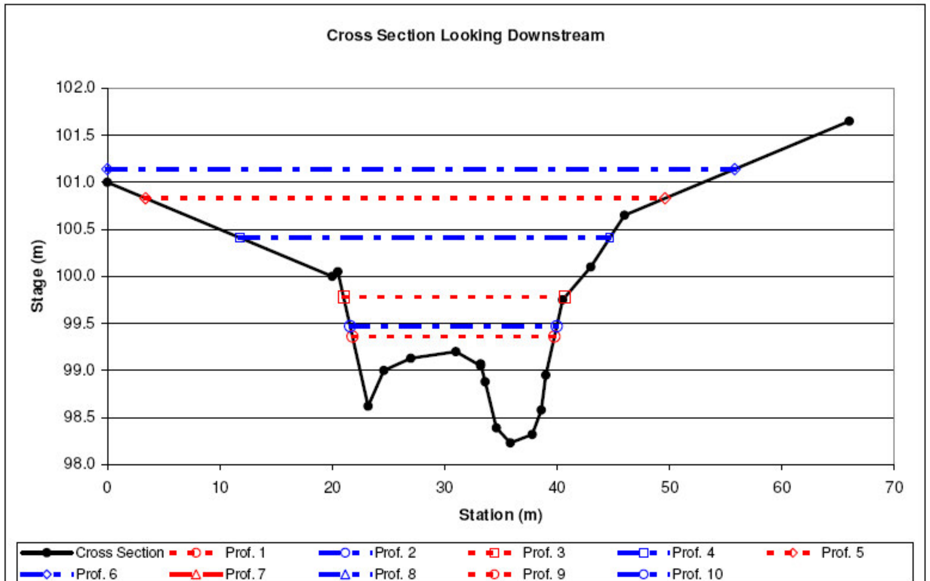

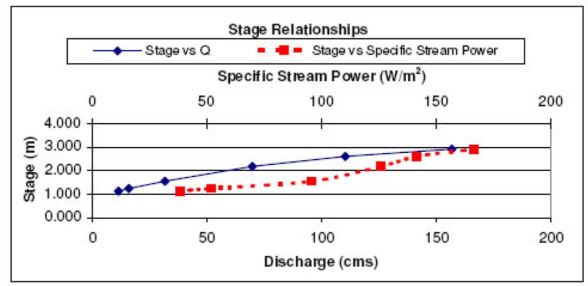

Prof. ID	Estimated n-value	L-Limit	R-Limit	WS (m)	Depth (m)	Left Sta (m)	Right Sta (m)	P_w (m)	Area (m^2)	W (m)	R (m)	D (m)	W/d	V (m/s)	Q (m^3/s)	U* (m/s)	τ (kg/ms^2)	τ^*	ω (W/m^2)	Ω (W/m)	F_r	R/d_{84}	n-value per Limerino	Floodplain Form
DCCR02P01	0.035			99.36	1.130	21.80	39.77	18.68	8.72	17.97	0.47	0.49	15.9	1.3	11.7	0.17	27.7	0.036	38	690	0.66	3.6	0.043	PR
DCCR02P02	0.035			99.47	1.240	21.60	39.98	19.15	10.72	18.38	0.56	0.58	14.8	1.5	16.2	0.18	33.2	0.043	52	958	0.68	4.3	0.042	PR
DCCR02P03	0.035			99.78	1.550	21.01	40.71	20.62	16.60	19.70	0.81	0.84	12.7	1.9	31.9	0.22	47.7	0.062	96	1890	0.72	6.2	0.039	PR
DCCR02P04	0.035			100.41	2.180	11.80	44.69	33.94	32.48	32.89	0.96	0.99	15.1	2.2	70.0	0.24	56.7	0.074	126	4149	0.74	7.4	0.039	PR
DCCR02P05	0.035			100.83	2.600	3.40	49.60	47.29	48.77	46.20	1.03	1.06	17.8	2.3	110.6	0.25	61.1	0.079	142	6549	0.76	8.0	0.038	PR
DCCR02P06	0.035			101.14	2.910	0.00	55.80	56.90	64.82	55.80	1.14	1.16	19.2	2.4	157.0	0.26	67.5	0.088	167	9301	0.77	8.8	0.038	PR
DCCR02P07	0.035																							PR
DCCR02P08	0.035																							PR
DCCR02P09	0.035																							PR
DCCR02P10	0.035																							PR

Cross Section Hydraulic Analyses: Hicks Canyon

Sta	22.273	267.208

Floodplain/Site Description: Hicks Canyon Modeling Reach Sta 22.3 m of Modeling Reach and Sta 267.2 m upstream of road crossing. Photograph view is looking upstream in Jan. 08 following a wildfire and ~ 5 to 10 yr flow event.

Location ID		HCMR01
d_{50} (mm) =		1.40
d_{84} (mm) =		66.30
So = Sf =		0.0171
Pt #	Sta (m)	Stage (m)
1	0.00	131.51
2	1.05	131.49
3	2.62	131.49
4	4.16	131.50
5	5.78	131.47
6	6.88	131.23
7	8.47	130.93
8	8.70	130.61
9	9.43	130.54
10	9.71	130.47
11	10.23	130.38
12	10.72	130.42
13	11.28	130.77
14	11.78	131.47
15	12.42	131.76
16	13.70	131.77
17	15.17	132.04
18		
19		
20		
21		
22		
23		
24		
25		
26		
27		
28		
29		
30		
31		
32		
33		
34		
35		
min. Stage =		130.38
Coninuum		1
CEM		3

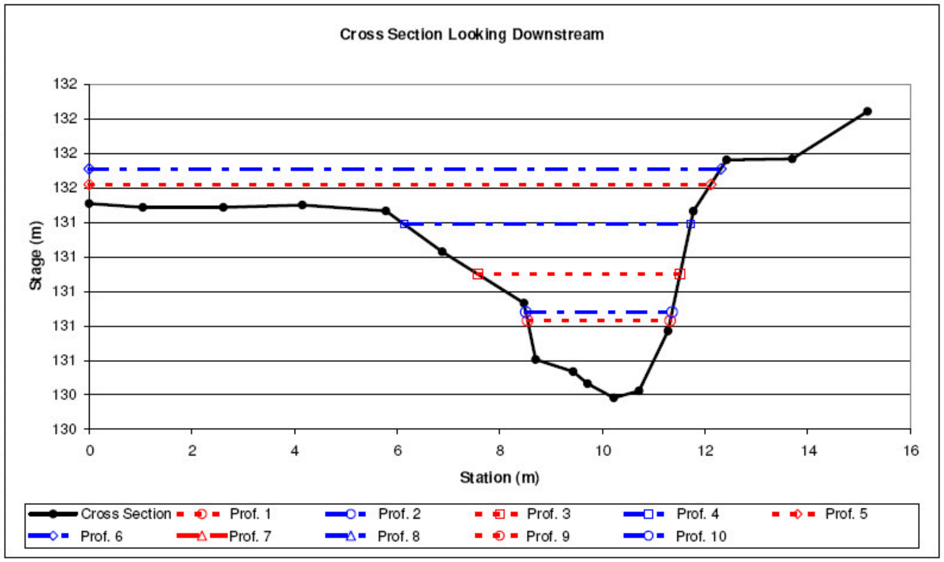

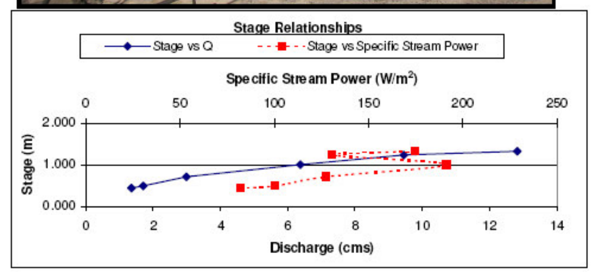

Prof. ID	Estimated n-value	L-Limit	R-Limit	WS (m)	Depth (m)	Left Sta (m)	Right Sta (m)	P_w (m)	Area (m^2)	W (m)	R (m)	D (m)	W/d	V (m/s)	Q (m^3/s)	U* (m/s)	τ (kg/ms²)	τ*	ω (W/m²)	Ω (W/m)	F_r	R/d_{84}	n-value per Limerino	Floodplain Form
HCMR01P01	0.035			130.83	0.447	8.55	11.32	3.04	0.85	2.78	0.28	0.31	6.2	1.6	1.4	0.22	46.8	2.070	82	228	0.99	4.2	0.037	PMB
HCMR01P02	0.035			130.88	0.497	8.51	11.36	3.17	0.99	2.85	0.31	0.35	5.7	1.7	1.7	0.23	52.5	2.320	100	286	1.00	4.7	0.036	PMB
HCMR01P03	0.040			131.10	0.717	7.58	11.52	4.41	1.72	3.94	0.39	0.44	5.5	1.7	3.0	0.26	65.2	2.884	127	502	0.90	5.9	0.035	PMB
HCMR01P04	0.040			131.39	1.007	6.14	11.72	6.24	3.11	5.59	0.50	0.56	5.5	2.1	6.4	0.29	83.5	3.689	191	1069	0.94	7.5	0.034	PMB
HCMR01P05	0.040			131.62	1.237	0.00	12.11	12.85	5.25	12.11	0.41	0.43	9.8	1.8	9.4	0.26	68.5	3.028	131	1584	0.94	6.2	0.035	PMB
HCMR01P06	0.040			131.71	1.327	0.00	12.31	13.06	6.35	12.31	0.49	0.52	9.3	2.0	12.8	0.29	81.5	3.601	175	2150	0.96	7.3	0.034	PMB
HCMR01P07	0.040																							PMB
HCMR01P08	0.040																							PMB
HCMR01P09	0.040																							PMB
HCMR01P10	0.040																							PMB

Cross Section Hydraulic Analyses: Hicks Canyon

Sta	38.465	283.400
Location ID	HCMR02	
d_{50} (mm) =	1.40	
d_{84} (mm) =	66.30	
So = Sf =	0.0171	

Floodplain/Site Description: Hicks Canyon Modeling Reach Sta 38.5 m of Modeling Reach and Sta 283.4 m upstream of road crossing. Photograph view is looking upstream in Jan. 08 following a wildfire and ~ 5 to 10 yr flow event.

Pt #	Sta (m)	Stage (m)
1	0.00	131.95
2	1.35	131.75
3	2.44	131.64
4	3.40	131.57
5	4.37	131.36
6	4.65	131.22
7	4.83	130.78
8	5.30	130.67
9	5.78	130.70
10	6.15	130.62
11	6.48	130.61
12	6.69	130.88
13	7.43	131.07
14	7.76	131.28
15	9.26	131.37
16	12.57	131.72
17	14.44	131.96
18	16.23	132.25
19	17.42	132.62
20		
21		
22		
23		
24		
25		
26		
27		
28		
29		
30		
31		
32		
33		
34		
35		
min. Stage =		130.61
Coninuum		1
CEM		3

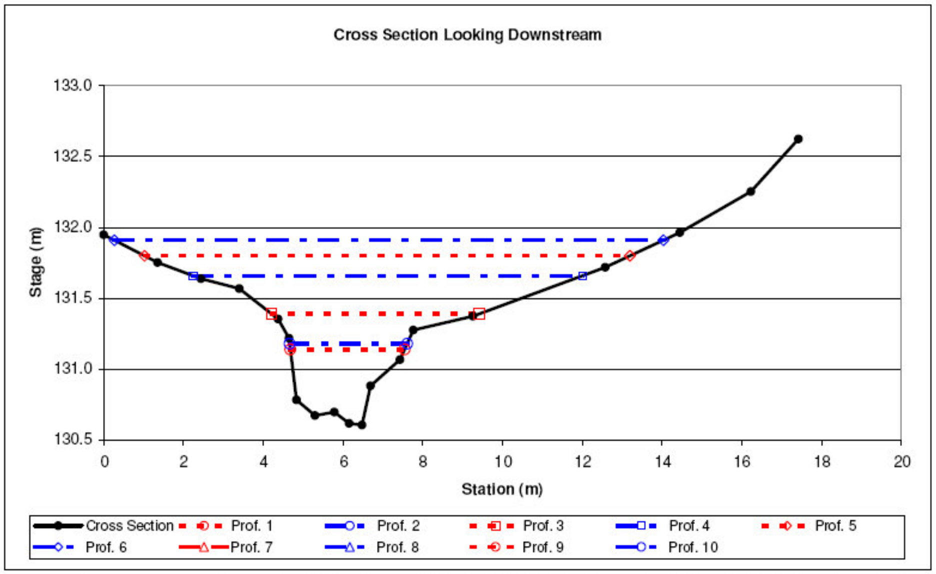

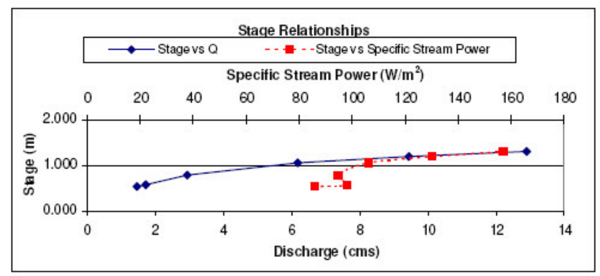

Prof. ID	Estimated n-value	L-Limit	R-Limit	WS (m)	Depth (m)	Left Sta (m)	Right Sta (m)	P_w (m)	Area (m^2)	W (m)	R (m)	D (m)	W/d	V (m/s)	Q (m^3/s)	U* (m/s)	τ (kg/ms²)	τ*	ω (W/m²)	Ω (W/m)	F_r	R/d_{84}	n-value per Limerino	Floodplain Form
HCMR02P01	0.040			131.14	0.533	4.68	7.55	3.30	1.00	2.87	0.30	0.35	5.4	1.5	1.5	0.23	50.7	2.241	86	246	0.85	4.6	0.036	PMB
HCMR02P02	0.040			131.18	0.573	4.66	7.61	3.42	1.11	2.95	0.33	0.38	5.1	1.5	1.7	0.23	54.6	2.414	98	289	0.86	4.9	0.036	PMB
HCMR02P03	0.040			131.39	0.783	4.21	9.41	5.77	1.89	5.20	0.33	0.36	6.6	1.6	2.9	0.23	55.0	2.431	95	493	0.88	4.9	0.036	PMB
HCMR02P04	0.042			131.66	1.053	2.24	12.01	10.37	3.85	9.77	0.37	0.39	9.3	1.6	6.2	0.25	62.2	2.749	106	1036	0.88	5.6	0.036	PMB
HCMR02P05	0.042			131.80	1.193	1.03	13.19	12.79	5.39	12.17	0.42	0.44	10.2	1.8	9.4	0.27	70.7	3.126	130	1583	0.90	6.4	0.035	PMB
HCMR02P06	0.042			131.91	1.303	0.27	14.03	14.40	6.82	13.76	0.47	0.50	10.6	1.9	12.9	0.28	79.4	3.510	157	2162	0.92	7.1	0.035	PMB
HCMR02P07	0.042																							PMB
HCMR02P08	0.042																							PMB
HCMR02P09	0.042																							PMB
HCMR02P10	0.042																							PMB

Cross Section Hydraulic Analyses: Hicks Canyon

Sta	50.238	295.174

Floodplain/Site Description: Hicks Canyon Modeling Reach Sta 50.2 m of Modeling Reach and Sta 295.2 m upstream of road crossing. Photograph view is looking downstream in Jan. 08 following a wildfire and ~ 5 to 10 yr flow event. Cutoff chute

	Location ID	HCMR03
	d_{50} (mm) =	1.40
	d_{84} (mm) =	66.30
	So = Sf =	0.0214
Pt #	Sta (m)	Stage (m)
1	0.00	132.12
2	1.29	132.03
3	2.09	131.77
4	3.29	131.50
5	3.45	131.29
6	4.46	131.17
7	4.67	131.40
8	6.00	131.30
9	6.81	131.23
10	8.14	131.25
11	10.07	131.34
12	10.96	131.47
13	11.93	131.16
14	12.07	131.00
15	12.53	130.90
16	12.79	130.94
17	13.12	131.12
18	14.10	131.36
19	15.25	131.60
20	15.69	132.44
21	17.18	132.70
22	17.94	132.78
23	19.30	132.94
24		
25		
26		
27		
28		
29		
30		
31		
32		
33		
34		
35		
	min. Stage =	130.90
	Coninuum	1
	CEM	3

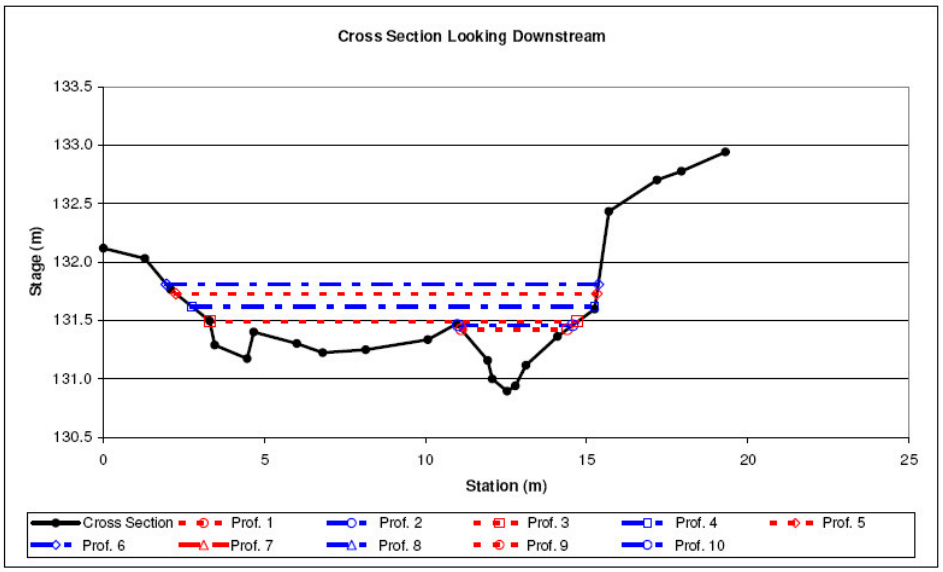

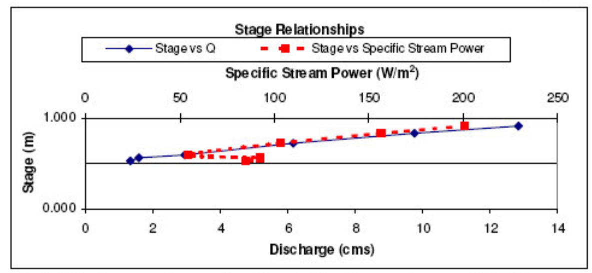

Prof. ID	Estimated n-value	L-Limit	R-Limit	WS (m)	Depth (m)	Left Sta (m)	Right Sta (m)	P_w (m)	Area (m^2)	W (m)	R (m)	D (m)	W/d	V (m/s)	Q (m^3/s)	U* (m/s)	τ (kg/ms²)	τ*	ω (W/m²)	Ω (W/m)	F_r	R/d_{84}	n-value per Limerino	Floodplain Form
HCMR03P01	0.035	10.96		131.43	0.530	11.11	14.40	3.50	0.83	3.29	0.24	0.25	6.2	1.6	1.3	0.22	49.7	2.196	85	278	1.09	3.6	0.039	PMB
HCMR03P02	0.035	10.96		131.46	0.565	11.00	14.57	3.79	0.95	3.57	0.25	0.27	6.3	1.7	1.6	0.23	52.5	2.322	93	330	1.10	3.8	0.038	PMB
HCMR03P03	0.045			131.49	0.595	3.30	14.72	11.86	2.54	11.41	0.21	0.22	19.2	1.2	2.9	0.21	44.8	1.980	54	617	0.84	3.2	0.040	PMB
HCMR03P04	0.045			131.62	0.725	2.75	15.26	13.00	4.10	12.51	0.31	0.33	17.3	1.5	6.2	0.26	66.0	2.916	103	1289	0.90	4.8	0.037	PMB
HCMR03P05	0.045			131.73	0.835	2.25	15.32	13.63	5.50	13.06	0.40	0.42	15.6	1.8	9.8	0.29	84.5	3.736	156	2043	0.94	6.1	0.035	PMB
HCMR03P06	0.045			131.81	0.915	1.96	15.36	14.03	6.56	13.40	0.47	0.49	14.6	2.0	12.8	0.31	97.9	4.330	201	2688	0.96	7.1	0.035	PMB
HCMR03P07	0.045																							PMB
HCMR03P08	0.045																							PMB
HCMR03P09	0.045																							PMB
HCMR03P10	0.045																							PMB

Cross Section Hydraulic Analyses: Hicks Canyon

Sta	59.748	304.684

Floodplain/Site Description: Hicks Canyon Modeling Reach Sta 559.8 m of Modeling Reach and Sta 304.7 m upstream of road crossing. Photograph view is looking downstream in Jan. 08 following a wildfire and ~ 5 to 10 yr flow event.

Location ID		HCMR04
d_{50} (mm) =		1.40
d_{84} (mm) =		66.30
So = Sf =		0.0214
Pt #	Sta (m)	Stage (m)
1	0.00	132.47
2	1.70	132.30
3	2.56	132.04
4	3.08	131.99
5	3.98	131.64
6	5.18	131.70
7	5.91	131.58
8	7.29	131.61
9	7.79	131.83
10	9.35	131.87
11	10.65	131.83
12	10.97	131.67
13	11.86	131.57
14	13.10	131.69
15	13.11	131.89
16	16.28	131.84
17	17.28	131.77
18	17.78	131.62
19	18.45	131.76
20	19.62	131.84
21	20.52	131.70
22	21.11	131.31
23	21.48	131.17
24	22.41	131.27
25	23.23	131.69
26	23.41	131.98
27	23.88	132.33
28	24.36	132.97
29	25.79	133.12
30		
31		
32		
33		
34		
35		
min. Stage =		131.17
Coninuum		1
CEM		3

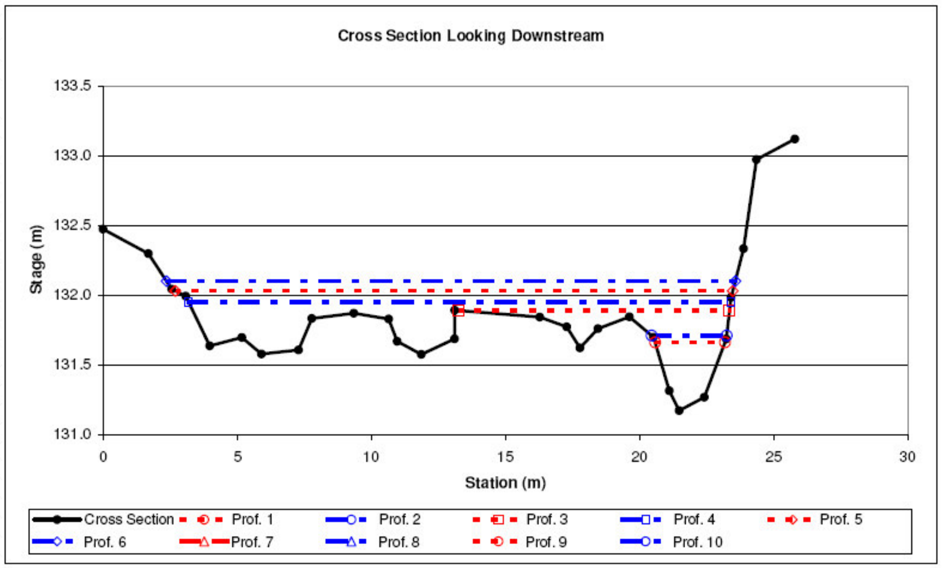

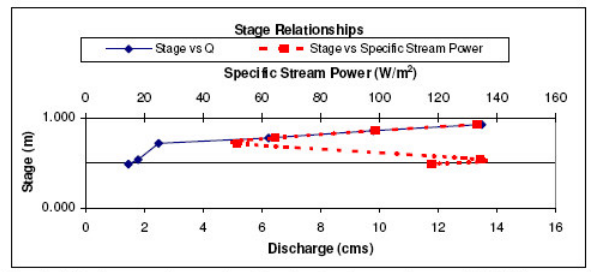

Prof. ID	Estimated n-value	L-Limit	R-Limit	WS (m)	Depth (m)	Left Sta (m)	Right Sta (m)	P_w (m)	Area (m^2)	W (m)	R (m)	D (m)	W/d	V (m/s)	Q (m^3/s)	U* (m/s)	τ (kg/ms²)	τ*	ω (W/m²)	Ω (W/m)	F_r	R/d_{84}	n-value per Limerino	Floodplain Form
HCMR04P01	0.035	19.62		131.66	0.489	20.58	23.18	2.83	0.81	2.60	0.29	0.31	5.3	1.8	1.5	0.24	59.8	2.645	118	307	1.11	4.3	0.037	PMB
HCMR04P02	0.035	19.62		131.71	0.539	20.45	23.25	3.06	0.94	2.80	0.31	0.34	5.2	1.9	1.8	0.25	64.6	2.854	134	376	1.12	4.6	0.037	PMB
HCMR04P03	0.040	13.11		131.89	0.719	13.24	23.36	10.54	2.04	10.12	0.19	0.20	14.1	1.2	2.5	0.20	40.6	1.793	52	523	0.93	2.9	0.041	PMB
HCMR04P04	0.045			131.95	0.779	3.19	23.39	21.03	5.00	20.21	0.24	0.25	25.9	1.2	6.2	0.22	49.8	2.203	65	1306	0.86	3.6	0.039	PMB
HCMR04P05	0.045			132.03	0.859	2.69	23.48	21.64	6.63	20.78	0.31	0.32	24.2	1.5	9.8	0.25	64.2	2.838	99	2051	0.89	4.6	0.037	PMB
HCMR04P06	0.045			13210	0.929	2.37	23.57	22.10	8.11	21.20	0.37	0.38	22.8	1.7	13.5	0.28	76.8	3.397	133	2825	0.92	5.5	0.036	PMB
HCMR04P07	0.045																							PMB
HCMR04P08	0.045																							PMB
HCMR04P09	0.045																							PMB
HCMR04P10	0.045																							PMB

Cross Section Hydraulic Analyses: Hicks Canyon

Sta	76.692	321.628

Floodplain/Site Description: Hicks Canyon Modeling Reach Sta 76.7 m of Modeling Reach and Sta 321.6 m upstream of road crossing. Photograph view is looking upstream in Jan. 08 following a wildfire and ~ 5 to 10 yr flow event.

Location ID	HCMR05	
d_{50} (mm) =	1.40	
d_{84} (mm) =	66.30	
So = Sf =	0.0196	
Pt #	Sta (m)	Stage (m)
1	0.00	132.48
2	1.12	132.34
3	2.47	132.19
4	3.18	131.98
5	3.47	131.90
6	4.83	132.07
7	5.00	132.22
8	5.62	132.44
9	7.06	132.37
10	8.22	131.92
11	9.72	131.96
12	11.27	132.03
13	12.24	132.07
14	12.88	131.89
15	13.99	131.64
16	15.06	131.75
17	15.63	131.84
18	15.97	132.03
19	16.68	132.10
20	17.13	132.42
21	17.49	133.13
22	18.96	133.26
23	20.60	133.39
24	22.25	133.38
25		
26		
27		
28		
29		
30		
31		
32		
33		
34		
35		
min. Stage =		131.64
Coninuum		1
CEM		3

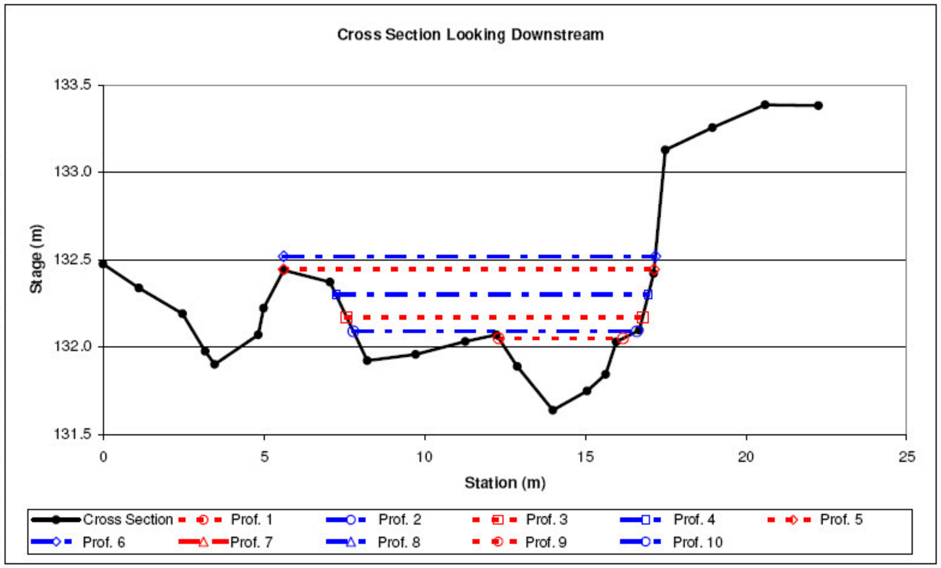

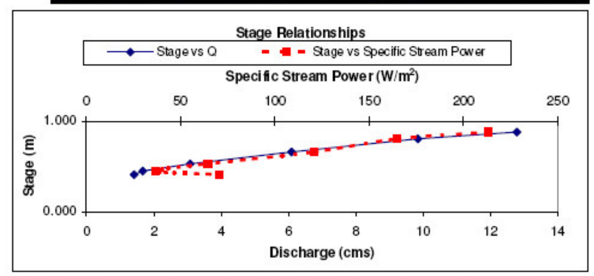

Prof. ID	Estimated n-value	L-Limit	R-Limit	WS (m)	Depth (m)	Left Sta (m)	Right Sta (m)	P_w (m)	Area (m^2)	W (m)	R (m)	D (m)	W/d	V (m/s)	Q (m^3/s)	U* (m/s)	τ (kg/ms²)	τ*	ω (W/m²)	Ω (W/m)	F_r	R/d_{84}	n-value per Limerino	Floodplain Form
HCMR05P01	0.035	12.24		132.05	0.412	12.31	16.18	3.99	0.93	3.87	0.23	0.24	9.4	1.5	1.4	0.21	45.0	1.989	70	272	1.06	3.5	0.039	PMB
HCMR05P02	0.040	7.06		132.09	0.452	7.79	16.61	8.97	1.54	8.82	0.17	0.17	19.5	1.1	1.7	0.18	33.1	1.465	37	322	0.89	2.6	0.042	PMB
HCMR05P03	0.040	7.06		132.17	0.532	7.58	16.78	9.39	2.27	9.20	0.24	0.25	17.3	1.4	3.1	0.22	46.5	2.055	64	593	0.94	3.6	0.039	PMB
HCMR05P04	0.040	7.06		132.30	0.662	7.24	16.96	9.98	3.50	9.72	0.35	0.36	14.7	1.7	6.1	0.26	67.6	2.986	121	1174	0.99	5.3	0.036	PMB
HCMR05P05	0.040	5.62		132.45	0.807	5.62	17.14	11.85	5.00	11.52	0.42	0.43	14.3	2.0	9.8	0.29	81.3	3.593	165	1897	1.02	6.4	0.035	PMB
HCMR05P06	0.040	5.62		132.52	0.882	5.62	17.18	11.93	5.86	11.56	0.49	0.51	13.1	2.2	12.8	0.31	94.7	4.185	213	2465	1.05	7.4	0.034	PMB
HCMR05P07	0.045																							PMB
HCMR05P08	0.045																							PMB
HCMR05P09	0.045																							PMB
HCMR05P10	0.045																							PMB

Cross Section Hydraulic Analyses: Hicks Canyon

Sta	96.023	340.959

Floodplain/Site Description: Hicks Canyon Modeling Reach Sta 96.0 m of Modeling Reach and Sta 341.0 m upstream of road crossing. Photograph view is looking upstream in Jan. 08 following a wildfire and ~ 5 to 10 yr flow event.

Location ID		HCMR06
d_{50} (mm) =		1.40
d_{84} (mm) =		66.30
So = Sf =		0.0196
Pt #	Sta (m)	Stage (m)
1	0.00	133.36
2	0.84	133.15
3	1.87	133.25
4	3.04	132.97
5	3.52	132.77
6	4.79	132.45
7	4.95	132.04
8	5.94	131.86
9	7.38	132.10
10	8.18	132.07
11	8.46	132.02
12	8.85	132.03
13	9.09	132.26
14	10.14	132.36
15	11.22	132.42
16	13.08	132.93
17	15.13	133.46
18	16.15	133.97
19	16.36	134.41
20	18.12	134.53
21	19.58	134.55
22	20.74	134.60
23		
24		
25		
26		
27		
28		
29		
30		
31		
32		
33		
34		
35		
min. Stage =		131.86
Coninuum		1
CEM		3

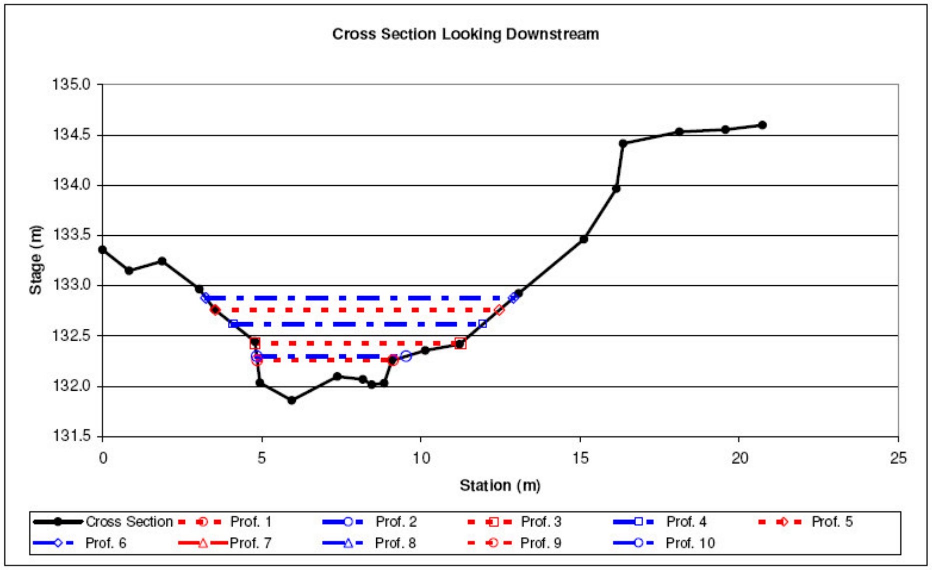

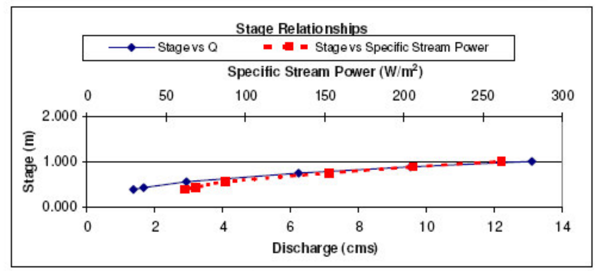

Prof. ID	Estimated n-value	L-Limit	R-Limit	WS (m)	Depth (m)	Left Sta (m)	Right Sta (m)	P_w (m)	Area (m^2)	W (m)	R (m)	D (m)	W/d	V (m/s)	Q (m^3/s)	U* (m/s)	τ (kg/ms²)	τ*	ω (W/m²)	Ω (W/m)	F_r	R/d_{84}	n-value per Limerino	Floodplain Form
HCMR06P01	0.040			132.26	0.399	4.86	9.13	4.55	1.04	4.27	0.23	0.24	10.7	1.3	1.4	0.21	44.2	1.955	62	264	0.91	3.5	0.039	PMB
HCMR06P02	0.040			132.30	0.439	4.85	9.54	5.01	1.22	4.70	0.24	0.26	10.7	1.4	1.7	0.22	47.1	2.081	69	323	0.92	3.7	0.038	PMB
HCMR06P03	0.040			132.43	0.569	4.80	11.26	6.87	1.94	6.46	0.28	0.30	11.4	1.5	2.9	0.23	54.5	2.409	87	565	0.94	4.3	0.037	PMB
HCMR06P04	0.040			132.62	0.759	4.10	11.96	8.32	3.30	7.85	0.40	0.42	10.3	1.9	6.2	0.28	76.4	3.376	153	1202	1.00	6.0	0.035	PMB
HCMR06P05	0.040			132.76	0.899	3.54	12.47	9.43	4.47	8.93	0.47	0.50	9.9	2.1	9.5	0.30	91.4	4.041	206	1837	1.03	7.2	0.034	PMB
HCMR06P06	0.040			132.88	1.019	3.25	12.91	10.20	5.59	9.66	0.55	0.58	9.5	2.3	13.1	0.32	105.5	4.666	262	2526	1.06	8.3	0.034	PMB
HCMR06P07	0.040																							PMB
HCMR06P08	0.040																							PMB
HCMR06P09	0.040																							PMB
HCMR06P10	0.040																							PMB

Cross Section Hydraulic Analyses: Hicks Canyon

Sta	134.898	379.833

Floodplain/Site Description: Hicks Canyon Modeling Reach Sta 134.9 m of Modeling Reach and Sta 379.8 m upstream of road crossing. Photograph view is looking downstream in Jan. 08 following a wildfire and ~ 5 to 10 yr flow event.

Location ID		HCMR07
d_{50} (mm) =		1.40
d_{84} (mm) =		66.30
So = Sf =		0.0196
Pt #	Sta (m)	Stage (m)
1	0.00	135.74
2	2.21	135.59
3	3.63	135.51
4	5.27	135.41
5	6.19	134.14
6	7.41	133.39
7	9.19	133.15
8	10.16	133.21
9	10.94	132.96
10	11.27	133.11
11	11.53	132.79
12	12.13	133.05
13	13.23	133.06
14	13.45	132.89
15	14.29	132.80
16	14.46	132.63
17	15.14	132.61
18	15.98	133.45
19	17.76	133.47
20	18.29	133.37
21	18.70	133.49
22	20.65	133.58
23	23.06	133.66
24	25.82	134.11
25		
26		
27		
28		
29		
30		
31		
32		
33		
34		
35		
min. Stage =		132.61
Coninuum		1
CEM		3

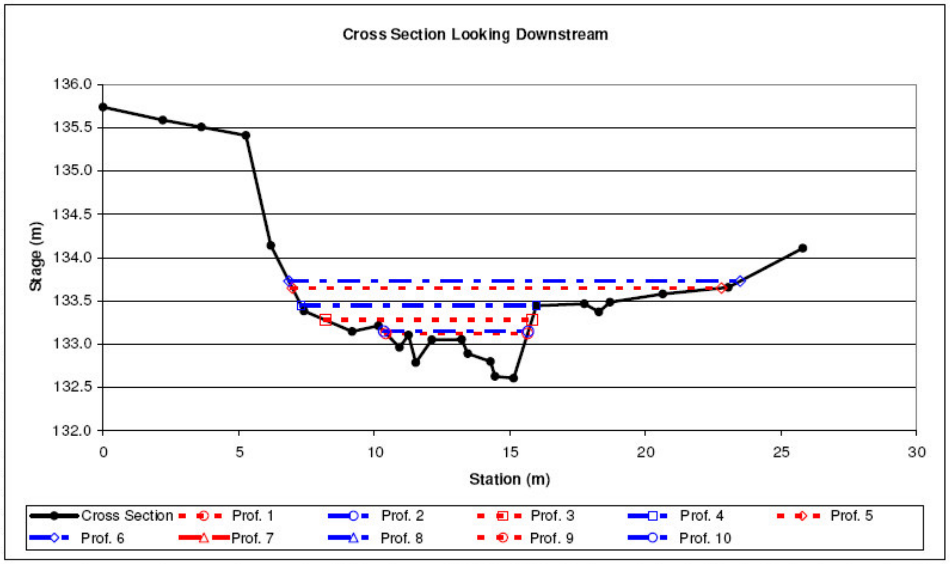

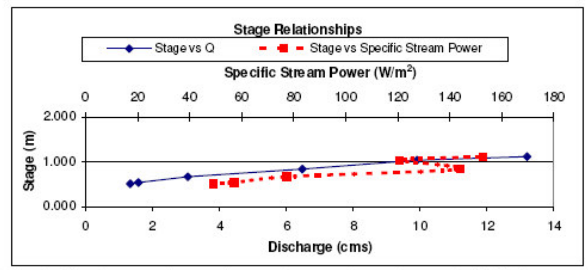

Prof. ID	Estimated n-value	L-Limit	R-Limit	WS (m)	Depth (m)	Left Sta (m)	Right Sta (m)	P_w (m)	Area (m^2)	W (m)	R (m)	D (m)	W/d	V (m/s)	Q (m^3/s)	U* (m/s)	τ (kg/ms²)	τ*	ω (W/m²)	Ω (W/m)	F_r	R/d_{84}	n-value per Limerino	Floodplain Form
HCMR07P01	0.040	10.16		133.13	0.517	10.43	15.66	5.83	1.13	5.23	0.19	0.22	10.1	1.2	1.3	0.19	37.5	1.656	49	257	0.86	2.9	0.040	PMB
HCMR07P02	0.040	10.16		133.15	0.542	10.36	15.69	5.95	1.27	5.33	0.21	0.24	9.8	1.2	1.6	0.20	41.0	1.812	57	305	0.88	3.2	0.039	PMB
HCMR07P03	0.040			133.28	0.672	8.20	15.82	8.31	2.15	7.62	0.26	0.28	11.3	1.4	3.1	0.22	49.8	2.202	77	588	0.92	3.9	0.038	PMB
HCMR07P04	0.040		15.98	133.45	0.842	7.31	15.98	9.46	3.55	8.68	0.38	0.41	10.3	1.8	6.5	0.27	72.4	3.199	144	1249	0.98	5.7	0.035	PMB
HCMR07P05	0.045			133.65	1.042	6.98	22.81	16.70	6.17	15.83	0.37	0.39	15.2	1.6	9.9	0.27	71.3	3.151	121	1910	0.88	5.6	0.036	PMB
HCMR07P06	0.045			133.73	1.122	6.86	23.50	17.55	7.48	16.65	0.43	0.45	14.8	1.8	13.2	0.29	82.2	3.633	153	2544	0.90	6.4	0.035	PMB
HCMR07P07	0.045																							PMB
HCMR07P08	0.045																							PMB
HCMR07P09	0.045																							PMB
HCMR07P10	0.045																							PMB

Cross Section Hydraulic Analyses: Hicks Canyon

Sta	162.556	407.491
Location ID	HCMR08	
d_{50} (mm) =	1.40	
d_{84} (mm) =	66.30	
So = Sf =	0.0196	

Floodplain/Site Description: Hicks Canyon Modeling Reach Sta 162.6 m of Modeling Reach and Sta 407.5 m upstream of road crossing. Photograph view is looking downstream shortly after the wildfires (January 08).

Pt #	Sta (m)	Stage (m)
1	0.00	136.08
2	2.59	135.89
3	4.87	135.69
4	6.86	135.20
5	9.34	134.38
6	10.94	134.08
7	12.94	134.01
8	14.67	134.09
9	15.90	134.10
10	17.05	134.10
11	17.18	133.99
12	18.00	133.95
13	18.71	134.08
14	21.05	134.09
15	22.37	134.05
16	23.68	133.75
17	24.58	133.22
18	25.15	133.17
19	25.28	133.39
20	25.85	133.58
21	27.19	134.67
22	28.38	135.56
23	28.71	136.23
24	30.19	136.29
25	31.29	136.27
26		
27		
28		
29		
30		
31		
32		
33		
34		
35		
min. Stage =		133.17
Coninuum		1
CEM		3

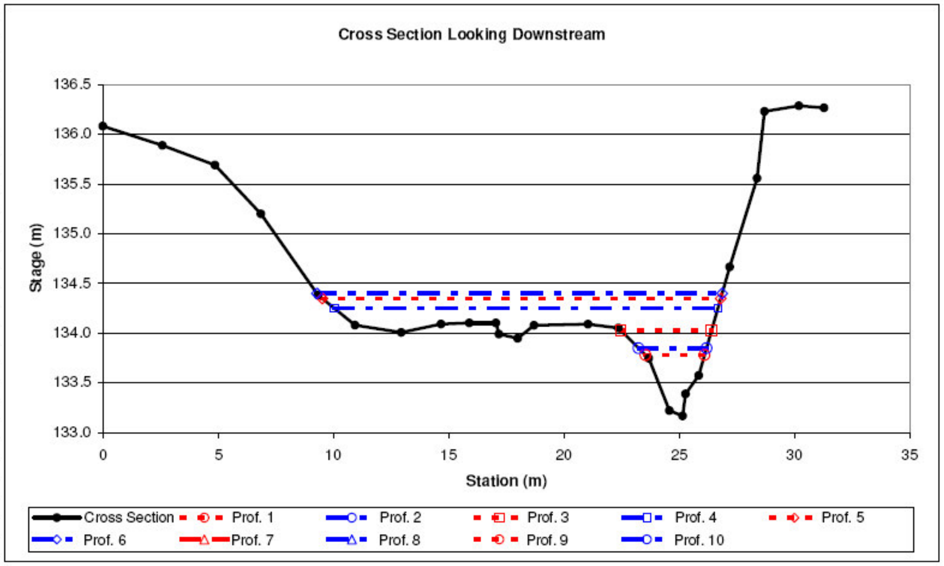

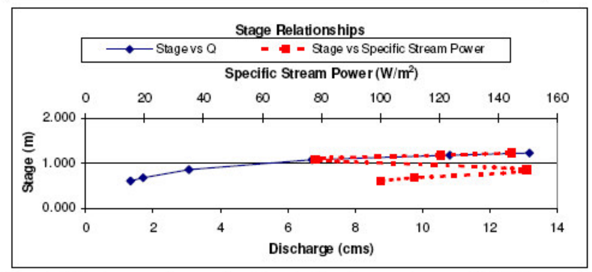

Prof. ID	Estimated n-value	L-Limit	R-Limit	WS (m)	Depth (m)	Left Sta (m)	Right Sta (m)	P_w (m)	Area (m^2)	W (m)	R (m)	D (m)	W/d	V (m/s)	Q (m^3/s)	U* (m/s)	τ (kg/ms²)	τ*	ω (W/m²)	Ω (W/m)	F_r	R/d_{84}	n-value per Limerino	Floodplain Form
HCMR08P01	0.040			133.78	0.612	23.54	26.10	2.94	0.86	2.56	0.29	0.34	4.2	1.5	1.3	0.24	56.5	2.498	100	257	0.91	4.4	0.037	PMB
HCMR08P02	0.040	22.37		133.85	0.682	23.24	26.19	3.36	1.05	2.95	0.31	0.36	4.3	1.6	1.7	0.25	60.5	2.674	112	329	0.93	4.7	0.036	PMB
HCMR08P03	0.040	21.05		134.03	0.862	22.46	26.41	4.44	1.67	3.95	0.38	0.42	4.6	1.8	3.1	0.27	72.7	3.215	150	591	0.96	5.7	0.035	PMB
HCMR08P04	0.043			134.25	1.082	10.05	26.68	17.28	4.83	16.63	0.28	0.29	15.4	1.4	6.7	0.23	53.8	2.380	78	1296	0.89	4.2	0.038	PMB
HCMR08P05	0.043			134.35	1.182	9.52	26.80	17.98	6.52	17.29	0.36	0.38	14.6	1.7	10.8	0.26	69.9	3.091	121	2085	0.92	5.5	0.036	PMB
HCMR08P06	0.043			134.40	1.232	9.29	26.87	18.29	7.39	17.58	0.40	0.42	14.3	1.8	13.2	0.28	77.9	3.445	145	2540	0.94	6.1	0.035	PMB
HCMR08P07	0.043																							PMB
HCMR08P08	0.043																							PMB
HCMR08P09	0.043																							PMB
HCMR08P10	0.043																							PMB

Cross Section Hydraulic Analyses: Hicks Canyon

Sta	192.838	437.774

Floodplain/Site Description: Hicks Canyon Modeling Reach Sta 192.8 m of Modeling Reach and Sta 437.8 m upstream of road crossing. Photograph view is looking downstream shortly after the wildfires (January 08).

Location ID		HCMR09
d_{50} (mm) =		1.40
d_{84} (mm) =		66.30
So = Sf =		0.0170
Pt #	Sta (m)	Stage (m)
1	0.00	136.48
2	2.72	136.30
3	6.02	136.37
4	8.45	136.52
5	11.07	134.90
6	14.14	134.89
7	16.93	134.86
8	18.35	134.79
9	19.04	134.56
10	20.27	134.67
11	21.25	134.62
12	22.29	133.91
13	22.72	133.82
14	24.50	134.07
15	25.64	134.62
16	28.52	136.34
17	28.83	137.02
18	30.70	137.25
19	31.96	137.74
20		
21		
22		
23		
24		
25		
26		
27		
28		
29		
30		
31		
32		
33		
34		
35		
min. Stage =		133.82
Coninuum		1
CEM		3

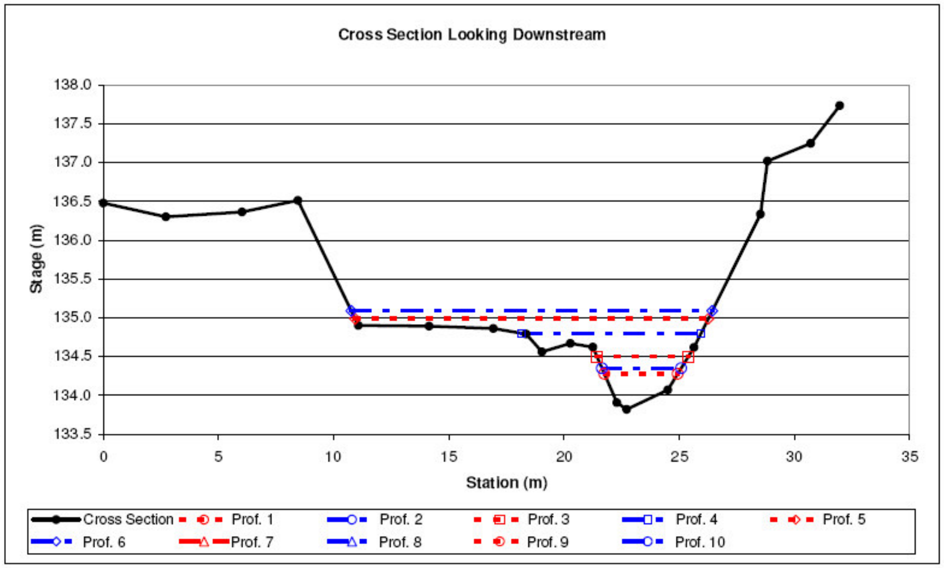

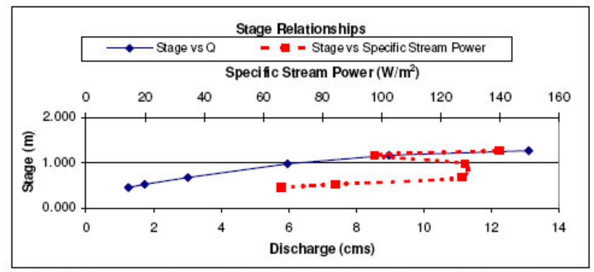

Prof. ID	Estimated n-value	L-Limit	R-Limit	WS (m)	Depth (m)	Left Sta (m)	Right Sta (m)	P_w (m)	Area (m^2)	W (m)	R (m)	D (m)	W/d	V (m/s)	Q (m^3/s)	U* (m/s)	τ (kg/ms²)	τ*	ω (W/m²)	Ω (W/m)	F_r	R/d_{84}	n-value per Limerino	Floodplain Form
HCMR09P01	0.040	21.25		134.28	0.459	21.75	24.93	3.38	0.92	3.19	0.27	0.29	6.9	1.4	1.3	0.21	45.5	2.011	66	210	0.87	4.1	0.038	PMB
HCMR09P02	0.040	21.25		134.35	0.529	21.64	25.08	3.66	1.15	3.43	0.31	0.34	6.5	1.5	1.7	0.23	52.5	2.322	84	290	0.89	4.7	0.037	PMB
HCMR09P03	0.040	21.25		134.50	0.679	21.43	25.39	4.27	1.71	3.96	0.40	0.43	5.8	1.8	3.0	0.26	66.7	2.949	127	504	0.92	6.0	0.035	PMB
HCMR09P04	0.043			134.80	0.979	18.17	25.94	8.24	3.49	7.77	0.42	0.45	7.9	1.7	6.0	0.27	70.7	3.127	128	997	0.87	6.4	0.035	PMB
HCMR09P05	0.043			134.99	1.169	10.93	26.26	15.88	5.79	15.33	0.36	0.38	13.1	1.5	9.0	0.25	60.9	2.694	98	1499	0.86	5.5	0.036	PMB
HCMR09P06	0.043			135.09	1.269	10.77	26.43	16.26	7.34	15.66	0.45	0.47	12.3	1.8	13.1	0.27	75.4	3.333	140	2190	0.89	6.8	0.035	PMB
HCMR09P07	0.043																							PMB
HCMR09P08	0.043																							PMB
HCMR09P09	0.043																							PMB
HCMR09P10	0.043																							PMB

Cross Section Hydraulic Analyses: Hicks Canyon

Sta	219.797	464.733

Floodplain/Site Description: Hicks Canyon Modeling Reach Sta 219.8 m of Modeling Reach and Sta 464.7 m upstream of road crossing. Photograph view is looking downstream shortly after the wildfires (January 08).

Location ID	HCMR10
d_{50} (mm) =	1.40
d_{84} (mm) =	66.30
So = Sf =	0.0170

Pt #	Sta (m)	Stage (m)
1	0.00	136.28
2	2.53	136.17
3	4.82	136.06
4	6.97	135.75
5	7.47	135.30
6	7.69	134.57
7	8.57	134.23
8	9.05	134.28
9	9.76	134.91
10	13.72	134.92
11	15.56	135.04
12	18.14	134.88
13	19.14	135.58
14	21.07	136.76
15	22.87	136.87
16	26.09	137.33
17	29.67	137.53
18		
19		
20		
21		
22		
23		
24		
25		
26		
27		
28		
29		
30		
31		
32		
33		
34		
35		
min. Stage =	134.23	
Coninuum	1	
CEM	2	

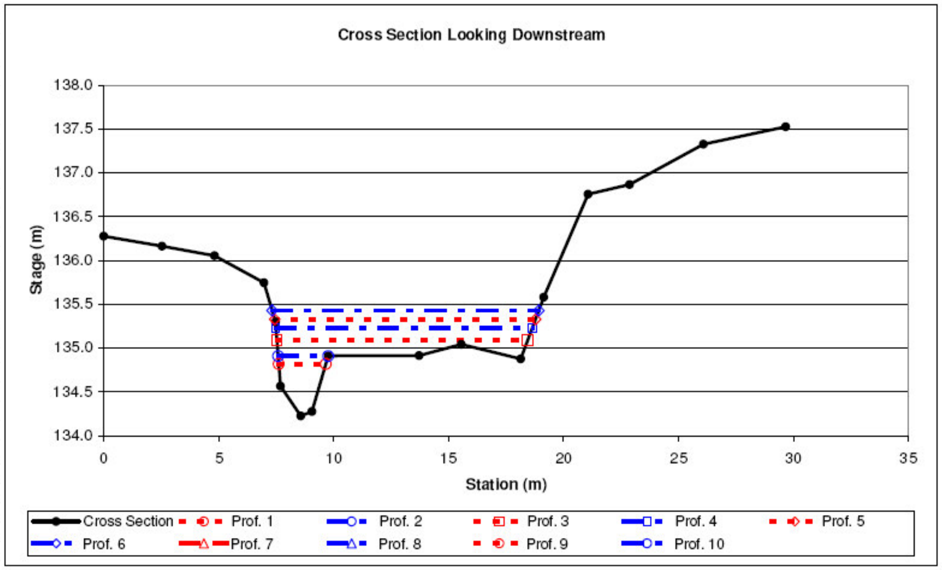

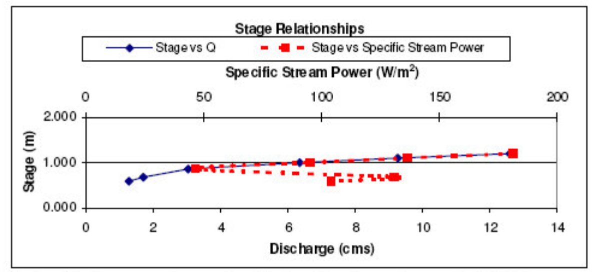

Prof. ID	Estimated n-value	L-Limit	R-Limit	WS (m)	Depth (m)	Left Sta (m)	Right Sta (m)	P_w (m)	Area (m^2)	W (m)	R (m)	D (m)	W/d	V (m/s)	Q (m^3/s)	U* (m/s)	τ (kg/ms^2)	τ*	ω (W/m^2)	Ω (W/m)	F_r	R/d_{84}	n-value per Limerino	Floodplain Form
HCMR10P01	0.040			134.82	0.594	7.61	9.66	2.51	0.82	2.05	0.33	0.40	3.4	1.6	1.3	0.23	54.7	2.420	104	213	0.84	4.9	0.036	PMB
HCMR10P02	0.040		15.56	134.91	0.684	7.59	9.76	2.74	1.01	2.17	0.37	0.47	3.2	1.7	1.7	0.25	61.8	2.730	131	284	0.84	5.6	0.035	PMB
HCMR10P03	0.043			135.09	0.864	7.54	18.44	11.68	2.67	10.90	0.23	0.25	12.6	1.1	3.0	0.20	38.2	1.690	46	507	0.79	3.5	0.039	PMB
HCMR10P04	0.043			135.23	1.004	7.49	18.64	12.07	4.22	11.15	0.35	0.38	11.1	1.5	6.3	0.24	58.3	2.579	95	1060	0.84	5.3	0.036	PMB
HCMR10P05	0.043			135.33	1.104	7.44	18.78	12.37	5.34	11.34	0.43	0.47	10.3	1.7	9.3	0.27	72.1	3.189	136	1546	0.87	6.5	0.035	PMB
HCMR10P06	0.043			135.43	1.204	7.33	18.93	12.69	6.49	11.60	0.51	0.56	9.6	1.9	12.6	0.29	85.4	3.775	181	2102	0.89	7.7	0.034	PMB
HCMR10P07	0.043																							PMB
HCMR10P08	0.043																							PMB
HCMR10P09	0.043																							PMB
HCMR10P10	0.043																							PMB

Cross Section Hydraulic Analyses: Hicks Canyon

Sta	265.296	510.231

Floodplain/Site Description: Hicks Canyon Modeling Reach Sta 265.3 m of Modeling Reach and Sta 510.2 m upstream of road crossing. Photograph view is looking from the right overbank to the left bank shortly after the wildfires (January 08).

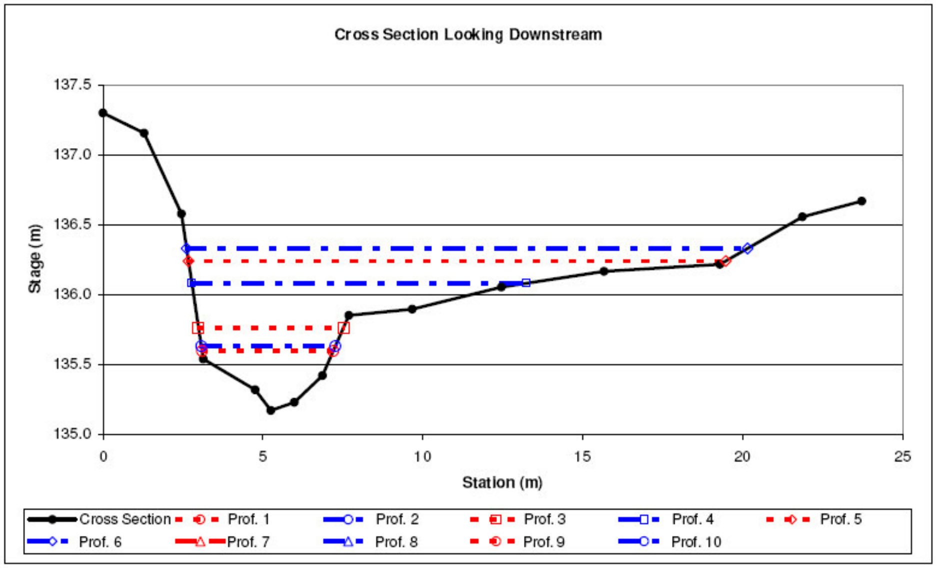

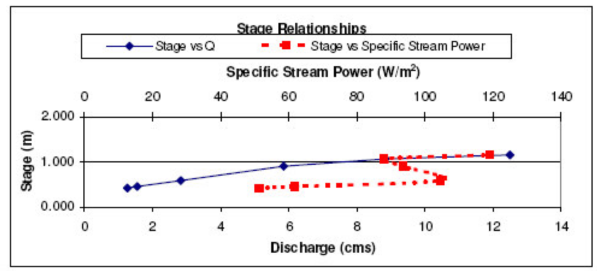

Location ID		HCMR12
d_{50} (mm) =		1.40
d_{84} (mm) =		66.30
So = Sf =		0.0170
Pt #	Sta (m)	Stage (m)
1	0.00	137.30
2	1.29	137.16
3	2.45	136.58
4	3.14	135.54
5	4.76	135.32
6	5.25	135.17
7	5.98	135.23
8	6.86	135.42
9	7.69	135.85
10	9.67	135.90
11	12.46	136.05
12	15.67	136.17
13	19.29	136.22
14	21.87	136.56
15	23.73	136.67
16		
17		
18		
19		
20		
21		
22		
23		
24		
25		
26		
27		
28		
29		
30		
31		
32		
33		
34		
35		
min. Stage =		135.17
Coninuum		1
CEM		2

Prof. ID	Estimated n-value	L-Limit	R-Limit	WS (m)	Depth (m)	Left Sta (m)	Right Sta (m)	P_w (m)	Area (m^2)	W (m)	R (m)	D (m)	W/d	V (m/s)	Q (m^3/s)	U* (m/s)	τ (kg/ms²)	τ*	ω (W/m²)	Ω (W/m)	F_r	R/d_{84}	n-value per Limerino	Floodplain Form
HCMR12P01	0.040			135.60	0.426	3.10	7.20	4.23	1.01	4.10	0.24	0.25	9.6	1.3	1.3	0.20	39.7	1.754	51	210	0.86	3.6	0.039	PMB
HCMR12P02	0.040			135.63	0.461	3.08	7.27	4.35	1.15	4.19	0.26	0.27	9.1	1.3	1.5	0.21	44.2	1.953	62	258	0.88	4.0	0.038	PMB
HCMR12P03	0.040			135.76	0.591	2.99	7.51	4.79	1.72	4.52	0.36	0.38	7.7	1.6	2.8	0.24	59.9	2.649	104	473	0.92	5.4	0.036	PMB
HCMR12P04	0.045			136.08	0.911	2.78	13.23	10.92	3.96	10.45	0.36	0.38	11.5	1.5	5.9	0.25	60.7	2.681	93	977	0.82	5.5	0.036	PMB
HCMR12P05	0.045			136.24	1.071	2.68	19.47	17.35	6.11	16.80	0.35	0.36	15.7	1.4	8.8	0.24	58.8	2.601	88	1477	0.82	5.3	0.036	PMB
HCMR12P06	0.045			136.33	1.161	2.62	20.16	18.15	7.66	17.54	0.42	0.44	15.1	1.6	12.5	0.27	70.5	3.116	119	2086	0.85	6.4	0.035	PMB
HCMR12P07	0.045																							PMB
HCMR12P08	0.045																							PMB
HCMR12P09	0.045																							PMB
HCMR12P10	0.045																							PMB

Cross Section Hydraulic Analyses: Hicks Canyon

Sta	274.432	519.368

Floodplain/Site Description: Hicks Canyon Modeling Reach Sta 274.4 m of Modeling Reach and Sta 519.4 m upstream of road crossing. Photograph view is looking downstream shortly after the wildfires (January 08).

Location ID		HCMR13
d_{50} (mm) =		1.40
d_{84} (mm) =		66.30
So = Sf =		0.0170
Pt #	Sta (m)	Stage (m)
1	0.00	137.49
2	2.74	137.48
3	5.04	137.04
4	5.98	136.64
5	8.27	136.46
6	10.48	136.05
7	10.82	135.53
8	12.04	135.31
9	13.03	135.46
10	13.29	136.02
11	16.65	136.18
12	19.48	136.28
13	20.13	135.87
14	21.05	135.86
15	21.99	136.22
16	24.92	136.31
17	25.39	136.04
18	26.81	136.23
19	29.20	136.39
20	29.72	135.84
21	31.91	136.06
22	33.20	137.71
23	35.30	137.74
24		
25		
26		
27		
28		
29		
30		
31		
32		
33		
34		
35		
min. Stage =		135.31
Coninuum		1
CEM		2

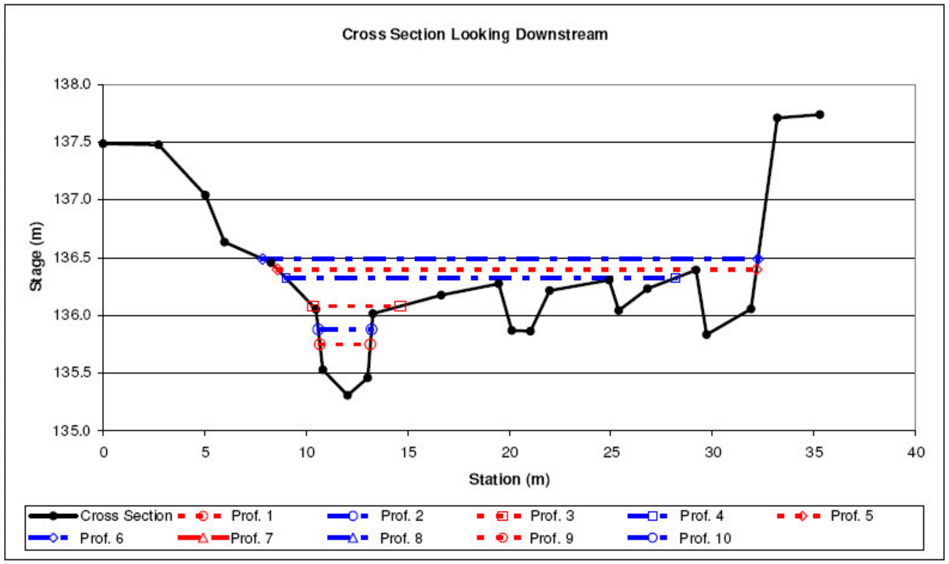

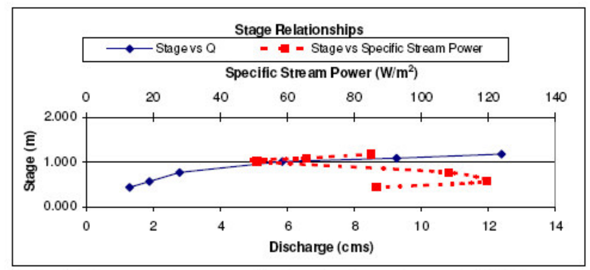

Prof. ID	Estimated n-value	L-Limit	R-Limit	WS (m)	Depth (m)	Left Sta (m)	Right Sta (m)	P_w (m)	Area (m^2)	W (m)	R (m)	D (m)	W/d	V (m/s)	Q (m^3/s)	U* (m/s)	τ (kg/ms²)	τ*	ω (W/m²)	Ω (W/m)	F_r	R/d_{84}	n-value per Limerino	Floodplain Form
HCMR13P01	0.035		19.48	135.75	0.441	10.68	13.16	2.82	0.80	2.49	0.28	0.32	5.6	1.6	1.3	0.22	47.4	2.094	87	215	0.97	4.3	0.037	PMB
HCMR13P02	0.040		19.48	135.88	0.571	10.59	13.22	3.12	1.13	2.63	0.36	0.43	4.6	1.7	1.9	0.25	60.6	2.681	120	314	0.87	5.5	0.035	PMB
HCMR13P03	0.040		19.48	136.08	0.771	10.34	14.63	4.97	1.72	4.29	0.35	0.40	5.6	1.6	2.8	0.24	58.0	2.562	108	464	0.87	5.2	0.036	PMB
HCMR13P04	0.045		29.20	136.33	1.016	9.00	28.18	20.16	5.06	19.19	0.25	0.26	18.9	1.2	5.8	0.20	42.0	1.855	51	976	0.77	3.8	0.038	PMB
HCMR13P05	0.050			136.40	1.091	8.58	32.18	24.99	7.75	23.59	0.31	0.33	21.6	1.2	9.3	0.23	51.8	2.289	66	1547	0.71	4.7	0.037	PMB
HCMR13P06	0.055			136.49	1.181	7.85	32.25	25.84	9.90	24.39	0.38	0.41	20.7	1.3	12.4	0.25	64.0	2.829	85	2069	0.67	5.8	0.036	PMB
HCMR13P07	0.055																							PMB
HCMR13P08	0.055																							PMB
HCMR13P09	0.055																							PMB
HCMR13P10	0.055																							PMB

Cross Section Hydraulic Analyses: Hicks Canyon

Sta	297.085	542.020

Floodplain/Site Description: Hicks Canyon Modeling Reach Sta 297.1 m of Modeling Reach and Sta 542.0 m upstream of road crossing. Photograph view is looking upstream shortly after the wildfires (January 08).

Location ID	HCMR14	
d_{50} (mm) =		1.40
d_{84} (mm) =		66.30
So = Sf =		0.0170
Pt #	Sta (m)	Stage (m)
1	0.00	138.11
2	1.32	137.97
3	4.05	137.02
4	7.19	136.80
5	9.70	136.76
6	9.93	136.09
7	10.88	135.86
8	11.93	135.86
9	12.68	136.28
10	13.03	136.68
11	15.56	136.76
12	20.84	137.04
13	26.14	137.20
14	29.07	138.49
15	30.06	138.69
16		
17		
18		
19		
20		
21		
22		
23		
24		
25		
26		
27		
28		
29		
30		
31		
32		
33		
34		
35		
min. Stage =		135.86
Coninuum		1
CEM		2

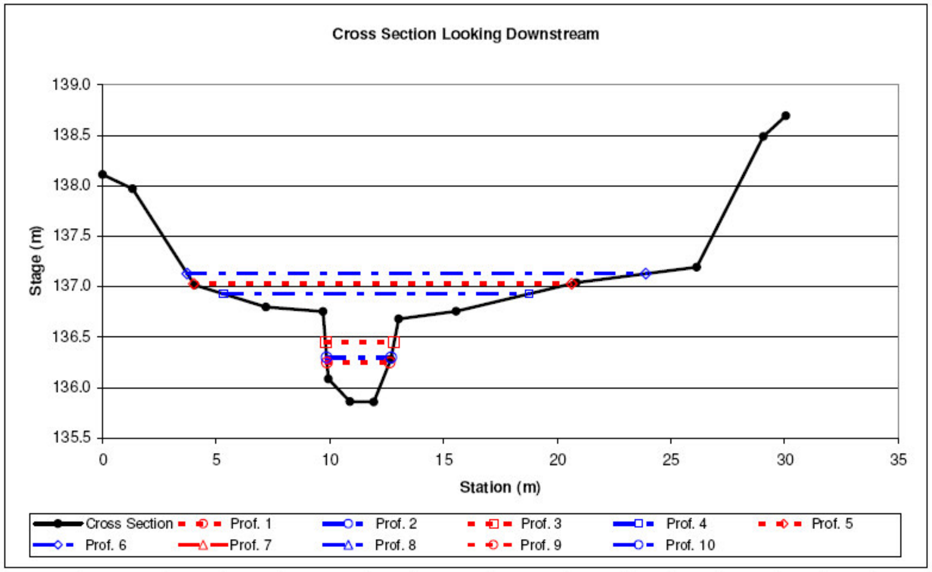

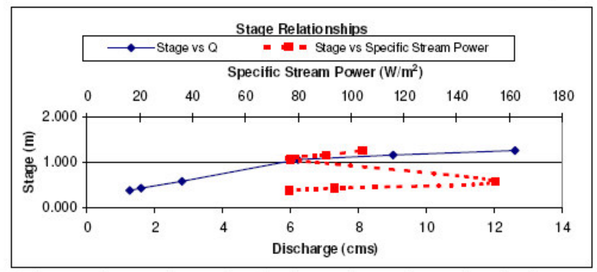

Prof. ID	Estimated n-value	L-Limit	R-Limit	WS (m)	Depth (m)	Left Sta (m)	Right Sta (m)	P_w (m)	Area (m^2)	W (m)	R (m)	D (m)	W/d	V (m/s)	Q (m^3/s)	U* (m/s)	τ (kg/ms^2)	τ^*	ω (W/m^2)	Ω (W/m)	F_r	R/d_{84}	n-value per Limerino	Floodplain Form
HCMR14P01	0.035			136.25	0.390	9.88	12.63	3.00	0.81	2.75	0.27	0.29	7.1	1.6	1.3	0.21	45.1	1.995	77	211	0.98	4.1	0.038	PMB
HCMR14P02	0.035			136.30	0.440	9.86	12.70	3.14	0.95	2.84	0.30	0.33	6.5	1.7	1.6	0.22	50.6	2.235	94	267	1.00	4.6	0.037	PMB
HCMR14P03	0.035			136.45	0.590	9.81	12.83	3.50	1.39	3.02	0.40	0.46	5.1	2.0	2.8	0.26	66.4	2.936	155	468	1.02	6.0	0.035	PMB
HCMR14P04	0.040			136.93	1.070	5.32	18.78	14.27	4.27	13.46	0.30	0.32	12.6	1.5	6.2	0.22	49.9	2.208	77	1039	0.89	4.5	0.037	PMB
HCMR14P05	0.040			137.03	1.170	4.01	20.64	17.44	5.78	16.62	0.33	0.35	14.2	1.6	9.0	0.24	55.3	2.446	91	1507	0.91	5.0	0.036	PMB
HCMR14P06	0.040			137.13	1.270	3.73	23.90	21.01	7.61	20.18	0.36	0.38	15.9	1.7	12.6	0.25	60.5	2.674	104	2106	0.92	5.5	0.036	PMB
HCMR14P07	0.040																							PMB
HCMR14P08	0.040																							PMB
HCMR14P09	0.040																							PMB
HCMR14P10	0.040																							PMB

Cross Section Hydraulic Analyses: Hicks Canyon

Sta	327.190	572.126

Floodplain/Site Description: Hicks Canyon Modeling Reach Sta 327.2 m of Modeling Reach and Sta 572.1 m upstream of road crossing. Photograph view is looking downstream shortly after the wildfires (January 08).

Location ID		HCMR15
d_{50} (mm) =		1.40
d_{84} (mm) =		66.30
So = Sf =		0.0187
Pt #	Sta (m)	Stage (m)
1	0.00	142.69
2	3.20	141.31
3	4.77	140.63
4	7.68	136.53
5	9.71	136.30
6	10.25	136.34
7	10.47	137.12
8	12.70	137.55
9	16.20	137.58
10	21.16	138.74
11	24.17	139.01
12	26.92	139.31
13		
14		
15		
16		
17		
18		
19		
20		
21		
22		
23		
24		
25		
26		
27		
28		
29		
30		
31		
32		
33		
34		
35		
min. Stage =		136.30
Coninuum		1
CEM		2

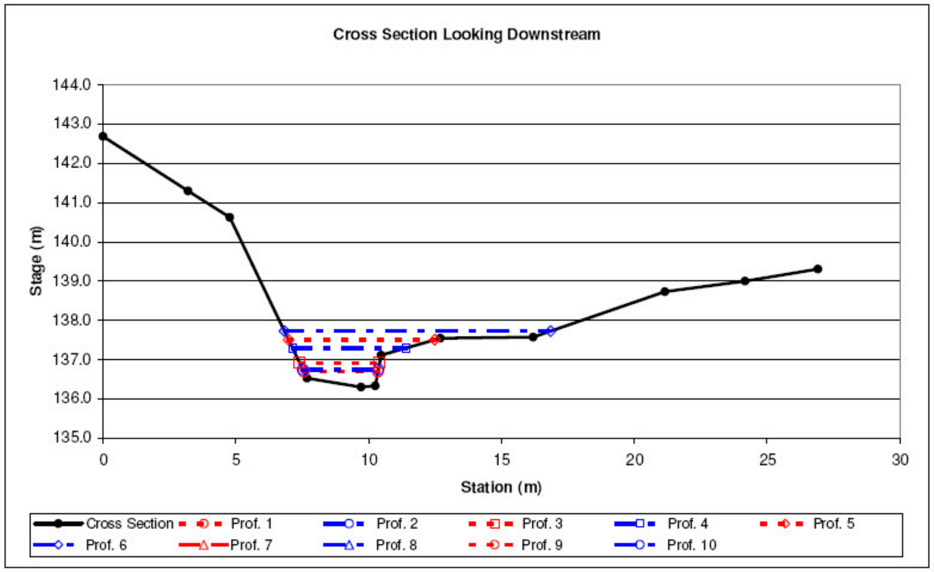

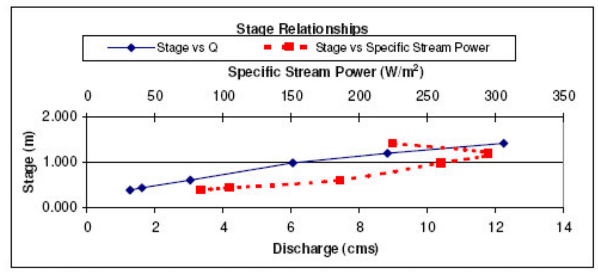

Prof. ID	Estimated n-value	L-Limit	R-Limit	WS (m)	Depth (m)	Left Sta (m)	Right Sta (m)	P_w (m)	Area (m^2)	W (m)	R (m)	D (m)	W/d	V (m/s)	Q (m^3/s)	U* (m/s)	τ (kg/ms²)	τ*	ω (W/m²)	Ω (W/m)	F_r	R/d_{84}	n-value per Limerino	Floodplain Form
HCMR15P01	0.035			136.70	0.396	7.56	10.35	3.17	0.81	2.79	0.25	0.29	7.0	1.6	1.3	0.22	46.8	2.070	84	233	1.00	3.8	0.038	PMB
HCMR15P02	0.035			136.75	0.446	7.53	10.37	3.28	0.95	2.84	0.29	0.33	6.4	1.7	1.6	0.23	53.1	2.347	105	298	1.01	4.4	0.037	PMB
HCMR15P03	0.035			136.92	0.616	7.41	10.42	3.67	1.44	3.01	0.39	0.48	4.9	2.1	3.0	0.27	72.5	3.203	186	558	1.04	5.9	0.035	PMB
HCMR15P04	0.040			137.30	0.996	7.14	11.41	5.29	2.74	4.28	0.52	0.64	4.3	2.2	6.0	0.31	95.2	4.208	260	1112	0.94	7.8	0.033	PMB
HCMR15P05	0.040			137.51	1.206	6.99	12.49	6.65	3.77	5.50	0.57	0.68	4.6	2.3	8.8	0.32	104.1	4.604	295	1623	0.97	8.5	0.033	PMB
HCMR15P06	0.040			137.73	1.426	6.83	16.85	11.30	5.67	10.02	0.50	0.57	7.0	2.2	12.2	0.30	92.2	4.076	225	2251	0.98	7.6	0.034	PMB
HCMR15P07	0.040																							PMB
HCMR15P08	0.040																							PMB
HCMR15P09	0.040																							PMB
HCMR15P10	0.040																							PMB

Cross Section Hydraulic Analyses: Hicks Canyon

Sta	398.871	643.806

Floodplain/Site Description: Hicks Canyon Modeling Reach Sta 398.9 m of Modeling Reach and Sta 643.8 m upstream of road crossing. Photograph view is looking upstream shortly after the wildfires (January 08).

Location ID		HCMR16
d_{50} (mm) =		1.40
d_{84} (mm) =		66.30
So = Sf =		0.0187
Pt #	Sta (m)	Stage (m)
1	0.00	138.55
2	1.79	138.30
3	3.56	137.54
4	5.22	137.60
5	6.13	137.78
6	6.88	138.37
7	7.54	138.95
8	8.01	139.50
9	9.49	139.48
10		
11		
12		
13		
14		
15		
16		
17		
18		
19		
20		
21		
22		
23		
24		
25		
26		
27		
28		
29		
30		
31		
32		
33		
34		
35		
min. Stage =		137.54
Coninuum		1
CEM		2

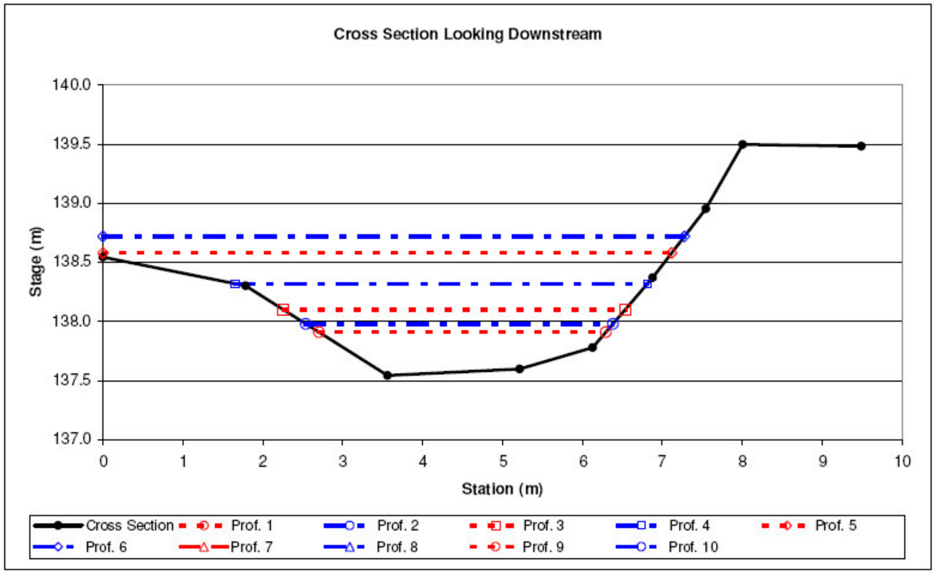

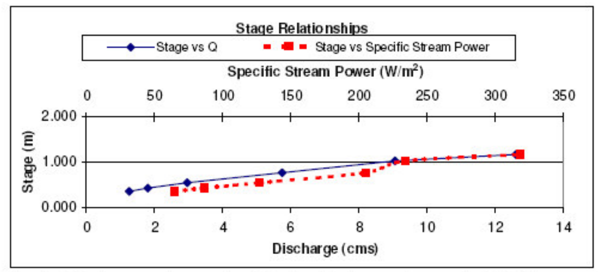

Prof. ID	Estimated n-value	L-Limit	R-Limit	WS (m)	Depth (m)	Left Sta (m)	Right Sta (m)	P_w (m)	Area (m^2)	W (m)	R (m)	D (m)	W/d	V (m/s)	Q (m^3/s)	U* (m/s)	τ (kg/ms²)	τ^*	ω (W/m²)	Ω (W/m)	F_r	R/d_{84}	n-value per Limerino	Floodplain Form
HCMR16P01	0.040			137.91	0.366	2.70	6.29	3.73	0.93	3.59	0.25	0.26	9.8	1.4	1.3	0.21	45.8	2.025	64	231	0.91	3.8	0.038	PMB
HCMR16P02	0.040			137.98	0.436	2.54	6.38	4.02	1.19	3.84	0.30	0.31	8.8	1.5	1.8	0.23	54.4	2.404	86	332	0.94	4.5	0.037	PMB
HCMR16P03	0.040			138.10	0.556	2.26	6.53	4.52	1.68	4.27	0.37	0.39	7.7	1.8	3.0	0.26	68.2	3.014	127	544	0.97	5.6	0.036	PMB
HCMR16P04	0.040			138.32	0.776	1.65	6.81	5.52	2.70	5.16	0.49	0.52	6.6	2.1	5.8	0.30	90.0	3.981	205	1057	1.01	7.4	0.034	PMB
HCMR16P05	0.045			138.58	1.036	0.00	7.12	7.59	4.33	7.12	0.57	0.61	6.9	2.1	9.1	0.32	104.9	4.636	234	1665	0.92	8.6	0.034	PMB
HCMR16P06	0.045			138.72	1.176	0.00	7.28	7.80	5.34	7.28	0.68	0.73	6.2	2.4	12.6	0.35	125.7	5.559	318	2317	0.94	10.3	0.033	PMB
HCMR16P07	0.045																							PMB
HCMR16P08	0.045																							PMB
HCMR16P09	0.045																							PMB
HCMR16P10	0.045																							PMB

Cross Section Hydraulic Analyses: Hicks Canyon

Sta	441.156	686.092

Floodplain/Site Description: Hicks Canyon Modeling Reach Sta 441.2 m of Modeling Reach and Sta 686.1 m upstream of road crossing. Photograph view is looking upstream shortly after the wildfires (January 08).

Location ID		HCMR17
d_{50} (mm) =		1.00
d_{84} (mm) =		43.50
So = Sf =		0.0137
Pt #	Sta (m)	Stage (m)
1	0.00	139.45
2	3.42	139.38
3	6.59	139.39
4	9.41	139.04
5	12.47	138.98
6	12.98	138.53
7	14.30	138.33
8	15.40	138.58
9	15.60	138.93
10	17.76	139.94
11	20.16	140.19
12	22.60	140.16
13	24.66	140.32
14		
15		
16		
17		
18		
19		
20		
21		
22		
23		
24		
25		
26		
27		
28		
29		
30		
31		
32		
33		
34		
35		
min. Stage =		138.33
Coninuum		1
CEM		2

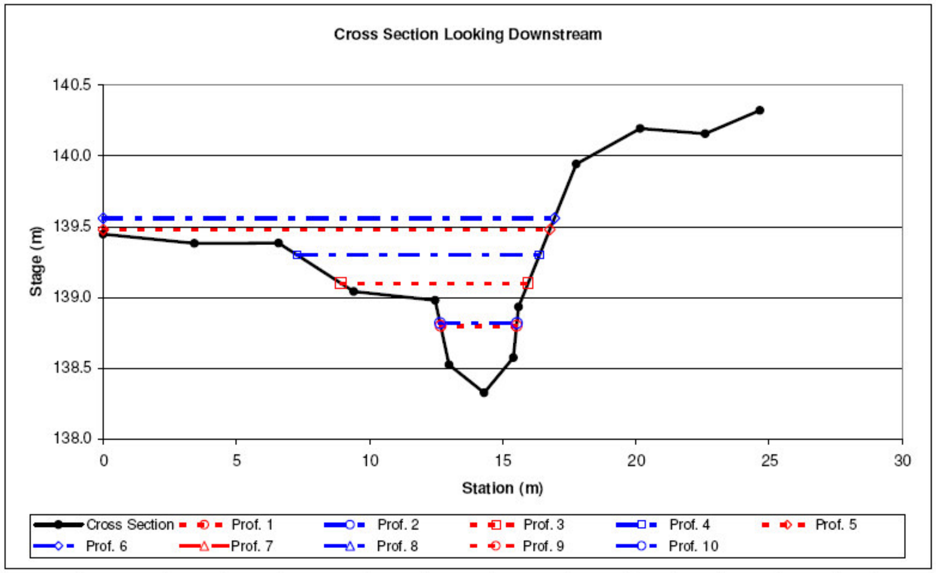

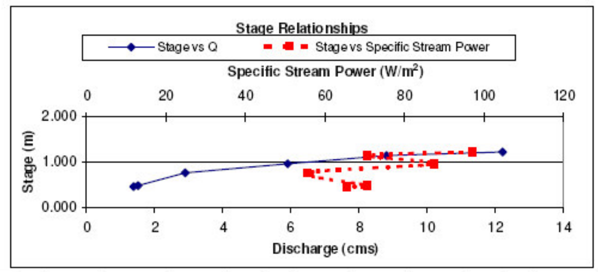

Prof. ID	Estimated n-value	L-Limit	R-Limit	WS (m)	Depth (m)	Left Sta (m)	Right Sta (m)	P_w (m)	Area (m^2)	W (m)	R (m)	D (m)	W/d	V (m/s)	Q (m^3/s)	U* (m/s)	τ (kg/ms^2)	τ^*	ω (W/m^2)	Ω (W/m)	F_r	R/d_{84}	n-value per Limerino	Floodplain Form
HCMR17P01	0.035			138.80	0.472	12.67	15.52	3.13	0.93	2.85	0.30	0.33	6.0	1.5	1.4	0.20	40.0	2.477	65	187	0.89	6.8	0.032	PMB
HCMR17P02	0.035			138.82	0.492	12.65	15.53	3.18	0.99	2.88	0.31	0.34	5.9	1.5	1.5	0.20	41.8	2.586	71	204	0.90	7.1	0.032	PMB
HCMR17P03	0.038			139.10	0.772	8.94	15.95	7.48	2.16	7.01	0.29	0.31	9.1	1.3	2.9	0.20	38.8	2.402	56	390	0.83	6.6	0.032	PMB
HCMR17P04	0.040			139.30	0.972	7.29	16.38	9.62	3.77	9.09	0.39	0.41	9.4	1.6	5.9	0.23	52.7	3.263	87	795	0.83	9.0	0.031	PMB
HCMR17P05	0.040			139.48	1.152	0.00	16.77	17.34	6.06	16.77	0.35	0.36	14.6	1.5	8.8	0.22	47.0	2.911	71	1185	0.83	8.0	0.032	PMB
HCMR17P06	0.040			139.56	1.232	0.00	16.94	17.53	7.41	16.94	0.42	0.44	13.8	1.6	12.2	0.24	56.9	3.520	97	1644	0.85	9.7	0.031	PMB
HCMR17P07	0.040																							PMB
HCMR17P08	0.040																							PMB
HCMR17P09	0.040																							PMB
HCMR17P10	0.040																							PMB

Cross Section Hydraulic Analyses: Hicks Canyon

Sta	464.267	709.202

Floodplain/Site Description: Hicks Canyon Modeling Reach Sta 464.3 m of Modeling Reach and Sta 709.2 m upstream of road crossing. Photograph view is looking downstream shortly after the wildfires (January 08).

Location ID		HCMR18
d_{50} (mm) =		1.00
d_{84} (mm) =		43.50
So = Sf =		0.0137
Pt #	Sta (m)	Stage (m)
1	0.00	139.53
2	3.00	139.51
3	5.75	139.69
4	8.55	139.70
5	10.88	139.73
6	13.70	139.20
7	14.24	138.74
8	14.76	138.64
9	15.86	138.78
10	16.18	139.32
11	17.26	139.79
12	19.28	139.91
13	22.26	139.94
14	25.80	139.89
15	28.20	140.66
16	29.57	140.89
17		
18		
19		
20		
21		
22		
23		
24		
25		
26		
27		
28		
29		
30		
31		
32		
33		
34		
35		
min. Stage =		138.64
Coninuum		1
CEM		1

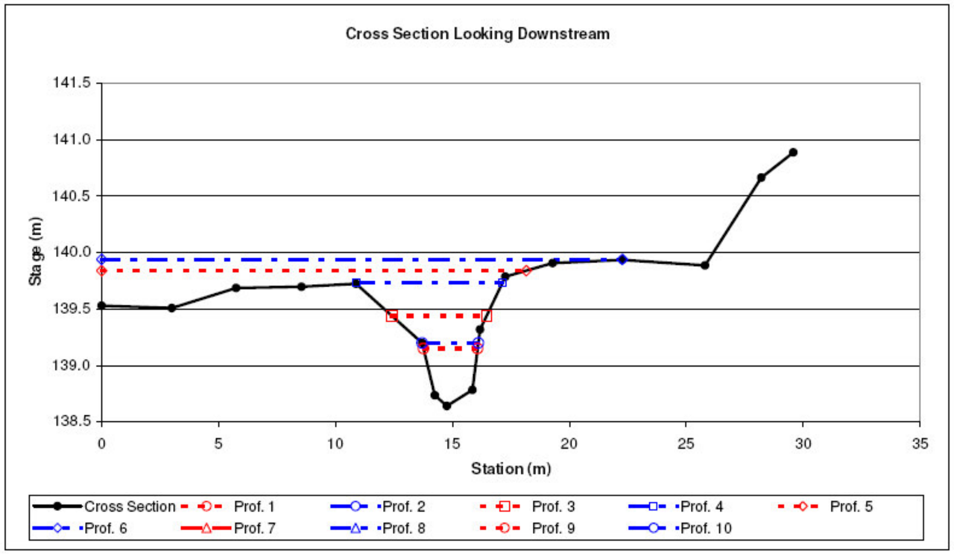

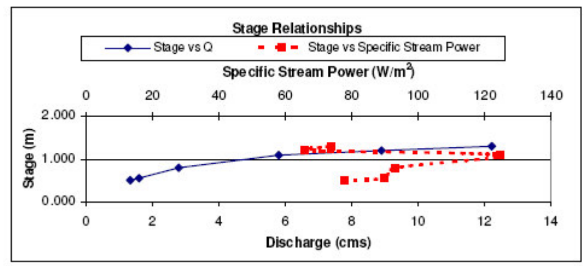

Prof. ID	Estimated n-value	L-Limit	R-Limit	WS (m)	Depth (m)	Left Sta (m)	Right Sta (m)	P_w (m)	Area (m^2)	W (m)	R (m)	D (m)	W/d	V (m/s)	Q (m^3/s)	U* (m/s)	τ (kg/ms²)	τ*	ω (W/m²)	Ω (W/m)	F_r	R/d_{84}	n-value per Limerino	Floodplain Form
HCMR18P01	0.035	10.88		139.15	0.509	13.76	16.08	2.69	0.86	2.31	0.32	0.37	4.5	1.6	1.3	0.21	42.9	2.654	78	180	0.88	7.3	0.032	PMB
HCMR18P02	0.035	10.88		139.20	0.559	13.70	16.10	2.83	0.98	2.40	0.35	0.41	4.3	1.6	1.6	0.22	46.4	2.875	90	216	0.88	7.9	0.031	PMB
HCMR18P03	0.038	10.88		139.44	0.799	12.41	16.46	4.59	1.74	4.04	0.38	0.43	5.1	1.6	2.8	0.23	51.0	3.155	93	377	0.84	8.7	0.031	PMB
HCMR18P04	0.040	10.88		139.74	1.094	10.88	17.14	6.89	3.27	6.26	0.47	0.52	5.7	1.8	5.8	0.25	63.8	3.946	125	782	0.84	10.9	0.031	PMB
HCMR18P05	0.040			139.84	1.199	0.00	18.15	18.80	6.30	18.15	0.34	0.35	15.1	1.4	8.9	0.21	45.1	2.792	66	1199	0.82	7.7	0.032	PMB
HCMR18P06	0.040		22.26	139.94	1.299	0.00	22.26	22.91	8.25	22.26	0.36	0.37	17.1	1.5	12.2	0.22	48.5	2.999	74	1645	0.83	8.3	0.032	PMB
HCMR18P07	0.040																							PMB
HCMR18P08	0.040																							PMB
HCMR18P09	0.040																							PMB
HCMR18P10	0.040																							PMB

Cross Section Hydraulic Analyses: Hicks Canyon

Sta	488.152	733.087

Floodplain/Site Description: Hicks Canyon Modeling Reach Sta 488.2 m of Modeling Reach and Sta 733.1 m upstream of road crossing. Photograph view is looking downstream at the main channel in June 07 .

Location ID		HCMR19
d_{50} (mm) =		1.00
d_{84} (mm) =		43.50
So = Sf =		0.0137
Pt #	Sta (m)	Stage (m)
1	0.00	139.81
2	2.31	139.89
3	5.84	139.96
4	7.68	140.12
5	9.83	139.67
6	10.21	139.27
7	11.01	139.04
8	12.10	139.08
9	12.66	139.22
10	12.83	139.61
11	15.28	140.01
12	18.72	140.08
13	22.06	140.15
14	25.63	140.14
15	28.58	140.22
16	32.54	140.21
17	37.17	140.32
18	42.24	140.51
19	45.12	141.59
20	46.75	141.73
21		
22		
23		
24		
25		
26		
27		
28		
29		
30		
31		
32		
33		
34		
35		
min. Stage =		139.04
Coninuum		1
CEM		1

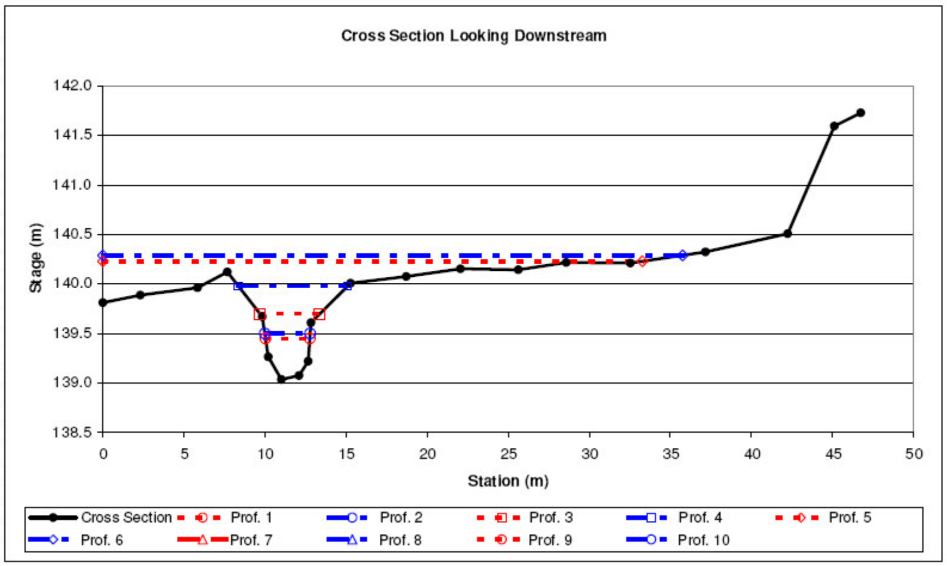

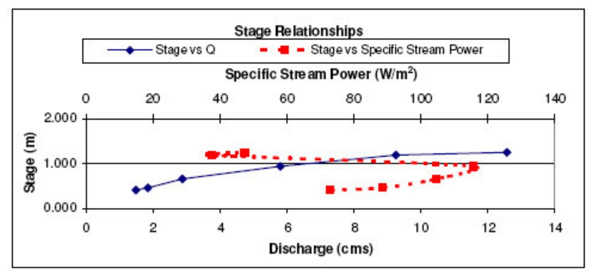

Prof. ID	Estimated n-value	L-Limit	R-Limit	WS (m)	Depth (m)	Left Sta (m)	Right Sta (m)	P_w (m)	Area (m^2)	W (m)	R (m)	D (m)	W/d	V (m/s)	Q (m^3/s)	U* (m/s)	τ (kg/ms²)	τ*	ω (W/m²)	Ω (W/m)	F_r	R/d_{84}	n-value per Limerino	Floodplain Form
HCMR19P01	0.030	7.68		139.45	0.414	10.04	12.76	3.01	0.87	2.73	0.29	0.32	6.6	1.7	1.5	0.20	38.8	2.400	73	199	1.03	6.6	0.032	PMB
HCMR19P02	0.030	7.68		139.50	0.464	9.99	12.79	3.13	1.01	2.80	0.32	0.36	6.0	1.8	1.8	0.21	43.2	2.674	89	248	1.04	7.4	0.032	PMB
HCMR19P03	0.035	7.68		139.70	0.664	9.70	13.39	4.19	1.62	3.69	0.39	0.44	5.6	1.8	2.9	0.23	52.0	3.216	105	386	0.92	8.9	0.031	PMB
HCMR19P04	0.035	7.68		139.98	0.944	8.36	15.10	7.29	3.08	6.75	0.42	0.46	7.1	1.9	5.8	0.24	56.8	3.514	116	780	0.95	9.7	0.031	PMB
HCMR19P05	0.045			140.23	1.194	0.00	33.28	33.86	8.76	33.28	0.26	0.26	27.9	1.1	9.2	0.19	34.8	2.153	37	1244	0.71	5.9	0.033	PMB
HCMR19P06	0.045			140.29	1.254	0.00	35.77	36.34	10.83	35.77	0.30	0.30	28.5	1.2	12.6	0.20	40.1	2.481	47	1691	0.72	6.8	0.033	PMB
HCMR19P07	0.045																							PMB
HCMR19P08	0.045																							PMB
HCMR19P09	0.045																							PMB
HCMR19P10	0.045																							PMB

Cross Section Hydraulic Analyses: Hasley Canyon Site 2

Floodplain/Site Description: Hasley Canyon downstream of Romero Canyon Rd. Photograph looking downstream from left bank (June 07).

Location ID		HCSA01
d_{50} (mm) =		1.60
d_{84} (mm) =		11.60
So = Sf =		0.0258
Pt#	Sta (m)	Stage (m)
1	0.00	415.46
2	4.60	415.29
3	8.14	415.31
4	12.48	415.20
5	15.03	415.21
6	15.14	414.62
7	18.64	414.66
8	21.35	414.77
9	24.78	414.72
10	27.77	414.67
11	31.65	414.76
12	35.66	414.70
13	40.53	414.83
14	43.88	414.83
15	47.17	414.92
16	50.73	414.80
17	54.23	414.81
18	54.39	414.44
19	55.99	414.35
20	58.81	414.31
21	61.96	414.50
22	65.38	414.65
23	67.95	414.51
24	70.18	414.51
25	72.22	414.55
26	74.89	414.72
27	75.19	415.59
28	77.47	415.63
29	79.40	415.64
30		
31		
32		
33		
34		
35		
min. Stage =		414.31
Continuum		1
CEM		3

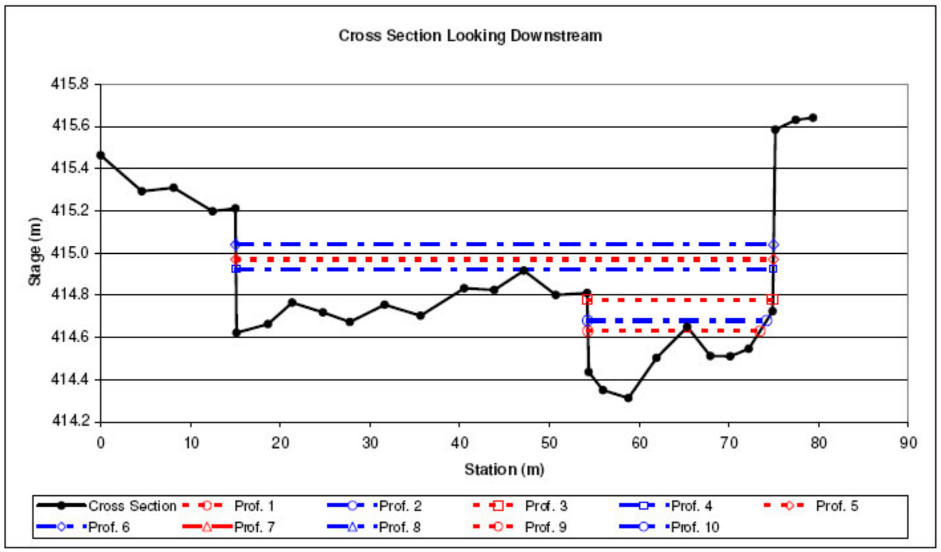

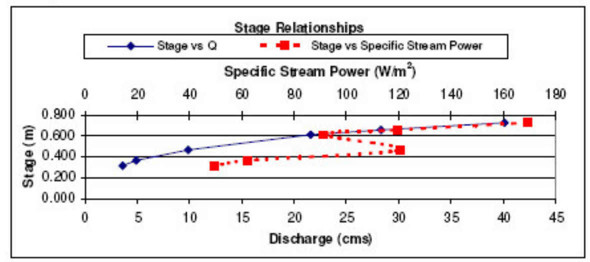

Prof. ID	Estimated n-value	L-Limit	R-Limit	WS (m)	Depth (m)	Left Sta (m)	Right Sta (m)	P_w (m)	Area (m^2)	W (m)	R (m)	D (m)	W/d	V (m/s)	Q (m^3/s)	U* (m/s)	τ (kg/ms²)	τ*	ω (W/m²)	Ω (W/m)	F_r	R/d_{84}	n-value per Limerino	Floodplain Form
HCSA01P01	0.035	47.17		414.63	0.317	54.31	73.48	18.48	2.77	18.34	0.15	0.15	57.9	1.3	3.6	0.19	37.9	1.467	50	908	1.14	12.9	0.024	BF
HCSA01P02	0.040	47.17		414.68	0.367	54.28	74.23	20.13	3.74	19.95	0.19	0.19	54.4	1.3	4.9	0.22	47.0	1.819	62	1238	1.03	16.0	0.024	BF
HCSA01P03	0.040	47.17		414.78	0.467	54.24	74.91	20.96	5.79	20.67	0.28	0.28	44.3	1.7	9.9	0.26	69.9	2.705	121	2496	1.10	23.8	0.023	BF
HCSA01P04	0.045			414.93	0.612	15.08	74.96	60.55	15.19	59.88	0.25	0.25	97.8	1.4	21.6	0.25	63.5	2.457	91	5461	0.97	21.6	0.023	BF
HCSA01P05	0.045			414.97	0.657	15.08	74.98	60.64	17.89	59.90	0.29	0.30	91.2	1.6	28.3	0.27	74.7	2.888	120	7162	0.99	25.4	0.023	BF
HCSA01P06	0.045			415.04	0.727	15.06	75.00	60.78	22.08	59.94	0.36	0.37	82.4	1.8	40.1	0.30	91.9	3.557	169	10157	1.03	31.3	0.023	BF
HCSA01P07	0.045																							BF
HCSA01P08	0.045																							BF
HCSA01P09	0.045																							BF
HCSA01P10	0.045																							BF

Cross Section Hydraulic Analyses: Hasley Canyon Site 2

Floodplain/Site Description: Hasley Canyon downstream of Romero Canyon Rd.

Location ID	HCSA02
d_{50} (mm) =	1.60
d_{84} (mm) =	11.60
So = Sf =	0.0203

Pt#	Sta (m)	Stage (m)
1	0.00	417.72
2	4.14	417.74
3	10.28	417.67
4	15.75	417.48
5	17.34	416.50
6	19.04	416.04
7	24.36	416.10
8	30.50	416.12
9	35.58	416.16
10	40.19	416.10
11	45.07	416.14
12	50.77	416.03
13	54.93	415.83
14	57.21	415.79
15	59.67	415.89
16	64.57	415.79
17	69.21	415.69
18	73.77	415.69
19	76.76	415.83
20	78.51	415.62
21	80.97	415.60
22	82.66	415.61
23	83.50	415.85
24	83.68	416.57
25	87.50	416.46
26		
27		
28		
29		
30		
31		
32		
33		
34		
35		
min. Stage =	415.60	
Continuum	1	
CEM	3	

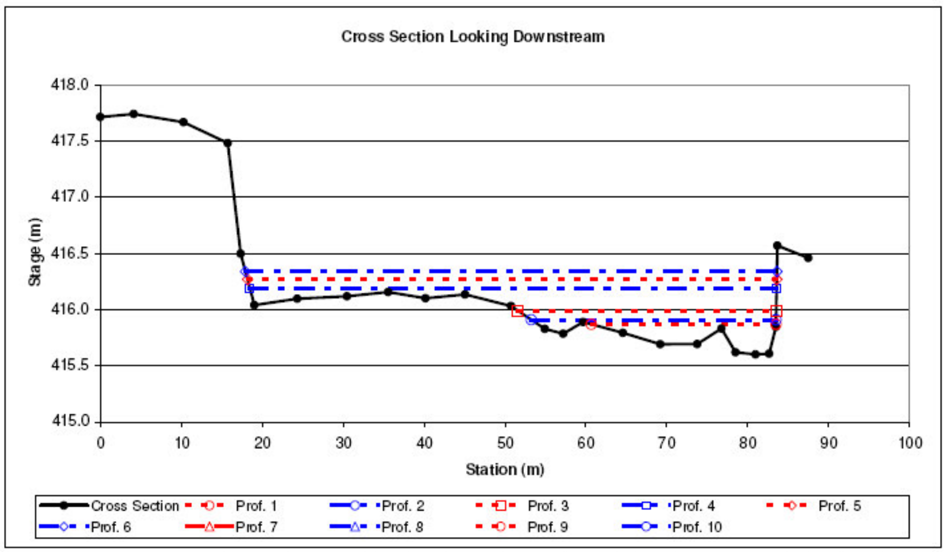

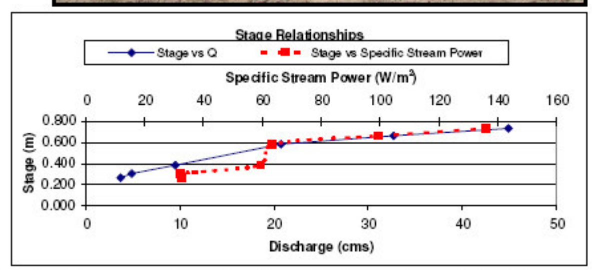

Prof. ID	Estimated n-value	L-Limit	R-Limit	WS (m)	Depth (m)	Left Sta (m)	Right Sta (m)	P_w (m)	Area (m^2)	W (m)	R (m)	D (m)	W/d	V (m/s)	Q (m^3/s)	U* (m/s)	τ (kg/ms²)	τ*	ω (W/m²)	Ω (W/m)	F_r	R/d_{84}	n-value per Limerino	Floodplain Form
HCSA02P01	0.035	59.67		415.87	0.268	60.69	83.51	22.89	3.31	22.82	0.14	0.15	85.1	1.1	3.7	0.17	28.8	1.116	32	741	1.01	12.5	0.024	BF
HCSA02P02	0.040	45.07		415.91	0.308	53.27	83.52	30.35	4.74	30.25	0.16	0.16	98.2	1.0	4.9	0.18	31.1	1.202	32	974	0.89	13.5	0.024	BF
HCSA02P03	0.040	45.07		415.99	0.388	51.63	83.54	32.08	7.22	31.91	0.23	0.23	82.2	1.3	9.5	0.21	44.8	1.734	59	1896	0.95	19.4	0.024	BF
HCSA02P04	0.045			416.19	0.588	18.49	83.59	65.45	16.45	65.10	0.25	0.25	110.7	1.3	20.7	0.22	50.0	1.936	63	4130	0.86	21.7	0.023	BF
HCSA02P05	0.045			416.27	0.668	18.19	83.61	65.84	21.67	65.42	0.33	0.33	97.9	1.5	32.7	0.26	65.5	2.535	100	6512	0.90	28.4	0.023	BF
HCSA02P06	0.045			416.34	0.738	17.93	83.62	66.18	26.26	65.69	0.40	0.40	89.0	1.7	44.9	0.28	79.0	3.056	136	8939	0.93	34.2	0.023	BF
HCSA02P07	0.045																							BF
HCSA02P08	0.045																							BF
HCSA02P09	0.045																							BF
HCSA02P10	0.045																							BF

Cross Section Hydraulic Analyses: Hasley Canyon Site 2

Floodplain/Site Description: Hasley Canyon downstream of Romero Canyon Rd. Photograph looking downstream along right bank (June 07)

Location ID		HCSA03
d_{50} (mm) =		2.60
d_{84} (mm) =		28.90
So = Sf =		0.0203
Pt #	Sta (m)	Stage (m)
1	0.00	419.08
2	3.61	418.91
3	7.69	418.78
4	10.59	418.67
5	12.47	417.93
6	13.32	417.43
7	16.07	417.43
8	20.70	417.31
9	22.96	417.22
10	23.24	417.02
11	25.27	416.99
12	25.45	417.13
13	29.22	417.03
14	33.07	416.95
15	36.15	416.80
16	37.27	416.83
17	37.49	417.00
18	40.03	416.60
19	42.50	416.80
20	44.31	416.68
21	46.72	417.12
22	47.05	418.16
23	51.06	418.21
24	51.88	418.52
25		
26		
27		
28		
29		
30		
31		
32		
33		
34		
35		
min. Stage =		416.60
Continuum		1
CEM		3

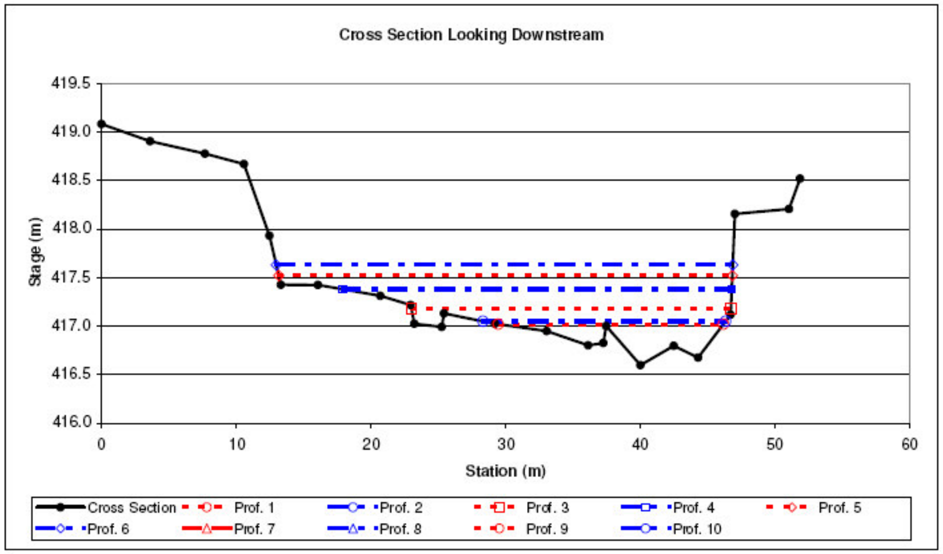

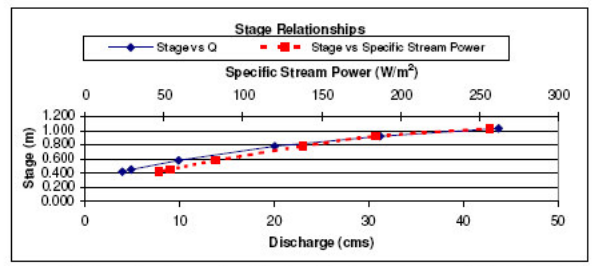

Prof. ID	Estimated n-value	L-Limit	R-Limit	WS (m)	Depth (m)	Left Sta (m)	Right Sta (m)	P_w (m)	Area (m^2)	W (m)	R (m)	D (m)	W/d	V (m/s)	Q (m^3/s)	U* (m/s)	τ (kg/ms²)	τ*	ω (W/m²)	Ω (W/m)	F_r	R/d_{84}	n-value per Limerino	Floodplain Form
HCSA03P01	0.035	25.45		417.02	0.423	29.48	46.19	16.86	3.03	16.72	0.18	0.18	39.5	1.3	3.9	0.19	35.8	0.852	47	782	1.04	6.2	0.031	BF
HCSA03P02	0.035	25.45		417.05	0.453	28.33	46.36	18.17	3.55	18.02	0.20	0.20	39.8	1.4	4.9	0.20	38.9	0.927	54	970	1.06	6.8	0.030	BF
HCSA03P03	0.040			417.18	0.583	23.02	46.74	24.02	6.58	23.73	0.27	0.28	40.7	1.5	9.9	0.23	54.5	1.298	83	1968	0.98	9.5	0.029	BF
HCSA03P04	0.045			417.38	0.783	17.92	46.81	29.35	11.69	28.89	0.40	0.40	36.9	1.7	20.0	0.28	79.4	1.889	138	3993	0.92	13.8	0.028	BF
HCSA03P05	0.045			417.52	0.923	13.17	46.85	34.27	16.22	33.68	0.47	0.48	36.5	1.9	31.2	0.31	94.3	2.244	184	6214	0.95	16.4	0.028	BF
HCSA03P06	0.045			417.63	1.033	12.98	46.88	34.60	19.94	33.90	0.58	0.59	32.8	2.2	43.7	0.34	114.8	2.732	257	8708	0.98	19.9	0.027	BF
HCSA03P07	0.045																							BF
HCSA03P08	0.045																							BF
HCSA03P09	0.045																							BF
HCSA03P10	0.045																							BF

Cross Section Hydraulic Analyses: Hasley Canyon Site 2

Floodplain/Site Description: Hasley Canyon downstream of Romero Canyon Rd.

Location ID	HCSA04
d_{50} (mm) =	2.60
d_{84} (mm) =	28.90
So = Sf =	0.0203

Pt #	Sta (m)	Stage (m)
1	0.00	421.76
2	1.69	421.68
3	1.83	420.93
4	3.21	420.42
5	3.44	420.00
6	7.01	419.79
7	7.79	419.51
8	10.38	419.49
9	11.23	419.74
10	13.68	419.52
11	15.89	419.81
12	16.80	419.94
13	18.78	420.02
14	19.44	419.43
15	20.93	419.31
16	22.40	419.39
17	22.53	419.67
18	24.97	419.79
19	26.72	419.65
20	28.84	419.80
21	30.58	421.14
22	33.04	421.37
23		
24		
25		
26		
27		
28		
29		
30		
31		
32		
33		
34		
35		
min. Stage =		419.31
Continuum		1
CEM		3

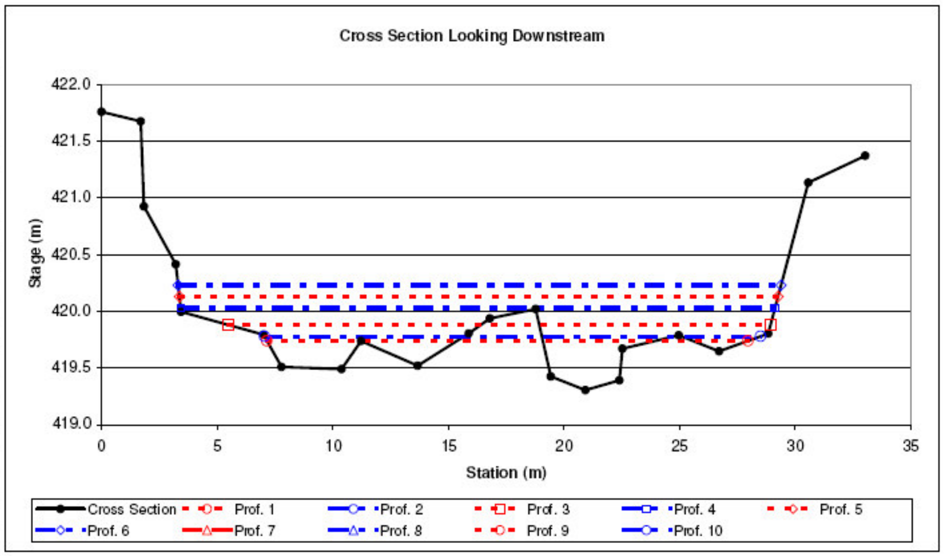

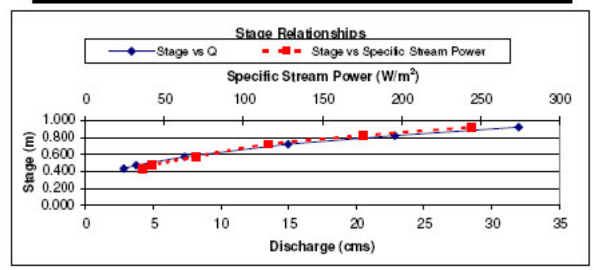

Prof. ID	Estimated n-value	L-Limit	R-Limit	WS (m)	Depth (m)	Left Sta (m)	Right Sta (m)	P_w (m)	Area (m^2)	W (m)	R (m)	D (m)	W/d	V (m/s)	Q (m^3/s)	U* (m/s)	τ (kg/ms²)	τ*	ω (W/m²)	Ω (W/m)	F_r	R/d_{84}	n-value per Limerino	Floodplain Form
HCSA04P01	0.040			419.74	0.435	7.15	27.97	15.92	2.64	15.51	0.17	0.17	35.6	1.1	2.8	0.18	33.0	0.785	36	564	0.89	5.7	0.031	BF
HCSA04P02	0.040			419.78	0.475	7.04	28.51	18.29	3.30	17.85	0.18	0.19	37.6	1.1	3.8	0.19	36.0	0.856	42	749	0.91	6.3	0.031	BF
HCSA04P03	0.040			419.88	0.575	5.49	28.94	21.44	5.26	20.92	0.25	0.25	36.4	1.4	7.3	0.22	48.8	1.163	70	1461	0.95	8.5	0.030	BF
HCSA04P04	0.040			420.03	0.725	3.42	29.13	26.36	8.76	25.71	0.33	0.34	35.5	1.7	15.0	0.26	66.2	1.575	116	2981	1.00	11.5	0.029	BF
HCSA04P05	0.040			420.13	0.825	3.37	29.26	26.64	11.34	25.90	0.43	0.44	31.4	2.0	22.9	0.29	84.8	2.018	176	4552	1.04	14.7	0.028	BF
HCSA04P06	0.040			420.23	0.925	3.31	29.40	26.92	13.94	26.08	0.52	0.53	28.2	2.3	32.0	0.32	103.1	2.454	244	6375	1.08	17.9	0.028	BF
HCSA04P07	0.040																							BF
HCSA04P08	0.040																							BF
HCSA04P09	0.040																							BF
HCSA04P10	0.040																							BF

Cross Section Hydraulic Analyses: Hasley Canyon Site 2

Floodplain/Site Description: Hasley Canyon downstream of Romero Canyon Rd.

Location ID	HCSA05
d_{50} (mm) =	2.60
d_{84} (mm) =	28.90
So = Sf =	0.0203

Pt #	Sta (m)	Stage (m)
1	0.00	424.16
2	1.79	424.01
3	2.41	422.56
4	5.26	421.40
5	7.83	421.39
6	9.46	421.47
7	9.85	420.91
8	12.71	420.81
9	13.77	421.04
10	16.03	421.09
11	18.34	420.94
12	21.27	420.77
13	22.23	420.82
14	22.53	421.04
15	23.41	421.20
16	25.37	423.05
17	26.55	423.23
18		
19		
20		
21		
22		
23		
24		
25		
26		
27		
28		
29		
30		
31		
32		
33		
34		
35		
min. Stage =		420.77
Continuum		1
CEM		3

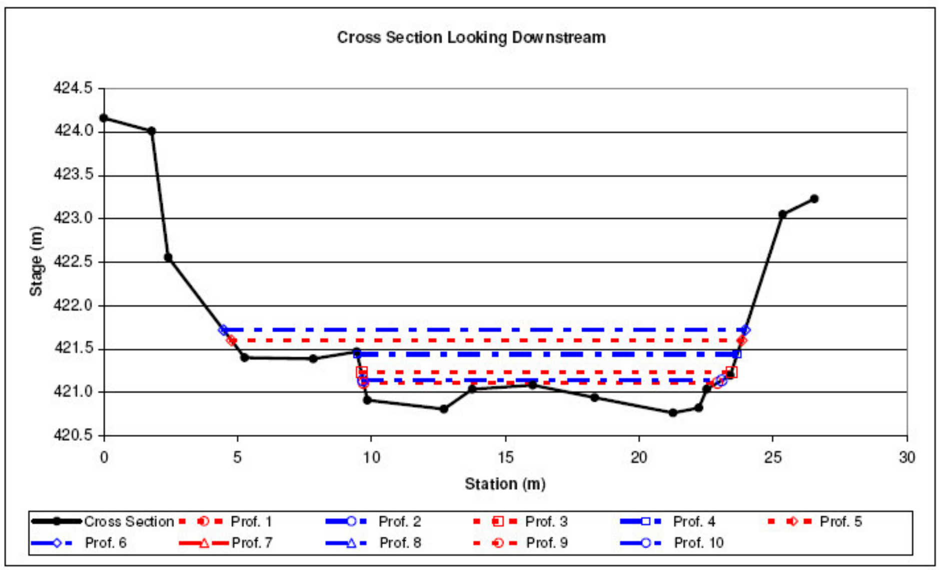

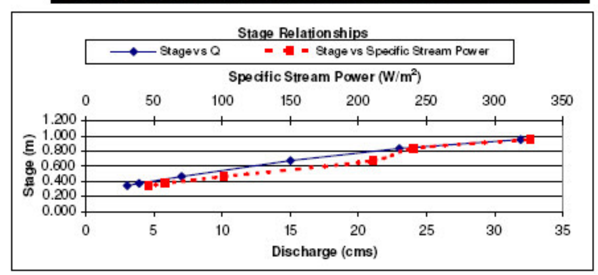

Prof. ID	Estimated n-value	L-Limit	R-Limit	WS (m)	Depth (m)	Left Sta (m)	Right Sta (m)	P_w (m)	Area (m^2)	W (m)	R (m)	D (m)	W/d	V (m/s)	Q (m^3/s)	U* (m/s)	τ (kg/ms^2)	τ*	ω (W/m^2)	Ω (W/m)	F_r	R/d_{84}	n-value per Limerino	Floodplain Form
HCSA05P01	0.035	9.46		421.11	0.344	9.71	22.93	13.44	2.38	13.22	0.18	0.18	38.4	1.3	3.0	0.19	35.2	0.838	46	606	1.04	6.1	0.031	PMB
HCSA05P02	0.035	9.46		421.14	0.374	9.69	23.09	13.64	2.77	13.41	0.20	0.21	35.8	1.4	3.9	0.20	40.5	0.964	58	778	1.06	7.0	0.030	PMB
HCSA05P03	0.035	9.46		421.23	0.464	9.62	23.44	14.12	4.00	13.82	0.28	0.29	29.8	1.8	7.0	0.24	56.5	1.344	101	1401	1.12	9.8	0.029	PMB
HCSA05P04	0.040	9.46		421.44	0.674	9.48	23.67	14.68	6.94	14.19	0.47	0.49	21.1	2.2	15.0	0.31	94.2	2.242	211	2990	1.06	16.4	0.028	PMB
HCSA05P05	0.040			421.60	0.834	4.77	23.83	19.68	10.08	19.06	0.51	0.53	22.9	2.3	23.0	0.32	102.1	2.429	240	4580	1.07	17.7	0.028	PMB
HCSA05P06	0.040			421.72	0.954	4.48	23.96	20.17	12.40	19.48	0.61	0.64	20.4	2.6	31.9	0.35	122.4	2.913	326	6356	1.11	21.3	0.027	PMB
HCSA05P07	0.040																							PMB
HCSA05P08	0.040																							PMB
HCSA05P09	0.040																							PMB
HCSA05P10	0.040																							PMB

Cross Section Hydraulic Analyses: Hasley Canyon Site 2

Floodplain/Site Description: Hasley Canyon downstream of Romero Canyon Rd.

Location ID	HCSA1T	
d_{50} (mm) =	1.50	
d_{84} (mm) =	40.00	
So = Sf =	0.0295	
Pt#	Sta (m)	Stage (m)
1	0.00	420.30
2	3.17	419.93
3	4.85	419.78
4	7.71	419.78
5	7.94	419.06
6	8.33	418.90
7	11.00	418.74
8	15.26	418.87
9	20.17	418.96
10	24.69	418.96
11	27.41	419.06
12	30.68	418.89
13	34.56	418.98
14	37.35	419.11
15	39.39	419.17
16	39.55	419.52
17	42.49	419.86
18	43.69	419.83
19	45.67	419.93
20	49.48	419.98
21	53.45	419.90
22	53.85	419.27
23	57.30	419.15
24	60.55	419.42
25	63.46	419.45
26	66.99	419.38
27	68.01	419.51
28	70.95	419.63
29	72.18	419.41
30	73.79	419.58
31	75.40	419.35
32	78.84	419.41
33	78.95	420.64
34	82.19	420.73
35	85.79	420.81
min. Stage =	418.74	
Continuum	1	
CEM	3	

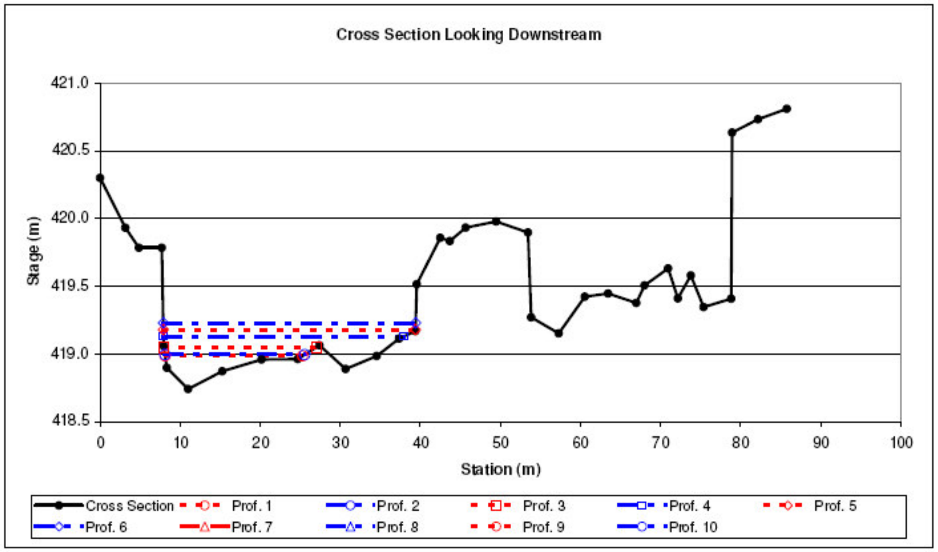

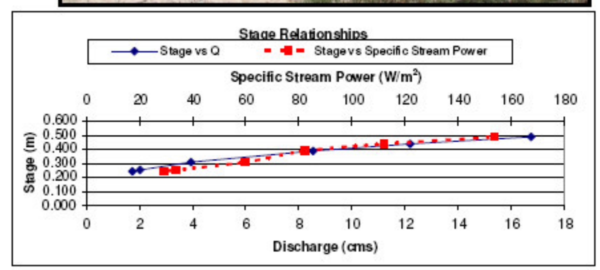

Prof. ID	Estimated n-value	L-Limit	R-Limit	WS (m)	Depth (m)	Left Sta (m)	Right Sta (m)	P_w (m)	Area (m^2)	W (m)	R (m)	D (m)	W/d	V (m/s)	Q (m^3/s)	U* (m/s)	τ (kg/ms^2)	τ^*	ω (W/m^2)	Ω (W/m)	F_r	R/d_{84}	n-value per Limerinos	Floodplain Form
HCSA1TP01	0.035		27.41	418.99	0.245	8.12	25.30	17.20	1.68	17.18	0.10	0.10	70.1	1.0	1.7	0.17	28.2	1.163	29	503	1.14	2.4	0.040	BF
HCSA1TP02	0.035		27.41	419.00	0.255	8.10	25.57	17.49	1.85	17.47	0.11	0.11	68.5	1.1	2.0	0.17	30.6	1.261	34	587	1.15	2.6	0.039	BF
HCSA1TP03	0.035		27.41	419.05	0.310	7.97	27.03	19.10	2.85	19.07	0.15	0.15	61.5	1.4	3.9	0.21	43.2	1.783	60	1140	1.22	3.7	0.036	BF
HCSA1TP04	0.040		39.55	419.13	0.390	7.92	37.97	30.15	5.90	30.05	0.20	0.20	77.0	1.4	8.5	0.24	56.6	2.336	82	2470	1.12	4.9	0.034	BF
HCSA1TP05	0.040		39.55	419.18	0.440	7.91	39.39	31.63	7.44	31.49	0.24	0.24	71.6	1.6	12.2	0.26	68.1	2.810	112	3526	1.15	5.9	0.033	BF
HCSA1TP06	0.040		39.55	419.23	0.490	7.89	39.42	31.74	9.02	31.53	0.28	0.29	64.3	1.9	16.7	0.29	82.2	3.393	154	4844	1.19	7.1	0.032	BF
HCSA1TP07	0.040																							BF
HCSA1TP08	0.040																							BF
HCSA1TP09	0.040																							BF
HCSA1TP10	0.040																							BF

Cross Section Hydraulic Analyses: Hasley Canyon Site 2

Floodplain/Site Description: Hasley Canyon downstream of Romero Canyon Rd. Photograph looking upstream at Romero Canyon.

Pt #	Sta (m)	Stage (m)
Location ID		HCSA2T
d_{50} (mm) =		1.50
d_{84} (mm) =		40.00
So = Sf =		0.0295
1	7.55	420.87
2	10.00	420.60
3	11.55	420.79
4	13.81	420.72
5	13.97	420.40
6	17.53	420.22
7	21.53	420.19
8	24.47	420.28
9	27.65	420.24
10	31.32	420.23
11	33.74	420.20
12	35.42	420.24
13	35.84	420.82
14	38.48	421.22
15	41.42	421.39
16	43.34	421.44
17		
18		
19		
20		
21		
22		
23		
24		
25		
26		
27		
28		
29		
30		
31		
32		
33		
34		
35		
min. Stage =		420.19
Continuum		1
CEM		3

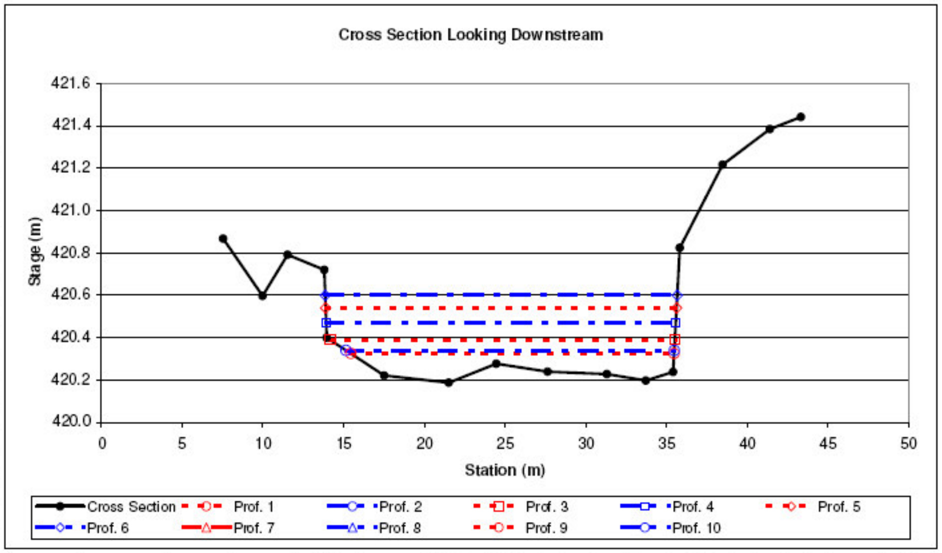

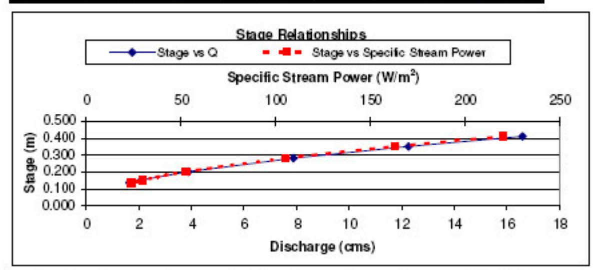

Prof. ID	Estimated n-value	L-Limit	R-Limit	WS (m)	Depth (m)	Left Sta (m)	Right Sta (m)	P_w (m)	Area (m^2)	W (m)	R (m)	D (m)	W/d	V (m/s)	Q (m^3/s)	U* (m/s)	τ (kg/ms²)	τ^*	ω (W/m²)	Ω (W/m)	F_r	R/d_{84}	n-value per Limerino	Floodplain Form
HCSA2TP01	0.040	11.55		420.33	0.138	15.46	35.48	20.07	1.87	20.02	0.09	0.09	145.1	0.9	1.6	0.16	27.0	1.112	24	477	0.99	2.3	0.040	BF
HCSA2TP02	0.040	11.55		420.34	0.153	15.16	35.49	20.39	2.17	20.33	0.11	0.11	132.9	1.0	2.1	0.18	30.8	1.272	30	607	1.01	2.7	0.039	BF
HCSA2TP03	0.040	11.55		420.39	0.203	14.16	35.53	21.45	3.21	21.36	0.15	0.15	105.2	1.2	3.9	0.21	43.4	1.790	53	1127	1.07	3.7	0.036	BF
HCSA2TP04	0.040	11.55		420.47	0.283	13.93	35.58	21.82	4.94	21.65	0.23	0.23	76.5	1.6	7.9	0.26	65.5	2.704	105	2282	1.14	5.7	0.033	BF
HCSA2TP05	0.040	11.55		420.54	0.353	13.90	35.63	21.99	6.46	21.74	0.29	0.30	61.6	1.9	12.3	0.29	85.0	3.509	163	3549	1.19	7.3	0.032	BF
HCSA2TP06	0.040	11.55		420.60	0.413	13.87	35.68	22.13	7.77	21.81	0.35	0.36	52.8	2.1	16.6	0.32	101.6	4.192	220	4803	1.23	8.8	0.031	BF
HCSA2TP07	0.040																							BF
HCSA2TP08	0.040																							BF
HCSA2TP09	0.040																							BF
HCSA2TP10	0.040																							BF

Cross Section Hydraulic Analyses: Hasley Canyon Site C

Floodplain/Site Description: Hasley Canyon Site C located approximately 2.4 kilometers upstream of Hasley Canyon Site A and Romero Canyon Road. Cross Section estimated based on tape measurements and photographs. Photograph view is looking downstream.

Location ID	HCSC01	
d_{50} (mm) =	4.70	
d_{84} (mm) =	12.90	
So = Sf =	0.0315	
Pt #	Sta (m)	Stage (m)
1	0.00	2.00
2	2.00	1.00
3	7.50	1.00
4	7.50	0.69
5	9.80	0.69
6	9.80	1.04
7	12.50	1.04
8	14.50	2.04
9		
10		
11		
12		
13		
14		
15		
16		
17		
18		
19		
20		
21		
22		
23		
24		
25		
26		
27		
28		
29		
30		
31		
32		
33		
34		
35		
min. Stage =	0.69	
Continuum	1	
CEM	1	

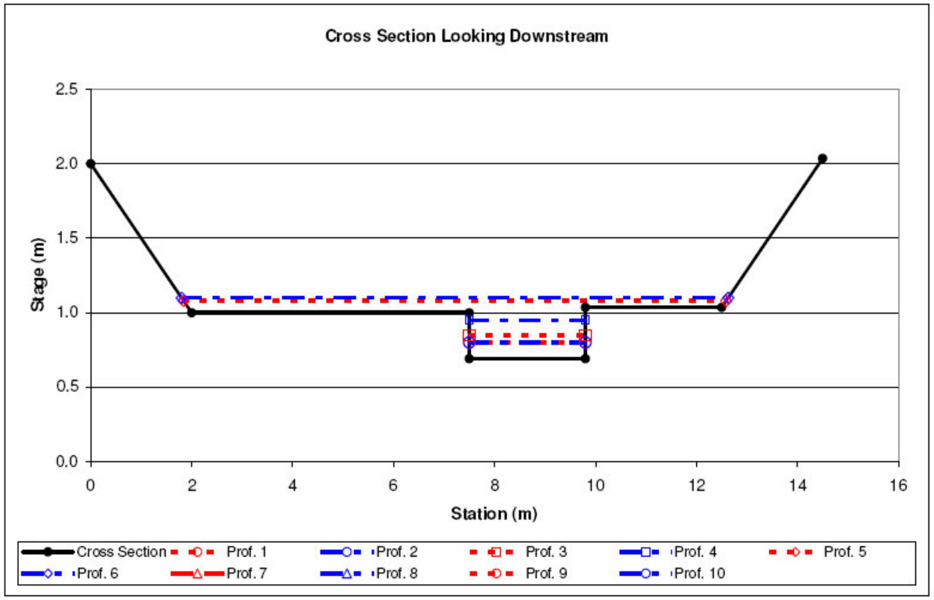

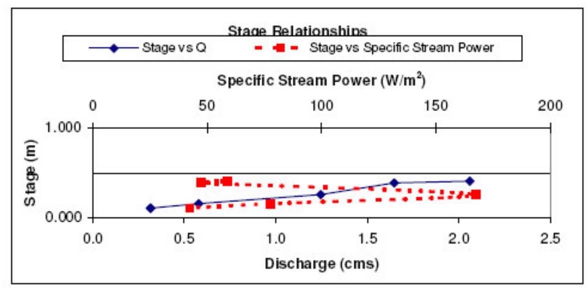

Prof. ID	Estimated n-value	L-Limit	R-Limit	WS (m)	Depth (m)	Left Sta (m)	Right Sta (m)	P_w (m)	Area (m^2)	W (m)	R (m)	D (m)	W/d	V (m/s)	Q (m^3/s)	U* (m/s)	τ (kg/ms²)	τ*	ω (W/m²)	Ω (W/m)	F_r	R/d_{84}	n-value per Limerino	Floodplain Form
HCSC01P01	0.030			0.80	0.108	7.50	9.80	2.52	0.25	2.30	0.10	0.11	21.2	1.3	0.3	0.17	30.6	0.403	42	97	1.32	7.7	0.026	PMB
HCSC01P02	0.030			0.80	0.108	7.50	9.80	2.52	0.25	2.30	0.10	0.11	21.2	1.3	0.3	0.17	30.6	0.403	42	97	1.32	7.7	0.026	PMB
HCSC01P03	0.030			0.85	0.158	7.50	9.80	2.62	0.36	2.30	0.14	0.16	14.5	1.6	0.6	0.21	43.0	0.566	78	179	1.37	10.8	0.025	PMB
HCSC01P04	0.030			0.95	0.258	7.50	9.80	2.82	0.59	2.30	0.21	0.26	8.9	2.1	1.2	0.26	65.2	0.858	167	385	1.41	16.3	0.024	PMB
HCSC01P05	0.040			1.08	0.388	1.84	12.59	11.43	1.46	10.75	0.13	0.14	27.7	1.1	1.6	0.20	39.5	0.520	47	508	1.05	9.9	0.025	PMB
HCSC01P06	0.040			1.10	0.408	1.80	12.63	11.52	1.68	10.83	0.15	0.15	26.5	1.2	2.1	0.21	45.0	0.592	59	636	1.07	11.3	0.025	PMB
HCSC01P07	0.045																							PMB
HCSC01P08	0.045																							PMB
HCSC01P09	0.045																							PMB
HCSC01P10	0.045																							PMB

Cross Section Hydraulic Analyses: Romero Canyon

Floodplain/Site Description: Romero Canyon located approximately 3.5 kilometers upstream of Hasley Canyon Site A (HCSA00). Photograph view is looking upstream. Suspect channel encroached by road.

Location ID	RCSA01	
d_{50} (mm) =		19.60
d_{84} (mm) =		127.20
So = Sf =		0.0587
Pt #	Sta (m)	Stage (m)
1	0.00	2.00
2	1.50	0.90
3	2.35	0.72
4	2.50	0.35
5	2.95	0.20
6	3.40	0.20
7	3.95	0.31
8	4.50	0.63
9	6.50	0.86
10	8.50	0.98
11	10.90	1.03
12	13.40	3.03
13		
14		
15		
16		
17		
18		
19		
20		
21		
22		
23		
24		
25		
26		
27		
28		
29		
30		
31		
32		
33		
34		
35		
min. Stage =		0.20
Continuum		1
CEM		3

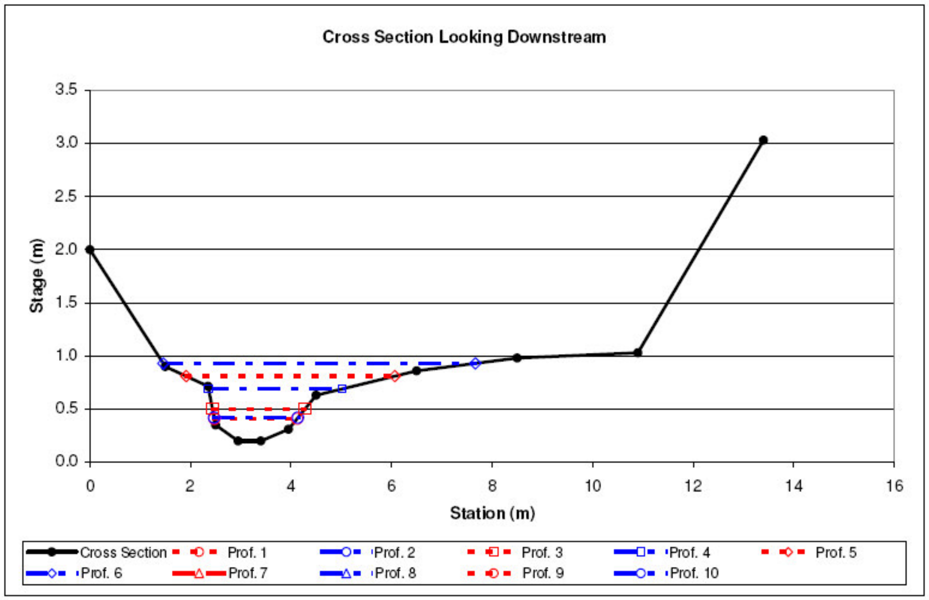

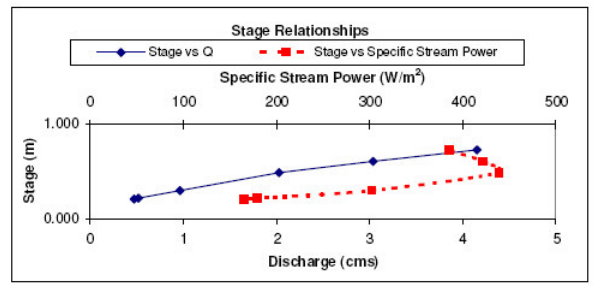

Prof. ID	Estimated n-value	L-Limit	R-Limit	WS (m)	Depth (m)	Left Sta (m)	Right Sta (m)	P_w (m)	Area (m^2)	W (m)	R (m)	D (m)	W/d	V (m/s)	Q (m^3/s)	U* (m/s)	τ (kg/ms^2)	τ^*	ω (W/m^2)	Ω (W/m)	F_r	R/d_{84}	n-value per Limerino	Floodplain Form
RCSA01P01	0.035			0.41	0.210	2.48	4.12	1.75	0.25	1.65	0.14	0.15	7.8	1.9	0.47	0.29	82.3	0.260	165	272	1.66	1.1	0.063	PMB
RCSA01P02	0.035			0.42	0.220	2.47	4.14	1.78	0.27	1.67	0.15	0.16	7.6	2.0	0.52	0.29	86.2	0.272	180	299	1.67	1.2	0.061	PMB
RCSA01P03	0.035			0.50	0.300	2.44	4.28	2.03	0.41	1.84	0.20	0.22	6.1	2.4	1.0	0.34	115.6	0.365	302	556	1.73	1.6	0.053	PMB
RCSA01P04	0.040			0.69	0.490	2.36	5.02	3.01	0.81	2.66	0.27	0.30	5.4	2.5	2.0	0.39	154.1	0.487	439	1169	1.56	2.1	0.048	PMB
RCSA01P05	0.040			0.81	0.610	1.91	6.07	4.54	1.21	4.15	0.27	0.29	6.8	2.5	3.0	0.39	153.6	0.485	422	1750	1.59	2.1	0.049	PMB
RCSA01P06	0.045			0.93	0.730	1.46	7.67	6.62	1.82	6.21	0.28	0.29	8.5	2.3	4.2	0.40	158.6	0.501	385	2392	1.44	2.2	0.049	PMB
RCSA01P07	0.040																							PMB
RCSA01P08	0.040																							PMB
RCSA01P09	0.040																							PMB
RCSA01P10	0.040																							PMB

Cross Section Hydraulic Analyses: Hicks Canyon Screening Reach

Floodplain/Site Description: Hicks Canyon approximately 25 meters (ie Sta 25) upstream of at-grade road crossing. (Q100 = ~13 cms)
Photograph view is looking downstream at the main channel of the downstream most cross section in the screening site reach.

Location ID	HCSR01	
d_{50} (mm) =	0.59	
d_{84} (mm) =	1.35	
So = Sf =	0.0132	
Pt #	Sta (m)	Stage (m)
1	0.00	101.60
2	1.00	101.44
3	3.40	101.24
4	4.00	101.13
5	5.00	100.71
6	6.20	100.53
7	6.23	100.40
8	6.50	100.33
9	8.30	100.34
10	9.10	100.38
11	9.55	100.55
12	10.65	100.75
13	11.55	101.02
14	12.60	101.40
15		
16		
17		
18		
19		
20		
21		
22		
23		
24		
25		
26		
27		
28		
29		
30		
31		
32		
33		
34		
35		
min. Stage =	100.33	
Continuum	1	
CEM	1.1	

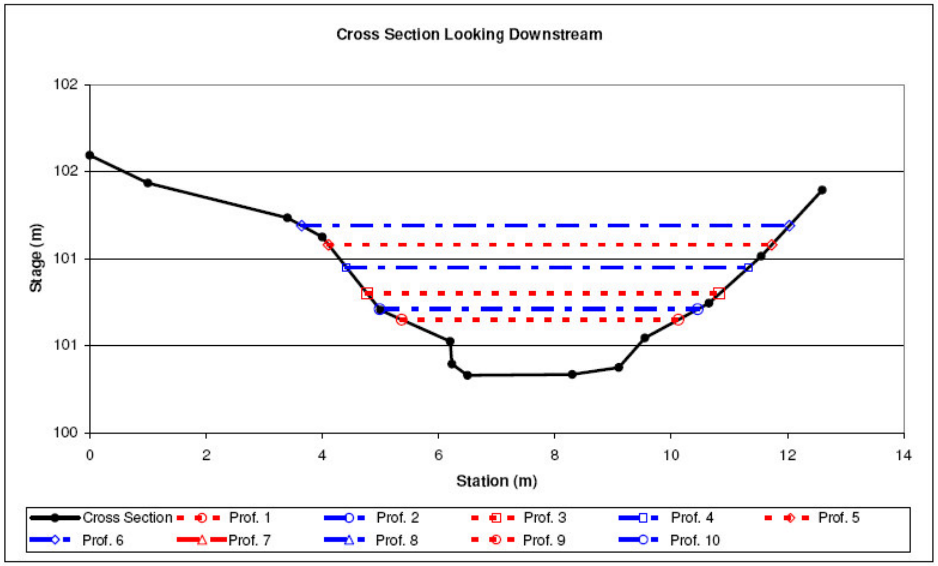

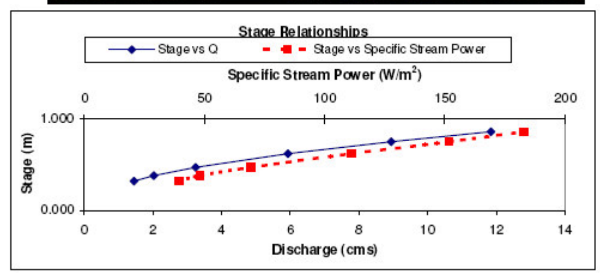

Prof. ID	Estimated n-value	L-Limit	R-Limit	WS (m)	Depth (m)	Left Sta (m)	Right Sta (m)	P_w (m)	Area (m^2)	W (m)	R (m)	D (m)	W/d	V (m/s)	Q (m^3/s)	U* (m/s)	τ (kg/ms²)	τ*	ω (W/m²)	Ω (W/m)	F_r	R/d_{84}	n-value per Limerino	Floodplain Form
HCSR01P01	0.030			100.65	0.320	5.37	10.13	4.92	1.06	4.76	0.22	0.22	14.9	1.4	1.5	0.17	27.8	2.921	40	188	1.00	159.3	0.016	PFB
HCSR01P02	0.030			100.71	0.380	4.99	10.46	5.64	1.37	5.47	0.24	0.25	14.4	1.5	2.0	0.18	31.4	3.289	48	263	1.02	179.4	0.016	PFB
HCSR01P03	0.030			100.80	0.470	4.77	10.83	6.26	1.89	6.06	0.30	0.31	12.9	1.7	3.2	0.20	39.0	4.094	69	421	1.06	223.3	0.016	PFB
HCSR01P04	0.030			100.95	0.620	4.42	11.33	7.17	2.86	6.92	0.40	0.41	11.2	2.1	5.9	0.23	51.7	5.419	111	769	1.10	295.5	0.016	PFB
HCSR01P05	0.030			101.08	0.750	4.11	11.73	7.92	3.81	7.62	0.48	0.50	10.2	2.3	8.9	0.25	62.2	6.526	152	1158	1.14	355.9	0.016	PFB
HCSR01P06	0.030			101.19	0.860	3.65	12.03	8.72	4.68	8.39	0.54	0.56	9.8	2.5	11.8	0.26	69.5	7.292	183	1534	1.16	397.6	0.016	PFB
HCSR01P07	0.030																							PFB
HCSR01P08	0.030																							PFB
HCSR01P09	0.030																							PFB
HCSR01P10	0.030																							PFB

Cross Section Hydraulic Analyses: Hicks Canyon Screening Reach

Floodplain/Site Description: Hicks Canyon approximately 150 m upstream of the road crossing (ie Sta 150) at upstream limit of single-thread channel. Photograph view is looking downstream at the main channel.

Location ID		HCSR02
d_{50} (mm) =		0.59
d_{84} (mm) =		1.35
So = Sf =		0.0141
Pt #	Sta (m)	Stage (m)
1	0.40	103.79
2	0.50	103.78
3	0.90	103.76
4	1.60	103.60
5	2.00	103.52
6	2.60	103.25
7	3.30	102.80
8	4.10	102.67
9	4.70	102.66
10	5.00	102.48
11	5.10	102.39
12	5.40	102.32
13	5.60	102.13
14	6.10	102.08
15	6.50	102.12
16	6.70	102.13
17	6.90	102.04
18	7.50	102.06
19	8.00	102.10
20	8.10	102.36
21	8.30	102.37
22	8.40	102.53
23	8.80	102.73
24	9.50	102.98
25	10.10	103.20
26	10.60	103.31
27	10.90	103.44
28	11.40	103.60
29		
30		
31		
32		
33		
34		
35		
min. Stage =		102.04
Continuum		1
CEM		3

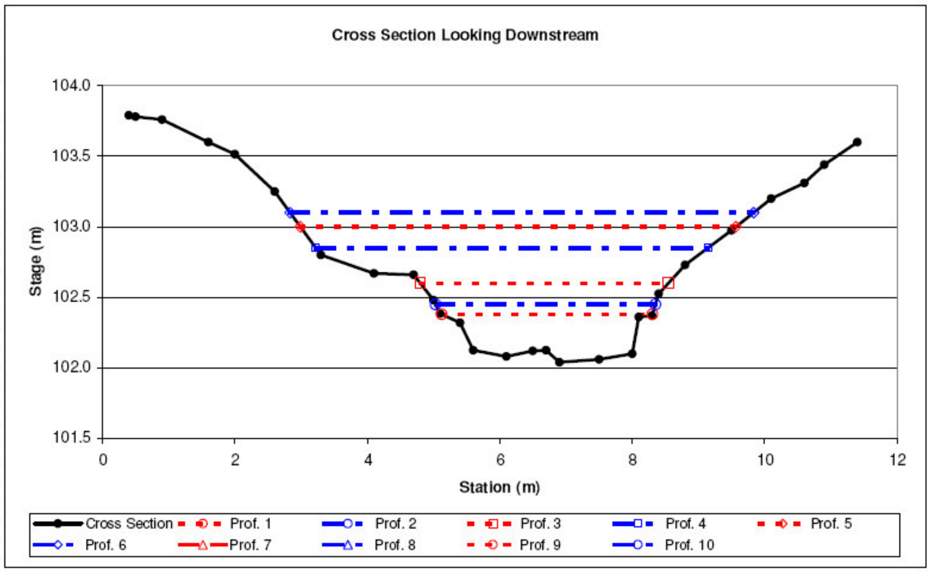

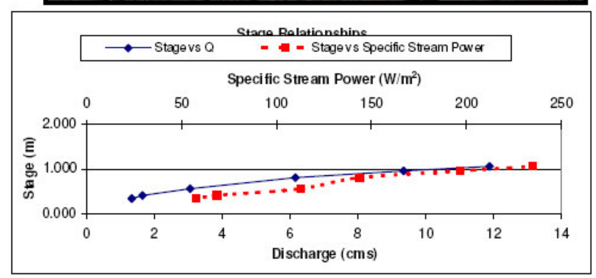

Prof. ID	Estimated n-value	L-Limit	R-Limit	WS (m)	Depth (m)	Left Sta (m)	Right Sta (m)	P_w (m)	Area (m^2)	W (m)	R (m)	D (m)	W/d	V (m/s)	Q (m^3/s)	U* (m/s)	τ (kg/ms²)	τ*	ω (W/m²)	Ω (W/m)	F_r	R/d_{84}	n-value per Limerino	Floodplain Form
HCSR02P01	0.025			102.38	0.340	5.12	8.31	3.48	0.77	3.18	0.22	0.24	9.4	1.7	1.3	0.17	30.5	3.20	58	184	1.21	163.5	0.016	PMB
HCSR02P02	0.030			102.45	0.410	5.03	8.35	3.68	1.00	3.32	0.27	0.30	8.1	1.7	1.6	0.19	37.4	3.93	69	228	1.04	200.5	0.016	PMB
HCSR02P03	0.030			102.60	0.560	4.80	8.55	4.21	1.52	3.75	0.36	0.41	6.7	2.0	3.1	0.22	50.0	5.24	113	423	1.08	267.7	0.016	PMB
HCSR02P04	0.030			102.85	0.810	3.22	9.14	6.48	2.75	5.92	0.42	0.46	7.3	2.2	6.2	0.24	58.8	6.17	144	852	1.12	314.8	0.016	PMB
HCSR02P05	0.030			103.00	0.960	2.99	9.57	7.20	3.69	6.58	0.51	0.56	6.9	2.5	9.3	0.27	70.9	7.43	197	1293	1.16	379.4	0.016	PMB
HCSR02P06	0.030			103.10	1.060	2.83	9.83	7.67	4.37	7.00	0.57	0.62	6.6	2.7	11.9	0.28	78.8	8.26	235	1643	1.18	421.7	0.016	PMB
HCSR02P07	0.030																							PMB
HCSR02P08	0.030																							PMB
HCSR02P09	0.030																							PMB
HCSR02P10	0.030																							PMB

Cross Section Hydraulic Analyses: Hicks Canyon Screening Reach

Floodplain/Site Description: Hicks Canyon approximately 175 m upstream of the road crossing (ie Sta 175), within the braided section of Screening Reach. Photograph view is looking downstream along the main channel. (Q100 ~ 13 cms)

Location ID		HCSR03
d_{50} (mm) =		1.60
d_{84} (mm) =		26.30
So = Sf =		0.0216
Pt #	Sta (m)	Stage (m)
1	2.10	103.73
2	2.80	103.36
3	3.20	103.23
4	4.40	103.18
5	4.80	102.88
6	5.00	102.85
7	5.10	102.69
8	5.30	102.64
9	5.40	102.55
10	5.60	102.55
11	5.80	102.59
12	6.40	102.58
13	6.60	102.60
14	6.90	102.69
15	7.20	102.72
16	7.50	102.66
17	7.80	102.68
18	7.90	102.77
19	8.20	102.83
20	8.40	102.97
21	9.00	102.97
22	9.50	102.91
23	10.20	103.13
24	10.80	103.21
25	12.60	103.21
26	13.10	103.09
27	13.10	103.09
28	13.50	103.12
29	14.60	103.13
30	14.90	103.04
31	17.00	103.05
32	18.80	103.15
33	19.30	103.27
34	20.00	103.29
35	22.00	103.66
min. Stage =		102.55
Continuum		1
CEM		3

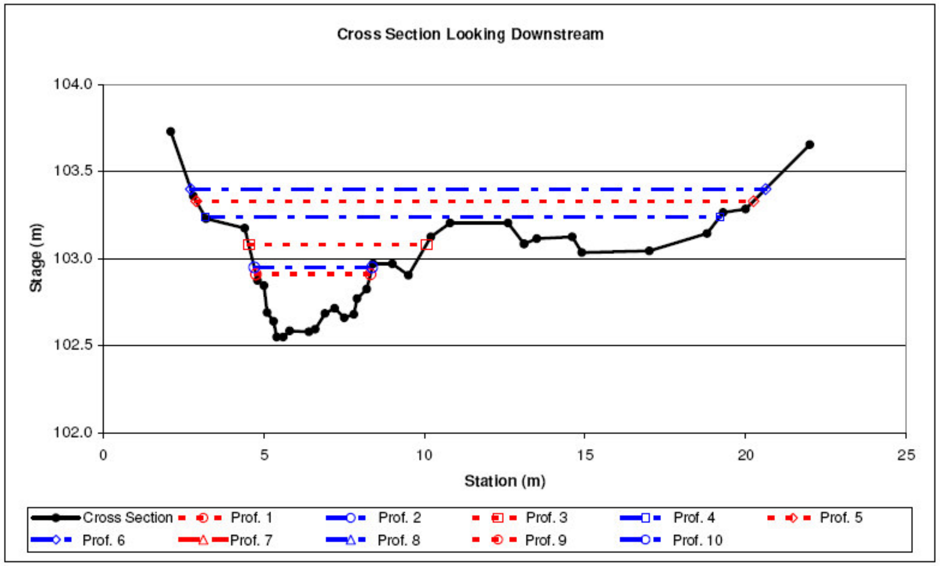

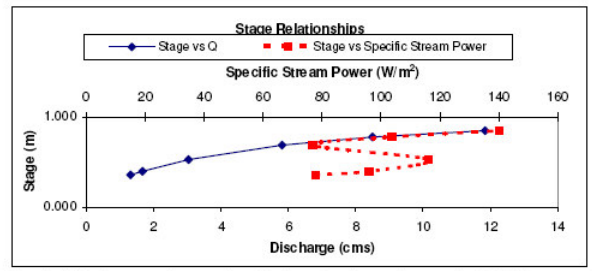

Prof. ID	Estimated n-value	L-Limit	R-Limit	WS (m)	Depth (m)	Left Sta (m)	Right Sta (m)	P_w (m)	Area (m^2)	W (m)	R (m)	D (m)	W/d	V (m/s)	Q (m^3/s)	U* (m/s)	τ (kg/ms²)	τ*	ω (W/m²)	Ω (W/m)	F_r	R/d_{84}	n-value per Limerino	Floodplain Form
HCSR03P01	0.035		8.40	102.91	0.360	4.75	8.32	3.79	0.85	3.56	0.22	0.24	9.9	1.5	1.3	0.22	47.3	1.830	78	277	1.09	8.5	0.029	PMB
HCSR03P02	0.035		8.40	102.95	0.400	4.70	8.37	3.93	0.99	3.67	0.25	0.27	9.2	1.7	1.7	0.23	53.5	2.069	96	352	1.11	9.6	0.029	PMB
HCSR03P03	0.035		10.20	103.08	0.530	4.53	10.06	5.87	1.67	5.53	0.28	0.30	10.4	1.8	3.0	0.25	60.3	2.333	116	643	1.13	10.8	0.028	PMB
HCSR03P04	0.035			103.24	0.690	3.17	19.20	16.45	3.72	16.03	0.23	0.23	23.2	1.6	5.8	0.22	48.0	1.856	77	1231	1.11	8.6	0.029	PMB
HCSR03P05	0.040			103.33	0.780	2.89	20.24	17.80	5.23	17.35	0.29	0.30	22.2	1.6	8.5	0.25	62.3	2.409	104	1801	1.01	11.2	0.028	PMB
HCSR03P06	0.040			103.40	0.850	2.72	20.62	18.37	6.47	17.90	0.35	0.36	21.1	1.8	11.8	0.27	74.6	2.886	140	2510	1.04	13.4	0.028	PMB
HCSR03P07	0.040																							PMB
HCSR03P08	0.040																							PMB
HCSR03P09	0.040																							PMB
HCSR03P10	0.040																							PMB

Cross Section Hydraulic Analyses: Upstream Screening Reach

Floodplain/Site Description: Hicks Canyon at ~ 283 m upstream of the road crossing (ie Sta 283 and HCMR02). (Q100` 12 cms)
Photograph view is looking upstream at the main channel. Note: Jan 08 gradation data for sta 290 applied.

Location ID	HCSR04
d_{50} (mm) =	1.40
d_{84} (mm) =	66.30
So = Sf =	0.0241

Pt #	Sta (m)	Stage (m)
1	0.00	106.06
2	1.00	105.93
3	1.70	105.79
4	2.50	105.77
5	3.00	105.70
6	3.90	105.72
7	4.30	105.57
8	4.70	105.32
9	4.90	104.86
10	5.20	104.80
11	5.30	104.75
12	5.50	104.75
13	5.80	104.72
14	6.10	104.72
15	6.40	104.67
16	6.60	104.70
17	7.00	104.70
18	7.20	105.02
19	7.50	105.23
20	7.70	105.27
21	7.80	105.35
22	9.50	105.49
23	10.20	105.65
24	11.00	105.67
25	13.40	105.88
26	14.50	106.06
27	15.40	106.21
28	16.60	106.42
29	17.60	106.72
30		
31		
32		
33		
34		
35		
min. Stage =		104.67
Continuum		1
CEM		3

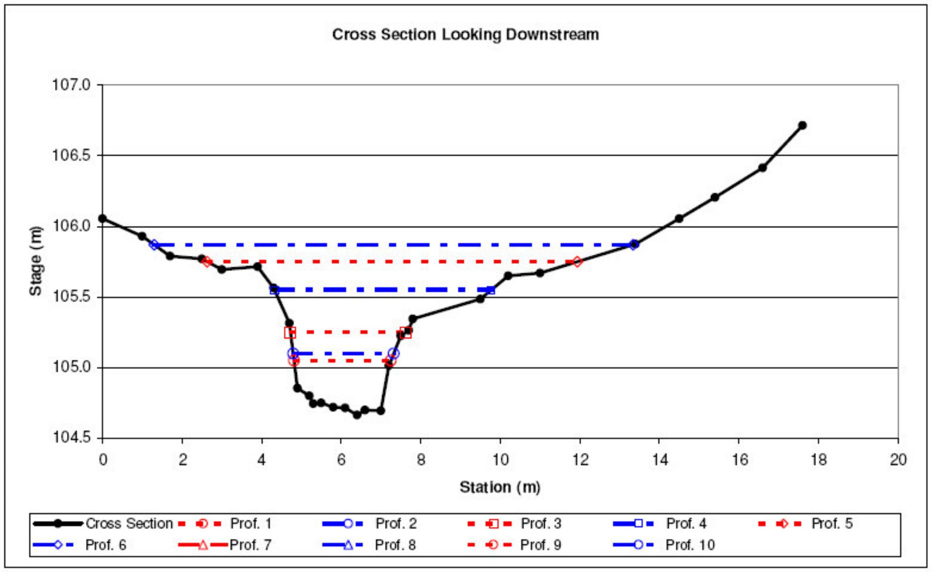

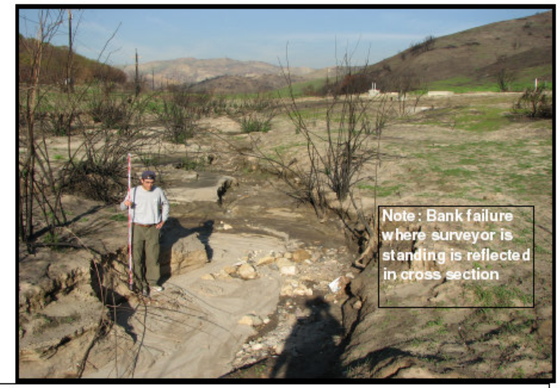

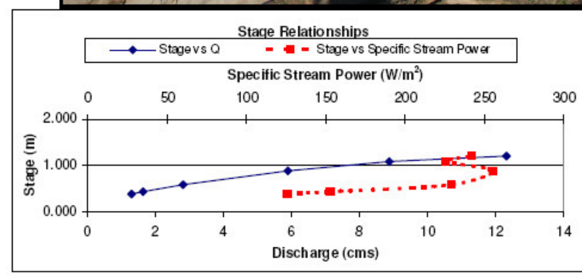

Prof. ID	Estimated n-value	L-Limit	R-Limit	WS (m)	Depth (m)	Left Sta (m)	Right Sta (m)	P_w (m)	Area (m^2)	W (m)	R (m)	D (m)	W/d	V (m/s)	Q (m^3/s)	U* (m/s)	τ (kg/ms^2)	τ*	ω (W/m^2)	Ω (W/m)	F_r	R/d_{84}	n-value per Limerino	Floodplain Form
HCSR04P01	0.035			105.05	0.385	4.82	7.25	2.78	0.72	2.43	0.26	0.30	6	1.8	1.3	0.25	61.2	2.708	126	307	1.13	3.9	0.037	PMB
HCSR04P02	0.035			105.10	0.435	4.79	7.32	2.92	0.84	2.53	0.29	0.33	6	1.9	1.6	0.26	68.3	3.020	153	387	1.15	4.4	0.037	PMB
HCSR04P03	0.035			105.25	0.585	4.73	7.63	3.43	1.25	2.90	0.36	0.43	5	2.3	2.8	0.29	85.8	3.795	229	665	1.18	5.5	0.035	PMB
HCSR04P04	0.035			105.55	0.885	4.32	9.78	6.14	2.45	5.45	0.40	0.45	6	2.4	5.9	0.31	94.4	4.174	256	1394	1.23	6.0	0.035	PMB
HCSR04P05	0.035			105.75	1.085	2.63	11.94	10.04	3.81	9.30	0.38	0.41	9	2.3	8.9	0.30	89.8	3.970	225	2097	1.24	5.7	0.035	PMB
HCSR04P06	0.035			105.87	1.205	1.30	13.34	12.79	5.12	12.04	0.40	0.42	10	2.4	12.3	0.31	94.6	4.180	242	2913	1.26	6.0	0.035	PMB
HCSR04P07	0.035																							PMB
HCSR04P08	0.035																							PMB
HCSR04P09	0.035																							PMB
HCSR04P10	0.035																							PMB

Cross Section Hydraulic Analyses: Upstream Screening Reach

Floodplain/Site Description: Hicks Canyon at ~ 534 m upstream of the road crossing (ie Sta 534 and ~20 m Upstream of HCMR10).
Photograph view is looking downstream at the main channel. Note: Jan 08 gradation data for sta 722 applied.

Location ID	HCSR05
d_{50} (mm) =	1.00
d_{84} (mm) =	43.50
So = Sf =	0.0167

Pt #	Sta (m)	Stage (m)
1	0.00	112.18
2	0.70	112.17
3	1.10	112.10
4	2.50	111.52
5	3.90	111.10
6	6.90	110.92
7	8.20	110.81
8	9.70	110.82
9	9.90	110.21
10	10.10	110.09
11	10.30	110.02
12	10.60	110.01
13	10.80	109.97
14	10.90	109.91
15	11.30	109.92
16	11.90	109.93
17	12.00	110.07
18	12.20	110.15
19	12.40	110.30
20	12.70	110.34
21	12.80	110.75
22	13.50	110.75
23	14.30	110.69
24	15.00	110.73
25	15.70	110.86
26	16.60	110.90
27	18.20	111.10
28	20.00	111.08
29	25.60	111.17
30	26.20	111.30
31	26.80	111.54
32	28.00	112.17
33	29.20	112.62
34	29.70	112.76
35	30.20	112.79
min. Stage =		109.91
Continuum		1
CEM		2

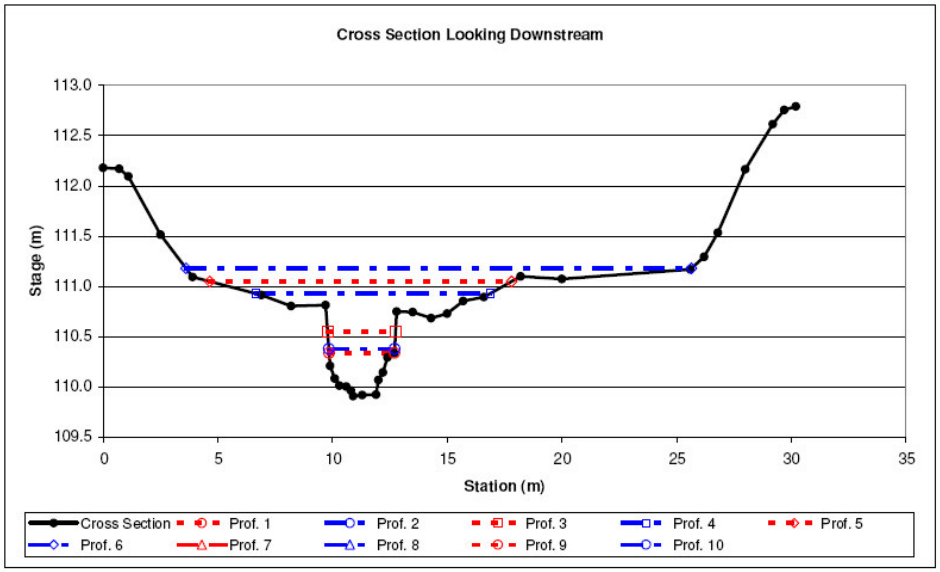

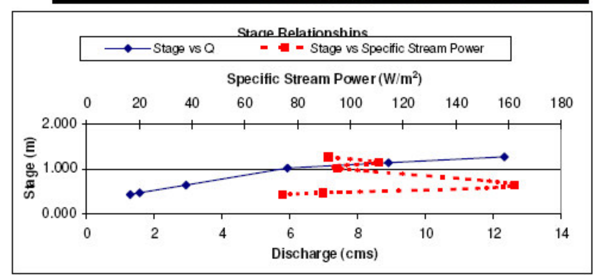

Prof. ID	Estimated n-value	L-Limit	R-Limit	WS (m)	Depth (m)	Left Sta (m)	Right Sta (m)	P_w (m)	Area (m^2)	W (m)	R (m)	D (m)	W/d	V (m/s)	Q (m^3/s)	U* (m/s)	τ (kg/ms²)	τ*	ω (W/m²)	Ω (W/m)	F_r	R/d_{84}	n-value per Limerino	Floodplain Form
HCSR05P01	0.035			110.34	0.430	9.86	12.70	3.15	0.84	2.84	0.27	0.30	7	1.5	1.3	0.21	43.8	2.711	74	211	0.96	6.1	0.033	PMB
HCSR05P02	0.035			110.38	0.470	9.84	12.71	3.23	0.96	2.87	0.30	0.33	6	1.6	1.6	0.22	48.5	2.999	90	257	0.97	6.8	0.032	PMB
HCSR05P03	0.035			110.55	0.640	9.79	12.75	3.59	1.45	2.96	0.40	0.49	5	2.0	2.9	0.26	66.3	4.104	162	481	0.99	9.3	0.031	PMB
HCSR05P04	0.035			110.93	1.020	6.65	16.87	11.22	3.49	10.22	0.31	0.34	10	1.7	5.9	0.23	51.0	3.157	95	970	0.99	7.2	0.032	PMB
HCSR05P05	0.035			111.05	1.140	4.65	17.81	14.17	4.90	13.16	0.35	0.37	12	1.8	8.9	0.24	56.6	3.504	111	1458	1.02	7.9	0.032	PMB
HCSR05P06	0.035			111.18	1.270	3.62	25.65	23.06	7.23	22.03	0.31	0.33	17	1.7	12.3	0.23	51.4	3.179	92	2018	1.02	7.2	0.032	PMB
HCSR05P07	0.035																							PMB
HCSR05P08	0.035																							PMB
HCSR05P09	0.035																							PMB
HCSR05P10	0.035																							PMB

Cross Section Hydraulic Analyses: Upstream Screening Reach

Floodplain/Site Description: Hicks Canyon at ~ 722 m upstream of the road crossing (ie Sta 722 and ~HCMR18).
Photograph view is looking downstream at the main channel . Note: Jan 08 gradation data for sta 722 applied.

Location ID	HCSR06	
d_{50} (mm) =	1.00	
d_{84} (mm) =	43.50	
So = Sf =	0.0153	
Pt #	Sta (m)	Stage (m)
1	0.00	113.85
2	5.40	114.05
3	7.70	114.19
4	8.20	114.16
5	8.50	114.11
6	8.90	113.94
7	9.30	113.83
8	9.80	113.77
9	10.00	113.64
10	10.20	113.34
11	10.60	113.21
12	10.80	113.11
13	11.00	113.07
14	11.30	113.07
15	11.50	113.08
16	11.70	113.05
17	11.90	113.10
18	12.10	113.14
19	12.30	113.20
20	12.40	113.27
21	12.60	113.36
22	12.70	113.63
23	13.20	113.69
24	13.50	113.78
25	14.00	113.87
26	14.40	113.91
27	14.70	113.97
28	15.00	114.03
29	20.20	114.21
30	25.00	114.18
31	30.00	114.21
32	35.00	114.31
33	41.90	114.56
34	43.40	115.15
35	45.00	115.65
min. Stage =	113.05	
Continuum	1	
CEM	1	

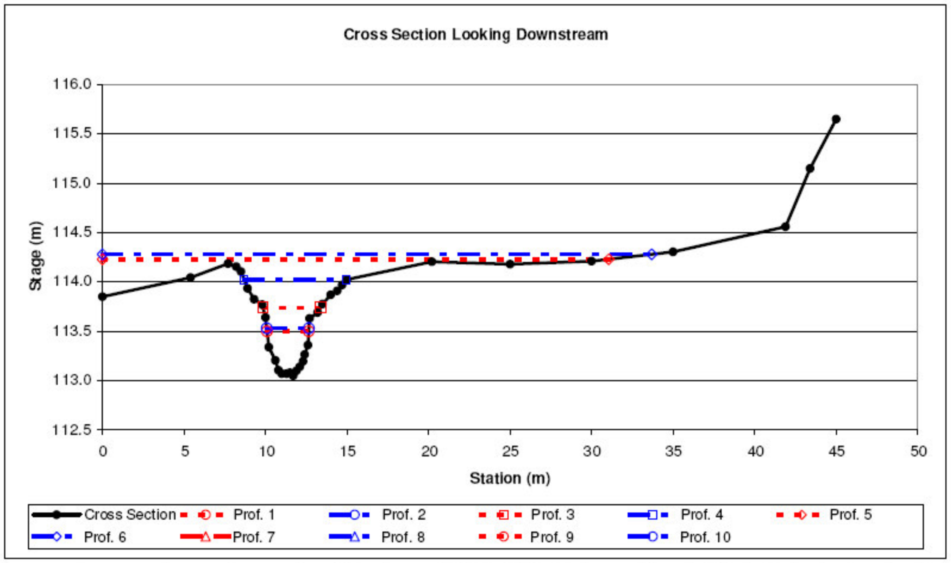

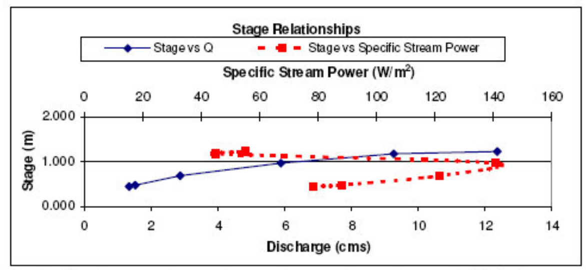

Prof. ID	Estimated n-value	L-Limit	R-Limit	WS (m)	Depth (m)	Left Sta (m)	Right Sta (m)	P_w (m)	Area (m^2)	W (m)	R (m)	D (m)	W/d	V (m/s)	Q (m^3/s)	U* (m/s)	τ (kg/ms²)	τ*	ω (W/m²)	Ω (W/m)	F_r	R/d_{84}	n-value per Limerino	Floodplain Form
HCSR06P01	0.035	7.70	20.20	113.50	0.450	10.09	12.65	2.85	0.85	2.56	0.30	0.33	6	1.6	1.3	0.21	44.6	2.759	78	200	0.94	6.8	0.032	PMB
HCSR06P02	0.035	7.70	20.20	113.53	0.480	10.07	12.66	2.92	0.92	2.59	0.32	0.36	5	1.6	1.5	0.22	47.5	2.940	88	228	0.94	7.3	0.032	PMB
HCSR06P03	0.035	7.70	20.20	113.74	0.690	9.85	13.38	4.03	1.54	3.53	0.38	0.44	5	1.9	2.9	0.24	57.3	3.544	122	429	0.96	8.8	0.031	PMB
HCSR06P04	0.035	7.70	20.20	114.02	0.970	8.70	14.97	6.84	2.93	6.27	0.43	0.47	6	2.0	5.9	0.25	64.2	3.975	141	882	1.01	9.8	0.031	PMB
HCSR06P05	0.035			114.23	1.180	0.00	31.05	31.66	7.10	31.05	0.22	0.23	26	1.3	9.3	0.18	33.7	2.083	45	1390	0.93	5.2	0.034	PMB
HCSR06P06	0.035			114.28	1.230	0.00	33.68	34.29	8.72	33.68	0.25	0.26	27	1.4	12.4	0.20	38.2	2.362	55	1856	0.95	5.8	0.033	PMB
HCSR06P07	0.035																							PMB
HCSR06P08	0.035																							PMB
HCSR06P09	0.035																							PMB
HCSR06P10	0.035																							PMB

Cross Section Hydraulic Analyses: Little Cedar Canyon

Floodplain/Site Description: Little Cedar Canyon upstream of Otay Lake Road. Photo shows main (right) channel looking downstream (Oct 07).
Note: Left channel appears to be the result of a upstream head-cut migration directly related to the downstream box culvert.

Location ID	LCOL05	
d_{50} (mm) =	20.30	
d_{84} (mm) =	62.80	
So = Sf =	0.0269	
Pt #	Sta (m)	Stage (m)
1	0.00	173.39
2	1.88	173.18
3	3.07	173.29
4	3.19	173.39
5	3.96	173.47
6	4.19	173.12
7	5.01	172.87
8	6.24	172.86
9	7.46	172.68
10	7.59	172.39
11	8.69	172.29
12	8.79	172.57
13	10.87	173.11
14	12.89	173.09
15	14.65	173.12
16	16.85	173.06
17	18.15	172.91
18	19.40	172.87
19	20.57	172.46
20	21.60	172.51
21	22.43	172.38
22	23.34	172.32
23	24.21	172.18
24	25.24	172.18
25	26.46	172.32
26	26.85	173.02
27	27.65	173.43
28	29.39	173.43
29		
30		
31		
32		
33		
34		
35		
min. Stage =	172.18	
Continuum	2	
CEM	3.0	

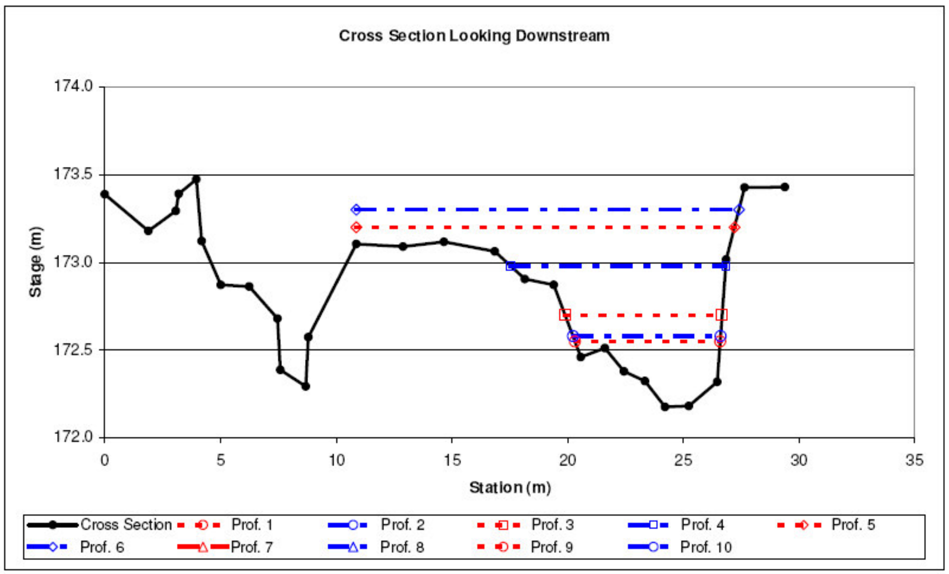

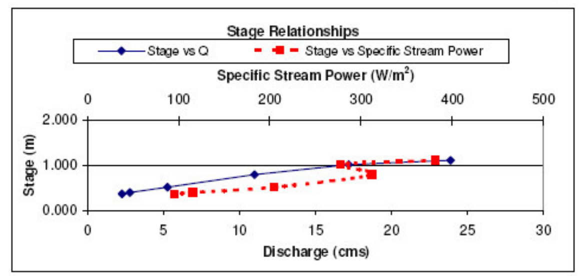

Prof. ID	Estimated n-value	L-Limit	R-Limit	WS (m)	Depth (m)	Left Sta (m)	Right Sta (m)	P_w (m)	Area (m^2)	W (m)	R (m)	D (m)	W/d	V (m/s)	Q (m^3/s)	U* (m/s)	τ (kg/ms²)	τ*	ω (W/m²)	Ω (W/m)	F_r	R/d_{84}	n-value per Limerino	Floodplain Form
LCOL05P01	0.035	19.40		172.55	0.373	20.32	26.59	6.46	1.37	6.28	0.21	0.22	16.8	1.7	2.3	0.24	55.8	0.170	96	600	1.22	3.4	0.039	PCB
LCOL05P02	0.035	19.40		172.58	0.403	20.23	26.61	6.59	1.56	6.38	0.24	0.24	15.8	1.8	2.8	0.25	62.4	0.190	115	736	1.24	3.8	0.038	PCB
LCOL05P03	0.035	19.40		172.70	0.523	19.89	26.68	7.08	2.35	6.79	0.33	0.35	13.0	2.2	5.3	0.30	87.4	0.267	205	1389	1.31	5.3	0.036	PCB
LCOL05P04	0.040	10.87		172.98	0.803	17.53	26.83	9.80	4.50	9.30	0.46	0.48	11.6	2.4	11.0	0.35	121.2	0.370	312	2900	1.20	7.3	0.034	PCB
LCOL05P05	0.040	10.87		173.20	1.023	10.87	27.21	16.91	7.32	16.34	0.43	0.45	16.0	2.3	17.2	0.34	114.3	0.349	278	4538	1.20	6.9	0.034	PCB
LCOL05P06	0.040	10.87		173.30	1.123	10.87	27.40	17.13	8.97	16.53	0.52	0.54	14.7	2.7	23.9	0.37	138.2	0.421	381	6306	1.24	8.3	0.034	PCB
LCOL05P07	0.040																							PCB
LCOL05P08	0.040																							PCB
LCOL05P09	0.040																							PCB
LCOL05P10	0.040																							PCB

Cross Section Hydraulic Analyses: Little Cedar Canyon

Floodplain/Site Description: Little Cedar Canyon upstream of Otay Lake Road. Photo shows main channel looking downstream.

Location ID	LCOL06	
d_{50} (mm) =	20.30	
d_{84} (mm) =	62.80	
So = Sf =	0.0269	
Pt #	Sta (m)	Stage (m)
1	0.00	173.70
2	3.61	173.68
3	6.19	173.66
4	8.18	173.73
5	10.25	173.76
6	12.01	173.68
7	13.22	173.60
8	14.04	173.61
9	14.95	173.43
10	15.37	173.17
11	16.30	173.03
12	17.27	172.96
13	18.34	172.91
14	19.56	172.95
15	20.42	173.05
16	21.42	173.47
17	22.67	173.49
18	23.86	173.46
19	25.72	173.63
20	27.29	173.74
21	29.18	173.75
22	31.54	173.80
23		
24		
25		
26		
27		
28		
29		
30		
31		
32		
33		
34		
35		
min. Stage =	172.91	
Continuum	2	
CEM	3.0	

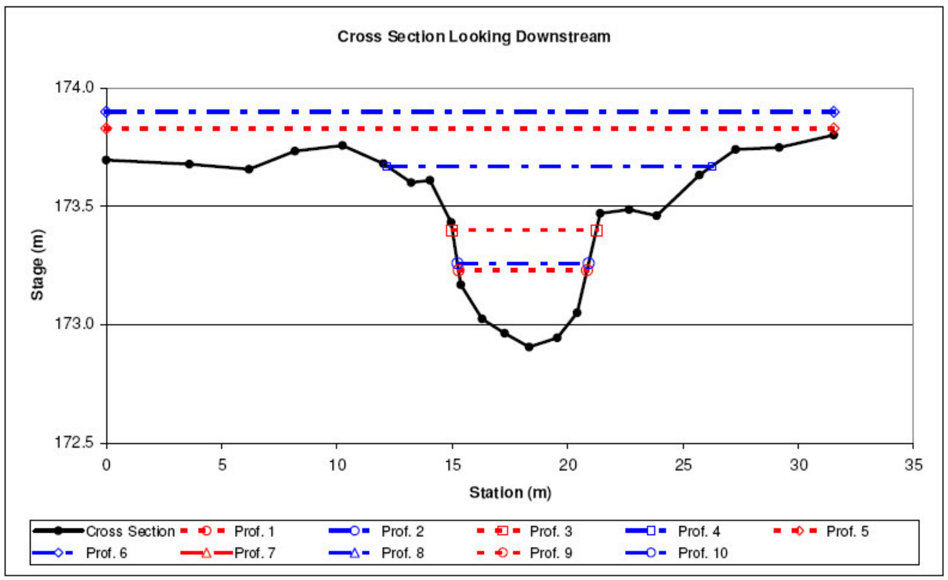

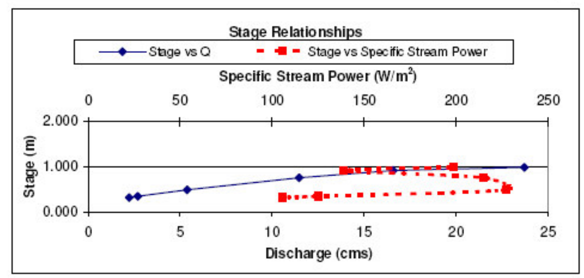

Prof. ID	Estimated n-value	L-Limit	R-Limit	WS (m)	Depth (m)	Left Sta (m)	Right Sta (m)	P_w (m)	Area (m^2)	W (m)	R (m)	D (m)	W/d	V (m/s)	Q (m^3/s)	U* (m/s)	τ (kg/ms²)	τ*	ω (W/m²)	Ω (W/m)	F_r	R/d_{84}	n-value per Limerino	Floodplain Form
LCOL06P01	0.035	10.25		173.23	0.324	15.28	20.84	5.64	1.28	5.57	0.23	0.23	17.2	1.7	2.2	0.24	59.8	0.182	106	588	1.24	3.6	0.039	PCB
LCOL06P02	0.035	10.25		173.26	0.354	15.23	20.91	5.78	1.45	5.69	0.25	0.25	16.1	1.9	2.7	0.26	66.2	0.202	125	712	1.26	4.0	0.038	PCB
LCOL06P03	0.035	10.25		173.40	0.494	15.00	21.25	6.40	2.28	6.24	0.36	0.37	12.6	2.4	5.4	0.31	94.1	0.287	227	1420	1.33	5.7	0.035	PCB
LCOL06P04	0.035	10.25		173.67	0.764	12.18	26.25	14.29	4.96	14.07	0.35	0.35	18.4	2.3	11.5	0.30	91.6	0.279	215	3028	1.34	5.5	0.036	PCB
LCOL06P05	0.040			173.83	0.924	0.00	31.54	31.76	9.22	31.54	0.29	0.29	34.1	1.8	16.6	0.28	76.6	0.234	139	4376	1.14	4.6	0.037	PCB
LCOL06P06	0.040			173.90	0.994	0.00	31.54	31.76	11.43	31.54	0.36	0.36	31.7	2.1	23.7	0.31	95.0	0.290	198	6259	1.18	5.7	0.036	PCB
LCOL06P07	0.040																							PCB
LCOL06P08	0.040																							PCB
LCOL06P09	0.040																							PCB
LCOL06P10	0.040																							PCB

Cross Section Hydraulic Analyses: Little Cedar Canyon

Floodplain/Site Description: Little Cedar Canyon upstream of Otay Lake Road. Photo shows main (left) channel looking downstream.

Note: The multiple channels appears to be a case of anastomising and not typical braiding.

Location ID	LCOL07	
d_{50} (mm) =	20.30	
d_{84} (mm) =	62.80	
So = Sf =	0.0269	
Pt #	Sta (m)	Stage (m)
1	0.00	174.68
2	2.48	174.67
3	4.17	174.66
4	8.39	174.17
5	10.27	174.12
6	10.87	173.99
7	11.80	173.95
8	13.11	173.67
9	14.26	173.84
10	15.10	174.28
11	15.91	174.35
12	17.03	174.74
13	19.43	174.81
14	21.31	174.83
15	23.33	174.26
16	25.32	174.36
17	26.30	174.18
18	29.52	173.90
19	30.21	174.03
20	30.89	174.33
21	32.09	174.39
22	33.49	174.71
23	36.05	174.69
24	38.44	174.57
25	41.12	174.54
26		
27		
28		
29		
30		
31		
32		
33		
34		
35		
min. Stage =	173.67	
Continuum	2	
CEM	3.0	

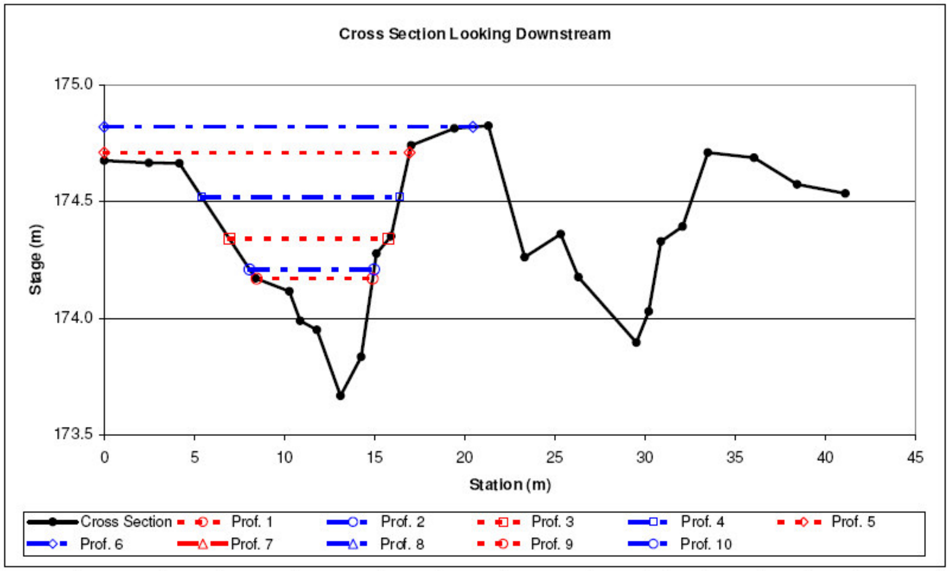

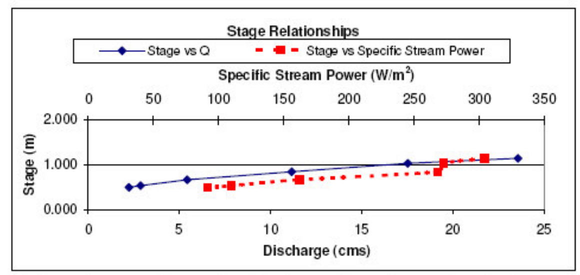

Prof. ID	Estimated n-value	L-Limit	R-Limit	WS (m)	Depth (m)	Left Sta (m)	Right Sta (m)	P_w (m)	Area (m^2)	W (m)	R (m)	D (m)	W/d	V (m/s)	Q (m^3/s)	U* (m/s)	τ (kg/ms²)	τ*	ω (W/m²)	Ω (W/m)	F_r	R/d_{84}	n-value per Limerino	Floodplain Form
LCOL07P01	0.035		17.03	174.17	0.501	8.46	14.89	6.58	1.36	6.44	0.21	0.21	12.8	1.6	2.2	0.23	54.7	0.167	92	590	1.22	3.3	0.039	PCB
LCOL07P02	0.035		17.03	174.21	0.541	8.06	14.97	7.06	1.63	6.91	0.23	0.24	12.8	1.8	2.9	0.25	60.9	0.186	110	759	1.24	3.7	0.038	PCB
LCOL07P03	0.035		17.03	174.34	0.671	6.95	15.78	9.01	2.63	8.83	0.29	0.30	13.2	2.1	5.4	0.28	77.1	0.235	162	1435	1.29	4.7	0.037	PCB
LCOL07P04	0.035		17.03	174.52	0.851	5.40	16.39	11.21	4.43	10.99	0.39	0.40	12.9	2.5	11.2	0.32	104.2	0.318	268	2947	1.36	6.3	0.035	PCB
LCOL07P05	0.035		21.31	174.71	1.041	0.00	16.94	17.20	6.88	16.94	0.40	0.41	16.3	2.5	17.5	0.33	105.7	0.322	273	4626	1.37	6.4	0.035	PCB
LCOL07P06	0.035		21.31	174.82	1.151	0.00	20.46	20.72	8.86	20.46	0.43	0.43	17.8	2.7	23.6	0.34	112.9	0.344	304	6222	1.38	6.8	0.035	PCB
LCOL07P07	0.040																							PCB
LCOL07P08	0.040																							PCB
LCOL07P09	0.040																							PCB
LCOL07P10	0.040																							PCB

Cross Section Hydraulic Analyses: Little Cedar Canyon

Floodplain/Site Description: Little Cedar Canyon upstream of Otay Lake Road. Photo shows main (left) channel looking downstream.
Note: The multiple channels appears to be a case of anastomising and not typical braiding.

Location ID	LCOL08	
d_{50} (mm) =	20.30	
d_{84} (mm) =	62.80	
So = Sf =	0.0269	
Pt #	Sta (m)	Stage (m)
1	0.00	175.45
2	3.92	175.53
3	6.56	175.50
4	10.38	175.41
5	12.01	175.41
6	13.64	174.97
7	17.05	174.74
8	18.11	174.89
9	19.43	174.92
10	20.25	175.03
11	22.27	174.78
12	23.04	174.94
13	25.30	174.76
14	26.38	175.34
15	29.39	175.36
16	32.67	175.29
17	35.44	175.37
18	38.62	175.26
19	41.68	175.30
20	44.04	175.20
21	45.58	175.13
22	47.04	174.97
23	48.90	175.16
24	49.73	175.66
25	52.50	176.23
26		
27		
28		
29		
30		
31		
32		
33		
34		
35		
min. Stage =	174.74	
Continuum	2	
CEM	3.0	

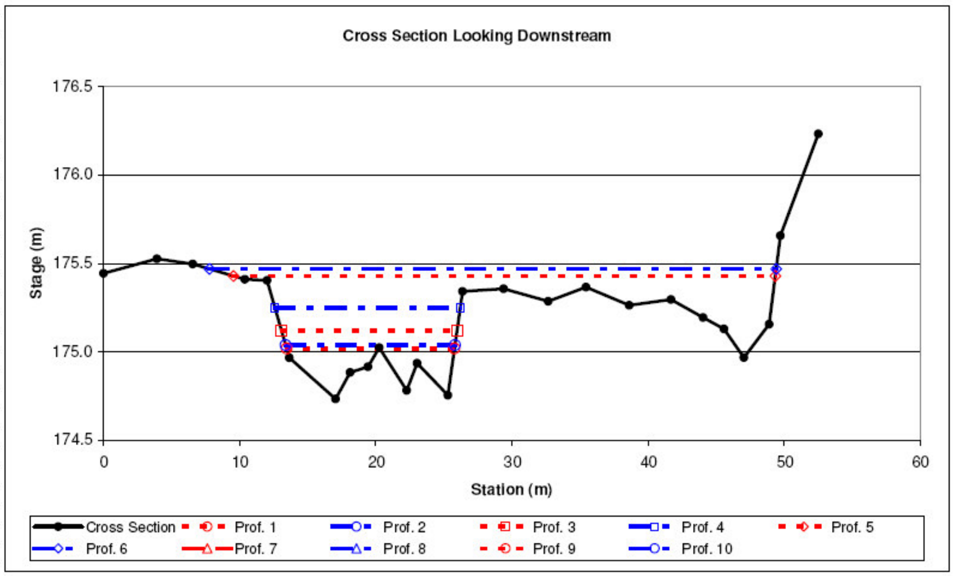

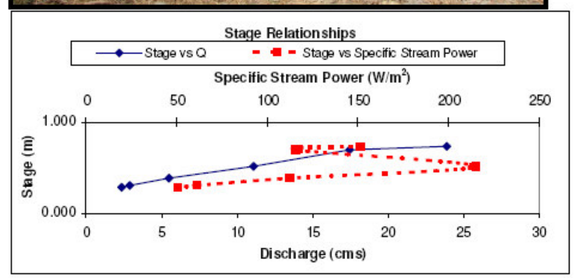

Prof. ID	Estimated n-value	L-Limit	R-Limit	WS (m)	Depth (m)	Left Sta (m)	Right Sta (m)	P_w (m)	Area (m^2)	W (m)	R (m)	D (m)	W/d	V (m/s)	Q (m^3/s)	U* (m/s)	τ (kg/ms²)	τ*	ω (W/m²)	Ω (W/m)	F_r	R/d_{84}	n-value per Limerino	Floodplain Form
LCOL08P01	0.035	3.92	26.38	175.02	0.285	13.45	25.78	12.39	1.81	12.25	0.15	0.15	43.0	1.3	2.4	0.20	38.6	0.118	51	623	1.16	2.3	0.043	PCB
LCOL08P02	0.035	3.92	26.38	175.04	0.305	13.38	25.82	12.59	2.06	12.44	0.16	0.17	40.8	1.4	2.9	0.21	43.2	0.132	61	763	1.18	2.6	0.042	PCB
LCOL08P03	0.035	3.92	26.38	175.12	0.385	13.08	25.97	13.06	3.07	12.89	0.24	0.24	33.5	1.8	5.5	0.25	62.1	0.189	112	1449	1.25	3.7	0.038	PCB
LCOL08P04	0.035	3.92	26.38	175.25	0.515	12.59	26.20	13.84	4.80	13.61	0.35	0.35	26.4	2.3	11.1	0.30	91.5	0.279	215	2927	1.33	5.5	0.036	PCB
LCOL08P05	0.045	3.92		175.43	0.695	9.54	49.35	40.18	11.21	39.80	0.28	0.28	57.3	1.6	17.5	0.27	73.7	0.225	116	4608	1.00	4.4	0.037	PCB
LCOL08P06	0.040	3.92		175.47	0.735	7.79	49.41	42.01	12.84	41.63	0.31	0.31	56.6	1.9	23.9	0.28	80.7	0.246	152	6308	1.15	4.9	0.036	PCB
LCOL08P07	0.040																							PCB
LCOL08P08	0.040																							PCB
LCOL08P09	0.040																							PCB
LCOL08P10	0.040																							PCB

Cross Section Hydraulic Analyses: Perris Lake Site B

Floodplain/Site Description: Un-Named wash within Lake Perris State Recreational Area. Photo view is looking upstream. (October, 2007).

Location ID	PLSB01
d_{50} (mm) =	0.88
d_{84} (mm) =	2.21
So = Sf =	0.0251

Pt #	Sta (m)	Stage (m)
1	0.00	499.56
2	3.61	499.49
3	7.27	499.51
4	8.88	499.24
5	10.00	499.22
6	10.56	499.40
7	11.37	499.39
8	12.48	499.53
9	18.27	499.62
10	25.44	499.86
min. Stage =		499.22
Continuum		1b
CEM		1

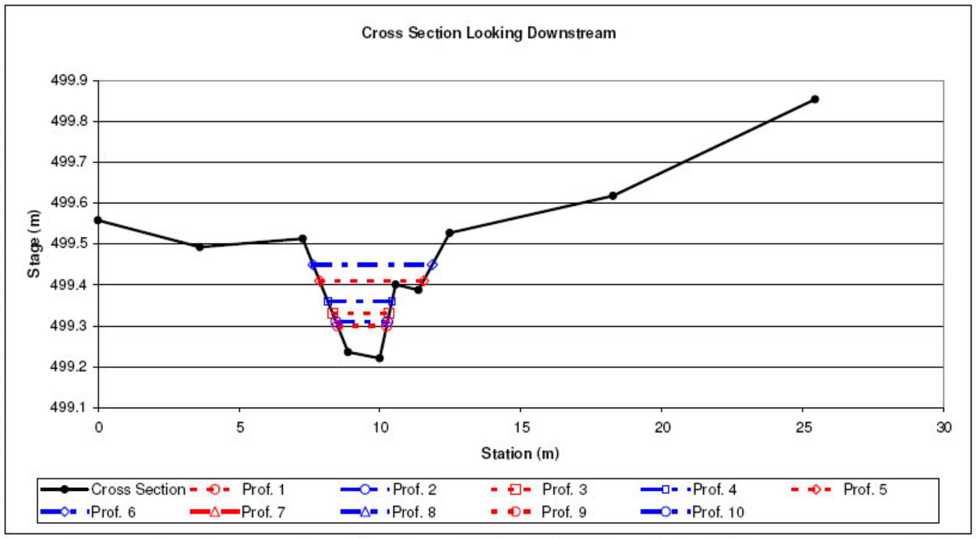

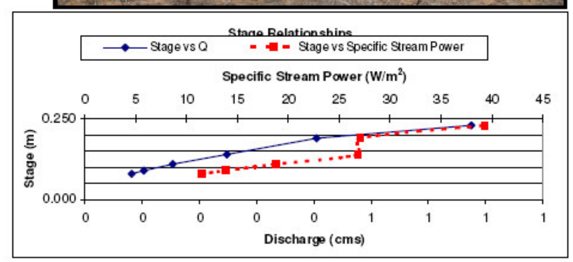

Prof. ID	Estimated n-value	L-Limit	R-Limit	WS (m)	Depth (m)	Left Sta (m)	Right Sta (m)	P_w (m)	Area (m^2)	W (m)	R (m)	D (m)	W/d	V (m/s)	Q (m^3/s)	U* (m/s)	τ (kg/ms²)	τ*	ω (W/m²)	Ω (W/m)	F_r	R/d_{84}	n-value per Limerino	Floodplain Form
PLSB01P01	0.030			499.30	0.080	8.50	10.24	1.76	0.10	1.74	0.06	0.06	21.9	0.8	0.081	0.12	14.4	1.009	12	20	1.12	26.4	0.018	PFB
PLSB01P02	0.030			499.31	0.090	8.45	10.28	1.85	0.12	1.83	0.07	0.07	20.4	0.9	0.103	0.13	16.0	1.126	14	25	1.14	29.4	0.017	PFB
PLSB01P03	0.030			499.33	0.110	8.33	10.34	2.03	0.16	2.01	0.08	0.08	18.3	1.0	0.15	0.14	19.2	1.352	19	38	1.17	35.3	0.017	PFB
PLSB01P04	0.030			499.36	0.140	8.16	10.43	2.31	0.22	2.28	0.10	0.10	16.3	1.1	0.2	0.15	23.8	1.673	27	61	1.22	43.7	0.017	PFB
PLSB01P05	0.030			499.41	0.190	7.87	11.55	3.73	0.36	3.68	0.10	0.10	19.4	1.1	0.4	0.15	23.9	1.684	27	100	1.22	44.0	0.017	PFB
PLSB01P06	0.030			499.45	0.230	7.64	11.87	4.28	0.52	4.23	0.12	0.12	18.4	1.3	0.7	0.17	30.0	2.107	39	166	1.27	55.0	0.017	PFB
PLSB01P07	0.030																							PFB
PLSB01P08	0.030																							PFB
PLSB01P09	0.030																							PFB
PLSB01P10	0.030																							PFB

Cross Section Hydraulic Analyses: Perris Lake Site B

Floodplain/Site Description: Photo view looking downstream, note hammer near center of photo.

Location ID	PLSB02
d_{50} (mm) =	0.88
d_{84} (mm) =	2.21
So = Sf =	0.0251

Pt #	Sta (m)	Stage (m)
1	0.00	501.23
2	4.79	500.71
3	11.49	500.67
4	17.34	500.64
5	21.97	500.32
6	23.97	500.38
7	24.85	500.80
8	29.78	501.10
9	34.62	501.53
10		
11		
12		
13		
14		
15		
16		
17		
18		
19		
20		
21		
22		
23		
24		
25		
26		
27		
28		
29		
30		
31		
32		
33		
34		
35		
min. Stage =	500.32	
Continuum	1b	
CEM	1	

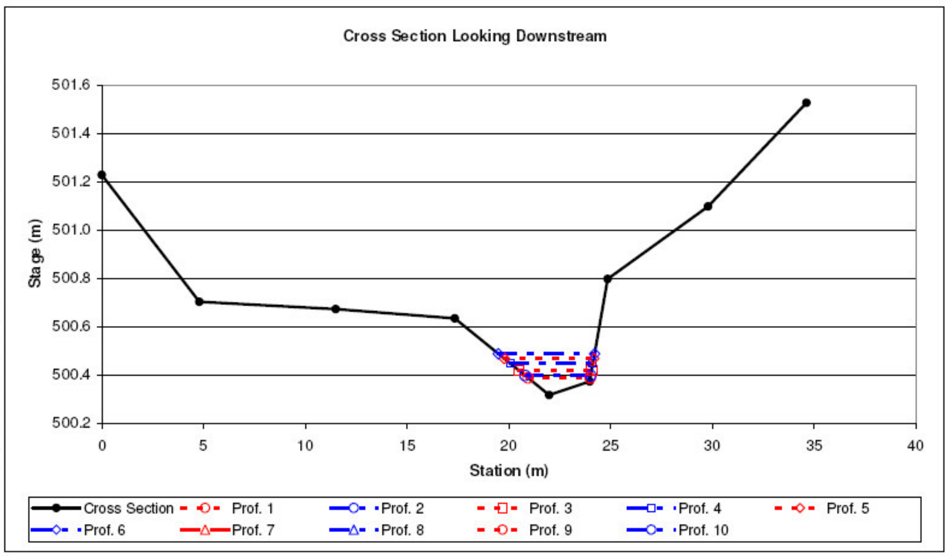

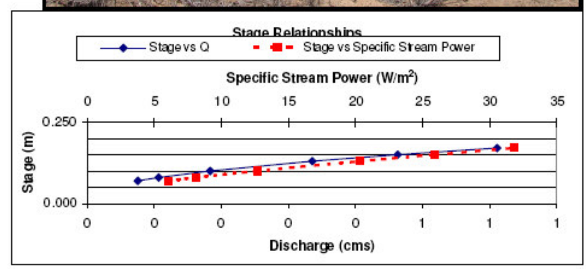

Prof. ID	Estimated n-value	L-Limit	R-Limit	WS (m)	Depth (m)	Left Sta (m)	Right Sta (m)	P_w (m)	Area (m^2)	W (m)	R (m)	D (m)	W/d	V (m/s)	Q (m^3/s)	U* (m/s)	τ (kg/ms²)	τ*	ω (W/m²)	Ω (W/m)	F_r	R/d_{84}	n-value per Limerino	Floodplain Form
PLSB02P01	0.030			500.39	0.071	20.94	24.00	3.07	0.12	3.06	0.04	0.04	43.2	0.6	0.08	0.10	9.8	0.691	6	19	1.06	18.1	0.018	PFB
PLSB02P02	0.030			500.40	0.081	20.79	24.02	3.24	0.15	3.23	0.05	0.05	39.9	0.7	0.11	0.11	11.7	0.823	8	26	1.09	21.5	0.018	PFB
PLSB02P03	0.030			500.42	0.101	20.50	24.06	3.57	0.22	3.56	0.06	0.06	35.3	0.8	0.18	0.12	15.3	1.074	13	45	1.14	28.1	0.017	PFB
PLSB02P04	0.030			500.45	0.131	20.06	24.12	4.08	0.34	4.06	0.08	0.08	31.0	1.0	0.34	0.14	20.3	1.425	20	83	1.19	37.2	0.017	PFB
PLSB02P05	0.030			500.47	0.151	19.77	24.16	4.42	0.42	4.39	0.10	0.10	29.1	1.1	0.46	0.15	23.4	1.647	26	114	1.22	43.0	0.017	PFB
PLSB02P06	0.030			500.49	0.171	19.48	24.21	4.76	0.51	4.73	0.11	0.11	27.7	1.2	0.61	0.16	26.5	1.862	32	150	1.24	48.6	0.017	PFB
PLSB02P07	0.030																							PFB
PLSB02P08	0.030																							PFB
PLSB02P09	0.030																							PFB
PLSB02P10	0.030																							PFB

Cross Section Hydraulic Analyses: Perris Lake Site B

Floodplain/Site Description: Photo view looking from right overbank toward left overbank.

Location ID		PLSB03
d_{50} (mm) =		0.88
d_{84} (mm) =		2.21
So = Sf =		0.0281
Pt #	Sta (m)	Stage (m)
1	0.00	504.39
2	7.23	503.40
3	10.31	503.15
4	13.47	502.93
5	15.97	502.83
6	16.47	502.92
7	16.97	503.24
8	18.32	503.38
9	21.37	503.57
10	25.20	503.58
11		
12		
13		
14		
15		
16		
17		
18		
19		
20		
21		
22		
23		
24		
25		
26		
27		
28		
29		
30		
31		
32		
33		
34		
35		
min. Stage =		502.83
Continuum		1b
CEM		1

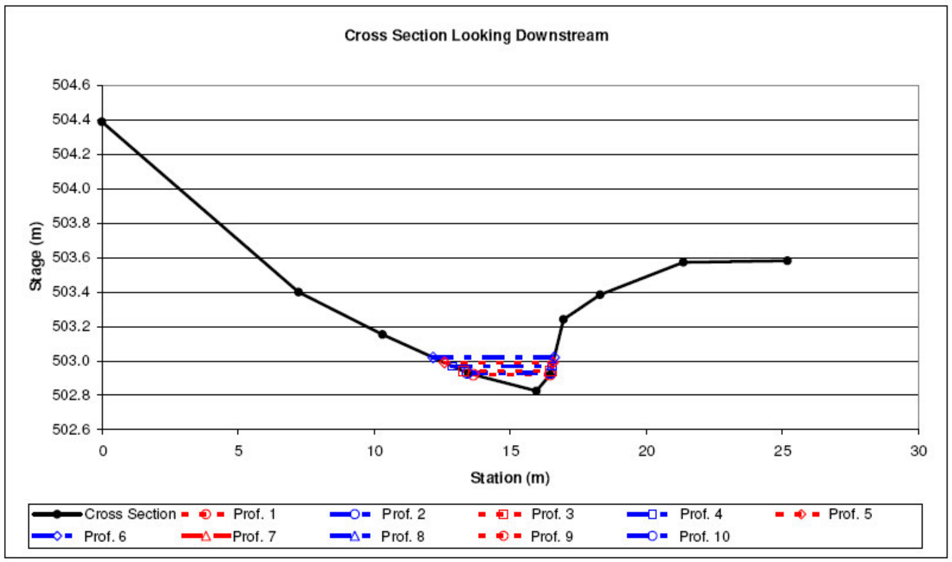

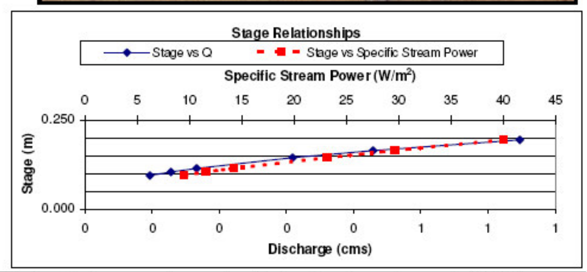

Prof. ID	Estimated n-value	L-Limit	R-Limit	WS (m)	Depth (m)	Left Sta (m)	Right Sta (m)	P_w (m)	Area (m^2)	W (m)	R (m)	D (m)	W/d	V (m/s)	Q (m^3/s)	U* (m/s)	τ (kg/ms²)	τ*	ω (W/m²)	Ω (W/m)	F_r	R/d_{84}	n-value per Limerino	Floodplain Form
PLSB03P01	0.030			502.92	0.094	13.66	16.48	2.83	0.13	2.82	0.05	0.05	29.9	0.7	0.097	0.11	13.0	0.912	9	27	1.15	21.3	0.018	PFB
PLSB03P02	0.030			502.93	0.104	13.44	16.49	3.07	0.16	3.05	0.05	0.05	29.3	0.8	0.13	0.12	14.6	1.028	12	35	1.17	24.0	0.018	PFB
PLSB03P03	0.030			502.94	0.114	13.30	16.51	3.23	0.19	3.21	0.06	0.06	28.1	0.9	0.17	0.13	16.6	1.166	14	46	1.19	27.2	0.018	PFB
PLSB03P04	0.030			502.97	0.144	12.88	16.55	3.70	0.30	3.68	0.08	0.08	25.5	1.0	0.31	0.15	22.1	1.556	23	85	1.25	36.3	0.017	PFB
PLSB03P05	0.030			502.99	0.164	12.60	16.58	4.02	0.37	3.99	0.09	0.09	24.3	1.1	0.43	0.16	25.6	1.803	30	118	1.28	42.1	0.017	PFB
PLSB03P06	0.030			503.02	0.194	12.18	16.63	4.50	0.50	4.45	0.11	0.11	22.9	1.3	0.65	0.18	30.7	2.158	40	178	1.32	50.4	0.017	PFB
PLSB03P07	0.030																							PFB
PLSB03P08	0.030																							PFB
PLSB03P09	0.030																							PFB
PLSB03P10	0.030																							PFB

Cross Section Hydraulic Analyses: Perris Lake Site B

Floodplain/Site Description: Photo view looking upstream.

Location ID	PLSB04	
d_{50} (mm) =	0.88	
d_{84} (mm) =	2.21	
So = Sf =	0.0281	
Pt #	Sta (m)	Stage (m)
1	0.00	505.31
2	3.62	504.71
3	7.30	504.19
4	8.47	503.68
5	9.51	503.70
6	10.29	503.94
7	15.07	504.37
8	20.76	504.72
9	27.26	505.06
10		
11		
12		
13		
14		
15		
16		
17		
18		
19		
20		
21		
22		
23		
24		
25		
26		
27		
28		
29		
30		
31		
32		
33		
34		
35		
min. Stage =	503.68	
Continuum	1b	
CEM	1	

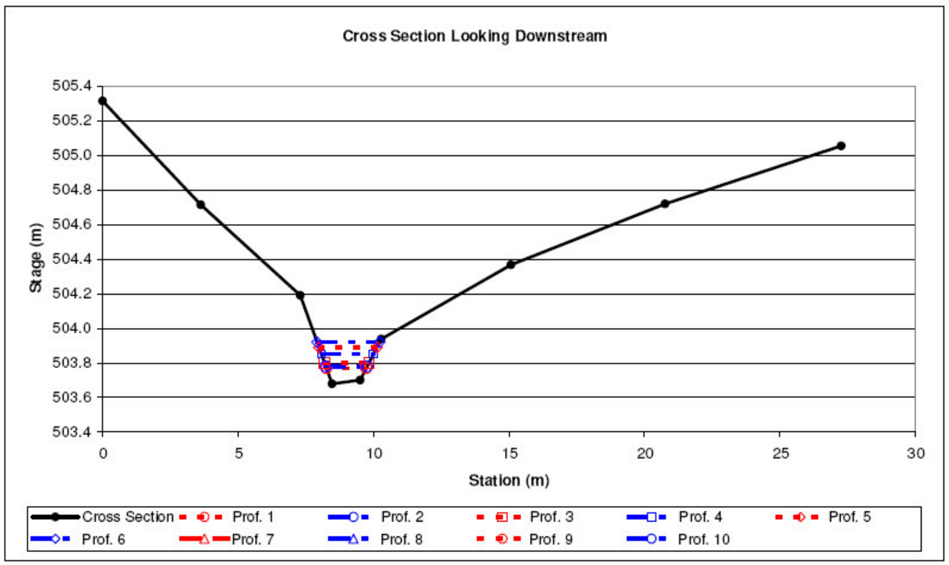

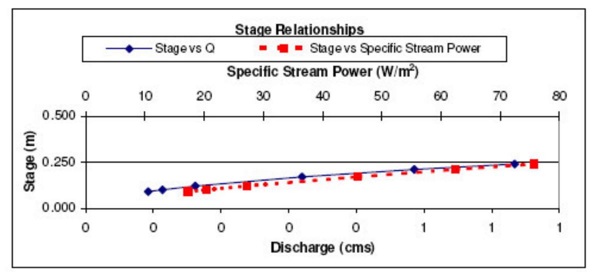

Prof. ID	Estimated n-value	L-Limit	R-Limit	WS (m)	Depth (m)	Left Sta (m)	Right Sta (m)	P_w (m)	Area (m^2)	W (m)	R (m)	D (m)	W/d	V (m/s)	Q (m^3/s)	U* (m/s)	τ (kg/ms²)	τ*	ω (W/m²)	Ω (W/m)	F_r	R/d_{84}	n-value per Limerino	Floodplain Form
PLSB04P01	0.030			503.77	0.091	8.26	9.73	1.50	0.10	1.47	0.07	0.07	16.2	0.9	0.092	0.14	18.4	1.295	17	25	1.21	30.2	0.017	PFB
PLSB04P02	0.030			503.78	0.101	8.24	9.77	1.56	0.12	1.53	0.07	0.08	15.1	1.0	0.113	0.14	20.4	1.432	20	31	1.23	33.4	0.017	PFB
PLSB04P03	0.030			503.80	0.121	8.19	9.83	1.68	0.15	1.64	0.09	0.09	13.6	1.1	0.162	0.16	24.1	1.696	27	45	1.26	39.6	0.017	PFB
PLSB04P04	0.030			503.85	0.171	8.08	10.00	1.98	0.24	1.92	0.12	0.12	11.2	1.4	0.320	0.18	32.9	2.315	46	88	1.32	54.0	0.017	PFB
PLSB04P05	0.030			503.89	0.211	7.99	10.13	2.21	0.32	2.14	0.14	0.15	10.2	1.5	0.485	0.20	39.5	2.778	62	134	1.36	64.8	0.017	PFB
PLSB04P06	0.030			503.92	0.241	7.92	10.23	2.39	0.38	2.31	0.16	0.17	9.6	1.7	0.634	0.21	44.3	3.113	76	175	1.39	72.6	0.017	PFB
PLSB04P07	0.030																							PFB
PLSB04P08	0.030																							PFB
PLSB04P09	0.030																							PFB
PLSB04P10	0.030																							PFB

Cross Section Hydraulic Analyses: Perris Lake Site B

Floodlplain/Site Description: Photo view looking downstream.

Location ID	PLSB05	
d_{50} (mm) =	0.88	
d_{84} (mm) =	2.21	
So = Sf =	0.0365	
Pt #	Sta (m)	Stage (m)
1	0.00	508.15
2	5.76	507.42
3	10.77	506.42
4	12.55	506.28
5	13.43	506.08
6	14.40	506.13
7	14.71	506.38
8	21.20	506.77
9	28.16	507.46
10		
11		
12		
13		
14		
15		
16		
17		
18		
19		
20		
21		
22		
23		
24		
25		
26		
27		
28		
29		
30		
31		
32		
33		
34		
35		
min. Stage =	506.08	
Continuum	1b	
CEM	1	

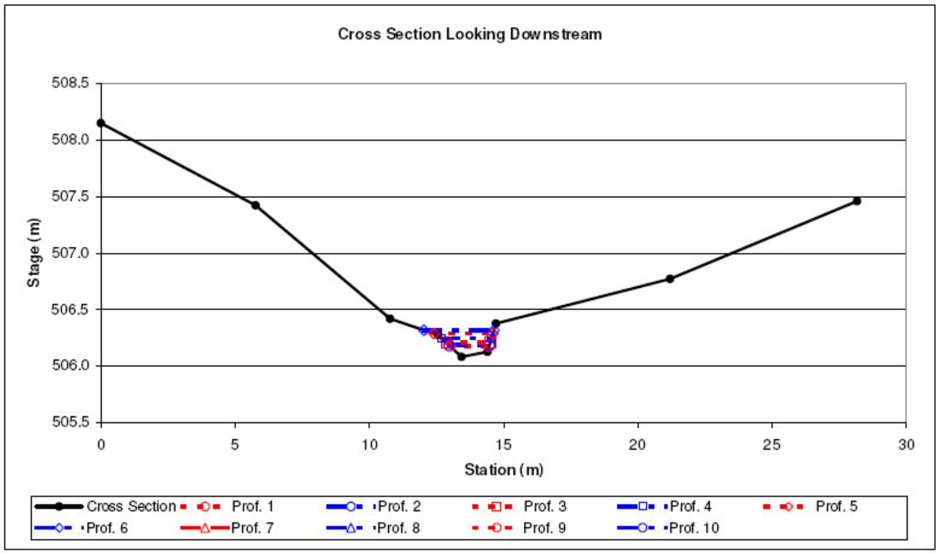

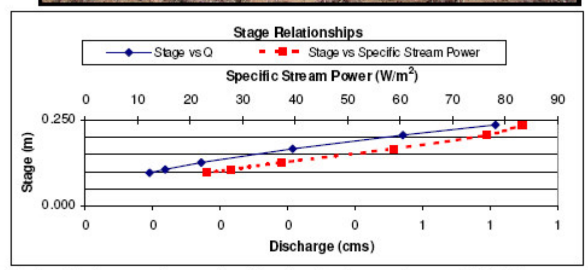

Prof. ID	Estimated n-value	L-Limit	R-Limit	WS (m)	Depth (m)	Left Sta (m)	Right Sta (m)	P_w (m)	Area (m^2)	W (m)	R (m)	D (m)	W/d	V (m/s)	Q (m^3/s)	U* (m/s)	τ (kg/ms^2)	τ*	ω (W/m^2)	Ω (W/m)	F_r	R/d_{84}	n-value per Limerino	Floodplain Form
PLSB05P01	0.030			506.18	0.097	12.99	14.46	1.50	0.09	1.47	0.06	0.06	15.2	1.0	0.095	0.15	22.5	1.585	23	34	1.36	28.5	0.017	PFB
PLSB05P02	0.030			506.19	0.107	12.95	14.48	1.56	0.11	1.53	0.07	0.07	14.3	1.1	0.118	0.16	25.1	1.764	28	42	1.38	31.7	0.017	PFB
PLSB05P03	0.030			506.21	0.127	12.86	14.50	1.69	0.14	1.64	0.08	0.09	13.0	1.2	0.172	0.17	30.0	2.107	37	62	1.42	37.8	0.017	PFB
PLSB05P04	0.030			506.25	0.167	12.68	14.55	1.94	0.21	1.87	0.11	0.11	11.2	1.5	0.308	0.20	39.1	2.750	59	110	1.48	49.4	0.017	PFB
PLSB05P05	0.030			506.29	0.207	12.40	14.60	2.28	0.29	2.20	0.13	0.13	10.7	1.6	0.471	0.21	45.8	3.218	77	169	1.52	57.8	0.017	PFB
PLSB05P06	0.030			506.32	0.237	12.03	14.64	2.70	0.36	2.61	0.13	0.14	11.0	1.7	0.608	0.22	48.2	3.388	83	218	1.53	60.9	0.017	PFB
PLSB05P07	0.030																							PFB
PLSB05P08	0.030																							PFB
PLSB05P09	0.030																							PFB
PLSB05P10	0.030																							PFB

Cross Section Hydraulic Analyses: Perris Lake Site C

Floodplain/Site Description: Photo view is looking downstream along left bank (October, 2007).

Location ID	PLSC02	
d_{50} (mm) =		0.76
d_{84} (mm) =		2.26
So = Sf =		0.0237
Pt #	Sta (m)	Stage (m)
1	0.00	502.80
2	4.80	502.46
3	8.97	502.32
4	11.28	502.00
5	16.83	501.98
6	20.19	502.00
7	23.77	502.00
8	28.99	502.05
9	31.72	501.85
10	36.23	502.14
11	39.08	501.97
12	44.33	502.05
13	47.84	502.32
14	53.09	502.73
15	56.26	503.13
16		
17		
18		
19		
20		
21		
22		
23		
24		
25		
26		
27		
28		
29		
30		
31		
32		
33		
34		
35		
min. Stage =		501.85
Continuum		1b
CEM		2

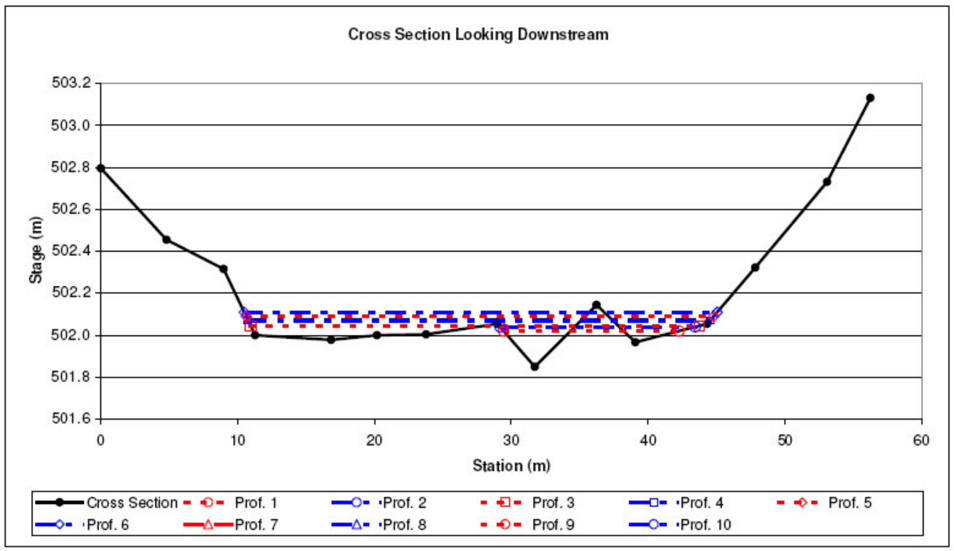

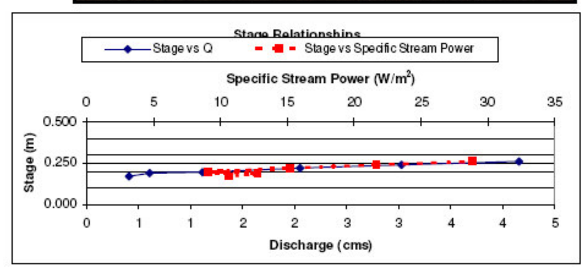

Prof. ID	Estimated n-value	L-Limit	R-Limit	WS (m)	Depth (m)	Left Sta (m)	Right Sta (m)	P_w (m)	Area (m^2)	W (m)	R (m)	D (m)	W/d	V (m/s)	Q (m^3/s)	U* (m/s)	τ (kg/ms²)	τ*	ω (W/m²)	Ω (W/m)	F_r	R/d_{84}	n-value per Limerino	Floodplain Form
PLSC02P01	0.030	28.99		502.02	0.171	29.44	42.26	8.94	0.53	8.93	0.06	0.06	52.3	0.8	0.41	0.12	13.7	1.112	11	95	1.09	26.0	0.018	BF
PLSC02P02	0.030	28.99		502.04	0.191	29.18	43.45	11.03	0.72	11.01	0.07	0.07	57.8	0.8	0.61	0.12	15.3	1.244	13	141	1.12	29.1	0.018	BF
PLSC02P03	0.030			502.05	0.196	10.95	43.75	28.62	1.53	28.60	0.05	0.05	146.3	0.7	1.1	0.11	12.4	1.012	9	259	1.08	23.6	0.018	BF
PLSC02P04	0.030			502.07	0.221	10.77	44.53	31.46	2.29	31.44	0.07	0.07	142.5	0.9	2.1	0.13	16.9	1.379	15	477	1.14	32.2	0.017	BF
PLSC02P05	0.030			502.09	0.241	10.62	44.79	32.50	2.93	32.47	0.09	0.09	135.0	1.0	3.0	0.14	21.0	1.708	22	703	1.18	39.9	0.017	BF
PLSC02P06	0.030			502.11	0.261	10.48	45.05	33.54	3.59	33.51	0.11	0.11	128.6	1.2	4.2	0.16	24.9	2.027	29	966	1.21	47.4	0.017	BF
PLSC02P07	0.030																							BF
PLSC02P08	0.030																							BF
PLSC02P09	0.030																							BF
PLSC02P10	0.030																							BF

Cross Section Hydraulic Analyses: Perris Lake Site C

Floodplain/Site Description: Photo view is looking downstream along left bank (October, 2007).

Location ID		PLSC03
d_{50} (mm) =		0.76
d_{84} (mm) =		2.26
So = Sf =		0.0237
Pt #	Sta (m)	Stage (m)
1	0.00	504.30
2	3.42	503.73
3	7.95	503.30
4	14.53	503.31
5	17.94	503.30
6	23.03	503.30
7	26.50	503.34
8	26.49	503.37
9	31.88	503.44
10	40.12	503.34
11	46.72	503.25
12	50.02	503.34
13	56.16	503.33
14	56.54	503.55
15	60.73	504.05
16	67.08	504.95
17	67.12	504.95
18		
19		
20		
21		
22		
23		
24		
25		
26		
27		
28		
29		
30		
31		
32		
33		
34		
35		
min. Stage =		503.25
Continuum		1b
CEM		2

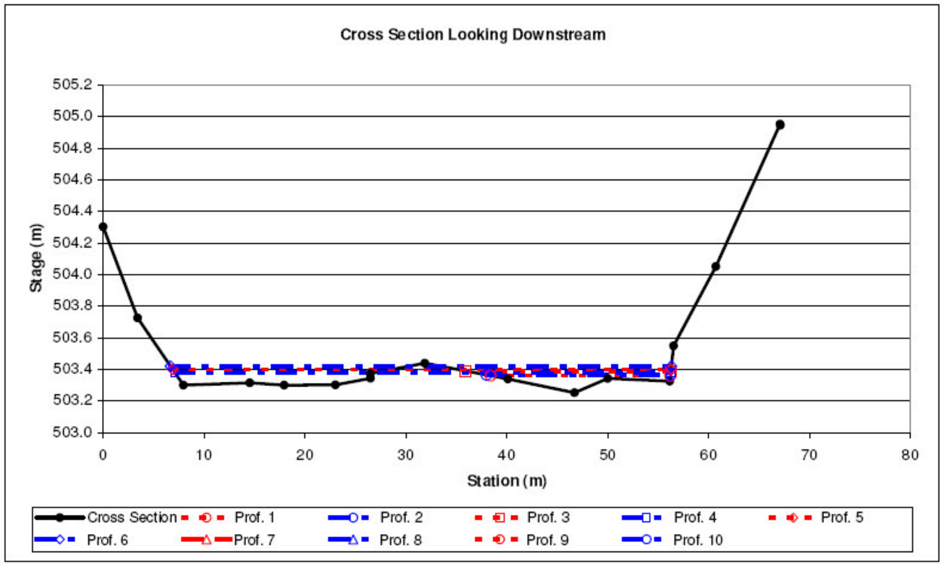

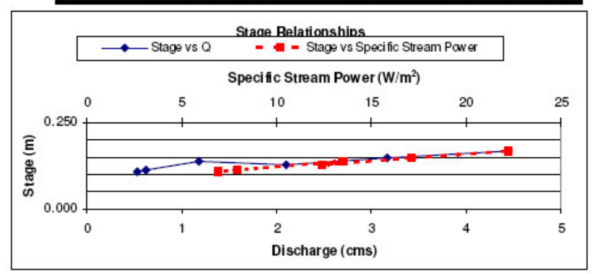

Prof. ID	Estimated n-value	L-Limit	R-Limit	WS (m)	Depth (m)	Left Sta (m)	Right Sta (m)	P_w (m)	Area (m^2)	W (m)	R (m)	D (m)	W/d	V (m/s)	Q (m^3/s)	U* (m/s)	τ (kg/ms²)	τ*	ω (W/m²)	Ω (W/m)	F_r	R/d_{84}	n-value per Limerino	Floodplain Form
PLSC03P01	0.030	31.88		503.36	0.108	38.41	56.22	17.82	0.81	17.81	0.05	0.05	165.0	0.7	0.53	0.10	10.6	0.860	7	123	1.05	20.1	0.018	BF
PLSC03P02	0.030	31.88		503.37	0.113	38.00	56.23	18.24	0.90	18.23	0.05	0.05	161.4	0.7	0.62	0.11	11.5	0.933	8	144	1.06	21.8	0.018	BF
PLSC03P03	0.030	31.88		503.39	0.138	35.93	56.27	20.35	1.38	20.33	0.07	0.07	147.4	0.9	1.18	0.13	15.8	1.285	13	274	1.12	30.0	0.018	BF
PLSC03P04	0.030			503.38	0.128	7.10	56.25	39.46	2.55	39.40	0.06	0.06	308.0	0.8	2.10	0.12	15.0	1.221	12	488	1.11	28.5	0.018	BF
PLSC03P05	0.030			503.40	0.148	6.89	56.29	43.01	3.37	42.94	0.08	0.08	290.3	0.9	3.16	0.13	18.2	1.483	17	736	1.15	34.7	0.017	BF
PLSC03P06	0.030			503.42	0.168	6.67	56.32	46.56	4.26	46.49	0.09	0.09	276.8	1.0	4.44	0.15	21.3	1.734	22	1033	1.18	40.5	0.017	BF
PLSC03P07	0.030																							BF
PLSC03P08	0.030																							BF
PLSC03P09	0.030																							BF
PLSC03P10	0.030																							BF

Cross Section Hydraulic Analyses: Perris Lake Site C

Floodplain/Site Description: Photo view is looking downstream along left bank (October, 2007). Due to downstream re-channelization, left channel appears abandoned and flood is cutting new channel.

Location ID		PLSC04
d_{50} (mm) =		0.76
d_{84} (mm) =		2.26
So = Sf =		0.0237
Pt #	Sta (m)	Stage (m)
1	0.00	504.74
2	4.62	504.37
3	9.67	504.07
4	14.53	504.01
5	16.49	504.17
6	20.27	504.11
7	24.09	504.09
8	28.25	504.49
9	34.88	504.75
10	44.77	504.64
11	47.85	504.49
12	53.09	504.46
13	58.99	504.90
14	68.40	506.56
15		
16		
17		
18		
19		
20		
21		
22		
23		
24		
25		
26		
27		
28		
29		
30		
31		
32		
33		
34		
35		
min. Stage =		504.01
Continuum		1b
CEM		2

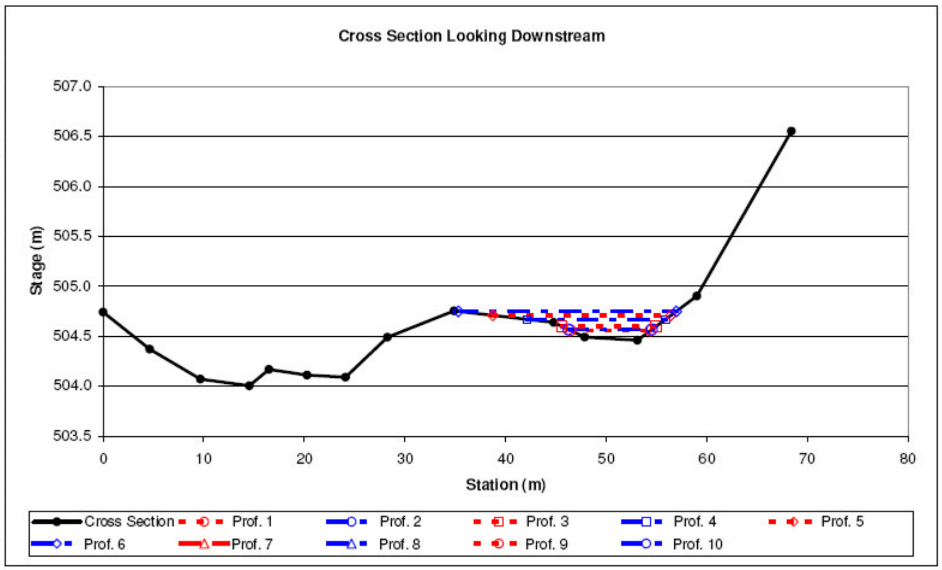

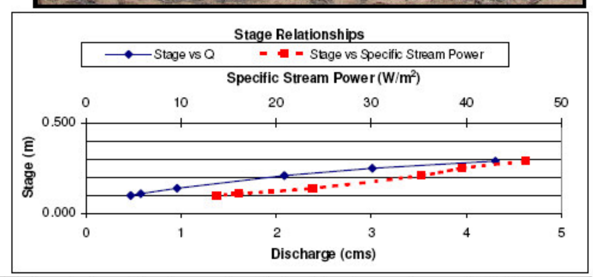

Prof. ID	Estimated n-value	L-Limit	R-Limit	WS (m)	Depth (m)	Left Sta (m)	Right Sta (m)	P_w (m)	Area (m^2)	W (m)	R (m)	D (m)	W/d	V (m/s)	Q (m^3/s)	U* (m/s)	τ (kg/ms²)	τ*	ω (W/m²)	Ω (W/m)	F_r	R/d_{84}	n-value per Limerino	Floodplain Form
PLSC04P01	0.030	34.88		504.56	0.099	46.44	54.41	7.98	0.55	7.97	0.07	0.07	80.7	0.9	0.471	0.13	16.0	1.300	14	110	1.12	30.4	0.017	BF
PLSC04P02	0.030	34.88		504.57	0.109	46.22	54.54	8.32	0.63	8.32	0.08	0.08	76.4	0.9	0.577	0.13	17.6	1.431	16	134	1.14	33.4	0.017	BF
PLSC04P03	0.030	34.88		504.60	0.139	45.59	54.94	9.36	0.89	9.35	0.10	0.10	67.3	1.1	0.96	0.15	22.2	1.809	24	223	1.19	42.3	0.017	BF
PLSC04P04	0.030	34.88		504.67	0.209	42.12	55.88	13.77	1.66	13.76	0.12	0.12	65.9	1.3	2.09	0.17	28.1	2.288	35	485	1.23	53.5	0.017	BF
PLSC04P05	0.030	34.88		504.71	0.249	38.71	56.41	17.71	2.29	17.70	0.13	0.13	71.1	1.3	3.0	0.17	30.1	2.452	40	700	1.25	57.3	0.017	BF
PLSC04P06	0.030	34.88		504.75	0.289	35.30	56.94	21.66	3.08	21.64	0.14	0.14	74.9	1.4	4.3	0.18	33.1	2.693	46	1001	1.27	62.9	0.017	BF
PLSC04P07	0.030																							BF
PLSC04P08	0.030																							BF
PLSC04P09	0.030																							BF
PLSC04P10	0.030																							BF

Cross Section Hydraulic Analyses: Perris Lake Site C

Floodplain/Site Description: Photo view is looking downstream along left bank (October, 2007).

Location ID		PLSC05
d_{50} (mm) =		0.90
d_{84} (mm) =		2.91
So = Sf =		0.0218
Pt #	Sta (m)	Stage (m)
1	0.00	507.61
2	4.81	506.96
3	7.23	506.71
4	10.73	506.55
5	17.74	506.39
6	25.78	506.22
7	33.55	506.11
8	41.97	506.04
9	49.20	505.94
10	52.18	505.66
11	55.84	505.56
12	61.62	506.28
13	67.98	506.62
14	72.04	507.00
15		
16		
17		
18		
19		
20		
21		
22		
23		
24		
25		
26		
27		
28		
29		
30		
31		
32		
33		
34		
35		
min. Stage =		505.56
Continuum		1b
CEM		1

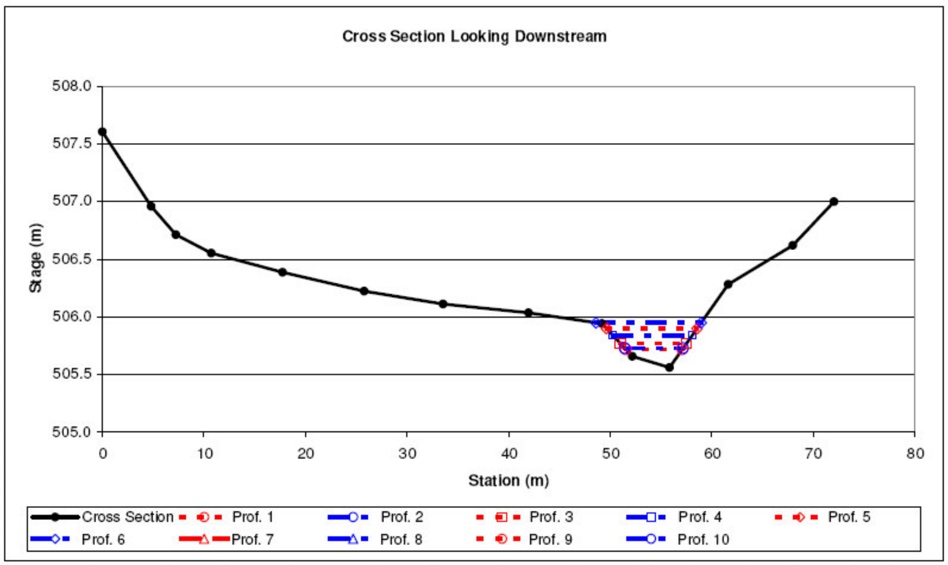

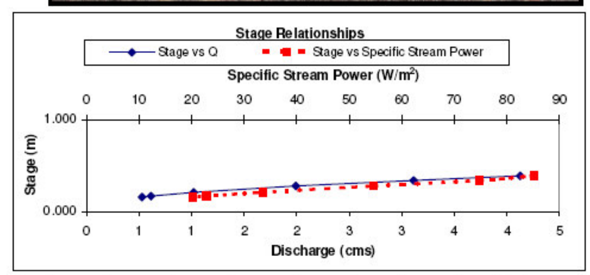

Prof. ID	Estimated n-value	L-Limit	R-Limit	WS (m)	Depth (m)	Left Sta (m)	Right Sta (m)	P_w (m)	Area (m^2)	W (m)	R (m)	D (m)	W/d	V (m/s)	Q (m^3/s)	U* (m/s)	τ (kg/ms^2)	τ*	ω (W/m^2)	Ω (W/m)	F_r	R/d_{84}	n-value per Limerino	Floodplain Form
PLSC05P01	0.030			505.72	0.158	51.54	57.11	5.59	0.52	5.57	0.09	0.09	35.2	1.0	0.53	0.14	20.0	1.373	20	113	1.13	32.1	0.018	PFB
PLSC05P02	0.030			505.73	0.168	51.43	57.19	5.77	0.58	5.76	0.10	0.10	34.2	1.1	0.61	0.15	21.4	1.473	23	131	1.15	34.4	0.018	PFB
PLSC05P03	0.030			505.77	0.208	51.01	57.51	6.52	0.82	6.50	0.13	0.13	31.2	1.2	1.02	0.16	27.0	1.858	34	218	1.19	43.4	0.018	PFB
PLSC05P04	0.030			505.84	0.278	50.28	58.07	7.82	1.32	7.79	0.17	0.17	28.0	1.5	1.99	0.19	36.2	2.489	55	426	1.25	58.2	0.018	PFB
PLSC05P05	0.030			505.90	0.338	49.65	58.55	8.94	1.82	8.90	0.20	0.20	26.3	1.7	3.11	0.21	43.6	3.002	75	666	1.29	70.1	0.018	PFB
PLSC05P06	0.030			505.95	0.388	48.60	58.95	10.39	2.29	10.35	0.22	0.22	26.7	1.8	4.13	0.22	47.2	3.247	85	882	1.31	75.9	0.018	PFB
PLSC05P07	0.030																							PFB
PLSC05P08	0.030																							PFB
PLSC05P09	0.030																							PFB
PLSC05P10	0.030																							PFB

Cross Section Hydraulic Analyses: Perris Lake Site C

Floodplain/Site Description: Photo view is looking downstream along left bank (October, 2007).

Location ID	PLSC06
d_{50} (mm) =	0.90
d_{84} (mm) =	2.91
So = Sf =	0.0218

Pt #	Sta (m)	Stage (m)
1	0.00	508.45
2	4.90	508.03
3	11.95	507.73
4	20.30	507.53
5	27.37	507.43
6	33.80	507.25
7	39.46	507.10
8	44.58	506.98
9	48.85	506.93
10	51.98	506.92
11	53.15	507.19
12	57.52	507.51
13	63.52	508.09
14		
15		
16		
17		
18		
19		
20		
21		
22		
23		
24		
25		
26		
27		
28		
29		
30		
31		
32		
33		
34		
35		
min. Stage =		506.92
Continuum		1b
CEM		1

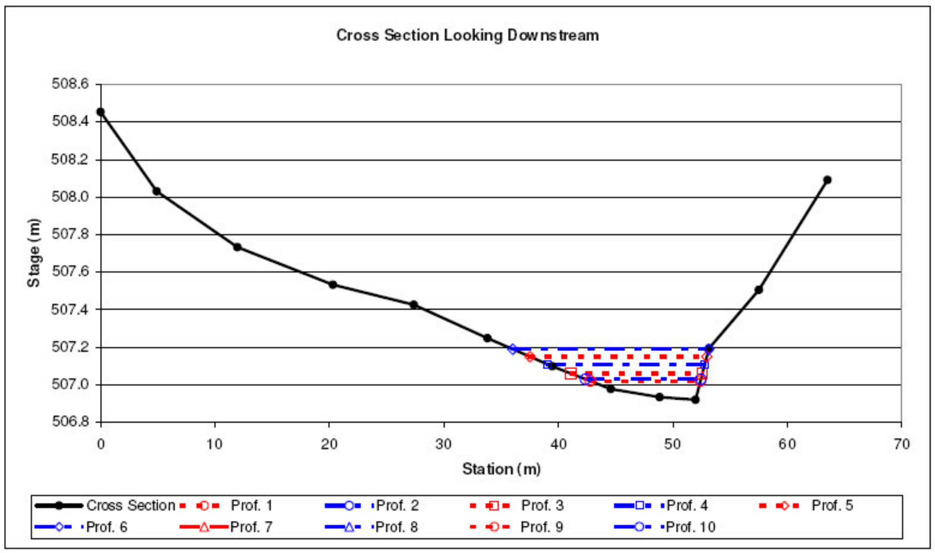

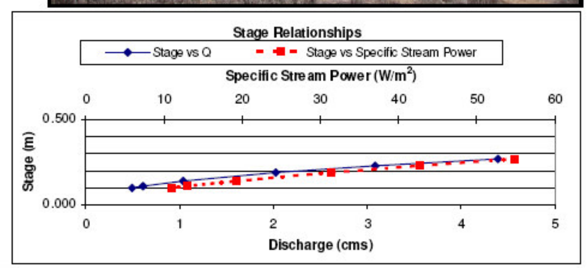

Prof. ID	Estimated n-value	L-Limit	R-Limit	WS (m)	Depth (m)	Left Sta (m)	Right Sta (m)	P_w (m)	Area (m^2)	W (m)	R (m)	D (m)	W/d	V (m/s)	Q (m^3/s)	U* (m/s)	τ (kg/ms^2)	τ*	ω (W/m^2)	Ω (W/m)	F_r	R/d_{84}	n-value per Limerino	Floodplain Form
PLSC06P01	0.030			507.02	0.100	42.79	52.41	9.63	0.62	9.62	0.06	0.06	96.6	0.8	0.49	0.12	13.8	0.949	11	105	1.07	22.2	0.019	PFB
PLSC06P02	0.030			507.03	0.110	42.36	52.45	10.10	0.72	10.09	0.07	0.07	92.1	0.8	0.61	0.12	15.2	1.049	13	130	1.08	24.5	0.018	PFB
PLSC06P03	0.030			507.06	0.140	41.09	52.58	11.51	1.04	11.49	0.09	0.09	82.3	1.0	1.04	0.14	19.4	1.334	19	222	1.13	31.2	0.018	PFB
PLSC06P04	0.030			507.11	0.190	39.02	52.80	13.79	1.68	13.77	0.12	0.12	72.6	1.2	2.02	0.16	26.0	1.787	31	433	1.18	41.8	0.018	PFB
PLSC06P05	0.030			507.15	0.230	37.52	52.97	15.48	2.26	15.45	0.15	0.15	67.3	1.4	3.09	0.18	31.2	2.148	43	660	1.22	50.2	0.018	PFB
PLSC06P06	0.030			507.19	0.270	36.01	53.14	17.16	2.91	17.13	0.17	0.17	63.5	1.5	4.39	0.19	36.3	2.496	55	940	1.25	58.3	0.018	PFB
PLSC06P07	0.030																							PFB
PLSC06P08	0.030																							PFB
PLSC06P09	0.030																							PFB
PLSC06P10	0.030																							PFB

Cross Section Hydraulic Analyses: Perris Lake Site C

Floodplain/Site Description: Photo view looking downstream to Section 7 from the left bank of Section 8.

Location ID	PLSC07
d_{50} (mm) =	0.90
d_{84} (mm) =	2.91
So = Sf =	0.0218

Pt #	Sta (m)	Stage (m)
1	0.00	510.99
2	4.62	510.12
3	10.03	509.24
4	15.49	509.05
5	20.15	509.23
6	25.56	509.58
7	33.45	509.67
8	37.08	509.72
9	44.50	509.92
10	49.91	509.87
11	55.89	509.87
12	62.27	509.87
13	66.76	509.88
14	69.62	510.04
15	72.61	510.24
16	76.15	510.51
17	79.29	510.81
18	82.95	511.24
19	86.95	511.75
20	90.65	512.32
21		
22		
23		
24		
25		
26		
27		
28		
29		
30		
31		
32		
33		
34		
35		
min. Stage =		509.05
Continuum		1b
CEM		1

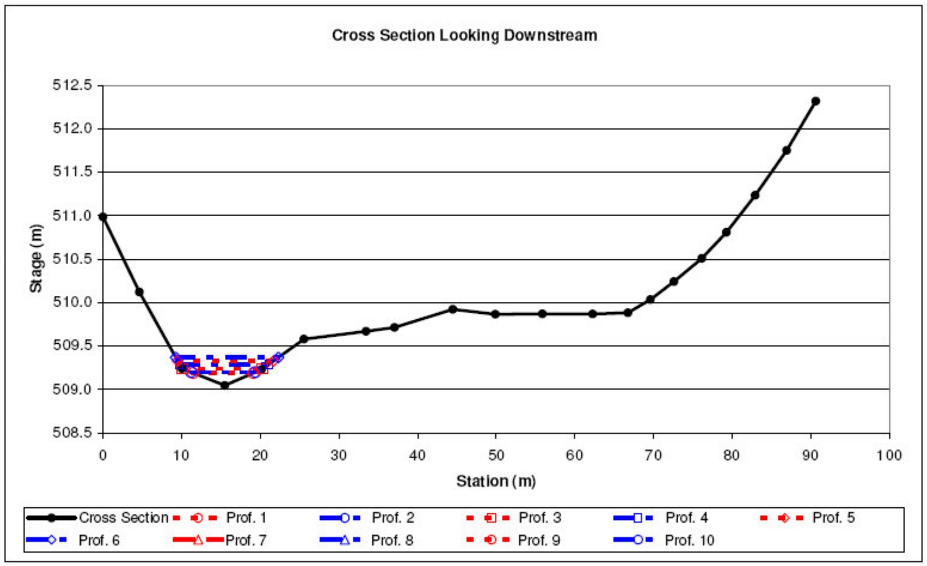

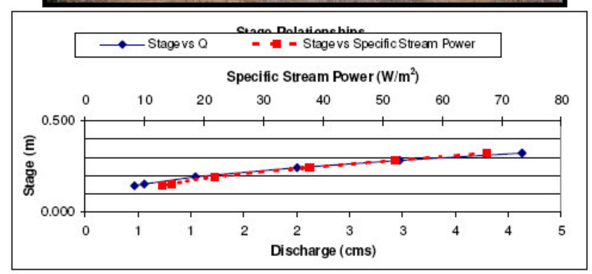

Prof. ID	Estimated n-value	L-Limit	R-Limit	WS (m)	Depth (m)	Left Sta (m)	Right Sta (m)	P_w (m)	Area (m^2)	W (m)	R (m)	D (m)	W/d	V (m/s)	Q (m^3/s)	U* (m/s)	τ (kg/ms²)	τ*	ω (W/m²)	Ω (W/m)	F_r	R/d_{84}	n-value per Limerino	Floodplain Form
PLSC07P01	0.030			509.19	0.143	11.47	19.15	7.69	0.55	7.68	0.07	0.07	53.6	0.8	0.47	0.12	15.3	1.054	13	100	1.09	24.6	0.018	PFB
PLSC07P02	0.030			509.20	0.153	11.18	19.40	8.22	0.63	8.22	0.08	0.08	53.6	0.9	0.56	0.13	16.4	1.127	15	120	1.10	26.3	0.018	PFB
PLSC07P03	0.030			509.24	0.193	10.06	20.32	10.26	1.00	10.25	0.10	0.10	53.0	1.0	1.04	0.14	20.9	1.435	22	223	1.14	33.5	0.018	PFB
PLSC07P04	0.030			509.29	0.243	9.73	21.08	11.37	1.54	11.35	0.14	0.14	46.6	1.3	2.00	0.17	29.0	1.995	38	428	1.21	46.6	0.018	PFB
PLSC07P05	0.030			509.33	0.283	9.49	21.70	12.23	2.01	12.21	0.16	0.16	43.1	1.5	2.98	0.19	35.2	2.421	52	636	1.25	56.6	0.018	PFB
PLSC07P06	0.030			509.37	0.323	9.24	22.32	13.10	2.52	13.08	0.19	0.19	40.4	1.6	4.13	0.20	41.1	2.828	68	883	1.28	66.1	0.018	PFB
PLSC07P07	0.030																							PFB
PLSC07P08	0.030																							PFB
PLSC07P09	0.030																							PFB
PLSC07P10	0.030																							PFB

Cross Section Hydraulic Analyses: Perris Lake Site C

Floodplain/Site Description: Photo view is looking upstream along left bank from Section 7 toward Section 8

Location ID	PLSC08
d_{50} (mm) =	0.90
d_{84} (mm) =	2.91
So = Sf =	0.0165

Pt #	Sta (m)	Stage (m)
1	0.00	511.33
2	5.29	511.05
3	11.02	510.75
4	17.23	510.51
5	23.76	510.34
6	24.99	510.12
7	30.03	510.37
8	34.13	510.52
9	35.21	510.85
10	36.47	510.92
11	41.08	510.88
12	46.25	510.77
13	50.05	510.64
14	54.73	510.50
15	61.11	510.41
16	64.65	510.46
17	67.31	510.59
18	70.26	510.86
19	73.90	511.36
20	78.40	511.89
21	81.82	512.32
22		
23		
24		
25		
26		
27		
28		
29		
30		
31		
32		
33		
34		
35		
min. Stage =		510.12
Continuum		1b
CEM		2

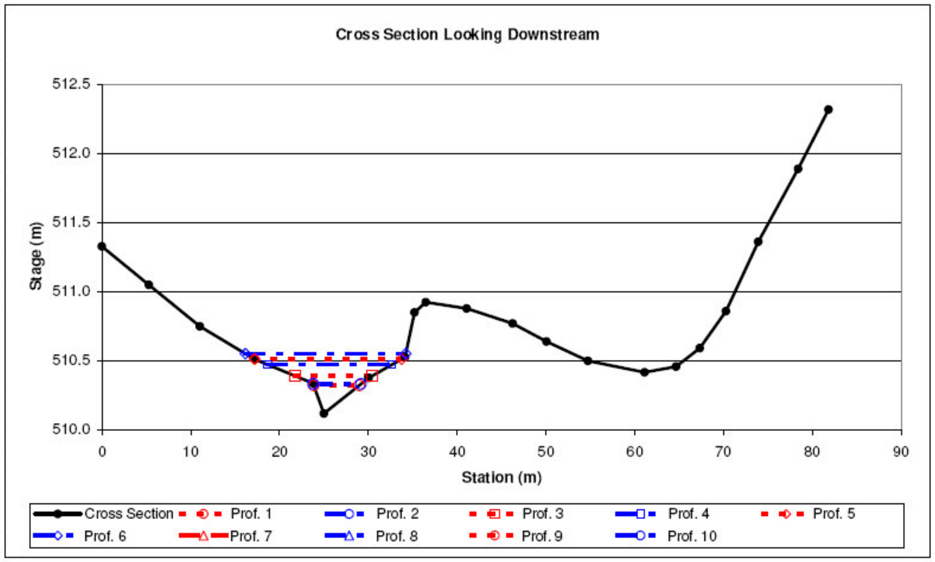

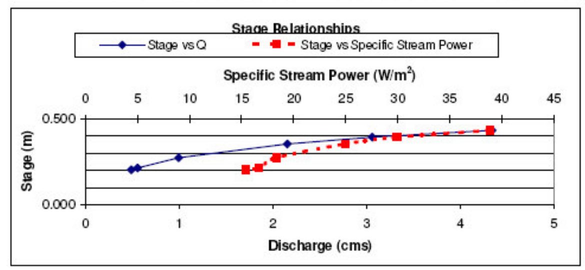

Prof. ID	Estimated n-value	L-Limit	R-Limit	WS (m)	Depth (m)	Left Sta (m)	Right Sta (m)	P_w (m)	Area (m^2)	W (m)	R (m)	D (m)	W/d	V (m/s)	Q (m^3/s)	U* (m/s)	τ (kg/ms^2)	τ*	ω (W/m^2)	Ω (W/m)	F_r	R/d_{84}	n-value per Limerino	Floodplain Form
PLSC08P01	0.030		36.47	510.32	0.204	23.85	28.98	5.16	0.52	5.14	0.10	0.10	25.2	0.9	0.49	0.13	16.5	1.131	15	79	1.00	34.9	0.018	PFB
PLSC08P02	0.030		36.47	510.33	0.214	23.79	29.18	5.41	0.58	5.39	0.11	0.11	25.2	1.0	0.56	0.13	17.3	1.187	17	90	1.01	36.6	0.018	PFB
PLSC08P03	0.030		36.47	510.39	0.274	21.70	30.48	8.80	0.99	8.77	0.11	0.11	32.0	1.0	0.99	0.14	18.3	1.257	18	161	1.02	38.8	0.018	PFB
PLSC08P04	0.030		36.47	510.47	0.354	18.68	32.66	14.01	1.90	13.98	0.14	0.14	39.5	1.1	2.16	0.15	22.0	1.513	25	349	1.05	46.7	0.018	PFB
PLSC08P05	0.030		36.47	510.51	0.394	17.19	33.75	16.59	2.52	16.56	0.15	0.15	42.0	1.2	3.06	0.16	24.5	1.688	30	496	1.07	52.1	0.018	PFB
PLSC08P06	0.030		36.47	510.55	0.434	16.15	34.21	18.10	3.21	18.07	0.18	0.18	41.6	1.4	4.34	0.17	28.7	1.975	39	703	1.10	61.0	0.018	PFB
PLSC08P07	0.030																							PFB
PLSC08P08	0.030																							PFB
PLSC08P09	0.030																							PFB
PLSC08P10	0.030																							PFB

Cross Section Hydraulic Analyses: Perris Lake Site D/Site 4

Floodplain/Site Description: Perris Lake Site D (Site 4). Photo shows downstream cross section looking upstream (Jan 08).

Location ID		PLSD01
d_{50} (mm) =		0.91
d_{84} (mm) =		1.91
So = Sf =		0.0094
Pt #	Sta (m)	Stage (m)
1	0.00	101.01
2	1.30	100.91
3	2.40	100.51
4	4.60	100.52
5	6.80	100.45
6	10.00	100.58
7	13.65	100.65
8	18.00	100.65
9	20.00	100.73
10	25.00	100.70
11	30.00	100.68
12	35.00	100.60
13	38.00	100.53
14	41.10	100.53
15	44.50	100.49
16	45.00	100.49
17	48.00	100.44
18	49.20	100.59
19	50.00	100.74
20	52.00	100.65
21	56.50	100.65
22	57.00	100.50
23	57.50	100.50
24	58.00	100.65
25		
26		
27		
28		
29		
30		
31		
32		
33		
34		
35		
min. Stage =		100.44
Continuum		1b
CEM		1.00

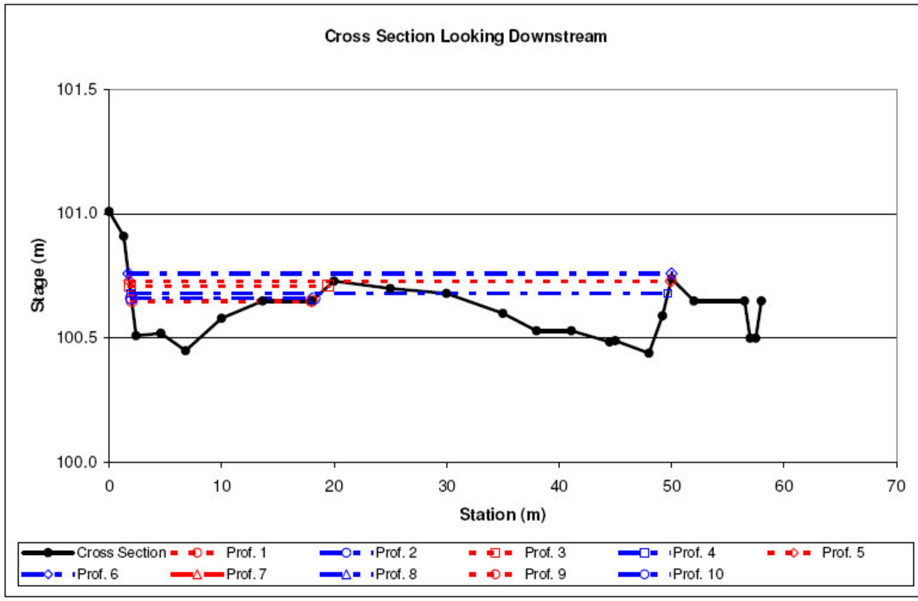

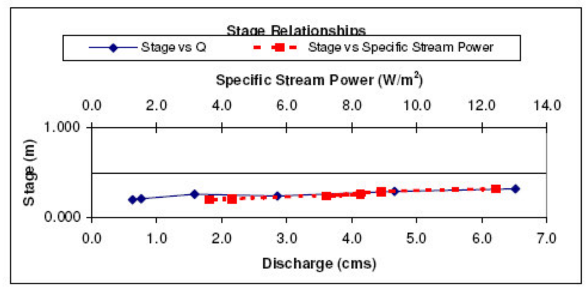

Prof. ID	Estimated n-value	L-Limit	R-Limit	WS (m)	Depth (m)	Left Sta (m)	Right Sta (m)	P_w (m)	Area (m^2)	W (m)	R (m)	D (m)	W/d	V (m/s)	Q (m^3/s)	U* (m/s)	τ (kg/ms²)	τ^*	ω (W/m²)	Ω (W/m)	F_r	R/d_{84}	n-value per Limerinos	Floodplain Form
PLSD01P01	0.035		20.00	100.65	0.200	2.01	18.00	16.01	1.25	15.99	0.08	0.08	80	0.5	0.6	0.08	7.2	0.488	3.6	58	0.62	40.8	0.017	BF
PLSD01P02	0.035		20.00	100.66	0.210	1.99	18.25	16.29	1.41	16.26	0.09	0.09	77	0.5	0.8	0.09	8.0	0.542	4.3	70	0.63	45.2	0.017	BF
PLSD01P03	0.035		20.00	100.71	0.260	1.85	19.50	17.69	2.26	17.65	0.13	0.13	68	0.7	1.6	0.11	11.8	0.800	8.3	146	0.67	66.8	0.017	BF
PLSD01P04	0.035		50.00	100.68	0.240	1.93	49.68	36.55	4.30	36.50	0.12	0.12	152	0.7	2.9	0.10	10.8	0.737	7.2	263	0.66	61.5	0.017	BF
PLSD01P05	0.035		50.00	100.73	0.290	1.79	49.95	48.22	6.44	48.15	0.13	0.13	166	0.7	4.7	0.11	12.3	0.837	8.9	430	0.68	69.9	0.017	BF
PLSD01P06	0.035		50.00	100.76	0.320	1.71	50.00	48.36	7.88	48.29	0.16	0.16	151	0.8	6.5	0.12	15.0	1.022	12.4	601	0.70	85.4	0.017	BF
PLSD01P07	0.035																							BF
PLSD01P08	0.035																							BF
PLSD01P09	0.035																							BF
PLSD01P10	0.035																							BF

Cross Section Hydraulic Analyses: Perris Lake Site D/Site 4

Floodplain/Site Description: Lake Perris Site D/4. Photo shows site looking downstream.

Location ID	PLSD02	
d_{50} (mm) =	0.94	
d_{84} (mm) =	1.79	
So = Sf =	0.0088	
Pt#	Sta (m)	Stage (m)
1	0.00	101.80
2	2.00	101.77
3	2.90	101.72
4	3.65	101.58
5	4.60	101.50
6	6.00	101.54
7	8.00	101.56
8	10.00	101.53
9	13.00	101.48
10	15.70	101.46
11	17.00	101.52
12	18.30	101.78
13	18.40	101.77
14	19.70	102.06
15	20.95	102.10
16		
17		
18		
19		
20		
21		
22		
23		
24		
25		
26		
27		
28		
29		
30		
31		
32		
33		
34		
35		
min. Stage =	101.46	
Continuum	1b	
CEM	1.00	

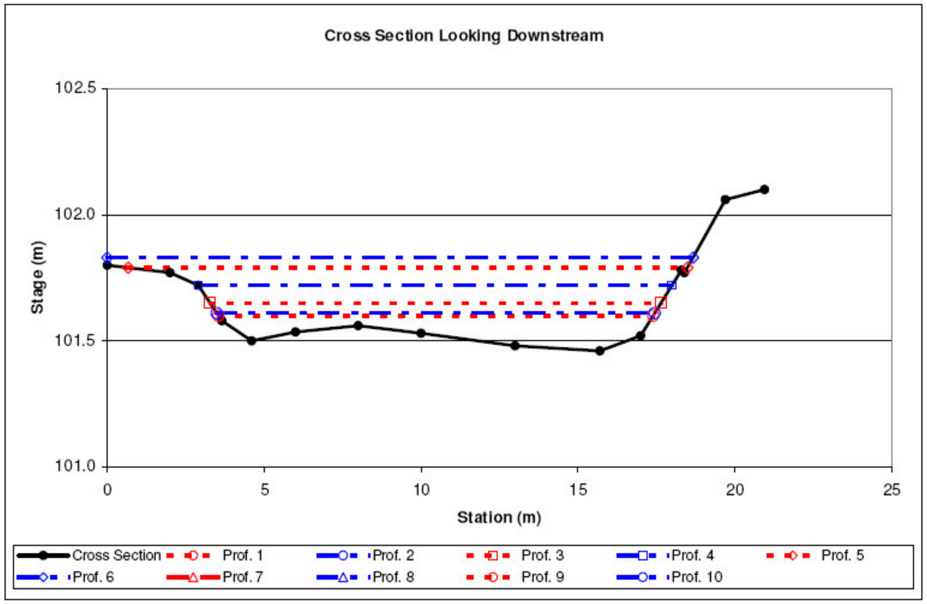

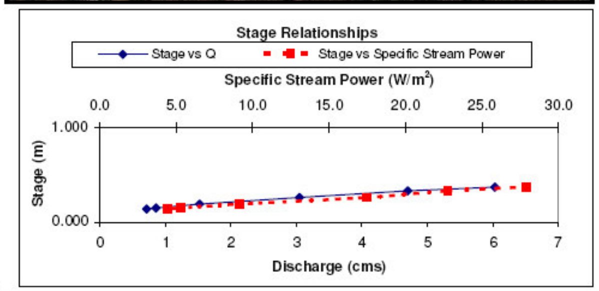

Prof. ID	Estimated n-value	L-Limit	R-Limit	WS (m)	Depth (m)	Left Sta (m)	Right Sta (m)	P_w (m)	Area (m^2)	W (m)	R (m)	D (m)	W/d	V (m/s)	Q (m^3/s)	U* (m/s)	τ (kg/ms²)	τ*	ω (W/m²)	Ω (W/m)	F_r	R/d_{84}	n-value per Limerino	Floodplain Form
PLSD02P01	0.030			101.60	0.140	3.54	17.40	13.87	1.18	13.86	0.09	0.09	99.0	0.6	0.7	0.09	7.4	0.485	4.5	62	0.71	47.7	0.017	PFB
PLSD02P02	0.030			101.61	0.150	3.49	17.45	13.98	1.32	13.96	0.09	0.09	93.1	0.6	0.9	0.09	8.2	0.538	5.3	74	0.72	52.9	0.017	PFB
PLSD02P03	0.030			101.65	0.190	3.27	17.65	14.40	1.89	14.38	0.13	0.13	75.7	0.8	1.5	0.11	11.3	0.746	9.2	132	0.76	73.3	0.016	PFB
PLSD02P04	0.030			101.72	0.260	2.90	18.00	15.14	2.92	15.10	0.19	0.19	58.1	1.0	3.0	0.13	16.7	1.097	17.4	263	0.81	107.8	0.016	PFB
PLSD02P05	0.030			101.79	0.330	0.67	18.49	17.87	4.05	17.82	0.23	0.23	54.0	1.2	4.7	0.14	19.5	1.287	22.8	406	0.83	126.5	0.016	PFB
PLSD02P06	0.030			101.83	0.370	0.00	18.67	18.72	4.79	18.67	0.26	0.26	50.5	1.3	6.0	0.15	22.1	1.453	27.9	520	0.85	142.8	0.016	PFB
PLSD02P07	0.030																							PFB
PLSD02P08	0.030																							PFB
PLSD02P09	0.030																							PFB
PLSD02P10	0.030																							PFB

Cross Section Hydraulic Analyses: Perris Lake Site D/Site 4

Floodplain/Site Description: Perris Lake Site D/4. Photo shows upstream cross section looking downstream (Jan 08).

Location ID		PLSD03
d_{50} (mm) =		0.76
d_{84} (mm) =		1.70
So = Sf =		0.0056
Pt #	Sta (m)	Stage (m)
1	0.00	102.69
2	2.00	102.38
3	2.80	102.33
4	3.30	102.19
5	4.00	102.11
6	4.90	102.15
7	5.60	102.17
8	6.30	102.14
9	7.00	102.09
10	9.10	102.07
11	9.70	102.13
12	10.40	102.39
13	12.00	102.38
14	13.00	102.67
15		
16		
17		
18		
19		
20		
21		
22		
23		
24		
25		
26		
27		
28		
29		
30		
31		
32		
33		
34		
35		
min. Stage =		102.07
Continuum		1b
CEM		1.00

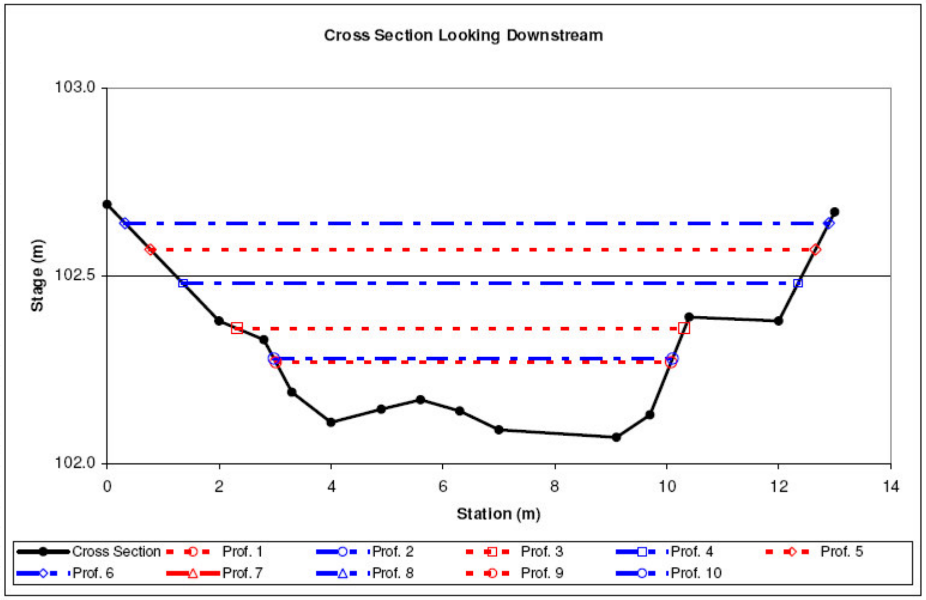

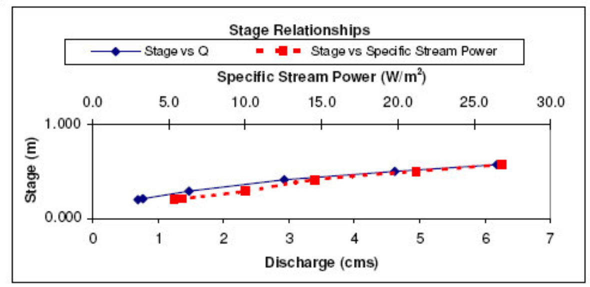

Prof. ID	Estimated n-value	L-Limit	R-Limit	WS (m)	Depth (m)	Left Sta (m)	Right Sta (m)	P_w (m)	Area (m^2)	W (m)	R (m)	D (m)	W/d	V (m/s)	Q (m^3/s)	U* (m/s)	τ (kg/ms^2)	τ^*	ω (W/m^2)	Ω (W/m)	F_r	R/d_{84}	n-value per Limerino	Floodplain Form
PLSD03P01	0.030			102.27	0.200	3.01	10.08	7.11	1.02	7.06	0.14	0.14	35.3	0.7	0.7	0.09	7.8	0.636	5.3	38	0.61	84.3	0.016	PFB
PLSD03P02	0.030			102.28	0.210	2.98	10.10	7.18	1.09	7.13	0.15	0.15	33.9	0.7	0.8	0.09	8.3	0.674	5.9	42	0.62	89.3	0.016	PFB
PLSD03P03	0.030			102.36	0.290	2.32	10.32	8.07	1.69	8.00	0.21	0.21	27.6	0.9	1.5	0.11	11.4	0.927	10.0	80	0.65	122.8	0.016	PFB
PLSD03P04	0.030			102.48	0.410	1.35	12.34	11.09	2.89	10.99	0.26	0.26	26.8	1.0	2.9	0.12	14.2	1.157	14.5	160	0.68	153.3	0.016	PFB
PLSD03P05	0.030			102.57	0.500	0.77	12.66	12.00	3.92	11.88	0.33	0.33	23.8	1.2	4.6	0.13	17.8	1.450	21.2	252	0.70	192.1	0.016	PFB
PLSD03P06	0.030			102.64	0.570	0.32	12.90	12.71	4.78	12.57	0.38	0.38	22.1	1.3	6.2	0.14	20.5	1.668	26.8	337	0.72	221.0	0.016	PFB
PLSD03P07	0.030																							PFB
PLSD03P08	0.030																							PFB
PLSD03P09	0.030																							PFB
PLSD03P10	0.030																							PFB

Cross Section Hydraulic Analyses: Un-Named Creek at Pigeon Pass

Floodplain/Site Description: Photo view looking upstream from cross section.

Pt #	Sta (m)	Stage (m)
Location ID		PPSB01
d_{50} (mm) =		1.53
d_{84} (mm) =		3.29
So = Sf =		0.0088
1	3.00	102.01
2	5.00	101.76
3	6.40	101.48
4	7.70	100.90
5	8.00	100.36
6	8.10	100.23
7	8.80	100.00
8	9.00	100.06
9	9.60	100.12
10	10.10	100.35
11	10.80	100.55
12	11.90	100.69
13	12.40	100.92
14	13.20	101.52
15	13.40	101.67
16	14.50	102.00
17		
18		
19		
20		
21		
22		
23		
24		
25		
26		
27		
28		
29		
30		
31		
32		
33		
34		
35		
min. Stage =		100.00
Continuum		1b
CEM		1

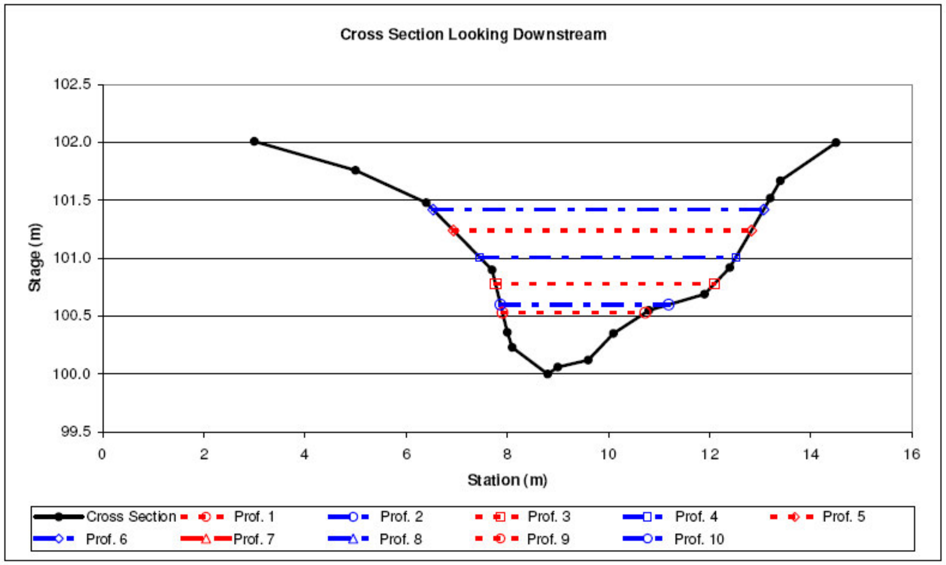

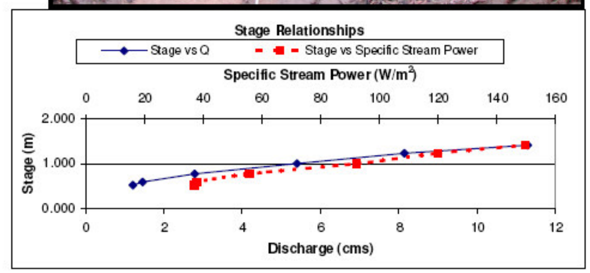

Prof. ID	Estimated n-value	L-Limit	R-Limit	WS (m)	Depth (m)	Left Sta (m)	Right Sta (m)	P_w (m)	Area (m^2)	W (m)	R (m)	D (m)	W/d	V (m/s)	Q (m^3/s)	U* (m/s)	τ (kg/ms²)	τ*	ω (W/m²)	Ω (W/m)	F_r	R/d_{84}	n-value per Limerino	Floodplain Form
PPSB01P01	0.030			100.53	0.530	7.91	10.73	3.11	0.89	2.82	0.29	0.32	5.3	1.4	1.21	0.16	24.8	1.003	37	105	0.83	86.9	0.018	PFB
PPSB01P02	0.032			100.60	0.600	7.87	11.19	3.66	1.10	3.33	0.30	0.33	5.5	1.3	1.46	0.16	26.1	1.057	38	126	0.78	91.6	0.018	PFB
PPSB01P03	0.032			100.78	0.780	7.77	12.10	4.80	1.82	4.33	0.38	0.42	5.5	1.5	2.79	0.18	32.8	1.327	56	242	0.81	115.1	0.018	PFB
PPSB01P04	0.032			101.01	1.010	7.45	12.52	5.69	2.89	5.07	0.51	0.57	5.0	1.9	5.4	0.21	44.0	1.782	92	469	0.85	154.4	0.018	PFB
PPSB01P05	0.035			101.24	1.240	6.94	12.83	6.64	4.15	5.89	0.63	0.70	4.7	2.0	8.2	0.23	54.2	2.193	120	707	0.80	190.1	0.018	PFB
PPSB01P06	0.035			101.42	1.420	6.53	13.07	7.38	5.27	6.53	0.71	0.81	4.6	2.1	11.3	0.25	61.9	2.504	150	980	0.82	217.0	0.018	PFB
PPSB01P07	0.035																							PFB
PPSB01P08	0.035																							PFB
PPSB01P09	0.035																							PFB
PPSB01P10	0.035																							PFB

Cross Section Hydraulic Analyses: Proctor Valley

Floodplain/Site Description: Proctor Valley Site with photograph looking upstream (October 07). Cross Section extended per field observations and DEM data.

Location ID		PVPV01
d_{50} (mm) =		1.62
d_{84} (mm) =		17.66
So = Sf =		0.0119
Pt #	Sta (m)	Stage (m)
1	0.00	247.79
2	4.00	247.45
3	5.13	247.35
4	5.95	247.20
5	6.68	247.11
6	6.92	247.01
7	7.34	247.13
8	8.18	247.14
9	8.88	246.96
10	9.55	247.10
11	10.41	247.02
12	11.12	246.95
13	11.81	246.98
14	12.19	246.88
15	12.65	246.66
16	13.00	246.63
17	13.44	246.61
18	13.83	246.81
19	14.23	246.88
20	14.62	246.91
21	14.97	247.01
22	15.64	247.10
23	16.61	247.20
24	17.57	247.33
25	29.57	247.45
26	32.57	247.85
27		
28		
29		
30		
31		
32		
33		
34		
35		
min. Stage =		246.61
Continuum		1b
CEM		1

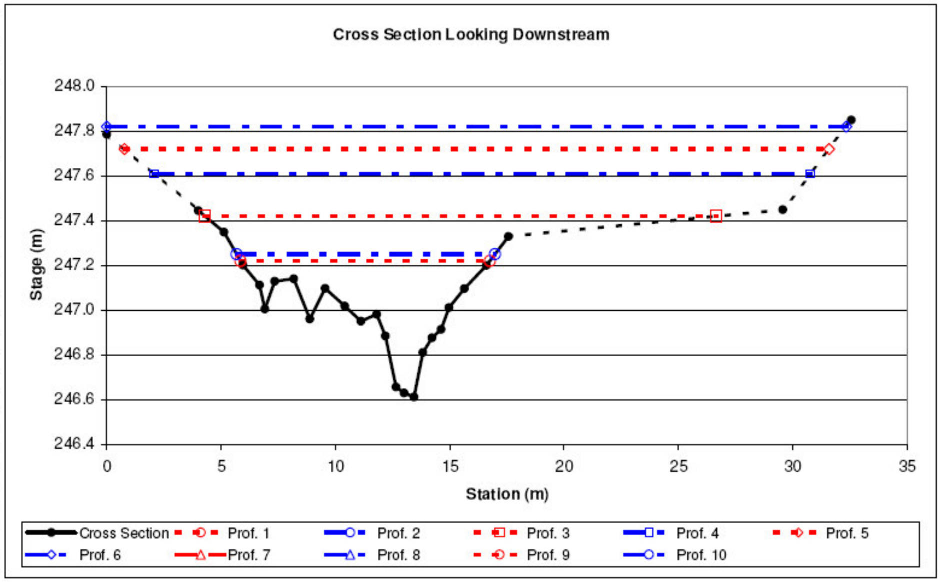

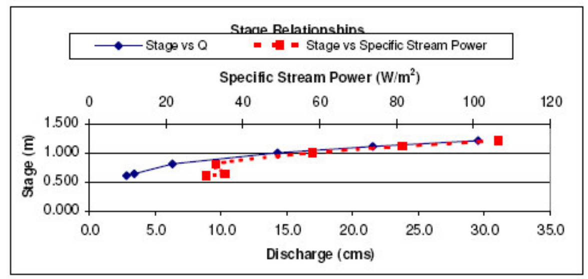

Prof. ID	Estimated n-value	L-Limit	R-Limit	WS (m)	Depth (m)	Left Sta (m)	Right Sta (m)	P_w (m)	Area (m^2)	W (m)	R (m)	D (m)	W/d	V (m/s)	Q (m^3/s)	U* (m/s)	τ (kg/ms^2)	τ*	ω (W/m^2)	Ω (W/m)	F_r	R/d_{84}	n-value per Limerino	Floodplain Form
PVPV01P01	0.035			247.22	0.609	5.85	16.76	11.15	2.48	10.91	0.22	0.23	17.9	1.1	2.8	0.16	26.0	0.993	30	332	0.82	12.6	0.026	PMB
PVPV01P02	0.035			247.25	0.639	5.68	16.98	11.55	2.82	11.30	0.24	0.25	17.7	1.2	3.4	0.17	28.5	1.088	35	400	0.83	13.8	0.026	PMB
PVPV01P03	0.035			247.42	0.809	4.29	26.67	22.64	5.32	22.38	0.24	0.24	27.7	1.2	6.3	0.17	27.5	1.049	33	738	0.83	13.3	0.026	PMB
PVPV01P04	0.040			247.61	0.999	2.06	30.78	28.99	10.39	28.71	0.36	0.36	28.7	1.4	14.3	0.20	41.8	1.599	58	1670	0.78	20.3	0.025	PMB
PVPV01P05	0.040			247.72	1.109	0.77	31.60	31.12	13.67	30.83	0.44	0.44	27.8	1.6	21.5	0.23	51.3	1.959	82	2514	0.81	24.9	0.025	PMB
PVPV01P06	0.040			247.82	1.209	0.00	32.35	32.65	16.84	32.35	0.52	0.52	26.8	1.8	29.5	0.25	60.2	2.300	107	3448	0.83	29.2	0.025	PMB
PVPV01P07	0.040																							PMB
PVPV01P08	0.040																							PMB
PVPV01P09	0.040																							PMB
PVPV01P10	0.040																							PMB

Cross Section Hydraulic Analyses: Proctor Valley

Floodplain/Site Description: Proctor Valley Site with photograph looking downstream (October 07). Cross Section extended per field observations and DEM data.

Location ID		PVPV02
d_{50} (mm) =		1.62
d_{84} (mm) =		17.66
So = Sf =		0.0119
Pt #	Sta (m)	Stage (m)
1	0.00	247.97
2	0.99	247.82
3	2.00	247.65
4	2.98	247.50
5	3.98	247.36
6	4.41	247.05
7	4.69	247.09
8	5.21	247.40
9	6.18	247.42
10	7.67	247.35
11	8.35	247.21
12	9.10	247.23
13	9.97	247.19
14	10.88	247.15
15	11.51	246.81
16	11.82	246.48
17	12.34	246.29
18	12.85	246.27
19	13.23	246.29
20	13.50	246.37
21	14.00	247.10
22	14.74	247.40
23	15.36	247.53
24	15.82	247.55
25	27.82	247.67
26	29.82	248.10
27		
28		
29		
30		
31		
32		
33		
34		
35		
min. Stage =		246.27
Continuum		1b
CEM		1

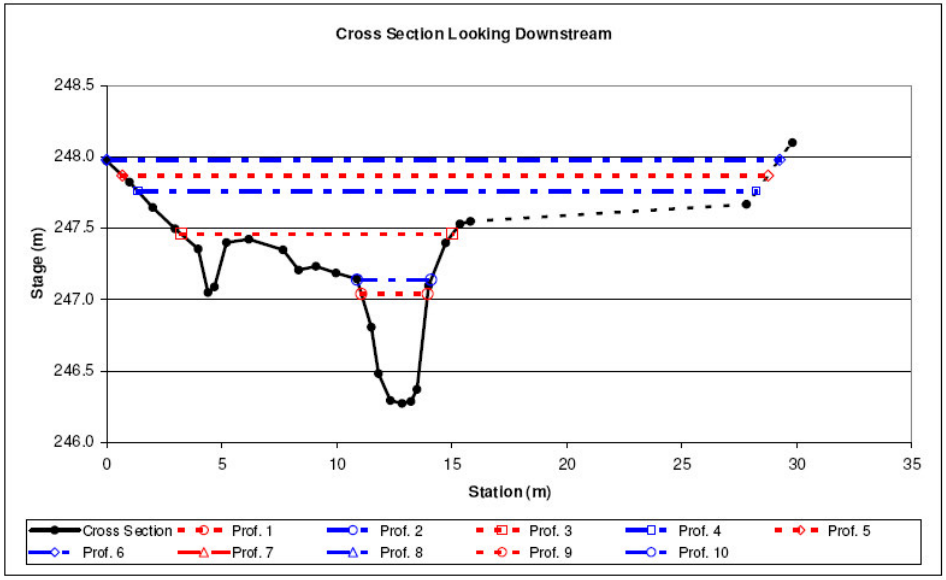

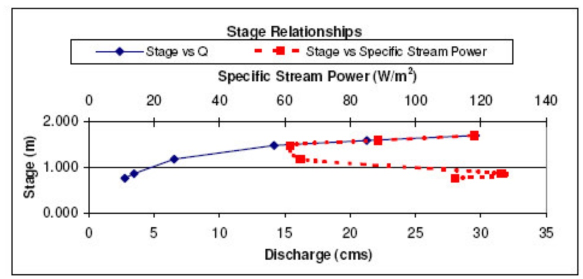

Prof. ID	Estimated n-value	L-Limit	R-Limit	WS (m)	Depth (m)	Left Sta (m)	Right Sta (m)	P_w (m)	Area (m^2)	W (m)	R (m)	D (m)	W/d	V (m/s)	Q (m^3/s)	U* (m/s)	τ (kg/ms²)	τ*	ω (W/m²)	Ω (W/m)	F_r	R/d_{84}	n-value per Limerino	Floodplain Form
PVPV02P01	0.035			247.04	0.768	11.07	13.96	3.48	1.53	2.89	0.44	0.53	3.8	1.8	2.8	0.23	51.5	1.966	112	323	0.85	25.0	0.025	PMB
PVPV02P02	0.035	9.97		247.14	0.868	10.89	14.10	3.88	1.84	3.22	0.47	0.57	3.7	1.9	3.5	0.24	55.3	2.114	126	406	0.86	26.8	0.025	PMB
PVPV02P03	0.035			247.46	1.188	3.24	15.03	12.73	4.32	11.80	0.34	0.37	9.9	1.5	6.5	0.20	39.6	1.513	65	764	0.86	19.2	0.025	PMB
PVPV02P04	0.040			247.76	1.488	1.36	28.25	27.86	10.18	26.89	0.37	0.38	18.1	1.4	14.2	0.21	42.7	1.630	62	1657	0.78	20.7	0.025	PMB
PVPV02P05	0.040			247.87	1.598	0.69	28.75	29.06	13.20	28.07	0.45	0.47	17.6	1.6	21.3	0.23	53.0	2.026	89	2484	0.80	25.7	0.025	PMB
PVPV02P06	0.040			247.98	1.708	0.00	29.26	30.28	16.36	29.26	0.54	0.56	17.1	1.8	29.6	0.25	63.1	2.410	118	3455	0.83	30.6	0.025	PMB
PVPV02P07	0.040																							PMB
PVPV02P08	0.040																							PMB
PVPV02P09	0.040																							PMB
PVPV02P10	0.040																							PMB

Cross Section Hydraulic Analyses: Proctor Valley

Floodplain/Site Description: Proctor Valley Site with photograph looking downstream (October 07). Cross Section extended per field observations and DEM data.

Location ID	PVPV03
d_{50} (mm) =	1.62
d_{84} (mm) =	17.66
So = Sf =	0.0119

Pt #	Sta (m)	Stage (m)
1	0.00	248.25
2	4.63	247.59
3	4.92	247.51
4	5.41	247.60
5	6.23	247.65
6	8.17	247.57
7	8.42	247.40
8	8.70	247.41
9	9.07	247.55
10	9.98	247.54
11	10.53	247.56
12	11.00	247.37
13	11.54	247.07
14	11.97	247.07
15	12.43	247.51
16	12.80	247.50
17	13.06	247.21
18	13.52	247.24
19	13.64	247.33
20	13.80	247.40
21	13.98	247.18
22	14.32	247.13
23	14.77	247.25
24	15.04	247.12
25	15.60	247.08
26	16.05	247.27
27	16.58	247.44
28	17.00	247.11
29	17.64	247.37
30	18.91	247.32
31	19.35	247.23
32	19.97	247.45
33	21.22	247.77
34	23.00	248.04
35	28.00	248.36
min. Stage =		247.07
Continuum		1b
CEM		1.00

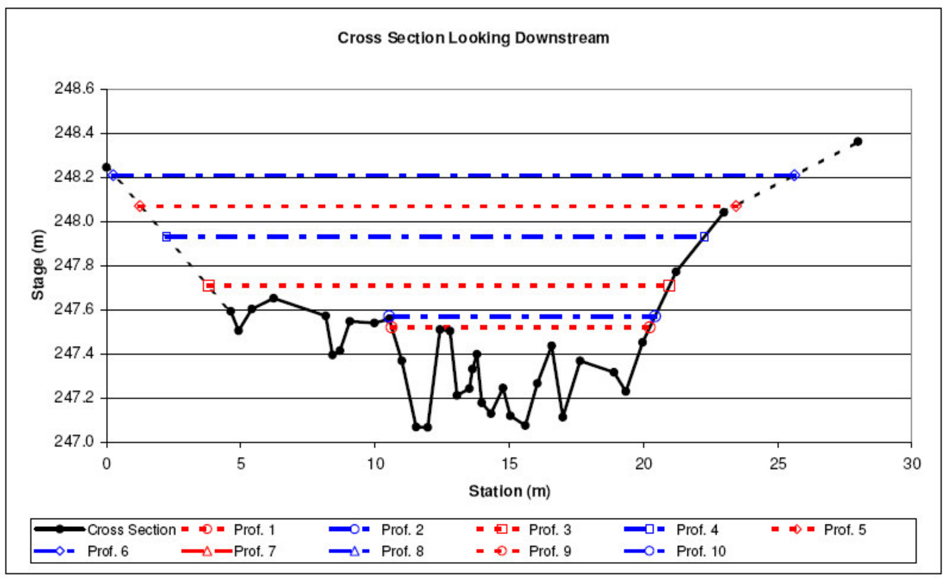

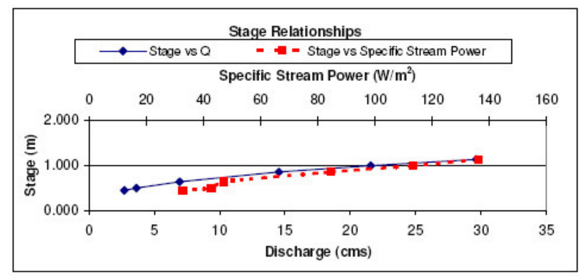

Prof. ID	Estimated n-value	L-Limit	R-Limit	WS (m)	Depth (m)	Left Sta (m)	Right Sta (m)	P_w (m)	Area (m^2)	W (m)	R (m)	D (m)	W/d	V (m/s)	Q (m^3/s)	U* (m/s)	τ (kg/ms²)	τ*	ω (W/m^2)	Ω (W/m)	F_r	R/d_{84}	n-value per Limerino	Floodplain Form
PVPV03P01	0.035	10.53		247.52	0.454	10.62	20.24	10.51	2.36	9.61	0.22	0.24	21.2	1.1	2.7	0.16	26.2	0.999	33	316	0.80	12.7	0.026	PMB
PVPV03P02	0.035	10.53		247.57	0.504	10.53	20.43	10.81	2.84	9.90	0.26	0.29	19.6	1.3	3.6	0.18	30.7	1.173	43	425	0.82	14.9	0.026	PMB
PVPV03P03	0.035			247.71	0.644	3.80	20.98	18.23	5.17	17.18	0.28	0.30	26.7	1.3	6.9	0.18	33.1	1.264	47	811	0.84	16.0	0.026	PMB
PVPV03P04	0.040			247.93	0.864	2.24	22.27	21.11	9.25	20.03	0.44	0.46	23.2	1.6	14.5	0.23	51.1	1.954	85	1698	0.79	24.8	0.025	PMB
PVPV03P05	0.040			248.07	1.004	1.25	23.45	23.30	12.19	22.21	0.52	0.55	22.1	1.8	21.6	0.25	61.1	2.333	113	2519	0.82	29.6	0.025	PMB
PVPV03P06	0.040			248.21	1.144	0.25	25.63	26.49	15.52	25.38	0.59	0.61	22.2	1.9	29.6	0.26	68.4	2.613	136	3459	0.84	33.2	0.025	PMB
PVPV03P07	0.040																							PMB
PVPV03P08	0.040																							PMB
PVPV03P09	0.040																							PMB
PVPV03P10	0.040																							PMB

Cross Section Hydraulic Analyses: Proctor Valley

Floodplain/Site Description: Proctor Valley Site with photograph looking downstream (October 07). Cross Section extended per field observations and DEM data.

Location ID	PVPV04
d_{50} (mm) =	1.62
d_{84} (mm) =	17.66
So = Sf =	0.0119

Pt #	Sta (m)	Stage (m)
1	0.00	248.77
2	3.00	248.28
3	3.63	248.17
4	4.40	248.07
5	5.44	248.10
6	6.05	248.06
7	6.62	248.00
8	7.32	247.96
9	8.04	247.74
10	8.34	247.79
11	8.98	247.69
12	9.42	247.68
13	9.56	247.53
14	9.87	247.27
15	10.49	247.20
16	10.93	247.61
17	11.39	247.78
18	11.80	247.68
19	12.29	247.75
20	12.96	247.93
21	13.82	247.94
22	14.80	247.96
23	15.79	248.10
24	16.87	248.12
25	17.67	248.11
26	18.45	248.22
27	30.45	248.34
28	33.45	248.74
29		
30		
31		
32		
33		
34		
35		
min. Stage =		247.20
Continuum		1b
CEM		1

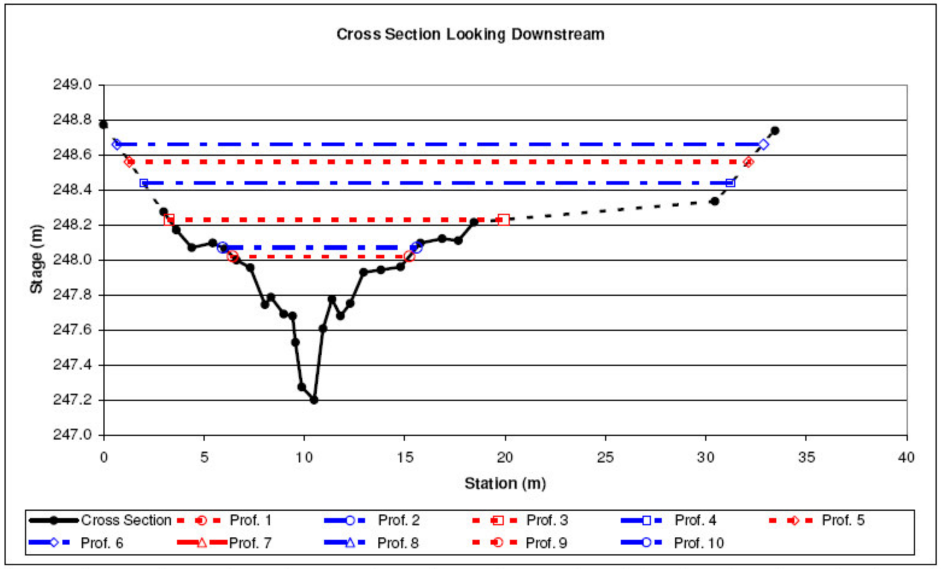

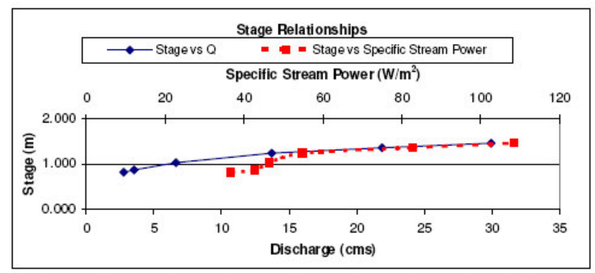

Prof. ID	Estimated n-value	L-Limit	R-Limit	WS (m)	Depth (m)	Left Sta (m)	Right Sta (m)	P_w (m)	Area (m^2)	W (m)	R (m)	D (m)	W/d	V (m/s)	Q (m^3/s)	U* (m/s)	τ (kg/ms^2)	τ*	ω (W/m^2)	Ω (W/m)	F_r	R/d_{84}	n-value per Limerino	Floodplain Form
PVPV04P01	0.035			248.02	0.821	6.43	15.24	9.24	2.26	8.80	0.24	0.26	10.7	1.2	2.8	0.17	28.6	1.092	37	322	0.82	13.9	0.026	PMB
PVPV04P02	0.035	5.44		248.07	0.871	5.94	15.60	10.11	2.72	9.66	0.27	0.28	11.1	1.3	3.5	0.18	31.4	1.202	43	413	0.84	15.3	0.026	PMB
PVPV04P03	0.035			248.23	1.031	3.27	19.95	17.15	4.90	16.68	0.29	0.29	16.2	1.4	6.6	0.18	33.4	1.276	46	774	0.85	16.2	0.026	PMB
PVPV04P04	0.040			248.44	1.241	2.01	31.23	29.72	10.23	29.23	0.34	0.35	23.5	1.3	13.7	0.20	40.2	1.536	55	1601	0.78	19.5	0.025	PMB
PVPV04P05	0.040			248.56	1.361	1.28	32.12	31.35	13.84	30.84	0.44	0.45	22.7	1.6	21.9	0.23	51.5	1.969	83	2554	0.81	25.0	0.025	PMB
PVPV04P06	0.040			248.66	1.461	0.68	32.87	32.71	16.99	32.19	0.52	0.53	22.0	1.8	29.9	0.25	60.6	2.317	109	3495	0.83	29.4	0.025	PMB
PVPV04P07	0.040																							PMB
PVPV04P08	0.040																							PMB
PVPV04P09	0.040																							PMB
PVPV04P10	0.040																							PMB

Cross Section Hydraulic Analyses: Proctor Valley

Floodplain/Site Description: Proctor Valley Site with photograph looking downstream (October 07). Cross Section extended per field observations and DEM data.

Location ID	PVPV05	
d_{50} (mm) =	1.62	
d_{84} (mm) =	17.66	
So = Sf =	0.0119	
Pt #	Sta (m)	Stage (m)
1	0.00	249.15
2	0.75	248.96
3	1.69	248.90
4	2.40	248.84
5	3.16	248.76
6	3.54	248.70
7	4.05	248.92
8	4.36	248.39
9	5.04	248.27
10	5.68	248.35
11	5.89	248.57
12	6.09	248.38
13	6.52	248.82
14	6.96	247.84
15	7.36	247.64
16	7.73	247.54
17	8.39	248.21
18	8.72	248.15
19	8.92	247.78
20	9.36	247.90
21	9.91	247.83
22	10.41	247.83
23	10.74	248.07
24	11.29	248.21
25	12.11	248.17
26	12.92	248.11
27	13.36	248.11
28	14.03	248.13
29	14.54	248.07
30	15.35	248.25
31	16.15	248.38
32	17.21	248.41
33	18.47	248.66
34	19.95	248.63
35	23.95	249.13
min. Stage =		247.54
Continuum		1b
CEM		1

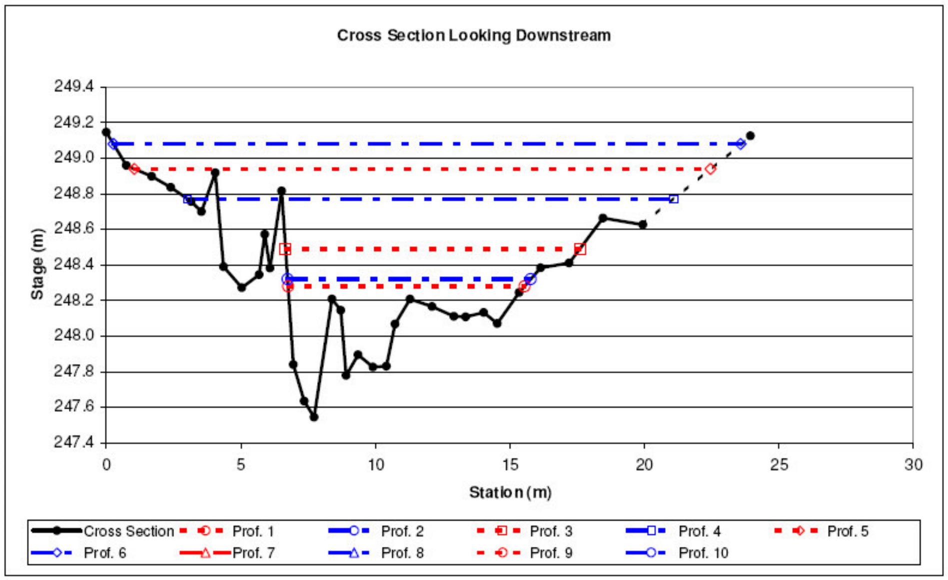

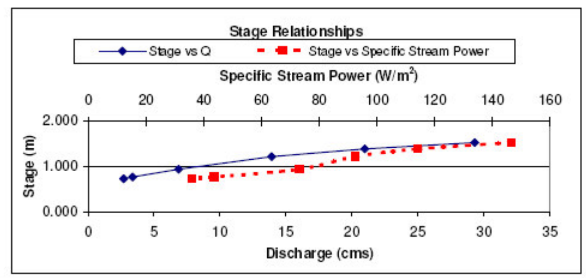

Prof. ID	Estimated n-value	L-Limit	R-Limit	WS (m)	Depth (m)	Left Sta (m)	Right Sta (m)	P_w (m)	Area (m^2)	W (m)	R (m)	D (m)	W/d	V (m/s)	Q (m^3/s)	U* (m/s)	τ (kg/ms^2)	τ*	ω (W/m^2)	Ω (W/m)	F_r	R/d_{84}	n-value per Limerino	Floodplain Form
PVPV05P01	0.035	6.52		248.28	0.736	6.76	15.55	9.78	2.29	8.79	0.23	0.26	11.9	1.2	2.7	0.17	27.3	1.043	36	316	0.79	13.2	0.026	PMB
PVPV05P02	0.035	6.52		248.32	0.776	6.74	15.78	10.06	2.64	9.04	0.26	0.29	11.7	1.3	3.4	0.18	30.7	1.173	44	395	0.81	14.9	0.026	PMB
PVPV05P03	0.035	6.52		248.49	0.946	6.66	17.60	12.08	4.35	10.94	0.36	0.40	11.6	1.6	6.9	0.21	42.1	1.607	73	802	0.86	20.4	0.025	PMB
PVPV05P04	0.040			248.77	1.226	3.03	21.10	19.51	8.73	17.57	0.45	0.50	14.3	1.6	13.9	0.23	52.2	1.995	92	1625	0.77	25.3	0.025	PMB
PVPV05P05	0.040			248.94	1.396	1.04	22.46	23.54	12.03	21.42	0.51	0.56	15.3	1.7	21.0	0.24	59.7	2.279	114	2448	0.80	28.9	0.025	PMB
PVPV05P06	0.040			249.08	1.536	0.26	23.58	25.46	15.18	23.32	0.60	0.65	15.2	1.9	29.3	0.26	69.6	2.658	147	3422	0.82	33.7	0.024	PMB
PVPV05P07	0.040																							PMB
PVPV05P08	0.040																							PMB
PVPV05P09	0.040																							PMB
PVPV05P10	0.040																							PMB

Cross Section Hydraulic Analyses: Proctor Valley

Floodplain/Site Description: Proctor Valley Site with photograph looking upstream (October 07).

Location ID		PVPV06
d_{50} (mm) =		1.62
d_{84} (mm) =		17.66
So = Sf =		0.0119
Pt #	Sta (m)	Stage (m)
1	0.00	249.17
2	0.73	249.06
3	1.47	249.10
4	2.11	248.99
5	2.77	248.78
6	3.43	248.71
7	4.09	248.64
8	4.67	248.47
9	5.00	248.19
10	5.26	248.03
11	5.79	247.95
12	5.85	247.52
13	6.80	247.46
14	7.83	247.36
15	8.60	247.36
16	9.34	247.49
17	9.88	247.54
18	10.55	247.68
19	11.29	248.00
20	12.09	248.29
21	12.74	248.42
22	13.36	248.60
23	14.23	248.69
24	15.18	248.75
25	16.26	248.80
26	17.23	248.90
27	18.03	248.95
28		
29		
30		
31		
32		
33		
34		
35		
min. Stage =		247.36
Continuum		1b
CEM		1

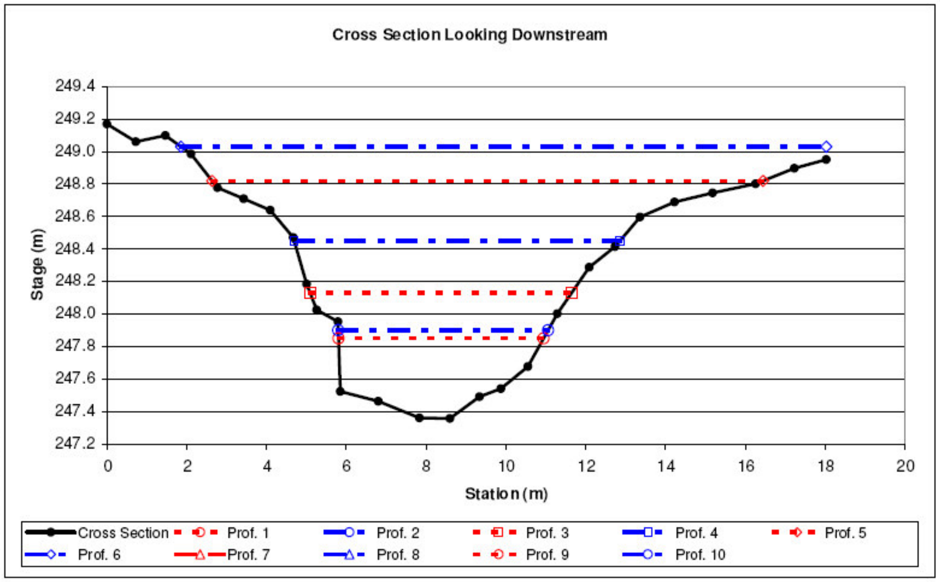

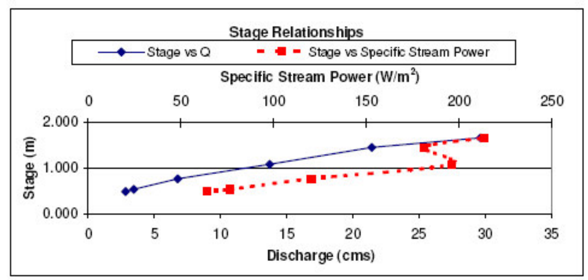

Prof. ID	Estimated n-value	L-Limit	R-Limit	WS (m)	Depth (m)	Left Sta (m)	Right Sta (m)	P_w (m)	Area (m^2)	W (m)	R (m)	D (m)	W/d	V (m/s)	Q (m^3/s)	U* (m/s)	τ (kg/ms^2)	τ^*	ω (W/m^2)	Ω (W/m)	F_r	R/d_{84}	n-value per Limerino	Floodplain Form
PVPV06P01	0.035			247.85	0.492	5.81	10.94	5.49	1.86	5.14	0.34	0.36	10.4	1.5	2.8	0.20	39.6	1.514	64	330	0.86	19.2	0.025	PMB
PVPV06P02	0.035			247.90	0.542	5.80	11.06	5.67	2.12	5.26	0.37	0.40	9.7	1.6	3.4	0.21	43.8	1.672	76	402	0.87	21.2	0.025	PMB
PVPV06P03	0.035			248.13	0.772	5.09	11.64	7.09	3.48	6.55	0.49	0.53	8.5	1.9	6.8	0.24	57.4	2.191	120	789	0.91	27.8	0.025	PMB
PVPV06P04	0.035			248.45	1.092	4.70	12.86	8.86	5.82	8.16	0.66	0.71	7.5	2.4	13.7	0.28	76.7	2.930	196	1600	0.96	37.2	0.024	PMB
PVPV06P05	0.037			248.82	1.462	2.64	16.44	14.58	9.60	13.81	0.66	0.70	9.4	2.2	21.4	0.28	76.9	2.938	181	2501	0.92	37.3	0.024	PMB
PVPV06P06	0.039			249.03	1.672	1.86	18.03	16.98	12.79	16.17	0.75	0.79	9.7	2.3	29.6	0.30	88.0	3.361	214	3459	0.89	42.7	0.024	PMB
PVPV06P07	0.035																							PMB
PVPV06P08	0.035																							PMB
PVPV06P09	0.035																							PMB
PVPV06P10	0.035																							PMB

Cross Section Hydraulic Analyses: Proctor Valley

Floodplain/Site Description: Proctor Valley Site with photograph looking downstream (October 07). Cross Section extended per field observations and DEM data.

Location ID		PVPV07
d_{50} (mm) =		1.62
d_{84} (mm) =		17.66
So = Sf =		0.0130
Pt #	Sta (m)	Stage (m)
1	0.00	249.26
2	5.17	249.18
3	6.24	249.13
4	7.28	249.04
5	8.05	248.96
6	8.72	248.81
7	9.36	248.61
8	9.99	248.39
9	10.24	248.32
10	10.51	248.17
11	10.73	248.12
12	10.89	247.98
13	11.38	247.95
14	11.62	247.86
15	11.92	247.86
16	12.11	247.90
17	12.38	248.09
18	12.95	248.31
19	13.72	248.32
20	14.52	248.29
21	14.66	248.03
22	15.15	248.03
23	15.59	248.27
24	16.31	248.43
25	17.22	248.57
26	18.21	248.72
27	19.00	248.88
28	19.50	248.93
29	20.26	248.95
30	32.26	249.29
31		
32		
33		
34		
35		
min. Stage =		247.86
Continuum		1b
CEM		1

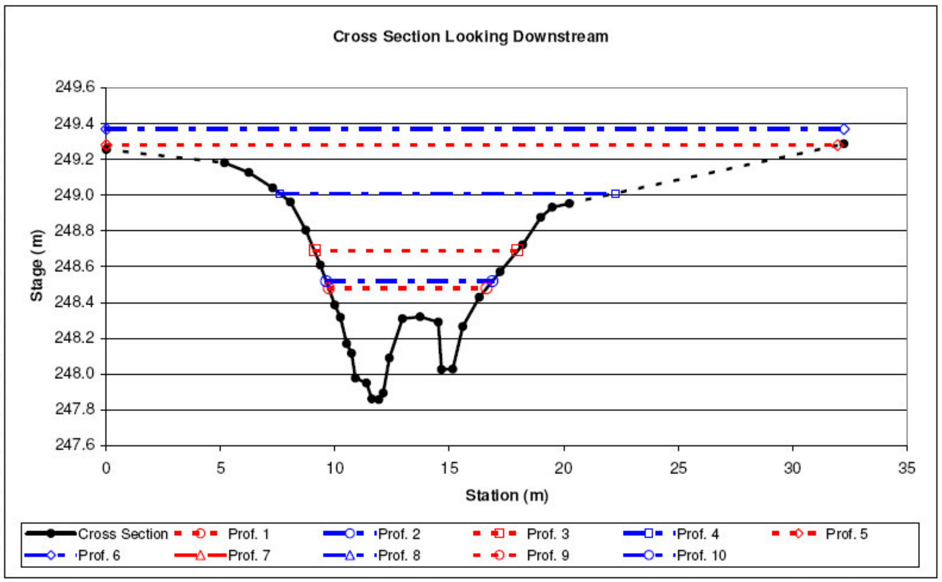

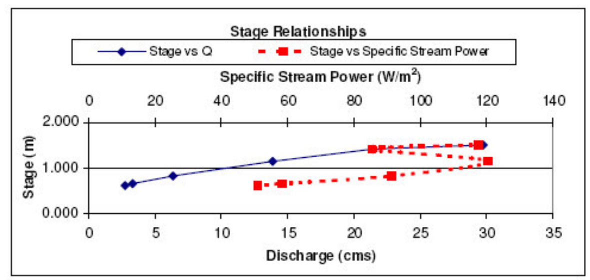

Prof. ID	Estimated n-value	L-Limit	R-Limit	WS (m)	Depth (m)	Left Sta (m)	Right Sta (m)	P_w (m)	Area (m^2)	W (m)	R (m)	D (m)	W/d	V (m/s)	Q (m^3/s)	U* (m/s)	τ (kg/ms²)	τ*	ω (W/m²)	Ω (W/m)	F_r	R/d_{84}	n-value per Limerino	Floodplain Form
PVPV07P01	0.035			248.48	0.622	9.73	16.63	7.39	2.02	6.90	0.27	0.29	11.1	1.4	2.8	0.19	34.8	1.329	51	352	0.87	15.4	0.026	PMB
PVPV07P02	0.035			248.52	0.662	9.62	16.88	7.77	2.30	7.27	0.30	0.32	11.0	1.4	3.3	0.19	37.7	1.442	58	424	0.88	16.8	0.025	PMB
PVPV07P03	0.035			248.69	0.832	9.10	17.99	9.43	3.67	8.89	0.39	0.41	10.7	1.7	6.4	0.22	49.6	1.896	91	813	0.93	22.0	0.025	PMB
PVPV07P04	0.035			249.01	1.152	7.58	22.27	15.29	7.10	14.69	0.46	0.48	12.7	2.0	13.9	0.24	59.2	2.264	121	1770	0.96	26.3	0.025	PMB
PVPV07P05	0.038			249.28	1.422	0.00	31.98	32.59	13.11	31.98	0.40	0.41	22.5	1.6	21.4	0.23	51.3	1.960	86	2735	0.87	22.8	0.025	PMB
PVPV07P06	0.038			249.37	1.512	0.00	32.26	32.87	16.01	32.26	0.49	0.50	21.3	1.9	29.8	0.25	62.1	2.374	118	3795	0.90	27.6	0.025	PMB
PVPV07P07	0.038																							PMB
PVPV07P08	0.038																							PMB
PVPV07P09	0.038																							PMB
PVPV07P10	0.038																							PMB

Cross Section Hydraulic Analyses: Proctor Valley

Floodplain/Site Description: Proctor Valley Site with photograph looking downstream (October 07). Cross Section extended per field observations and DEM data.

Location ID	PVPV06
d_{50} (mm) =	1.62
d_{84} (mm) =	17.66
So = Sf =	0.0130

Pt #	Sta (m)	Stage (m)
1	0.00	249.82
2	4.07	249.07
3	4.64	248.91
4	5.24	248.66
5	5.97	248.58
6	6.72	248.56
7	7.08	248.51
8	7.53	248.36
9	7.87	248.36
10	8.38	248.52
11	8.67	248.56
12	9.39	248.46
13	10.11	248.37
14	10.62	248.52
15	11.32	248.55
16	11.70	248.61
17	12.38	248.83
18	13.21	249.08
19	14.26	249.23
20	15.13	249.29
21	15.86	249.31
22	27.86	249.64
23		
24		
25		
26		
27		
28		
29		
30		
31		
32		
33		
34		
35		
min. Stage =	248.36	
Continuum	1b	
CEM	1	

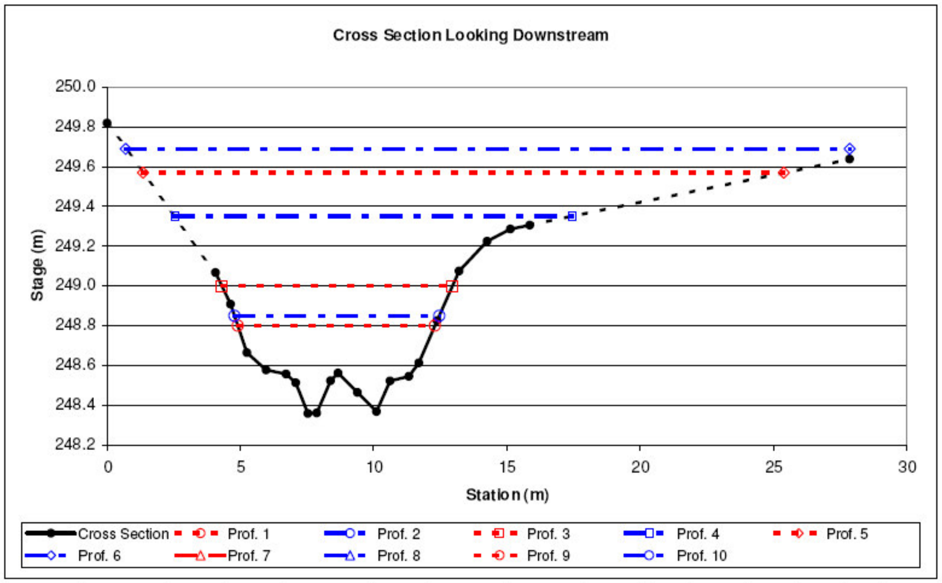

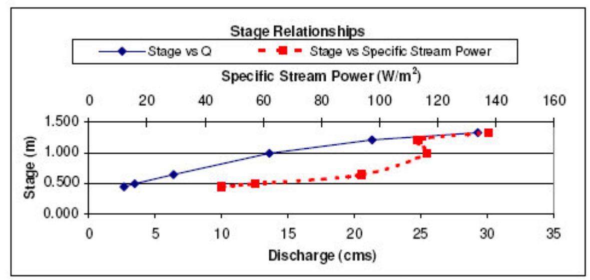

Prof. ID	Estimated n-value	L-Limit	R-Limit	WS (m)	Depth (m)	Left Sta (m)	Right Sta (m)	P_w (m)	Area (m^2)	W (m)	R (m)	D (m)	W/d	V (m/s)	Q (m^3/s)	U* (m/s)	τ (kg/ms^2)	τ^*	ω (W/m^2)	Ω (W/m)	F_r	R/d_{84}	n-value per Limerino	Floodplain Form
PVPV06P01	0.035			248.80	0.442	4.90	12.30	7.55	1.98	7.39	0.26	0.27	16.7	1.3	2.7	0.18	33.5	1.280	46	338	0.88	14.9	0.026	PMB
PVPV06P02	0.035			248.85	0.492	4.78	12.46	7.86	2.36	7.68	0.30	0.31	15.6	1.5	3.5	0.20	38.3	1.464	57	440	0.90	17.0	0.025	PMB
PVPV06P03	0.035			249.00	0.642	4.31	12.96	8.87	3.58	8.65	0.40	0.41	13.5	1.8	6.4	0.23	51.5	1.968	94	814	0.95	22.9	0.025	PMB
PVPV06P04	0.038			249.35	0.992	2.54	17.44	15.19	7.35	14.91	0.48	0.49	15.0	1.8	13.6	0.25	61.7	2.358	116	1733	0.90	27.4	0.025	PMB
PVPV08P05	0.038			249.57	1.212	1.35	25.39	24.34	11.63	24.04	0.48	0.48	19.8	1.8	21.3	0.25	60.9	2.329	113	2721	0.90	27.1	0.025	PMB
PVPV08P06	0.038			249.69	1.332	0.70	27.86	27.47	14.77	27.16	0.54	0.54	20.4	2.0	29.3	0.26	68.6	2.619	138	3736	0.92	30.4	0.025	PMB
PVPV08P07	0.035																							PMB
PVPV06P08	0.035																							PMB
PVPV06P09	0.035																							PMB
PVPV06P10	0.035																							PMB

Cross Section Hydraulic Analyses: Proctor Valley

Floodplain/Site Description: Proctor Valley Site with photograph looking downstream (October 07). Cross Section extended per field observations and DEM data.

Location ID	PVPV09
d_{50} (mm) =	1.62
d_{84} (mm) =	17.66
So = Sf =	0.0130

Pt #	Sta (m)	Stage (m)
1	0.00	249.91
2	8.00	249.69
3	10.15	249.72
4	12.71	249.64
5	13.63	249.57
6	14.42	249.51
7	15.20	249.49
8	15.55	249.36
9	16.16	249.30
10	16.66	249.22
11	17.28	249.19
12	17.82	249.22
13	18.27	249.32
14	18.85	249.25
15	19.25	249.04
16	19.74	249.06
17	20.03	249.36
18	20.61	249.22
19	20.78	249.07
20	20.98	249.06
21	21.15	248.98
22	21.26	249.00
23	21.36	249.12
24	21.52	249.18
25	21.73	249.30
26	22.64	249.29
27	23.29	249.29
28	23.89	249.50
29	24.64	249.68
30	25.41	249.78
31	26.22	249.86
32	30.22	250.25
33		
34		
35		
min. Stage =		248.98
Continuum		1b
CEM		1

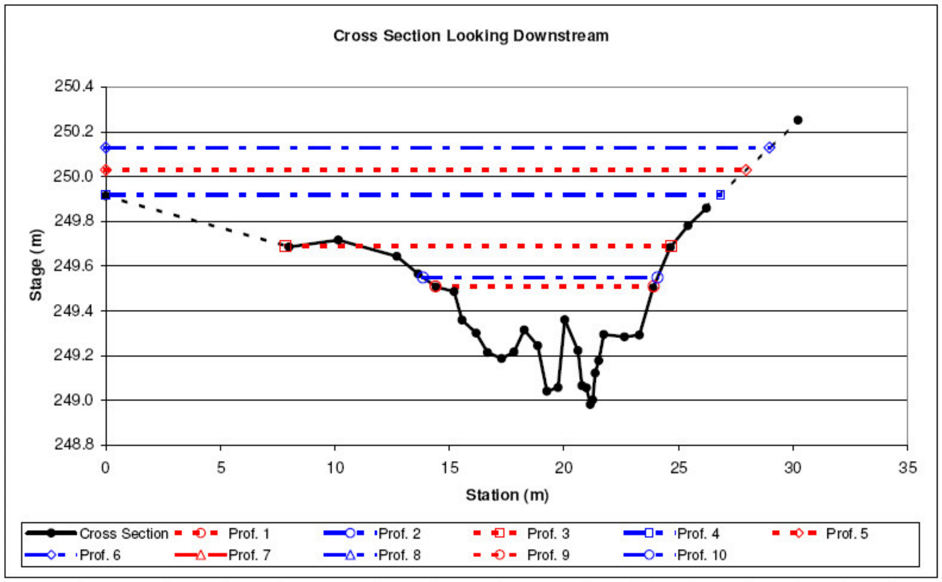

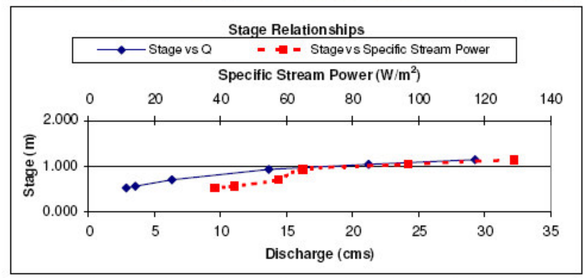

Prof. ID	Estimated n-value	L-Limit	R-Limit	WS (m)	Depth (m)	Left Sta (m)	Right Sta (m)	P_w (m)	Area (m^2)	W (m)	R (m)	D (m)	W/d	V (m/s)	Q (m^3/s)	U* (m/s)	τ (kg/ms²)	τ^*	ω (W/m²)	Ω (W/m)	F_r	R/d_{84}	n-value per Limerino	Floodplain Form
PVPV09P01	0.035			249.51	0.527	14.39	23.92	9.97	2.32	9.52	0.23	0.24	18.1	1.2	2.9	0.17	29.7	1.135	38	365	0.85	13.2	0.026	PMB
PVPV09P02	0.035			249.55	0.567	13.85	24.08	10.69	2.72	10.23	0.25	0.27	18.0	1.3	3.6	0.18	32.4	1.239	44	453	0.87	14.4	0.026	PMB
PVPV09P03	0.035			249.69	0.707	7.86	24.68	14.49	4.34	14.01	0.30	0.31	19.8	1.5	6.3	0.20	38.2	1.459	58	806	0.90	17.0	0.025	PMB
PVPV09P04	0.038			249.92	0.937	0.00	26.83	27.32	9.33	26.83	0.34	0.35	28.6	1.5	13.7	0.21	43.5	1.663	65	1743	0.85	19.3	0.025	PMB
PVPV09P05	0.038			250.03	1.047	0.00	27.95	28.45	12.34	27.95	0.43	0.44	26.7	1.7	21.2	0.24	55.3	2.113	97	2705	0.89	24.6	0.025	PMB
PVPV09P06	0.038			250.13	1.147	0.00	28.97	29.47	15.19	28.97	0.52	0.52	25.3	1.9	29.3	0.26	65.7	2.510	129	3734	0.91	29.2	0.025	PMB
PVPV09P07	0.038																							PMB
PVPV09P08	0.038																							PMB
PVPV09P09	0.038																							PMB
PVPV09P10	0.038																							PMB

Cross Section Hydraulic Analyses: San Antonio Creek

Floodplain/Site Description: San Antonio Creek at East Ojai Avenue. Photo looking upstream from top of right bank, upstream from East Ojai Avenue.

Location ID	SAOA01
d_{50} (mm) =	16.00
d_{84} (mm) =	70.20
So = Sf =	0.0111

Pt #	Sta (m)	Stage (m)
1	0.00	100.46
2	0.10	99.26
3	1.40	98.36
4	5.40	98.59
5	9.40	98.59
6	14.40	98.58
7	15.50	98.41
8	17.80	98.64
9	20.50	98.54
10	22.40	98.77
11	25.45	98.81
12	30.90	98.93
13	35.10	99.02
14	39.90	99.06
15	42.90	99.04
16	48.35	98.78
17	49.10	98.53
18	51.60	98.35
19	52.90	98.24
20	55.90	98.14
21	57.40	98.44
22	58.90	98.34
23	61.90	98.45
24	62.95	98.53
25	64.15	99.07
26	65.40	100.00
27	66.40	102.04
28		
29		
30		
31		
32		
33		
34		
35		
min. Stage =		98.14
Continuum		2
CEM		3

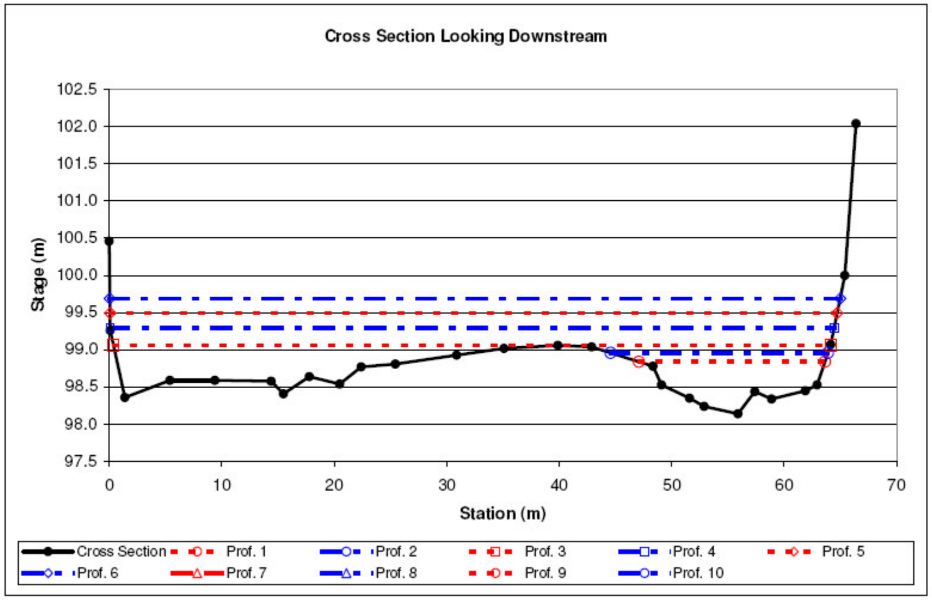

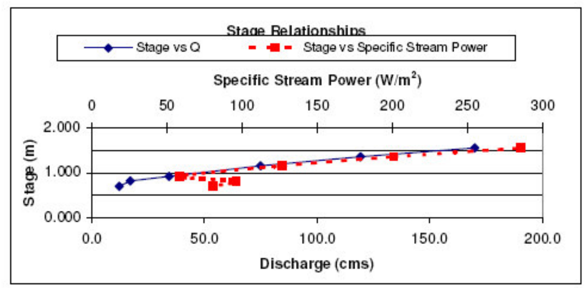

Prof. ID	Estimated n-value	L-Limit	R-Limit	WS (m)	Depth (m)	Left Sta (m)	Right Sta (m)	P_w (m)	Area (m^2)	W (m)	R (m)	D (m)	W/d	V (m/s)	Q (m^3/s)	U* (m/s)	τ (kg/ms^2)	τ^*	ω (W/m^2)	Ω (W/m)	F_r	R/d_{84}	n-value per Limerino	Floodplain Form
SAOA01P01	0.035	42.90		98.84	0.700	47.09	63.64	16.71	7.14	16.55	0.43	0.43	23.6	1.7	12.2	0.22	46.6	0.180	80	1331	0.89	6.1	0.036	BF
SAOA01P02	0.035	42.90		98.96	0.820	44.58	63.91	19.52	9.30	19.33	0.48	0.48	23.6	1.8	17.1	0.23	51.9	0.201	96	1861	0.91	6.8	0.035	BF
SAOA01P03	0.040			99.06	0.920	0.39	64.13	64.22	24.65	63.74	0.38	0.39	69.3	1.4	34.3	0.20	41.8	0.162	59	3741	0.77	5.5	0.036	BF
SAOA01P04	0.040			99.30	1.155	0.10	64.45	65.01	39.58	64.36	0.61	0.62	55.7	1.9	74.9	0.26	66.4	0.257	127	8167	0.83	8.7	0.034	BF
SAOA01P05	0.040			99.50	1.355	0.08	64.72	65.54	52.48	64.64	0.80	0.81	47.7	2.3	119.2	0.30	87.3	0.338	201	12998	0.86	11.4	0.033	BF
SAOA01P06	0.040			99.69	1.550	0.06	64.98	66.06	65.11	64.92	0.99	1.00	41.9	2.6	169.9	0.33	107.4	0.416	285	18522	0.89	14.0	0.033	BF
SAOA01P07	0.040																							BF
SAOA01P08	0.040																							BF
SAOA01P09	0.040																							BF
SAOA01P10	0.040																							BF

Cross Section Hydraulic Analyses: Acton Site

Floodplain/Site Description: Santa Clara River Tributary at Acton Site. Photo looking upstream up center line of main or left channel (Jan 08).
Note: Downstream box culvert providing grade control resulting in aggradation and channel widening in response to increase in inflowing sed. load.

Location ID		SCAT01
d_{50} (mm) =		4.95
d_{84} (mm) =		12.05
So = Sf =		0.0379
Pt #	Sta (m)	Stage (m)
1	0.50	72.75
2	1.50	72.70
3	2.30	72.60
4	2.70	72.40
5	3.60	72.38
6	4.10	72.40
7	4.90	72.36
8	5.80	72.34
9	6.40	72.47
10	7.70	72.51
11	8.50	72.65
12	9.00	72.70
13	10.40	72.67
14	10.80	72.55
15	12.00	72.54
16	14.00	72.52
17	15.00	72.50
18	16.00	72.47
19	16.40	72.47
20	16.60	72.53
21	17.20	72.65
22	18.60	72.65
23	20.00	72.97
24		
25		
26		
27		
28		
29		
30		
31		
32		
33		
34		
35		
min. Stage =		72.34
Continuum		1b
CEM		4

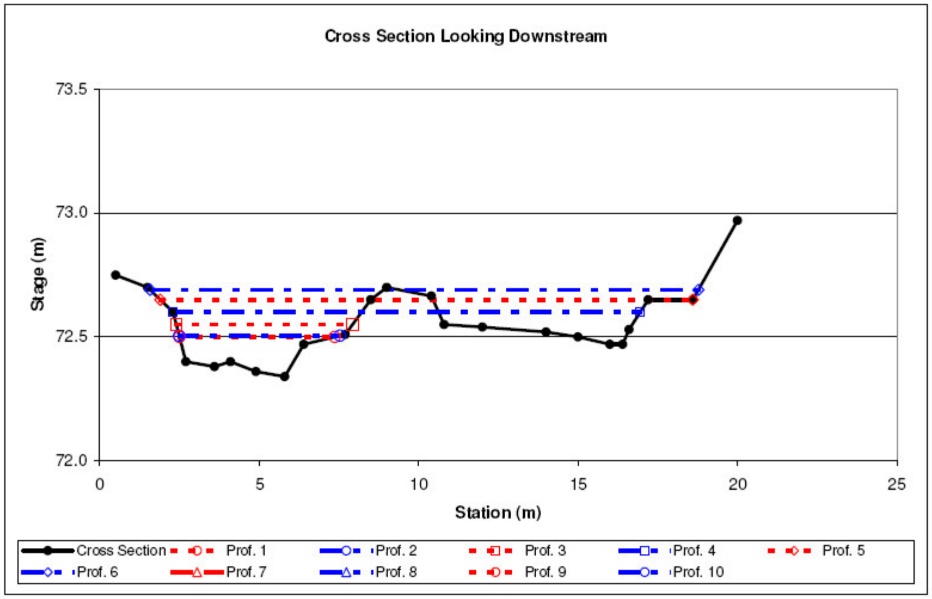

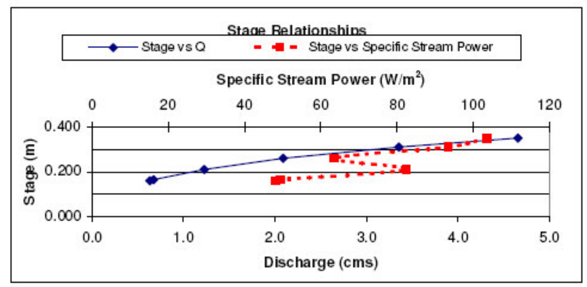

Prof. ID	Estimated n-value	L-Limit	R-Limit	WS (m)	Depth (m)	Left Sta (m)	Right Sta (m)	P_w (m)	Area (m^2)	W (m)	R (m)	D (m)	W/d	V (m/s)	Q (m^3/s)	U* (m/s)	τ (kg/ms²)	τ*	ω (W/m²)	Ω (W/m)	F_r	R/d_{84}	n-value per Limerino	Floodplain Form
SCAT01P01	0.030		9.00	72.50	0.160	2.50	7.37	4.91	0.47	4.87	0.09	0.10	30.5	1.4	0.6	0.19	35.3	0.441	48	234	1.49	7.9	0.026	BF
SCAT01P02	0.030		9.00	72.51	0.165	2.49	7.54	5.09	0.49	5.05	0.10	0.10	30.6	1.4	0.7	0.19	35.9	0.449	49	250	1.50	8.0	0.026	BF
SCAT01P03	0.030		9.00	72.55	0.210	2.40	7.93	5.58	0.73	5.53	0.13	0.13	26.3	1.7	1.2	0.22	48.7	0.609	82	456	1.58	10.9	0.025	BF
SCAT01P04	0.035			72.60	0.260	2.30	16.95	12.33	1.52	12.24	0.12	0.12	47.1	1.4	2.1	0.21	45.8	0.572	63	777	1.34	10.2	0.025	BF
SCAT01P05	0.035			72.65	0.310	1.90	18.60	13.46	2.09	13.35	0.16	0.16	43.1	1.6	3.4	0.24	57.7	0.721	93	1247	1.39	12.9	0.024	BF
SCAT01P06	0.035			72.69	0.350	1.58	18.78	16.82	2.78	16.69	0.17	0.17	47.7	1.7	4.7	0.25	61.4	0.768	104	1731	1.41	13.7	0.024	BF
SCAT01P07	0.035																							BF
SCAT01P08	0.035																							BF
SCAT01P09	0.035																							BF
SCAT01P10	0.035																							BF

Cross Section Hydraulic Analyses: Acton Site

Floodplain/Site Description: Lake Perris Site D/4. Photo shows site looking downstream (Jan 08).

Location ID	SCAT02
d_{50} (mm) =	3.76
d_{84} (mm) =	8.76
So = Sf =	0.0377

Pt #	Sta (m)	Stage (m)
1	0.00	86.93
2	1.60	86.96
3	2.50	86.60
4	3.10	86.38
5	3.20	86.17
6	3.70	86.19
7	4.20	86.20
8	4.70	86.21
9	5.20	86.21
10	5.70	86.21
11	6.20	86.21
12	6.70	86.19
13	7.00	86.19
14	7.40	86.43
15	7.70	86.70
16	8.50	86.65
17	8.70	86.93
18	10.00	86.88
19		
20		
21		
22		
23		
24		
25		
26		
27		
28		
29		
30		
31		
32		
33		
34		
35		
min. Stage =		86.17
Continuum		1b
CEM		3

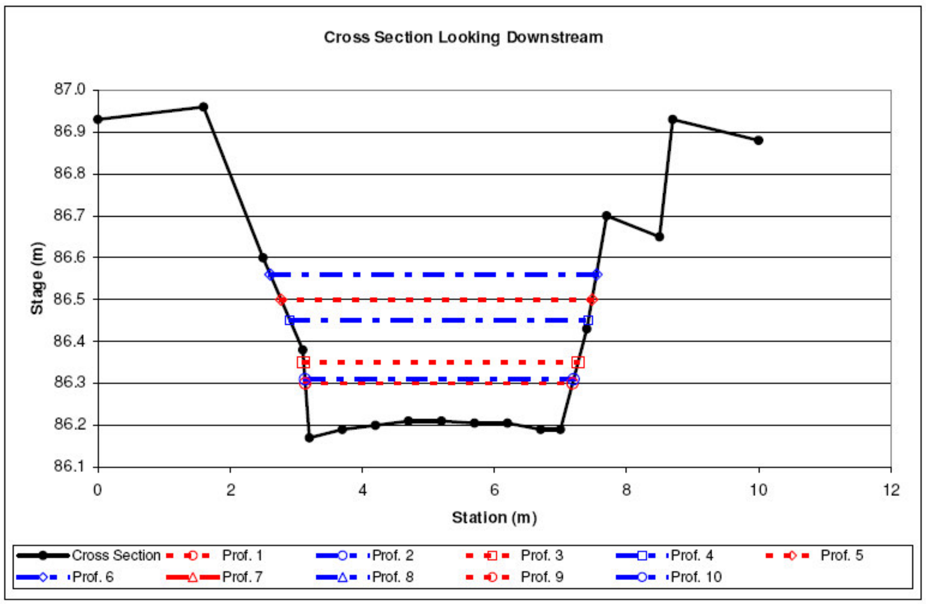

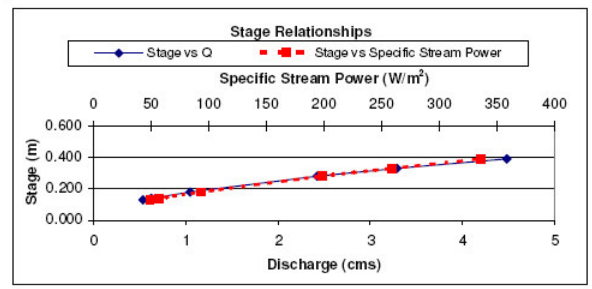

Prof. ID	Estimated n-value	L-Limit	R-Limit	WS (m)	Depth (m)	Left Sta (m)	Right Sta (m)	P_w (m)	Area (m^2)	W (m)	R (m)	D (m)	W/d	V (m/s)	Q (m^3/s)	U* (m/s)	τ (kg/ms²)	τ*	ω (W/m²)	Ω (W/m)	F_r	R/d_{84}	n-value per Limerino	Floodplain Form
SCAT02P01	0.030			86.30	0.130	3.14	7.18	4.16	0.40	4.05	0.10	0.10	31.1	1.4	0.5	0.19	35.3	0.581	49	199	1.48	10.9	0.024	PMB
SCAT02P02	0.030			86.31	0.140	3.13	7.20	4.19	0.44	4.07	0.10	0.11	29.0	1.4	0.6	0.20	38.6	0.636	57	232	1.50	11.9	0.023	PMB
SCAT02P03	0.030			86.35	0.180	3.11	7.27	4.31	0.60	4.15	0.14	0.14	23.1	1.7	1.0	0.23	51.6	0.850	93	388	1.57	15.9	0.023	PMB
SCAT02P04	0.030			86.45	0.280	2.91	7.42	4.73	1.03	4.51	0.22	0.23	16.1	2.3	2.4	0.28	80.7	1.329	199	897	1.68	24.9	0.022	PMB
SCAT02P05	0.030			86.50	0.330	2.77	7.48	4.95	1.26	4.71	0.26	0.27	14.3	2.6	3.3	0.31	94.4	1.553	259	1217	1.72	29.1	0.022	PMB
SCAT02P06	0.030		7.70	86.56	0.390	2.61	7.54	5.22	1.55	4.94	0.30	0.31	12.7	2.9	4.5	0.33	110.1	1.812	336	1657	1.76	34.0	0.022	PMB
SCAT02P07	0.030																							PMB
SCAT02P08	0.030																							PMB
SCAT02P09	0.030																							PMB
SCAT02P10	0.030																							PMB

Cross Section Hydraulic Analyses: Acton Site

Floodplain/Site Description: Lake Perris Site D/4. Photo shows site looking downstream (Jan 08).

Location ID		SCAT03
d_{50} (mm) =		5.03
d_{84} (mm) =		16.85
So = Sf =		0.0308
Pt #	Sta (m)	Stage (m)
1	0.00	101.97
2	0.05	100.82
3	1.00	100.49
4	1.60	100.28
5	2.20	100.27
6	2.50	99.77
7	3.00	99.51
8	4.80	99.49
9	5.30	99.37
10	6.45	99.29
11	7.20	99.24
12	7.60	99.12
13	8.40	99.14
14	8.80	99.09
15	9.10	99.17
16	9.60	99.22
17	10.10	99.30
18	10.60	99.29
19	10.70	101.79
20		
21		
22		
23		
24		
25		
26		
27		
28		
29		
30		
31		
32		
33		
34		
35		
min. Stage =		99.09
Continuum		1b
CEM		3

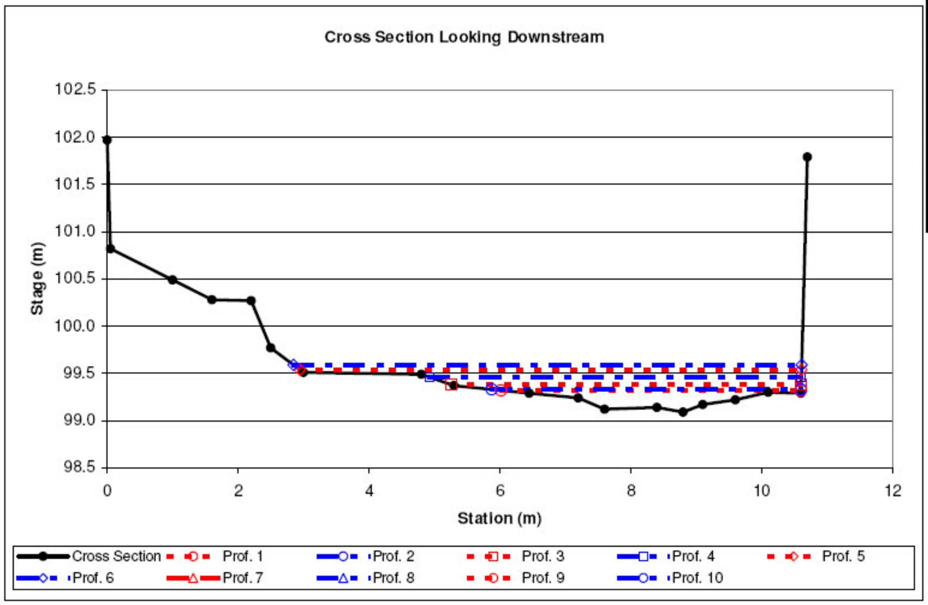

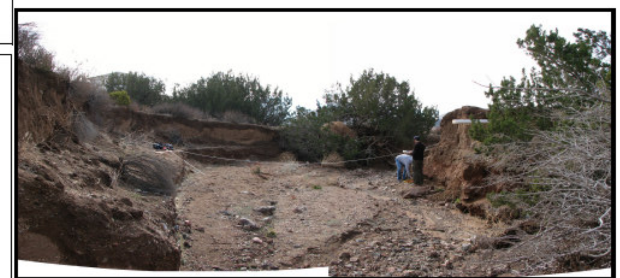

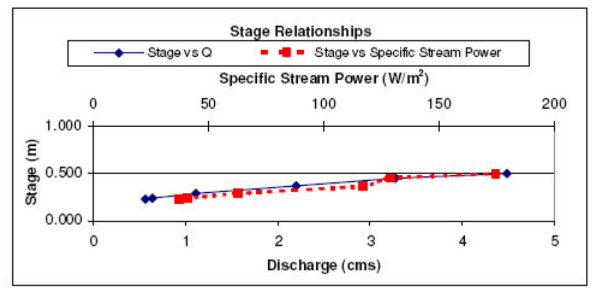

Prof. ID	Estimated n-value	L-Limit	R-Limit	WS (m)	Depth (m)	Left Sta (m)	Right Sta (m)	P_w (m)	Area (m^2)	W (m)	R (m)	D (m)	W/d	V (m/s)	Q (m^3/s)	U* (m/s)	τ (kg/ms^2)	τ^*	ω (W/m^2)	Ω (W/m)	F_r	R/d_{84}	n-value per Limerino	Floodplain Form
SCAT03P01	0.035			99.32	0.230	6.02	10.60	4.65	0.50	4.58	0.11	0.11	19.9	1.1	0.6	0.18	32.4	0.399	37	171	1.17	6.4	0.028	PMB
SCAT03P02	0.035			99.33	0.240	5.88	10.60	4.81	0.55	4.73	0.11	0.12	19.7	1.2	0.6	0.19	34.3	0.422	41	194	1.18	6.7	0.028	PMB
SCAT03P03	0.035			99.38	0.290	5.26	10.60	5.48	0.80	5.35	0.15	0.15	18.4	1.4	1.1	0.21	44.1	0.543	63	336	1.23	8.7	0.027	PMB
SCAT03P04	0.035			99.46	0.370	4.93	10.61	5.90	1.24	5.68	0.21	0.22	15.4	1.8	2.2	0.25	63.6	0.782	117	665	1.30	12.5	0.026	PMB
SCAT03P05	0.035			99.54	0.450	2.94	10.61	7.97	1.78	7.67	0.22	0.23	17.0	1.8	3.3	0.26	67.3	0.828	129	989	1.31	13.2	0.026	PMB
SCAT03P06	0.035			99.59	0.500	2.85	10.61	8.13	2.16	7.77	0.27	0.28	15.5	2.1	4.5	0.28	80.3	0.989	174	1355	1.35	15.8	0.025	PMB
SCAT03P07	0.035																							PMB
SCAT03P08	0.035																							PMB
SCAT03P09	0.035																							PMB
SCAT03P10	0.035																							PMB

Cross Section Hydraulic Analyses: Stewart Canyon

Floodplain/Site Description: Photo view looking downstream from cross section.

Location ID	SCNS01	
d_{50} (mm) =	151.79	
d_{84} (mm) =	724.00	
So = Sf =	0.1004	
Pt #	Sta (m)	Stage (m)
1	1.05	100.00
2	1.20	100.21
3	2.50	99.53
4	3.40	99.32
5	4.15	99.10
6	4.20	98.97
7	4.75	98.92
8	5.00	99.22
9	5.50	99.17
10	5.55	98.90
11	5.85	99.15
12	6.00	98.90
13	6.30	98.89
14	6.90	98.71
15	7.40	98.90
16	7.40	99.16
17	7.90	99.26
18	8.45	99.33
19	8.95	99.68
20	9.50	99.68
21	10.15	99.61
22	10.80	99.91
23		
24		
25		
26		
27		
28		
29		
30		
31		
32		
33		
34		
35		
min. Stage =	98.71	
Continuum	2	
CEM	1	

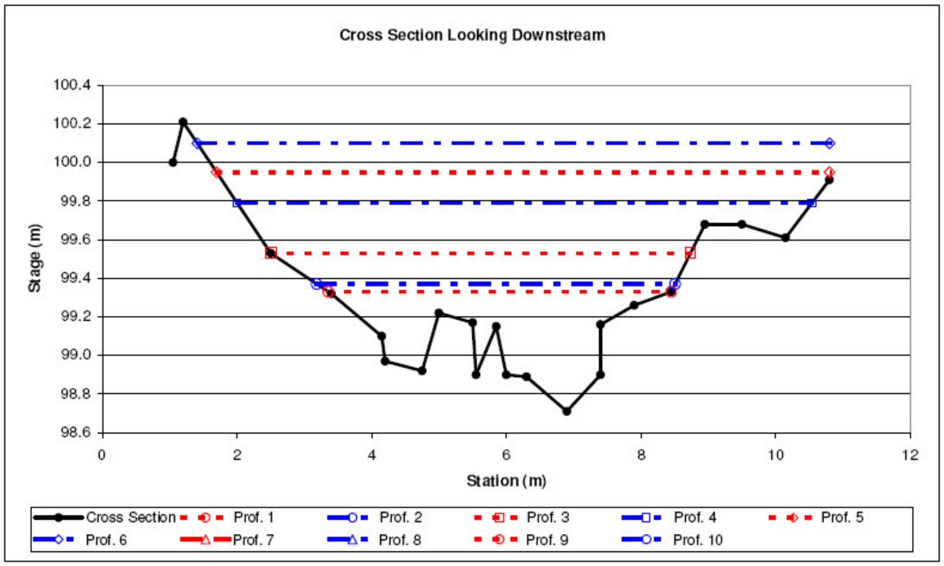

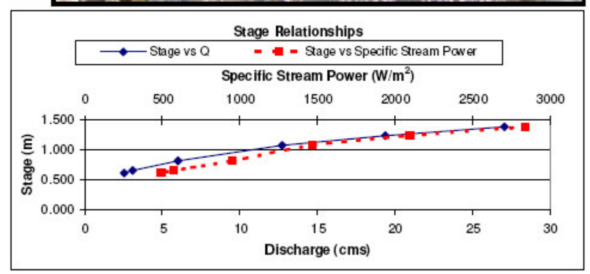

Prof. ID	Estimated n-value	L-Limit	R-Limit	WS (m)	Depth (m)	Left Sta (m)	Right Sta (m)	P_w (m)	Area (m^2)	W (m)	R (m)	D (m)	W/d	V (m/s)	Q (m^3/s)	U* (m/s)	τ (kg/ms^2)	τ*	ω (W/m^2)	Ω (W/m)	F_r	R/d_{84}	n-value per Limerino	Floodplain Form
SCNS01P01	0.065			99.33	0.620	3.36	8.45	6.15	1.40	5.09	0.23	0.28	8.2	1.8	2.55	0.47	224.4	0.092	493	2511	1.19	0.3	0.285	CA
SCNS01P02	0.065			99.37	0.660	3.19	8.51	6.40	1.60	5.32	0.25	0.30	8.1	1.9	3.10	0.50	246.3	0.100	573	3049	1.21	0.3	0.233	CA
SCNS01P03	0.065			99.53	0.820	2.50	8.74	7.38	2.52	6.24	0.34	0.40	7.6	2.4	6.02	0.58	336.9	0.137	951	5929	1.28	0.5	0.148	CA
SCNS01P04	0.065			99.79	1.080	2.00	10.54	9.84	4.44	8.54	0.45	0.52	7.9	2.9	12.7	0.67	444.6	0.181	1470	12547	1.36	0.6	0.116	CA
SCNS01P05	0.065			99.95	1.240	1.70	10.80	10.47	5.86	9.10	0.56	0.64	7.3	3.3	19.4	0.74	551.1	0.225	2098	19096	1.41	0.8	0.099	CA
SCNS01P06	0.065	1.20		100.10	1.390	1.41	10.80	10.79	7.24	9.39	0.67	0.77	6.8	3.7	27.1	0.81	661.2	0.270	2840	26667	1.46	0.9	0.089	CA
SCNS01P07	0.065																							CA
SCNS01P08	0.065																							CA
SCNS01P09	0.065																							CA
SCNS01P10	0.065																							CA

Cross Section Hydraulic Analyses: Silverado Canyon

Floodplain/Site Description: Silverado Canyon upstream of Oak Lane. Photo is looking upstream from the right overbank.

Location ID	SCOL01	
d_{50} (mm) =	141.50	
d_{84} (mm) =	353.73	
So = Sf =	0.0315	
Pt #	Sta (m)	Stage (m)
1	0.30	101.01
2	1.15	100.84
3	1.45	100.62
4	2.15	100.23
5	2.50	100.17
6	3.00	100.08
7	3.60	100.19
8	5.50	99.71
9	6.20	99.43
10	7.10	98.98
11	7.70	98.91
12	9.00	98.74
13	9.70	98.89
14	10.10	98.71
15	11.50	99.81
16	12.50	100.24
17	13.00	100.39
18	13.80	100.73
19	14.00	100.86
20		
21		
22		
23		
24		
25		
26		
27		
28		
29		
30		
31		
32		
33		
34		
35		
min. Stage =	98.71	
Continuum	2	
CEM	1.00	

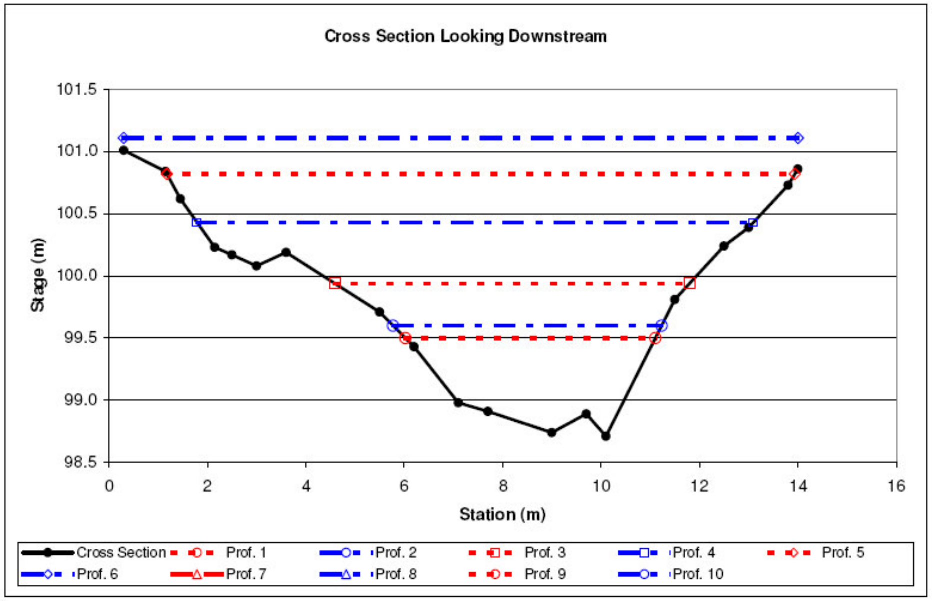

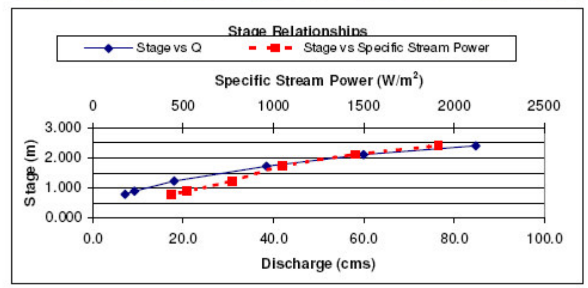

Prof. ID	Estimated n-value	L-Limit	R-Limit	WS (m)	Depth (m)	Left Sta (m)	Right Sta (m)	P_w (m)	Area (m^2)	W (m)	R (m)	D (m)	W/d	V (m/s)	Q (m^3/s)	U* (m/s)	τ (kg/ms^2)	τ*	ω (W/m^2)	Ω (W/m)	F_r	R/d_{84}	n-value per Limerino	Floodplain Form
SCOL01P01	0.040			99.50	0.790	6.02	11.11	5.54	2.64	5.08	0.48	0.52	6.4	2.7	7.1	0.38	147.1	0.064	434	2206	1.29	1.3	0.068	SP
SCOL01P02	0.040			99.60	0.890	5.78	11.23	5.97	3.17	5.46	0.53	0.58	6.1	2.9	9.2	0.40	163.7	0.072	521	2842	1.31	1.5	0.065	SP
SCOL01P03	0.040			99.94	1.230	4.59	11.80	7.88	5.29	7.21	0.67	0.73	5.9	3.4	18.0	0.46	207.4	0.091	770	5556	1.36	1.9	0.060	SP
SCOL01P04	0.040			100.43	1.720	1.79	13.09	12.17	9.92	11.30	0.82	0.88	6.6	3.9	38.4	0.50	252.1	0.110	1051	11880	1.42	2.3	0.057	SP
SCOL01P05	0.045			100.82	2.110	1.18	13.94	13.83	14.64	12.76	1.06	1.15	6.0	4.1	60.0	0.57	327.1	0.143	1452	18528	1.31	3.0	0.053	SP
SCOL01P06	0.045			101.11	2.400	0.30	14.00	14.80	18.52	13.70	1.25	1.35	5.7	4.6	84.8	0.62	386.6	0.169	1913	26206	1.35	3.5	0.051	SP
SCOL01P07	0.040																							SP
SCOL01P08	0.040																							SP
SCOL01P09	0.040																							SP
SCOL01P10	0.040																							SP

Cross Section Hydraulic Analyses: Silverado Canyon

Floodplain/Site Description: Silverado Canyon upstream of Oak Lane. Photo is looking upstream from the right overbank.

Location ID	SCOL02
d_{50} (mm) =	124.30
d_{84} (mm) =	383.98
So = Sf =	0.0540

Pt #	Sta (m)	Stage (m)
1	0.00	100.83
2	1.00	100.39
3	2.00	100.02
4	3.00	99.77
5	4.00	99.80
6	5.00	99.83
7	6.00	99.57
8	7.00	99.41
9	7.80	99.18
10	8.60	98.77
11	9.20	98.68
12	9.90	99.08
13	10.30	98.67
14	10.50	98.87
15	11.20	98.60
16	12.20	99.93
17	13.60	101.00
18		
19		
20		
21		
22		
23		
24		
25		
26		
27		
28		
29		
30		
31		
32		
33		
34		
35		
min. Stage =		98.60
Continuum		2
CEM		1.00

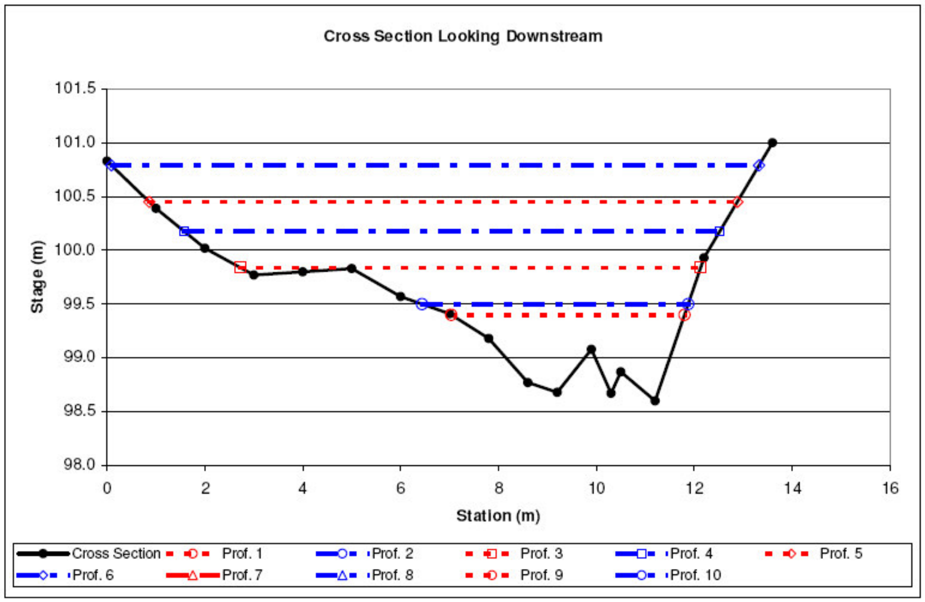

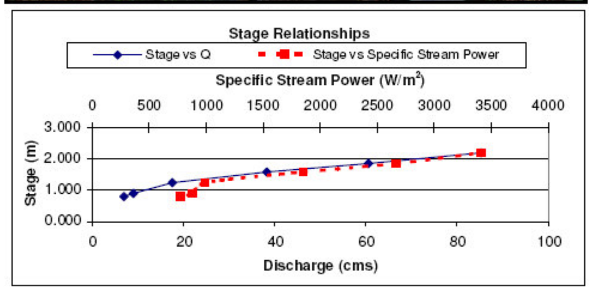

Prof. ID	Estimated n-value	L-Limit	R-Limit	WS (m)	Depth (m)	Left Sta (m)	Right Sta (m)	P_w (m)	Area (m^2)	W (m)	R (m)	D (m)	W/d	V (m/s)	Q (m^3/s)	U* (m/s)	τ (kg/ms^2)	τ*	ω (W/m^2)	Ω (W/m)	F_r	R/d_{84}	n-value per Limerino	Floodplain Form
SCOL02P01	0.040			99.40	0.800	7.03	11.80	5.71	2.24	4.77	0.39	0.47	6.0	3.1	6.9	0.46	207.2	0.103	772	3679	1.55	1.0	0.075	SP
SCOL02P02	0.040			99.50	0.900	6.44	11.88	6.45	2.74	5.44	0.43	0.50	6.0	3.3	9.0	0.47	225.5	0.112	879	4780	1.58	1.1	0.072	SP
SCOL02P03	0.040			99.84	1.240	2.72	12.13	10.64	5.00	9.41	0.47	0.53	7.6	3.5	17.6	0.50	249.0	0.124	988	9304	1.65	1.2	0.070	SP
SCOL02P04	0.040			100.18	1.580	1.57	12.53	12.36	8.48	10.96	0.69	0.77	6.9	4.5	38.3	0.60	363.1	0.181	1850	20280	1.76	1.8	0.061	SP
SCOL02P05	0.040			100.45	1.850	0.86	12.88	13.56	11.58	12.02	0.85	0.96	6.5	5.2	60.5	0.67	452.3	0.225	2669	32075	1.82	2.2	0.057	SP
SCOL02P06	0.045			100.79	2.190	0.09	13.33	14.97	15.87	13.23	1.06	1.20	6.0	5.4	85.2	0.75	561.8	0.280	3412	45156	1.68	2.8	0.054	SP
SCOL02P07	0.045																							SP
SCOL02P08	0.030																							SP
SCOL02P09	0.030																							SP
SCOL02P10	0.030																							SP

Cross Section Hydraulic Analyses: Santiago Creek Modeling Reach

Floodplain/Site Description: Santiago Creek~ 0.25 mi downstream of Santiago Canyon Bridge and USGS guaging station. Photograph view is looking downstream at only the main channel (see cross section tab for full section view). Flow of Record 1998 6200 cfs = 175 cms.

Location ID		SCSA01
d_{50} (mm) =		22.00
d_{84} (mm) =		70.80
So = Sf =		0.0150
Pt #	Sta (m)	Stage (m)
1	1.21	366.30
2	2.89	366.25
3	4.17	364.25
4	5.61	364.07
5	7.35	363.67
6	8.45	363.67
7	11.99	364.20
8	14.67	364.09
9	15.88	364.43
10	17.77	364.60
11	18.18	364.96
12	21.69	365.39
13	25.15	365.55
14	28.72	365.45
15	32.26	365.45
16	33.88	364.99
17	36.10	365.04
18	38.90	364.94
19	41.34	365.15
20	43.97	364.29
21	45.78	364.26
22	47.07	364.51
23	48.84	364.88
24	51.66	364.96
25	55.22	365.39
26	61.13	365.31
27	63.54	364.86
28	65.81	365.12
29	67.48	364.94
30	69.48	365.05
31	70.24	364.71
32	72.33	364.95
33	75.64	365.24
34	77.36	366.42
35	78.11	366.46
min. Stage =		363.67
Continuum		2
CEM		1

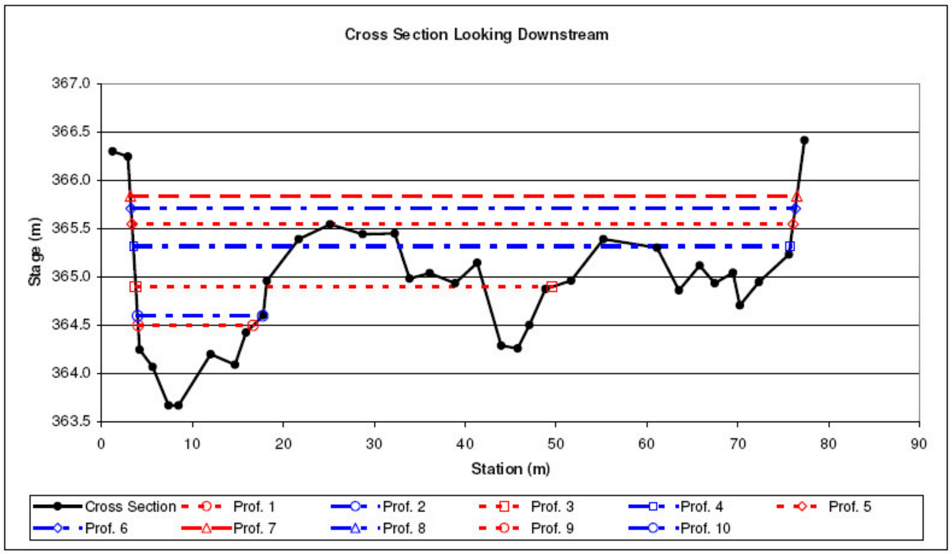

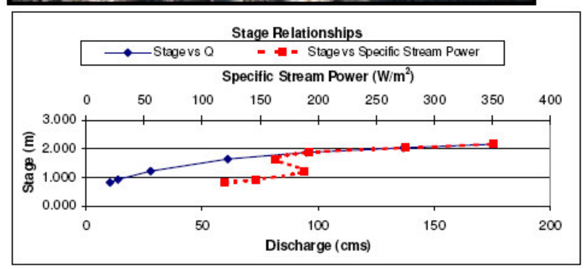

Prof. ID	Estimated n-value	L-Limit	R-Limit	WS (m)	Depth (m)	Left Sta (m)	Right Sta (m)	P_w (m)	Area (m^2)	W (m)	R (m)	D (m)	W/d	V (m/s)	Q (m^3/s)	U* (m/s)	τ (kg/ms^2)	τ^*	ω (W/m^2)	Ω (W/m)	F_r	R/d_{84}	n-value per Limerino	Floodplain Form
SCSA01P01	0.040		25.15	364.50	0.828	4.01	16.66	12.93	5.76	12.65	0.45	0.46	15.3	1.8	10.3	0.26	65.5	0.184	120	1513	0.91	6.3	0.036	BF
SCSA01P02	0.040		25.15	364.60	0.928	3.95	17.72	14.12	7.08	13.78	0.50	0.51	14.8	1.9	13.7	0.27	73.8	0.208	146	2013	0.92	7.1	0.035	BF
SCSA01P03	0.045		55.22	364.90	1.228	3.75	49.59	22.62	14.04	21.84	0.62	0.64	17.8	2.0	27.8	0.30	91.4	0.257	187	4093	0.85	8.8	0.034	BF
SCSA01P04	0.045			365.32	1.648	3.49	75.76	56.45	32.43	55.09	0.57	0.59	33.4	1.9	61.0	0.29	84.5	0.238	163	8975	0.84	8.1	0.034	BF
SCSA01P05	0.045			365.55	1.878	3.34	76.10	74.35	47.24	72.76	0.64	0.65	38.7	2.0	95.0	0.31	93.5	0.263	192	13984	0.85	9.0	0.034	BF
SCSA01P06	0.045			365.71	2.038	3.24	76.33	74.82	58.91	73.09	0.79	0.81	35.9	2.3	136.7	0.34	115.9	0.326	275	20117	0.89	11.1	0.033	BF
SCSA01P07	0.045			365.84	2.168	3.15	76.52	75.21	68.43	73.36	0.91	0.93	33.8	2.6	174.9	0.37	133.9	0.377	351	25734	0.91	12.9	0.033	BF
SCSA01P08	0.045																							BF
SCSA01P09	0.045																							BF
SCSA01P10	0.045																							BF

Cross Section Hydraulic Analyses: Santiago Creek Modeling Reach

Floodplain/Site Description: Santiago Creek~ 0.20 mi downstream of Santiago Canyon Bridge and USGS guaging station. Photograph view is looking downstream at only the main channel (see cross section tab for full section view).

Location ID	SCSA02
d_{50} (mm) =	22.00
d_{84} (mm) =	70.80
So = Sf =	0.0150

Pt #	Sta (m)	Stage (m)
1	0.00	366.63
2	2.68	365.61
3	3.64	364.60
4	6.11	364.38
5	8.59	364.20
6	12.02	364.35
7	15.68	364.85
8	17.74	365.11
9	20.05	365.17
10	23.25	365.36
11	25.87	365.62
12	29.13	365.92
13	31.34	365.86
14	35.15	365.85
15	38.75	365.78
16	41.37	365.51
17	45.54	365.00
18	48.66	365.09
19	51.03	365.23
20	53.79	365.48
21	54.39	365.73
22	56.79	365.75
23	59.41	365.46
24	61.67	365.67
25	66.16	365.33
26	68.81	365.88
27	71.57	367.24
28	72.52	367.29
29		
30		
31		
32		
33		
34		
35		
min. Stage =		364.20
Continuum		2
CEM		1

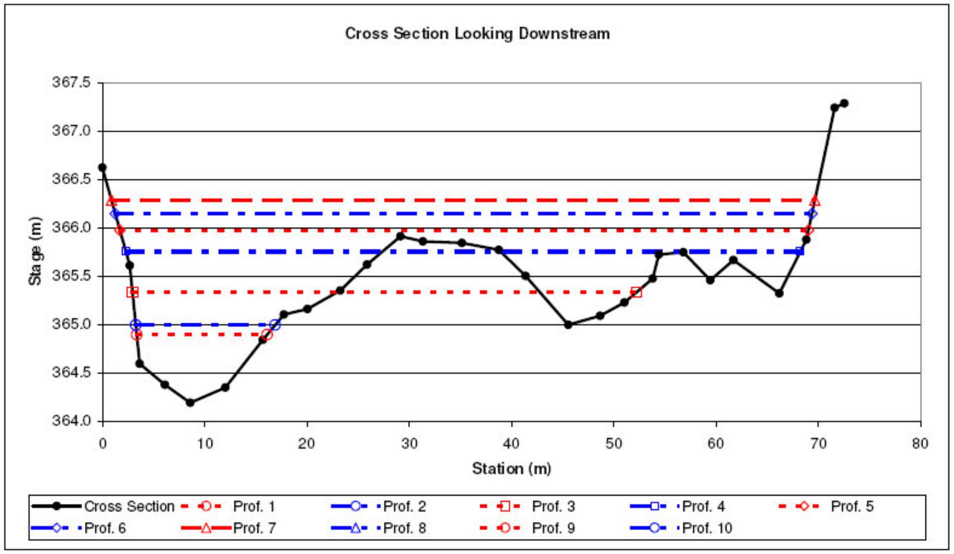

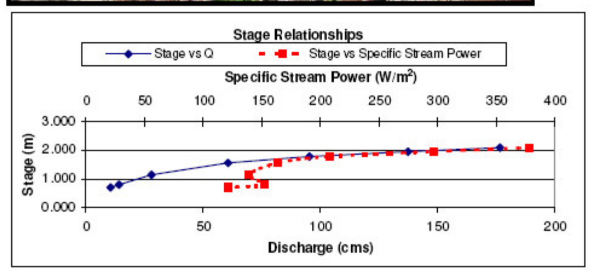

Prof. ID	Estimated n-value	L-Limit	R-Limit	WS (m)	Depth (m)	Left Sta (m)	Right Sta (m)	P_w (m)	Area (m^2)	W (m)	R (m)	D (m)	W/d	V (m/s)	Q (m^3/s)	U* (m/s)	τ (kg/ms^2)	τ^*	ω (W/m^2)	Ω (W/m)	F_r	R/d_{84}	n-value per Limerino	Floodplain Form
SCSA02P01	0.040		29.13	364.90	0.704	3.36	16.10	12.93	5.83	12.75	0.45	0.46	18.1	1.8	10.5	0.26	66.3	0.186	121	1542	0.91	6.4	0.036	BF
SCSA02P02	0.040		29.13	365.00	0.804	3.26	16.89	13.86	7.14	13.63	0.52	0.52	16.9	2.0	14.1	0.28	75.8	0.213	152	2069	0.93	7.3	0.035	BF
SCSA02P03	0.040		54.39	365.34	1.144	2.94	52.23	29.92	14.66	29.50	0.49	0.50	25.8	1.9	27.9	0.27	72.1	0.203	139	4105	0.92	6.9	0.035	BF
SCSA02P04	0.045			365.76	1.564	2.29	68.22	55.16	32.00	54.41	0.58	0.59	34.8	1.9	60.6	0.29	85.4	0.240	164	8913	0.85	8.2	0.034	BF
SCSA02P05	0.045			365.98	1.784	1.71	69.00	68.13	45.68	67.29	0.67	0.68	37.7	2.1	95.3	0.31	98.7	0.278	208	14017	0.87	9.5	0.034	BF
SCSA02P06	0.045			366.15	1.954	1.26	69.35	68.99	57.19	68.09	0.83	0.84	34.8	2.4	137.4	0.35	122.0	0.343	297	20212	0.90	11.7	0.033	BF
SCSA02P07	0.045			366.29	2.094	0.89	69.63	69.71	66.77	68.74	0.96	0.97	32.8	2.6	176.6	0.38	141.0	0.397	378	25985	0.92	13.5	0.033	BF
SCSA02P08	0.045																							BF
SCSA02P09	0.045																							BF
SCSA02P10	0.045																							BF

Cross Section Hydraulic Analyses: Santiago Creek Modeling Reach

Floodplain/Site Description: Santiago Creek~ 0.15 mi downstream of Santiago Canyon Bridge and USGS guaging station. Photograph view is looking downstream at only the main channel (see cross section tab for full section view).

Location ID	SCSA03	
d_{50} (mm) =	22.00	
d_{84} (mm) =	70.80	
So = Sf =	0.0150	
Pt #	Sta (m)	Stage (m)
1	0.00	369.14
2	2.94	366.62
3	5.00	366.49
4	6.60	365.77
5	8.37	365.30
6	9.63	365.26
7	11.46	365.48
8	13.06	366.31
9	13.67	366.38
10	14.63	366.19
11	17.02	365.05
12	20.28	365.20
13	22.85	365.40
14	25.30	365.36
15	27.73	365.60
16	29.43	365.96
17	30.88	366.31
18	33.37	366.31
19	35.08	366.24
20	38.01	366.03
21	41.12	365.88
22	44.14	366.06
23	47.24	366.51
24	50.47	366.04
25	52.43	366.46
26	55.73	366.31
27	58.61	365.83
28	59.77	365.88
29	61.29	366.44
30	65.40	366.40
31	66.71	367.44
32	68.60	367.67
33		
34		
35		
min. Stage =	365.05	
Continuum	2	
CEM	1	

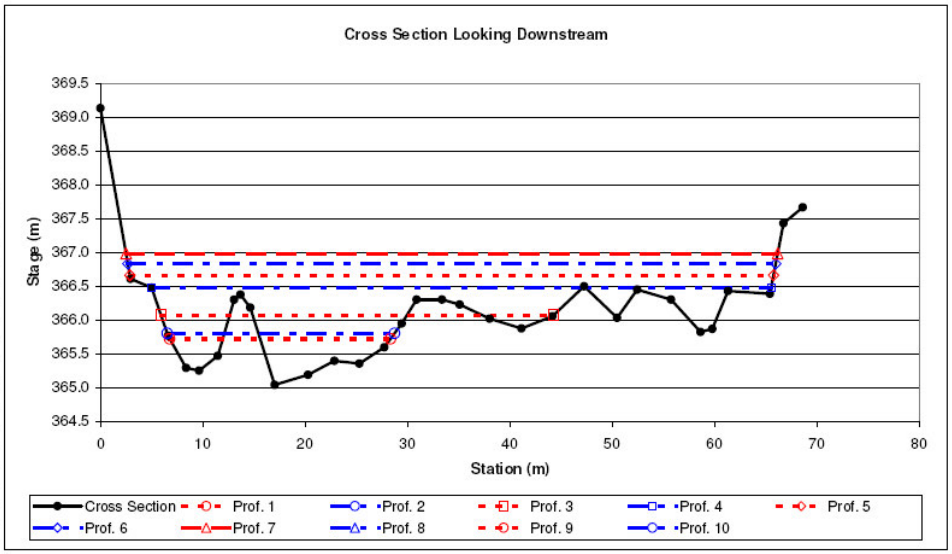

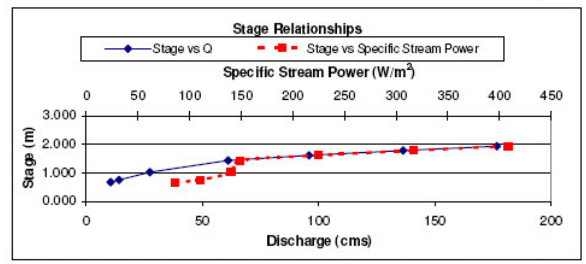

Prof. ID	Estimated n-value	L-Limit	R-Limit	WS (m)	Depth (m)	Left Sta (m)	Right Sta (m)	P_w (m)	Area (m^2)	W (m)	R (m)	D (m)	W/d	V (m/s)	Q (m^3/s)	U* (m/s)	τ (kg/ms²)	τ*	ω (W/m²)	Ω (W/m)	F_r	R/d_{84}	n-value per Limerino	Floodplain Form
SCSA03P01	0.040		30.88	365.73	0.683	6.76	28.34	18.25	6.69	17.93	0.37	0.37	26.3	1.6	10.5	0.23	54.0	0.152	86	1545	0.88	5.2	0.037	BF
SCSA03P02	0.040		30.88	365.81	0.762	6.52	28.73	19.27	8.17	18.89	0.42	0.43	24.8	1.7	14.1	0.25	62.4	0.175	110	2076	0.90	6.0	0.036	BF
SCSA03P03	0.040		47.24	366.08	1.032	5.91	44.26	29.38	14.40	28.77	0.49	0.50	27.9	1.9	27.4	0.27	72.1	0.203	140	4032	0.92	6.9	0.035	BF
SCSA03P04	0.045			366.49	1.443	4.94	65.52	61.47	33.57	60.36	0.55	0.56	41.8	1.8	61.0	0.28	80.4	0.226	149	8983	0.83	7.7	0.035	BF
SCSA03P05	0.045			366.67	1.623	2.88	65.74	64.07	44.73	62.87	0.70	0.71	38.7	2.1	95.8	0.32	102.7	0.289	224	14097	0.87	9.9	0.034	BF
SCSA03P06	0.045			366.84	1.792	2.68	65.96	64.61	55.45	63.28	0.86	0.88	35.3	2.5	136.3	0.36	126.3	0.355	317	20057	0.90	12.1	0.033	BF
SCSA03P07	0.045			366.99	1.943	2.50	66.15	65.08	64.97	63.64	1.00	1.02	32.8	2.7	176.6	0.38	146.9	0.413	408	25992	0.92	14.1	0.033	BF
SCSA03P08	0.045																							BF
SCSA03P09	0.045																							BF
SCSA03P10	0.045																							BF

Cross Section Hydraulic Analyses: Santiago Creek Modeling Reach

Floodplain/Site Description: Santiago Creek~ 0.15 mi downstream of Santiago Canyon Bridge and USGS guaging station. Photograph view is looking downstream at only the main channel (see cross section tab for full section view).

Location ID	SCSA04	
d_{50} (mm) =	22.00	
d_{84} (mm) =	70.80	
So = Sf =	0.0140	
Pt #	Sta (m)	Stage (m)
1	0.00	371.33
2	0.68	370.77
3	2.29	370.34
4	2.85	368.94
5	4.27	368.25
6	5.99	368.02
7	8.11	367.94
8	8.97	367.67
9	10.59	367.46
10	13.48	367.61
11	14.22	367.90
12	16.62	368.07
13	19.46	368.29
14	21.99	369.65
15	42.01	369.35
16	48.68	370.47
17		
18		
19		
20		
21		
22		
23		
24		
25		
26		
27		
28		
29		
30		
31		
32		
33		
34		
35		
min. Stage =	367.46	
Continuum	2	
CEM	1.1	

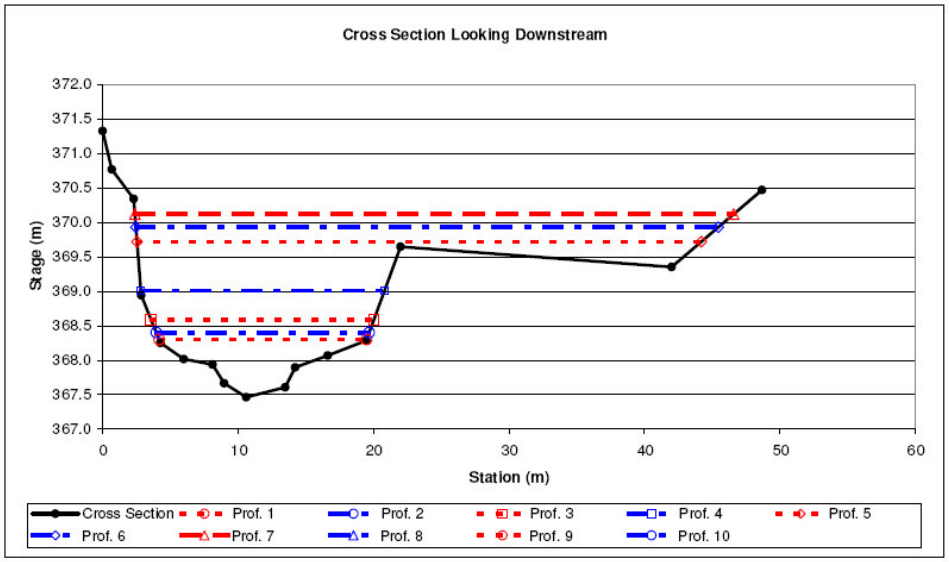

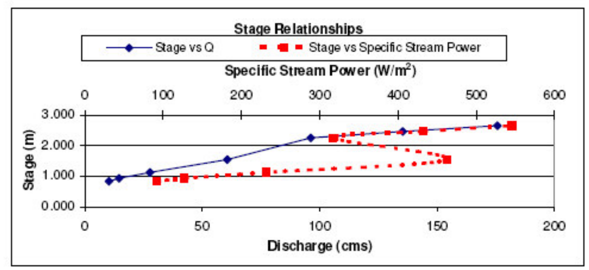

Prof. ID	Estimated n-value	L-Limit	R-Limit	WS (m)	Depth (m)	Left Sta (m)	Right Sta (m)	P_w (m)	Area (m^2)	W (m)	R (m)	D (m)	W/d	V (m/s)	Q (m^3/s)	U* (m/s)	τ (kg/ms²)	τ*	ω (W/m²)	Ω (W/m)	F_r	R/d_{84}	n-value per Limerino	Floodplain Form
SCSA04P01	0.040		21.99	368.30	0.836	4.17	19.49	15.47	6.32	15.31	0.41	0.41	18.3	1.6	10.3	0.24	56.1	0.158	92	1413	0.87	5.8	0.036	PCB
SCSA04P02	0.040		21.99	368.40	0.936	3.97	19.67	15.91	7.87	15.71	0.49	0.50	16.8	1.8	14.6	0.26	67.9	0.191	127	2000	0.89	7.0	0.035	PCB
SCSA04P03	0.035		21.99	368.59	1.126	3.57	20.03	16.75	10.93	16.45	0.65	0.66	14.6	2.5	27.8	0.30	89.6	0.252	232	3815	1.07	9.2	0.034	PCB
SCSA04P04	0.035		21.99	369.01	1.546	2.82	20.81	18.52	18.18	17.99	0.98	1.01	11.6	3.3	60.7	0.37	134.8	0.379	463	8335	1.14	13.9	0.033	PCB
SCSA04P05	0.040			369.72	2.256	2.54	44.19	42.86	36.32	41.65	0.85	0.87	18.5	2.6	96.2	0.34	116.4	0.327	317	13211	0.97	12.0	0.033	PCB
SCSA04P06	0.040			369.93	2.466	2.46	45.45	44.36	45.20	42.99	1.02	1.05	17.4	3.0	135.4	0.37	140.0	0.394	433	18597	1.00	14.4	0.032	PCB
SCSA04P07	0.040			370.12	2.656	2.38	46.58	45.71	53.49	44.20	1.17	1.21	16.6	3.3	175.7	0.40	160.7	0.452	546	24128	1.02	16.5	0.032	PCB
SCSA04P08	0.040																							PCB
SCSA04P09	0.040																							PCB
SCSA04P10	0.040																							PCB

Cross Section Hydraulic Analyses: Santiago Creek Modeling Reach

Floodplain/Site Description: Santiago Creek upstream of Santiago Canyon Bridge and USGS guaging station. Photograph view is looking downstream at channel (see cross section tab for full section view).

Location ID	SCSA06	
d_{50} (mm) =		34.00
d_{84} (mm) =		127.40
So = Sf =		0.0140
Pt #	Sta (m)	Stage (m)
1	0.00	371.78
2	1.45	371.01
3	1.84	370.37
4	3.65	369.48
5	5.73	369.26
6	7.82	369.41
7	8.52	369.64
8	10.41	369.85
9	13.04	369.96
10	15.90	370.34
11	19.41	370.30
12	22.28	370.17
13	22.68	370.00
14	23.76	369.95
15	24.60	370.01
16	25.80	370.70
17	28.26	370.64
18	30.89	370.73
19	33.97	370.85
20	36.82	372.85
21	37.47	372.86
22		
23		
24		
25		
26		
27		
28		
29		
30		
31		
32		
33		
34		
35		
min. Stage =		369.26
Continuum		2
CEM		1.1

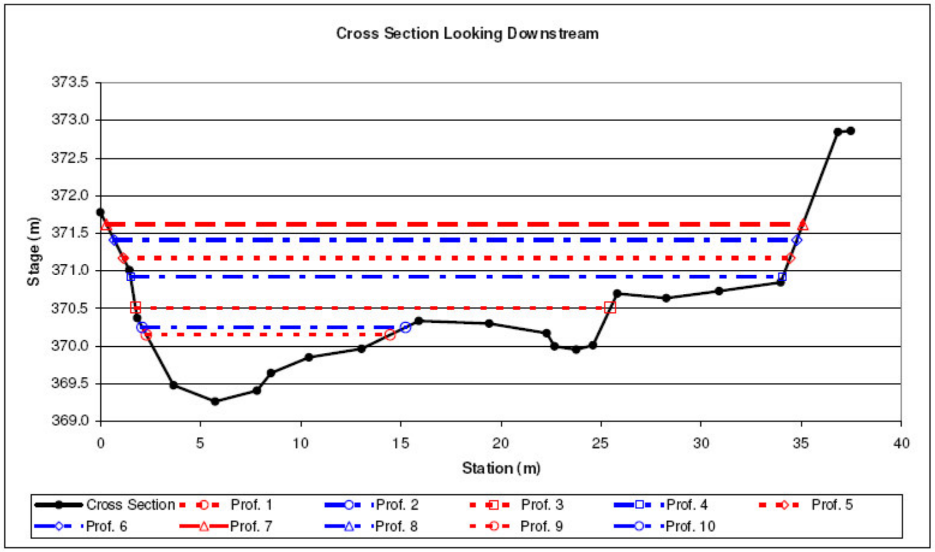

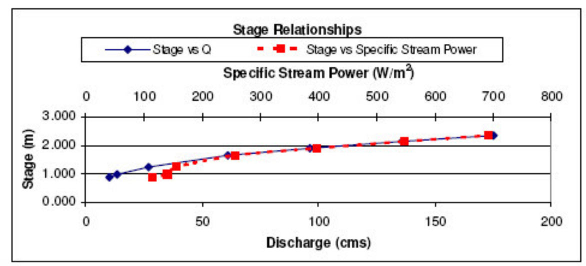

Prof. ID	Estimated n-value	L-Limit	R-Limit	WS (m)	Depth (m)	Left Sta (m)	Right Sta (m)	P_w (m)	Area (m^2)	W (m)	R (m)	D (m)	W/d	V (m/s)	Q (m^3/s)	U* (m/s)	τ (kg/ms²)	τ*	ω (W/m²)	Ω (W/m)	F_r	R/d_{84}	n-value per Limerino	Floodplain Form
SCSA06P01	0.040		15.90	370.15	0.886	2.29	14.47	12.41	5.74	12.18	0.46	0.47	13.7	1.8	10.2	0.25	63.5	0.116	115	1395	0.88	3.6	0.043	PR
SCSA06P02	0.040		15.90	370.25	0.986	2.09	15.24	13.42	7.01	13.15	0.52	0.53	13.3	1.9	13.4	0.27	71.7	0.131	140	1846	0.90	4.1	0.042	PR
SCSA06P03	0.040		25.80	370.51	1.246	1.75	25.47	24.27	13.49	23.72	0.56	0.57	19.0	2.0	27.0	0.28	76.4	0.139	156	3705	0.91	4.4	0.042	PR
SCSA06P04	0.040			370.92	1.656	1.50	34.07	33.42	25.01	32.57	0.75	0.77	19.7	2.4	61.0	0.32	102.8	0.187	257	8376	0.95	5.9	0.040	PR
SCSA06P05	0.040			371.17	1.906	1.15	34.43	34.31	33.24	33.28	0.97	1.00	17.5	2.9	96.3	0.36	133.1	0.242	397	13220	0.99	7.6	0.038	PR
SCSA06P06	0.040			371.41	2.147	0.70	34.77	35.24	41.32	34.07	1.17	1.21	15.9	3.3	135.9	0.40	161.0	0.293	548	18665	1.02	9.2	0.037	PR
SCSA06P07	0.040			371.62	2.356	0.30	35.07	36.05	48.55	34.77	1.35	1.40	14.8	3.6	175.1	0.43	184.9	0.337	692	24051	1.05	10.6	0.037	PR
SCSA06P08	0.040																							PR
SCSA06P09	0.040																							PR
SCSA06P10	0.040																							PR

Cross Section Hydraulic Analyses: Santiago Creek Modeling Reach

Floodplain/Site Description: Santiago Creek upstream of Santiago Canyon Bridge and USGS guaging station. Photograph view is looking downstream at channel (see cross section tab for full section view).

Location ID	SCSA07	
d_{50} (mm) =	34.00	
d_{84} (mm) =	127.40	
So = Sf =	0.0140	
Pt #	Sta (m)	Stage (m)
1	0.00	372.70
2	0.34	372.50
3	1.78	370.74
4	4.72	370.76
5	7.38	370.89
6	9.80	370.75
7	12.04	370.53
8	14.97	370.44
9	17.37	370.32
10	19.68	370.53
11	23.19	372.05
12	26.11	373.35
13	28.64	373.52
14		
15		
16		
17		
18		
19		
20		
21		
22		
23		
24		
25		
26		
27		
28		
29		
30		
31		
32		
33		
34		
35		
min. Stage =	370.32	

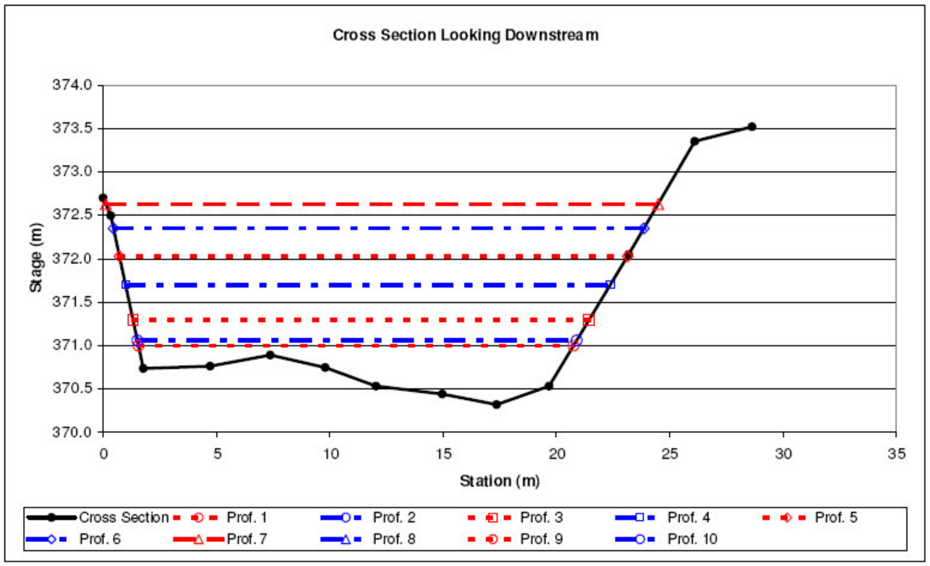

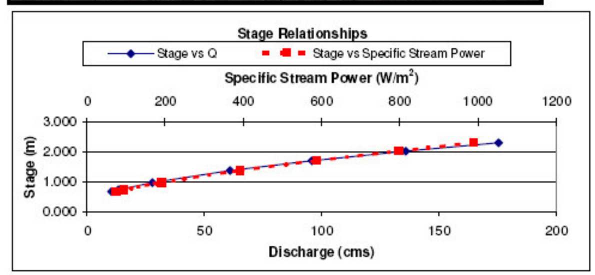

Prof. ID	Estimated n-value	L-Limit	R-Limit	WS (m)	Depth (m)	Left Sta (m)	Right Sta (m)	P_w (m)	Area (m^2)	W (m)	R (m)	D (m)	W/d	V (m/s)	Q (m^3/s)	U* (m/s)	τ (kg/ms²)	τ*	ω (W/m²)	Ω (W/m)	F_r	R/d_{84}	n-value per Limerino	Floodplain Form
SCSA07P01	0.040			371.00	0.678	1.56	20.76	19.45	7.01	19.20	0.36	0.37	28.3	1.5	10.5	0.22	49.5	0.090	75	1443	0.85	2.8	0.046	PR
SCSA07P02	0.040			371.06	0.738	1.51	20.90	19.68	8.17	19.39	0.42	0.42	26.2	1.6	13.4	0.24	57.0	0.104	95	1847	0.87	3.3	0.044	PR
SCSA07P03	0.040			371.30	0.978	1.32	21.46	20.59	12.91	20.14	0.63	0.64	20.6	2.2	28.0	0.29	86.1	0.157	191	3843	0.93	4.9	0.041	PR
SCSA07P04	0.040			371.70	1.378	0.99	22.38	22.12	21.22	21.39	0.96	0.99	15.5	2.9	61.0	0.36	131.7	0.240	392	8384	0.99	7.5	0.038	PR
SCSA07P05	0.040			372.03	1.708	0.72	23.15	23.38	28.45	22.42	1.22	1.27	13.1	3.4	95.9	0.41	167.1	0.304	587	13172	1.02	9.6	0.037	PR
SCSA07P06	0.040			372.35	2.029	0.46	23.86	24.58	35.78	23.40	1.46	1.53	11.5	3.8	135.9	0.45	199.9	0.364	798	18671	1.05	11.4	0.037	PR
SCSA07P07	0.040			372.63	2.308	0.12	24.49	25.71	42.46	24.37	1.65	1.74	10.6	4.1	175.5	0.48	226.8	0.413	989	24099	1.07	13.0	0.036	PR
SCSA07P08	0.040																							PR
SCSA07P09	0.040																							PR
SCSA07P10	0.040																							PR

Cross Section Hydraulic Analyses: Santiago Creek Modeling Reach

Floodplain/Site Description: Santiago Creek upstream of Santiago Canyon Bridge and USGS guaging station. Photograph view is looking downstream at channel (see cross section tab for full section view).

Location ID	SCSA08	
d_{50} (mm) =	34.00	
d_{84} (mm) =	127.40	
So = Sf =	0.0140	
Pt #	Sta (m)	Stage (m)
1	0.00	373.33
2	0.78	372.95
3	2.62	371.17
4	4.79	371.21
5	6.56	371.22
6	7.98	371.26
7	10.38	370.95
8	11.84	370.79
9	14.71	370.71
10	17.33	370.54
11	18.60	370.73
12	20.26	371.01
13	23.83	372.05
14	27.84	373.81
15		
16		
17		
18		
19		
20		
21		
22		
23		
24		
25		
26		
27		
28		
29		
30		
31		
32		
33		
34		
35		
min. Stage =		370.54

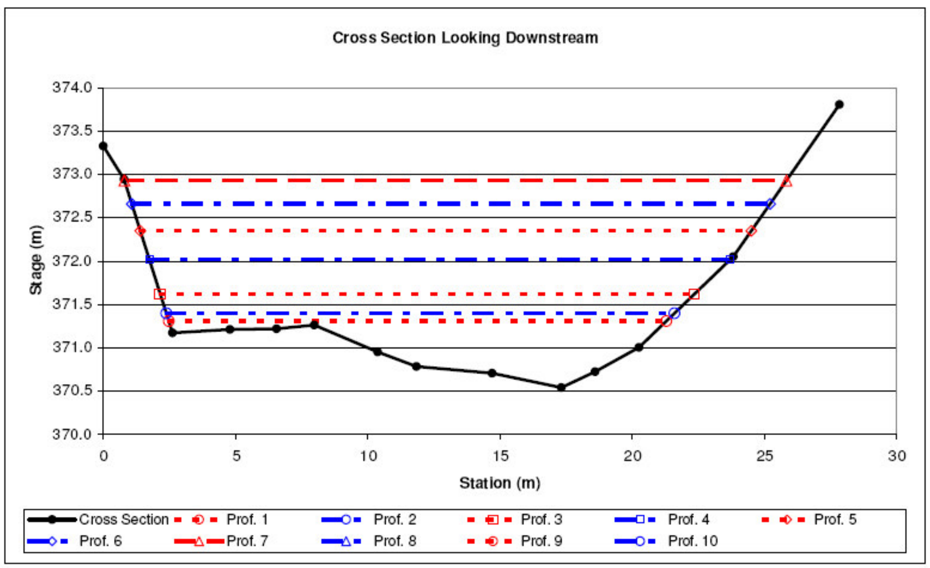

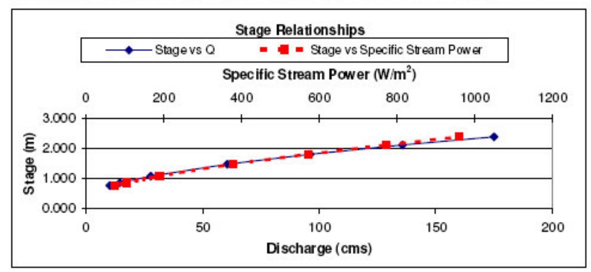

Prof. ID	Estimated n-value	L-Limit	R-Limit	WS (m)	Depth (m)	Left Sta (m)	Right Sta (m)	P_w (m)	Area (m^2)	W (m)	R (m)	D (m)	W/d	V (m/s)	Q (m^3/s)	U* (m/s)	τ (kg/ms²)	τ^*	ω (W/m²)	Ω (W/m)	F_r	R/d_{84}	n-value per Limerino	Floodplain Form
SCSA08P01	0.040			371.31	0.767	2.48	21.30	18.99	6.81	18.82	0.36	0.36	24.5	1.5	10.2	0.22	49.2	0.090	74	1395	0.85	2.8	0.046	PR
SCSA08P02	0.040			371.40	0.857	2.38	21.60	19.44	8.52	19.22	0.44	0.44	22.4	1.7	14.5	0.25	60.2	0.110	104	1996	0.88	3.4	0.044	PR
SCSA08P03	0.040			371.62	1.077	2.16	22.35	20.54	12.85	20.20	0.63	0.64	18.7	2.2	27.8	0.29	86.0	0.156	189	3821	0.93	4.9	0.041	PR
SCSA08P04	0.040			372.02	1.477	1.74	23.72	22.53	21.29	21.97	0.94	0.97	14.9	2.8	60.6	0.36	129.7	0.236	379	8327	0.99	7.4	0.038	PR
SCSA08P05	0.040			372.35	1.808	1.40	24.51	23.87	28.73	23.11	1.20	1.24	12.8	3.3	96.2	0.41	165.3	0.301	572	13209	1.03	9.4	0.037	PR
SCSA08P06	0.040			372.66	2.118	1.08	25.22	25.09	36.06	24.14	1.44	1.49	11.4	3.8	135.8	0.44	197.4	0.359	773	18653	1.06	11.3	0.037	PR
SCSA08P07	0.040			372.93	2.387	0.80	25.83	26.15	42.69	25.04	1.63	1.71	10.5	4.1	175.1	0.47	224.2	0.408	961	24047	1.08	12.8	0.036	PR
SCSA08P08	0.040																							PR
SCSA08P09	0.040																							PR
SCSA08P10	0.040																							PR

Cross Section Hydraulic Analyses: Santiago Creek At Tucker Sanctuary

Floodplain/Site Description: Santiago Creek just upstream of the Tucker Sanctuary following a significant flow event:
Photograph view is looking upstream at the main channel, during active degradation of recent depositon following a fire.

Location ID	SCSB01
d_{50} (mm) =	14.10
d_{84} (mm) =	98.30
So = Sf =	0.0208

Pt#	Sta (m)	Stage (m)
1	2.50	107.20
2	5.00	102.11
3	6.00	101.50
4	6.95	101.31
5	8.70	101.03
6	9.45	100.70
7	10.05	100.75
8	11.00	100.68
9	12.20	100.56
10	12.30	100.39
11	12.80	100.30
12	13.65	100.34
13	14.00	100.29
14	14.50	100.27
15	14.95	100.28
16	15.55	100.36
17	15.75	100.32
18	16.20	100.23
19	16.55	100.32
20	18.10	100.46
21	18.60	100.73
22	18.90	101.35
23	20.35	101.13
24	21.95	101.17
25	23.30	101.22
26	23.90	101.20
27	25.00	100.91
28	25.70	100.88
29	26.40	100.93
30	27.05	101.16
31	27.85	101.14
32	29.70	101.22
33	31.60	101.57
34	34.10	103.27
35		
min. Stage =		100.23
Continuum		2
CEM		2.10

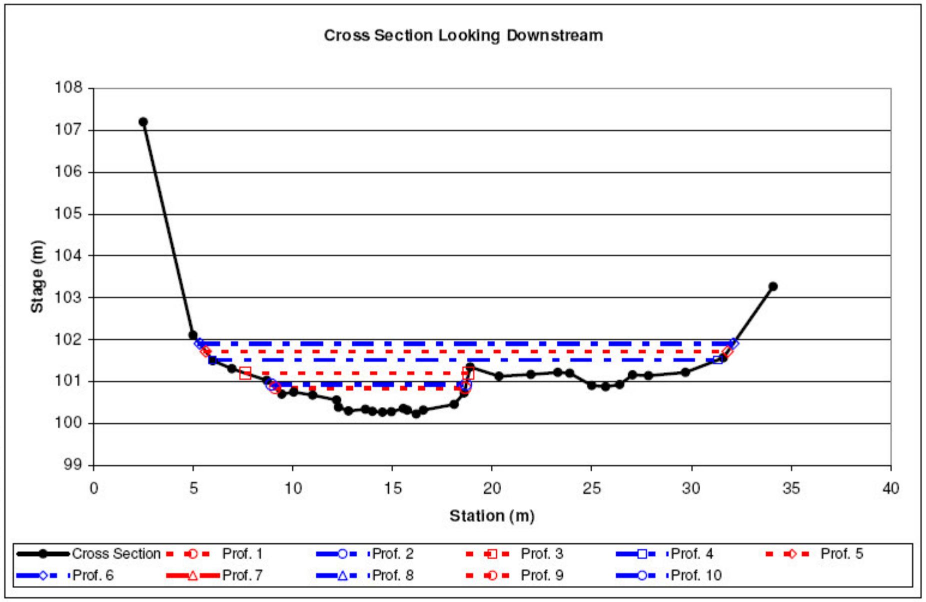

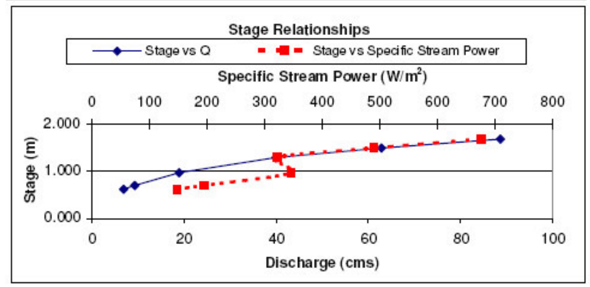

Prof. ID	Estimated n-value	L-Limit	R-Limit	WS (m)	Depth (m)	Left Sta (m)	Right Sta (m)	P_w (m)	Area (m^2)	W (m)	R (m)	D (m)	W/d	V (m/s)	Q (m^3/s)	U* (m/s)	τ (kg/ms^2)	τ*	ω (W/m^2)	Ω (W/m)	F_r	R/d_{84}	n-value per Limerino	Floodplain Form
SCSB01P01	0.040		18.90	100.65	0.620	9.11	18.66	9.88	3.70	9.55	0.37	0.39	15.4	1.9	6.9	0.28	76.4	0.335	148	1414	1.03	3.8	0.041	PMB
SCSB01P02	0.040		18.90	100.93	0.700	8.93	18.70	10.17	4.47	9.77	0.44	0.46	14.0	2.1	9.3	0.30	89.8	0.394	195	1903	1.06	4.5	0.040	PMB
SCSB01P03	0.040		18.90	101.20	0.970	7.64	18.83	11.79	7.27	11.19	0.62	0.65	11.5	2.6	19.0	0.35	125.8	0.552	346	3873	1.11	6.3	0.038	PMB
SCSB01P04	0.040			101.52	1.290	5.97	31.33	26.22	15.64	25.36	0.60	0.62	19.7	2.6	40.0	0.35	121.7	0.534	321	8153	1.11	6.1	0.038	PMB
SCSB01P05	0.040			101.72	1.490	5.64	31.82	27.15	20.81	26.18	0.77	0.79	17.6	3.0	62.8	0.40	156.4	0.687	490	12823	1.16	7.8	0.037	PMB
SCSB01P06	0.040			101.91	1.680	5.33	32.10	27.85	25.84	26.77	0.93	0.97	15.9	3.4	88.6	0.44	189.3	0.831	675	18084	1.20	9.4	0.036	PMB
SCSB01P07	0.040																							PMB
SCSB01P08	0.035																							PMB
SCSB01P09	0.035																							PMB
SCSB01P10	0.035																							PMB

Cross Section Hydraulic Analyses: Santiago Creek At Tucker Sanctuary

Floodplain/Site Description: Santiago Creek just upstream of the Tucker Sanctuary following a significant flow event: Photograph view is looking downstream at the main channel, during active degradation of recent depositon following a fire.

Location ID	SCSB02	
d_{50} (mm) =	14.10	
d_{84} (mm) =	98.30	
So = Sf =	0.0193	
Pt#	Sta (m)	Stage (m)
1	5.00	102.99
2	6.10	102.32
3	7.40	101.94
4	8.40	102.18
5	9.20	102.17
6	10.25	102.09
7	11.50	101.90
8	12.30	101.86
9	13.30	101.80
10	13.70	101.78
11	14.30	101.82
12	15.00	101.84
13	15.75	101.89
14	16.35	101.81
15	16.75	101.74
16	17.40	101.85
17	17.60	101.75
18	18.00	101.74
19	18.70	101.79
20	19.70	101.89
21	20.65	101.99
22	20.80	102.12
23	21.10	102.19
24	22.60	102.15
25	24.60	102.65
26		
27		
28		
29		
30		
31		
32		
33		
34		
35		
min. Stage =	101.74	
Continuum	2	
CEM	2.10	

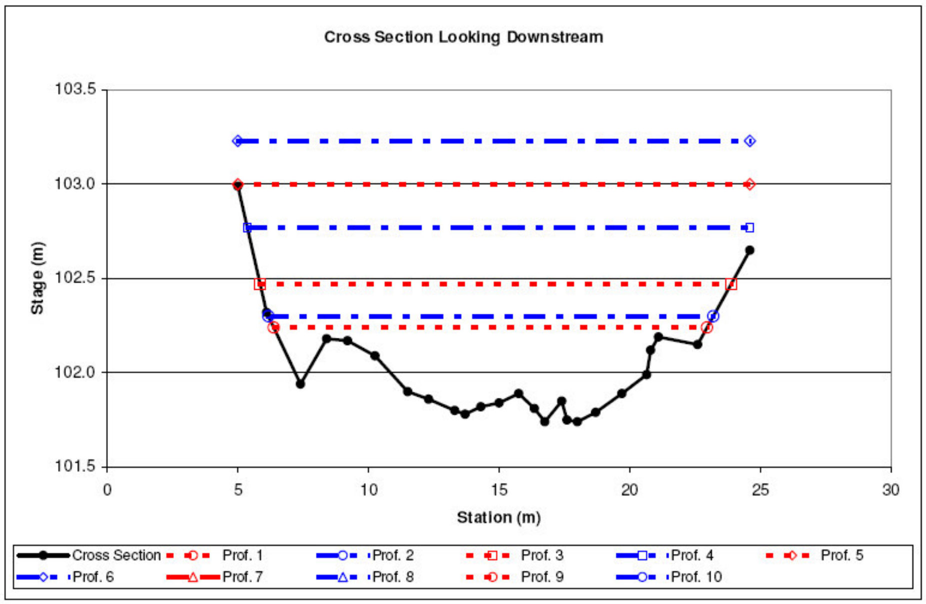

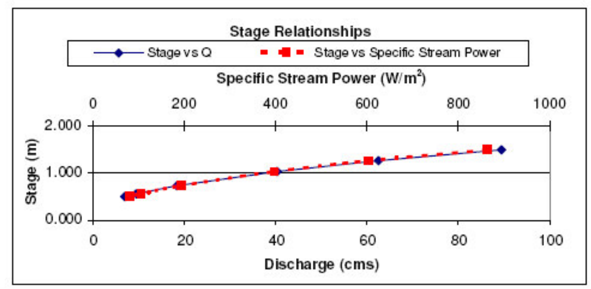

Prof. ID	Estimated n-value	L-Limit	R-Limit	WS (m)	Depth (m)	Left Sta (m)	Right Sta (m)	P_w (m)	Area (m^2)	W (m)	R (m)	D (m)	W/d	V (m/s)	Q (m^3/s)	U* (m/s)	τ (kg/ms^2)	τ*	ω (W/m^2)	Ω (W/m)	F_r	R/d_{84}	n-value per Limerino	Floodplain Form
SCSB02P01	0.040			102.24	0.500	6.37	22.96	16.81	4.71	16.59	0.28	0.28	33.2	1.5	7.0	0.23	53.0	0.233	80	1324	0.96	2.8	0.044	PMB
SCSB02P02	0.040			102.30	0.560	6.17	23.20	17.27	5.71	17.03	0.33	0.34	30.4	1.7	9.5	0.25	62.6	0.275	106	1797	0.98	3.4	0.042	PMB
SCSB02P03	0.040			102.47	0.730	5.85	23.88	18.33	8.70	18.03	0.47	0.48	24.7	2.1	18.4	0.30	89.8	0.394	193	3479	1.04	4.8	0.039	PMB
SCSB02P04	0.040			102.77	1.030	5.36	24.60	19.65	14.33	19.24	0.73	0.74	18.7	2.8	40.3	0.37	138.1	0.606	397	7635	1.12	7.4	0.037	PMB
SCSB02P05	0.040			103.00	1.260	5.00	24.60	20.07	18.80	19.60	0.94	0.96	15.6	3.3	62.5	0.42	177.3	0.778	604	11833	1.16	9.5	0.036	PMB
SCSB02P06	0.040			103.23	1.490	5.00	24.60	20.07	23.31	19.60	1.16	1.19	13.2	3.8	89.4	0.47	219.9	0.965	864	16931	1.20	11.8	0.035	PMB
SCSB02P07	0.040																							PMB
SCSB02P08	0.040																							PMB
SCSB02P09	0.040																							PMB
SCSB02P10	0.040																							PMB

Cross Section Hydraulic Analyses: Santiago Creek At Tucker Sanctuary

Floodplain/Site Description: Santiago Creek just upstream of the Tucker Sanctuary following a significant flow event:
Photograph view is looking upstream at the main channel, during active degradation of recent depositon following a fire.

Location ID	SCSB03	
d_{50} (mm) =	14.10	
d_{84} (mm) =	98.30	
So = Sf =	0.0193	
Pt#	Sta (m)	Stage (m)
1	4.00	105.51
2	5.00	103.51
3	6.00	102.90
4	6.95	102.71
5	8.70	102.67
6	13.70	102.51
7	18.70	102.67
8	18.90	102.75
9	20.00	102.97
10	25.00	104.67
11		
12		
13		
14		
15		
16		
17		
18		
19		
20		
21		
22		
23		
24		
25		
26		
27		
28		
29		
30		
31		
32		
33		
34		
35		
min. Stage =	102.51	
Continuum	2	
CEM	2.10	

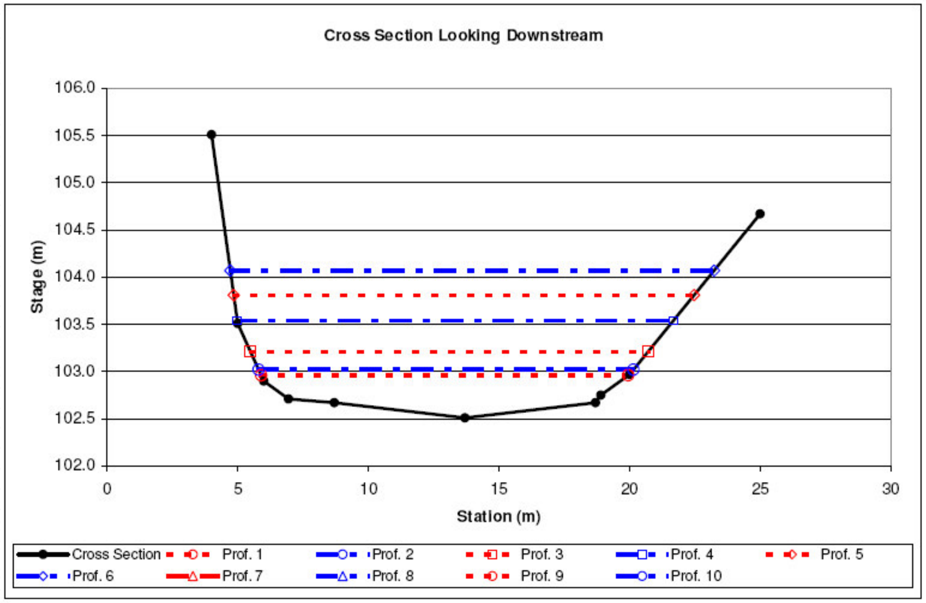

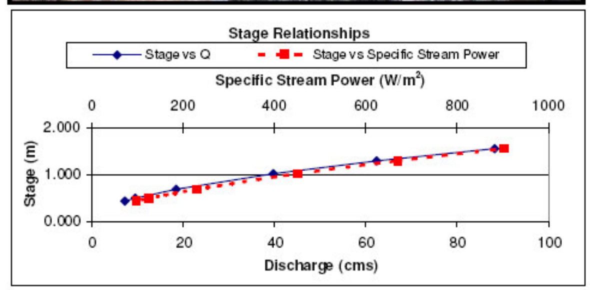

Prof. ID	Estimated n-value	L-Limit	R-Limit	WS (m)	Depth (m)	Left Sta (m)	Right Sta (m)	P_w (m)	Area (m^2)	W (m)	R (m)	D (m)	W/d	V (m/s)	Q (m^3/s)	U* (m/s)	τ (kg/ms^2)	τ^*	ω (W/m^2)	Ω (W/m)	F_r	R/d_{84}	n-value per Limerino	Floodplain Form
SCSB03P01	0.040			102.96	0.450	5.90	19.95	14.13	4.48	14.05	0.32	0.32	31.2	1.6	7.2	0.25	60.1	0.264	98	1372	0.98	3.2	0.043	PMB
SCSB03P02	0.040			103.02	0.510	5.80	20.15	14.45	5.34	14.34	0.37	0.37	28.1	1.8	9.5	0.26	69.9	0.307	126	1806	1.00	3.8	0.041	PMB
SCSB03P03	0.040			103.21	0.700	5.49	20.71	15.40	8.14	15.21	0.53	0.54	21.7	2.3	18.5	0.32	100.1	0.439	230	3501	1.06	5.4	0.039	PMB
SCSB03P04	0.040			103.54	1.030	4.98	21.68	17.04	13.41	16.69	0.79	0.80	16.2	3.0	39.7	0.39	149.1	0.654	451	7520	1.13	8.0	0.036	PMB
SCSB03P05	0.040			103.81	1.300	4.85	22.47	18.18	18.04	17.62	0.99	1.02	13.6	3.5	62.4	0.43	187.9	0.825	670	11808	1.17	10.1	0.035	PMB
SCSB03P06	0.040			104.07	1.560	4.72	23.24	19.28	22.74	18.52	1.18	1.23	11.9	3.9	88.2	0.47	223.4	0.981	902	16698	1.20	12.0	0.035	PMB
SCSB03P07	0.040																							PMB
SCSB03P08	0.040																							PMB
SCSB03P09	0.040																							PMB
SCSB03P10	0.040																							PMB

Cross Section Hydraulic Analyses: Santiago Creek Natural Loadings Site

Floodplain/Site Description: Santiago Creek just upstream of the SCCWRP Natural Loadings monitoring Site following a significant flow event: Photograph view is looking downstream at the main channel, during active degradation of recent deposition following a fire.

Location ID	SCSC01	
d_{50} (mm) =		7.20
d_{84} (mm) =		21.10
So = Sf =		0.0242
Pt#	Sta (m)	Stage (m)
1	0.00	3.63
2	0.10	1.63
3	1.80	1.47
4	2.50	1.17
5	4.30	0.78
6	5.00	0.54
7	5.10	0.40
8	5.90	0.15
9	6.70	0.01
10	8.90	0.00
11	10.70	0.02
12	11.00	0.07
13	12.30	0.19
14	13.30	0.53
15	14.60	1.36
16	15.60	2.00
17	16.60	2.64
18		
19		
20		
21		
22		
23		
24		
25		
26		
27		
28		
29		
30		
31		
32		
33		
34		
35		
min. Stage =		0.00
Continuum		2
CEM		2.10

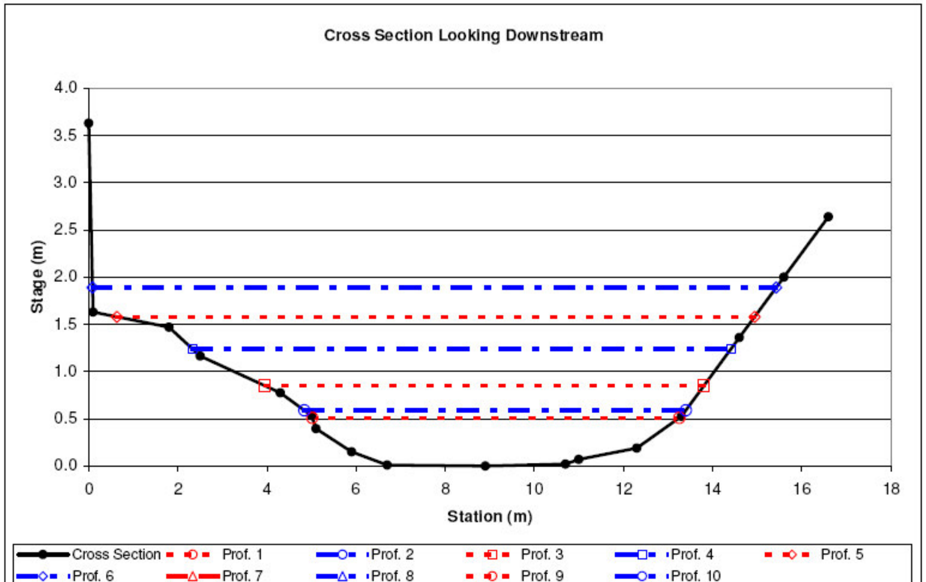

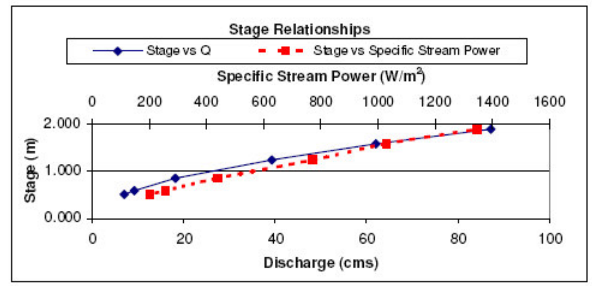

Prof. ID	Estimated n-value	L-Limit	R-Limit	WS (m)	Depth (m)	Left Sta (m)	Right Sta (m)	P_w (m)	Area (m^2)	W (m)	R (m)	D (m)	W/d	V (m/s)	Q (m^3/s)	U* (m/s)	τ (kg/ms^2)	τ*	ω (W/m^2)	Ω (W/m)	F_r	R/d_{84}	n-value per Limerino	Floodplain Form
SCSC01P01	0.040			0.51	0.510	5.02	13.26	8.41	3.34	8.24	0.40	0.40	16.2	2.1	7.0	0.31	94.2	0.810	202	1663	1.13	18.8	0.026	PMB
SCSC01P02	0.040			0.59	0.590	4.84	13.40	8.78	4.01	8.56	0.46	0.47	14.5	2.3	9.2	0.33	108.4	0.932	256	2194	1.15	21.6	0.026	PMB
SCSC01P03	0.040			0.85	0.850	3.95	13.81	10.18	6.39	9.85	0.63	0.65	11.6	2.9	18.2	0.39	149.0	1.281	439	4324	1.21	29.7	0.025	PMB
SCSC01P04	0.038			1.24	1.240	2.33	14.41	12.58	10.69	12.09	0.85	0.88	9.7	3.7	39.3	0.45	201.9	1.735	772	9328	1.34	40.3	0.025	PMB
SCSC01P05	0.038			1.58	1.580	0.63	14.94	14.96	15.08	14.31	1.01	1.05	9.1	4.1	62.0	0.49	239.3	2.057	1029	14730	1.37	47.8	0.025	PMB
SCSC01P06	0.040			1.89	1.890	0.09	15.43	16.33	19.74	15.34	1.21	1.29	8.1	4.4	87.1	0.54	287.1	2.468	1348	20687	1.33	57.3	0.025	PMB
SCSC01P07	0.040																							PMB
SCSC01P08	0.040																							PMB
SCSC01P09	0.040																							PMB
SCSC01P10	0.040																							PMB

Cross Section Hydraulic Analyses: Santiago Creek Natural Loadings Site

Floodplain/Site Description: Santiago Creek upstream of the SCCWRP Natural Loadings monitoring site following a significant flow event: Photograph view is looking downstream at the main channel, during active degradation of recent deposition following a fire.

Location ID		SCSC02
d_{50} (mm) =		26.20
d_{84} (mm) =		298.60
So = Sf =		0.0273
Pt #	Sta (m)	Stage (m)
1	0.00	2.33
2	2.60	1.93
3	3.10	1.58
4	4.40	1.38
5	5.30	0.20
6	5.80	0.00
7	6.40	0.30
8	7.10	0.09
9	8.00	0.14
10	8.30	0.35
11	8.80	0.40
12	9.20	0.50
13	10.00	0.58
14	10.40	0.90
15	11.70	1.03
16	13.50	1.18
17	14.80	1.53
18	16.60	1.97
19		
20		
21		
22		
23		
24		
25		
26		
27		
28		
29		
30		
31		
32		
33		
34		
35		
min. Stage =		0.00
Continuum		2
CEM		2.10

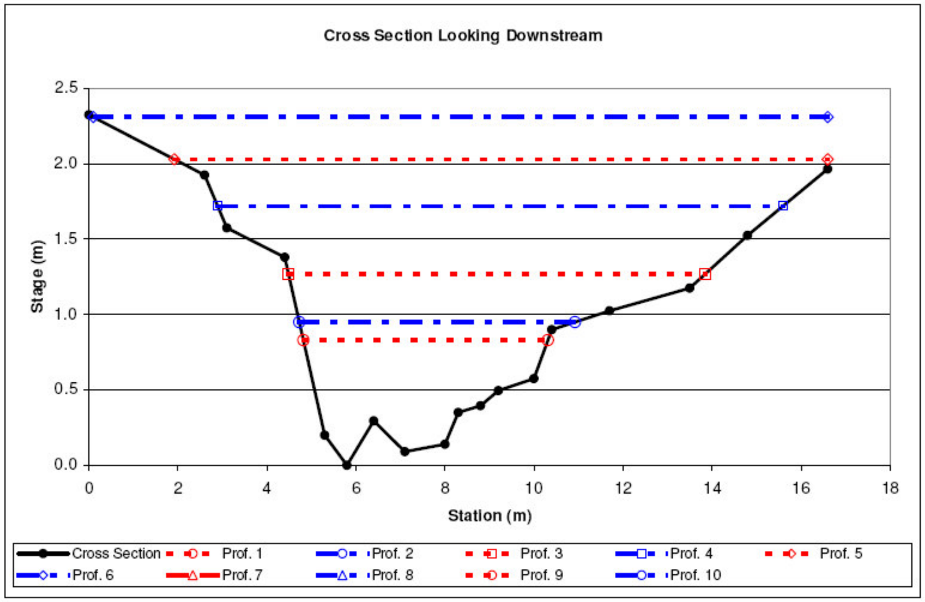

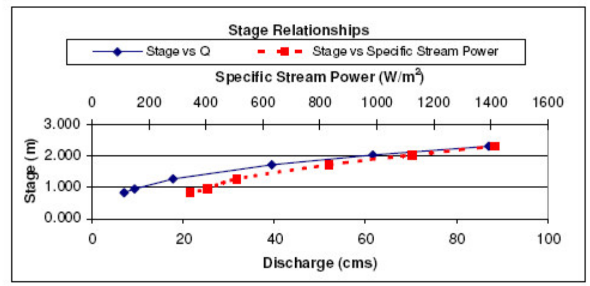

Prof. ID	Estimated n-value	L-Limit	R-Limit	WS (m)	Depth (m)	Left Sta (m)	Right Sta (m)	P_w (m)	Area (m^2)	W (m)	R (m)	D (m)	W/d	V (m/s)	Q (m^3/s)	U* (m/s)	τ (kg/ms²)	τ*	ω (W/m²)	Ω (W/m)	F_r	R/d_{84}	n-value per Limerino	Floodplain Form
SCSC02P01	0.040			0.83	0.830	4.82	10.31	6.12	2.85	5.49	0.47	0.52	6.6	2.5	7.1	0.35	124.7	0.295	345	1894	1.18	1.6	0.062	PMB
SCSC02P02	0.040			0.95	0.950	4.73	10.92	6.90	3.54	6.19	0.51	0.57	6.5	2.6	9.3	0.37	137.1	0.324	404	2503	1.20	1.7	0.060	PMB
SCSC02P03	0.040			1.27	1.270	4.48	13.85	10.26	6.10	9.37	0.59	0.65	7.4	2.9	17.8	0.40	159.2	0.376	509	4769	1.24	2.0	0.057	PMB
SCSC02P04	0.040			1.72	1.720	2.89	15.60	13.77	11.06	12.70	0.80	0.87	7.4	3.6	39.5	0.46	215.1	0.508	832	10575	1.31	2.7	0.053	PMB
SCSC02P05	0.040			2.03	2.030	1.92	16.60	15.85	15.28	14.68	0.96	1.04	7.2	4.0	61.6	0.51	258.3	0.610	1124	16504	1.35	3.2	0.051	PMB
SCSC02P06	0.040			2.31	2.310	0.10	16.60	17.69	19.65	16.50	1.11	1.19	7.1	4.4	87.1	0.55	297.5	0.703	1413	23315	1.39	3.7	0.049	PMB
SCSC02P07	0.040																							PMB
SCSC02P08	0.040																							PMB
SCSC02P09	0.040																							PMB
SCSC02P10	0.040																							PMB

Cross Section Hydraulic Analyses: Santiago Creek Site D Reach

Floodplain/Site Description: The Site D reach is located approximately 1000 meters upstream of the Santiago Canyon Natural Loadings Site and has a drainage area of approximately 7 sq. miles.

Location ID		SCSD01
d_{50} (mm) =		10.70
d_{84} (mm) =		62.20
So = Sf =		0.0324
Pt #	Sta (m)	Stage (m)
1	0.00	2.00
2	1.00	1.00
3	1.60	0.78
4	2.45	0.75
5	3.10	0.77
6	4.90	0.65
7	5.50	0.66
8	6.90	0.71
9	7.30	1.06
10	8.50	1.14
11	9.90	1.26
12	10.30	1.29
13	10.40	0.94
14	10.90	0.75
15	12.10	0.62
16	12.20	0.50
17	13.60	0.44
18	14.90	0.50
19	15.60	0.57
20	16.30	0.45
21	17.00	0.44
22	17.30	0.52
23	17.80	0.67
24	18.50	1.07
25	19.50	1.31
26	20.90	1.31
27	22.40	1.62
28	24.90	1.49
29	26.50	1.64
30	30.90	2.30
31	32.30	3.30
32		
33		
34		
35		
min. Stage =		0.44
Continuum		2
CEM		1.0

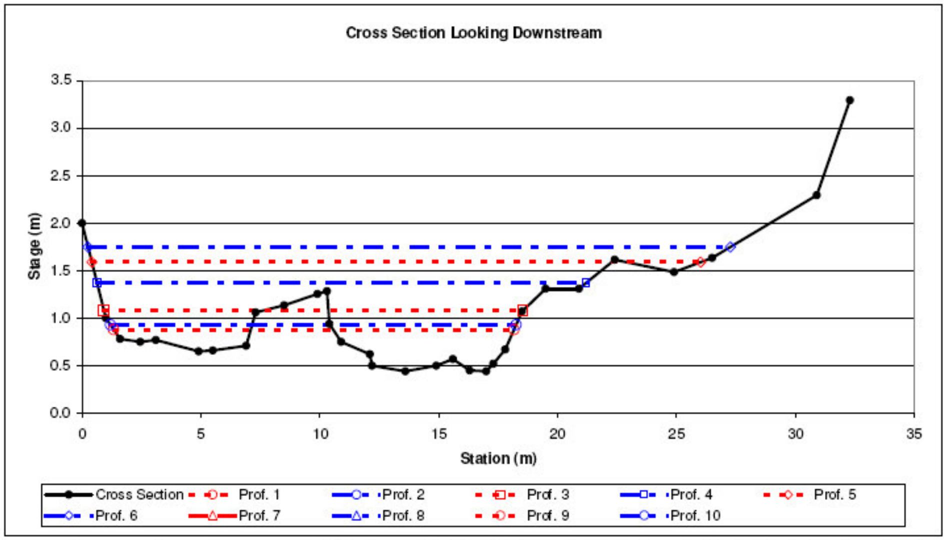

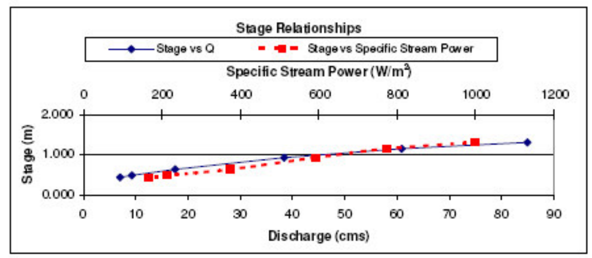

Prof. ID	Estimated n-value	L-Limit	R-Limit	WS (m)	Depth (m)	Left Sta (m)	Right Sta (m)	P_w (m)	Area (m^2)	W (m)	R (m)	D (m)	W/d	V (m/s)	Q (m^3/s)	U* (m/s)	τ (kg/ms²)	τ*	ω (W/m²)	Ω (W/m)	F_r	R/d_{84}	n-value per Limerinos	Floodplain Form
SCSD01P01	0.035		19.50	0.88	0.440	1.33	18.17	13.66	3.42	13.38	0.25	0.26	30.4	2.0	7.0	0.28	79.6	0.461	166	2223	1.38	4.0	0.038	PMB
SCSD01P02	0.035			0.93	0.490	1.19	18.26	14.12	4.10	13.79	0.29	0.30	28.1	2.3	9.2	0.30	92.3	0.534	213	2939	1.42	4.7	0.037	PMB
SCSD01P03	0.035			1.08	0.640	0.92	18.54	15.45	6.24	14.88	0.40	0.42	23.3	2.8	17.5	0.36	128.3	0.742	374	5567	1.49	6.5	0.035	PMB
SCSD01P04	0.035		22.40	1.37	0.930	0.63	21.20	21.45	11.38	20.57	0.53	0.55	22.1	3.4	38.4	0.41	168.7	0.976	593	12194	1.55	8.5	0.033	PMB
SCSD01P05	0.035			1.59	1.150	0.41	26.02	26.01	16.21	25.01	0.62	0.65	21.7	3.8	60.8	0.45	198.1	1.146	773	19340	1.60	10.0	0.033	PMB
SCSD01P06	0.035			1.75	1.310	0.25	27.27	28.10	20.43	27.02	0.73	0.76	20.6	4.2	84.9	0.48	231.0	1.336	999	26994	1.64	11.7	0.032	PMB
SCSD01P07	0.040																							PMB
SCSD01P08	0.040																							PMB
SCSD01P09	0.040																							PMB
SCSD01P10	0.040																							PMB

Cross Section Hydraulic Analyses: Un-Named Tributary to the San Jacinto River

Floodplain/Site Description: Un-named tributary to the San Jacinto River within the Badlands area, also known as RC Site 2 Alternate. Photograph view is looking upstream at the main channel.

Location ID		SJBL00
d_{50} (mm) =		0.25
d_{84} (mm) =		0.63
So = Sf =		0.0359
Pt #	Sta (m)	Stage (m)
1	0.00	101.86
2	1.00	101.82
3	1.60	101.67
4	2.80	101.14
5	4.30	100.38
6	5.10	100.12
7	5.50	100.00
8	5.80	100.09
9	6.75	100.61
10	8.00	101.38
11	9.00	101.71
12	10.00	101.81
13		
14		
15		
16		
17		
18		
19		
20		
21		
22		
23		
24		
25		
26		
27		
28		
29		
30		
31		
32		
33		
34		
35		
min. Stage =		100.00
Continuum		1
CEM		1.00

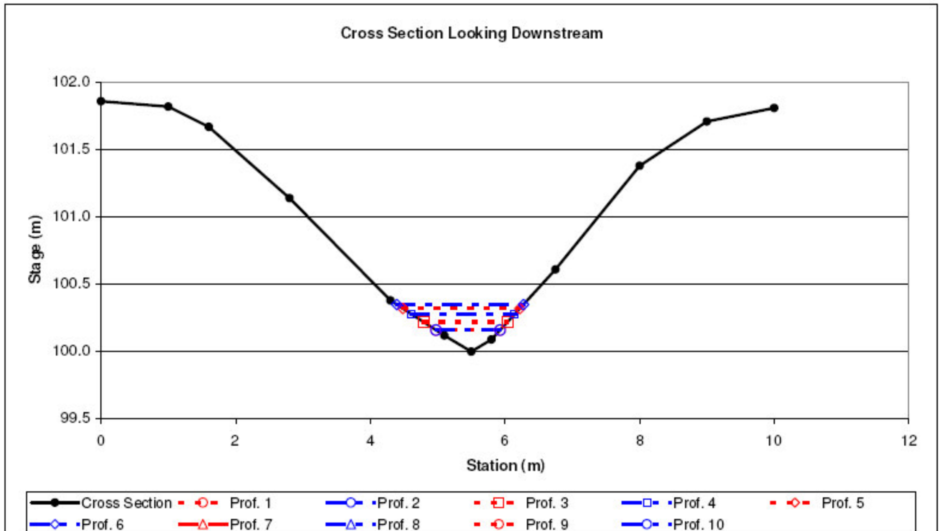

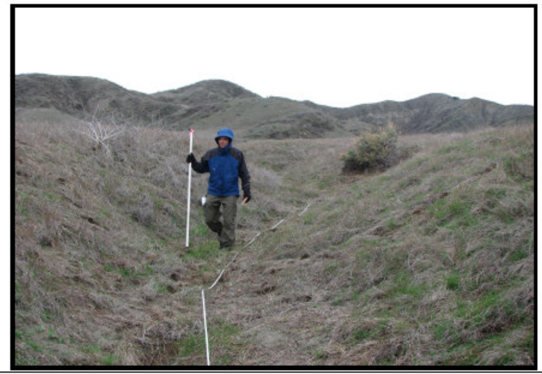

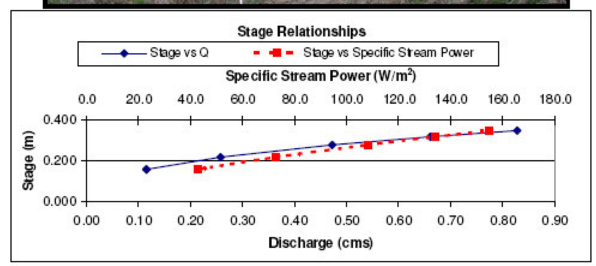

Prof. ID	Estimated n-value	L-Limit	R-Limit	WS (m)	Depth (m)	Left Sta (m)	Right Sta (m)	P_w (m)	Area (m^2)	W (m)	R (m)	D (m)	W/d	V (m/s)	Q (m^3/s)	U* (m/s)	τ (kg/ms²)	τ*	ω (W/m²)	Ω (W/m)	F_r	R/d_{84}	n-value per Limerino	Floodplain Form
SJBL01P01	0.025			100.16	0.160	4.98	5.93	1.01	0.08	0.95	0.08	0.09	5.9	1.4	0.115	0.17	28.5	7.06	42.8	41	1.66	128.5	0.014	PR
SJBL01P02	0.025			100.16	0.160	4.98	5.93	1.01	0.08	0.95	0.08	0.09	5.9	1.4	0.115	0.17	28.5	7.06	42.8	41	1.66	128.5	0.014	PR
SJBL01P03	0.025			100.22	0.220	4.79	6.04	1.33	0.15	1.25	0.11	0.12	5.7	1.8	0.258	0.20	39.2	9.69	73.0	91	1.74	176.5	0.014	PR
SJBL01P04	0.025			100.28	0.280	4.61	6.15	1.64	0.23	1.54	0.14	0.15	5.5	2.0	0.473	0.22	49.4	12.24	108.1	166	1.81	222.9	0.014	PR
SJBL01P05	0.025			100.32	0.320	4.48	6.22	1.86	0.30	1.74	0.16	0.17	5.4	2.2	0.661	0.24	56.2	13.92	134.1	233	1.85	253.3	0.014	PR
SJBL01P06	0.025			100.35	0.350	4.39	6.27	2.02	0.35	1.88	0.17	0.19	5.4	2.4	0.828	0.25	61.2	15.16	154.9	292	1.87	276.0	0.014	PR
SJBL01P07	0.025																							PR
SJBL01P08	0.025																							PR
SJBL01P09	0.025																							PR
SJBL01P10	0.025																							PR

Cross Section Hydraulic Analyses: San Juan Creek

Floodplain/Site Description: Photo views looking upstream along the main channel only. Low flow channel is channel has a step-pool or pool-riffle configuration, but the entire cross section is braided.

Location ID	SJOH01
d_{50} (mm) =	34.36
d_{84} (mm) =	104.76
So = Sf =	0.0132

Pt #	Sta (m)	Stage (m)
1	0.00	100.00
2	5.00	99.52
3	6.80	99.08
4	8.10	98.93
5	10.80	98.92
6	14.70	98.80
7	16.20	98.67
8	18.00	98.66
9	19.90	99.34
10	20.70	99.46
11	26.50	99.18
12	26.80	98.91
13	28.10	98.31
14	28.90	98.22
15	30.00	98.12
16	31.40	98.31
17	32.90	98.19
18	33.70	98.40
19	35.00	98.55
20	36.00	98.73
21	38.90	98.59
22	40.10	98.96
23	42.60	98.95
24	46.50	98.84
25	49.60	98.79
26	51.00	98.70
27	52.40	98.58
28	53.20	98.70
29	53.70	98.71
30	55.20	98.95
31	55.80	99.02
32	57.20	98.96
33	59.90	98.98
34	61.70	98.86
35	64.00	100.16
min. Stage =		98.12
Continuum		2
CEM		1

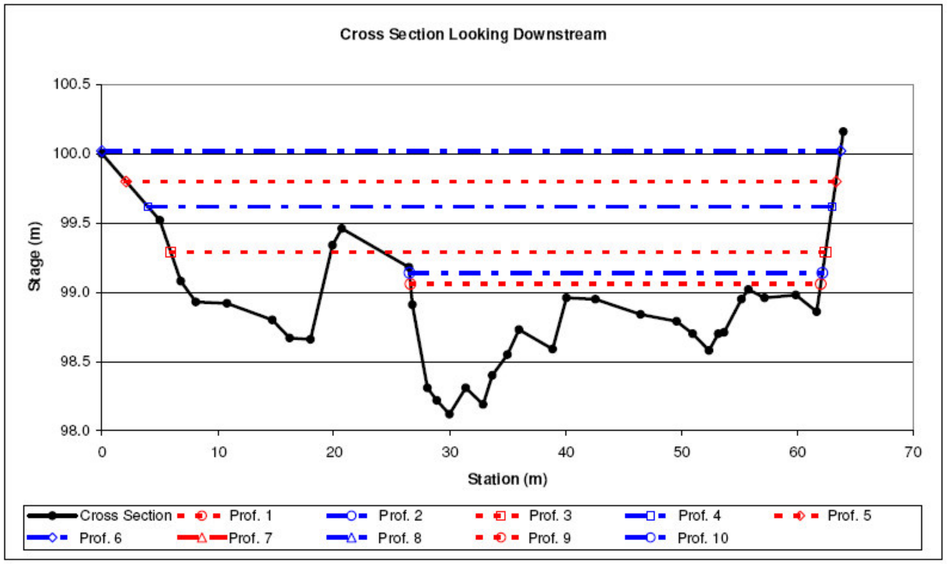

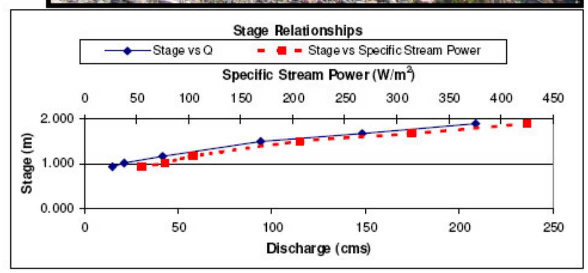

Prof. ID	Estimated n-value	L-Limit	R-Limit	WS (m)	Depth (m)	Left Sta (m)	Right Sta (m)	P_w (m)	Area (m^2)	W (m)	R (m)	D (m)	W/d	V (m/s)	Q (m^3/s)	U* (m/s)	τ (kg/ms²)	τ*	ω (W/m²)	Ω (W/m)	F_r	R/d_{84}	n-value per Limerino	Floodplain Form
SJOH01P01	0.045	20.70		99.06	0.940	26.63	62.05	35.85	12.13	35.42	0.34	0.34	37.7	1.2	15.06	0.21	44.0	0.079	55	1956	0.73	3.2	0.043	BF
SJOH01P02	0.045	20.70		99.14	1.020	26.54	62.20	36.13	14.97	35.65	0.41	0.42	35.0	1.4	21.28	0.23	53.8	0.097	78	2764	0.75	4.0	0.041	BF
SJOH01P03	0.045			99.29	1.170	5.94	62.46	52.75	26.11	52.06	0.49	0.50	44.5	1.6	41.77	0.25	64.3	0.116	104	5425	0.77	4.7	0.040	BF
SJOH01P04	0.045			99.62	1.500	3.96	63.04	59.91	44.72	59.09	0.75	0.76	39.4	2.1	94.1	0.31	96.9	0.175	207	12220	0.83	7.1	0.037	BF
SJOH01P05	0.040			99.80	1.680	2.08	63.36	62.16	55.55	61.28	0.89	0.91	36.5	2.7	148.3	0.34	116.1	0.209	314	19256	0.96	8.5	0.037	BF
SJOH01P06	0.040			100.02	1.900	0.00	63.75	64.70	69.33	63.75	1.07	1.09	33.6	3.0	208.8	0.37	139.2	0.251	425	27120	0.99	10.2	0.036	BF
SJOH01P07	0.045																							BF
SJOH01P08	0.045																							BF
SJOH01P09	0.045																							BF
SJOH01P10	0.045																							BF

Cross Section Hydraulic Analyses: San Juan Creek

Floodplain/Site Description: Aliso Canyon near the Hovnanian development. Photo view looking downstream.

Location ID	SJOH02
d_{50} (mm) =	61.24
d_{84} (mm) =	252.42
So = Sf =	0.0143

Pt #	Sta (m)	Stage (m)
1	0.00	100.00
2	1.00	99.79
3	2.50	99.67
4	4.30	99.43
5	6.20	99.48
6	7.30	99.29
7	8.60	98.69
8	9.50	98.46
9	10.20	98.28
10	11.10	98.00
11	12.30	97.88
12	13.90	97.92
13	16.60	98.05
14	17.60	98.34
15	19.60	98.50
16	21.70	98.78
17	23.60	99.01
18	24.60	98.98
19	26.90	99.17
20	29.70	100.13
21	31.80	100.49
22		
23		
24		
25		
26		
27		
28		
29		
30		
31		
32		
33		
34		
35		
min. Stage =		97.88
Continuum		2
CEM		1

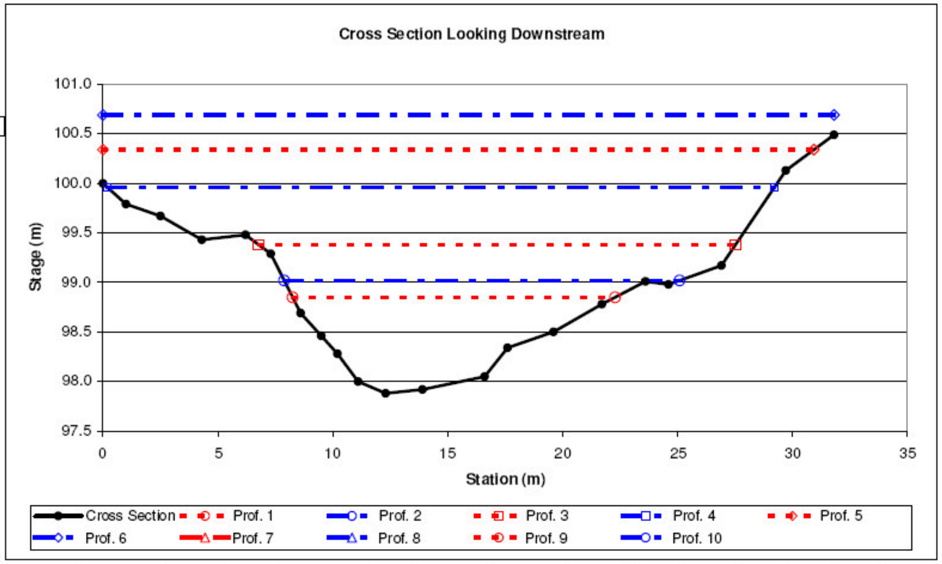

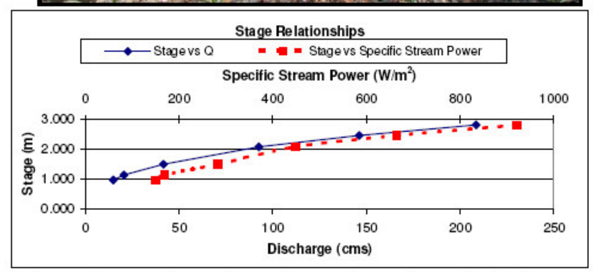

Prof. ID	Estimated n-value	L-Limit	R-Limit	WS (m)	Depth (m)	Left Sta (m)	Right Sta (m)	P_w (m)	Area (m^2)	W (m)	R (m)	D (m)	W/d	V (m/s)	Q (m^3/s)	U* (m/s)	τ (kg/ms^2)	τ*	ω (W/m^2)	Ω (W/m)	F_r	R/d_{84}	n-value per Limerino	Floodplain Form
SJOH02P01	0.045			98.85	0.970	8.25	22.28	14.23	8.17	14.02	0.57	0.58	14.5	1.8	15.0	0.28	80.7	0.082	151	2111	0.82	2.3	0.055	PR
SJOH02P02	0.045			99.02	1.140	7.89	25.08	17.46	10.74	17.20	0.62	0.62	15.1	1.9	20.7	0.29	86.5	0.087	169	2906	0.83	2.4	0.054	PR
SJOH02P03	0.045			99.38	1.500	6.78	27.51	21.10	17.67	20.73	0.84	0.85	13.8	2.4	41.8	0.34	117.7	0.119	283	5870	0.88	3.3	0.050	PR
SJOH02P04	0.045			99.96	2.080	0.19	29.20	29.52	32.61	29.01	1.10	1.12	13.9	2.8	92.7	0.39	155.2	0.157	449	13023	0.92	4.4	0.047	PR
SJOH02P05	0.045			100.34	2.460	0.00	30.93	31.49	43.97	30.93	1.40	1.42	12.6	3.3	146.1	0.44	196.3	0.198	664	20540	0.95	5.5	0.045	PR
SJOH02P06	0.045			100.69	2.810	0.00	31.80	32.37	55.04	31.80	1.70	1.73	11.3	3.8	208.5	0.49	238.9	0.241	922	29309	0.99	6.7	0.044	PR
SJOH02P07	0.045																							PR
SJOH02P08	0.045																							PR
SJOH02P09	0.045																							PR
SJOH02P10	0.045																							PR

Cross Section Hydraulic Analyses: Topanga Canyon

Floodplain/Site Description: Topanga Canyon looking upstream toward cross section.

Location ID		TCBD01
d_{50} (mm) =		87.80
d_{84} (mm) =		240.10
So = Sf =		0.0192
Pt #	Sta (m)	Stage (m)
1	0.00	100.80
2	1.50	100.30
3	2.00	100.25
4	3.00	99.35
5	3.50	99.75
6	4.00	99.80
7	5.00	100.15
8	6.00	100.20
9	8.00	100.80
10	10.00	100.80
11	12.00	100.64
12	13.00	100.47
13	14.00	100.11
14	15.00	99.76
15	16.00	99.38
16	16.20	99.30
17	16.80	99.30
18	17.60	99.12
19	18.20	99.29
20	18.50	99.10
21	19.00	99.16
22	19.50	99.15
23	20.00	99.12
24	20.50	99.33
25	21.40	99.43
26	22.40	99.75
27	23.50	99.99
28	24.60	100.31
29	25.60	100.58
30	25.90	100.90
31		
32		
33		
34		
35		
min. Stage =		99.10
Continuum		2
CEM		1.00

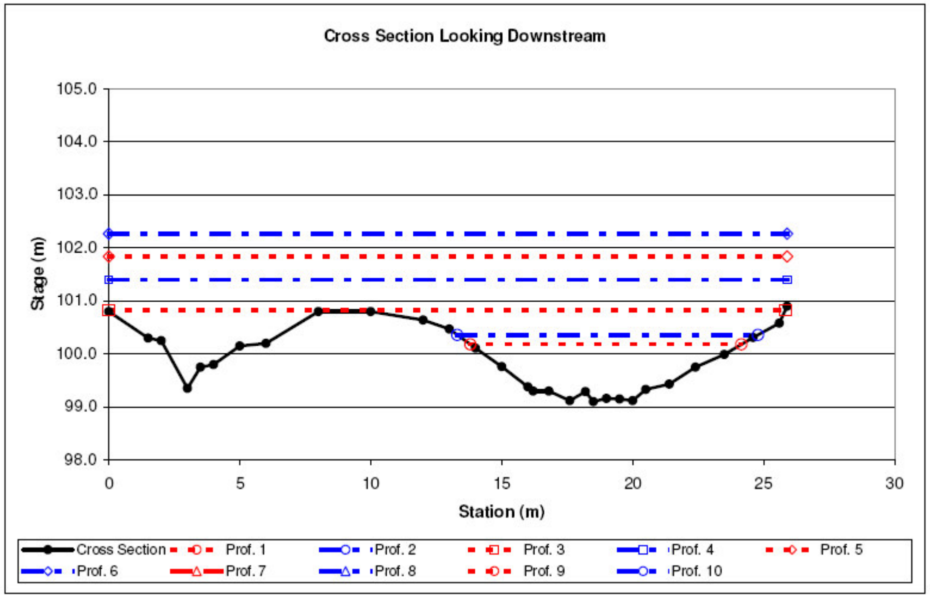

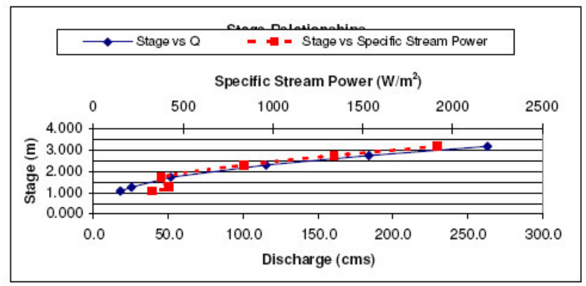

Prof. ID	Estimated n-value	L-Limit	R-Limit	WS (m)	Depth (m)	Left Sta (m)	Right Sta (m)	P_w (m)	Area (m^2)	W (m)	R (m)	D (m)	W/d	V (m/s)	Q (m^3/s)	U* (m/s)	τ (kg/ms²)	τ*	ω (W/m²)	Ω (W/m)	F_r	R/d_{84}	n-value per Limerino	Floodplain Form
TCBD01P01	0.040	10.00		100.18	1.080	13.81	24.15	10.76	6.96	10.35	0.65	0.67	9.6	2.6	18.1	0.35	121.9	0.086	329	3401	1.08	2.7	0.051	PR
TCBD01P02	0.040	10.00		100.36	1.260	13.31	24.79	11.95	8.93	11.48	0.75	0.78	9.1	2.9	25.5	0.38	140.8	0.099	418	4797	1.11	3.1	0.050	PR
TCBD01P03	0.045			100.83	1.730	0.00	25.83	27.20	20.39	25.83	0.75	0.79	14.9	2.5	51.8	0.38	141.2	0.100	378	9761	0.98	3.1	0.049	PR
TCBD01P04	0.050			101.40	2.300	0.00	25.90	27.30	35.15	25.90	1.29	1.36	11.3	3.3	115.3	0.49	242.6	0.171	839	21721	0.96	5.4	0.045	PR
TCBD01P05	0.050			101.84	2.740	0.00	25.90	27.30	46.55	25.90	1.71	1.80	9.5	4.0	184.1	0.57	321.2	0.226	1339	34683	1.01	7.1	0.043	PR
TCBD01P06	0.050			102.27	3.170	0.00	25.90	27.30	57.69	25.90	2.11	2.23	8.2	4.6	263.3	0.63	398.1	0.281	1915	49589	1.05	8.8	0.042	PR
TCBD01P07	0.050																							PR
TCBD01P08	0.050																							PR
TCBD01P09	0.050																							PR
TCBD01P10	0.050																							PR

Cross Section Hydraulic Analyses: Topanga Canyon

Floodplain/Site Description: Photograph view is looking upstream.

Location ID	TCBD02	
d_{50} (mm) =	100.00	
d_{84} (mm) =	331.70	
So = Sf =	0.0175	
Pt #	Sta (m)	Stage (m)
1	0.25	105.53
2	0.50	101.53
3	1.80	101.24
4	2.20	101.10
5	3.00	101.06
6	3.60	101.08
7	4.10	101.12
8	4.50	101.19
9	5.10	101.31
10	5.90	101.27
11	6.20	101.35
12	6.70	101.25
13	7.30	101.33
14	8.50	101.26
15	9.50	101.25
16	9.90	101.29
17	10.40	101.36
18	11.20	101.39
19	12.40	101.48
20	13.40	101.73
21	15.00	101.71
22	15.70	101.50
23	16.60	101.83
24	17.00	101.88
25	18.70	101.81
26	19.50	101.63
27	20.60	102.04
28	22.00	101.96
29	23.80	102.20
30	25.30	102.25
31	27.60	102.53
32	28.90	102.48
33	32.60	103.16
34	34.50	103.25
35	36.50	103.25
min. Stage =		101.06
Continuum		2
CEM		1.00

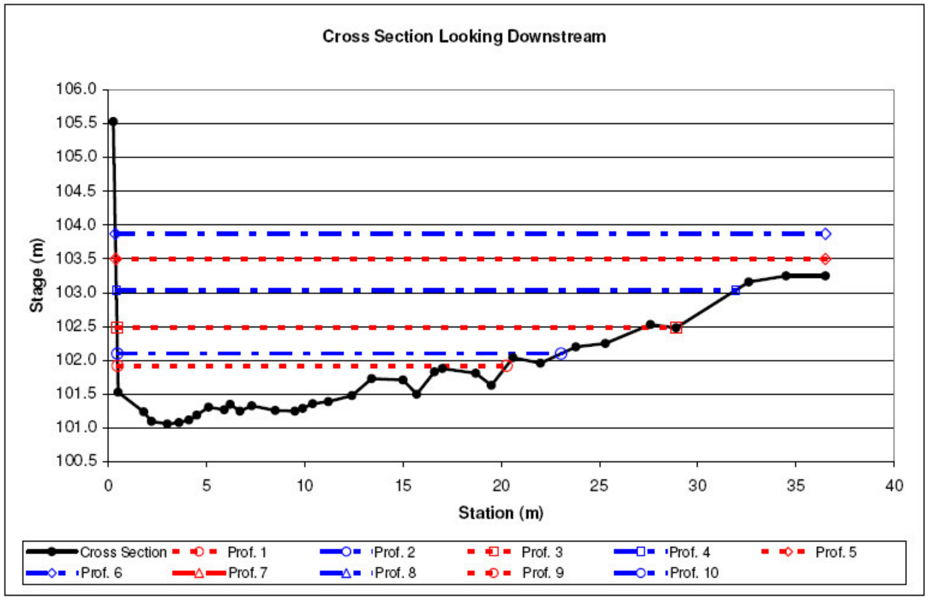

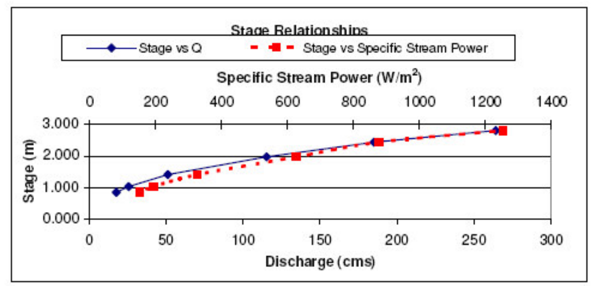

Prof. ID	Estimated n-value	L-Limit	R-Limit	WS (m)	Depth (m)	Left Sta (m)	Right Sta (m)	P_w (m)	Area (m^2)	W (m)	R (m)	D (m)	W/d	V (m/s)	Q (m^3/s)	U* (m/s)	τ (kg/ms²)	τ*	ω (W/m²)	Ω (W/m)	F_r	R/d_{84}	n-value per Limerino	Floodplain Form
TCBD02P01	0.040			101.92	0.860	0.48	20.28	20.48	9.18	19.80	0.45	0.46	23.0	1.9	17.8	0.28	76.9	0.048	154	3051	0.97	1.4	0.068	PR
TCBD02P02	0.045			102.10	1.040	0.46	23.05	23.47	12.99	22.59	0.55	0.58	21.7	2.0	25.8	0.31	95.1	0.059	196	4422	0.89	1.7	0.063	PR
TCBD02P03	0.050			102.48	1.420	0.44	28.90	28.01	22.43	26.75	0.80	0.84	18.8	2.3	51.2	0.37	137.5	0.085	328	8785	0.85	2.4	0.056	PR
TCBD02P04	0.050			103.04	1.980	0.41	31.95	33.38	39.19	31.54	1.17	1.24	15.9	2.9	115.4	0.45	201.5	0.125	628	19806	0.90	3.5	0.051	PR
TCBD02P05	0.050			103.50	2.440	0.38	36.50	38.41	55.02	36.12	1.43	1.52	14.8	3.4	185.0	0.50	245.9	0.152	879	31760	0.93	4.3	0.049	PR
TCBD02P06	0.050			103.87	2.810	0.35	36.50	38.78	68.39	36.15	1.76	1.89	12.9	3.9	264.1	0.55	302.8	0.187	1255	45346	0.96	5.3	0.047	PR
TCBD02P07	0.050																							PR
TCBD02P08	0.050																							PR
TCBD02P09	0.050																							PR
TCBD02P10	0.050																							PR

Cross Section Hydraulic Analyses: Yucaipa Creek U/S of Mesa Grande

Floodplain/Site Description: Yucaipa Creek upstream of Mesa Grande. Floodplain appears to have been encroached or narrowed significantly during construction of the adjacent park. Photo is looking upstream.

Location ID	YCMG01
d_{50} (mm) =	3.50
d_{84} (mm) =	8.40
So = Sf =	0.0371

Pt #	Sta (m)	Stage (m)
1	0.00	102.67
2	0.01	100.67
3	1.00	100.12
4	5.60	100.01
5	9.60	100.00
6	12.10	100.32
7	17.70	101.72
8		
9		
10		
11		
12		
13		
14		
15		
16		
17		
18		
19		
20		
21		
22		
23		
24		
25		
26		
27		
28		
29		
30		
31		
32		
33		
34		
35		
min. Stage =		100.00
Continuum		1
CEM		3.00

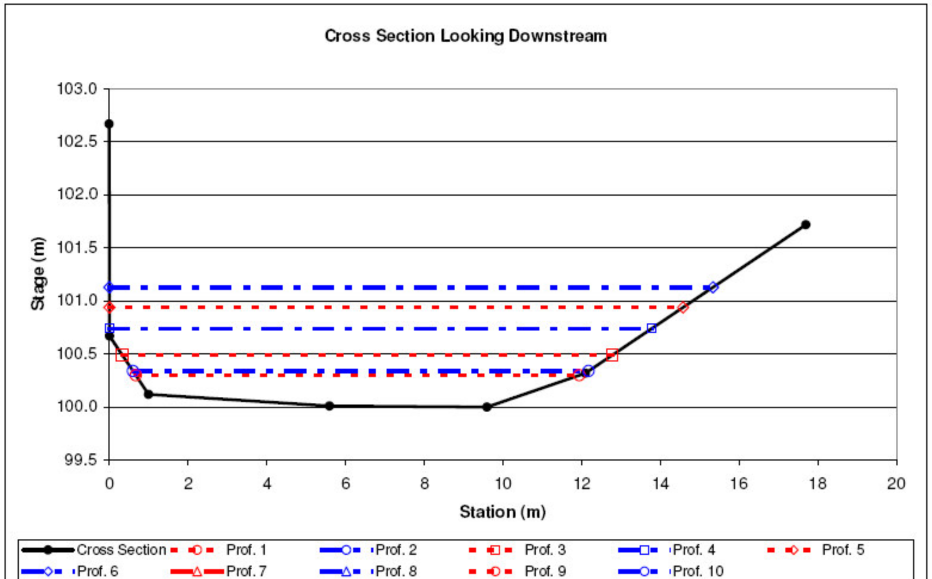

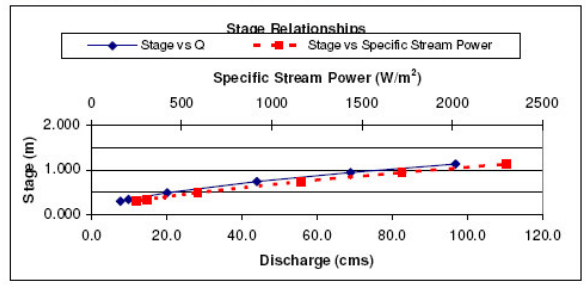

Prof. ID	Estimated n-value	L-Limit	R-Limit	WS (m)	Depth (m)	Left Sta (m)	Right Sta (m)	P_w (m)	Area (m^2)	W (m)	R (m)	D (m)	W/d	V (m/s)	Q (m^3/s)	U* (m/s)	τ (kg/ms²)	τ*	ω (W/m²)	Ω (W/m)	F_r	R/d_{84}	n-value per Limerino	Floodplain Form
YCMG01P01	0.025			100.30	0.300	0.68	11.94	11.33	2.64	11.27	0.23	0.23	37.6	2.9	7.7	0.29	84.8	1.500	249	2805	2.06	27.7	0.022	PMB
YCMG01P02	0.025			100.34	0.340	0.60	12.18	11.66	3.10	11.58	0.27	0.27	34.0	3.2	9.9	0.31	96.8	1.711	310	3593	2.11	31.7	0.022	PMB
YCMG01P03	0.025			100.49	0.490	0.33	12.78	12.58	4.90	12.45	0.39	0.39	25.4	4.1	20.1	0.38	141.7	2.506	589	7329	2.24	46.4	0.021	PMB
YCMG01P04	0.025			100.74	0.740	0.01	13.78	14.06	8.19	13.77	0.58	0.59	18.6	5.4	44.0	0.46	212.0	3.750	1163	16019	2.39	69.4	0.021	PMB
YCMG01P05	0.025			100.94	0.940	0.01	14.58	15.08	11.02	14.57	0.73	0.76	15.5	6.3	68.9	0.52	266.0	4.705	1721	25083	2.46	87.0	0.021	PMB
YCMG01P06	0.025			101.13	1.130	0.01	15.34	16.05	13.86	15.33	0.86	0.90	13.6	7.0	96.9	0.56	314.3	5.558	2299	35256	2.52	102.8	0.021	PMB
YCMG01P07	0.025																							PMB
YCMG01P08	0.025																							PMB
YCMG01P09	0.025																							PMB
YCMG01P10	0.025																							PMB

Cross Section Hydraulic Analyses: Yucaipa Creek U/S of Mesa Grande

Floodplain/Site Description: Yucaipa Creek upstream of Mesa Grande. At this location both the left and right banks are actively failing. Photo view is looking downstream.

Location ID	YCMG02	
d_{50} (mm) =		4.80
d_{84} (mm) =		18.60
So = Sf =		0.0383
Pt #	Sta (m)	Stage (m)
1	0.00	103.25
2	0.01	101.25
3	1.60	100.25
4	7.00	100.07
5	10.20	100.17
6	10.50	100.40
7	11.50	100.45
8	12.50	100.34
9	14.00	100.29
10	15.50	100.32
11	16.50	100.40
12	18.00	100.23
13	20.33	100.25
14	21.20	100.02
15	22.90	100.00
16	24.20	100.04
17	24.45	100.06
18	25.80	100.03
19	26.60	100.03
20	26.60	101.53
21	28.60	102.53
22		
23		
24		
25		
26		
27		
28		
29		
30		
31		
32		
33		
34		
35		
min. Stage =		100.00

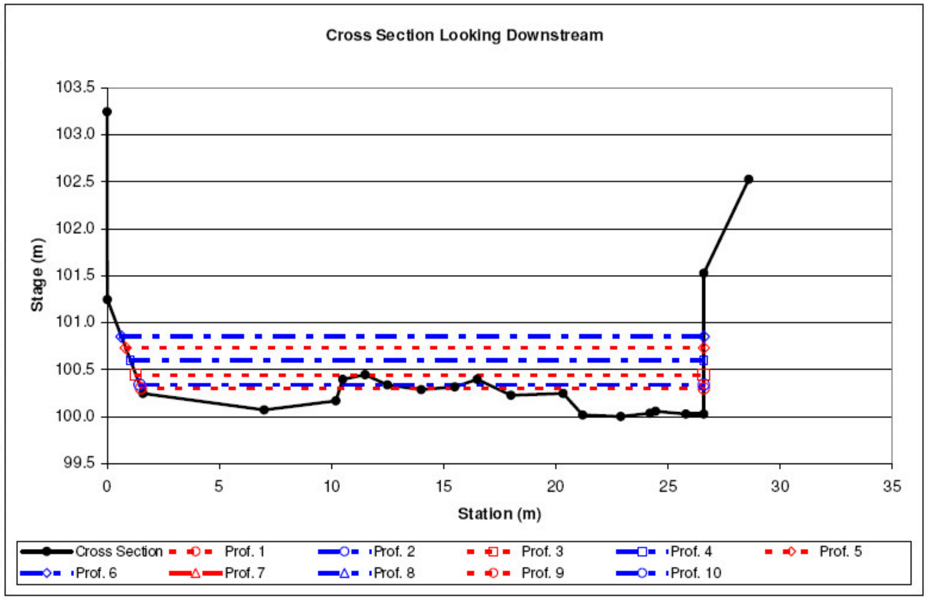

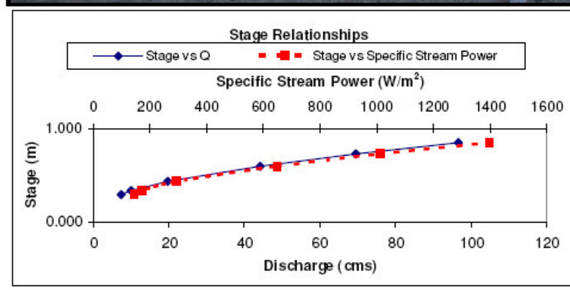

Prof. ID	Estimated n-value	L-Limit	R-Limit	WS (m)	Depth (m)	Left Sta (m)	Right Sta (m)	P_w (m)	Area (m^2)	W (m)	R (m)	D (m)	W/d	V (m/s)	Q (m^3/s)	U* (m/s)	τ (kg/ms²)	τ*	ω (W/m²)	Ω (W/m)	F_r	R/d_{84}	n-value per Limerino	Floodplain Form
YCMG02P01	0.025			100.30	0.300	1.51	26.60	19.70	3.20	19.33	0.16	0.17	64.4	2.3	7.5	0.25	61.0	0.786	145	2800	1.96	8.7	0.027	BF
YCMG02P02	0.025			100.34	0.340	1.45	26.60	22.40	4.03	21.95	0.18	0.18	64.6	2.5	10.1	0.26	67.6	0.872	172	3782	1.99	9.7	0.027	BF
YCMG02P03	0.025			100.44	0.440	1.29	26.60	25.77	6.39	25.16	0.25	0.25	57.2	3.1	19.8	0.31	93.2	1.201	295	7419	2.10	13.3	0.026	BF
YCMG02P04	0.025			100.60	0.600	1.04	26.60	26.38	10.46	25.56	0.40	0.41	42.6	4.2	44.2	0.39	149.0	1.921	649	16600	2.26	21.3	0.025	BF
YCMG02P05	0.025			100.73	0.730	0.83	26.60	26.75	13.80	25.77	0.52	0.54	35.3	5.0	69.5	0.44	193.7	2.498	1012	26085	2.36	27.7	0.025	BF
YCMG02P06	0.025			100.85	0.850	0.64	26.60	27.10	16.90	25.96	0.62	0.65	30.5	5.7	96.6	0.48	234.3	3.021	1397	36268	2.42	33.5	0.025	BF
YCMG02P07	0.025																							BF
YCMG02P08	0.025																							BF
YCMG02P09	0.025																							BF
YCMG02P10	0.025																							BF

Cross Section Hydraulic Analyses: Un-Named Tributary to Yucaipa Creek

Floodplain/Site Description: Photo view looking downstream from right overbank.

Location ID		YTLC01
d_{50} (mm) =		0.88
d_{84} (mm) =		6.00
So = Sf =		0.0795
Pt #	Sta (m)	Stage (m)
1	0.70	568.07
2	1.69	568.07
3	3.17	568.09
4	4.02	568.06
5	4.52	568.16
6	5.87	568.00
7	6.45	567.55
8	7.66	562.77
9	7.77	562.74
10	7.80	562.61
11	8.12	562.60
12	8.21	562.47
13	8.94	562.28
14	9.33	562.61
15	9.90	562.68
16	10.13	562.77
17	10.40	562.80
18	11.30	562.97
19	12.14	563.22
20	13.46	565.28
21	13.93	567.31
22	14.56	567.83
23	15.14	568.00
24	16.79	568.05
25	17.91	568.04
26	18.68	567.90
27	19.40	567.83
28		
29		
30		
31		
32		
33		
34		
35		
min. Stage =		562.28
Continuum		1
CEM		3

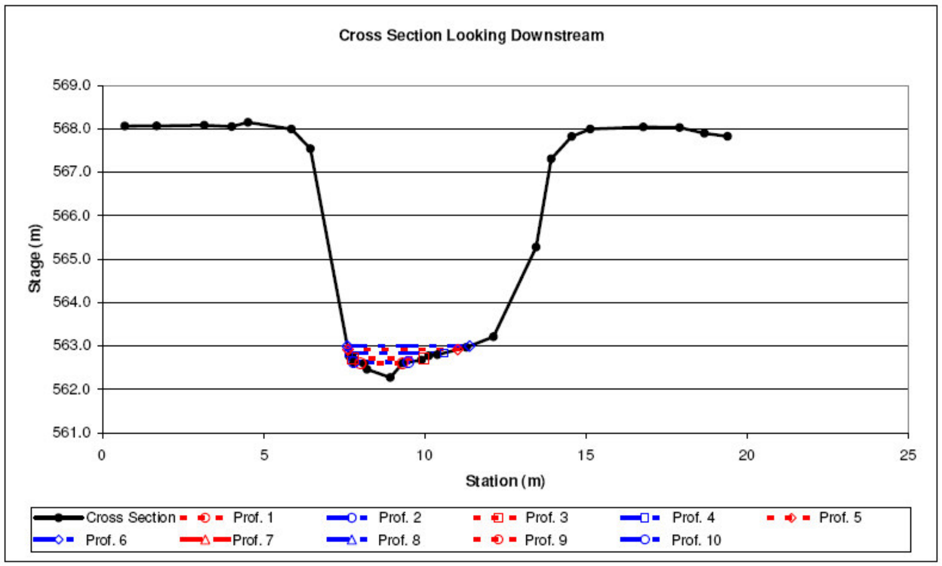

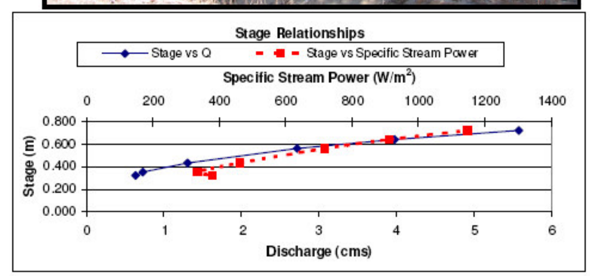

Prof. ID	Estimated n-value	L-Limit	R-Limit	WS (m)	Depth (m)	Left Sta (m)	Right Sta (m)	P_w (m)	Area (m^2)	W (m)	R (m)	D (m)	W/d	V (m/s)	Q (m^3/s)	U* (m/s)	τ (kg/ms^2)	τ*	ω (W/m^2)	Ω (W/m)	F_r	R/d_{84}	n-value per Limerino	Floodplain Form
YTLC01P01	0.030			562.60	0.324	8.02	9.32	1.51	0.23	1.30	0.15	0.18	4.0	2.7	0.63	0.35	120.7	8.468	380	495	2.19	25.8	0.021	PMB
YTLC01P02	0.030			562.63	0.354	7.80	9.50	1.93	0.28	1.70	0.15	0.16	4.8	2.6	0.73	0.34	113.3	7.947	334	568	2.19	24.2	0.021	PMB
YTLC01P03	0.030			562.71	0.434	7.77	9.98	2.51	0.44	2.20	0.18	0.20	5.1	3.0	1.31	0.37	137.5	9.647	462	1019	2.26	29.4	0.021	PMB
YTLC01P04	0.030			562.84	0.564	7.64	10.60	3.36	0.77	2.96	0.23	0.26	5.2	3.5	2.7	0.42	179.0	12.558	717	2121	2.36	38.2	0.020	PMB
YTLC01P05	0.030			562.92	0.644	7.62	11.03	3.87	1.03	3.40	0.26	0.30	5.3	3.9	4.0	0.45	206.6	14.494	912	3103	2.42	44.1	0.020	PMB
YTLC01P06	0.030			563.00	0.724	7.60	11.40	4.34	1.32	3.79	0.30	0.35	5.2	4.2	5.6	0.49	236.6	16.598	1148	4354	2.47	50.5	0.020	PMB
YTLC01P07	0.030																							PMB
YTLC01P08	0.030																							PMB
YTLC01P09	0.030																							PMB
YTLC01P10	0.030																							PMB

Cross Section Hydraulic Analyses: Un-Named Tributary to Yucaipa Creek

Floodplain/Site Description: Photo view looking downstream from left overbank.

Pt #	Sta (m)	Stage (m)
Location ID		YTLC02
d_{50} (mm) =		0.88
d_{84} (mm) =		6.00
So = Sf =		0.0795
1	0.00	568.72
2	1.22	568.64
3	1.70	568.72
4	2.77	568.79
5	3.75	568.85
6	4.34	568.78
7	4.89	568.76
8	5.79	568.28
9	6.32	567.79
10	6.90	566.38
11	7.87	565.80
12	9.50	564.98
13	10.37	564.91
14	10.71	564.12
15	11.10	563.78
16	11.87	563.76
17	12.77	563.81
18	13.65	563.87
19	13.74	564.17
20	14.06	564.59
21	14.22	564.37
22	14.71	564.51
23	14.78	564.48
24	15.50	567.84
25	15.92	568.62
26	17.11	568.59
27	18.06	568.52
28		
29		
30		
31		
32		
33		
34		
35		
min. Stage =		563.76
Continuum		1
CEM		3

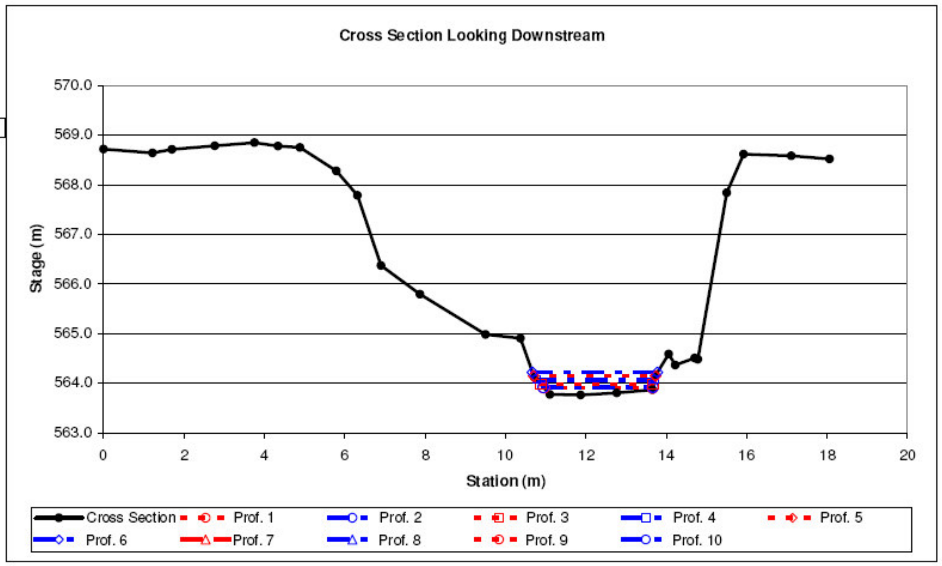

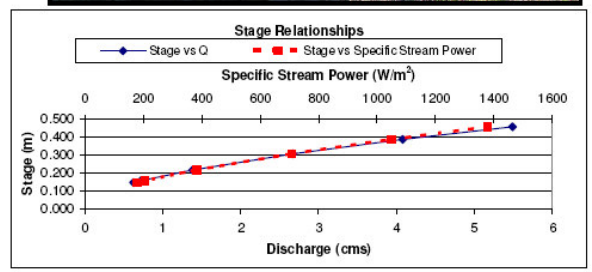

Prof. ID	Estimated n-value	L-Limit	R-Limit	WS (m)	Depth (m)	Left Sta (m)	Right Sta (m)	P_w (m)	Area (m^2)	W (m)	R (m)	D (m)	W/d	V (m/s)	Q (m^3/s)	U* (m/s)	τ (kg/ms^2)	τ*	ω (W/m^2)	Ω (W/m)	F_r	R/d_{84}	n-value per Limerino	Floodplain Form
YTLC02P01	0.030			563.91	0.147	10.95	13.66	2.80	0.30	2.72	0.11	0.11	18.5	2.1	0.6	0.29	82.6	5.793	179	487	2.18	17.6	0.021	PMB
YTLC02P02	0.030			563.92	0.157	10.94	13.67	2.83	0.32	2.73	0.11	0.12	17.4	2.2	0.7	0.30	89.4	6.268	205	560	2.20	19.1	0.021	PMB
YTLC02P03	0.030			563.98	0.217	10.87	13.68	2.98	0.49	2.81	0.16	0.17	13.0	2.8	1.4	0.36	128.3	8.999	383	1079	2.32	27.4	0.021	PMB
YTLC02P04	0.030			564.07	0.307	10.77	13.71	3.21	0.75	2.94	0.23	0.25	9.6	3.6	2.7	0.43	182.1	12.771	708	2083	2.42	38.9	0.020	PMB
YTLC02P05	0.030			564.15	0.387	10.70	13.73	3.40	0.99	3.03	0.29	0.33	7.8	4.1	4.1	0.48	226.8	15.911	1050	3182	2.47	48.4	0.020	PMB
YTLC02P06	0.030			564.22	0.457	10.67	13.78	3.56	1.20	3.11	0.34	0.39	6.8	4.6	5.5	0.51	263.6	18.489	1377	4281	2.51	56.3	0.020	PMB
YTLC02P07	0.030																							PMB
YTLC02P08	0.030																							PMB
YTLC02P09	0.030																							PMB
YTLC02P10	0.030																							PMB

Cross Section Hydraulic Analyses: Un-Named Tributary to Yucaipa Creek

Floodplain/Site Description: Photo view looking downstream from left overbank.

Location ID	YTLC03
d_{50} (mm) =	0.88
d_{84} (mm) =	6.00
So = Sf =	0.0582

Pt #	Sta (m)	Stage (m)
1	0.00	570.70
2	1.64	570.72
3	3.13	570.72
4	4.17	570.76
5	4.95	570.61
6	5.48	569.79
7	5.89	567.03
8	7.10	567.08
9	7.88	567.06
10	8.73	567.05
11	9.25	567.09
12	9.71	567.17
13	9.78	567.42
14	10.59	567.85
15	10.98	568.27
16	11.28	569.43
17	12.05	569.64
18	13.08	569.64
19	14.00	569.89
20	15.09	570.20
21	16.37	570.48
22	17.40	570.76
23	18.49	570.72
24	20.02	570.72
25		
26		
27		
28		
29		
30		
31		
32		
33		
34		
35		
min. Stage =		567.03
Continuum		1
CEM		3

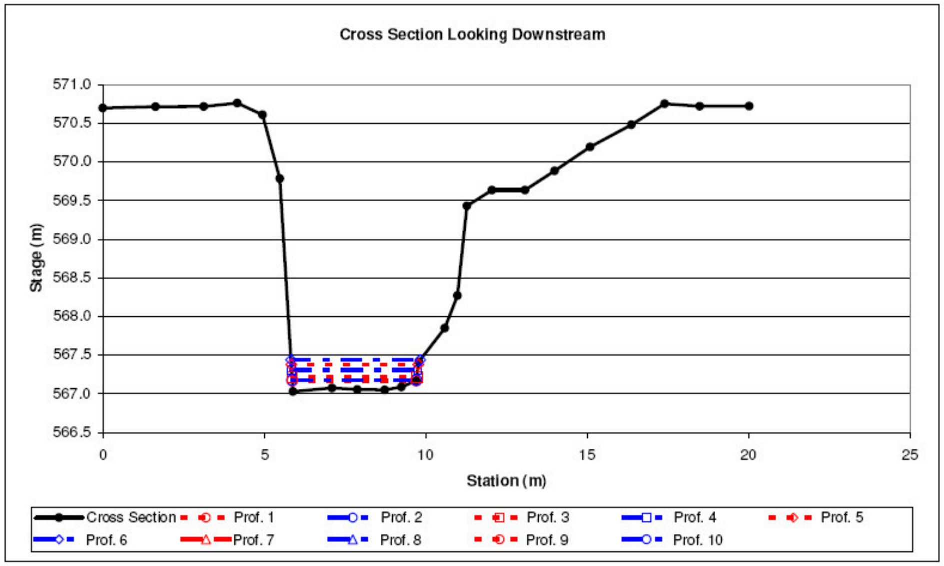

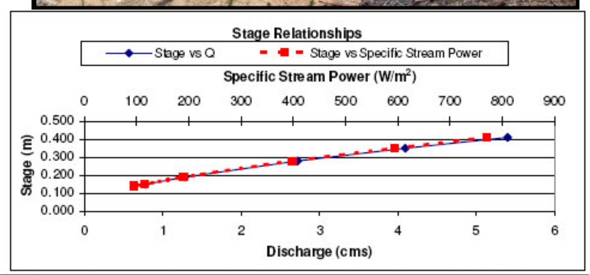

Prof. ID	Estimated n-value	L-Limit	R-Limit	WS (m)	Depth (m)	Left Sta (m)	Right Sta (m)	P_w (m)	Area (m^2)	W (m)	R (m)	D (m)	W/d	V (m/s)	Q (m^3/s)	U* (m/s)	τ (kg/ms^2)	τ*	ω (W/m^2)	Ω (W/m)	F_r	R/d_{84}	n-value per Limerino	Floodplain Form
YTLC03P01	0.030			567.17	0.140	5.87	9.71	3.97	0.38	3.84	0.10	0.10	27.4	1.7	0.64	0.23	54.5	3.820	95	363	1.83	15.9	0.021	PMB
YTLC03P02	0.030			567.18	0.150	5.87	9.71	3.99	0.43	3.84	0.11	0.11	25.6	1.8	0.78	0.25	61.4	4.308	116	446	1.86	17.9	0.021	PMB
YTLC03P03	0.030			567.22	0.190	5.86	9.72	4.07	0.58	3.86	0.14	0.15	20.3	2.2	1.3	0.29	81.8	5.736	190	733	1.94	23.9	0.021	PMB
YTLC03P04	0.030			567.31	0.280	5.85	9.75	4.26	0.93	3.90	0.22	0.24	13.9	2.9	2.7	0.35	125.0	8.770	399	1555	2.05	36.5	0.020	PMB
YTLC03P05	0.030			567.38	0.350	5.84	9.77	4.40	1.21	3.93	0.27	0.31	11.2	3.4	4.1	0.40	156.5	10.977	594	2337	2.10	45.7	0.020	PMB
YTLC03P06	0.030			567.44	0.410	5.83	9.83	4.55	1.44	4.00	0.32	0.36	9.8	3.7	5.4	0.43	181.1	12.702	770	3083	2.13	52.9	0.020	PMB
YTLC03P07	0.030																							PMB
YTLC03P08	0.030																							PMB
YTLC03P09	0.030																							PMB
YTLC03P10	0.030																							PMB

Cross Section Hydraulic Analyses: Un-Named Tributary to Yucaipa Creek

Floodplain/Site Description: Photo view looking downstream from left overbank.

Location ID	YTLC04
d_{50} (mm) =	0.89
d_{84} (mm) =	3.34
So = Sf =	0.0479

Pt #	Sta (m)	Stage (m)
1	0.00	574.38
2	2.13	574.05
3	3.39	573.97
4	5.02	573.55
5	6.25	573.20
6	7.39	573.00
7	8.20	572.77
8	9.18	570.08
9	9.40	569.93
10	10.73	569.90
11	12.04	569.92
12	12.29	570.08
13	13.34	570.08
14	13.54	570.01
15	14.55	569.96
16	15.13	570.03
17	15.60	570.00
18	15.96	570.05
19	16.71	570.00
20	17.59	570.04
21	18.46	569.99
22	19.48	570.09
23	20.59	570.08
24	21.43	570.55
25	22.55	571.78
26	23.18	572.36
27	24.36	572.71
28	25.35	573.30
29	26.39	573.79
30	28.54	573.80
31		
32		
33		
34		
35		
min. Stage =		569.90
Continuum		1
CEM		3.0

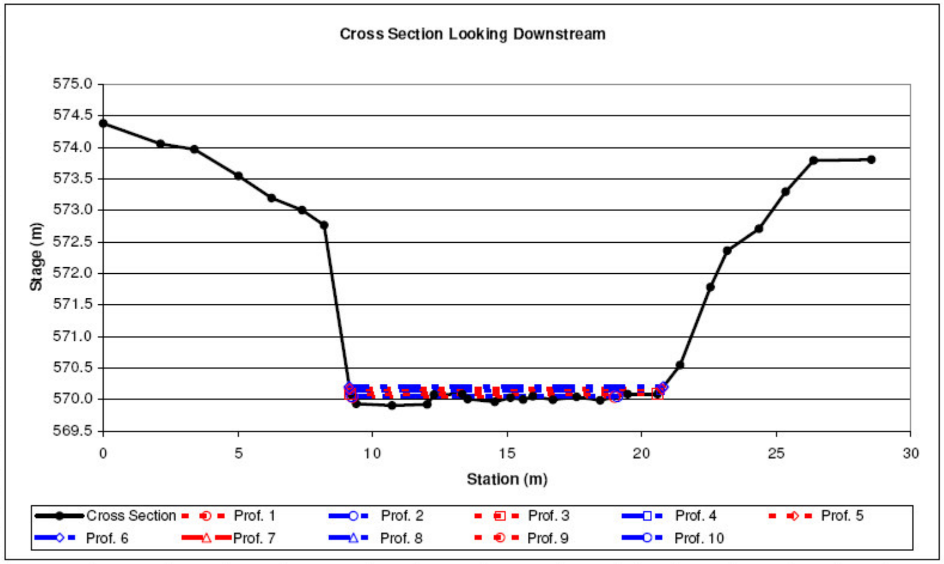

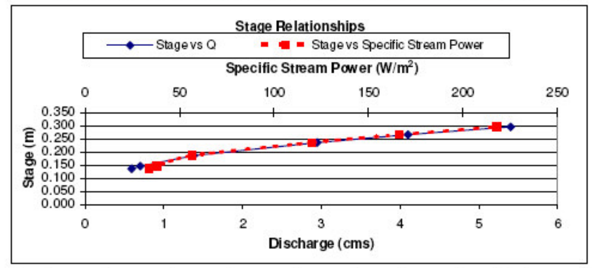

Prof. ID	Estimated n-value	L-Limit	R-Limit	WS (m)	Depth (m)	Left Sta (m)	Right Sta (m)	P_w (m)	Area (m^2)	W (m)	R (m)	D (m)	W/d	V (m/s)	Q (m^3/s)	U* (m/s)	τ (kg/ms²)	τ*	ω (W/m²)	Ω (W/m)	F_r	R/d_{84}	n-value per Limerino	Floodplain Form
YTLC04P01	0.030			570.04	0.136	9.25	19.00	8.35	0.52	8.26	0.06	0.06	60.7	1.1	0.6	0.17	29.2	2.018	34	279	1.56	18.6	0.019	BF
YTLC04P02	0.030			570.05	0.146	9.23	19.11	8.79	0.59	8.69	0.07	0.07	59.5	1.2	0.7	0.18	31.3	2.166	38	330	1.58	20.0	0.019	BF
YTLC04P03	0.030			570.09	0.186	9.18	20.60	11.55	0.98	11.42	0.08	0.09	61.4	1.4	1.4	0.20	39.8	2.756	57	648	1.65	25.4	0.019	BF
YTLC04P04	0.030			570.14	0.236	9.16	20.69	11.71	1.55	11.53	0.13	0.13	48.9	1.9	2.9	0.25	62.3	4.311	120	1385	1.77	39.7	0.018	BF
YTLC04P05	0.030			570.17	0.266	9.15	20.75	11.80	1.90	11.60	0.16	0.16	43.6	2.2	4.1	0.28	75.6	5.232	166	1928	1.83	48.2	0.018	BF
YTLC04P06	0.030			570.20	0.296	9.14	20.80	11.90	2.25	11.66	0.19	0.19	39.4	2.4	5.4	0.30	88.8	6.143	218	2539	1.87	56.6	0.018	BF
YTLC04P07	0.030																							BF
YTLC04P08	0.030																							BF
YTLC04P09	0.030																							BF
YTLC04P10	0.030																							BF

Cross Section Hydraulic Analyses: Un-Named Tributary to Yucaipa Creek

Floodplain/Site Description: Photo view looking downstream from left overbank.

Location ID	YTLC05	
d_{50} (mm) =	0.89	
d_{84} (mm) =	3.34	
So = Sf =	0.0479	
Pt #	Sta (m)	Stage (m)
1	0.00	574.78
2	1.83	574.17
3	2.98	574.13
4	3.87	574.10
5	4.86	573.79
6	5.97	574.09
7	6.52	574.08
8	6.78	573.86
9	7.89	573.68
10	8.37	572.22
11	8.93	572.07
12	9.74	572.06
13	10.77	572.09
14	10.95	572.03
15	12.05	572.02
16	13.16	572.09
17	13.62	572.27
18	14.01	572.13
19	14.53	572.14
20	14.91	572.28
21	15.94	572.32
22	16.18	572.25
23	16.83	572.27
24	17.57	572.35
25	18.39	572.34
26	19.36	572.31
27	19.53	573.20
28	20.30	573.61
29	20.72	575.19
30	22.42	575.17
31	24.08	575.27
32		
33		
34		
35		
min. Stage =		572.02
Continuum		1
CEM		3.0

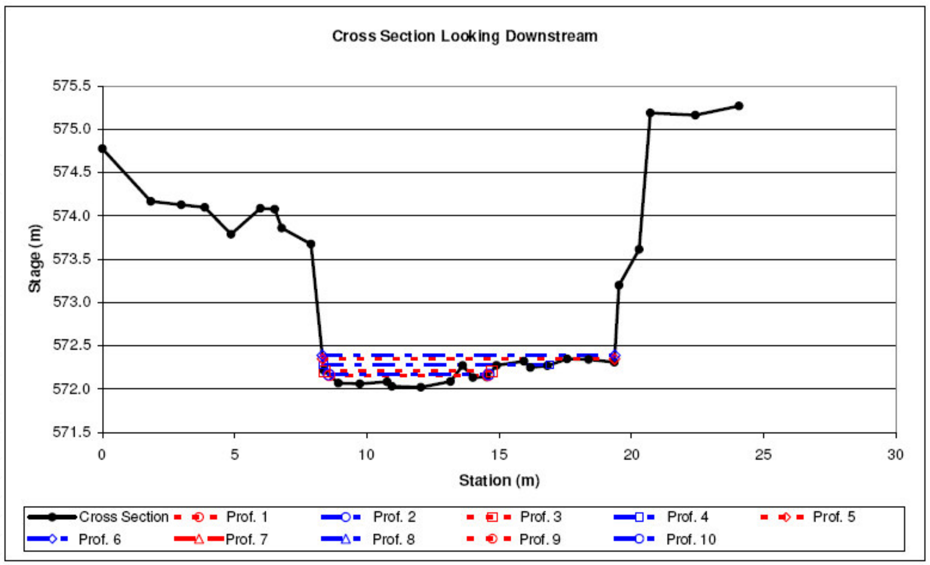

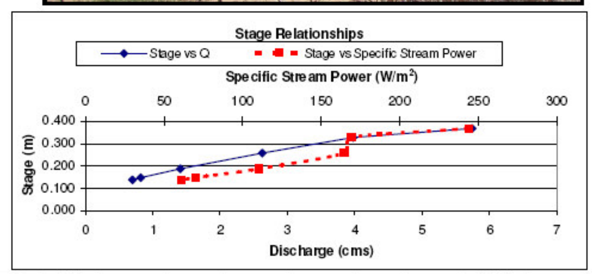

Prof. ID	Estimated n-value	L-Limit	R-Limit	WS (m)	Depth (m)	Left Sta (m)	Right Sta (m)	P_w (m)	Area (m^2)	W (m)	R (m)	D (m)	W/d	V (m/s)	Q (m^3/s)	U* (m/s)	τ (kg/ms²)	τ*	ω (W/m²)	Ω (W/m)	F_r	R/d_{84}	n-value per Limerino	Floodplain Form
YTLC05P01	0.030			572.16	0.138	8.59	14.59	5.44	0.48	5.40	0.09	0.09	39.1	1.4	0.7	0.20	41.6	2.878	61	328	1.66	26.5	0.019	PMB
YTLC05P02	0.030			572.17	0.148	8.55	14.61	5.57	0.54	5.52	0.10	0.10	37.3	1.5	0.8	0.21	45.3	3.132	70	387	1.68	28.9	0.019	PMB
YTLC05P03	0.030			572.21	0.188	8.40	14.73	6.07	0.77	5.99	0.13	0.13	31.9	1.8	1.4	0.24	59.4	4.108	111	662	1.76	37.9	0.019	PMB
YTLC05P04	0.030			572.28	0.258	8.35	16.91	7.66	1.22	7.49	0.16	0.16	29.0	2.1	2.6	0.27	75.1	5.191	165	1234	1.82	47.9	0.018	PMB
YTLC05P05	0.030			572.35	0.328	8.33	19.36	11.29	1.83	11.03	0.16	0.17	33.6	2.2	4.0	0.28	76.2	5.272	169	1868	1.82	48.6	0.018	PMB
YTLC05P06	0.030			572.39	0.368	8.32	19.37	11.37	2.29	11.06	0.20	0.21	30.0	2.5	5.7	0.31	94.6	6.545	244	2698	1.89	60.3	0.018	PMB
YTLC05P07	0.030																							PMB
YTLC05P08	0.030																							PMB
YTLC05P09	0.030																							PMB
YTLC05P10	0.030																							PMB

Cross Section Hydraulic Analyses: Un-Named Tributary to Yucaipa Creek

Floodplain/Site Description: Photo view looking downstream from left overbank.

Location ID	YTLC06
d_{50} (mm) =	0.89
d_{84} (mm) =	3.34
So = Sf =	0.0479

Pt #	Sta (m)	Stage (m)
1	0.00	577.96
2	1.11	577.58
3	2.16	577.18
4	2.65	577.12
5	3.43	576.72
6	4.03	575.65
7	5.34	573.26
8	5.78	573.26
9	6.08	573.18
10	6.92	573.24
11	7.53	573.26
12	7.70	574.51
13	8.62	574.79
14	9.25	574.93
15	9.36	575.13
16	10.77	575.24
17	12.23	575.30
18	13.50	575.32
19	14.54	575.63
20	15.27	575.89
21	16.05	576.34
22	16.75	576.64
23	17.41	576.68
24	17.94	576.67
25		
26		
27		
28		
29		
30		
31		
32		
33		
34		
35		
min. Stage =		573.18
Continuum		1
CEM		3

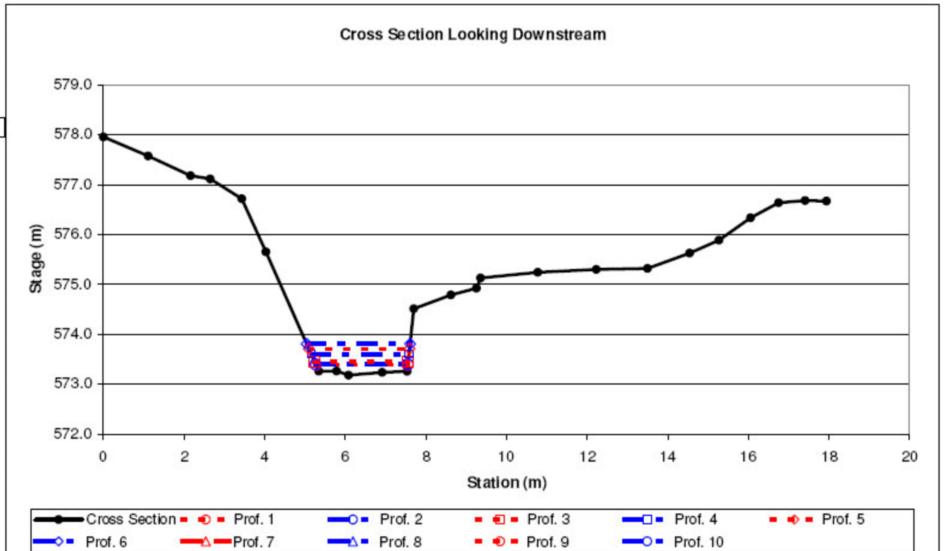

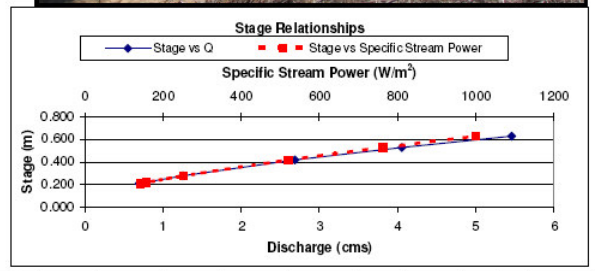

Prof. ID	Estimated n-value	L-Limit	R-Limit	WS (m)	Depth (m)	Left Sta (m)	Right Sta (m)	P_w (m)	Area (m^2)	W (m)	R (m)	D (m)	W/d	V (m/s)	Q (m^3/s)	U* (m/s)	τ (kg/ms^2)	τ^*	ω (W/m^2)	Ω (W/m)	F_r	R/d_{84}	n-value per Limerino	Floodplain Form
YTLC06P01	0.030			573.39	0.209	5.27	7.55	2.49	0.35	2.28	0.14	0.15	10.9	2.0	0.7	0.26	66.3	4.586	143	326	1.73	42.3	0.018	PMB
YTLC06P02	0.030			573.40	0.219	5.26	7.55	2.51	0.37	2.29	0.15	0.16	10.4	2.1	0.8	0.26	70.0	4.842	157	360	1.74	44.6	0.018	PMB
YTLC06P03	0.030			573.46	0.279	5.23	7.56	2.64	0.51	2.33	0.19	0.22	8.3	2.4	1.3	0.30	91.3	6.313	253	589	1.79	58.2	0.018	PMB
YTLC06P04	0.030			573.60	0.419	5.16	7.58	2.94	0.84	2.42	0.29	0.35	5.8	3.2	2.7	0.37	135.2	9.347	521	1262	1.84	86.2	0.018	PMB
YTLC06P05	0.030			573.71	0.529	5.09	7.59	3.17	1.12	2.50	0.35	0.45	4.7	3.6	4.1	0.41	165.2	11.423	762	1905	1.86	105.3	0.018	PMB
YTLC06P06	0.030			573.81	0.629	5.04	7.61	3.39	1.37	2.57	0.40	0.53	4.1	4.0	5.5	0.44	189.8	13.128	999	2565	1.87	121.0	0.018	PMB
YTLC06P07	0.030																							PMB
YTLC06P08	0.030																							PMB
YTLC06P09	0.030																							PMB
YTLC06P10	0.030																							PMB

Cross Section Hydraulic Analyses: Un-Named Tributary to Yucaipa Creek

Floodplain/Site Description: Photo view lookingupstream.

Location ID	YTLC07
d_{50} (mm) =	0.89
d_{84} (mm) =	3.34
So = Sf =	0.0479

Pt #	Sta (m)	Stage (m)
1	0.00	578.97
2	0.39	578.90
3	0.53	578.70
4	1.53	578.44
5	2.29	578.35
6	2.90	577.93
7	3.45	577.47
8	4.67	574.44
9	5.54	574.46
10	6.35	574.51
11	6.95	574.67
12	7.61	574.77
13	7.78	576.29
14	8.52	576.33
15	9.35	576.54
16	10.30	576.94
17	11.24	577.34
18	12.35	577.68
19	13.86	577.85
20	15.21	577.79
21		
22		
23		
24		
25		
26		
27		
28		
29		
30		
31		
32		
33		
34		
35		
min. Stage =		574.44
Continuum		1
CEM		3

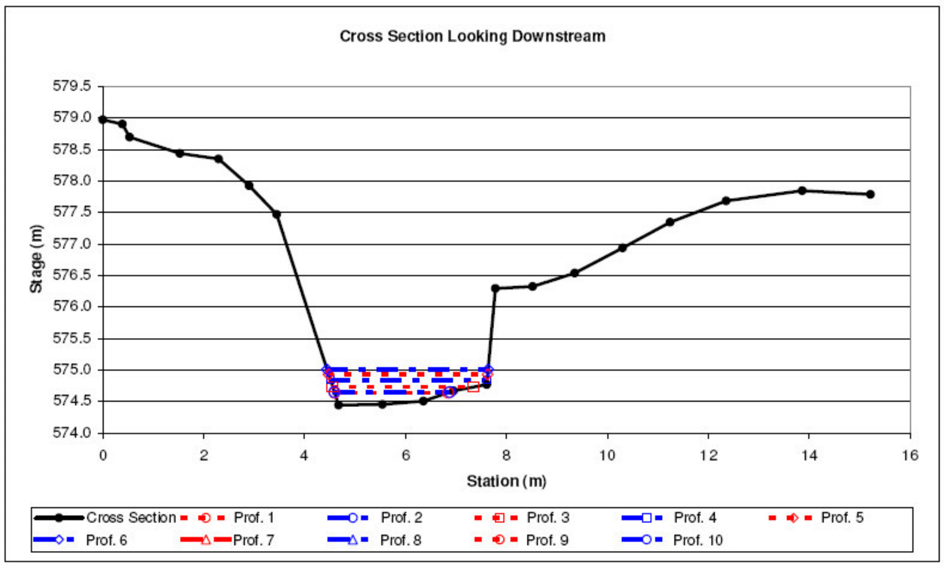

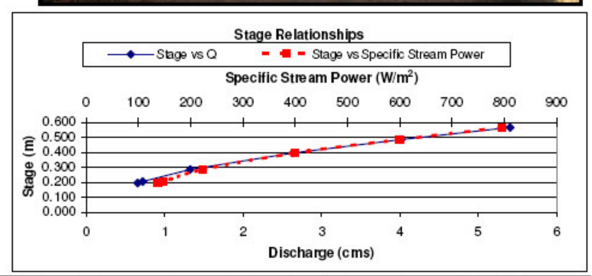

Prof. ID	Estimated n-value	L-Limit	R-Limit	WS (m)	Depth (m)	Left Sta (m)	Right Sta (m)	P_w (m)	Area (m^2)	W (m)	R (m)	D (m)	W/d	V (m/s)	Q (m^3/s)	U* (m/s)	τ (kg/ms^2)	τ^*	ω (W/m^2)	Ω (W/m)	F_r	R/d_{84}	n-value per Limerino	Floodplain Form
YTLC07P01	0.030			574.64	0.196	4.59	6.85	2.40	0.33	2.25	0.14	0.15	11.5	2.0	0.66	0.26	65.5	4.531	137	309	1.74	41.8	0.018	PMB
YTLC07P02	0.030			574.65	0.206	4.59	6.88	2.45	0.36	2.29	0.15	0.16	11.1	2.0	0.72	0.26	68.6	4.741	148	340	1.75	43.7	0.018	PMB
YTLC07P03	0.030			574.73	0.286	4.56	7.35	3.02	0.56	2.79	0.19	0.20	9.8	2.4	1.3	0.30	87.2	6.030	223	624	1.82	55.6	0.018	PMB
YTLC07P04	0.030			574.84	0.396	4.51	7.62	3.46	0.89	3.10	0.26	0.29	7.8	3.0	2.6	0.35	121.1	8.376	399	1240	1.89	77.2	0.018	PMB
YTLC07P05	0.030			574.93	0.486	4.48	7.63	3.65	1.17	3.15	0.32	0.37	6.5	3.4	4.0	0.39	151.1	10.449	600	1889	1.92	96.3	0.018	PMB
YTLC07P06	0.030			575.01	0.566	4.44	7.64	3.82	1.43	3.19	0.37	0.45	5.6	3.8	5.4	0.42	175.7	12.152	796	2541	1.94	112.0	0.018	PMB
YTLC07P07	0.030																							PMB
YTLC07P08	0.030																							PMB
YTLC07P09	0.030																							PMB
YTLC07P10	0.030																							PMB

Cross Section Hydraulic Analyses: Un-Named Tributary to Yucaipa Creek

Floodplain/Site Description: Photo view looking downstream from left overbank.

Location ID	YTLC08	
d_{50} (mm) =	0.89	
d_{84} (mm) =	3.34	
So = Sf =	0.0479	
Pt #	Sta (m)	Stage (m)
1	0.00	580.03
2	1.50	579.38
3	2.47	579.24
4	3.53	579.03
5	5.02	578.53
6	5.53	577.21
7	6.32	575.21
8	6.88	575.09
9	7.70	575.17
10	8.49	575.04
11	8.90	575.17
12	9.83	575.21
13	10.71	575.16
14	11.40	575.05
15	11.97	575.08
16	12.49	575.13
17	12.59	575.42
18	13.04	575.55
19	13.49	575.53
20	13.58	575.04
21	14.52	574.99
22	14.90	575.02
23	15.26	575.11
24	16.40	577.34
25	17.36	577.74
26	18.54	577.83
27	19.49	577.79
28		
29		
30		
31		
32		
33		
34		
35		
min. Stage =	574.99	
Continuum	1	
CEM	3.0	

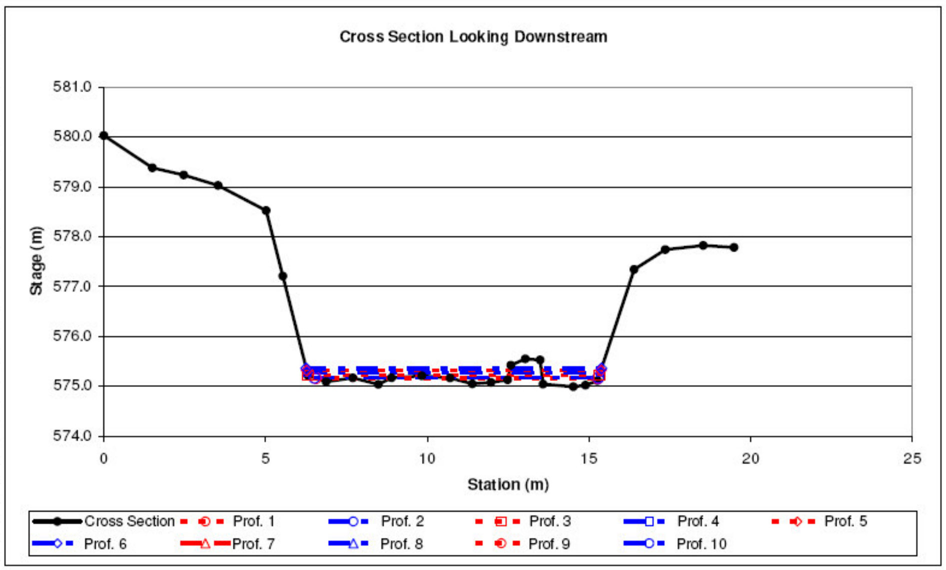

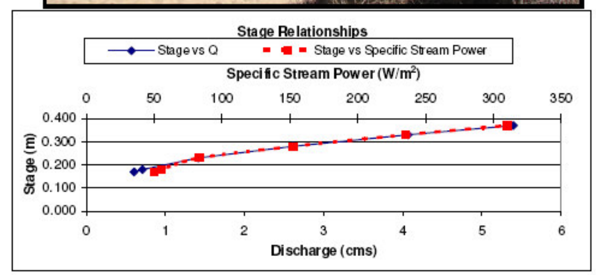

Prof. ID	Estimated n-value	L-Limit	R-Limit	WS (m)	Depth (m)	Left Sta (m)	Right Sta (m)	P_w (m)	Area (m^2)	W (m)	R (m)	D (m)	W/d	V (m/s)	Q (m^3/s)	U* (m/s)	τ (kg/ms^2)	τ*	ω (W/m^2)	Ω (W/m)	F_r	R/d_{84}	n-value per Limerino	Floodplain Form
YTLC08P01	0.030			575.16	0.170	6.56	15.29	5.89	0.46	5.68	0.08	0.08	33.4	1.3	0.6	0.19	36.4	2.517	50	284	1.60	23.2	0.019	PMB
YTLC08P02	0.030			575.17	0.180	6.51	15.29	6.26	0.52	6.02	0.08	0.09	33.5	1.4	0.7	0.20	38.6	2.672	55	334	1.62	24.6	0.019	PMB
YTLC08P03	0.030			575.22	0.230	6.31	15.32	8.33	0.87	7.97	0.10	0.11	34.7	1.6	1.4	0.22	49.2	3.406	83	665	1.68	31.4	0.019	PMB
YTLC08P04	0.030			575.27	0.280	6.29	15.34	8.55	1.27	8.05	0.15	0.16	28.7	2.1	2.6	0.26	70.0	4.843	153	1228	1.76	44.7	0.018	PMB
YTLC08P05	0.030			575.32	0.330	6.27	15.37	8.76	1.68	8.12	0.19	0.21	24.6	2.4	4.1	0.30	90.0	6.224	235	1911	1.83	57.4	0.018	PMB
YTLC08P06	0.030			575.36	0.370	6.26	15.39	8.93	2.00	8.17	0.22	0.25	22.1	2.7	5.4	0.32	105.4	7.291	310	2536	1.86	67.2	0.018	PMB
YTLC08P07	0.030																							PMB
YTLC08P08	0.030																							PMB
YTLC08P09	0.030																							PMB
YTLC08P10	0.030																							PMB

Cross Section Hydraulic Analyses: Un-Named Tributary to Yucaipa Creek

Floodplain/Site Description: Photo view looking upstream from left overbank.

Location ID	YTLC09
d_{50} (mm) =	0.89
d_{84} (mm) =	3.34
So = Sf =	0.0479

Pt #	Sta (m)	Stage (m)
1	0.00	579.18
2	1.54	578.70
3	3.05	578.08
4	4.42	577.58
5	5.02	577.46
6	6.34	577.38
7	7.71	577.41
8	8.93	577.33
9	9.14	577.10
10	9.54	577.01
11	9.72	576.31
12	9.80	576.25
13	9.86	575.98
14	9.97	575.90
15	10.03	575.57
16	11.14	575.57
17	11.31	575.68
18	11.37	575.57
19	11.53	575.58
20	11.67	575.68
21	12.52	575.70
22	13.05	575.73
23	13.69	575.79
24	14.47	575.90
25	14.54	576.07
26	14.85	576.21
27	14.98	576.35
28	15.58	576.45
29	16.12	576.72
30	16.72	578.20
31	17.41	578.27
32	18.60	578.09
33	20.26	577.98
34	21.78	577.93
35		
min. Stage =		575.57
Continuum		1
CEM		3.0

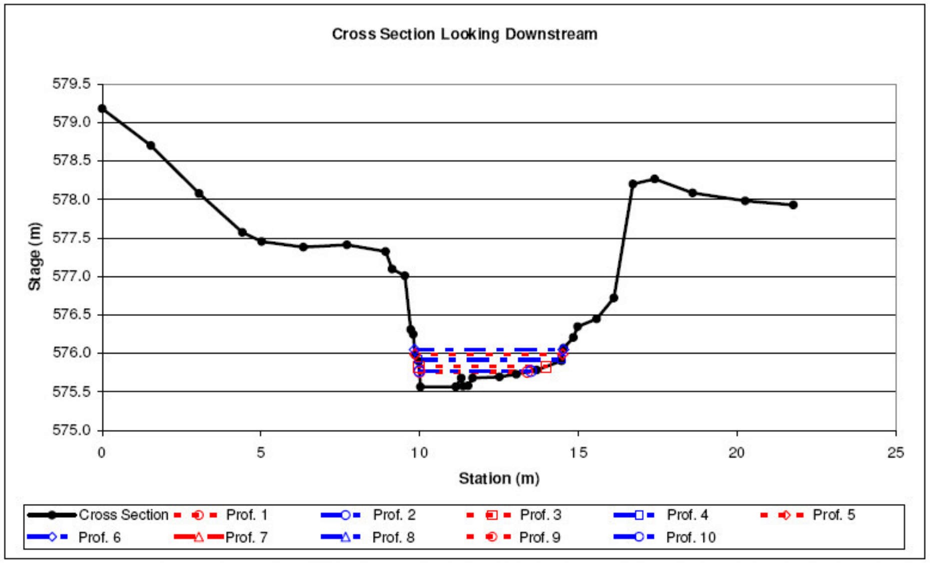

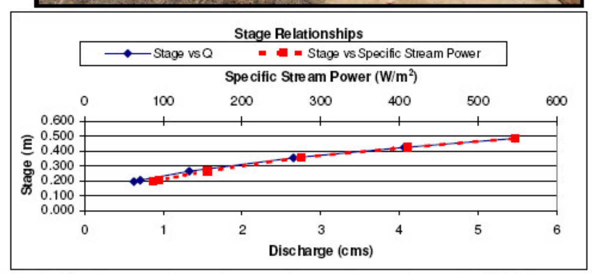

Prof. ID	Estimated n-value	L-Limit	R-Limit	WS (m)	Depth (m)	Left Sta (m)	Right Sta (m)	P_w (m)	Area (m^2)	W (m)	R (m)	D (m)	W/d	V (m/s)	Q (m^3/s)	U* (m/s)	τ (kg/ms²)	τ*	ω (W/m²)	Ω (W/m)	F_r	R/d_{84}	n-value per Limerino	Floodplain Form
YTLC09P01	0.030			575.76	0.195	10.00	13.40	3.70	0.39	3.40	0.10	0.11	17.4	1.6	0.6	0.22	49.2	3.404	87	296	1.64	31.4	0.019	PMB
YTLC09P02	0.030			575.77	0.205	10.00	13.52	3.83	0.42	3.52	0.11	0.12	17.2	1.7	0.7	0.23	51.8	3.585	95	333	1.66	33.1	0.019	PMB
YTLC09P03	0.030			575.83	0.265	9.99	13.98	4.37	0.65	4.00	0.15	0.16	15.1	2.0	1.3	0.26	69.9	4.838	156	626	1.74	44.6	0.018	PMB
YTLC09P04	0.030			575.92	0.355	9.95	14.48	4.98	1.04	4.53	0.21	0.23	12.8	2.6	2.7	0.31	97.8	6.764	275	1248	1.83	62.4	0.018	PMB
YTLC09P05	0.030			575.99	0.425	9.86	14.51	5.17	1.36	4.65	0.26	0.29	10.9	3.0	4.1	0.35	123.4	8.537	411	1910	1.90	78.7	0.018	PMB
YTLC09P06	0.030			576.05	0.485	9.85	14.53	5.30	1.64	4.69	0.31	0.35	9.7	3.3	5.5	0.38	145.3	10.051	548	2568	1.93	92.7	0.018	PMB
YTLC09P07	0.030																							PMB
YTLC09P08	0.030																							PMB
YTLC09P09	0.030																							PMB
YTLC09P10	0.030																							PMB

Cross Section Hydraulic Analyses: Un-Named Tributary to Yucaipa Creek

Floodplain/Site Description: Photo view looking upstream from left overbank.

Location ID		YTLC10
d_{50} (mm) =		0.89
d_{84} (mm) =		3.34
So = Sf =		0.0479
Pt #	Sta (m)	Stage (m)
1	0.00	580.71
2	1.09	580.21
3	2.39	579.88
4	3.54	579.64
5	4.95	579.49
6	6.39	579.40
7	7.74	579.24
8	9.53	578.80
9	10.59	578.44
10	11.37	578.29
11	12.25	578.30
12	12.58	577.41
13	12.81	576.85
14	13.84	576.83
15	14.82	576.83
16	15.62	576.84
17	16.37	576.94
18	17.36	576.94
19	18.53	576.96
20	18.84	577.10
21	19.81	578.32
22	20.51	579.19
23	21.35	579.36
24	22.71	579.18
25	24.03	579.08
26	25.13	579.10
27	25.65	579.12
28		
29		
30		
31		
32		
33		
34		
35		
min. Stage =		576.83
Continuum		1
CEM		3

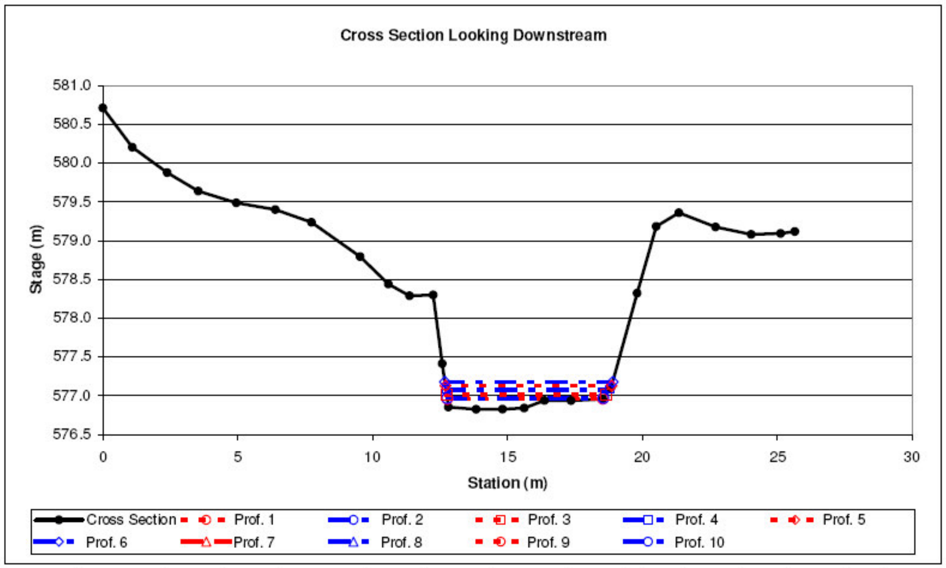

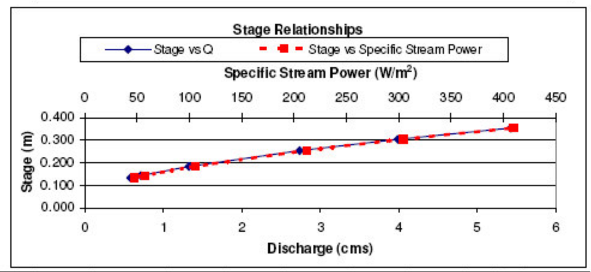

Prof. ID	Estimated n-value	L-Limit	R-Limit	WS (m)	Depth (m)	Left Sta (m)	Right Sta (m)	P_w (m)	Area (m^2)	W (m)	R (m)	D (m)	W/d	V (m/s)	Q (m^3/s)	U* (m/s)	τ (kg/ms^2)	τ*	ω (W/m^2)	Ω (W/m)	F_r	R/d_{84}	n-value per Limerino	Floodplain Form
YTLC10P01	0.030			576.96	0.134	12.77	18.54	5.85	0.45	5.77	0.08	0.08	43.1	1.3	0.59	0.19	35.9	2.480	48	275	1.62	22.9	0.019	PMB
YTLC10P02	0.030			576.97	0.144	12.76	18.56	5.88	0.50	5.80	0.09	0.09	40.3	1.4	0.71	0.20	40.3	2.785	58	336	1.65	25.7	0.019	PMB
YTLC10P03	0.030			577.01	0.184	12.75	18.64	6.02	0.74	5.90	0.12	0.13	32.0	1.8	1.3	0.24	57.6	3.985	106	624	1.74	36.7	0.019	PMB
YTLC10P04	0.030			577.08	0.254	12.72	18.79	6.26	1.16	6.07	0.18	0.19	23.9	2.4	2.7	0.29	86.9	6.009	212	1287	1.86	55.4	0.018	PMB
YTLC10P05	0.030			577.13	0.304	12.70	18.86	6.40	1.46	6.16	0.23	0.24	20.3	2.7	4.0	0.33	107.4	7.431	304	1875	1.92	68.5	0.018	PMB
YTLC10P06	0.030			577.18	0.354	12.68	18.90	6.52	1.77	6.22	0.27	0.28	17.6	3.1	5.4	0.36	127.8	8.840	410	2551	1.96	81.5	0.018	PMB
YTLC10P07	0.030																							PMB
YTLC10P08	0.030																							PMB
YTLC10P09	0.030																							PMB
YTLC10P10	0.030																							PMB

Cross Section Hydraulic Analyses: Un-Named Tributary to Yucaipa Creek

Floodplain/Site Description: Photo view looking upstream.

Location ID		YTLC11
d_{50} (mm) =		0.89
d_{84} (mm) =		3.34
So = Sf =		0.0479
Pt #	Sta (m)	Stage (m)
1	0.00	581.57
2	0.81	581.25
3	2.32	580.70
4	3.60	579.92
5	4.43	579.60
6	5.29	579.59
7	5.65	578.75
8	6.05	578.34
9	6.58	578.36
10	6.90	578.35
11	7.33	578.29
12	7.80	578.33
13	7.90	578.31
14	8.29	578.28
15	8.47	578.25
16	9.73	578.25
17	10.46	578.23
18	10.72	578.25
19	11.65	578.25
20	12.96	578.26
21	13.57	580.10
22	14.32	580.12
23	15.28	580.16
24	16.65	580.10
25	18.03	580.05
26	19.39	580.09
27		
28		
29		
30		
31		
32		
33		
34		
35		
min. Stage =		578.23
Continuum		1
CEM		3.0

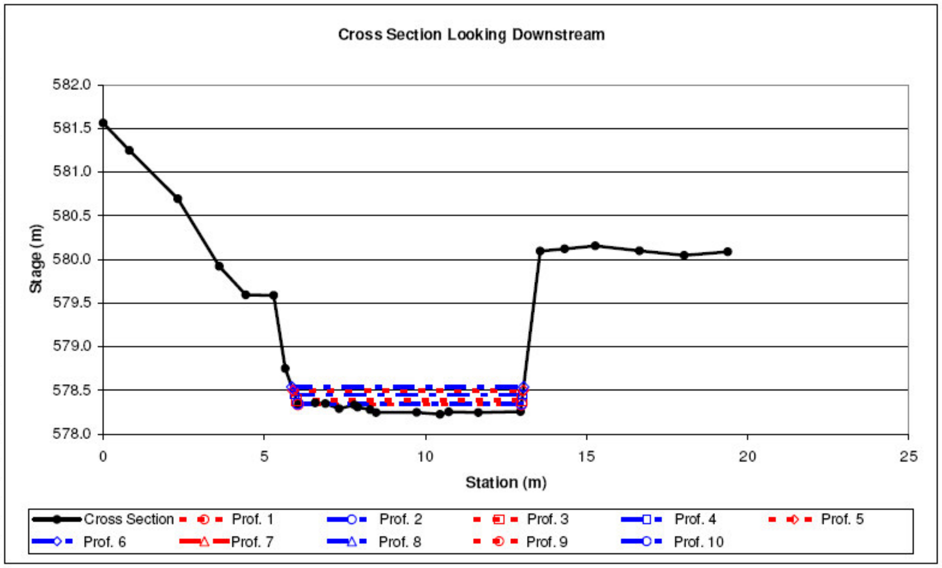

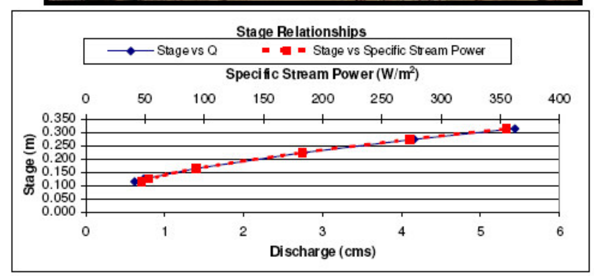

Prof. ID	Estimated n-value	L-Limit	R-Limit	WS (m)	Depth (m)	Left Sta (m)	Right Sta (m)	P_w (m)	Area (m^2)	W (m)	R (m)	D (m)	W/d	V (m/s)	Q (m^3/s)	U* (m/s)	τ (kg/ms²)	τ*	ω (W/m²)	Ω (W/m)	F_r	R/d_{84}	n-value per Limerino	Floodplain Form
YTLC11P01	0.030			578.34	0.114	6.05	12.98	6.19	0.47	6.12	0.08	0.08	53.7	1.3	0.6	0.19	35.8	2.477	48	291	1.62	22.8	0.019	PMB
YTLC11P02	0.030			578.35	0.124	6.04	12.99	6.56	0.53	6.47	0.08	0.08	52.2	1.4	0.7	0.20	38.3	2.649	53	345	1.63	24.4	0.019	PMB
YTLC11P03	0.030			578.39	0.164	6.00	13.00	7.14	0.81	7.00	0.11	0.12	42.7	1.7	1.4	0.23	53.5	3.698	93	654	1.72	34.1	0.019	PMB
YTLC11P04	0.030			578.45	0.224	5.94	13.02	7.28	1.23	7.08	0.17	0.17	31.6	2.2	2.8	0.28	79.7	5.509	183	1296	1.83	50.8	0.018	PMB
YTLC11P05	0.030			578.50	0.274	5.89	13.04	7.40	1.59	7.14	0.21	0.22	26.1	2.6	4.2	0.32	100.9	6.979	274	1955	1.90	64.4	0.018	PMB
YTLC11P06	0.030			578.54	0.314	5.85	13.05	7.50	1.88	7.20	0.25	0.26	22.9	2.9	5.4	0.34	117.6	8.131	355	2555	1.94	75.0	0.018	PMB
YTLC11P07	0.030																							PMB
YTLC11P08	0.030																							PMB
YTLC11P09	0.030																							PMB
YTLC11P10	0.030																							PMB

Cross Section Hydraulic Analyses: Un-Named Tributary to Yucaipa Creek

Floodplain/Site Description: Photo view looking from right overbank toward left overbank.

Location ID	YTLC12	
d_{50} (mm) =	0.89	
d_{84} (mm) =	3.34	
So = Sf =	0.0479	
Pt #	Sta (m)	Stage (m)
1	0.00	582.75
2	0.97	582.80
3	2.05	582.78
4	3.22	582.81
5	4.84	582.83
6	5.08	582.62
7	5.85	582.30
8	6.67	582.23
9	7.50	582.10
10	7.61	581.85
11	7.75	581.79
12	9.37	581.74
13	9.58	581.79
14	9.92	581.76
15	10.10	581.81
16	10.64	581.79
17	11.50	581.80
18	11.99	581.84
19	12.49	581.80
20	12.56	581.76
21	13.14	581.73
22	13.61	581.76
23	14.58	581.72
24	16.28	581.76
25	17.24	582.06
26	17.48	582.98
27	17.96	582.99
28	18.56	582.91
29	20.07	583.10
30	21.58	583.11
31	23.20	583.19
32		
33		
34		
35		
min. Stage =		581.72
Continuum		1
CEM		3.0

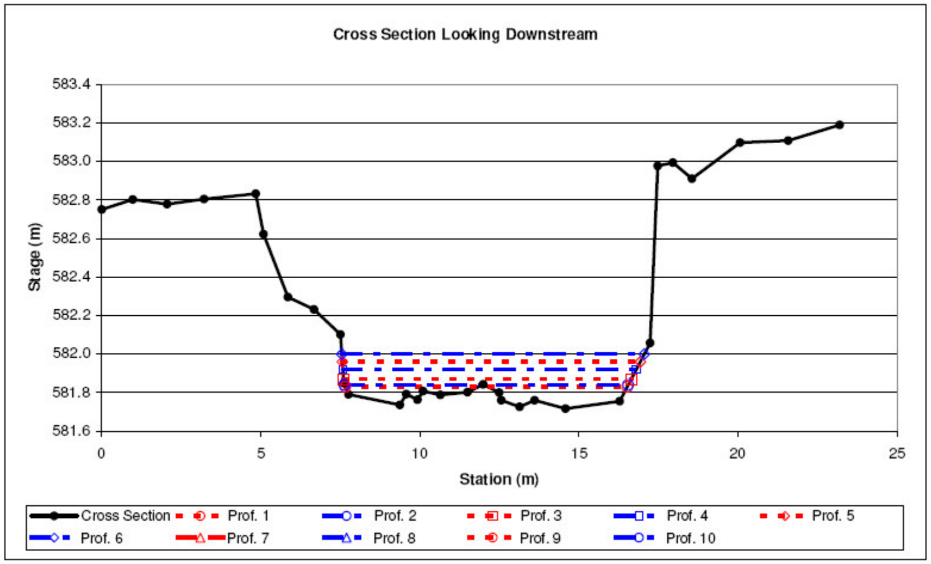

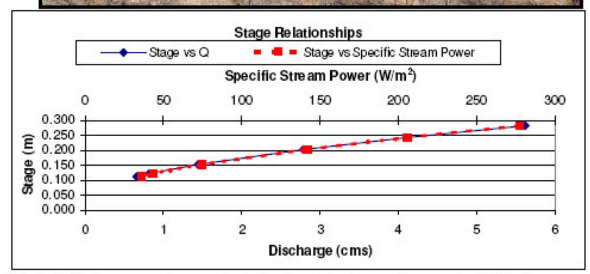

Prof. ID	Estimated n-value	L-Limit	R-Limit	WS (m)	Depth (m)	Left Sta (m)	Right Sta (m)	P_w (m)	Area (m^2)	W (m)	R (m)	D (m)	W/d	V (m/s)	Q (m^3/s)	U* (m/s)	τ (kg/ms^2)	τ*	ω (W/m^2)	Ω (W/m)	F_r	R/d_{84}	n-value per Limerino	Floodplain Form
YTLC12P01	0.030			581.83	0.113	7.66	16.52	8.61	0.56	8.56	0.06	0.07	75.7	1.2	0.7	0.17	30.5	2.109	36	309	1.58	19.4	0.019	BF
YTLC12P02	0.030			581.84	0.123	7.63	16.55	8.90	0.65	8.85	0.07	0.07	71.9	1.3	0.8	0.18	34.1	2.357	43	385	1.61	21.7	0.019	BF
YTLC12P03	0.030			581.87	0.153	7.60	16.65	9.12	0.92	9.05	0.10	0.10	59.1	1.6	1.4	0.22	47.1	3.261	75	677	1.70	30.1	0.019	BF
YTLC12P04	0.030			581.92	0.203	7.58	16.80	9.34	1.37	9.22	0.15	0.15	45.4	2.0	2.8	0.26	69.0	4.773	142	1309	1.80	44.0	0.018	BF
YTLC12P05	0.030			581.96	0.243	7.56	16.93	9.52	1.74	9.37	0.18	0.19	38.5	2.4	4.1	0.29	86.1	5.955	206	1928	1.87	54.9	0.018	BF
YTLC12P06	0.030			582.00	0.283	7.55	17.06	9.69	2.12	9.51	0.22	0.22	33.6	2.6	5.6	0.32	102.8	7.113	278	2641	1.92	65.6	0.018	BF
YTLC12P07	0.030																							BF
YTLC12P08	0.030																							BF
YTLC12P09	0.030																							BF
YTLC12P10	0.030																							BF